

NASA CR-112145

FINAL REPORT

INTEGRATED DYNAMIC ANALYSIS SIMULATION OF SPACE STATIONS WITH CONTROLLABLE SOLAR ARRAYS (SUPPLEMENTAL DATA AND ANALYSES)

By

Joseph A. Heinrichs
Fairchild Industries, Inc.

Joseph J. Fee
Wolf Research and Development Corp.

Prepared Under Contract No. NAS1-10155

By



FAIRCHILD

Fairchild Industries
Germantown, Maryland 20767

For

NATIONAL AERONAUTICS AND SPACE ADMINISTRATION

September 1972

(NASA-CR-112145) INTEGRATED DYNAMIC
ANALYSIS SIMULATION OF SPACE STATIONS WITH
CONTROLLABLE SOLAR ARRAYS J. A. Heinrichs,
et al (Fairchild Industries, Inc.,
Germantown, Md.) Sep. 1972 464 p CSCI 22B G3/31

Unclas
41646

N72-32849

FINAL REPORT

INTEGRATED DYNAMIC ANALYSIS SIMULATION OF SPACE STATIONS WITH CONTROLLABLE SOLAR ARRAYS (SUPPLEMENTAL DATA AND ANALYSES)

By

Joseph A. Heinrichs
Fairchild Industries, Inc.

Joseph J. Fee
Wolf Research and Development Corp.

Prepared Under Contract No. NAS1-10155

By



FAIRCHILD

Fairchild Industries
Germantown, Maryland 20767

For

NATIONAL AERONAUTICS AND SPACE ADMINISTRATION

September 1972

TABLE OF CONTENTS

<u>SECTION</u>	<u>SUBJECT</u>	<u>PAGE</u>
1.0	INTRODUCTION	1-1
2.0	SPACE STATION/SOLAR ARRAY STRUCTURAL CONFIGURATIONS	2-1
3.0	GUIDANCE AND CONTROL SYSTEM CONSIDERATIONS	3-1
3.1	Space Station Attitude Control System	3-1
3.1.1	CMG Control System	3-1
3.1.2	Reaction Jet Control System	3-3
3.2	Solar Array Orientation Control System	3-6
3.2.1	Continuous Array Drive System	3-6
3.2.2	Non-Linear Drive System	3-9
3.3	References	3-10
4.0	DYNAMIC INTERACTIONS ANALYSIS FORMULATION AND DIGITAL SIMULATION	4-1
4.1	Rigid Space Station/Flexible Controlled Appendages	4-1
4.1.1	Conventions and Coordinate Systems	4-3
4.1.2	Initialization Procedures	4-11
4.1.3	Rigid Body Equations of Motion	4-15
4.1.4	Flexible Array Dynamics	4-34
4.1.5	Guidance and Control	4-56
4.1.6	Orbit Generator	4-78
4.1.7	Equations of Constrained Motion of Three Rigid Bodies	4-80
4.2	Flexible Space Station/Flexible Appendage, Zero "G" Condition	4-102
4.2.1	Modal Analysis of Freely Translating and Translating and Rotating Space Station	4-104
4.2.2	Rigidly Attached Appendages	4-115
4.2.3	Rotating Arrays	4-123
4.2.4	Total System Equation	4-130
4.2.5	Auxiliary Equations	4-151
4.3	Flexible Spinning Space Station	4-157
4.3.1	Modal Equations	4-157
4.3.2	Rigid Body Equations	4-162

(TABLE OF CONTENTS - CONTINUED)

<u>SECTION</u>	<u>SUBJECT</u>	<u>PAGE</u>
4.3.3	Equations of Flexible Appendages Attached to the Spinning Space Station	4-166
4.3.4	Interaction Forces and Torques	4-171
4.3.5	Total System Equation	4-176
4.3.6	Transformation Matrix [V]	4-184
4.3.7	Computational Considerations	4-190
4.4	References	4-192
5.0	SOLAR ARRAY AND SPACE STATION STRUCTURAL DYNAMIC ANALYSES AND DATA	5-1
5.1	Phase I Study Analysis	5-1
5.1.1	Flexible Rollup Array	5-2
5.1.2	Foldout Panel Array	5-40
5.2	Phase II Study Analyses	5-65
5.2.1	Zero "G" Space Station Configuration	5-65
5.2.2	Artificial "G" Space Station Configuration	5-70
5.2.3	Zero "G" Solar Array Configuration	5-79
5.2.4	Artificial "G" Solar Array Configuration	5-85
5.3	References	
6.0	SIMULATION VERIFICATION ANALYSIS	6-1
6.1	Structural Dynamics Verification	6-1
6.1.1	Simulation of Flexible Appendages and Rigid Space Station	6-1
6.1.2	Simulation of Rigid Appendages and Rigid Space Station	6-3
6.1.3	Simulation of Flexible Appendages and Flexible Space Station	6-3
6.1.4	Verification of Complex Eigenvalue-Eigenvector Routine	6-5
6.2	Subprogram Verification	6-6
6.3	References	6-8
APPENDIX A	- Vibration Mode Data	A-1

1.0 INTRODUCTION

This volume of the final report presents space station and solar array data and the analyses which were performed in support of the integrated dynamic analysis study. It is intended to supplement the information included in NASA CR-112118.

The presented analysis methods and the formulated digital simulation were developed by the combined efforts of Fairchild Industries and its associate, Wolf Research and Development Corporation.

Section 2 of this volume presents the space station and solar array configurations which were considered during the course of this study. These are resulting configurations from studies performed by various aerospace companies. Control systems for space station altitude control and solar array orientation control (Report Section 3) include generic type control systems. These systems have been digitally coded and included in the simulation.

Report Section 4 presents the detailed analytical formulations which were derived and digitally simulated to provide an automated method of dynamic analysis. These formulations and corresponding simulations were derived for two study phases. The first study phase considered only the rigid body dynamics of the space station; while the second study phase included the flexible body dynamics of space station as well as the rigid and flexible dynamics of spinning space stations. Required input to the simulation includes the vibration mode data associated with the controllable and non-controllable appendages, and the space station. Therefore, extensive structural analyses were performed on the structures in support of the study work and analyses results are presented in Report Section 5. Appendix A presents detailed information and structural analyses data associated with the models utilized.

Verification analyses performed with the simulation are presented in Report Section 6. These analyses used simple structural configurations for the subsequent comparison with the simulation. Numerous documents were written during the course of this study which present interim study results and user information for the simulations.

2. SPACE STATION/SOLAR ARRAY STRUCTURAL CONFIGURATIONS

The formulation of an interaction analysis method for the determination of solar array structural requirement required structural concept definitions for purposes of providing analytical baselines. By direction from NASA/LRC, two solar array configurations were specified as analytical baselines for this study. One configuration consisted of the flexible rollup array studied by the Lockheed Missile and Space Company (Reference 2.1) and is sized to meet a 100 kilowatt power requirement. An initial version of the fully extended array and space station configurations is shown in Figure 2-1. The other solar array configuration which was used in this study was the foldout panel concept shown in Figure 2-2. The structural configuration of this array is based upon a Boeing Aircraft Corporation design which was proposed for a Mars mission vehicle. This design was updated to meet the 100 kw power requirement and to meet the geometrical constraints of the space station's shroud for the launch phase of powered flight. These two array configurations were utilized to derive structural vibration mode data which are required in the implementation of the dynamic interactions analysis.

A space station configuration concept utilized was that presented by the North American Rockwell Corporation (NAR) in Reference 2.2. The configuration is comprised of one or more modules which can be assembled in space in "cruciform" and "bar bell" arrangements. Typical arrangements are depicted in Figure 2-3. The specific arrangement of modules analyzed for vibration mode properties, is that given in Figure 2-4. It is comprised of a power boom, a core module, and eight attached modules arranged in a cruciform configuration. An artificial "G" space station configuration was also chosen and analyzed and is shown in Figure 2-5.

An updated version of the rollup solar array configuration was also analyzed. This design was configured by Lockheed under Contract NAS9-11039. A review of their study is given in Reference 2.3 and a sketch of the array is shown in

Figure 2-6. It is comprised of a series of 10 flexible solar cell substrates deployed with a center boom and tensioned between an inner and outer boom. During a proposed artificial "G" mode of operation, the roll up array configuration is changed to that shown in Figure 2-7. All array configurations were analyzed for cantilever vibration mode properties.

REFERENCES

Reference 2.1 - "Space Station Solar Array Technology Program Mid-Term Review", Lockheed Missile and Space Company, May 1971.

Reference 2.2 - "Modular Space Station - Phase B Extension, First Quarterly Review", North American Rockwell, Space Division, PDS-71-2, May 1971.

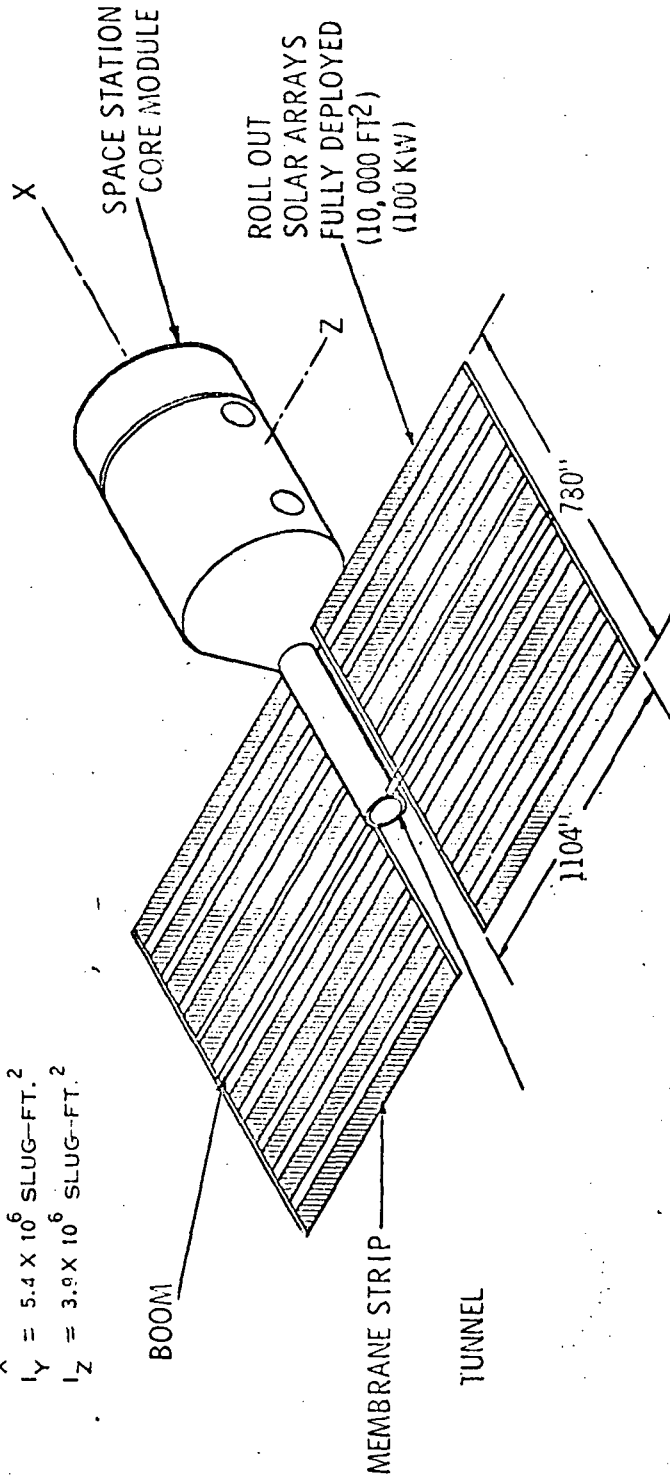
Reference 2.3 - "Space Array Technology Evaluation Program, Second Topical Report", Lockheed Missile and Space Company (LMSC-A981486), November 1971.

ARRAY INERTIAS

$I_x = 2.3 \times 10^6 \text{ SLUG-FT.}^2$

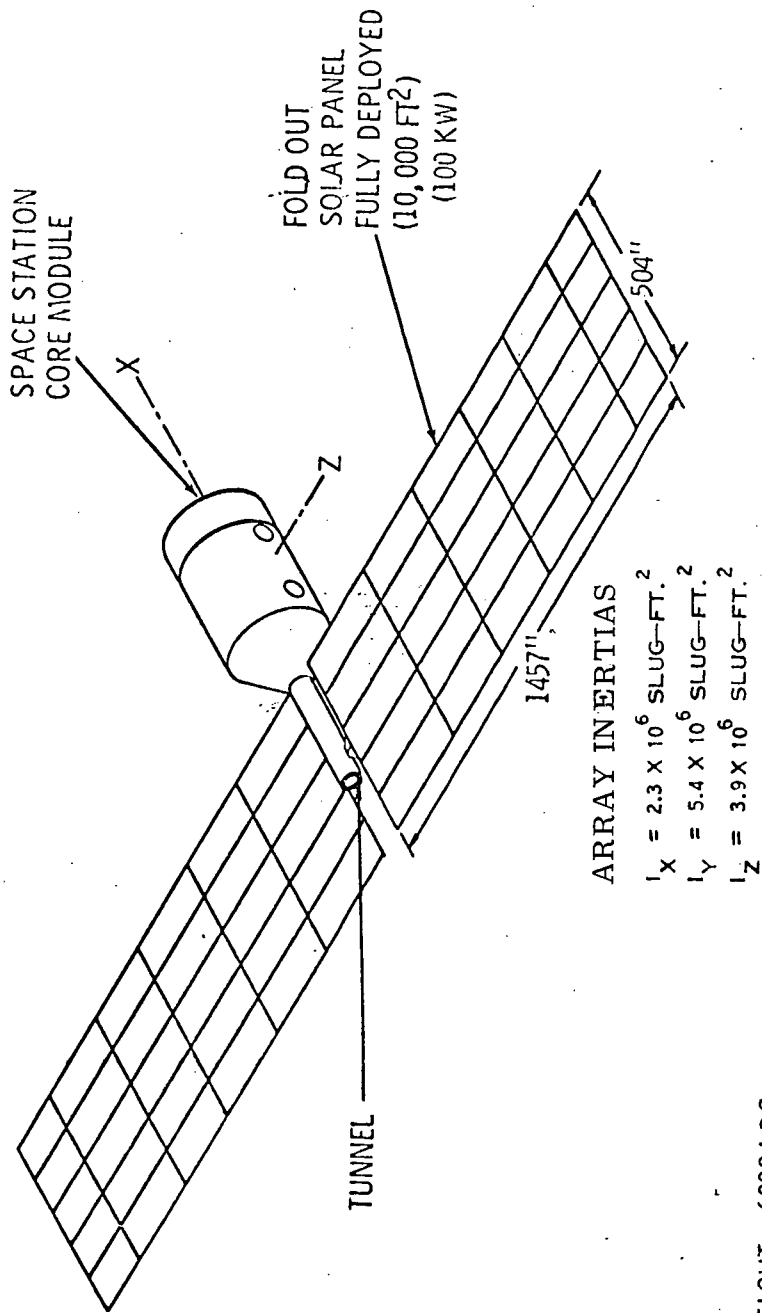
$I_y = 5.4 \times 10^6 \text{ SLUG-FT.}^2$

$I_z = 3.9 \times 10^6 \text{ SLUG-FT.}^2$



ARRAY WEIGHT - 7590 LBS.
 CORE MODULE WEIGHT - 210,000 LBS.

Figure 2-1. Space Station/Rollup Flexible Array



ARRAY WEIGHT - 6090 LBS.
 CORE MODULE WEIGHT = 210,000 LBS.

Figure 2-2. Space Station/Foldout Panel Array

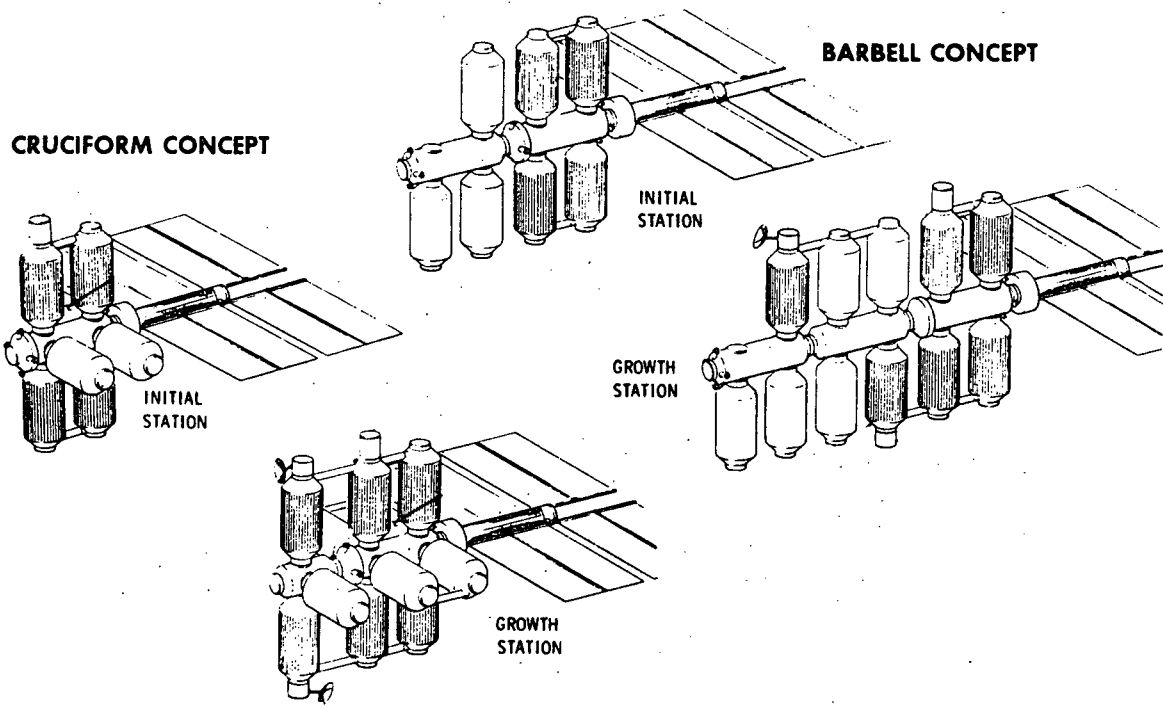
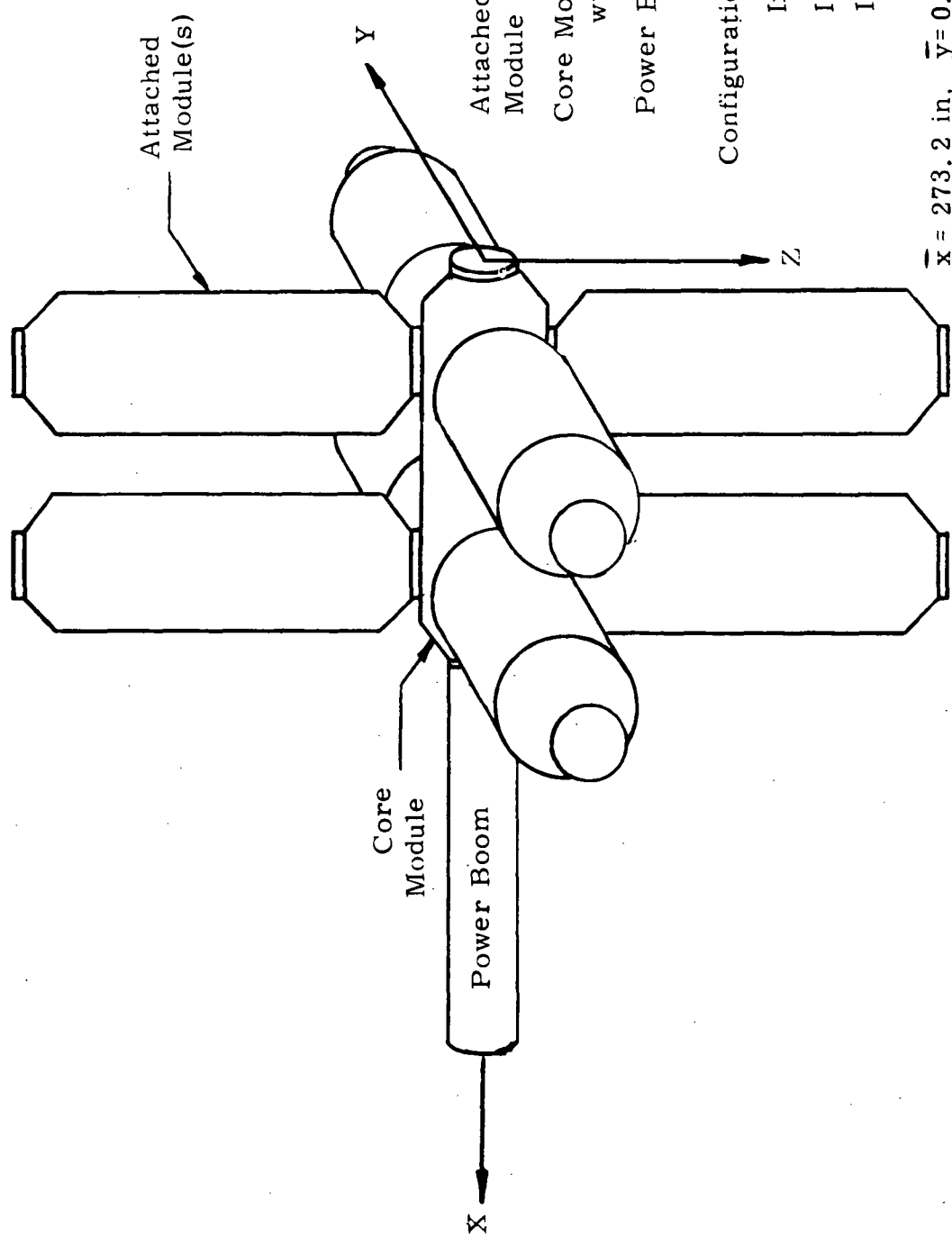


Figure 2-3. Space Station - Modular Concept



Attached Module wt. = 25,000 lb/ Module

Core Module wt. = 25,000 lb.

Power Boom wt. = 17,500 lb.

Configuration Wt. = 242,500 lb.

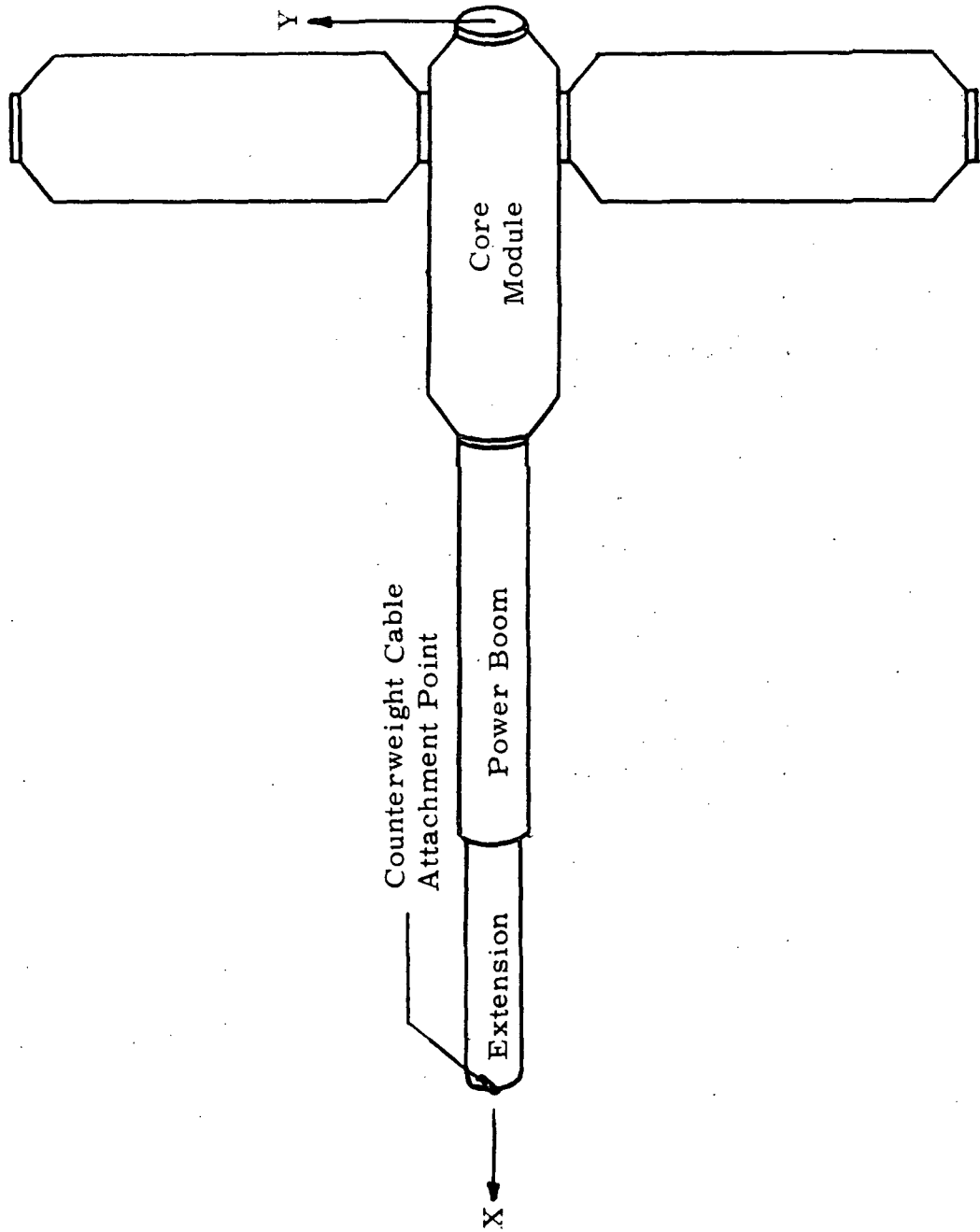
$I_x = 6.0 \times 10^7 \text{ lb} \cdot \text{in}^2$

$I_y = 10.0 \times 10^7 \text{ lb} \cdot \text{in}^2$

$I_z = 10.0 \times 10^7 \text{ lb} \cdot \text{in}^2$

$\bar{x} = 273.2 \text{ in}, \bar{y} = 0. \text{ in.}, \bar{z} = .0 \text{ in.}$

Figure 2-4 Zero "G" Space Station Configuration



Configuration Wt. = 92,500 lb.

$$I_x = 1.56 \times 10^7 \text{ lb-in-sec}^2$$

$$I_y = 3.0 \times 10^7 \text{ lb-in-sec}^2$$

$$I_z = 4.5 \times 10^7 \text{ lb-in-sec}^2$$

$$\bar{x} = 249.5 \text{ in.}, \bar{y} = 0. \text{ in.}, \bar{z} = 0. \text{ in.}$$

Figure 2-5 Artificial "G" Space Station Configuration

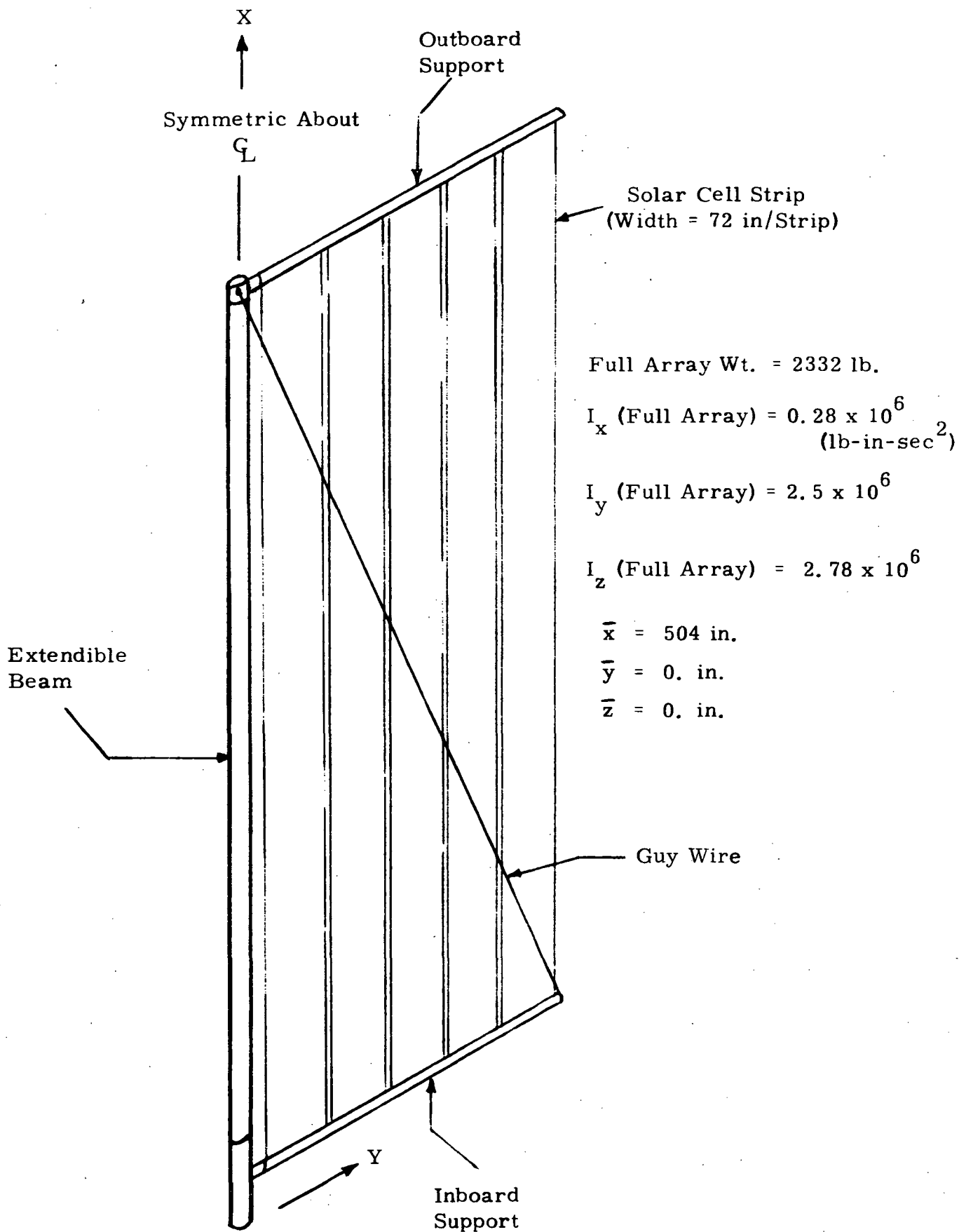
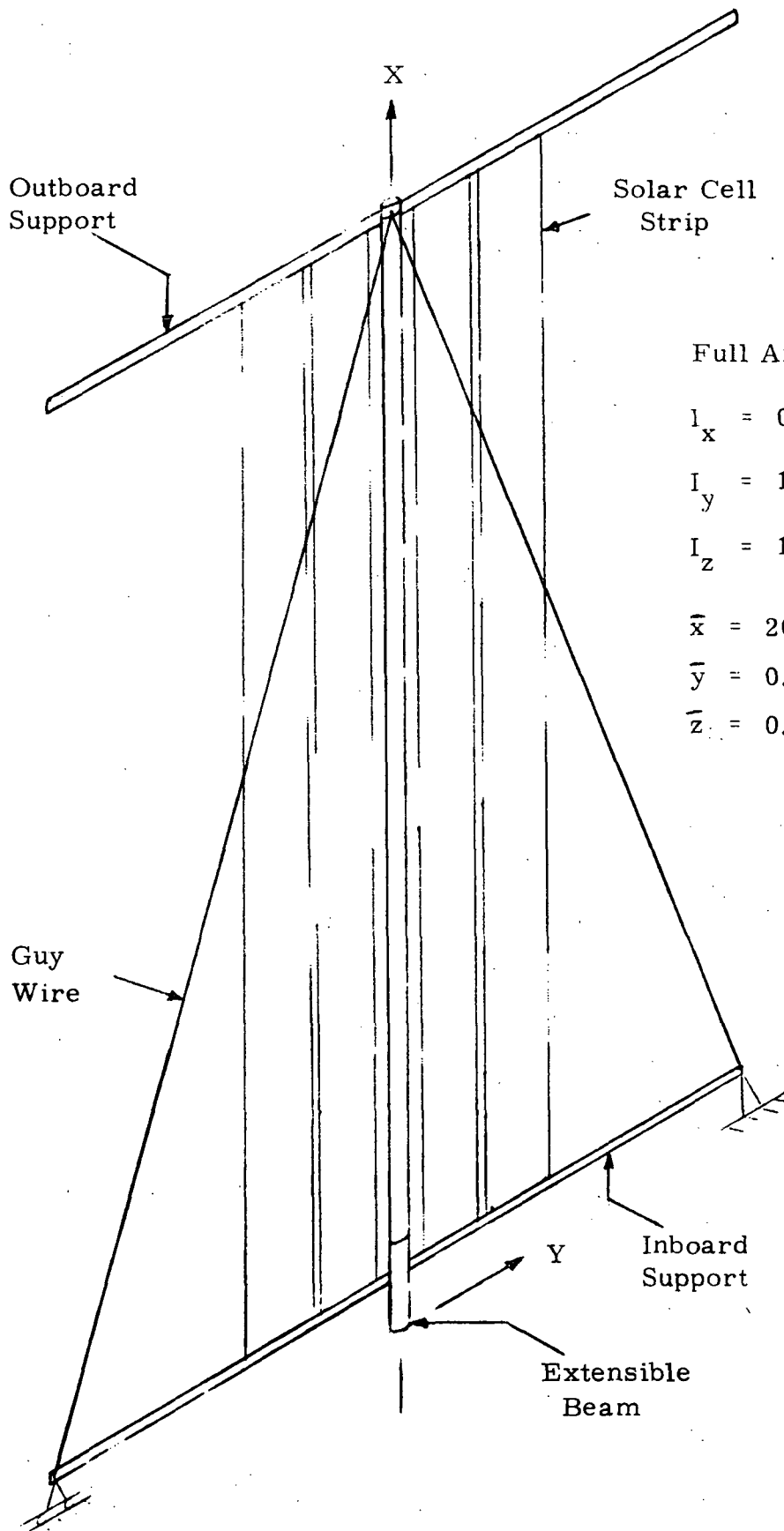


Figure 2-6 Zero "G" Roll-Up Solar Array Configuration
2-8



Full Array Wt. = 2044 lbs.

$$I_x = 0.16 \times 10^6 \text{ lb-in-sec}^2$$

$$I_y = 1.34 \times 10^6 \text{ lb-in-sec}^2$$

$$I_z = 1.5 \times 10^6 \text{ lb-in-sec}^2$$

$$\bar{x} = 205. \text{ in.}$$

$$\bar{y} = 0. \text{ in.}$$

$$\bar{z} = 0. \text{ in.}$$

Figure 2-7 Artificial "G" Rollup Solar Array Configuration

3. GUIDANCE AND CONTROL SYSTEM CONSIDERATIONS

3.1 SPACE STATION ATTITUDE CONTROL SYSTEM

The guidance and control system for the North American space station incorporates two generic types of control laws/torquers for attitude control. A control moment gyro (CMG) control system is used for precision attitude stabilization without the need for propellant expenditure. A reaction jet control system (RCS) is used for reference attitude acquisition maneuvers and for momentum desaturation, as required, for the CMG system.

The attitude control requirements as given in Reference 3.1 during zero G operations are as follows:

- Stabilization of the Station, prior to manning, to an accuracy of ± 5 degrees
- Stabilization during initial docking to an accuracy of ± 1 degree
- Stabilization during routine experiment operations to a ± 0.25 degree attitude tolerance, and with angular rate excursions below 0.05 degree per second.

3.1.1 CMG CONTROL SYSTEM

The CMG control system has been designed by the General Electric Company for North American.

A simulation model has been developed and is based upon a number of reports provided by G. E. A block diagram of this simulation model as given in Reference 3.2 is presented in Figure 3-1. The detailed equations for the control law are in accordance with the system selected by GE, which can be characterized as follows. It consists of three two-degree-of-freedom control moment gyros with parallel outer gimbals and with their momentum vectors initially equally spaced in the orbit plane. This configuration permits simpler steering laws and a planar, rather than three dimensional, anti-hangup law.

Reference 3.1 indicates that this control system has a natural frequency of 1.414 Hz and a damping ratio of 0.707. It was found that during the performance of various digital simulations, that a relatively small numerical integration interval ($\Delta t = .005$ second) was required to stabilize solutions to motion equations when the CMG was chosen as the active control system. This was due to high frequencies of inner control loops. Since small integration time steps were required for stability of solution with the CMG of Reference 3.2, a simpler system for the control structural motions was also derived to represent CMG controlling torques. This system which was suggested by NAR, produces a more efficient computer simulation time to real time ratio when the CMG is chosen as the active control. It is programmed in the simulation as represented by the diagram shown in Figure 3-2. It is comprised of a lead-lag compensator, a constant multiplying the moment of inertia properties of the spacecraft under investigation and an output torque limiter. The time constants of the lead-lag compensator, the constant multiplying spacecraft inertia and the limiting torque are allowed as input quantities to the control subroutine in the simulation. This simplified representation thus allows a certain degree of flexibility when analyzing general space station configurations. The commanded position angle is obtained from parameters calculated within the computer program (Reference 3.3). The actual angle is calculated within the program logic and is comprised of rigid plus flexible spacecraft body structural motions. Since space station structural flexibility is considered in the feedback control loop, the position of angle sensors and angular rate within the structural system is allowed to be specified. In like manner, the position of the control torque is specified so that generalized modal torques produced by the control system can be considered as input to modal degrees of freedom.

A simple wobble damper control representation is included in the simulation for control of spinning structural configurations. It consists of a single degree-of-freedom control moment gyro with its gimbal axis along the nominal spin axis and its momentum vector normal to that axis. With reference to Figure 3-3, the spinning structural system is considered to be about the X axis. The control moment gyro is torqued so that its momentum

vector \bar{h} always lags the wobble rate, ω_T , by 90° . A correction torque is applied to the space station which is equal to the following.

$$T_C = -(\omega_S + \dot{\alpha}) \times \bar{h}$$

An increase in the nominal spin rate also occurs to the correction wobble torque and is given as

$$\bar{T}_S = -\omega_T \times \bar{h}$$

The magnitudes of parameters associated with the wobble damper control system are an option when performing the simulation of a spinning space station.

3.1.2 REACTION JET CONTROL SYSTEM (RCS)

The reaction jet control system (RCS) is used for reference attitude acquisition maneuvers, momentum unloading of the control moment gyro, and as an alternate to the CMG for controlling the attitude of the space station. A RCS is composed of four thruster modules and each module has four thrusters. The modules are located at the periphery of a space station, as shown in Figure 3-4. All sixteen thrusters compose a fully redundant three axes attitude control system.

A jet thrust level is indicated in Reference 3.1 to be 10 pounds in order to provide the same torque magnitude with the RCS as with the CMG control system. Reference 3.1 further states that this small jet size requires significant pulse durations for most maneuvers and thus should minimize the need for a minimum impulse provision which was a major problem area for Apollo. Expected orbit makeup (correction) firing times are indicated to range from 7 to 14 seconds. Reference 3.1 indicates that the preprocessing electronics for the RCS sums the outer loop attitude and rate signals with any attitude maneuver command signals. It also includes the phase-plane deadband logic which then feeds the jet drive electronics.

Based upon the foregoing information, a suitable model of the RCS for the North American space station should be as depicted in Figure 3-5. Because of the indicated comparable torque levels of the CMG control system

and the RCS (and the low thrust levels and relatively long firing times) the former will represent a dynamic excitation element for the space station/array that is comparable to the latter. All maneuvers using the RCS are performed by firing two thrusters as a couple. The primary thrusters for each maneuver are selected by choosing the pair of thrusters with the longest lever arm.

The torque equations in the simulation of a rigid space station, and based upon the block diagram in Figure 3-5, are

$$\begin{bmatrix} T_R \\ T_P \\ T_Y \end{bmatrix} = \begin{bmatrix} B_R \\ B_P \\ B_Y \end{bmatrix} \begin{bmatrix} K_{\Theta} \phi_e + K_{\dot{\Theta}} \dot{\phi} \\ K_{\Theta} \theta_e + K_{\dot{\Theta}} \dot{\theta} \\ K_{\Theta} \psi_e + K_{\dot{\Theta}} \dot{\psi} \end{bmatrix}$$

where

T_R, T_P, T_Y are the torques applied to the space station about the roll, pitch and yaw axes respectively.

B_R, B_P, B_Y are the torque dead bands for each axis

K_{Θ} is the gain proportional to the space station angle error

$K_{\dot{\Theta}}$ is the gain proportional to the space station rate about each axis

ϕ_e, θ_e, ψ_e are the angle errors in roll, pitch and yaw respectively

$\dot{\phi}, \dot{\theta}, \dot{\psi}$ are the space station rates in roll, pitch and yaw.

These equations are used in the RCS digital subroutine in the simulation to develop the control torques for the thruster system. This proportional control system, when used as an alternate to the CMG control system, will permit more economical computation of the interaction dynamics.

Since the computerized method of simulating space station motions was modified in Phase II study efforts to account for space station flexibility, the reaction jet control system in the simulation consists of six individual constant-thrust-magnitude thrusters at specified structural locations to control the three angular rigid body motions. Location of each thruster, thrust magnitude and thrust direction, are allowed to be specified prior to performing a simulation. Program logic computes the generalized forces into space station modal degrees of freedom using other appropriate input structural mode constants. The typical applied torque equation is

$$T = K \cdot 1(E_C - E_{DB})$$

where

T = output torque of the reaction jets at any given time for which the computed "error" is E_C .

K = torque capability of the reaction jets

$1(\)$ = unit step function having the value zero for negative or zero arguments and the value unity for positive arguments.

E_C = computed equivalent attitude/rate error of the space station determined by

$$E_C = K_1(K_2 \phi - \omega)$$

where K_1 and K_2 are input constants and ϕ and ω are attitude and rate errors of the space station respectively.

E_{DB} = deadband threshold level for equivalent attitude/rate error which determines when the reaction jets are active.

3.2 SOLAR ARRAY ORIENTATION CONTROL SYSTEM (OCS)

The operating characteristics of the Orientation Control System (OCS) for the solar arrays being considered in this study effort can have a major impact on the latter's design requirements. Hence, in developing an analysis method to evaluate the design of such arrays, the significant dynamic characteristics of the OCS must be properly modeled. Two generic types of OCS drive systems have been considered and are characterized by the following:

- The continuous array drive system.
- The non-linear (bang-bang) drive system.

3.2.1 CONTINUOUS ARRAY DRIVE SYSTEM

A block diagram of the continuous OCS is shown in Figure 3-6. The difference between the commanded array angle and actual array angle are used to generate the angle error signal. This error signal is then filtered by the provided compensation in the control loop. The array angular rate $\dot{\theta}$ is multiplied by the back EMF coefficient K_B and added (negatively) to the filtered error signal. This gives the effective drive signal for the motor. The drive motor is modeled as a first order lag with K_M as the torque gain of the motor and τ_M as the motor time constant. The output torque of the motor is reduced by the friction in the reduction gear unit as shown by the K_F feedback loop. The effective torque of the motor is increased by the ratio of the reduction gear and delivered to the solar array. To determine the stability of the OCS, the solar array is assumed to be rigid and have an inertia I_A about its axis of rotation.

To assess the effects of the two rate feedback loops in Figure 3-6 the value of $K_F \dot{\theta}$ and T_M were compared for $\dot{\theta}$ equal to orbital rate. The results showed $K_F \dot{\theta}$ to be significantly smaller than T_M and hence the K_F feedback loop can be dropped from the simulation without any loss of generality. This is generally expected to occur for this class of control systems. With one of the feedback loops removed, the OCS continuous drive model can be simplified. The drive mechanism can then be modeled by two first order

filters to smooth the array angle error and rate signals. The two signals are weighted by the appropriate gains and added together. The sum is then filtered by a third first order filter (i.e., the motor) where the gain of the filter is the product of the torque gain of the motor and the gear ratio of the drive system. This is shown schematically in Figure 3-7.

To evaluate the stability of the continuous drive OCS, the T-2170 Inland torque motor is assumed as the prime mover in the system. The characteristics of this motor are generally representative of the class of DC torque motors that would be suitable for the array drive system. These characteristics are:

$$\begin{aligned}
 L_M &= 3 \times 10^{-3} \text{ Henrys} \\
 K_T &= 18.9 \text{ oz-in/amp} \\
 R_T &= 3.3 \text{ ohms} \\
 K_B &= 1.3 \text{ volts/rad/sec}
 \end{aligned}$$

The motor gain and time constant are defined as

$$\begin{aligned}
 K_M &= K_T / R_T = 5.727 \text{ oz-in/volt} \\
 \tau_M &= L_M / R_T = 0.00091 \text{ sec.}
 \end{aligned}$$

A larger torque motor than required was chosen to allow the motor to operate near its rated speed without an unusually high gear reduction ratio.

The chosen motor requires the use of a 6800:1 reduction gear.

The open loop transfer function of the simplified continuous drive OCS is given by equation 1.

$$\frac{\theta}{\theta_c} = G(S) = \frac{K_\theta K_M K_G}{S \left\{ \tau_\theta \tau_M I_A S^3 + I_A (\tau_\theta + \tau_M) S^2 + (K_M K_G^2 K \tau_\theta + I_A) S + K_M K_G^2 K_\beta \right\}} \quad (\text{Equation 1})$$

The steady state hang off error for the system when following a velocity input (orbit rate) is given by equation 2.

$$e_{ss} = \frac{\dot{\Theta}_c}{\lim_{S \rightarrow 0} S G(S)} \quad (\text{Equation 2})$$

Hence, by selecting a suitable steady state following error, the value of K_{Θ} can be determined. The steady state error is chosen to be 1 degree for the determination of K_{Θ} . This is somewhat tighter than required but it allows for other components in the system to contribute to the steady state error without exceeding the desired overall system value. Substituting equation 1 into equation 2 gives an expression for K_{Θ} in terms of known quantities.

$$K_{\Theta} = \frac{K_B K_G \dot{\Theta}}{e_{ss}} \quad (\text{Equation 3})$$

Using the values for K_B , K_G , and e_{ss} previously given and assuming an orbit period of 100 minutes, the gain of the loop compensation is

$$K_{\Theta} = 530$$

The time constant for the loop compensation is selected by restricting the maximum overshoot to be less than 1 db. Using the characteristics of the T-2170 torque motor and an array inertia of 77,000 slug ft², Equation 1 reduces to

$$G(s) = \frac{1/166.8 T_{\Theta}}{s (s + \frac{1}{T_{\Theta}})} \quad (\text{Equation 4})$$

when all small terms are neglected. An appropriate time constant for equation 4 is

$$T_{\Theta} \approx 0.01 \text{ sec.}$$

The values presented in this section are considered representative of the continuous drive control system. If other values are desired, provisions are available to include them in the digital simulation.

3.2.2 NON-LINEAR DRIVE SYSTEM

The non-linear drive OCS is similar to the continuous drive system with the exception that the control logic is operated in an on-off manner. When the error signal exceeds some pre-selected threshold value, the motor is turned on until the array is driven to the null position at which point the motor is switched off. The time that the motor takes to reach its running speed when switched on is very small compared to the total time that the motor is operated to drive the array back to the null position. Similarly, the time the motor takes to coast to a stop when the power is turned off is small compared to its total on-time. This would allow the motor to be modeled as a square wave rate generator, i. e., when the motor is commanded on, the array begins rotating at a constant velocity and when the motor is commanded off the array stops rotating.

A non-linear orientation control drive system has been formulated by the Ball Brothers Research Corporation (Reference 3. 4), and this system is included as a control subroutine in the simulation. It is represented by the diagram shown in Figure 3-8. Values of the various constants shown are those received as representative of the BBRC system. In order that simulations could be performed with the many constants varied as parameters, the following were allowed to be input variables to the program subroutine representing this system.

- Deadband angle
- Bus Voltage Generator time constant,
- Bus Voltage Generator amplification constant, A
- Motor Gain ($K_T N/R$)
- Coulomb Friction
- Scaling constant, G

- Gear Ratio, K_G
- Back EMF

The relative velocity vector and angular error are computed by the simulation program for the space station rigid body and flexible degrees of freedom and the solar array degrees of freedom.

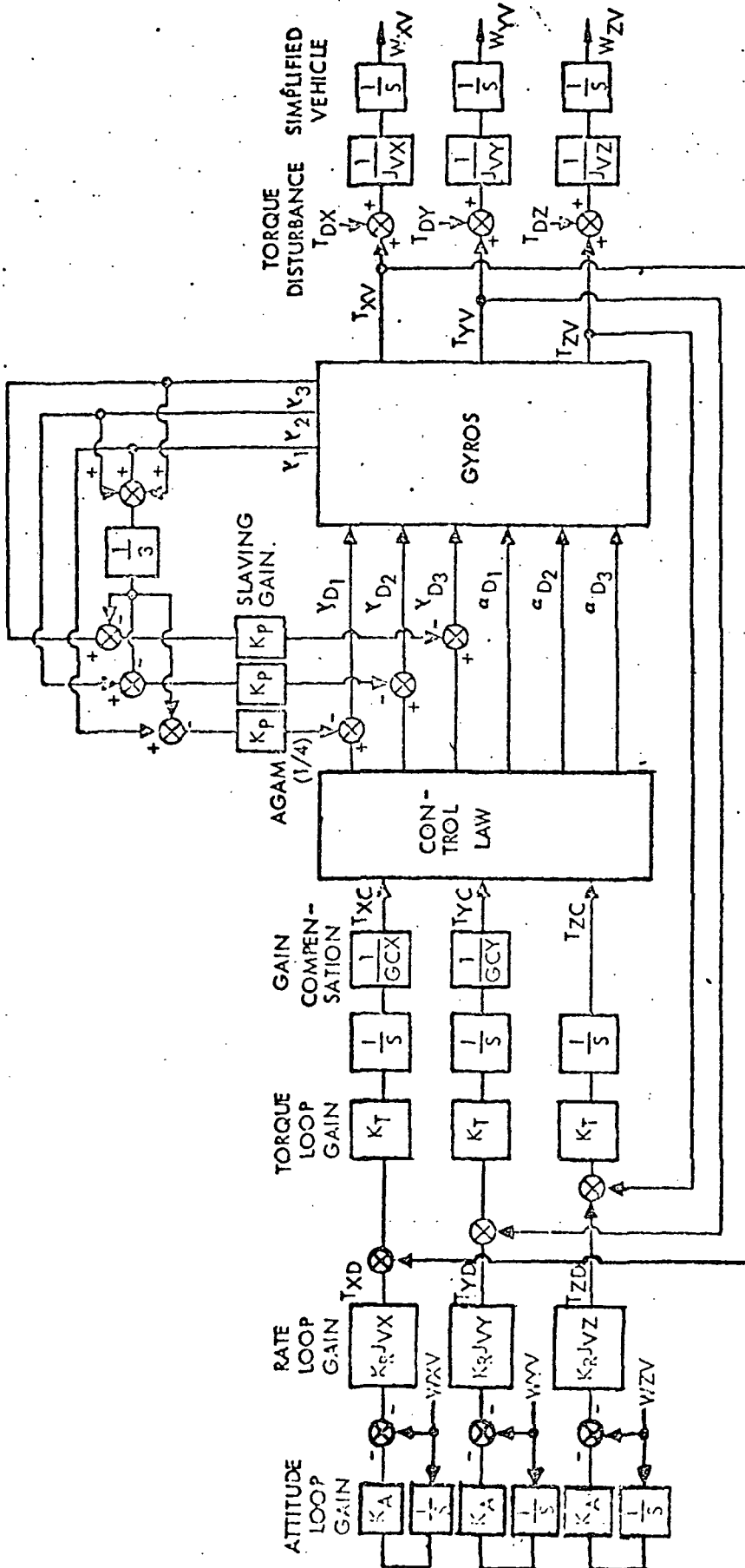
3.3 REFERENCES

Reference 3.1. "Solar-Powered Space Station Preliminary Design," Vol. III, Guidance and Control Subsystem, North American Rockwell, July 1970.

Reference 3.2. "Preliminary Synthesis and Simulation of the Selected CMG Attitude Control System," G. E. Report EL-506-D, 5 March 1970.

Reference 3.3. "Small Eccentricities or Inclinations in the Brower Theory of the Artificial Satellite," R. H. Lyddane, Astronomical Journal, Vol. 68, No. 8, October 1963, pg. 555.

Reference 3.4. "Space Station Solar Array Technology Evaluation Program," Second Topical Report, Lockheed Missile and Space Company (LMSC-A981486), November 1971.



FOR TRANSPOSE CONTROL LAW:

$$\begin{aligned}
 GCX &= \cos^3 \theta_1 + \cos^2 \theta_2 + \cos^2 \theta_3 \\
 GCY &= \sin^2 \theta_1 + \sin^2 \theta_2 + \sin^2 \theta_3 \\
 \gamma_{D1} &= TZC/3H \cos \theta_1 \\
 \gamma_{D2} &= (TXC \cos \theta_1 + TYC \sin \theta_1)/H \cos \theta_1
 \end{aligned}$$

Figure 3.1 Simulation Diagram - CMG Control System

CMG CONTROL SYSTEM

(Simplified)

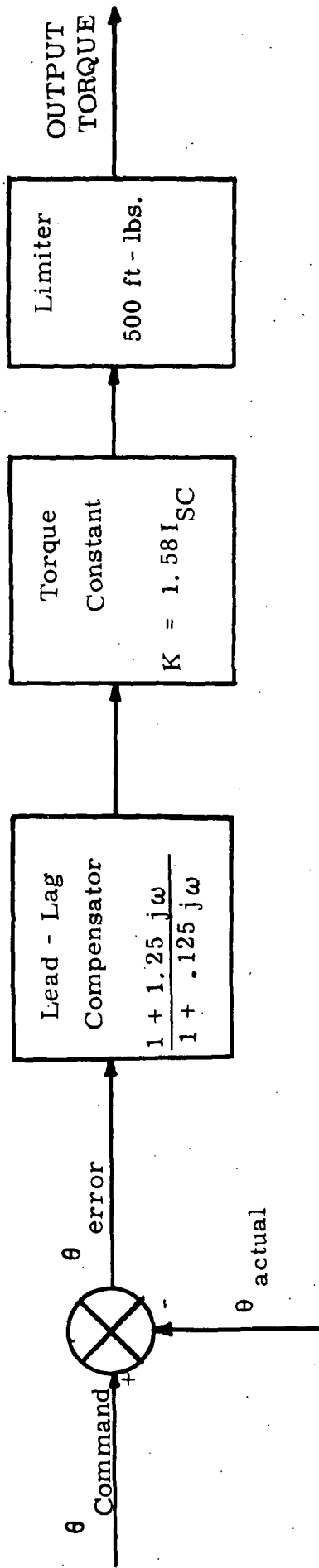
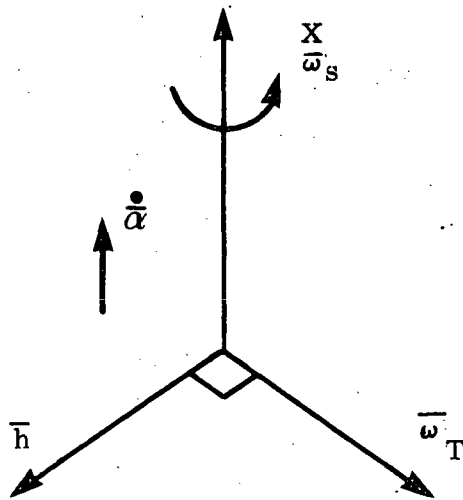


FIGURE 3-2



- $\dot{\alpha}$ - Gimbal Rate of CMG
- \bar{h} - Momentum Vector
- ω_s - Spin Axis Component of Spin Rate
- ω_T - Transverse Component of Spin Rate

Applied Torques

$$\bar{T}_c = -(\omega_s + \dot{\alpha}) \times \bar{h} \text{ (opposes } \omega_T)$$

$$\bar{T}_s = -\omega_T \times \bar{h} \text{ (increases spin rate)}$$

FIGURE 3-3 Wobble Damper Control Torques

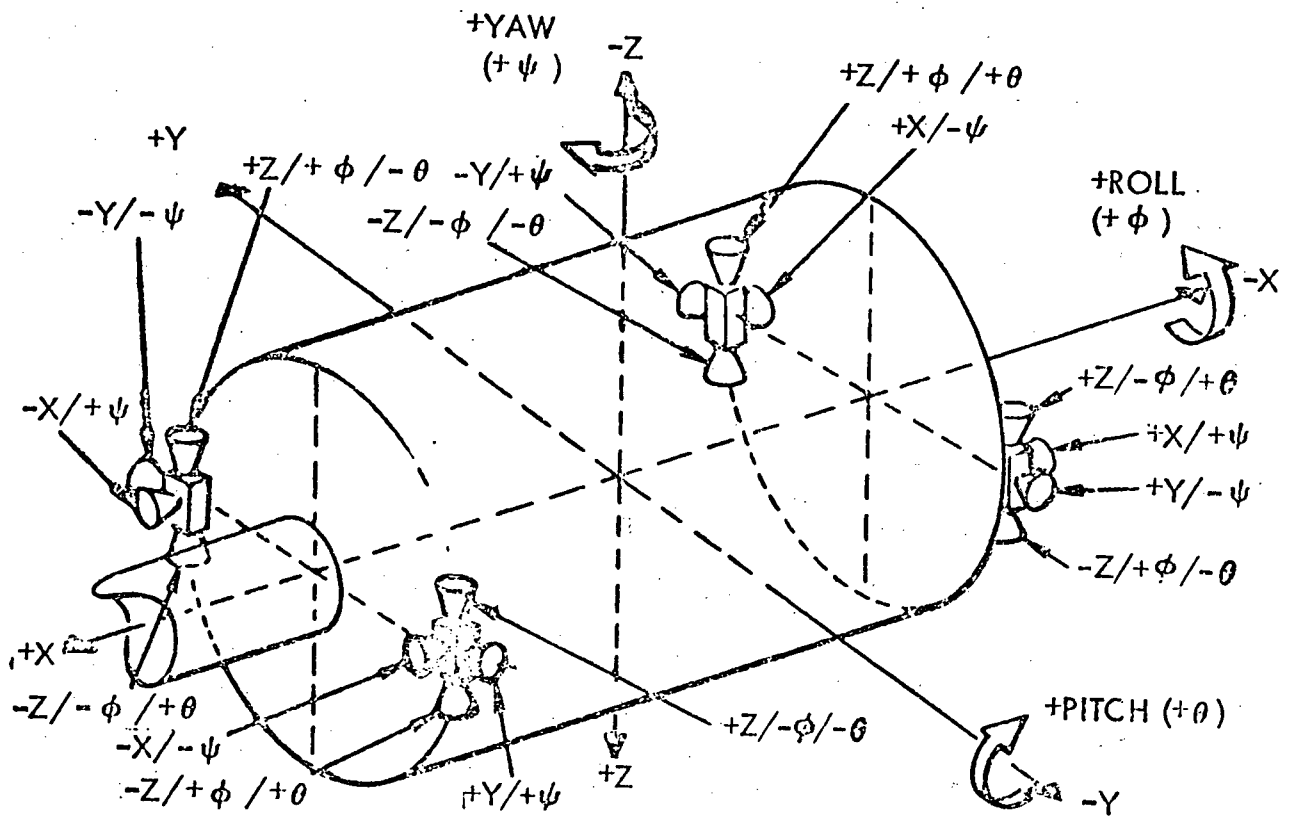
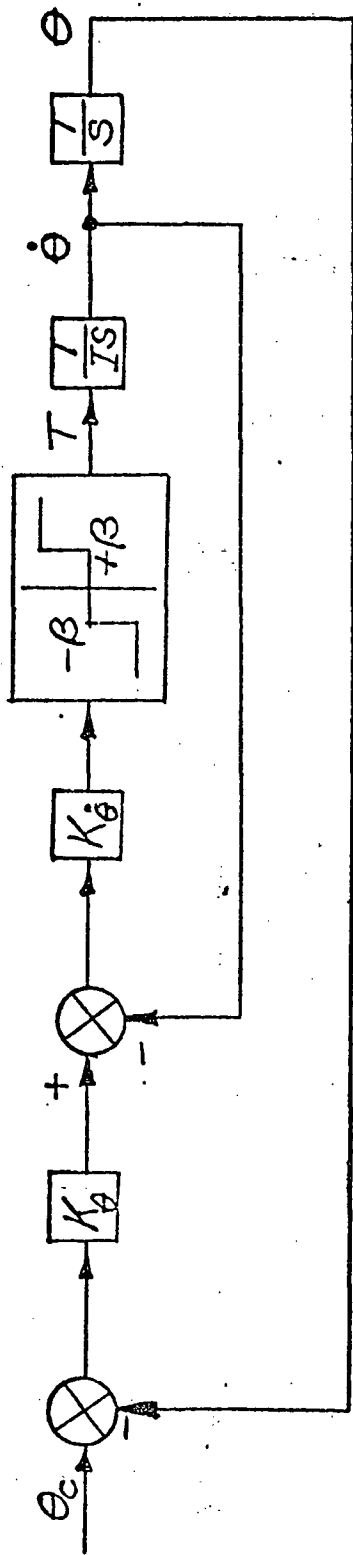


Figure 3-4 RCS Jet Location/Function



LEGEND

- θ_c = Commanded Attitude Angle
- θ = Attitude Angle, Rate
- $K_\theta, K_{\dot{\theta}}$ = Attitude Angle Gain, Rate Gain
- β = Control Loop Deadband
- T = RCS Torque Level
- I = Space Station Moment of Inertia

Figure 3-5. RCS Model

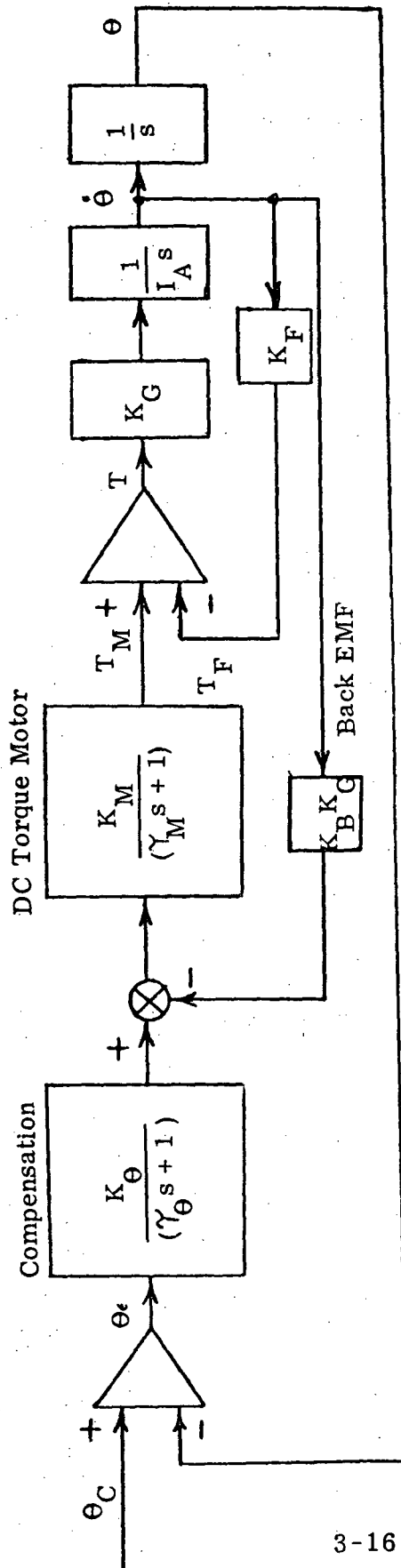


Figure 3-6. Model for Continuous Drive OCS for Solar Arrays
(one continuous motion axis)

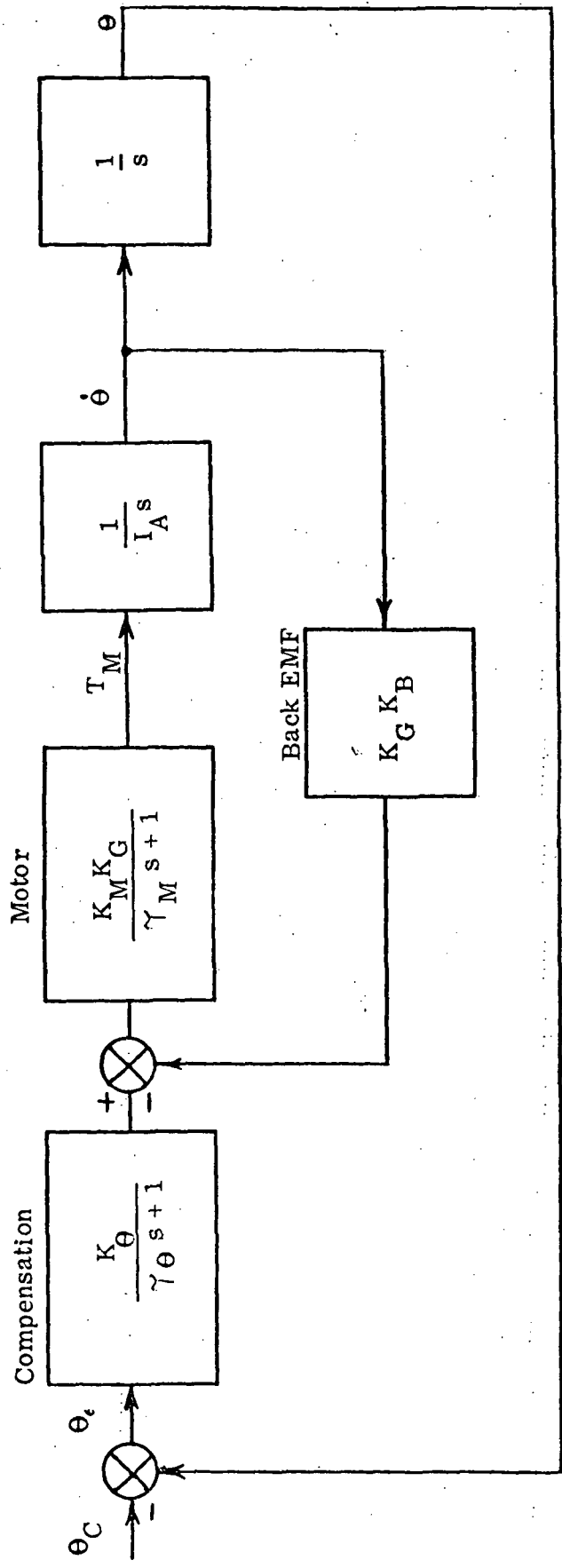
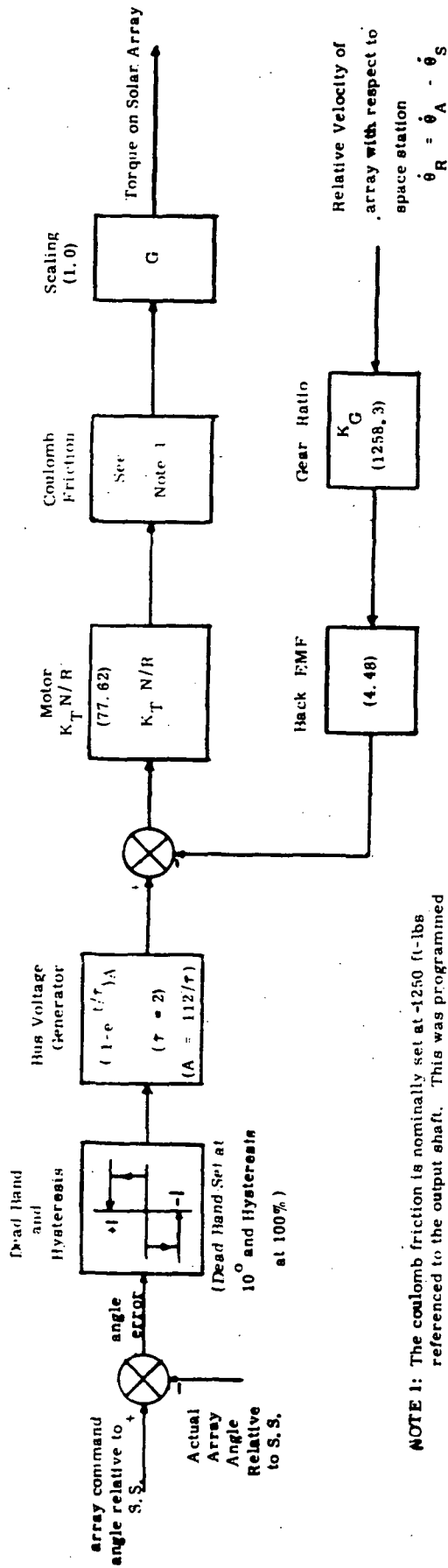


Figure 3-7. Simplified Continuous Drive OCS Model



NOTE 1: The coulomb friction is nominally set at -1250 (1-lbs referred to the output shaft). This was programmed so that the torque on the array is zero if the motor torque is less than 1250 ft-lbs when the array is not moving relative to the space station. When the array is moving and the motor torque is less than 1250 ft-lbs, the torque on the array is the coulomb torque minus the motor torque. When the motor torque is greater than 1250 ft-lbs, the torque on the array is the difference between the motor torque and coulomb torque.

Figure 3-8. Non-Linear Orientation Control System

4. DYNAMIC INTERACTIONS ANALYSIS FORMULATION AND DIGITAL SIMULATION

Three phases of interaction analysis formulations and corresponding simulations resulted during the study period. Separate digital simulations and the associated user information were derived on the basis of each analytical formulation. The formulations are categorized by the following:

- Rigid space station with two flexible controllable appendages in a zero "G" orbit environment
- Flexible space station with two flexible controllable appendages and four flexible non-controllable appendages in a zero "G" orbital environment
- Flexible space station with four flexible non-controllable appendages in an artificial "G" orbital environment.

A detailed description and derivation of each of the formulations that were digitally programmed are contained in the following report subsections.

4.1 RIGID SPACE STATION/FLEXIBLE CONTROLLED APPENDAGES

The interaction dynamics study simulation is designed to determine the effects of important solar array structural characteristics on the motion of an orbiting space station. Two flexible solar arrays are connected to the space station by means of rigid driver assemblies which are totally constrained in translation and allowed two rotational degrees of freedom for each driver about the attachment point. The array drivers are rotated to obtain the desired sun/solar array aspect. The space station is attitude stabilized by a Control Moment Gyro System (CMG) which is augmented by a reaction control system to provide maneuver capability and "momentum dumping". The simulation model utilized for this system is described below:

- The space station and the two rigid array drivers are each modeled as rigid bodies with each of the rigid drivers permitted to rotate about the spacecraft attachment points along an axis parallel to the spacecraft roll axis and an axis normal to that in the plane of the solar array. The rigid array driver rotation may be additionally constrained in rotational freedom by user input to the digital simulation.
- The flexible array is modeled by the synthetic modes technique of Likins (Reference 4.1), i.e., the array is modeled in terms of a finite number of orthogonal cantilever modes suitably augmented by six synthetic modes to assure that the steady state (rigid) conditions for constant acceleration are met. The appendage equation is an exact formulation which includes all accelerations of the appendage base. In accord with the synthetic modes approach, the effect of the two flexible arrays upon the rigid body system is obtained in the form of the equivalent force and torque exerted by the flexible arrays upon the system by the modal accelerations. The effects of the rigid system motion upon the flexible arrays is accounted for by system acceleration in the appendage equation of each array.
- Maneuver and attitude control of the space station together with the solar array orientation control are modeled in terms of the appropriate time varying forces and torques produced by closed loop guidance equations. The guidance and steering commands are computed external to the dynamics section and provide the space station with a fixed orientation relative to orbit coordinates.

Formulation of these equations is given in the Command and Control description.

- The array driver gear train for the axis parallel to the space station roll axis is modeled as an ideal mechanical transformer referenced to the spacecraft side of the gear train. The other driver axis is directly driven. Either axis of both drivers may be locked.
- The simulation orbit generator uses Lyddane's method for near earth orbits which may be circular. (Ref. 4.2).

A block diagram representation of the simulation program is presented in the following where important logical switches and function interconnection have been delineated (Figures 4-1 thru 4-5).

4.1.1 CONVENTIONS AND COORDINATE SYSTEMS

The coordinate systems given below represent the main computational frames utilized in the simulation.

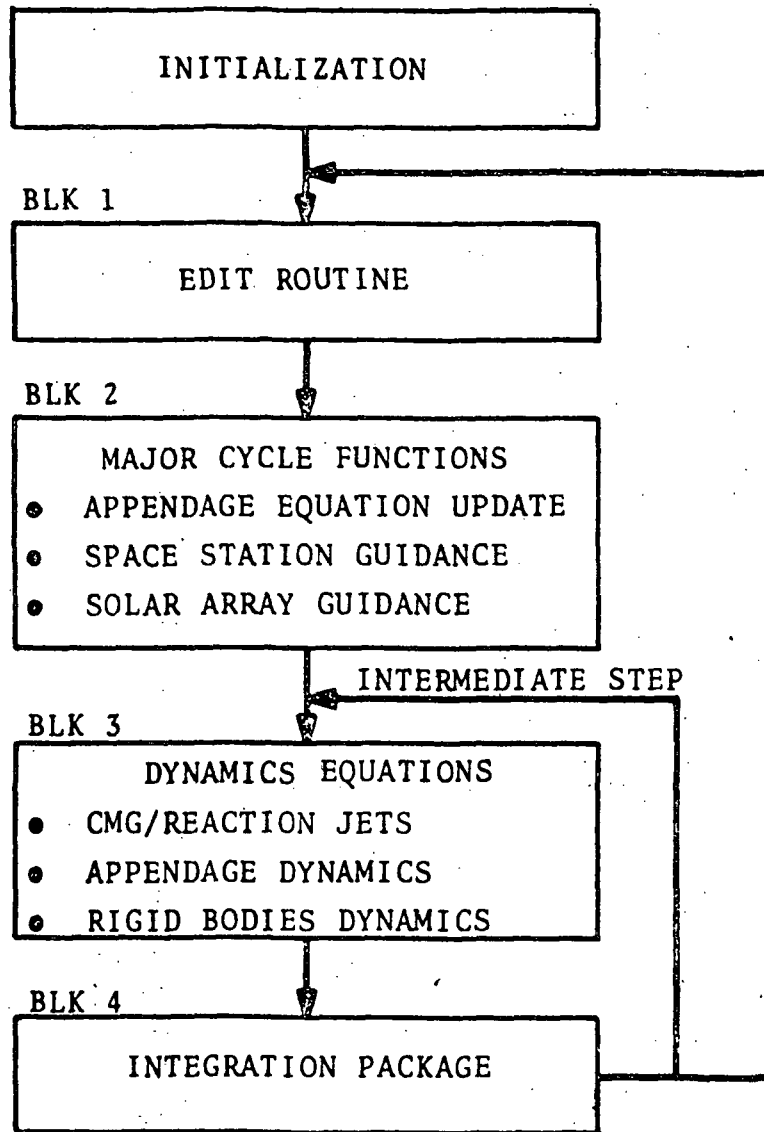


Figure 4-1 Overall Flow Chart

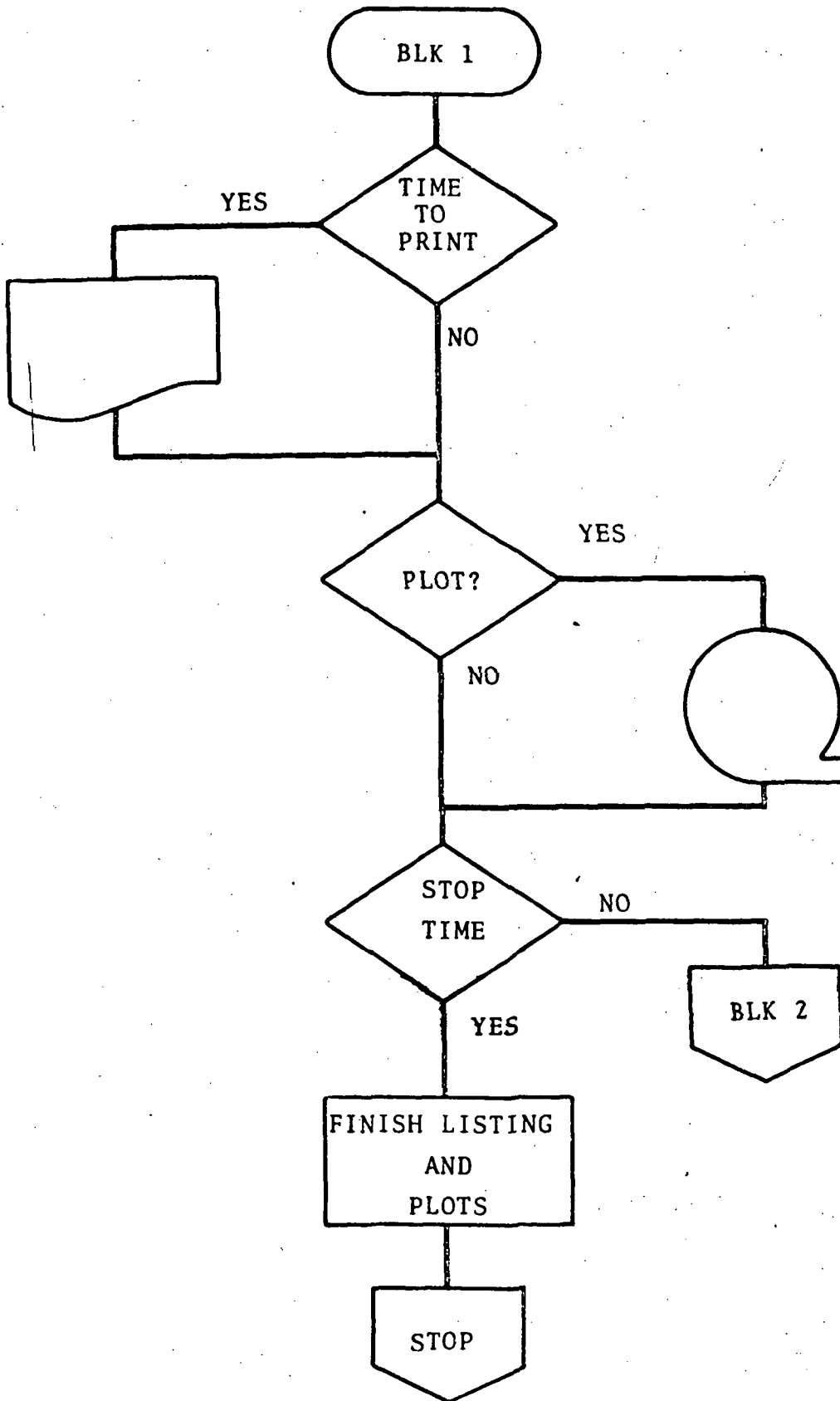


Figure 4-2 Blk 1 Edit Routine Flow Chart

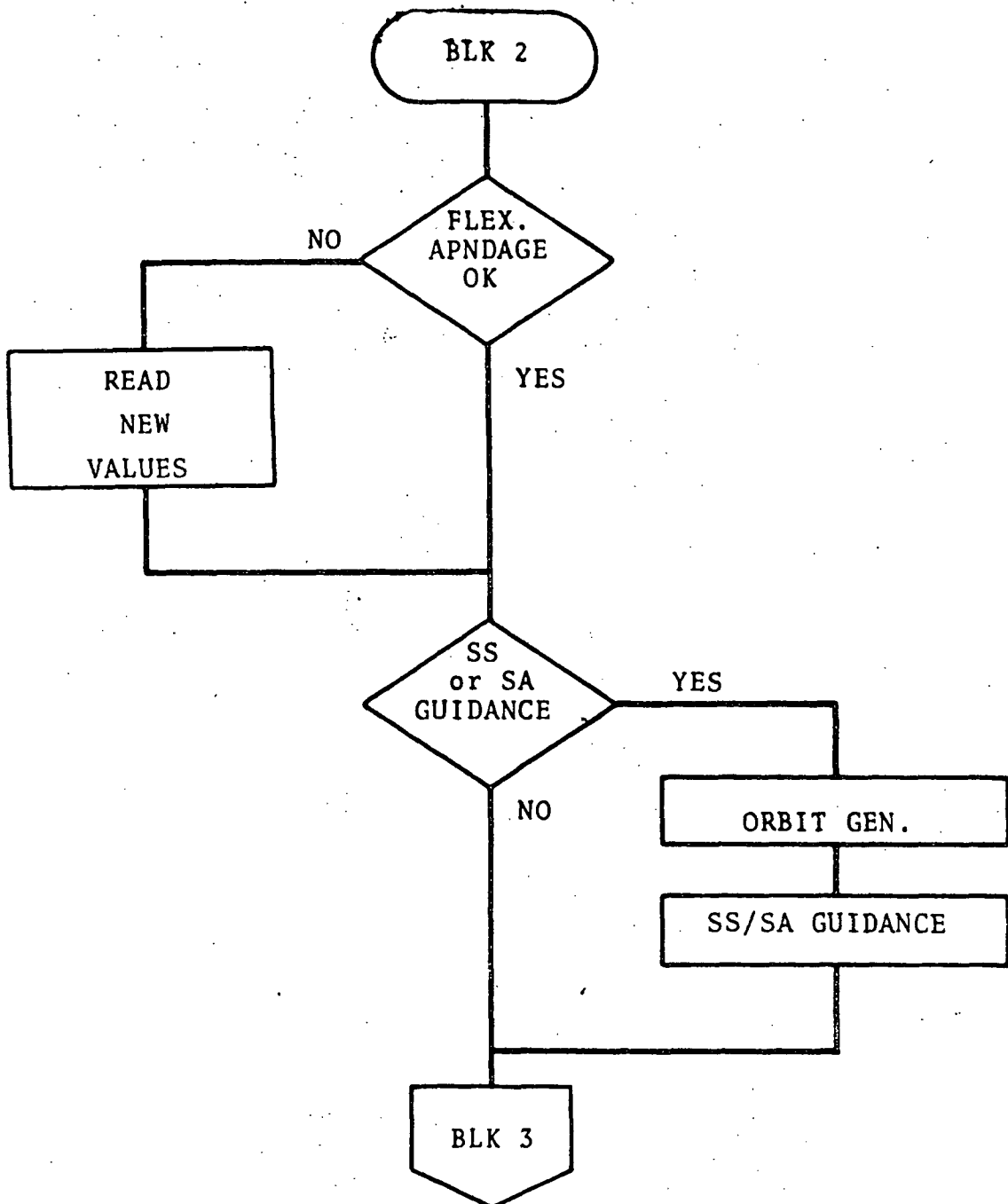


Figure 4-3 Blk 2 - Major Cycle Flow Chart

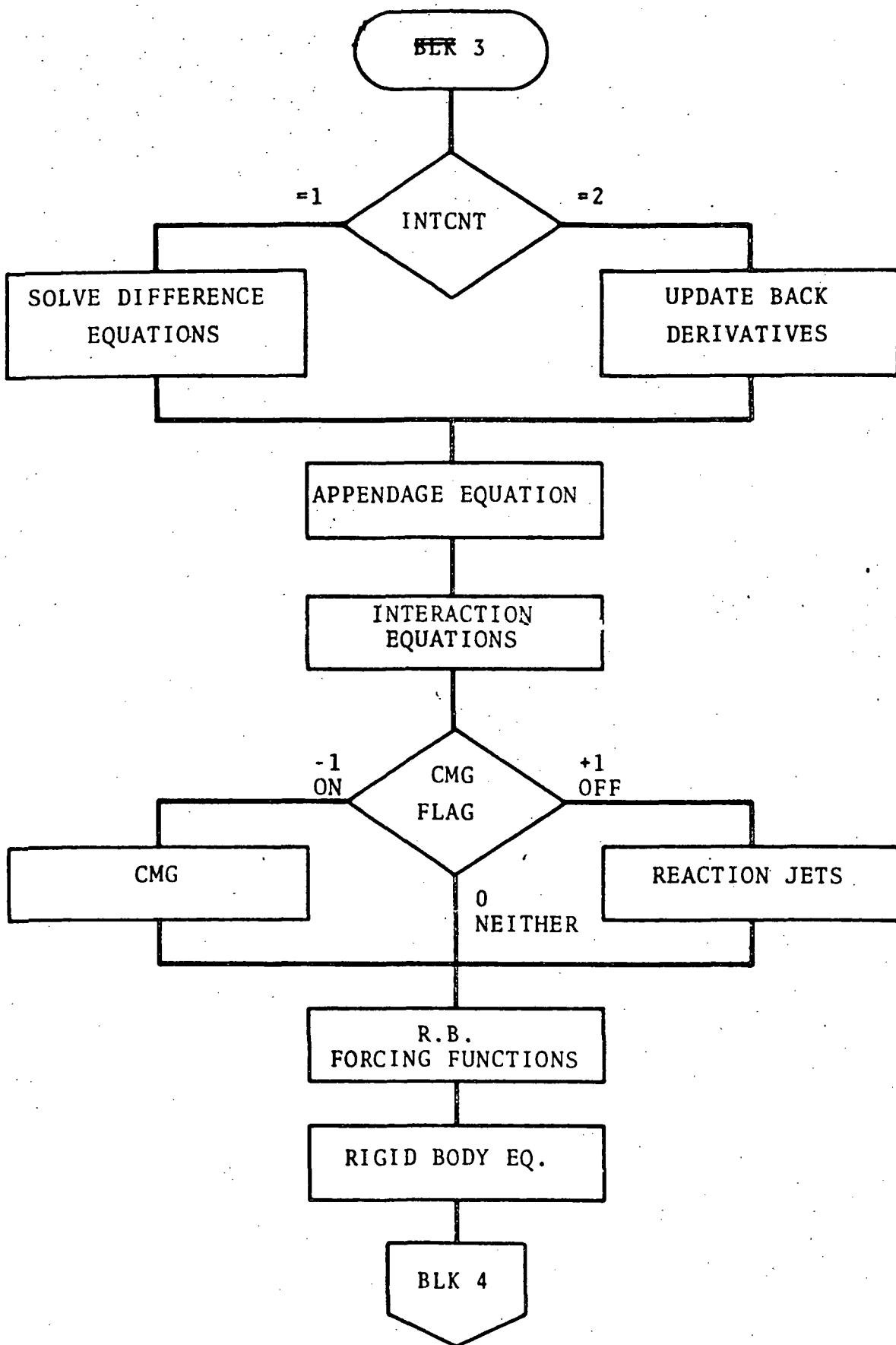


Figure 4-4 Blk 3 - Dynamics Equations Flow Chart

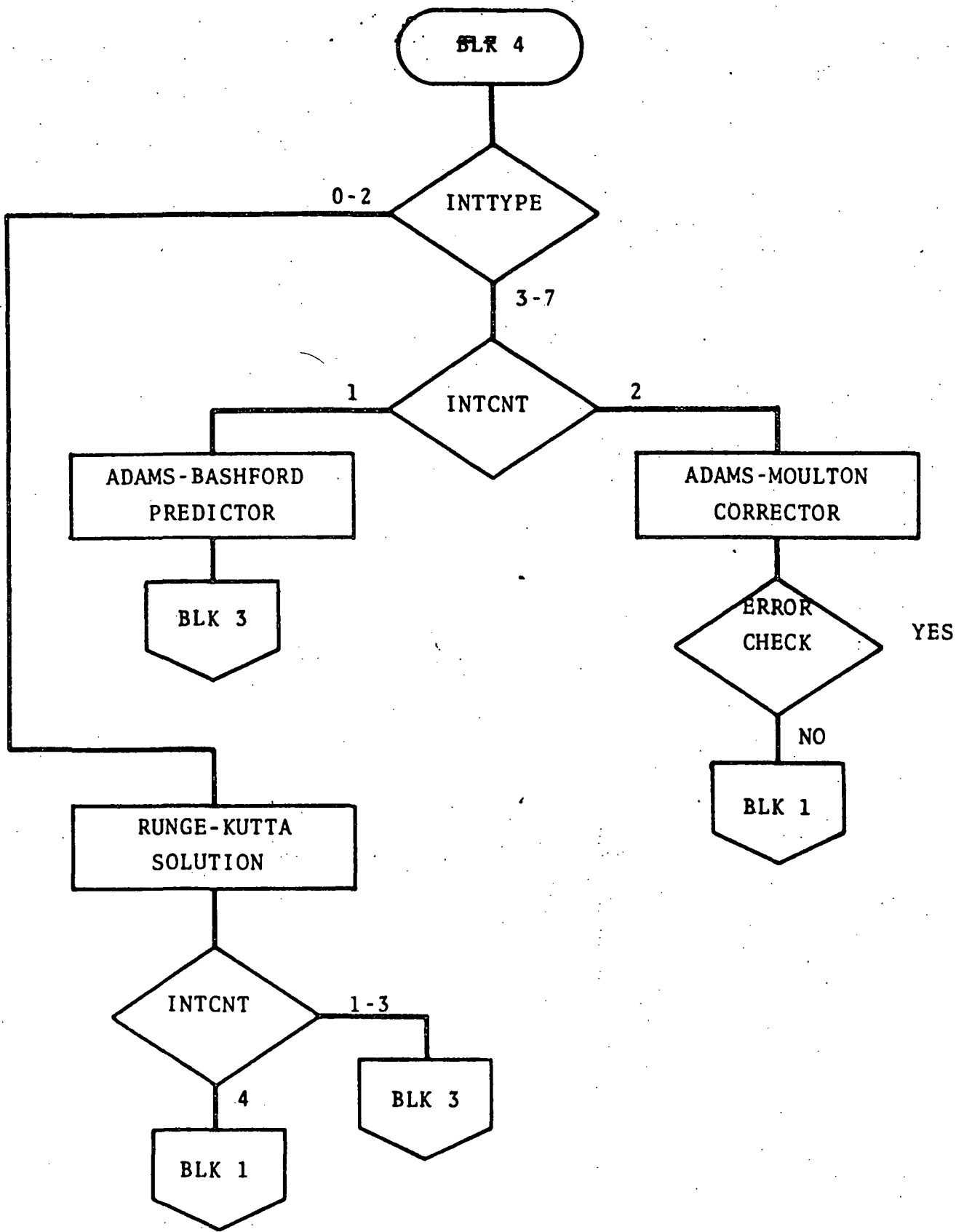
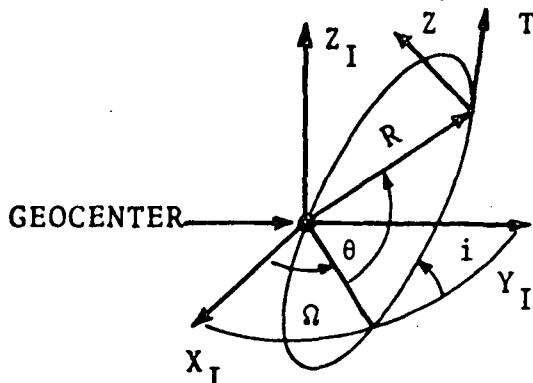


Figure 4-5 Blk 4 - Integration Package Flow Chart

4.1.1.1 COORDINATE FRAME 1

Earth Centered Inertial (ECI) Coordinates



X_I - In equatorial plane pointing at Aries

Z_I - Points to geocentric north pole

Y_I - Provides right handed set in order X_I, Y_I, Z_I

4.1.1.2 COORDINATE FRAME 2

Local Level (RTN) Coordinate

$$\begin{bmatrix} R \\ T \\ N \end{bmatrix} = \begin{bmatrix} C\theta & S\theta & 0 \\ -S\theta & C\theta & 0 \\ 0 & 0 & 1 \end{bmatrix} \begin{bmatrix} 1 & 0 & 0 \\ 0 & Ci & Si \\ 0 & -Si & Ci \end{bmatrix} \begin{bmatrix} C\Omega & S\Omega & 0 \\ -S\Omega & C\Omega & 0 \\ 0 & 0 & 1 \end{bmatrix} \begin{bmatrix} X_I \\ Y_I \\ Z_I \end{bmatrix}$$

R - directed along geocenter to space station radius vector

N - normal to orbit plane

T - completes right handed set (R, T, N)

where Ω - longitude of ascending node

i - orbital inclination

θ - sum of argument of perigee (ω), plus the true anomaly (ν)

C, S - cosine and sine functions

As indicated above, the Euler rotations are about the Z_I , the X_I and the N axis where X_I is the X_I axis after rotation through Ω .

4.1.1.3 COORDINATE FRAME 3

Commanded Space Station Coordinates

The desired space station orientation X_c, Y_c, Z_c represent, in order,

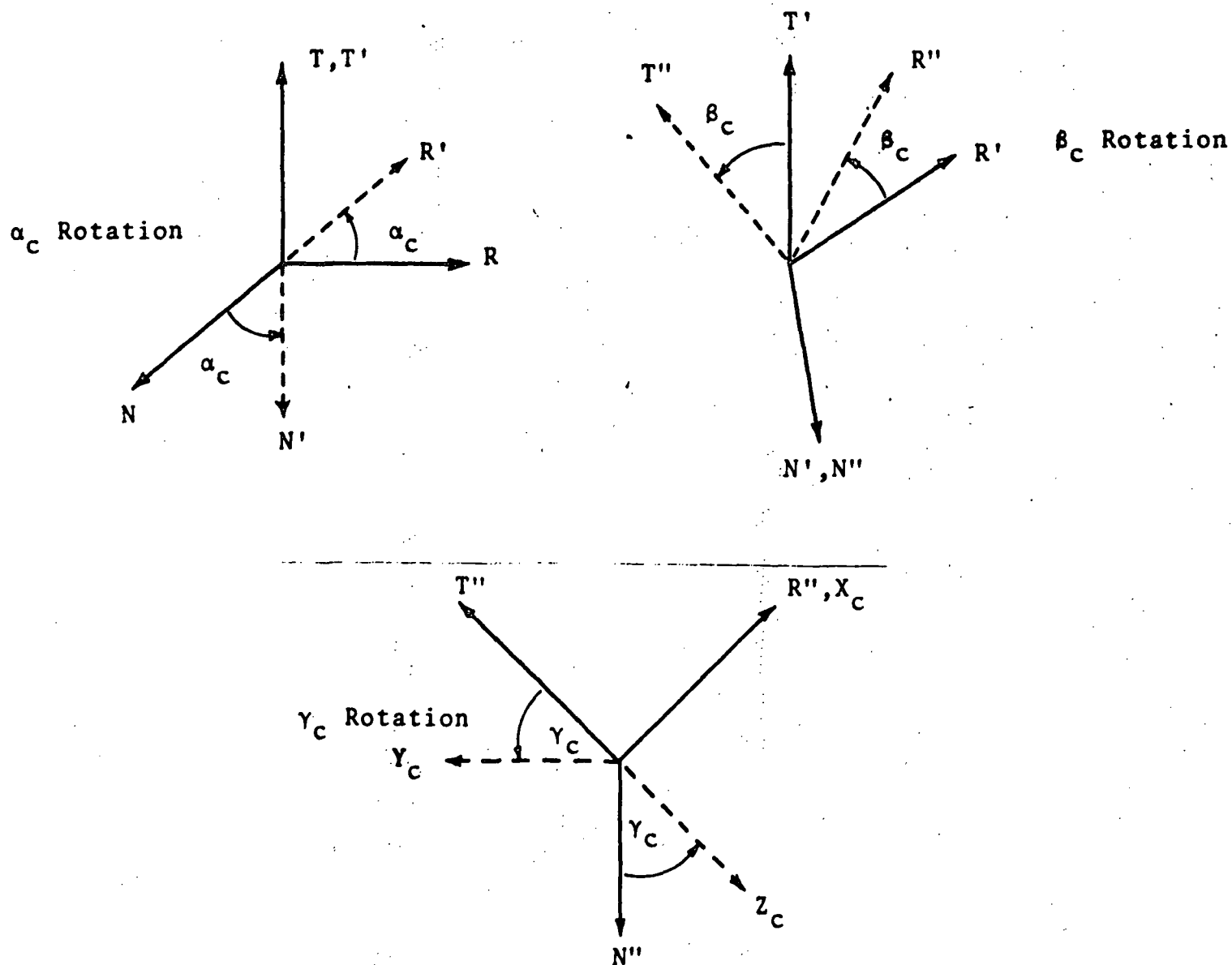
the commanded orientation of the space station roll, pitch and yaw axes. The vehicle command orientation is related to the R, T, N set by means of three Euler rotations:

α_c about T axis

β_c about N' axis

γ_c about X_c (commanded roll) axis

where N' is the N axis after rotation by α_c



4.1.1.4 COORDINATE FRAME 4

Actual Space Station Coordinates

The actual orientation of the space station is similarly related to the RTN frame by a set of Euler angles α, β, γ . The order of rotations is the same as for the command angles and the resultant direction cosine matrix is given below in expanded form

$$\begin{bmatrix} X_S \\ Y_S \\ Z_S \end{bmatrix} = \begin{bmatrix} 1 & 0 & 0 \\ 0 & C\gamma & S\gamma \\ 0 & -S\gamma & C\gamma \end{bmatrix} \begin{bmatrix} C\beta & S\beta & 0 \\ -S\beta & C\beta & 0 \\ 0 & 0 & 1 \end{bmatrix} \begin{bmatrix} C\alpha & 0 & -S\alpha \\ 0 & 1 & 0 \\ S\alpha & 0 & C\alpha \end{bmatrix} \begin{bmatrix} R \\ T \\ N \end{bmatrix}$$

X_S, Y_S, Z_S - actual roll, pitch, and yaw axes of the space station.

α, β, γ - Euler angles

in more condensed form

$$\begin{bmatrix} X_S \\ Y_S \\ Z_S \end{bmatrix} = \begin{bmatrix} C_A \end{bmatrix} \begin{bmatrix} R \\ T \\ N \end{bmatrix}$$

4.1.1.5 COORDINATE FRAME 5

Solar Array Driver Coordinates

Each rigid solar array driver is constrained to rotate about an axis parallel to the space station roll (X_S) axis and about the array vane (Z_{A_1}) axis where the resultant set of axes for the first driver are X_{A_1}, Y_{A_1} and Z_{A_1} as shown below.

The resultant direction cosine relation is in expanded form

$$\begin{bmatrix} X_c \\ Y_c \\ Z_c \end{bmatrix} = \begin{bmatrix} 1 & 0 & 0 \\ 0 & C\gamma_c & S\gamma_c \\ 0 & -S\gamma_c & C\gamma_c \end{bmatrix} \begin{bmatrix} C\beta_c & S\beta_c & 0 \\ -S\beta_c & C\beta_c & 0 \\ 0 & 0 & 1 \end{bmatrix} \begin{bmatrix} C\alpha_c & 0 & -S\alpha_c \\ 0 & 1 & 0 \\ S\alpha_c & 0 & C\alpha_c \end{bmatrix} \begin{bmatrix} R \\ T \\ N \end{bmatrix}$$

X_c - commanded roll axis

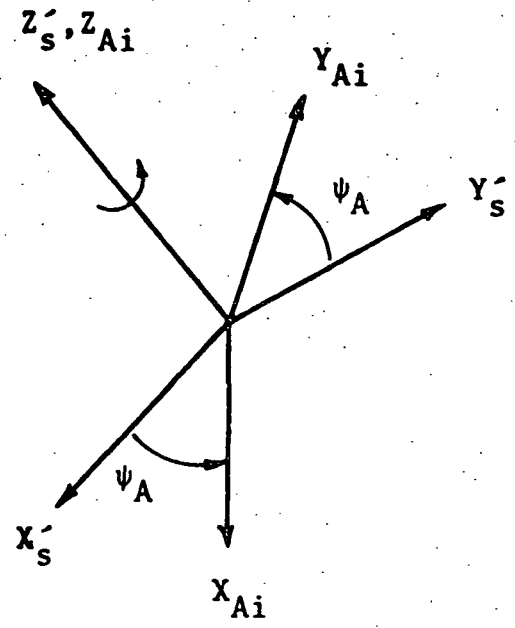
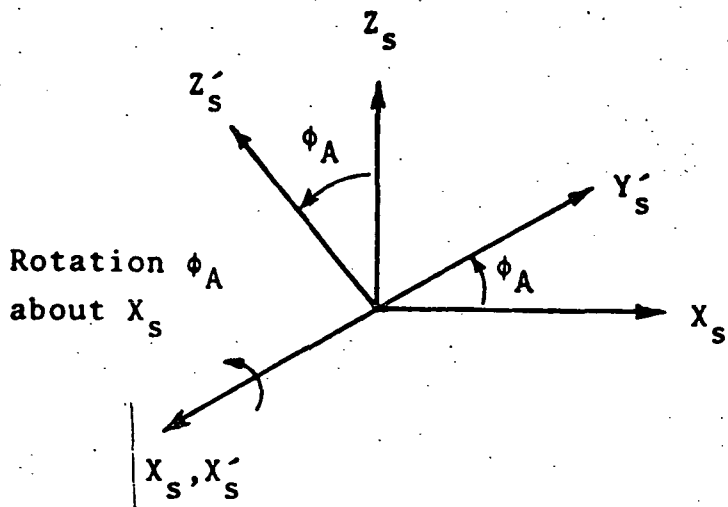
Y_c - commanded pitch axis

Z_c - commanded yaw axis

$\alpha_c, \beta_c, \gamma_c$ - commanded Euler angles

or in more condensed fashion

$$\begin{bmatrix} X_c \\ Y_c \\ Z_c \end{bmatrix} = \begin{bmatrix} C_{A_c} \end{bmatrix} \begin{bmatrix} R \\ T \\ N \end{bmatrix}$$



$$\begin{bmatrix} X_A \\ Y_A \\ Z_A \end{bmatrix} = \begin{bmatrix} \cos\psi_A & \sin\psi_A & 0 \\ -\sin\psi_A & \cos\psi_A & 0 \\ 0 & 0 & 1 \end{bmatrix} \cdot \begin{bmatrix} 1 & 0 & 0 \\ 0 & \cos\phi_A & \sin\phi_A \\ 0 & -\sin\phi_A & \cos\phi_A \end{bmatrix} \begin{bmatrix} X_s \\ Y_s \\ Z_s \end{bmatrix}$$

In condensed form

$$\begin{bmatrix} X_{A1} \\ Y_{A1} \\ Z_{A1} \end{bmatrix} = \begin{bmatrix} \\ C_1 \\ \end{bmatrix} \begin{bmatrix} X_s \\ Y_s \\ Z_s \end{bmatrix}$$

The second rigid driver nominally has the same Y_A axis as the first and the remaining axes are reversed.

$$\begin{bmatrix} X_{A_2} \\ Y_{A_2} \\ Z_{A_2} \end{bmatrix} = \begin{bmatrix} -1 & 0 & 0 \\ 0 & 1 & 0 \\ 0 & 0 & -1 \end{bmatrix} \begin{bmatrix} C_1 \\ \\ \end{bmatrix} \begin{bmatrix} X_s \\ Y_s \\ Z_s \end{bmatrix}$$

$$\begin{bmatrix} C_2 \\ \\ \end{bmatrix} = \begin{bmatrix} -1 & 0 & 0 \\ 0 & 1 & 0 \\ 0 & 0 & -1 \end{bmatrix} \begin{bmatrix} C_1 \\ \\ \end{bmatrix}$$

$$\begin{bmatrix} X_{A_2} \\ Y_{A_2} \\ Z_{A_2} \end{bmatrix} = \begin{bmatrix} C_2 \\ \\ \end{bmatrix} \begin{bmatrix} X_s \\ Y_s \\ Z_s \end{bmatrix}$$

where

$Y_{A(1,2)}$ is normal to the plane of the (1,2) array and is pointed to the sun.

$Z_{A(1,2)}$ is normal to the space station roll axis and in the plane of the array.

The Z_A axis provides the seasonal adjustment and is referred to as the vane axis.

$X_{A(1,2)}$ makes X_A, Y_A, Z_A a right handed set.

4.1.1.6 COORDINATE FRAME 6

Control Moment Gyro Orientation

The Control Moment Gyro is oriented with respect to the spacecraft axes in the following manner:

$$\begin{bmatrix} X_G \\ Y_G \\ Z_G \end{bmatrix} \text{Outer Gimbal} = \begin{bmatrix} 0 & 1 & 0 \\ 0 & 0 & 1 \\ 1 & 0 & 0 \end{bmatrix} \begin{bmatrix} X_S \\ Y_S \\ Z_S \end{bmatrix}$$

or

$$\begin{bmatrix} X_G \\ Y_G \\ Z_G \end{bmatrix} = \begin{bmatrix} \\ C_G \\ \end{bmatrix} \begin{bmatrix} X_S \\ Y_S \\ Z_S \end{bmatrix}$$

Transformation from outer gimbal axes to inner gimbal axes is treated in the discussion of CMG dynamics.

Direction Cosine Identities

$$\begin{bmatrix} X_S \\ Y_S \\ Z_S \end{bmatrix} = \begin{bmatrix} C_O \end{bmatrix}^T \begin{bmatrix} X_I \\ Y_I \\ Z_I \end{bmatrix}$$

$$\begin{bmatrix} C_O \end{bmatrix}^T = \begin{bmatrix} C_A \end{bmatrix} \begin{bmatrix} C_S \end{bmatrix}$$

$$\begin{bmatrix} C_A \end{bmatrix} = \begin{bmatrix} C_O \end{bmatrix}^T \begin{bmatrix} C_S \end{bmatrix}^T$$

$$\alpha = \tan^{-1} \left(\frac{-C_{A 13}}{C_{A 11}} \right)$$

$$\beta = \sin^{-1} \left(C_{A 12} \right)$$

$$\gamma = \tan^{-1} \left(\frac{-C_{A 32}}{C_{A 22}} \right)$$

$$\begin{bmatrix} \dot{C}_i \end{bmatrix} = \begin{bmatrix} C_i \end{bmatrix} \begin{bmatrix} 0 & -w_{i3} & w_{i2} \\ w_{i3} & 0 & -w_{i1} \\ -w_{i2} & w_{i1} & 0 \end{bmatrix}$$

$i = i^{\text{TH}}$ coordinate frame

0 - space station basis

1,2 - driver bases

$w_i =$ rotation of i^{TH} rigid body about its C of G.

1.2 INITIALIZATION PROCEDURES

4.1.2.1 GENERAL INITIALIZATION PROCEDURES

The program is capable of initializing the simulation with any of the integrals or key parameters to user specified values. The input will utilize the Namelist feature of FORTRAN IV and the default (no input data) will be to use the values given in the Data Statements. Such a procedure will assure that any run will not fail because of omitted data and is at the same time extremely flexible.

4.1.2.2 DIRECTION COSINE INITIALIZATION

Space Station Commanded Attitude (C_c)

The basic philosophy used for space station orientation is "belly down" or earth pointing attitude control. Therefore the desired orientation can be specified in terms of the three Euler angles given in Section 1, α_c about T, β_c about N' and γ_c about R'' (or yaw). Specification of these three commanded angles will give any desired space station attitude with respect to the (R, T, N) orbit unit vector set. The steps in computing (C_c), the direction cosine matrix of desired space station orientation are as follows:

A. Computation of Inertial to RTN Direction Cosine Matrix (C_s)

$$\hat{R} = \frac{\bar{R} \cdot \bar{R}}{|\bar{R}^2|}$$

$$\hat{V} = \frac{\bar{V} \cdot \bar{V}}{|\bar{V}^2|}$$

$$\hat{N} = \frac{\hat{R} \times \hat{V}}{|\hat{R} \times \hat{V}|}$$

$$\hat{T} = \hat{N} \times \hat{R}$$

where \bar{R} is the vector position of the orbiting space station in ECI coordinates and \bar{V} is the vector velocity.

$$\begin{bmatrix} C_S \end{bmatrix}_{\text{Initial}} = \begin{bmatrix} \hat{R}_1 & \hat{R}_2 & \hat{R}_3 \\ \hat{T}_1 & \hat{T}_2 & \hat{T}_3 \\ \hat{N}_1 & \hat{N}_2 & \hat{N}_3 \end{bmatrix}_{\text{Initial}}$$

(RTN + ECI)

Note that $\begin{bmatrix} C_S \end{bmatrix}$ is computed throughout the simulation.

B. Computation of the Commanded Attitude Matrix (C_{Ac})

Performing the multiplications in the order indicated in Section 4.1.3 we find:

$$\begin{bmatrix} C_{Ac} \end{bmatrix} = \begin{bmatrix} C\beta_c C\alpha_c & S\beta_c & -S\alpha_c C\beta_c \\ \begin{pmatrix} S\gamma_c & S\alpha_c \\ -C\gamma_c & S\beta_c C\alpha_c \end{pmatrix} & C\gamma_c C\beta_c & C\gamma_c S\beta_c S\alpha_c + C\alpha_c S\gamma_c \\ S\gamma_c S\beta_c C\alpha_c & & -S\gamma_c S\beta_c S\alpha_c \\ C\gamma_c S\alpha_c & -S\gamma_c C\beta_c & C\gamma_c C\alpha_c \end{bmatrix}$$

(Command S/S + RTN)

where

C and S imply cosine and sine respectively. (C_{Ac}) is computed once, at the start of the simulation.

C. Computation of the Command Direction Cosine Matrix (C_c)

$$\begin{bmatrix} C_c \end{bmatrix} = \begin{bmatrix} C_{Ac} \end{bmatrix} \begin{bmatrix} C_s \end{bmatrix}$$

($[C_c]$ is computed throughout the simulation) in which the commanded roll axis unit vector and commanded pitch axis unit vector are respectively:

$$R_{o_c} \Big|_{ECI} = (C_c(11), C_c(12), C_c(13))$$

$$P_{i_c} \Big|_{ECI} = (C_c(21), C_c(22), C_c(23))$$

Space Station Attitude (C_o)

$$\begin{bmatrix} C_o \end{bmatrix}^T_{\text{Initial}} = \begin{bmatrix} C_A \end{bmatrix} \begin{bmatrix} C_s \end{bmatrix}_{\text{Initial}}$$

where $[C_A]$ is the direction cosine matrix of actual space station attitude relative to the RTN set. This matrix is identical in structure to the $[C_{Ac}]$ matrix except that α , β and γ are used in place of α_c , β_c , and γ_c respectively. $[C_o]^T$ is defined as the transpose of $[C_o]$ matrix.

SOLAR ARRAY

The solar array drivers are allowed to rotate about an axis parallel to the roll axis and about the array vane axis. In addition, the two vane axes are 180 degrees apart and the two axes normal to the arrays are parallel. Therefore only two angles are needed to specify the direction cosines of both arrays relative to the spacecraft. ϕ_{A_0} is the rotation of the vane axis of Driver 1 about the space station roll axis. ψ_{A_0} is the rotation of the solar array about the vane axis.

$$\begin{bmatrix} X_{A1} \\ Y_{A1} \\ Z_{A1} \end{bmatrix} = \begin{bmatrix} C\psi_{A_0} & S\psi_{A_0} & 0 \\ S\psi_{A_0} & C\psi_{A_0} & 0 \\ 0 & 0 & 1 \end{bmatrix} \begin{bmatrix} 1 & 0 & 0 \\ 0 & C\phi_{A_0} & S\phi_{A_0} \\ 0 & -S\phi_{A_0} & C\phi_{A_0} \end{bmatrix} \begin{bmatrix} X_s \\ Y_s \\ Z_s \end{bmatrix}$$

or

$$\begin{bmatrix} X_{A1} \\ Y_{A1} \\ Z_{A1} \end{bmatrix} = \begin{bmatrix} C_1 \end{bmatrix} \text{Initial} \begin{bmatrix} X_s \\ Y_s \\ Z_s \end{bmatrix}$$

and

$$\begin{bmatrix} X_{A2} \\ Y_{A2} \\ Z_{A2} \end{bmatrix} = \begin{bmatrix} -1 & 0 & 0 \\ 0 & 1 & 0 \\ 0 & 0 & -1 \end{bmatrix} \begin{bmatrix} X_{A1} \\ Y_{A1} \\ Z_{A1} \end{bmatrix}$$

$$\begin{bmatrix} C_2 \end{bmatrix}_{\text{Initial}} = \begin{bmatrix} -C_1(11) & -C_1(12) & -C_1(13) \\ C_1(21) & C_1(22) & C_1(23) \\ -C_1(31) & -C_1(32) & -C_1(33) \end{bmatrix}$$

4.1.3 RIGID BODY EQUATIONS OF MOTION

4.1.3.1 GENERAL RIGID BODY DYNAMICS FORMULATION

The space station and the rigid array drivers are modeled as a subsystem of interconnected rigid bodies whose motion is described by the Newton-Euler equations of motion. This is shown in Figure 4.6. As stated earlier the effect of appendage dynamics is modeled as an external force and torque. The pertinent equations are given below:

- System Force

$$m_T \left. \frac{d^2(\bar{R}_0 + \bar{C})}{dt^2} \right|_I = \bar{F}_{AJ} + \bar{F}_R$$

- Space Station Moment

$$\left. \frac{d}{dt} (\bar{L}_0 (CG_{SS})) \right|_I = (\bar{C} - \bar{r}_R) \times \bar{F}_R - \sum_J \bar{r}'_J \times \bar{F}_{HJ} - \sum_J \bar{T}_J + \bar{T}_{AC} + \bar{T}_{CMG}$$

- Hinged Body Moment

$$\left. \frac{d}{dt} (\bar{L}_J (CG_J)) \right|_I = \bar{T}_{AJ} + \bar{T}_J + \bar{r}_J \times \bar{F}_{HJ}$$

- J - Index of solar array. J is equal to 1 or 2
- F_{AJ}, T_{AJ} - are the force and torque exerted by the flexible array on each rigid driver
- T_{AC} - torque exerted on spacecraft by rigid driver along constrained axes.
- m_T - total system mass
- O_N - Newtonian reference point
- O_B - Spacecraft reference point
- $CG_{S.S.}$ - Space Station center of gravity
- CG_{SYS} - Center of gravity for the entire rigid body system
- CG_J - Center of gravity for the J^{TH} rigid driver
- R_0 - Distance space station has moved from unperturbed orbital position
- F_R - External force applied by reaction control system
- L_J - Angular Momentum of J^{TH} rigid body
- J = 0,1,2

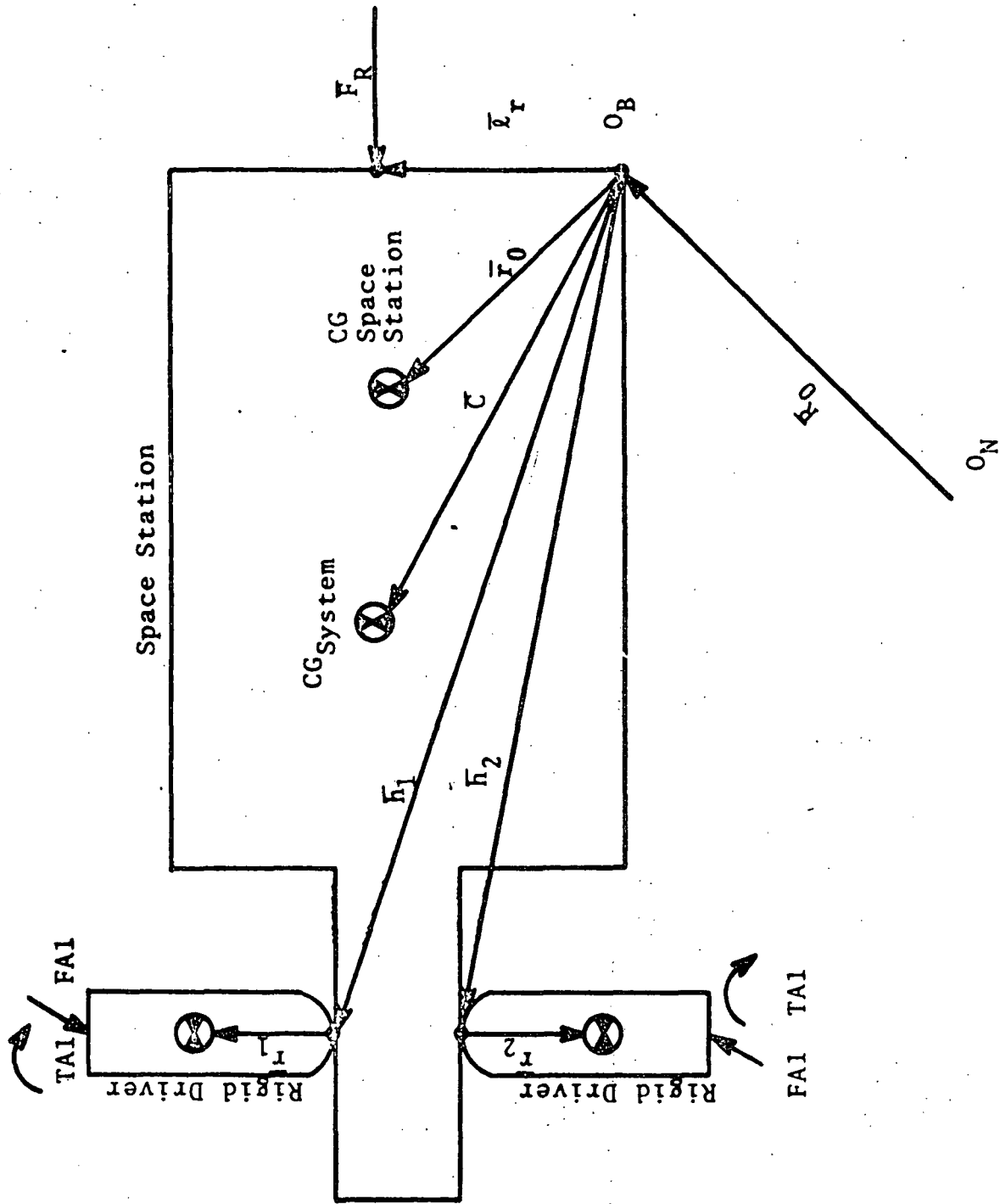


Figure 4-6 Rigid Body System Geometry

- \bar{h}_J - Vector from space station reference point to hinge point for rigid drivers and CMG package
- \bar{r}_J - vector from the respective hinge point to the J^{TH} rigid body (on space station)
- \bar{r}_R - vector from space station reference point to rocket location
- \bar{c} - vector from space station reference to rigid system CG
- \bar{T}_J - hinge torque on J^{TH} driver produced by control system
- \bar{r}_J - $(\bar{r}_O - \bar{h}_J)$ hinge force moment arm
- F_{HJ} - hinge force exerted by space station on J^{TH} body
- $\frac{d}{dt} () \Big|_I$ - implies differentiation w.r.t. an inertial reference frame
- \bar{T}_{CMG} - control torque exerted by the control moment gyros

Before proceeding further, it is instructive to present the principal coordinate frames and direction cosine identities to be utilized in the matrix formulation of these equations.

$$\{X_s\} = [C_0]^T \{X_I\}$$

$$\{X_{A_1}\} = [C_1]^T \{X_s\}$$

$$\{X_{A_2}\} = [C_2]^T \{X_s\}$$

where

$\{X_I\}$ is the vector basis defined by unit vectors in the X_I, Y_I, Z_I directions

$\{X_s\}$ is the vector basis defined by unit vectors along X_s, Y_s and Z_s directions

$\{X_{A_i}\}$ is the vector basis for the i^{TH} solar array

$[]^T$ indicates that the transpose of the matrix is required.

We have previously shown how the C_0, C_1 and C_2 matrices are initialized in terms of Euler angles. The updating of these time varying matrices during the course of the simulation will be performed by the following equation.

$$\begin{bmatrix} \dot{C}_i \end{bmatrix} = \begin{bmatrix} C_i \end{bmatrix} \begin{bmatrix} 0 & -w_{i3} & w_{i2} \\ w_{i3} & 0 & -w_{i1} \\ -w_{i2} & w_{i1} & 0 \end{bmatrix}$$

$$= \begin{bmatrix} C_1 \end{bmatrix} \begin{bmatrix} \tilde{w}_i \end{bmatrix}$$

where

w_{i1} are the rotational rates about i^{TH} coordinate frame axes ($i = 0, 1, 2$).
 w_{i2} For i equals zero, these rates are the spacecraft roll, pitch and
 w_{i3} yaw rates.

This equation is derived in Section 4.1.7. The four vector equations presented may now be formulated as a matrix equation in a convenient coordinate frame. In the equations that follow the space station frame was chosen for the system force and space station moment equations. Each driver moment equation is written in terms of driver coordinates.

In the following formulation the square brackets used to denote a matrix are dropped and it is assumed that all quantities given are in matrix format. A few useful identities are given below.

$$A \times B \rightarrow \tilde{A}B$$

$$\tilde{A}B \equiv -\tilde{B}A$$

$$m_T \left[\begin{array}{l} \ddot{R}_0 + 2 \tilde{w}_0 \dot{R}_0 + (\tilde{w}_0 \tilde{w}_0 + \dot{\tilde{w}}_0) R_0 \\ + (\tilde{w}_0 \tilde{w}_0 + \dot{\tilde{w}}_0) (\mu_0 r_0 + \sum_J \mu_J (h_J + C_J r_J)) \\ + \sum_J \mu_J \left(\begin{array}{l} C_J (\tilde{w}_J \tilde{w}_J + \dot{\tilde{w}}_J) r_J \\ + 2 \tilde{w}_0 C_J \tilde{w}_J r_J \end{array} \right) \end{array} \right] = F_R + \sum_{J=1}^2 C_J F_{A_J}$$

(SYSTEM FORCE)

$$\begin{aligned} \bar{I}_0 \ddot{w}_0 + \tilde{w}_0 \bar{I}_0 \dot{w}_0 &= \ell_R F_R - \sum_{J=1}^2 T_J + T_{CMG} \\ &- \sum_{J=1}^2 \tilde{r}_J \dot{F}_{H_J} + T_{AC} \end{aligned}$$

(SPACE STATION MOMENT)

$$\begin{aligned} \bar{I}_J (C_J^T \dot{w}_0 + \dot{w}_J + (C_J^T w_0) \tilde{w}_J) &= T_{A_J} + C_J^T T_J \\ + (C_J^T w_0 + w_J) \bar{I}_J (w_J + C_J^T w_0) &+ \tilde{r}_J C_J^T F_{H_J} \end{aligned}$$

$$J = 1, 2$$

(RIGID DRIVER MOMENT)

where

$$F_{H_J} = m_J \left[\begin{array}{l} (\tilde{w}_0 \tilde{w}_0 + \dot{\tilde{w}}_0) (R_0 + h_J) + 2 \tilde{w}_0 \dot{R}_0 + \ddot{R}_0 \\ + (2 \tilde{w}_0 C_J \tilde{w}_i + \tilde{w}_0 \tilde{w}_0 C_J + \dot{\tilde{w}}_0 C_J) r_J \\ + C_J (\tilde{w}_J \tilde{w}_J + \dot{\tilde{w}}_J) r_J \end{array} \right] - C_J F_{A_J}$$

(HINGE FORCE)

where

- \ddot{R}_0, \dot{R}_0 and R_0 - The "apparent" (space station
(3x1 matrix) referenced) acceleration of the
space station reference point
and its first two integrals.
- μ_J (scalar) - m_J/m_T
- I_J - Inertia tensor of the J^{TH} rigid
(3x3 matrices) driver referenced to the driver
basis and center of gravity.
- I_0 - Space station inertia tensor
(3x3 matrix) referenced to the space station
basis and center of gravity.
- \dot{w}_0, w_0 - Space station angular accelera-
(3x1 matrix) tion and rate.
- \dot{w}_1, w_1 Driver angular accelerations
(3x1 matrix) and rates.
- \dot{w}_2, w_2
(3x1 matrix)

4. 1. 3. 2 MATRIX FORMULATION OF RIGID BODY DYNAMICS

The equations developed must now be rearranged in a form suitable for solution. This involves formulating the problem in terms of coefficients of \ddot{R}_0 , \dot{w}_0 , \dot{w}_1 and \dot{w}_2 and then inverting the coefficient matrix to obtain these derivatives.

In addition some changes are required in the form of the equations to obtain the following model requirements:

- The rotational motion of the rigid solar array drivers is constrained to motion about an axis parallel to the spacecraft roll axis and an axis in the plane of the solar array normal to the space station roll axis.
- The gear ratio for the array rotation in the roll direction is explicitly incorporated into the moment equations by considering all array driver rotation on the space station side of the gear train.

In effect, this reduces the three equations for each rigid driver to two, the first of which is solved for the scalar variable \hat{w}_{Ai} which is the driver rotation referred to the space station side of the gear box. The roll axis rotation of the driver is taken to be the orbit adjustment while the rotation about the array axis of symmetry is considered nominally to be the seasonal adjustment.

In addition the effect of the constrained axis of driver rotation (rotation about an axis normal to the roll axis and the vane or Z_A axis) must be included in the Space Station Moment Equation. This is done by solving for the constraint torque in terms of \ddot{R}_0 and \dot{w}_0 and adding the terms in these variables to the equation of space station moment to obtain the set of ten scalar equations presented on the following page in matrix form.

RIGID BODY DYNAMICS MATRIX

$$\begin{bmatrix}
 [A_1] & [A_5] & [A_9] & [A_{13}] \\
 [A_2] & [A_6] & [A_{10}] & [A_{14}] \\
 [A_3] & [A_7] & [A_{11}] & [A_{15}] \\
 [A_4] & [A_8] & [A_{12}] & [A_{16}]
 \end{bmatrix}
 \begin{bmatrix}
 \ddot{R}_{01} \\
 \ddot{R}_{02} \\
 \ddot{R}_{03} \\
 \dot{w}_{01} \\
 \dot{w}_{02} \\
 \dot{w}_{03} \\
 \hat{w}A_{11} \\
 \dot{w}A_{12} \\
 \hat{w}A_{21} \\
 \dot{w}A_{22}
 \end{bmatrix}
 =
 \begin{bmatrix}
 F_1 & F_2 & F_3 & F_4
 \end{bmatrix}$$

Definitions -

- $C_1, [C_2]$ - Direction cosine matrix (3x3) relating driver bases to space station basis

$$\begin{bmatrix} X_s \\ Y_s \\ Z_s \end{bmatrix} = [C_i] \begin{bmatrix} X_{Ai} \\ Y_{Ai} \\ Z_{Ai} \end{bmatrix}$$

- C_1^*, C_2^* - direction cosines relating array basis to normally unconstrained axes

- C_1^{**}, C_1^{**} - direction cosines relating array basis to normally constrained axes

- h_1, h_2 - 3x1 vectors in space station basis giving hinge position from reference point

- I_0, I_1, I_2 - inertia matrices of space station, driver 1 and driver 2 respectively. Each is expressed in its own basis

- K_G - gear ratio for array driver orbit adjust mechanism

- l_1, l_2 - vector from driver CG to appendage connection point given in the driver basis

- m_1, m_2, m_T - masses of array drivers and total system respectively

- R_0 - vector from Newtonian reference to space station reference point in space station basis
- r_0 - vector from reference point to space station CG in space station basis
- r_1, r_2 - vectors from hinge point to driver CG in the driver basis
- r_1', r_2' - vectors from hinge point to space station CG
- w_0 - rotation rate of space station
- w_1, w_2 - rotation rate of rigid driver (on array side of gear train)
- $\hat{w}_{A1}, \hat{w}_{A2}$ - rotation rate of rigid driver on space station side of gear box
- $[\tilde{ }]$ - matrix equivalent of vector cross product
- μ_1, μ_2 - mass fractions

$$\mu_1 = \frac{m_1}{m_2} \quad \mu_2 = \frac{m_2}{m_T}$$

Equation Set I - System Translation

$$[A_1] \ddot{R}_0 + [A_5] \dot{w}_0 + [A_9] \dot{w}_{A1} + [A_{13}] \dot{w}_{A2} = F_1]$$

$$[A_1] = m_T [I]$$

$$[A_5] = -m_T \left(\begin{array}{l} [\tilde{R}_0] + \mu_0 [\tilde{r}_0] + \mu_1 (h_1 + [C_1] r_1) \\ + \mu_2 (h_2 + [C_2] r_2) \end{array} \right)$$

$$[A_9] = -m_T \mu_1 [C_1] [\tilde{r}_1] [C_1^*]^T \begin{bmatrix} 1 & 0 \\ KG & 1 \end{bmatrix}$$

$$[A_{13}] = -m_T \mu_2 [C_2] [\tilde{r}_2] [C_2^*]^T \begin{bmatrix} 1 & 0 \\ KG & 1 \end{bmatrix}$$

$$F_1] = \begin{array}{l} F_R] + [C_1] F_{A1}] + [C_2] F_{A2}] \\ -m_T \left(\begin{array}{l} 2 [\tilde{w}_0] \dot{R}_0 + [\tilde{w}_0] [\tilde{w}_0] (R_0 + [\mu_0 r_0]) \\ + [\tilde{w}_0] [\tilde{w}_0] ((h_1 + [C_1] r_1) \mu_1 + (h_2 + [C_2] r_2) \mu_2) \\ + \mu_1 ([C_1] [\tilde{w}_1] [\tilde{w}_1] r_1 + 2 [\tilde{w}_0] [C_1] [\tilde{w}_1] r_1) \\ + \mu_2 ([C_2] [\tilde{w}_2] [\tilde{w}_2] r_2 + 2 [\tilde{w}_0] [C_2] [\tilde{w}_2] r_2) \end{array} \right) \end{array}$$

where

[I] is the identity matrix,

$\tilde{[]}$ and $(\quad)^{\sim}$ indicate that the cross product form is required

$$\begin{bmatrix} \tilde{X}_1 \\ \tilde{X}_2 \\ \tilde{X}_3 \end{bmatrix} = \begin{bmatrix} 0 & -X_3 & X_2 \\ X_3 & 0 & -X_1 \\ -X_2 & X_1 & 0 \end{bmatrix}$$

KG is the gear ratio for the array driver

$[C_i^*]^T$ = transforms \hat{w}_{Ai} to array basis (X_{Ai}, Y_{Ai}, Z_{Ai})

$$[C_i^*]^T = \begin{bmatrix} C_{i1} & 0 \\ C_{i2} & 0 \\ 0 & 1 \end{bmatrix}$$

C_{i1} is the direction cosine between the X_s space station axis (roll) and X_{Ai}

C_{i2} is the direction cosine relating X_s and Y_{Ai}

$$w_i = \begin{bmatrix} C_{i1} & 0 \\ C_{i2} & 0 \\ 0 & 1 \end{bmatrix} \begin{bmatrix} 1/KG & 0 \\ 0 & 1 \end{bmatrix} \begin{bmatrix} \hat{w}_{Ai1} \\ w_{Ai2} \end{bmatrix}$$

Equation Set II - Space Station Rotation

$$[A_2] \ddot{R}_0 + [A_6] \dot{w}_0 + [A_{10}] \dot{w}_{A1} + [A_{14}] \dot{w}_{A2} = F_2$$

$$[A_2] = m_1 \left(-[\tilde{r}'_1] + [C_1^{**}] [\tilde{r}_1] [C_1]^T \right) + m_2 \left(-[\tilde{r}'_2] + [C_2^{**}] [\tilde{r}_2] [C_2]^T \right)$$

$$[A_6] = [I_0] + m_1 [\tilde{r}'_1] \left(R_0 + h_1 + [C_1] r_1 \right) + m_2 [\tilde{r}'_2] \left(R_0 + h_2 + [C_2] r_2 \right) + [C_1^{**}] \left([I_1] [C_1]^T - m_1 [\tilde{r}_1] [C_1]^T \left(R_0 + h_1 + [C_1] r_1 \right) \right) + [C_2^{**}] \left([I_2] [C_2]^T - m_2 [\tilde{r}_2] [C_2]^T \left(R_0 + h_2 + [C_2] r_2 \right) \right)$$

$$[A_{10}] = + m_1 [\tilde{r}'_1] [C_1] [\tilde{r}_1] [C_1^*]^T \begin{bmatrix} 1/KG^2 & 0 \\ 0 & 1 \end{bmatrix}$$

$$[A_{14}] = + m_2 [\tilde{r}'_2] [C_2] [\tilde{r}_2] [C_2^*]^T \begin{bmatrix} 1/KG^2 & 0 \\ 0 & 1 \end{bmatrix}$$

$$\begin{aligned}
[F_2] = & - [\tilde{l}_r] [F_R] - T_1 - T_2 \\
& - [\tilde{w}_0] [I_0] w_0 + \begin{bmatrix} 1/KG & 0 & 0 \\ 0 & 1 & 0 \\ 0 & 0 & 1 \end{bmatrix} [\tilde{r}_1] F_{H1}' \\
& + \begin{bmatrix} 1/KG & 0 & 0 \\ 0 & 1 & 0 \\ 0 & 0 & 1 \end{bmatrix} [\tilde{r}_2] F_{H2}' + T_{CMG} \\
& + C_1^{**} \left(T_{A1} - ([C_1]^T w_0) \right) [I_1] [C_1] w_0 - [\tilde{r}_1] [C_1]^T F_{H1}' \\
& + C_2^{**} \left(T_{A2} - ([C_2] w_0) \right) [I_2] [C_2] w_0 - [\tilde{r}_2] [C_2]^T F_{H2}'
\end{aligned}$$

and

$$F_{H1}' = m_1 \begin{bmatrix} [\tilde{w}_0] [\tilde{w}_0] (R_0 + h_1) + 2 [\tilde{w}_0] \dot{R}_0 \\ (2 [\tilde{w}_0] [C_1] [\tilde{w}_1] + [\tilde{w}_0] [\tilde{w}_0] [C_1]) r_1 + \\ [C_1] [\tilde{w}_1] [\tilde{w}_1] r_1 \end{bmatrix} + [C_1] F_{A1}$$

$$F_{H2}' = m_2 \begin{bmatrix} [\tilde{w}_0] [\tilde{w}_0] (R_0 + h_2) + 2 [\tilde{w}_0] \dot{R}_0 \\ (2 [\tilde{w}_0] [C_2] [\tilde{w}_2] + [\tilde{w}_0] [\tilde{w}_0] [C_2]) r_2 + \\ [C_2] [\tilde{w}_2] [\tilde{w}_2] r_2 \end{bmatrix} + [C_2] F_{A2}$$

where

$$r_1] = r_0] - h_i]$$

$F_{H1}]$ & $F_{H2}]$ - are the hinge force equations less the linear terms in R_0 , w_0 , and w_i

The terms in C_i^{**} represent the effect of the normally constrained rigid driver axis moment on the space station moment equation

$$C_i^{**} = [C_i] \begin{array}{l} +C_{i12} \\ -C_{i11} \\ 0 \end{array} \quad \underline{C_{i12} - C_{i11} \quad 0}$$

$i = 1, 2$ gives the projection of constrained axis component of the i^{TH} driver variables onto the space station axes.

Equation Set III - Rigid Driver 1 Dynamics

The dynamics of the X_{A1} and Y_{A1} axes are restricted to rotation about the X_s direction.

$$[A_3] \ddot{R}_0 + [A_7] \dot{w}_0 + [A_{11}] \dot{w}_{A1} + [A_{15}] \dot{w}_{A2} = F_3$$

$$[A_3] = + [C_1^*] [m_1] [\tilde{r}_1] [C_1]^T$$

$$[A_7] = \begin{bmatrix} 1/KG & 0 \\ 0 & 1 \end{bmatrix} \left[[C_1^*] [I_1] [C_1]^T - m_1 [\tilde{r}_1] [C_1]^T (R_0 + h_1 + [C_1] r_1) \right]$$

$$[A_{11}] = \begin{bmatrix} 1/KG^2 & 0 \\ 0 & 1 \end{bmatrix} [C_1^*] ([I_1] - m_1 [\tilde{r}_1] [\tilde{r}_1]) [C_1^*]^T$$

$$[A_{15}] = 0$$

$$F_3 = \begin{bmatrix} 1/KG & 0 \\ 0 & 1 \end{bmatrix} [C_1^*] \left[\begin{array}{l} T_{A1} + ([C_1]^T T_1) \text{ KG} \\ - [I_1] ([C_1]^T w_0) \tilde{w}_1 \\ - \left(([C_1]^T w_0) \tilde{w}_1 + [\tilde{w}_1] \right) [I_1] (w_1 + [C_1]^T w_0) \\ - [\tilde{r}_1] [C_1]^T F_{H1} \end{array} \right]$$

Equation Set IV - Rigid Driver 2 Dynamics

$$[A_4] \ddot{R}_0 + [A_8] \dot{w}_0 + [A_{12}] \dot{w}_{A1} + [A_{16}] \dot{w}_{A2} = F_4$$

$$[A_4] = + [C_2^*] m_2 [\tilde{r}_2] [C_2]^T$$

$$[A_8] = \begin{bmatrix} 1/KG & 0 \\ 0 & 1 \end{bmatrix} \left[[C_2^*] [I_2] [C_2]^T - m_2 [\tilde{r}_2] [C_2]^T (R_0 + h_2) + [C_2] r_2 \right]$$

$$[A_{12}] = 0$$

$$[A_{16}] = \begin{bmatrix} 1/KG^2 & 0 \\ 0 & 1 \end{bmatrix} [C_2^*] ([I_2] - m_2 [\tilde{r}_2] [\tilde{r}_2]) [C_2^*]^T$$

$$F_4 = \begin{bmatrix} 1/KG & 0 \\ 0 & 1 \end{bmatrix} [C_2^*] \left[\begin{array}{l} T_{A2} + ([C_2]^T T_2) \cdot KG \\ -[I_2] ([C_2]^T w_0) \tilde{w}_2 - [\tilde{r}_2] [C_2]^T F_{H2} \\ - \left(([C_2]^T w_0) \tilde{w}_2 + [\tilde{w}_2] \right) \cdot [I_2] (w_2) + [C_2]^T w_0 \end{array} \right]$$

where

$$w_1] = [C_1^*]^T \begin{bmatrix} 1/KG & 0 \\ 0 & 1 \end{bmatrix} \begin{bmatrix} \hat{w}_{A11} \\ \hat{w}_{A12} \end{bmatrix}$$

$$w_2] = [C_2^*]^T \begin{bmatrix} 1/KG & 0 \\ 0 & 1 \end{bmatrix} \begin{bmatrix} \hat{w}_{A21} \\ \hat{w}_{A22} \end{bmatrix}$$

and

$$[\dot{C}_1] = [C_1] [\tilde{w}_1]$$

$$[\dot{C}_2] = [C_2] [\tilde{w}_2]$$

4.1.3.3 APPLICATION OF ADDITIONAL CONSTRAINTS

The constraint torque imposed by the rigid driver axis simultaneously normal to the roll axis and the array vane axis has been incorporated into simulation by:

- Solving the driver equations for the constraint torque about the locked axis.

$$T_{\text{Con}} = f(\ddot{R}_0, \dot{w}_0, w_0, T_{A_i}, F_{H_i})$$

- The moment applied to the space station is the negative of this constraint torque which is applied by combining the terms in \ddot{R}_0 and \dot{w}_0 with those of A_2 and A_6 for the unconstrained case and adding the remaining terms to F_2 .

This results, as we have previously noted, in the addition of a set of terms preceded by C_i^{**} which is the direction cosine matrix relating the normally constrained driver axis to the space station axes.

We could perform the same procedure for additional constraints imposed by the user and solve a further reduced matrix. However, since the values of these constraints are of real interest for engineering analysis an alternative scheme is utilized:

- The matrix equation for the affected axis is changed from an equation in \ddot{R}_0 , \dot{w}_0 and \dot{w}_A to an equation in \ddot{R}_0 , \dot{w}_0 and T_C , the constraint torque. In other words, we now solve for the constraint torque instead of the rotational acceleration.

In terms of matrix changes the appropriate row of matrix A_{11} and A_{16} is changed to $\begin{bmatrix} -1 & 0 \end{bmatrix}$ if the axis parallel to the roll axis is constrained or $\begin{bmatrix} 0 & -1 \end{bmatrix}$ if the vane axis is constrained.

- Since the affected matrix variable is now constraint torque, the columns of A_{10} and A_{14} are changed to give the projection of the negative of constraint torque in space station coordinates. If the vane axis is constrained,

the second column of these matrices become

$$\begin{bmatrix} C_{131} \\ C_{132} \\ C_{133} \end{bmatrix} \quad i = 1, 2$$

If the other axis is constrained the first column is changed to

$$\begin{bmatrix} 1 \\ 0 \\ 0 \end{bmatrix}$$

and both are changed accordingly if the drivers are completely locked.

4.1.4 FLEXIBLE ARRAY DYNAMICS

4.1.4.1 GENERAL FORMULATION OF A FLEXIBLE APPENDAGE EQUATION

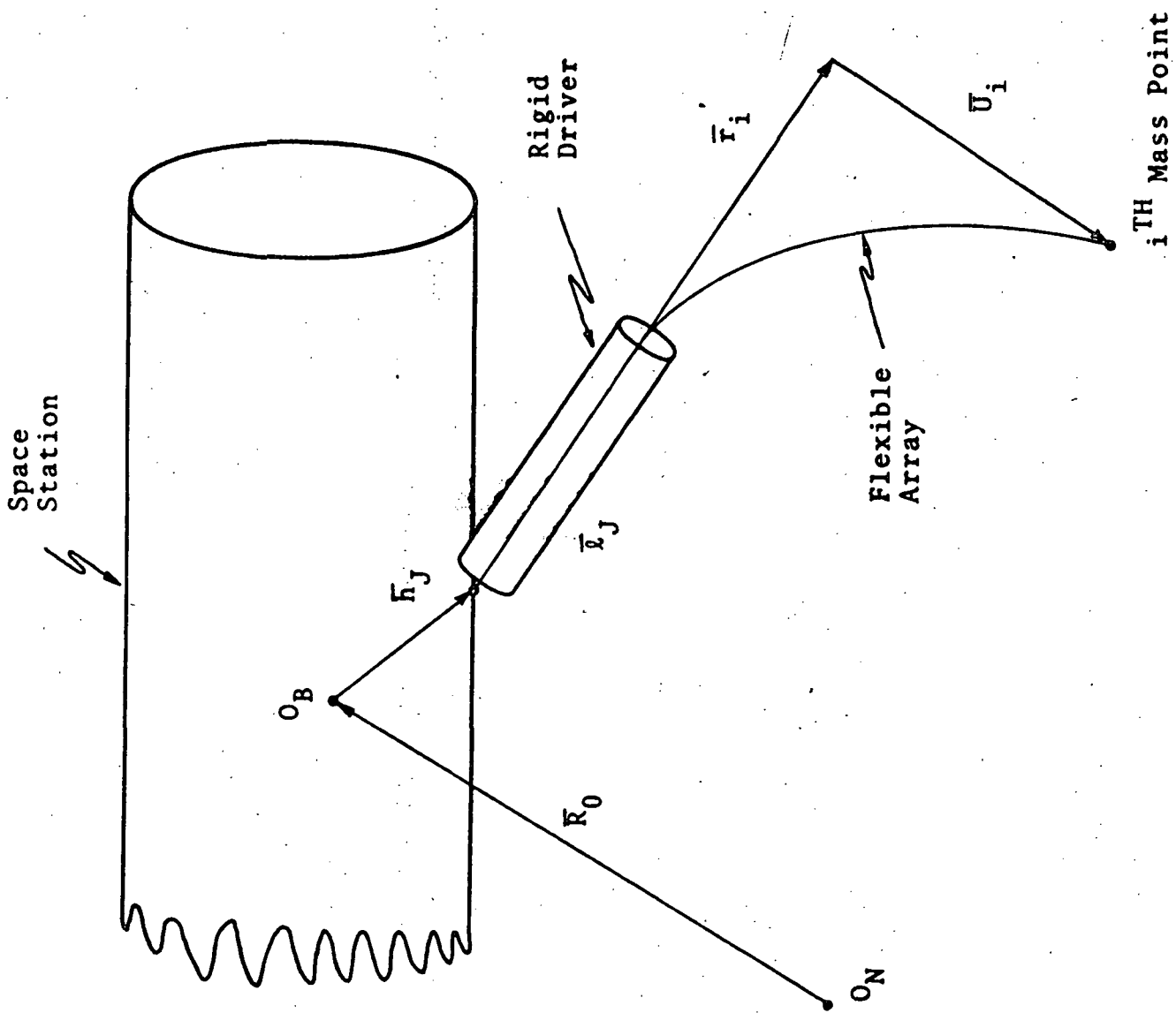
The model for the flexible array dynamics is adapted from the synthetic modes approach developed by Likens in Reference 4.1. The utilization of orthogonal modes augmented by a set of synthetic modes is an attractive approach for simulating the dynamics of large, driven, flexible structures from both a modeling and a computational efficiency viewpoint. The geometry of the system considered is shown in Figure 4-7.

Major Assumptions and Conventions

- Each flexible array utilizes the basis associated with the rigid driver to which it is fixed. This is the basis in which the equations are solved.
- The particle masses have negligible inertias about their respective CG's
- The appendage deflections are sufficiently small that conventional structural analysis is valid; i.e., the system is linear.

Force on iTH Particle

$$F_i = m_i \frac{d^2}{dt^2} (\bar{R}_0 + \bar{h}_J + \bar{l}_J + \bar{r}_i + U_i) \Big|_I$$



$$\bar{P}_i = \bar{R}_0 + \bar{r}_J + \bar{r}_i + \bar{U}_i$$

\bar{P}_i - vector position of i^{th} mass particle of flexible appendage J

\bar{r}_i - vector position of i^{th} mass particle for undeformed appendage

\bar{U}_i - vector deflection of mass particle

Figure 4-7 Flexible Array Geometry

In order to simplify the notation in the following list:

$$\underline{R}_0 = C_J^T R_0$$

$$\underline{w}_0 = C_J^T w_0 C_J$$

$$F_i = m_i \left[\begin{array}{l} \ddot{\underline{R}}_0 + 2\underline{\tilde{w}}_0 \dot{\underline{R}}_0 + (\dot{\underline{w}}_0 + \underline{\tilde{w}}_0 \underline{\tilde{w}}_0) (\underline{R}_0 + \underline{h}_J + \ell_J + r_i + U_i) \\ + (\dot{\underline{w}}_J + \underline{\tilde{w}}_J \underline{\tilde{w}}_J) (\ell_J + r_i + U_i) + 2\underline{\tilde{w}}_0 \underline{\tilde{w}}_J (\ell_J + r_i + U_i) \\ + 2 (\underline{\tilde{w}}_0 + \underline{w}_J) \dot{U}_i + \ddot{U}_i \end{array} \right]$$

$$J=1,2 \quad i=1,2,\dots,n$$

Because of the linear elastic properties of the flexible array the force F_J is also related to the deformation of the array and the applied loads:

$$[M] \dot{q} + [K] q = - [G] \dot{q} - [B] q + L$$

where

$$q = [U_1^1 \quad U_2^1 \quad U_3^1 \quad U_1^2 \quad U_2^2 \quad U_3^2 \quad \dots \quad U_1^N \quad U_2^N \quad U_3^N]$$

K is the symmetric stiffness matrix

L is the matrix of applied loads and rigid body forcing functions.

$$M = \begin{bmatrix} m_1 & 0 & 0 & 0 & 0 & 0 \\ 0 & m_2 & 0 & 0 & 0 & 0 \\ 0 & 0 & m_3 & 0 & 0 & 0 \\ 0 & 0 & 0 & m_4 & 0 & 0 \\ 0 & 0 & 0 & 0 & \ddots & \ddots \\ 0 & 0 & 0 & 0 & \ddots & \ddots \end{bmatrix}$$

3n x 3n

$$G = \begin{bmatrix} \begin{matrix} \tilde{2w}_T m_1 \\ 3 \times 3 \end{matrix} & 0 & 0 & 0 & 0 \\ 0 & \tilde{2w}_T m_2 & 0 & 0 & 0 \\ 0 & 0 & \tilde{2w}_T m_3 & 0 & 0 \\ 0 & 0 & 0 & \ddots & \ddots \\ 0 & 0 & 0 & \ddots & \ddots \end{bmatrix}$$

3n x 3n

$$w_T = \underline{w_0} + w_J$$

$$B = \begin{bmatrix} m_1 \dot{\underline{\Omega}} & 0 & 0 & 0 & 0 \\ 3 \times 3 & & & & \\ 0 & m_2 \dot{\underline{\Omega}} & 0 & 0 & 0 \\ & 3 \times 3 & & & \\ 0 & 0 & m_3 \dot{\underline{\Omega}} & 0 & 0 \\ & & & & \ddots \end{bmatrix}$$

$$\begin{aligned} \dot{\underline{\Omega}} &= \dot{\underline{w}}_T + \underline{\underline{w}}_0 \underline{\underline{w}}_0 + \underline{\underline{w}}_J \underline{\underline{w}}_J + 2 \underline{\underline{w}}_0 \underline{\underline{w}}_J \\ &= \dot{\underline{w}}_T + \underline{\underline{w}}_T \underline{\underline{w}}_T \end{aligned}$$

Before formulating the expression for the L term the following identities are useful

$$\sum_E = \begin{bmatrix} E & \vdots & E & \vdots & \dots & E \\ 3 \times 3 & \vdots & 3 \times 3 & \vdots & & \end{bmatrix}^T$$

$$\sum_{EO} \begin{bmatrix} E & \vdots & 0 \\ 3 \times 3 & \vdots & 3 \times 3 \end{bmatrix}^T$$

$$\sum_{OE} \begin{bmatrix} 0 & \vdots & E \\ 3 \times 3 & \vdots & 3 \times 3 \end{bmatrix}^T$$

where

$$\begin{bmatrix} E \\ 3 \times 3 \end{bmatrix} = \begin{bmatrix} 1 & 0 & 0 \\ 0 & 1 & 0 \\ 0 & 0 & 1 \end{bmatrix}$$

$$\bar{r} = [r_1 \ r_2 \ r_3 \ \dots \ r_n]^T$$

$$\tilde{A}B = -\tilde{B}A$$

$$\ddot{R}_J = \ddot{R}_0 - (\dot{R}_0 + h_J) \dot{w}_0$$

$$w_T = w_0 + w_J$$

$$L = -M \sum_E [\ddot{R}_J - \tilde{L}_J \dot{w}_T] + M \tilde{r} \dot{w}_T$$

$$-M \sum_E C - M D \bar{r} + \lambda$$

where

$$\tilde{r} = \begin{bmatrix} \tilde{r}_1 & 0 & 0 & 0 \\ 3 \times 3 & & & \\ & \tilde{r}_2 & 0 & 0 \\ & 3 \times 3 & & \\ \text{SYMMETRIC} & & & 0 \end{bmatrix},$$

3n x 3n

$$\lambda = \begin{bmatrix} \lambda_1 \\ \lambda_2 \\ \vdots \\ \lambda_{3n} \end{bmatrix}$$

3n x 1

$$[C] = 2 \underline{w_0} \underline{\dot{R}_0} + \underline{\tilde{w}_0} \underline{\tilde{w}_0} (\underline{R_0} + \underline{h_J}) + \underline{\tilde{w}_T} \underline{w_T} \underline{\ell_J} + \underline{\tilde{r}_J} \underline{\dot{w}_T}$$

$$\begin{bmatrix} D \end{bmatrix}_{3n \times 3n} = \begin{bmatrix} \left(\sum_E \underline{w_0} \right)^{\sim} \left(\sum_E \underline{w_0} \right)^{\sim} + \left(\sum_E \underline{w_J} \right)^{\sim} \left(\sum_E \underline{w_J} \right)^{\sim} \\ + 2 \left(\sum_E \underline{w_0} \right)^{\sim} \left(\sum_E \underline{w_J} \right)^{\sim} \end{bmatrix}$$

$$\left(\sum_E \underline{w} \right)^{\sim} = \begin{bmatrix} \underline{\tilde{w}} & 0 & 0 & 0 \\ 0 & \underline{\tilde{w}} & 0 & 0 \\ 0 & 0 & \underline{\tilde{w}} & 0 \\ 0 & 0 & 0 & \underline{\tilde{w}} \end{bmatrix}$$

Let

$$\ddot{\underline{U}} = \begin{bmatrix} \ddot{\underline{R}_J} \\ \dot{\underline{w}_T} \end{bmatrix}$$

$$L = -M \left(\sum_E \hat{\Sigma}_{EO}^T - \left(\sum_E \underline{\tilde{\ell}'_J} - \underline{\tilde{r}} \right) \hat{\Sigma}_{OE}^T \right) \ddot{\underline{U}}$$

$$- M \left(\sum_E C + D \bar{F} \right) + \lambda$$

where

$$\underline{\ell}'_J = \underline{\ell}_J - \underline{r}_J$$

Conversion to Normal Coordinates

There exists a unique orthogonal transformation which has the following properties:

a. $\phi^T M \phi = [E]$

b. $\phi^T K \phi = \begin{bmatrix} \sigma_1^2 & & & \\ & \sigma_2^2 & & \\ & & \ddots & \\ & & & \sigma_N^2 \end{bmatrix} = \bar{\sigma}^2$

such that

$$q(R,t) = \phi(R) \eta(t)$$

A finite number of cantilever modes ($\bar{\phi}$) satisfying (a) and (b) are utilized to transform the appendage equation:

$$M\ddot{\phi}\eta + K\phi\eta = -G\dot{\phi}\eta - B\phi\eta + L$$

Premultiplying by $\bar{\phi}^T$ we have

$$\ddot{\bar{\eta}} + 2\xi\bar{\sigma}\dot{\bar{\eta}} + \bar{\sigma}^2 \bar{\eta} = \bar{\phi}^T G\bar{\phi}\dot{\bar{\eta}} - \bar{\phi}^T B\bar{\phi}\bar{\eta} + \bar{\phi}^T L$$

$\bar{\eta}, \dot{\bar{\eta}}, \ddot{\bar{\eta}}$ are $N \times 1$ matrices where

N is the number of cantilevered modes utilized. Note that a modal damping term has been arbitrarily inserted in the classic manner of structural analysis.

Now since the appendage mass, mode shape, and geometry are all known a priori and remain invariant, the appendage equation can be reformulated to reduce the required computational effort

$$\begin{aligned} \ddot{\bar{\eta}} + 2\xi\bar{\sigma}\dot{\bar{\eta}} + \bar{\sigma}^2 \bar{\eta} = & -A_1 \dot{\bar{\eta}} - A_3 \bar{\eta} \\ & -A_4 \dot{C} - A_5 \\ & -\Delta' \ddot{U} + \phi^T L \end{aligned}$$

where

$\ddot{\bar{\eta}}, \dot{\bar{\eta}}, \bar{\eta}$ are $N \times 1$ vectors

4.1.4.2 ADDITION OF SYNTHETIC MODES

A particularly important term in the Appendage Equation is the next to the last term $\Delta' \ddot{U}$ where

$$\Delta' = -\bar{\phi}^T M \left(\sum_E \hat{\sum}_{EO}^T - \sum_E \hat{\sum}_{OE} \tilde{\ell}'_J - \tilde{r} \hat{\sum}_{OE} \right)$$

If we define $\Delta = \lim_{N \rightarrow \infty} \Delta'$ it can be shown that

$$N \rightarrow \infty$$

$$\Delta^T \Delta = \begin{bmatrix} M_A & -P_A M_A \\ 3 \times 3 & 3 \times 3 \\ \hline P_A M_A & I_A \end{bmatrix}$$

where

M_A - Appendage mass

I_A - Appendage inertia

P_A - Centroid vector for appendage relative to attachment point.

Since $\Delta'^T \Delta' \neq \Delta^T \Delta$, the rigid or steady state representation of the appendage is inaccurate. In order to circumvent this difficulty, synthetic modes may be added in terms of additional rows for Δ' .

$$\text{Let } \Delta = \left[\begin{array}{c} \Delta' \\ \Delta'' \end{array} \right]$$

The synthetic modes are then defined as

$$\ddot{\eta}_s + 2 \bar{\xi}_s \bar{\sigma}_s \dot{\eta}_s + \bar{\sigma}_s^2 \eta_s = \Delta'^T \ddot{U}_J$$

To avoid impacting the frequency range of interest the following procedure is utilized:

$$(\sigma_s)_{\text{MIN}} \gg \sigma_{\text{MAX}}$$

$$\xi_s > .71$$

The synthetic modes are computed in terms of a difference equation to avoid potential integration instability:

$$\eta_s(NT) = a \Delta'^T \ddot{U}(NT) + b \Delta'^T \ddot{U}(NT-T)$$

$$-d \eta_s(NT-T) - e \eta_s(NT-2T)$$

for each synthetic mode.

Six synthetic modes will be employed, each one will be chosen to satisfy the constraints for a given column and thus the first synthetic mode will have six coefficients, the second will have five and so forth, until the sixth mode which has only one coefficient.

The capability of using a steady state mode function is also included in this case

where $\eta_s(NT) = K \Delta^{-1} \ddot{U}(NT)$

$$K = \frac{a+b}{1+d+e}$$

Forces and Torques Induced by the Flexible Appendage (from Likins)

$$f' = \sum_E^T M \phi \sigma^2 \eta$$

$$l' = \left(\sum_E^T \tilde{r} + \tilde{l}_J \sum_E^T \right) M \phi \sigma^2 \eta$$

where f' and l' are respectively, the force and torque upon the rigid driver.

Let

$$\Lambda' = \begin{bmatrix} f' \\ l' \end{bmatrix}$$

$$\Lambda' = \left(\sum_{EO}^{\hat{}} \sum_E + \sum_{OE}^{\hat{}} \left(\sum_E^{\hat{T}} \tilde{r} + \tilde{l}_J \sum_E^{\hat{T}} \right) \right) M \phi \sigma^2 \eta$$

$$\Lambda' = -\Delta^T \sigma^2 \eta \text{ (for ideal } \Delta^T)$$

For the case where Δ is approximated by a finite number of cantilever modes augmented by the synthetic modes as discussed earlier

$$\Lambda' = - \bar{\Delta}^T \bar{\sigma}^2 \bar{\eta}$$

$$\bar{\Delta}^T = [\bar{\Delta}_1 \quad \bar{\Delta}_2]^T$$

where

$$\bar{\Delta}_1^T \bar{\sigma}^2 \bar{\eta} \quad - \quad \text{external force impressed upon } J^{\text{TH}} \text{ rigid driver } (F_{AJ})$$

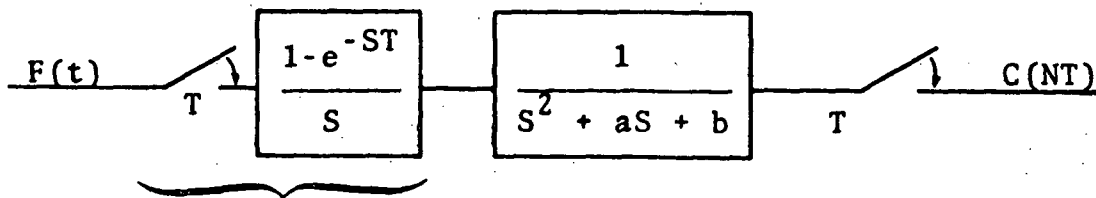
$$\bar{\Delta}_2^T \bar{\sigma}^2 \bar{\eta} \quad - \quad \text{external torque impressed upon } J^{\text{TH}} \text{ rigid driver } (T_J)$$

Difference Equation Formulation for Synthetic Modes

Given an equation of the form

$$\ddot{q} + a \dot{q} + b q = F(t),$$

A difference equation formulation utilizing a staircase step representation of $F(t)$ can be readily obtained by the use of Z transform theory. The equivalent block diagram corresponding to this approach is shown in the following figure.



Sample and Hold

- $C(NT)$ - Output of system to staircase step representation of $F(t)$ at $t = NT$
- T - Sampling interval
- S - Laplace transform variable

In terms of the sampled data Z transform:

$$\frac{C(Z)}{F(Z)} = \frac{Z-1}{Z} \mathcal{Z} \left(\frac{1}{S(S^2+aS+b)} \right)$$

Let

\mathcal{Z} = Z transformation

$$\alpha = a/2$$

$$\beta^2 = b - \alpha^2$$

$$\frac{1}{S[(S+\alpha)^2 + \beta^2]} = \left[\frac{1}{S} - \frac{S + \alpha}{(S+\alpha)^2 + \beta^2} - \frac{\alpha}{(S+\alpha)^2 + \beta^2} \right] \left[\frac{1}{\alpha^2 + \beta^2} \right]$$

Laplace Transform

Z Transform

1/S

Z/Z-1

$$-(S+\alpha)/[(S+\alpha)^2 + \beta^2]$$

$$-\frac{(Z^2 - Ze^{-\alpha T} \cos \beta T)}{(Z^2 - 2Ze^{-\alpha T} \cos \beta T + e^{-2\alpha T})}$$

$$-\frac{\alpha}{(S+\alpha)^2 + \beta^2}$$

$$-\frac{\alpha}{\beta} \frac{(Ze^{-\alpha T} \sin \beta T)}{(Z^2 - 2Ze^{-\alpha T} \cos \beta T + e^{-2\alpha T})}$$

$$\frac{C(Z)}{F(Z)} = \frac{Z-1}{Z} \frac{1}{\beta} \left[\begin{array}{l} Z^3 - 2Z^2 e^{-\alpha T} \cos \beta T + e^{-2\alpha T} Z \\ -Z^3 + Z^2 (e^{-\alpha T} \cos \beta T - \frac{\alpha}{\beta} e^{-\alpha T} \sin \beta T) \\ +Z^2 - Ze^{-\alpha T} \cos \beta T + \frac{\alpha}{\beta} Ze^{-\alpha T} \sin \beta T \\ \hline (Z-1) (Z^2 - 2Ze^{-\alpha T} \cos \beta T + e^{-2\alpha T}) \end{array} \right]$$

$$= \frac{1}{\beta} \left[\begin{array}{l} Z (1 - e^{-\alpha T} \cos \beta T - \alpha/\beta e^{-\alpha T} \sin \beta T) \\ + (e^{-2\alpha T} - e^{-\alpha T} \cos \beta T + \frac{\alpha}{\beta} e^{-\alpha T} \sin \beta T) \\ \hline Z^2 - 2Ze^{-\alpha T} \cos \beta T + e^{-2\alpha T} \end{array} \right]$$

The equivalent difference equation is:

$$C(NT) = a_1 F(NT-T) + a_2 F(NT-2T) \\ - a_3 C(NT-T) - a_4 C(NT-2T)$$

where

$$a_1 = (1 - e^{-\alpha T} \cos \beta T - \alpha/\beta e^{-\alpha T} \sin \beta T)$$

$$a_2 = (e^{-2\alpha T} - e^{-\alpha T} \cos \beta T + \alpha/\beta e^{-\alpha T} \sin \beta T)$$

$$a_3 = -2e^{-\alpha T} \cos \beta T$$

$$a_4 = e^{-2\alpha T}$$

$X(NT)$ - present sampled value of X

$X(NT-T)$ - previous sampled value of X

4.1.4.3 PRESIMULATION COMPUTATIONS

The form of the appendage equation given in the preceding section is:

$$\ddot{\bar{\eta}} + 2\xi\sigma \dot{\bar{\eta}} + \sigma^2 \bar{\eta} = -A_1 \ddot{\bar{\eta}} - A_3 \bar{\eta} - A_4 C - A_5 - \Delta \ddot{U}$$

In their most general form these equations require the multiplication of $3 \times 3n$ matrices where n is the number of mass points used to define the appendage. The form of the mass matrix employed allows considerable simplification of the computation and permits the calculation of a set of coefficients of much reduced order prior to the actual simulation.

Computation of A_2, A_4, A_6

From the preceding equation we can define the A_1 and A_3 matrices in terms of rigid body rotation parameters and A_2 , a constant matrix:

$$A_{1\ell m} = \sum_{i=1}^3 \sum_{J=1}^3 2 \tilde{w}_{iJ} A_{2iJ\ell m}$$

$$A_{3\ell m} = \sum_{i=1}^3 \sum_{J=1}^3 \tilde{\Omega}_{iJ} A_{2iJ\ell m}$$

where

$$A_{2iJ\ell m} = \sum_{k=1}^n \phi_{kJ}^m \phi_{ki}^{\ell} m_k$$

ℓ, m - cantilever mode numbers ($0 < \ell, m \leq N$)

k - mass point number ($0 < k \leq n$)

i, J - identify the three components of the n mode shape displacements ($0 < i, J \leq 3$)

m_k - k^{TH} mass element ($0 < k \leq n$)

A_4 is an $N \times 3$ matrix which multiplies the 3×1 C matrix which is a summation of rigid acceleration terms

$$A_{4\ell i} = \sum_{k=1}^n \phi_{ki}^{\ell} m_k$$

ℓ - cantilever mode number ($0 < \ell \leq N$)

i - component identifier ($0 < i \leq 3$)

The A_5 matrix can be reduced to the product of a constant matrix and a matrix of rigid angular accelerations:

$$A_{5\ell} = \sum_{J=1}^3 \sum_{i=1}^3 d_{Ji} A_{6Ji\ell}$$

where

$$A_{6Ji\ell} = \sum_{k=1}^n m_k \phi_{ki}^{\ell} r_{ki}$$

where

d_{Ji} are rigid acceleration terms

r_{ki} are the coordinates of the undeflected mass points relative to the attachment point.

Computation of the Δ Matrix

The Δ matrix is an $(N+6 \times 6)$ matrix which is composed entirely of constant parameters. It is formed by calculating the unaugmented Δ matrix Δ' ($N \times 6$) shown below and augmenting this matrix to obtain the desired $\Delta^T \Delta$ product.

$$\Delta' = -\phi^T M \begin{pmatrix} \Sigma & \hat{\Sigma}^T - \tilde{b}_i & \Sigma & \hat{\Sigma}^T \\ E & EO & E & OE \end{pmatrix}$$

where each \tilde{b}_i is a 3×3 matrix formed by $\tilde{b}_i = (r_i + 1_j)$

The matrix multiplication may be performed yielding the general formula for Δ' , an $(N \times 6)$ matrix shown below:

$$a) \quad \Delta'_{lm} = \sum_{i=1}^n m_i \phi_{im}^1$$

for l and m such that $1 \leq l \leq N$ and $1 \leq m \leq 3$

$$b) \quad \Delta'_{lm} = \sum_{i=1}^n m_i \left(\phi_{ik}^1 b_{ij} - \phi_{ij}^1 b_{ik} \right)$$

for l and m such that $1 \leq l \leq N$ and $4 \leq m \leq 6$

where the J 's and k 's are related to m by:

m	j	k
4	2	3
5	3	1
6	1	2

Six rows will be added to the Δ matrix to form the Δ matrix. These rows will be added in such a manner so that the new Δ matrix will represent the real world. This is accomplished by performing the multiplication $\Delta^T \Delta$. This multiplication should equal.

$$\Delta^T \Delta = \begin{bmatrix}
 M_A & 0 & 0 & 0 & P_{A3}M_A & -P_{A2}M_A \\
 0 & M_A & 0 & -P_{A3}M_A & 0 & P_{A1}M_A \\
 0 & 0 & M_A & P_{A2}M_A & -P_{A1}M_A & 0 \\
 0 & -P_{A3}M_A & P_{A2}M_A & I_{A11} & I_{A12} & I_{A13} \\
 P_{A3}M_A & 0 & -P_{A1}M_A & I_{A21} & I_{A22} & I_{A23} \\
 -P_{A2}M_A & P_{A1}M_A & 0 & I_{A31} & I_{A32} & I_{A33}
 \end{bmatrix}$$

(ideal)

where

- M_A is the total mass of the flexible appendage
- $P_{A1,2,3}$ is the coordinates of the appendage mass centroid, with respect to the attachment point.

$$P_{Ai} = \left[\sum_{k=1}^n (r_{ki} + 1) m_k \right] / M_A$$

- c. I_A is the moment of inertia with respect to the attachment point.

$$I_A = \sum_{k=1}^n m_k \tilde{b}_k^2$$

Since every element of the $\Delta^T \Delta$ product has the form:

$$(\Delta^T \Delta)_{iJ} = \Delta_{1i} \Delta_{1J} + \Delta_{2i} \Delta_{2J} + \dots + \Delta_{Ni} \Delta_{NJ}$$

We can add a row of augmenting Δ 's to obtain a perfect row in the $\Delta^T \Delta$ matrix; e.g., add

$$\Delta_{N+1,1} \quad \Delta_{N+1,1} \quad \text{to idealize 1, 1 element}$$

$$\Delta_{N+1,1} \quad \Delta_{N+1,2} \quad \text{to idealize 1, 2 element}$$

and so forth.

We can perform the same function for the second row and by making its first entry zero, avoid changing the previously obtained result. This process continues until six rows of augmenting Δ 's have been developed. (The last row is a single element.)

The six augmenting Δ rows are defined by the following set of equations:

$$\Delta_{(N+1)1} = \left[M_A - \sum_{i=1}^N \Delta_{i1} \Delta_{i1} \right]^{1/2}$$

$$\Delta_{(N+1)j} = - \left(\sum_{i=1}^N \Delta_{ij} \Delta_{i1} \right) / \Delta_{(N+1)1} \quad j = 2, 3, 4$$

$$\Delta_{(N+1)5} = \left(P_{A3} M_A - \sum_{i=1}^N \Delta_{i5} \Delta_{i1} \right) / \Delta_{(N+1)1}$$

$$\Delta_{(N+1)6} = \left(-P_{A2} M_A - \sum_{i=1}^N \Delta_{i6} \Delta_{i1} \right) / \Delta_{(N+1)1}$$

$$\Delta_{ij} = 0 \quad \begin{array}{l} i = N+k \\ j = 1, 2, \dots, k-1 \\ k = 2, 3, 4, 5, 6 \end{array}$$

$$\Delta_{(N+2)2} = \left[M_A - \sum_{i=1}^{N+1} \Delta_{i2} \Delta_{i2} \right]^{1/2}$$

$$\Delta_{(N+2)j} = - \left(\sum_{i=1}^{N+1} \Delta_{ij} \Delta_{i2} \right) / \Delta_{(N+2)2} \quad J = 3, 5$$

$$\Delta_{(N+2)4} = -P_{A3} M_A \sum_{i=1}^{N+1} \Delta_{i4} \Delta_{i2} / \Delta_{(N+2)2}$$

$$\Delta_{(N+2)6} = P_{A1} M_A - \sum_{i=1}^{N+1} \Delta_{i4} \Delta_{i2} / \Delta_{(N+2)2}$$

$$\Delta_{(N+3)3} = \left[M_A - \sum_{i=1}^{N+2} \Delta_{i3} \Delta_{i3} \right]^{1/2}$$

$$\Delta_{(N+3)4} = P_{A2} M_A - \sum_{i=1}^{N+2} \Delta_{i4} \Delta_{i3} / \Delta_{(N+3)3}$$

$$\Delta_{(N+3)5} = P_{A2} M_A - \sum_{i=1}^{N+2} \Delta_{i5} \Delta_{i3} / \Delta_{(N+3)3}$$

$$\Delta_{(N+3)6} = P_{A2} M_A - \sum_{i=1}^{N+2} \Delta_{i6} \Delta_{i3} / \Delta_{(N+3)3}$$

$$\Delta_{(N+4)4} = \left[I_{A11} - \sum_{i=1}^{N+3} \Delta_{i4} \Delta_{i4} \right]^{1/2}$$

$$\Delta_{(N+4)5} = I_{A21} - \sum_{i=1}^{N+3} \Delta_{i5} \Delta_{i4} / \Delta_{(N+4)4}$$

$$\Delta_{(N+4)5} = I_{A21} - \sum_{i=1}^{N+3} \Delta_{i5} \Delta_{i4} / \Delta_{(N+4)4}$$

$$\Delta_{(N+4)6} = I_{A31} - \sum_{i=1}^{N+3} \Delta_{i6} \Delta_{i4} / \Delta_{(N+4)6}$$

$$\Delta_{(N+5)5} = \left[I_{A22} - \sum_{i=1}^{N+4} \Delta_{i5} \Delta_{i5} \right]^{1/2}$$

$$\Delta_{(N+5)6} = I_{A23} - \sum_{i=1}^{N+4} \Delta_{i6} \Delta_{i5} / \Delta_{(N+5)5}$$

$$\Delta_{(N+6)6} = \left[I_{A33} - \sum_{i=1}^{N+5} \Delta_{i6} \Delta_{i6} \right]^{1/2}$$

As we have shown the equations, the inertial quantities not absorbed by the modal representation are accounted for by the synthetic modes representation. For the specific case which we are considering, the allocation of some of the mass and inertia to the rigid body driver is advisable. This requires that biased values of mass, moment of inertia and centroid location be used in lieu of the values now used.

4.1.5 GUIDANCE AND CONTROL

The STRISS simulation has two principal guidance and control functions:

- The space station is to be oriented with the roll axis normal to the orbit plane and yaw axis along the negative of the radius vector from the geocenter to the spacecraft.
- The two solar arrays are driven normal to the space station to sun line within the limits of permissible array motion.

4.1.5.1 SPACE STATION GUIDANCE

Since the commanded attitude is fixed relative to the R, T, N frame, computation of the space station commands consist of updating the (C_s) matrix as a function of orbit position and then multiplying by the constant (C_{Ac}) matrix to obtain the current value of \bar{R}_{0c} and \bar{P}_{ic} .

$$[C_c] = [C_{Ac}] [C_s]$$

$$\bar{R}_{0c} = \text{row 1 of } [C_c] \quad (\text{Commanded roll axis})$$

$$\bar{P}_{ic} = \text{row 2 of } [C_c] \quad (\text{Commanded pitch axis})$$

where the vectors given above are expressed in inertial coordinates. For the nominal case where the roll axis is normal to the orbit plane and yaw is along the $-\bar{R}$ direction, the required Euler angle commands are:

$$\alpha_c = -90^\circ$$

$$\beta_c = \gamma_c = 0$$

4.1.5.2 SOLAR ARRAY GUIDANCE

Orientation commands for the solar array drivers are obtained by using the cross product of the array Y_A axis and the earth-to-sun unit vector as an

error signal. When the Y_A axis, which is normal to the plane of the solar array, is pointing toward the sun the error is null. Other orientations result in an error signal of proper sign being generated. The components of the error signal along the permitted axes of notation are then input to the array driver control equations.

Earth-to-Sun Unit Vector

$$\hat{S} \Big|_{EC1} = \begin{bmatrix} C\Gamma \\ S\Gamma \ C\Delta \\ S\Gamma \ S\Delta \end{bmatrix}$$

Γ - rotation of sun in ecliptic plane

Δ - deflection of ecliptic

$$\hat{S} \Big|_{ss} = [C_0]^T \hat{S} \Big|_{EC1}$$

Cross Product Law

$$\hat{E1} = \hat{Y}_{A1} \times \hat{S} \Big|_{ss}$$

$$\hat{E2} = \hat{Y}_{A2} \times \hat{S} \Big|_{ss}$$

$$\phi_{AE1} = \hat{E1}(1)$$

$$\phi_{AE2} = -\hat{E2}(1)$$

$$\psi_{AE1} = \hat{i}_{\psi1} \cdot \hat{E1}$$

$$\psi_{AE2} = \hat{i}_{\psi2} \cdot \hat{E2}$$

where

$$\hat{i}_{\psi 1} = \begin{bmatrix} 0 \\ -S\phi_{A1} \\ C\phi_{A1} \end{bmatrix}$$

$$\hat{i}_{\psi 2} = \begin{bmatrix} 0 \\ -S\phi_{A2} \\ C\phi_{A2} \end{bmatrix}$$

ϕ_{AEi} and ψ_{AEi} are the solar array error components along the axes of allowable rotation for the i^{TH} driver.

4.1.5.3 SPACE STATION CONTROL

The space station attitude controls are affected by one of two methods:

- Control Moment Gyro (CMG)
- Reaction Control System

The program permits the selection of one or the other by setting a logical flag.

4.1.5.3.1 Control Moment Gyro (CMG) Dynamics

The CMG modelled in the simulation is the Three Parallel Mount (3 PM) configuration shown in Figure 4-8. This CMG and the mathematical description utilized were developed by the General Electric Company Defense Electronics Division (References 4.3 through 4.5) and utilizes three individual two degree of freedom CMG's mounted with their outer gimbal axes parallel. The CMG is mounted in the spacecraft with the parallel outer gimbal axes aligned with the space station axis of minimum moment of inertia which is, in the present case, the roll axis.

CMG COORDINATE FRAMES

The CMG will be mounted in the space station with the following orientation of the Outer Gimbal basis relative to the space station axes.

$$\begin{bmatrix} X_G \\ Y_G \\ Z_G \end{bmatrix}_{\text{Outer Gimbal}} = \begin{bmatrix} 0 & 1 & 0 \\ 0 & 0 & 1 \\ 1 & 0 & 0 \end{bmatrix} \begin{bmatrix} X_S \\ Y_S \\ Z_S \end{bmatrix}$$

This orientation assumes that minimum momentum requirement is along the X_S (roll) spacecraft axis where

$$\begin{bmatrix} X_S \\ Y_S \\ Z_S \end{bmatrix} \quad \left\{ \begin{array}{l} \text{roll} \\ \text{pitch} \\ \text{yaw} \end{array} \right\} \quad \left\{ \begin{array}{l} w_{ro} \\ w_{pi} \\ w_{ya} \end{array} \right\} \quad \left\{ \begin{array}{l} \phi \\ \theta \\ \psi \end{array} \right\}$$

The i^{TH} CMG Inner Gimbal axis is defined by the following transformation

$$\begin{bmatrix} X \\ Y \\ Z \end{bmatrix} \text{ Inner Gimbal} = \begin{bmatrix} \cos \theta_i & \sin \theta_i & 0 \\ -\sin \theta_i & \cos \theta_i & 0 \\ 0 & 0 & 1 \end{bmatrix} \begin{bmatrix} X \\ Y \\ Z \end{bmatrix} \text{ Outer Gimbal}$$

$$\theta_i = \alpha_i + \delta_i$$

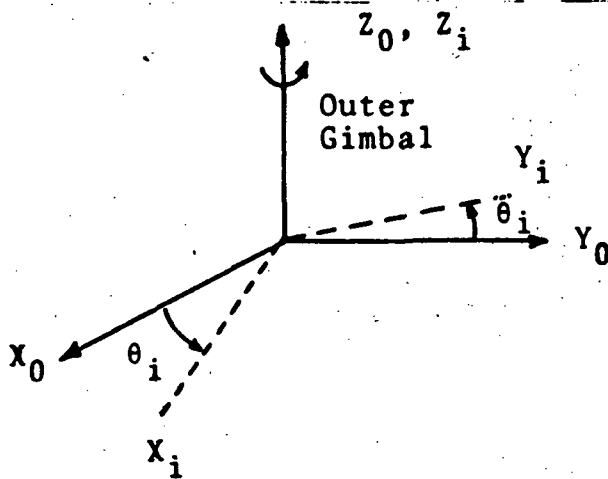
where $\delta_1 = 0$

$$\delta_2 = 120^\circ$$

$$\delta_3 = 240^\circ$$

and the δ 's are fixed

α_i is the outer gimbal angle



In the parallel mount configuration employed there are three individual CMG gyros.

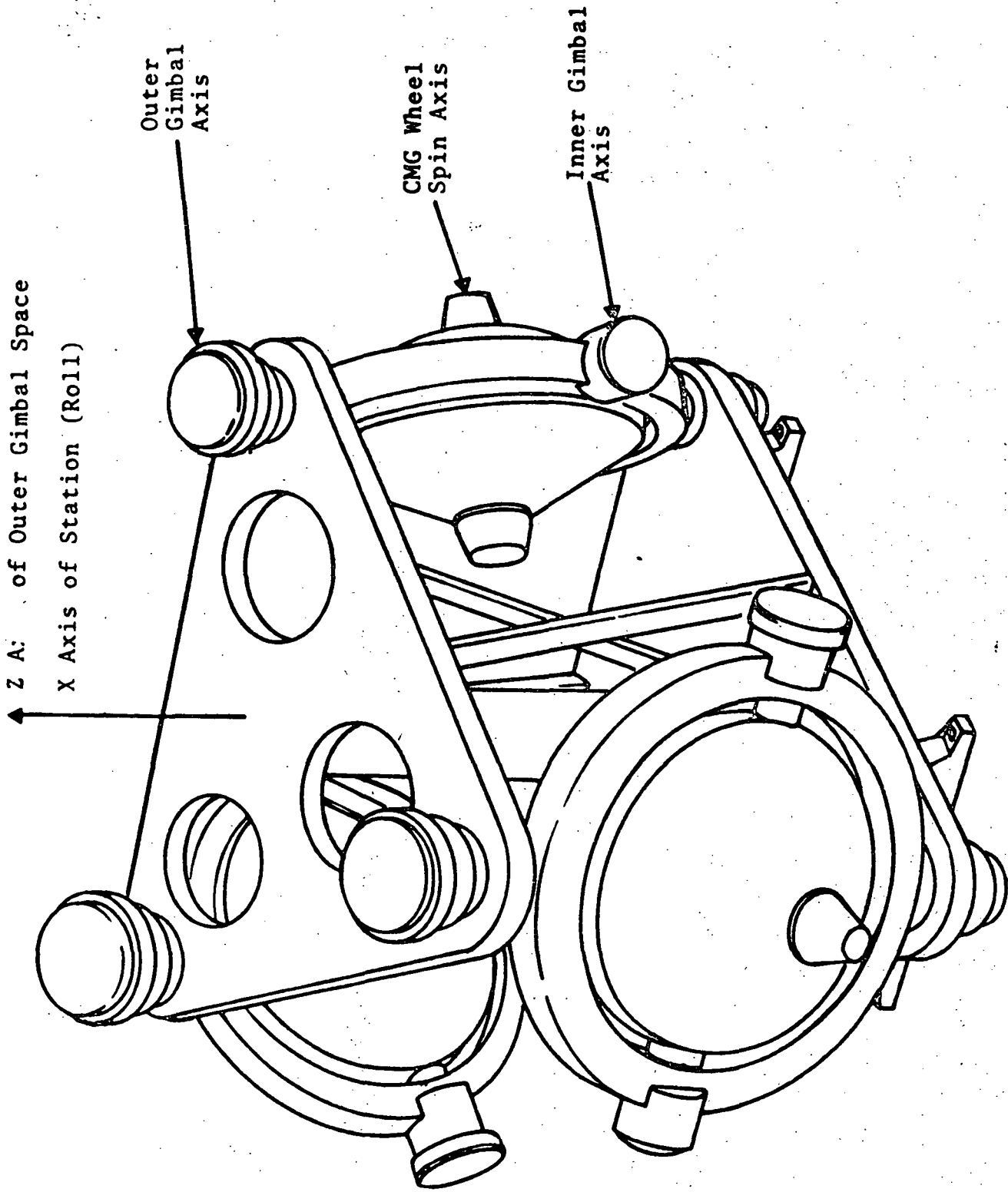
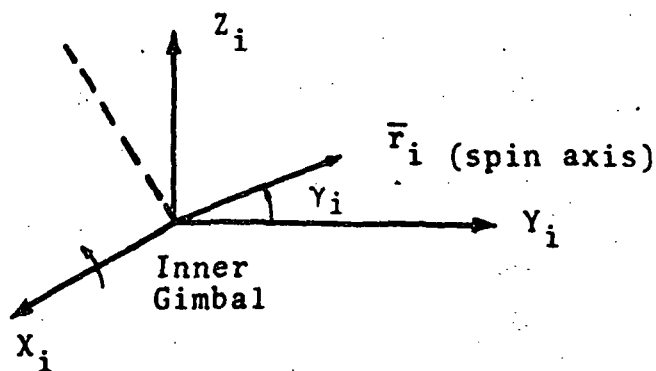


Figure 4-8 3 PM Control Moment Gyro Array

~~4.60a~~
4.60a

The I^{TH} CMG wheel momentum vector, \bar{h} , in the inner gimbal space is

$$\begin{aligned} h_{x_i} &= 0 & h & \text{- magnitude of each CMG momentum} \\ h_{y_i} &= h \cos \gamma_i & \gamma_i & \text{- inner gimbal angle of } I^{TH} \text{ CMG} \\ h_{z_i} &= h \sin \gamma_i \end{aligned}$$



The CMG momentum wheel vector is, in Outer Gimbal space:

$$\begin{aligned} h_{x_o} &= - h \cos \gamma_i \sin \theta_i \\ h_{y_o} &= h \cos \gamma_i \cos \theta_i \\ h_{z_o} &= h \sin \gamma_i \end{aligned}$$

The I^{TH} CMG Inner Gimbal axis is defined by the following transformation

$$\begin{bmatrix} X \\ Y \\ Z \end{bmatrix}_{\text{Inner Gimbal}} = \begin{bmatrix} \cos \theta_i & \sin \theta_i & 0 \\ -\sin \theta_i & \cos \theta_i & 0 \\ 0 & 0 & 1 \end{bmatrix} \begin{bmatrix} X \\ Y \\ Z \end{bmatrix}_{\text{Outer Gimbal}}$$

$$\theta_i = \alpha_i + \delta_i$$

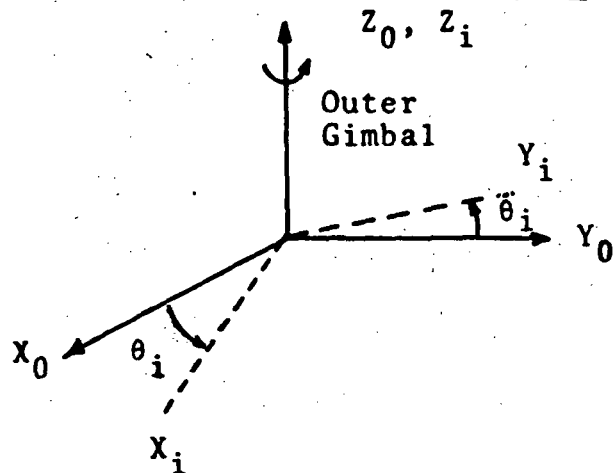
where $\delta_1 = 0$

$$\delta_2 = 120^\circ$$

$$\delta_3 = 240^\circ$$

and the δ 's are fixed

α_i is the outer gimbal angle



In the parallel mount configuration employed there are three individual CMG gyros.

CMG TORQUE EQUATIONS

$$\bar{T}_g = \dot{\bar{H}}_g = \overset{o}{\dot{H}} + \bar{w}_g \times H \quad (\text{Torque Equation})$$

where

T_g - external torque exerted on CMG

$\overset{o}{\dot{H}}_g$ - change in magnitude of momentum vector in CMG coordinates

\bar{w}_g - rotation rate of CMG in inertial space

H - CMG momentum vector

$$H = \bar{H}_{\text{wheel}} + \overset{=}{I}_{\text{Gimbal}} \bar{w}_g$$

$$\overset{o}{\dot{H}} = \overset{o}{\dot{H}} + \overset{=}{I}_{\text{Gimbal}} \overset{o}{\dot{w}}_g$$

$$\bar{w}_g \times H \approx \bar{w}_g \times \bar{H}$$

where

$\overset{=}{I}_{\text{Gimbal}}$ is the CMG moment of inertia matrix (inertia tensor)

- implies the derivative with respect to inertial coordinates

- o implies the derivative with respect to CMG coordinates

Initial Conditions

Initially the CMG's have, for the nominal case, zero inner and outer gimbal angles. Thus we have

$$\theta_1 = 0^\circ$$

$$\theta_2 = 120^\circ$$

$$\theta_3 = 240^\circ$$

and the net momentum of the system is identically zero.

The torque on the space station is equal to $-T_G$

$$T_{out} = -\left(\bar{I}_{Gimbal} \cdot \frac{0}{\bar{w}_g} + \bar{w}_g \times \bar{h} \right)$$

Performing all computations in the Inner Gimbal space we have

$$T_{out_{xi}} = -I_{Gi} \ddot{\gamma}_i + w_{zi} h \cos \gamma - w_{yi} h \sin \gamma$$

$$T_{out_{yi}} = w_{xi} h \sin \gamma$$

$$T_{out_{zi}} = -I_{Go} \ddot{\alpha} - w_{xi} h \cos \gamma$$

where

w_i is the total inertial rate of the i^{TH} CMG gyro with respect to inertial space

$$w_{xi} = \dot{\gamma} + \Omega_{xi}$$

$$w_{yi} = \Omega_{yi}$$

$$w_{zi} = \dot{\alpha} + \Omega_{zi}$$

where Ω is defined as:

$$\begin{bmatrix} \Omega_{xi} \\ \Omega_{yi} \\ \Omega_{zi} \end{bmatrix} = \begin{bmatrix} \cos \theta_i & \sin \theta_i & 0 \\ -\sin \theta_i & \cos \theta_i & 0 \\ 0 & 0 & 1 \end{bmatrix} \begin{bmatrix} 0 & 1 & 0 \\ 0 & 0 & 1 \\ 1 & 0 & 0 \end{bmatrix} \begin{bmatrix} w_{ro} \\ w_{pi} \\ w_{ya} \end{bmatrix}$$

$\begin{bmatrix} \Omega_{xi} \\ \Omega_{yi} \\ \Omega_{zi} \end{bmatrix}$ is the rotation rate of vehicle transformed to inner gimbal space

and

$\dot{\alpha}, \dot{\gamma}; \ddot{\alpha}, \ddot{\gamma}$ are the scalar derivatives of outer and inner gimbal angles and gimbal rates, respectively.

Therefore,

$$\begin{bmatrix} \ddot{x}_i \\ \ddot{y}_i \\ \ddot{z}_i \end{bmatrix} \begin{matrix} \text{out} \\ \text{TH} \\ \text{CMG} \end{matrix} \left. \begin{array}{l} x_i = I_{Gi} \ddot{\gamma} + (\dot{\alpha} + w_{ro}) h \cos \gamma - \Omega_{yi} h \sin \gamma \\ y_i = (\dot{\gamma} + \Omega_{xi}) h \sin \gamma \\ z_i = I_{Go} \ddot{\alpha} - (\dot{\gamma} + \Omega_{xi}) h \cos \gamma \end{array} \right\}$$

$$I_{Gi} = J_{Gi}$$

$$I_{Go} = J_{Go} + J_{Gi(Z)} \cos^2 \gamma + J_{Gi(Y)} \sin^2 \gamma$$

let

$$\dot{\alpha}_I = \dot{\alpha} + \omega_{ro}$$

$$\dot{\gamma}_I = \dot{\gamma} + \Omega_{xi}$$

$$T_{out} \begin{matrix} x_i \\ y_i \\ z_i \end{matrix} \begin{matrix} I_{Gi} \ddot{\gamma} + \dot{\alpha}_I h \cos \gamma - \Omega_{yi} h \sin \gamma \\ \dot{\gamma}_I h \sin \gamma \\ I_{Go} \ddot{\alpha} - \dot{\gamma}_I h \cos \gamma \end{matrix}$$

where

I_{Gi} - inertia tensor of inner gimbal expressed in the inner gimbal coordinate frame

J_{Gi} - inertia matrix of inner gimbal in inner gimbal coordinate

I_{Go} - inertia tensor of outer gimbal plus inner gimbal (suitably transformed) expressed in inner gimbal coordinates

J_{Go} - inertia matrix of outer gimbal in inner gimbal coordinates

CMG MOTOR TORQUE CONTROL LAW

$$T_{M1} = \left(\dot{\gamma}_{pi} - \dot{\gamma}_i - \frac{\dot{\alpha}_i H \cos \gamma}{K_{M1}} + \gamma_{Ai} \right) K_{M1}$$

$$T_{M2} = \left(\dot{\alpha}_{pi} - \dot{\alpha}_i + \frac{\dot{\gamma} H \cos \gamma}{K_{M2}} \right) K_{M2}$$

are the equations for the motor torque for inner and outer gimbals respectively, where the terms divided by KM1 and KM2 are used to decouple the torque motor dynamics between gimbals in a given CMG. KM1 and KM2 are, respectively, the inner and outer torque motor gains. If the motor torque exceeds the stiction torque plus the reaction torque produced by the CMG motion, the gimbal accelerates

$$\bar{T}_{GIMBAL} = \bar{T}_{M1_i} - \bar{T}_{REACT1} - \bar{T}_{RUN1}$$

if

$$(\bar{T}_{M1_i} - \bar{T}_{REACT1} - \bar{T}_{STICK1}) > 0$$

otherwise

$$T_{GIMBAL} = 0$$

(INNER)

Similarly for

$T_{\text{GIMBAL (OUTER)}}$

where

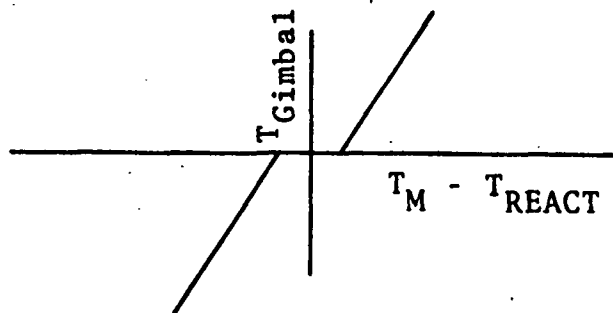
$$\bar{T}_{\text{REACT1}} = T_{\text{OUT}_{xi}} - I_{Gi} \ddot{\gamma}$$

in other words, T_{REACT} is the torque exerted by the gyro about the inner gimbal axis when the gimbal is not accelerated.

$$T_{\text{REACT2}} = T_{\text{OUT}_{3i}} - I_{Go} \ddot{\alpha}$$

T_{STICK} is the stiction torque

T_{RUN} is the running torque



$$\gamma = T_{\text{Gimbal}_i} / J_{Gi}$$

$$\ddot{\alpha} = T_{\text{Gimbal}_0} / J_{Go}$$

If $T_{\text{GIMBAL}} = 0$, it is necessary to set the gimbal rates about the affected axes to the component of body rate on the axis, e.g.

$$T_{\text{GIMBAL}} = 0 \quad \dot{\gamma}_I = \Omega_{xi} \quad , \quad \ddot{\gamma} = 0$$

(INNER)

$$T_{\text{GIMBAL}} = 0 \quad \dot{\alpha}_1 = \Omega_{zi} \quad , \quad \ddot{\alpha} = 0$$

(OUTER)

COMPUTATION OF CMG GIMBAL COMMAND RATES

The terms $\dot{\gamma}_{pi}$ and $\dot{\alpha}_{pi}$ represent the commanded gimbal rates and are obtained from the following computation:

$$T_{xc} = \int (T_{xe} - T_{xv}) dt$$

$$T_{yc} = \int (T_{ye} - T_{yv}) dt$$

$$T_{zc} = \int (T_{ze} - T_{zv}) dt$$

where

$T_{()e}$ is the disturbance torque applied to the CMG by the control law.

$T_{()v}$ is the torque presently applied by the gyro to the vehicle

$$\dot{\gamma}_{pi} = -T_{zc} / 3h \cos \gamma$$

$$\dot{\alpha}_{pi} = T_{xc} \cos \theta_i + T_{yc} \sin \theta_i + T_{AH_i}$$

The last term in the second equation represents the torque term to eliminate "hang-up" or antiparallelism.

Another term

$$\gamma_{A1} = [(\gamma_1 + \gamma_2 + \gamma_3)/3 - \gamma_i] \cdot K_p$$

is added to the inner gimbal commanded angle to assure an equal distribution of orientation and reduce the possibility of gimbal limits being encountered

$$\begin{array}{l} T_{xe} \\ T_{ye} \\ T_{ze} \end{array} = \begin{bmatrix} 0 & 1 & 0 \\ 0 & 0 & 1 \\ 1 & 0 & 0 \end{bmatrix} \begin{array}{l} (K_D \phi_\epsilon - K_R w_{ro}) \\ (K_D \theta_\epsilon - K_R w_{pi}) \\ (K_D \psi_\epsilon - K_R w_{ya}) \end{array}$$

where ϕ_ϵ , θ_ϵ , and ψ_ϵ are the space station attitude errors.

ATTITUDE ERROR EQUATIONS

$$\bar{E}_1 = \bar{R}_0 \times \bar{R}_{0C}$$

$$\theta_\epsilon = \begin{bmatrix} 0 & 0 & 0 \\ 0 & 1 & 0 \\ 0 & 0 & 0 \end{bmatrix} [C_0]^T E_1$$

$$\bar{E}_2 = \bar{P}_i \times \bar{P}_{iC}$$

$$\begin{matrix} \phi_\epsilon \\ \psi_\epsilon \end{matrix} = \begin{bmatrix} 1 & 0 & 0 \\ 0 & 0 & 1 \end{bmatrix} [C_0]^T E_2$$

where

- \bar{R}_0, \bar{P}_i - unit vectors of roll and pitch axes in inertial coordinates
- $\bar{R}_{0C}, \bar{P}_{iC}$ - unit vectors of roll and pitch axes in in inertial coordinates
- \bar{E}_1, \bar{E}_2 - error vectors in inertial coordinates
- $E_1], E_2]$ - 3x1 matrix representation of \bar{E}_1 and \bar{E}_2

and $[C_0^T]$ is used to transform the attitude errors into the space station frame.

CMG CONTROL TORQUE

The computation of the CMG control torque involves the transformation of the output torque of each CMG to the space station basis followed by the summation of the three torque terms:

$$\begin{bmatrix} T_{o_i} \\ (i^{\text{TH}} \text{ CMG}) \end{bmatrix}_{\text{SS}} = \begin{bmatrix} \cos \theta_i & -\sin \theta_i & 0 \\ \sin \theta_i & +\cos \theta_i & 0 \\ 0 & 0 & 1 \end{bmatrix} \begin{bmatrix} T_o \\ (i^{\text{TH}} \text{ CMG}) \end{bmatrix}_{\text{Inner Gimbal}}$$

$$\begin{bmatrix} T_o \\ (\text{TOTAL}) \end{bmatrix}_{\text{SS}} = \begin{bmatrix} T_{o_1} \\ \end{bmatrix}_{\text{SS}} + \begin{bmatrix} T_{o_2} \\ \end{bmatrix}_{\text{SS}} + \begin{bmatrix} T_{o_3} \\ \end{bmatrix}_{\text{SS}}$$

4.1.5.3.2 Reaction Control System

A perfect proportional control system is modelled as an alternative to the Control Moment Gyro. The utilization of this alternative control system will permit more economical computation of the interaction dynamics.

$$T_o = \begin{bmatrix} I_o(11) & & \\ & I_o(22) & \\ & & I_o(33) \end{bmatrix} \begin{bmatrix} (K\theta \phi_\epsilon + K\dot{\theta} w_{ro}) \\ (K\theta \theta_\epsilon + K\dot{\theta} w_{pi}) \\ (K\theta \psi_\epsilon + K\dot{\theta} w_{ya}) \end{bmatrix}$$

$K\theta$, $K\dot{\theta}$ are control gains chosen to satisfy frequency and damping characteristics.

ϕ_ϵ , θ_ϵ , and ψ_ϵ are computed in identical fashion to that presented in the previous section.

4.1.5.4 SOLAR ARRAY CONTROL EQUATIONS

The solar array drive controller mechanism consists of two first order filters which smooth the attitude error and driver rate signals. The two signals are weighted by appropriate gains, added together and then the sum is filtered by a third first order lag filter. The control system equations are adaptive with respect to driver inertia and roll axis gear ratio.

Filter Input Signals

$$\begin{aligned}\hat{w}_{11} &= b_{11} w_{11} + a_{11} \hat{w}_{11-1} \\ \hat{w}_{12} &= b_{12} w_{12} + a_{12} \hat{w}_{12-1} \\ \hat{w}_{21} &= b_{21} \hat{w}_{21} + a_{21} \hat{w}_{21-1} \\ \hat{w}_{22} &= b_{22} w_{22} + a_{22} \hat{w}_{22-1} \\ \hat{\phi}_{AE1} &= b_{11} \phi_{AE1} + a_{11} \hat{\phi}_{AE1-1} \\ \hat{\psi}_{AE1} &= b_{12} \psi_{AE1} + a_{12} \hat{\psi}_{AE1-1} \\ \hat{\phi}_{AE2} &= b_{21} \phi_{AE2} + a_{21} \hat{\phi}_{AE2-1} \\ \hat{\psi}_{AE2} &= b_{22} \psi_{AE2} + a_{22} \hat{\psi}_{AE2-1}\end{aligned}$$

where

- w_{iJ} - J^{TH} component of i^{TH} driver rotation rate
- ϕ_{AEi} - roll axis error of i^{TH} driver
- ψ_{AEi} - vane axis error of i^{TH} driver
- \hat{X} - implies "smoothed" or filtered value of X
- X_{-1} - implies immediately previous value of X
- a_{iJ} - difference equation coefficient $a_{iJ} = \exp\left(\frac{\text{INT.STEP}}{\tau_{iJ}}\right)$
- b_{iJ} - $1 - a_{iJ}$
- τ_{iJ} - filter time constant

Computation of Hinge Torque

$$T_{C11} = K_{\theta A} \cdot I_{1(R0)} \cdot \hat{\phi}_{AE1} + K_{\dot{\theta} A} \cdot I_{1(R0)} \cdot \hat{w}_{11}$$

$$T_{C12} = K_{\theta A} \cdot I_{1(33)} \cdot \hat{\psi}_{AE1} + K_{\dot{\theta} A} \cdot I_{1(33)} \cdot \hat{w}_{12}$$

$$T_{C21} = K_{\theta A} \cdot I_{2(R0)} \cdot \hat{\phi}_{AE2} + K_{\dot{\theta} A} \cdot I_{2(R0)} \cdot \hat{w}_{21}$$

$$T_{C22} = K_{\theta A} \cdot I_{2(33)} \cdot \hat{\psi}_{AE2} + K_{\dot{\theta} A} \cdot I_{2(33)} \cdot \hat{w}_{22}$$

Filtered Hinge Torque

$$\hat{T}_{C11} = b_{13} T_{C11} + a_{13} \hat{T}_{C11-1}$$

$$\hat{T}_{C12} = b_{13} T_{C12} + a_{13} \hat{T}_{C12-1}$$

$$\hat{T}_{C21} = b_{13} T_{C21} + a_{13} \hat{T}_{C21-1}$$

$$\hat{T}_{C22} = b_{13} T_{C22} + a_{13} \hat{T}_{C22-1}$$

where

$K_{\theta A}, K_{\dot{\theta} A}$ - displacement and rate gains

$I_{J(R0)}$ - root sum square (RSS) of 11 and 22 elements of the J^{TH} inertia matrix divided by KG

$I_{J(33)}$ - vane axis moment of inertia for J^{TH} rigid driver

a_{13} - $\exp\left(\frac{\text{Integration Step}}{\tau_{13}}\right)$

b_{13} - $1 - a_{13}$

4.1.6 ORBIT GENERATOR

The calculation of the space station orbit is required to perform the previously specified guidance functions. Lyddane's method is employed in this simulation to obtain the desired orbital state vector. This method provides a closed form of solution and is much more efficient and economical than numerical integration techniques. WOLF R & D has developed a standardized Lyddane's method subroutine which will be utilized in the simulation. A complete analytic treatment is presented in Reference 4.2 and will not be repeated here. Lyddane's method is an extension of Brouwer's theory which provides closed form solution of orbits from mean orbital elements. A brief exposition of the method is given below.

- Brouwer/Lyddane Theory

Brouwer's theory utilizes the standard elliptic elements a, e, I, w, M . The end product is typified by

$$w_{osc_{t-t_0}} = w'' + (t-t_0) f_1(a'', e'', I'') + f_2(a'', e'', I'', w'', M'')$$

where

$w_{osc_{t-t_0}}$ = "real world" or "osculating" value of the argument of perigee at time $t-t_0$.

w'' = "mean" value of the argument of perigee at time t_0 .
 These "mean" values are related to the constants of integration of the differential equations of motion. They do not represent real world values, but are required for the prediction of osculating elements.

The difficulty with Brouwer's theory is that the function f_2 involves terms with e'' and $\sin I''$ in the denominator, and for very small values of e'' and/or I'' , these terms present a situation which violates the basic foundations of "small perturbation" theory.

3

In order to overcome these difficulties, Lyddane used a different set of parameters, which were first suggested in the 1800's by Poincare'. These variables, which do not produce divisions by e or $\sin I$, are:

$$\begin{aligned}
 & a \\
 & e \sin M \\
 & e \cos M \\
 & (\sin I) (\sin \Omega) \\
 & (\sin I) (\cos \Omega) \\
 & w + \Omega + M
 \end{aligned}$$

With these parameters, numerical values are computed for each of the above six quantities from equations similar to those given by Brouwer. Then the individual values for e and M are obtained from

$$e^2 = (e \sin M)^2 + (e \cos M)^2$$

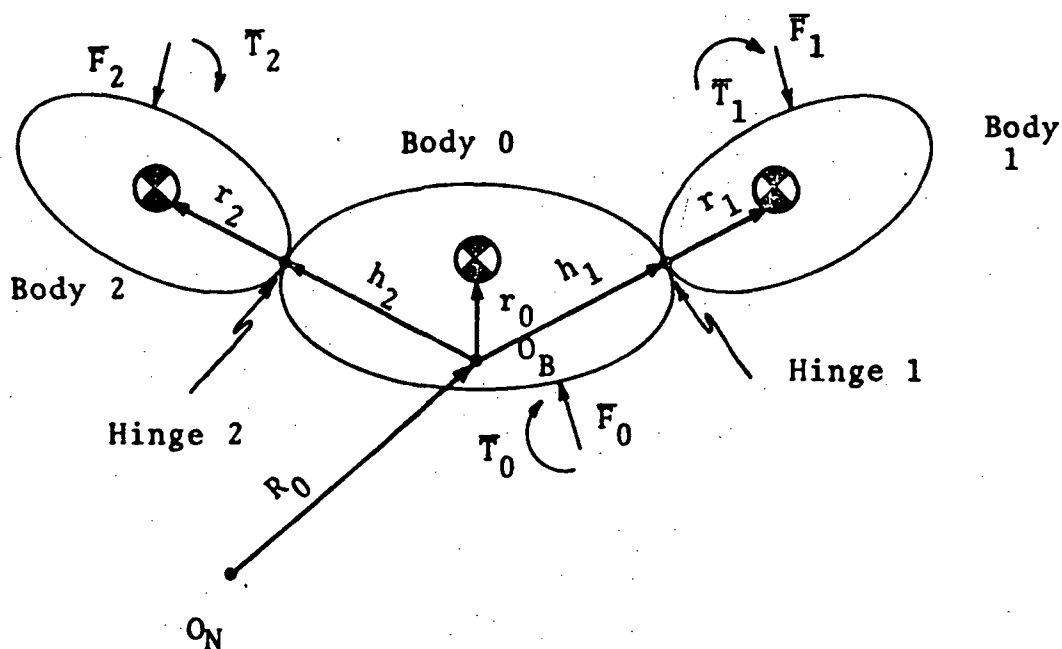
$$\tan M = \frac{e \sin M}{e \cos M}$$

Similar Procedures are performed for I and Ω , and finally, w is computed from

$$w = (w + \Omega + M) - \Omega - M$$

4.1.7 EQUATIONS OF CONSTRAINED MOTION FOR A
SYSTEM OF THREE RIGID BODIES

Case A - Unconstrained Rotation



Consider the three body system presented above in which bodies one and two have unconstrained rotation about the two hinge points and neither of the two bodies can have translational motion with respect to the central (zero) body.

Definitions:

- O_N - Newtonian reference point
- O_B - Zero body reference point
- R_0 - Distance of body reference point from Newtonian reference
- r_0 - Distance of zero body CG from body reference point
- h_i - Distance between body reference point and i^{TH} hinge point
 $i=1,2$
- r_i - distance between i^{TH} hinge point and i^{TH} body center of gravity
 $i=1,2$
- F_0, T_0 - Vector force and torque applied to body zero
- F_1, T_1 - Vector force and torque applied to body one
- F_2, T_2 - Vector force and torque applied to body two

Coordinate Frames and Relationships

- {I} - Inertially fixed coordinate basis
- {X} - Coordinate basis fixed to body zero
- {x₁} - Coordinate basis fixed to body one
- {x₂} - Coordinate basis fixed to body two

where {I} can be represented as the unity matrix and each of the others as a triad of orthogonal unit vectors in the form of a 3x3 matrix.

$$\{I\} = C_0 \{X\}; \{I\}^T = \{X\}^T C_0^T$$

$$\{X\} = C_1 \{x_1\}; \{X\}^T = \{x_1\}^T C_1^T$$

$$\{X\} = C_2 \{x_2\}; \{X\}^T = \{x_2\}^T C_2^T$$

where

C_i are the direction cosine matrices
 $i=0,1,2$

Vector Representation of Variables

Each of the variables defined as distances represent the scalar magnitude of the related vector quantity. Each of the vectors defined below is given in a "convenient" frame and choice of basis is, of course, arbitrary.

$$\bar{R}_0 = \{X\}^T R_0$$

$$\bar{r}_0 = \{X\}^T r_0$$

$$\bar{h}_i = \{X\}^T h_i$$

$$\bar{r}_i = \{x_i\} r_i$$

where the bars designate a vector quantity.

The following identity is offered

$$\dot{C}_i = C_i \tilde{w}_i \quad i = 0, 1, 2$$

where

$$\tilde{w}_i = \begin{bmatrix} 0 & -w_{i3} & w_{i2} \\ w_{i3} & 0 & -w_{i1} \\ -w_{i2} & w_{i1} & 0 \end{bmatrix}$$

EQUATIONS OF MOTION

1. Acceleration of the System Mass Center

$$m_T \frac{d^2}{dt^2} (\bar{R}_0 + \bar{C}) \Big|_I = \bar{F}_1 + \bar{F}_2 \quad \left(\begin{array}{l} \text{Forces external to the} \\ \text{System} \end{array} \right)$$

m_T = total system mass

m_0 = mass of body zero

m_1 = mass of body one

m_2 = mass of body two

$$\bar{C} = \frac{m_0 \bar{r}_0 + m_1 (\bar{h}_1 + \bar{r}_1) + m_2 (\bar{h}_2 + \bar{r}_2)}{m_T}$$

C is the system mass center relative to O_B

$$\begin{aligned} m_T \frac{d^2 \bar{R}_0}{dt^2} \Big|_I + m_0 \frac{d^2 \bar{r}_0}{dt^2} \Big|_I \\ + m_1 \frac{d^2 (\bar{h}_1 + \bar{r}_1)}{dt^2} \Big|_I + m_2 \frac{d^2 (\bar{h}_2 + \bar{r}_2)}{dt^2} \Big|_I = \bar{F}_1 + \bar{F}_2 \end{aligned}$$

Noting that \bar{F}_1 is in body one coordinates and \bar{F}_2 in those of body two, we have in the inertial basis ($\frac{d}{dt}\{\bar{I}\} \equiv 0$):

$$\begin{aligned} & \bar{m}_T \frac{d^2}{dt^2} (\{\bar{I}\}^T \bar{c}_0 \bar{R}_0) \\ & + \bar{m}_0 \frac{d^2}{dt^2} (\{\bar{I}\}^T \bar{c}_0 \bar{r}_0) \\ & + \bar{m}_1 \frac{d^2}{dt^2} (\{\bar{I}\}^T (\bar{c}_0 \bar{h}_1 + \bar{c}_0 \bar{c}_1 \bar{r}_1)) \\ & + \bar{m}_2 \frac{d^2}{dt^2} (\{\bar{I}\}^T (\bar{c}_0 \bar{h}_2 + \bar{c}_0 \bar{c}_2 \bar{r}_1)) \end{aligned} = \{\bar{I}\}^T \begin{pmatrix} \bar{c}_0 \bar{c}_1 \bar{F}_1 \\ + \bar{c}_0 \bar{c}_2 \bar{F}_2 \end{pmatrix}$$

where

$$\begin{aligned} \frac{d}{dt} (\{\bar{I}\}^T \bar{c}_0 \bar{R}_0) &= \{\bar{I}\}^T \bar{c}_0 (\dot{\bar{R}}_0 + \tilde{\omega}_0 \bar{R}_0) \\ \frac{d^2}{dt^2} (\{\bar{I}\} \bar{c}_0 \bar{R}_0) &= \{\bar{I}\}^T \bar{c}_0 (\ddot{\bar{R}}_0 + 2\tilde{\omega}_0 \dot{\bar{R}}_0 + \dot{\tilde{\omega}}_0 \bar{R}_0 + \tilde{\omega}_0 \tilde{\omega}_0 \bar{R}_0 + \tilde{\omega}_0 \dot{\bar{R}}_0) \\ &= \{\bar{X}\}^T (\ddot{\bar{R}}_0 + 2\tilde{\omega}_0 \dot{\bar{R}}_0 + \dot{\tilde{\omega}}_0 \bar{R}_0 + \tilde{\omega}_0 \tilde{\omega}_0 \bar{R}_0) \end{aligned}$$

and

$$\frac{d}{dt} (\{\bar{I}\} \bar{c}_0 \bar{c}_1 \bar{r}_1) = \{\bar{I}\}^T (\cancel{\bar{c}_0} \dot{\bar{c}}_1 \bar{r}_1 + \bar{c}_0 \tilde{\omega}_0 \bar{c}_1 \bar{r}_1 + \bar{c}_0 \bar{c}_1 \dot{\tilde{\omega}}_1 \bar{r}_1)$$

$$\frac{d^2}{dt^2} (\{I\} C_0 C_1 r_1) = \{I\}^T \left[\begin{array}{l} C_0 \ddot{w}_0 \ddot{w}_0 C_1 r_1 + C_0 \ddot{w}_0 C_1 \ddot{w}_1 r_1 \\ + C_0 \ddot{w}_0 C_1 \ddot{w}_1 r_1 + C_0 C_1 \ddot{w}_1 \ddot{w}_1 r_1 \\ + C_0 \dot{\ddot{w}}_0 C_1 r_1 + C_0 C_1 \dot{\ddot{w}}_1 r_1 \end{array} \right]$$

$$= \{X\}^T \left(\begin{array}{l} \ddot{w}_0 \ddot{w}_0 C_1 r_1 + 2\ddot{w}_0 C_1 \ddot{w}_1 r_1 \\ + C_1 \ddot{w}_1 \ddot{w}_1 r_1 \\ + \dot{\ddot{w}}_0 C_1 r_1 + C_1 \dot{\ddot{w}}_1 r_1 \end{array} \right)$$

This gives us, in the body zero basis

$$m_T \{X\}^T \left[\begin{array}{l} \ddot{R}_0 + 2\tilde{w}_0 \dot{R}_0 + \tilde{w}_0 \tilde{w}_0 R_0 + \ddot{\tilde{w}}_0 R_0 \\ + \mu_0 (\tilde{w}_0 \tilde{w}_0 + \ddot{\tilde{w}}_0) r_0 \\ + \mu_1 \left[\begin{array}{l} (\tilde{w}_0 \tilde{w}_0 + \ddot{\tilde{w}}_0) (h_1 + C_1 r_1) \\ + 2\tilde{w}_0 C_1 \tilde{w}_1 r_1 + C_1 \ddot{\tilde{w}}_1 r_1 \\ + C_1 \tilde{w}_1 \tilde{w}_1 r_1 \end{array} \right] \\ + \mu_2 \left[\begin{array}{l} (\tilde{w}_0 \tilde{w}_0 + \ddot{\tilde{w}}_0) (h_2 + C_2 r_2) \\ + 2\tilde{w}_0 C_2 \tilde{w}_2 r_2 \\ + C_2 \tilde{w}_2 \tilde{w}_2 r_2 \\ + C_2 \ddot{\tilde{w}}_2 r_2 \end{array} \right] \end{array} \right] = \{X\}^T \left[\begin{array}{l} C_1 F_1 \\ + \\ C_2 F_2 \\ + F_0 \end{array} \right]$$

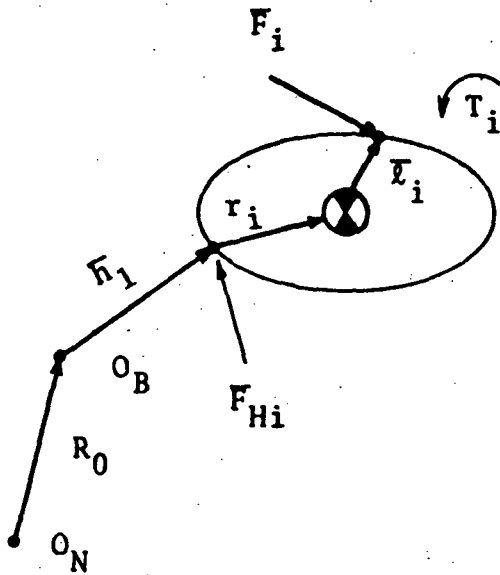
$$\mu_0 = \frac{m_0}{m_T}$$

$$\mu_1 = \frac{m_1}{m_T}$$

$$\mu_2 = \frac{m_2}{m_T}$$

2. Hinge Force Applied To The i^{TH} Body

($i = 1, 2$)



F_{Hi} , the hinge force, is given in the body zero, $\{X\}$, basis

$$m_i \{I\}^T \frac{d^2}{dt^2} \left(C_0 (R_0 + h_i) + C_0 C_i r_i \right) = \{I\}^T C_0 (F_{Hi} + C_i F_i)$$

$$\{X\}^T F_{Hi} = \{X\}^T m_i \begin{bmatrix} \ddot{R}_0 + 2\dot{\omega}_0 \dot{R}_0 \\ + (\tilde{\omega}_0 \tilde{\omega}_0 + \dot{\tilde{\omega}}_0) (R_0 + h_i + C_i r_i) \\ + 2\tilde{\omega}_0 C_i \tilde{\omega}_i r_i \\ + C_i (\tilde{\omega}_i \tilde{\omega}_i + \dot{\tilde{\omega}}_i) r_i \end{bmatrix} - C_i F_i$$

3. Torque Equation For The i^{TH} Body

$$\frac{d}{dt} \bar{L}_i \Big|_I = \bar{T}_i + \tilde{L}_i F_i - \tilde{r}_i \bar{F}_{Hi} + \bar{T}_{Hi}$$

\bar{L}_i - Angular momentum about CG of i^{TH} Body

$$\bar{L}_i = \{x_i\}^T \begin{matrix} [I_i] \\ 3 \times 3 \end{matrix} \{x_i\} \cdot \left[\{x_i\}^T w_i + \{X\}^T w_0 \right]$$

T_{Hi} - hinge torque

$$\begin{aligned} \frac{d}{dt} \bar{L}_i \Big|_I &= \frac{d}{dt} \{I\}^T C_0 C_i [I_i] C_i^T C_0^T \{I\} \left(\{I\}^T (C_0 C_i w_i + C_0 w_0) \right) \\ &= \{I\}^T (C_0 \dot{w}_0 C_i + C_0 C_i \dot{w}_i) [I_i] \{x_i\} \cdot \{x_i\}^T (w_i + C_i^T w_0) \\ &+ \{x_i\}^T [I_i] \left(\tilde{w}_i^T C_i^T C_0^T + C_i^T \tilde{w}_0^T C_0^T \right) \{I\} \cdot \{I\}^T \left(C_0 C_i w_i + C_0 w_0 \right) \\ &+ \{x_i\}^T [I_i] \{x_i\} \cdot \{I\}^T \left(C_0 \tilde{w}_0 C_i w_i + C_0 C_i \tilde{w}_i w_i \right. \\ &\quad \left. + C_0 \tilde{w}_0 w_0 \right. \\ &\quad \left. + C_0 C_i \dot{w}_i + C_0 \dot{w}_0 \right) \end{aligned}$$

noting that $\{x\} \cdot \{x\}^T$ equals the identity matrix

$$\begin{aligned}
 \frac{d}{dt} L_i \Big|_I &= \{x_i\}^T \left(C_i^T \tilde{w}_0 C_i + \tilde{w}_i \right) [I_i] \left(w_i + C_i^T w_0 \right) \\
 &+ \{x_i\}^T [I_i] \left(\tilde{w}_i^T - C_i^T \tilde{w}_0 C_i \right) \left(w_i + C_i^T w_0 \right) \\
 &+ \{x_i\}^T [I_i] \left(C_i^T \tilde{w}_0 C_i w_i + \dot{w}_i + C_i^T \dot{w}_0 \right) \\
 &= \{x_i\}^T \left(C_i^T \tilde{w}_0 C_i + \tilde{w}_i \right) [I_i] \left(w_i + C_i^T w_0 \right) \\
 &+ \{x_i\}^T [I_i] \left(\dot{w}_i + C_i^T \dot{w}_0 \right) \\
 &+ \{x_i\}^T [I_i] \left(\begin{array}{l} \tilde{w}_i^T C_i^T w_0 - C_i^T \tilde{w}_0 C_i w_i \\ + C_i^T \tilde{w}_0 C_i w_i \end{array} \right)
 \end{aligned}$$

We note that

$$(C_i w_0)^{\sim} = C_i \tilde{w}_0 C_i^T$$

$$\tilde{A} B = -\tilde{B} A$$

$$\tilde{A}^T = -\tilde{A}$$

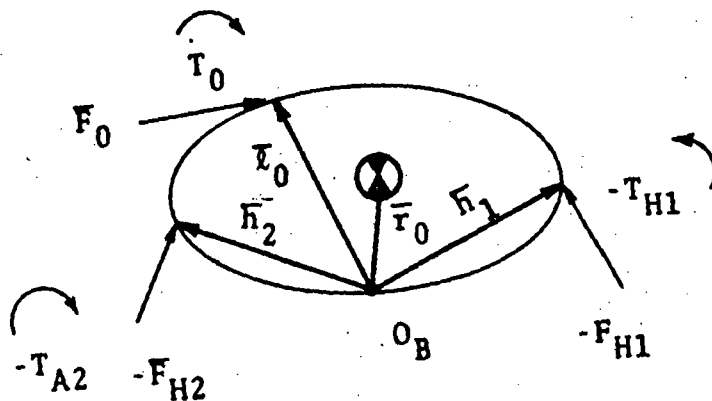
$$\tilde{w}_i^T C_i^T w_0 = -\tilde{w}_i C_i^T w_0 = C_i^T \tilde{w}_0 C_i w_i$$

∴ Two of the terms cancel giving

$$(x_i)^T \begin{bmatrix} ((C_i^T w_0)^{\sim} + \tilde{w}_i) [I_i] (w_i^T C_i^T w_0) \\ + [I_i] \dot{w}_i + C_i^T \dot{w}_0 \\ + [I_i] C_i^T \tilde{w}_0 C_i w_i \end{bmatrix} = (x_i)^T \begin{bmatrix} C_i^T T_{Hi} \\ -\tilde{F}_i C_i^T F_{Hi} \\ \tilde{A}_i F_i + T_i \end{bmatrix}$$

where T_{Hi} and F_{Hi} are given in the zero body basis and T_i , F_i are in the i^{TH} body basis.

4. Torque Equation for Body Zero



External Moments on Body Zero

$$(-r_0 + h_1) \times -F_{H1} \quad -T_{H1}$$

$$(-r_0 + h_2) \times -F_{H2} \quad -T_{H2}$$

$$(-r_0 + l_0) \times F_0 \quad +T_0$$

Reaction Torque

$$\left. \frac{d \bar{L}_0}{dt} \right|_I = \{X\}^T \begin{bmatrix} \tilde{w}_0 [I_0] w_0 \\ [I_0] \dot{w}_0 \end{bmatrix}$$

$$\{X\}^T \begin{bmatrix} \tilde{w}_0 [I_0] w_0 \\ [I_0] \dot{w}_0 \end{bmatrix} = \begin{bmatrix} (r_0 + h_1) \tilde{F}_{H1} \\ (-r_0 + h_2) \tilde{F}_{H2} \\ (-r_0 + l_0) \tilde{F}_0 \end{bmatrix} \quad +T_0 \quad -T_{H1} \quad -T_{H2}$$

Matrix Equations

Since $\{x\} \cdot \{x\}^T$ is equal to the identity matrix we can obtain a set of scalar matrix equations from the preceding by formally taking this product on both sides of the equation. For purposes of computer solution we shall also require a formulation of the form

$$[A] \dot{X} = B$$

$$\dot{X}^T = \underline{\ddot{R}_0, \dot{w}_0, \dot{w}_1, \dot{w}_2}$$

and B is a function of external forces and terms in w_0, w_1, w_2, \dot{R}_0 and R_0 . Noting the identity

$$X\tilde{Y} = -\tilde{Y}X$$

System Acceleration Equation

L.H.S.

$$m_T \ddot{R}_0] - m_T \left(\ddot{R}_0] + N_0 \ddot{r}_0] + N_1 (\ddot{h}_1] + C_1 \ddot{r}_1] \right) + N_2 (\ddot{h}_2] + C_2 \ddot{r}_2] \right) \dot{w}_0$$

$$- m_1 C_1 \ddot{r}_1 \dot{w}_1 - m_2 C_2 \ddot{r}_2 \dot{w}_2$$

R.H.S.

$$- m_T (2\dot{w}_0 \dot{R}_0 + \dot{w}_0 \dot{w}_0 R_0)$$

$$- m_0 \dot{w}_0 \dot{w}_0 r_0 - m_1 \dot{w}_0 \dot{w}_0 (h_1 + C_1 r_1)$$

$$- m_1 (2\dot{w}_0 C_1 \dot{w}_1 r_1 + C_1 \dot{w}_1 \dot{w}_1 r_1)$$

$$- m_2 (\dot{w}_0 \dot{w}_0 (h_2 + C_2 r_2) - 2\dot{w}_0 C_2 \dot{w}_2 r_2)$$

$$- m_2 (C_2 \dot{w}_2 \dot{w}_2 r_2)$$

$$+ C_1 F_1 + C_2 F_2 + F_0$$

NOTE: L.H.S. - implies "lefthand side"

R.H.S. - implies "righthand side"

ITH Body Torque Equation

L.H.S

$$m_i \tilde{r}_i C_i^T \ddot{R}_0 + \left[[I_i] C_i^T - m_i \tilde{r}_i C_i^T (R_0 + h_i + C_i r_i)^{\sim} \right] \dot{w}_0$$

$$+ ([I_i] - m_i \tilde{r}_i \tilde{r}_i) \dot{w}_i$$

R.H.S.

$$-m_i \tilde{r}_i C_i^T \left(\ddot{R}_0 + 2\tilde{w}_0 \dot{R}_0 + \tilde{w}_0 \tilde{w}_0 (R_0 + h_i + C_i r_i)^{\sim} \right)$$

$$\left(+ 2\tilde{w}_0 C_i \tilde{w}_i r_i + C_i \tilde{w}_i \tilde{w}_i r_i \right)$$

$$- \left[(C_i^T w_0)^{\sim} + \tilde{w}_i \right] [I_i] (w_i + C_i^T w_0)$$

$$- [I_i] (C_i^T \tilde{w}_0 C_i w_i) + C_i^T T_{Hi}$$

$$+ \tilde{l}_i F_i + T_i$$

$$+ m_i \tilde{r}_i F_i$$

Body Zero Torque Equation

L.H.S.

Terms in \ddot{R}_0

$$\left(m_1 (-r_0 + h_1)^{\sim} + m_2 (-r_0 + h_2)^{\sim} \right)$$

Terms in \dot{w}_0

$$\left(\begin{array}{cc} -m_1 (-r_0 + h_1)^{\sim} & (R_0 + h_1 + C_1 r_1)^{\sim} \\ -m_2 (-r_0 + h_2)^{\sim} & (R_0 + h_2 + C_2 r_2)^{\sim} \end{array} + [I_0] \right)$$

Terms in $\dot{w}_1 + \dot{w}_2$

$$\left(-m_1 (-r_0 + h_1)^{\sim} C_1 \tilde{r}_1 \right) \dot{w}_1 + \left(-m_2 (-r_0 + h_2)^{\sim} C_2 \tilde{r}_2 \right) \dot{w}_2$$

R.H.S.

$$-m_1 (-r_0 + h_1) \tilde{\left[\begin{array}{l} 2\tilde{w}_0 \quad \tilde{w}_0 (R_0 + h_1 + C_1 r_1) \\ + 2\tilde{w}_0 C_1 \tilde{w}_1 r_1 + C_1 \tilde{w}_1 \tilde{w}_1 r_1 \end{array} \right]}$$

$$-m_2 (-r_0 + h_2) \tilde{\left[\begin{array}{l} 2\tilde{w}_0 \dot{R}_0 + \tilde{w}_0 \tilde{w}_0 (R_0 + h_2 + C_2 r_2) \\ + 2\tilde{w}_0 C_1 \tilde{w}_1 r_1 + C_1 \tilde{w}_1 \tilde{w}_1 r_1 \end{array} \right]}$$

$$- (-r_0 + l_0) \tilde{F}_0 - \tilde{w}_0 [I_0] w_0$$

$$-T_{H1} \quad -T_{H2} \quad +T_0$$

$$+ m_1 (-r_0 + h_1) \tilde{C}_1 F_1$$

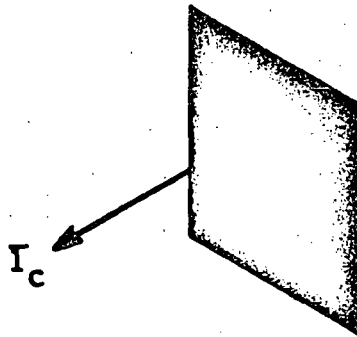
$$+ m_2 (-r_0 + h_1) \tilde{C}_2 F_2$$

Case B - Constrained Rotation

In the previous case the hinge torques were assumed to be arbitrary functions which completely accounted for the rotational interaction between the bodies 1 and 2 and the central element. In general, one or more axes of rotation may be constrained and the equations given previously must be modified to handle the rotational constraints.

- Modification to the Driver Moment Equation

If we consider the constrained axes in terms of unit vectors, the modification procedure is easily visualized:



Consider the unit vector of constraint shown above. The remaining two degrees of rotation must be about mutually orthogonal axes lying in the plane normal to \hat{l}_c . An additional constraint, if it exists, must lie within the plane and for this case the single degree of rotational freedom is about the unit vector normal to both of the constraint axes.

The moment equation is altered by the elimination of constrained degree of freedom. This can most easily be done by taking the dot product of the unconstrained equations with unit vectors along the axes of allowable rotation. The reduction in dimension may be utilized advantageously by then reformulating the equations in terms of the new driver rotational acceleration components thereby eliminating a variable for each constraint.

Modification of the Zero Body Moment Equation

The constraint application effects this equation in two ways:

1. The negative of the constraint torque which nulls the outer body rotation about the axis of constraint must be applied to body zero.
2. If the driver moment equations are written in terms of the reduced set of variables the zero body moment equation must be modified appropriately.

Computation of the constraint torque is simply the reaction torque of the outer body minus the external outer body torque; this difference projected onto the constrained axis. The implementation of this computation can be done in either of two ways.

1. The constraint torque can be solved for formally and the terms in R_0 and w_0 added to the L.H.S. of the zero body moment equation while all other terms are added to the R.H.S. of the equation.
2. The scalar equation of the outer body rotational acceleration about the constrained axis can be changed to an equation in terms of constraint torque (with suitable coupling to the zero body moment equation).

The former is recommended for constraints which are always applied while the latter is useful if the application of constraints is optional.

4.2 FLEXIBLE SPACE STATION/FLEXIBLE APPENDAGE, ZERO "G" CONDITION

The flexible body considerations used in the initial study phase have been extended to include the space station as a non-rigid structure and in addition, the capability of simulating the flexible dynamics of four non-controlled appendages has also been included. Extension of the initial digital simulation to include the capability of modeling the space station as a flexible structure necessitated a major revision of the systems dynamic equations which had been previously derived. Basically, appendage and array base motion must now include translation and rotation due to space station flexibility. Likewise, space station flexible modes must be excited by external forces and torques, and appendage and array interaction forces and torques. However, much of the philosophy and equation development techniques established in Section 4.1 are still applicable. Space station guidance and orbital motion, solar array guidance, ability to constrain solar array motions and so forth remain essentially unchanged from those descriptions given in Section 4.1.

The equation derivations logically fall into four separate categories:

1. Modal analysis of a freely translating and rotating space station.
2. Modal analysis of an appendage rigidly fixed to a base which is arbitrarily moving in space.
3. Modal analysis of appendage hinged to a base which is moving arbitrarily in space.
4. Total system equation which can be simultaneously solved for both rigid and flexible motions of a flexible space station with a maximum of two hinged arrays and up to four rigidly attached appendages.

4.2.1

MODAL ANALYSIS OF A FREELY TRANSLATING AND ROTATING SPACE STATION*

The space station, taken as a rigid body, rotates with an angular velocity $\bar{\omega}_0$ with respect to inertial space. Its translation is measured by \bar{R}_0 , a vector from O_N , the origin of an inertial coordinate frame, to point O_B , a point fixed on the space station. This "rigid body" motion is conveniently described by a coordinate frame X_s fixed in the space station with origin at point O_B .

Determination of the flexible motion of the space station assumes that the station may be described by a collection of n discrete rigid bodies interconnected by massless elastic constraints. This system is idealized as initially undamped. The flexible motion of each discrete rigid body is measured relative to the X_s coordinate frame defined in the preceding paragraph. Thus, for example, the i^{th} rigid body's center of mass is located by the vector

$$\vec{p}_i = \vec{q}_i + \vec{x}_i$$

where

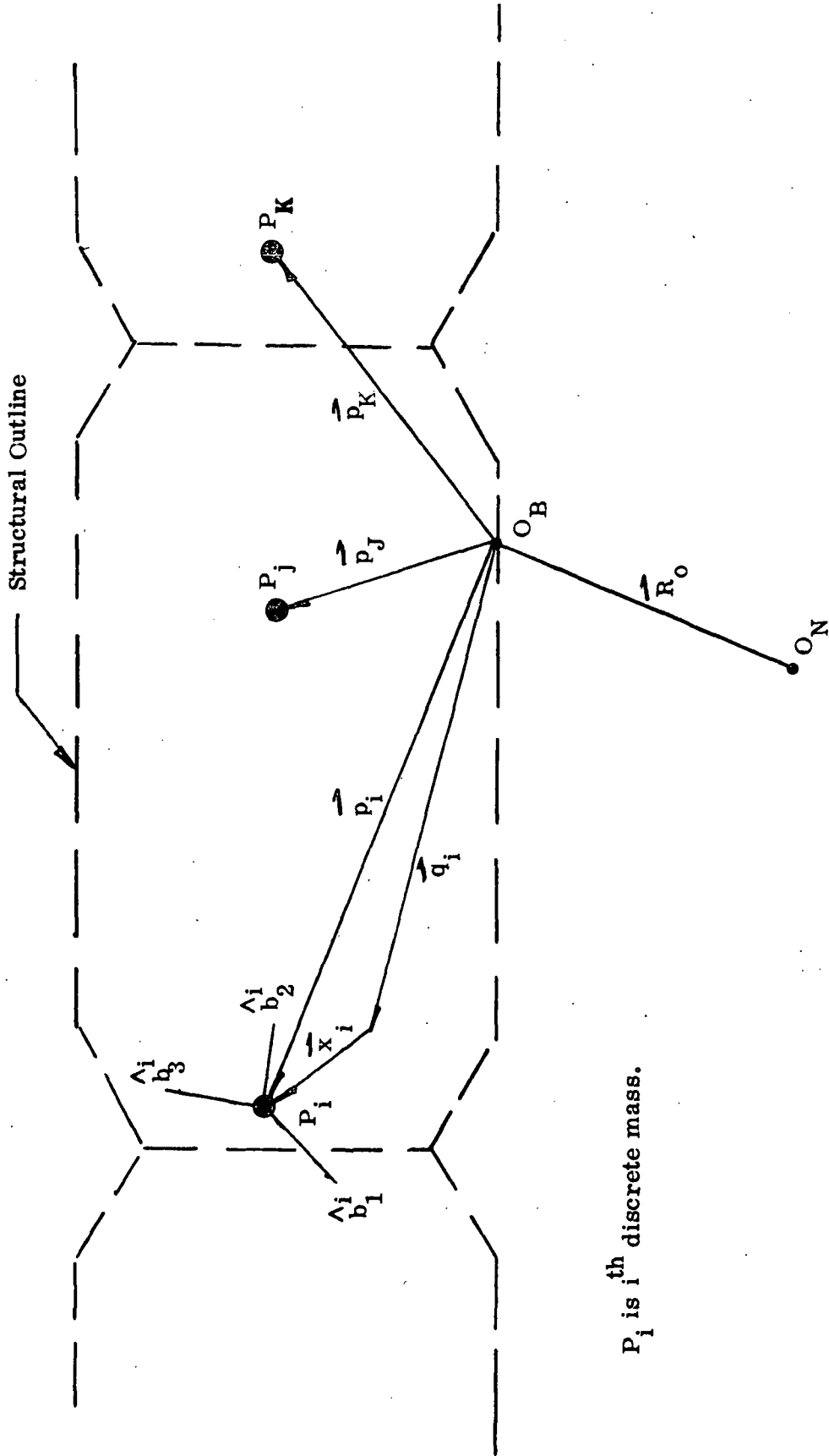
\vec{p}_i - center of mass of i^{th} rigid body P_i

\vec{q}_i - vector fixed in X_s ; it accommodates in its changes of orientation the motion of P_i due to "rigid body" motion of the space station (Figure 4-9).

\vec{x}_i - describes small deformations of system at P_i

Likewise, the i^{th} rigid body's angular velocity - measured in its own principal axes frame - is $\vec{\omega}_{b_i}$ with respect to the X_s coordinate system. Thus flexible motion of the i^{th} body may be represented by the variables $x_{i_1}, x_{i_2}, x_{i_3}, \theta_{i_1}, \theta_{i_2}, \theta_{i_3}$, and their respective derivatives.

*See Reference 4.6.



P_i is i^{th} discrete mass.

FIGURE 4-9 SPACE STATION COORDINATE SYSTEM

4.2.1.1 Coordinate Frames and Relationships

- $[I]$ - inertially fixed coordinates
- $[X_s]$ - coordinate basis fixed to and moving with the space station taken as a rigid body (origin at O_B , angular velocity $\bar{\omega}_o$ with respect to inertial space)
- $[B_i]$ - coordinate basis with origin at the center of mass of the i^{th} elastically connected rigid body used to define space station flexible motion (angular velocity Ω^i with respect to inertial space). This basis is initially oriented along $[X_s]$.

The relationships between these frames are defined by the following direction cosine matrices:

$$\begin{aligned} \begin{bmatrix} I \\ X_s \end{bmatrix} &= C_O \begin{bmatrix} X_s \\ B_i \end{bmatrix} \\ \begin{bmatrix} X_s \\ B_i \end{bmatrix} &= C_{B_i} \begin{bmatrix} X_s \\ B_i \end{bmatrix} \end{aligned} \quad i = 1, 2, \dots, n$$

where

$$C_{B_i} \cong \begin{bmatrix} 1 & \theta_{i_3} & -\theta_{i_2} \\ -\theta_{i_3} & 1 & \theta_{i_1} \\ \theta_{i_2} & -\theta_{i_1} & 1 \end{bmatrix} = E - \tilde{\theta}_i$$

E is the identity matrix. The \sim operation is basically used in cross product calculations and is defined by

$$\tilde{y} = \begin{bmatrix} y_1 \\ y_2 \\ y_3 \end{bmatrix} = \begin{bmatrix} 0 & -y_3 & y_2 \\ y_3 & 0 & -y_1 \\ -y_2 & y_1 & 0 \end{bmatrix}$$

As shown in Section 4.1

$$\begin{aligned}\dot{C}_o &= C_o \tilde{\omega}_o \\ \dot{C}_{B_i} &= C_{B_i} \tilde{\omega}_{b_i}, \quad \dot{C}_{b_i}^T = -\tilde{\omega}_{b_i} C_{b_i}^T\end{aligned}$$

4.2.1.2 Equation Derivation

Using D'Alembert's principle, the total external force acting on the i^{th} rigid body is

$$F_i = m_i \frac{d^2}{dt^2} \left[\vec{R}_o + \vec{q}_i + \vec{x}_i \right]_I$$

Defining \vec{R}_o , \vec{q}_i , and \vec{x}_i in the X_s frame, and derivation in Reference 4.1, representative calculations are

$$\begin{aligned}\frac{d}{dt} (\vec{R}_o)_I &= \frac{d}{dt} \left[I^T C_o R_o \right] = I^T (C_o \tilde{\omega}_o R_o + C_o \dot{R}_o) \\ \frac{d^2}{dt^2} (\vec{R}_o)_I &= I^T \left[C_o \tilde{\omega}_o \dot{R}_o + C_o \ddot{R}_o + C_o \tilde{\omega}_o \tilde{\omega}_o R_o \right. \\ &\quad \left. + C_o \dot{\tilde{\omega}}_o R_o + C_o \tilde{\omega}_o \dot{R}_o \right] \\ &= X_s^T \left[\tilde{\omega}_o \tilde{\omega}_o R_o + 2 \tilde{\omega}_o \dot{R}_o + \dot{\tilde{\omega}}_o R_o + \ddot{R}_o \right]\end{aligned}$$

Therefore, remembering that \vec{q}_i does not vary with respect to time in the X_s frame, the translational equation of motion for the i^{th} rigid body becomes

$$\begin{aligned}\{F_i\} &= m_i X_s^T \left[\tilde{\omega}_o \tilde{\omega}_o (R_o + q_i + x_i) + 2 \tilde{\omega}_o \dot{(R_o + x_i)} \right. \\ &\quad \left. + \dot{\tilde{\omega}}_o (R_o + q_i + x_i) + \ddot{R}_o + \ddot{x}_i \right] \quad (4.1)\end{aligned}$$

Thus F_i must be expressed in $\{X_S\}$ frame.

Rotational motion of the rigid body in the $[B_i]$ frame is expressed by Euler's equation for principal axes

$$\{T_i\}_B = [I^i] \{\dot{\Omega}^i\} + \tilde{\Omega}^i [I^i] \{\Omega^i\} \quad (4.2)$$

where

$$[I^i] = \begin{bmatrix} I_1^i & 0 & 0 \\ 0 & I_2^i & 0 \\ 0 & 0 & I_3^i \end{bmatrix} \equiv \text{inertia matrix for } i^{\text{th}} \text{ rigid body}$$

$\{\Omega^i\}$ - angular velocity of i^{th} body with respect to inertial space.

$\{\Omega^i\} = \{\omega_{bi}\} + C_{bi} \{\omega_o\}$ in the $[B_i]$ frame. Therefore, substitution into equation (4.2) gives

$$\begin{aligned} \{T_i\}_B &= [I^i] \{\dot{\omega}_{bi}\} - [I^i] \tilde{\omega}_{bi} C_{bi}^T \{\omega_o\} + [I^i] C_{bi}^T \{\dot{\omega}_o\} \\ &+ \tilde{\omega}_{bi} [I^i] \{\omega_{bi}\} + \tilde{\omega}_{bi} [I^i] C_{bi}^T \{\omega_o\} + \left[\widetilde{C_{bi}^T \{\omega_o\}} [I^i] \right] \{\omega_{bi}\} \quad (4.3) \\ &+ \left[\widetilde{C_{bi}^T \{\omega_o\}} \right] [I^i] C_{bi}^T \{\omega_o\} \end{aligned}$$

For small flexible rotations of the i^{th} rigid body $C_{bi}^T \cong E + \tilde{\theta}_i$ as shown above. Substituting this along with the simplification

$$\left[\widetilde{C_{bi}^T \{\omega_o\}} \right] \cong \tilde{\omega}_o + \left[\tilde{\theta}^i \widetilde{\{\omega_o\}} \right]$$

into equation (4.3) gives

$$\begin{aligned}
\{T_i\}_B &= \begin{bmatrix} I^i \\ \vdots \end{bmatrix} \{\dot{\omega}_{bi}\} - \begin{bmatrix} I^i \\ \vdots \end{bmatrix} \tilde{\omega}_{bi} \{\omega_o\} - \begin{bmatrix} I^i \\ \vdots \end{bmatrix} \tilde{\theta}^i \tilde{\omega}_{bi} \{\omega_o\} \\
&+ \begin{bmatrix} I^i \\ \vdots \end{bmatrix} \{\dot{\omega}_o\} + \begin{bmatrix} I^i \\ \vdots \end{bmatrix} \tilde{\theta}^i \{\dot{\omega}_o\} + \tilde{\omega}_{bi} \begin{bmatrix} I^i \\ \vdots \end{bmatrix} \{\omega_{bi}\} + \tilde{\omega}_{bi} \begin{bmatrix} I^i \\ \vdots \end{bmatrix} \{\omega_o\} \\
&+ \tilde{\omega}_{bi} \begin{bmatrix} I^i \\ \vdots \end{bmatrix} \tilde{\theta}^i \{\omega_o\} + \tilde{\omega}_o \begin{bmatrix} I^i \\ \vdots \end{bmatrix} \{\omega_{bi}\} - \begin{bmatrix} \tilde{\theta}^i \\ \vdots \end{bmatrix} \{\omega_o\} \begin{bmatrix} I^i \\ \vdots \end{bmatrix} \{\omega_{bi}\} \\
&+ \tilde{\omega}_o \begin{bmatrix} I^i \\ \vdots \end{bmatrix} \{\omega_o\} - \tilde{\omega}_o \begin{bmatrix} I^i \\ \vdots \end{bmatrix} \tilde{\theta}^i \{\omega_o\} + \begin{bmatrix} \tilde{\theta}^i \\ \vdots \end{bmatrix} \{\omega_o\} \begin{bmatrix} I^i \\ \vdots \end{bmatrix} \{\omega_o\} \\
&+ \begin{bmatrix} \tilde{\theta}^i \\ \vdots \end{bmatrix} \{\omega_o\} \begin{bmatrix} I^i \\ \vdots \end{bmatrix} \tilde{\theta}^i \{\omega_o\}
\end{aligned} \tag{4.4}$$

Note that linearization of the above equation has been assumed since terms containing products of small variables have been neglected.

The force equation is written in the X_s coordinate basis. Transforming Equation 4.4 to the X_s frame involves multiplication by $C_{bi}^T \cong E - \tilde{\theta}^i$.

This procedure results in Equation 4.5.

$$\begin{aligned}
\{T_i\} &= \begin{bmatrix} I^i \\ \vdots \end{bmatrix} \{\dot{\omega}_{bi}\} - \tilde{\theta}^i \begin{bmatrix} I^i \\ \vdots \end{bmatrix} \{\dot{\omega}_{bi}\} - \begin{bmatrix} I^i \\ \vdots \end{bmatrix} \tilde{\omega}_{bi} \{\omega_o\} \\
&+ \tilde{\theta}^i \begin{bmatrix} I^i \\ \vdots \end{bmatrix} \tilde{\omega}_{bi} \{\omega_o\} + \begin{bmatrix} I^i \\ \vdots \end{bmatrix} \{\dot{\omega}_o\} - \tilde{\theta}^i \begin{bmatrix} I^i \\ \vdots \end{bmatrix} \{\dot{\omega}_o\} - \begin{bmatrix} I^i \\ \vdots \end{bmatrix} \tilde{\theta}^i \{\dot{\omega}_o\} \\
&- \tilde{\theta}^i \begin{bmatrix} I^i \\ \vdots \end{bmatrix} \tilde{\theta}^i \{\dot{\omega}_o\} + \tilde{\omega}_{bi} \begin{bmatrix} I^i \\ \vdots \end{bmatrix} \{\omega_o\} - \tilde{\theta}^i \tilde{\omega}_{bi} \begin{bmatrix} I^i \\ \vdots \end{bmatrix} \{\omega_o\} \\
&+ \tilde{\omega}_o \begin{bmatrix} I^i \\ \vdots \end{bmatrix} \{\omega_{bi}\} - \tilde{\theta}^i \tilde{\omega}_o \begin{bmatrix} I^i \\ \vdots \end{bmatrix} \{\omega_{bi}\} + \tilde{\omega}_o \begin{bmatrix} I^i \\ \vdots \end{bmatrix} \{\omega_o\} \\
&- \tilde{\theta}^i \tilde{\omega}_o \begin{bmatrix} I^i \\ \vdots \end{bmatrix} \{\omega_o\} + \tilde{\omega}_o \begin{bmatrix} I^i \\ \vdots \end{bmatrix} \tilde{\theta}^i \{\omega_o\} - \tilde{\theta}^i \tilde{\omega}_o \begin{bmatrix} I^i \\ \vdots \end{bmatrix} \tilde{\theta}^i \{\omega_o\} \\
&+ \begin{bmatrix} \tilde{\theta}^i \\ \vdots \end{bmatrix} \{\omega_o\} \begin{bmatrix} I^i \\ \vdots \end{bmatrix} \{\omega_o\} - \tilde{\theta}^i \begin{bmatrix} \tilde{\theta}^i \\ \vdots \end{bmatrix} \{\omega_o\} \begin{bmatrix} I^i \\ \vdots \end{bmatrix} \{\omega_o\}
\end{aligned} \tag{4.5}$$

Using the following identity

$$\tilde{u} \{v\} = - \tilde{v} \{u\}$$

and defining

$$\{h_i\} = [I^i] \{\omega_o\}$$

Therefore

$$\tilde{h}_i = \left[[I^i] \widetilde{\{\omega_o\}} \right]$$

$$\left[\tilde{\theta}^i \widetilde{\{\omega_o\}} \right] [I^i] \{\omega_o\} = - \tilde{h}_i \tilde{\theta}^i \{\omega_o\} = \tilde{h}_i \tilde{\omega}_o \{\theta^i\}$$

Substitution of these identities into Equation 4.5 yields the rotational equation of motion for the i^{th} rigid body of the space station.

$$\{T_i\} = [I^i] \{\dot{\omega}_{bi}\} + [I^i] \tilde{\omega}_o \{\omega_{bi}\} + [I^i] \{\dot{\omega}_o\}$$

$$\tilde{h}_i \{\tilde{\theta}^i\} - [I^i] \tilde{\omega}_o \{\theta^i\} - \tilde{h}_i \{\omega_{bi}\} + \tilde{\omega}_o [I^i] \{\omega_{bi}\} + \tilde{\omega}_o \{h^i\} \quad (4.6)$$

$$+ \left[\tilde{\omega}_o [I^i] \{\omega_2\} \right] \{\theta^i\} - \tilde{\omega}_o [I^i] \tilde{\omega}_o \{\theta^i\} + \tilde{h}_i \tilde{\omega}_o \{\theta^i\}$$

Combining Equations 4.1 and 4.6 for all n rigid bodies into one large matrix equation of column dimension $6n$ yields

$$\begin{aligned} [m] \{\ddot{q}\} + [K] \{q\} &= -[G] \{\dot{q}\} - [B] \{q\} + [R] \{RB\} \\ &+ \{F^1\} + \{L\} \end{aligned} \quad (4.7)$$

$\{F^1\}$ - discretely applied forces and torques on those elastically connected rigid bodies which define the space station to which either

- (a) fixed appendage is attached
- (b) rotating array is hinged
- (c) external force is applied (\vec{F}_R)
- (d) external torque is applied ($\vec{T}_R - \tilde{l}_R F_R$)

The applied forces and torques include those resulting from appendage base constraints.

$$\left[B \right] = \begin{bmatrix} \bar{m}_1 (\ddot{\tilde{\omega}}_0 + \tilde{\omega}_0 \tilde{\omega}_0) & 0 \\ -\bar{I}^{-1} \ddot{\tilde{\omega}}_0 - \tilde{\omega}_0 \bar{I}^{-1} \tilde{\omega}_0 + \tilde{h}_1 \tilde{\omega}_0 + \tilde{h}_1 + \left[\tilde{\omega}_0 \bar{I} \tilde{\omega}_0 \right] & 0 \\ 0 & \vdots \\ 0 & \vdots \end{bmatrix}$$

6n x 6n

$$\{L\} = \begin{bmatrix} -\bar{m}_1 \left[\tilde{\omega}_0 \tilde{\omega}_0 (R_0 + q_1) + 2 \tilde{\omega}_0 \dot{R}_0 \right] \\ -\tilde{\omega}_0 \bar{I}^{-1} \{\omega_0\} \\ -\bar{m}_2 \left[\tilde{\omega}_0 \tilde{\omega}_0 (R_0 + q_2) + 2 \tilde{\omega}_0 \dot{R}_0 \right] \\ -\tilde{\omega}_0 \bar{I}^{-2} \{\omega_0\} \\ \vdots \\ \vdots \\ \vdots \end{bmatrix}$$

6n x 1

4.2.1.3 Modal Analysis

Subjecting Equation 4.7 to the orthogonal transformation

$$\{q\} = [\gamma] \{n_s\}$$

and premultiplying by $[\gamma]^T$ yields, if $[\gamma]$ is a matrix whose columns are eigenvectors of the system, $[\gamma]^T [m] [\gamma] = I$,

$$\begin{aligned} \ddot{n}_s + \begin{bmatrix} 2\xi_s & \omega_s \end{bmatrix} \dot{n}_s + \begin{bmatrix} \omega_s^2 \end{bmatrix} n_s = -[\gamma]^T [G] [\gamma] \dot{n}_s \\ + [\gamma]^T \{L\} - [\gamma]^T [B] [\gamma] n_s \\ + [\gamma]^T [R] \{RB\} + [\gamma]^T \{F^1\} \end{aligned} \quad (4.8)$$

Note that modal damping has been added in the classical manner of structural analysis.

For this simulation, space station "rigid body" motion is considered to be small. Thus, Equation 4.8 may be linearized to the following form

$$\ddot{n}_s + \begin{bmatrix} 2\xi_s & \omega_s \end{bmatrix} \dot{n}_s + \begin{bmatrix} \omega_s^2 \end{bmatrix} n_s = [\gamma]^T \{F^1\} + [\gamma]^T [R] \{RB\} \quad (4.9)$$

Derivations in Section 4.2.5 also show that $[\gamma]^T [R] \{RB\} = 0$. Thus Equation 4.9 becomes

$$\left\langle \ddot{n}_s + \begin{bmatrix} 2\xi_s & \omega_s \end{bmatrix} \dot{n}_s + \begin{bmatrix} \omega_s^2 \end{bmatrix} n_s = [\gamma]^T \{F^1\} \right\rangle$$

The above equation in diamond brackets is the equation modeled in the simulation. The diamond bracket will hence forth be utilized solely for indicating equations to be programmed.

In summary, the above equation was derived assuming:

- (a) linearization of equations because of
 1. small flexible motions of system
 2. small space station angular velocity, and translation with respect to osculating orbit position
- (b) free-free modes of space station are available for generation of $[\gamma]$ modal matrix
- (c) moments of inertia for each of the n discrete rigid bodies are initially defined along axes parallel to the X_s coordinate basis
- (d) external forces and torques acting on the space station to be expressed in the space station axes system

4.2.2 RIGIDLY ATTACHED APPENDAGES

Appendages, as in previous derivations, are modeled as elastically connected masses. Cantilevered mode shapes are used to represent the fixed appendage flexibility. The base of a fixed appendage must be rigidly attached to one of those rigid bodies which comprise the space station. Therefore base motion of the appendage includes translational and rotational motion of that rigid body to which it is attached plus translational and rotational motion of the entire space station with respect to inertial space.

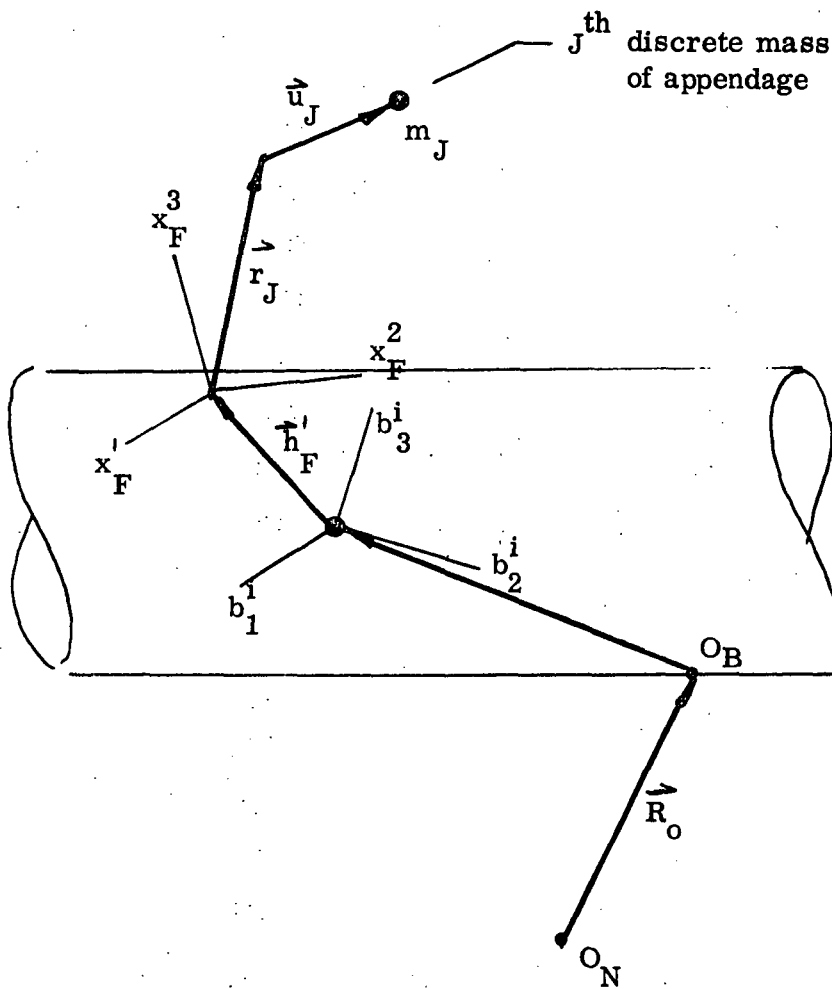


FIGURE 4-10 FIXED APPENDAGE COORDINATE SYSTEM

4.2.2.1 Coordinate Frames and Relationships

$\begin{bmatrix} X \\ S \end{bmatrix}$ - previously defined S/S "rigid body" basis

$\begin{bmatrix} I \end{bmatrix}$ - previously defined inertial basis

$\begin{bmatrix} B \\ i \end{bmatrix}$ - previously defined basis fixed to i^{th} rigid body of space station

$\begin{bmatrix} X \\ F \end{bmatrix}$ - coordinate basis defined with origin at attachment point of appendage and axes directed along principal axes of the appendage

$\begin{bmatrix} C \\ F \end{bmatrix}$ - direction cosine matrix relating coordinate frames $\begin{bmatrix} B \\ i \end{bmatrix}$ and $\begin{bmatrix} X \\ F \end{bmatrix}$

$$\begin{bmatrix} B \\ i \end{bmatrix} = \begin{bmatrix} C \\ F \end{bmatrix} \begin{bmatrix} X \\ F \end{bmatrix}$$

4.2.2.2 Equation Derivation

The total force acting on the j^{th} mass particle m_J of the appendage is, by D'Alembert's principle

$$F_J = m_J \frac{d^2}{dt^2} \left[\vec{R}_O + \vec{q}_i + \vec{x}_i + \vec{h}'_F + \vec{r}_J + \vec{u}_J \right]_I$$

where

\vec{h}'_F - location of attachment point of appendage with respect to the center of mass of the i^{th} rigid body of the space station to which the appendage is rigidly attached.

\vec{r}_J - undeformed location of j^{th} particle m_J of appendage.

\vec{u}_J - location of m_J with respect to undeformed position.

Representative calculations, assuming \vec{h}'_F is defined in the $[B_i]$ basis and \vec{r}_J and \vec{u}_J are defined in the $[X_F]$ basis, and noting that $C_F = 0$ are

$$\begin{aligned} \frac{d}{dt} \vec{u}_J &= \frac{d}{dt} \left[I^T C_o C_{bi} C_F u_J \right] = \\ I^T &\left[C_o \tilde{\omega}_o C_{bi} C_F u_J + C_o C_{bi} \tilde{\omega}_{bi} C_F u_J + C_o C_{bi} C_F \dot{u}_J \right] \\ \frac{d^2}{dt^2} \left[u_J \right]_I &= I^T \left[C_o \tilde{\omega}_o \dot{\tilde{\omega}}_o C_{bi} C_F u_J + C_o \dot{\tilde{\omega}}_o C_{bi} C_F u_J \right. \\ &+ C_o \tilde{\omega}_o C_{bi} \dot{\tilde{\omega}}_{bi} C_F u_J + C_o \tilde{\omega}_o C_{bi} \ddot{u}_J + C_o \tilde{\omega}_o C_{bi} \tilde{\omega}_{bi} C_G u_J \\ &+ C_o C_{bi} \dot{\tilde{\omega}}_{bi} \tilde{\omega}_{bi} C_F u_J + C_o C_{bi} \tilde{\omega}_{bi} \dot{C}_F u_J + C_o C_{bi} \tilde{\omega}_{bi} C_F \dot{u}_J \\ &\left. + C_o \dot{\tilde{\omega}}_o C_{bi} C_F \dot{u}_J + C_o C_{bi} \dot{\tilde{\omega}}_{bi} C_F \dot{u}_J + C_o C_{bi} C_F \ddot{u}_J \right] \\ &= X^T \left[\tilde{\omega}_o \tilde{\omega}_o C_{bi} C_F u_J + \dot{\tilde{\omega}}_o C_{bi} C_F u_J + 2 \tilde{\omega}_o C_{bi} \dot{\tilde{\omega}}_{bi} C_F u_J \right. \\ &+ 2 \dot{\tilde{\omega}}_o C_{bi} C_F \dot{u}_J + C_{bi} \dot{\tilde{\omega}}_{bi} \tilde{\omega}_{bi} C_F u_J + C_{bi} \dot{\tilde{\omega}}_{bi} C_F u_J + 2 C_{bi} \tilde{\omega}_{bi} C_F \dot{u}_J \\ &\left. + C_{bi} C_F \ddot{u}_J \right] \end{aligned}$$

$\vec{q}'_I, \vec{h}'_F, \vec{r}_J$ do not vary with time in their respective frames.

$$\begin{aligned}
\left\{ F_J \right\} &= m_J X_F^T \left[(\tilde{\omega}_o \tilde{\omega}_o (R_o + q_i + x_i) + 2 \dot{\tilde{\omega}}_o (\dot{R}_o + \dot{x}_i) \right. \\
&+ \ddot{\tilde{\omega}}_o (R_o + q_i + x_i) + \ddot{R}_o + \ddot{x}_i) + (\tilde{\omega}_o \tilde{\omega}_o C_{bi} + 2 \dot{\tilde{\omega}}_o C_{bi} \dot{\tilde{\omega}}_{bi} \\
&+ \ddot{\tilde{\omega}}_o C_{bi} + C_{bi} \ddot{\tilde{\omega}}_{bi} \tilde{\omega}_{bi} + C_{bi} \dot{\tilde{\omega}}_{bi}) h'_F + (\tilde{\omega}_o \tilde{\omega}_o C_{bi} C_F \\
&+ \dot{\tilde{\omega}}_o C_{bi} C_F + 2 \tilde{\omega}_o C_{bi} \dot{\tilde{\omega}}_{bi} C_F + C_{bi} \tilde{\omega}_{bi} \dot{\tilde{\omega}}_{bi} C_F + C_{bi} \ddot{\tilde{\omega}}_{bi} C_F)^* \\
&\left. (r_J + u_J) + (2 \tilde{\omega}_o C_{bi} C_F + C_{bi} \tilde{\omega}_{bi} C_F) \dot{u}_J + C_{bi} C_F \ddot{u}_J \right] \\
&= m_J X_F^T \left\{ \begin{matrix} C_F^T \\ C_{bi}^T \end{matrix} \right\} (\tilde{\omega}_o \tilde{\omega}_o (R_o + q_i + x_i) + 2 \dot{\tilde{\omega}}_o (\dot{R}_o + \dot{x}_i) \\
&+ \ddot{\tilde{\omega}}_o (R_o + q_i + x_i) + \ddot{R}_o + \ddot{x}_i) + (\tilde{\omega}_o \tilde{\omega}_o C_{bi} + 2 \dot{\tilde{\omega}}_o C_{bi} \dot{\tilde{\omega}}_{bi} + \ddot{\tilde{\omega}}_o C_{bi} \\
&+ C_{bi} \dot{\tilde{\omega}}_{bi} \tilde{\omega}_{bi} + C_{bi} \ddot{\tilde{\omega}}_{bi}) h'_F + (\tilde{\omega}_o \tilde{\omega}_o C_{bi} C_F + \dot{\tilde{\omega}}_o C_{bi} C_F \\
&+ 2 \tilde{\omega}_o C_{bi} \dot{\tilde{\omega}}_{bi} C_F + C_{bi} \tilde{\omega}_{bi} \dot{\tilde{\omega}}_{bi} C_F + C_{bi} \ddot{\tilde{\omega}}_{bi} C_F) (r_J + u_J) \\
&+ (2 \tilde{\omega}_o C_{bi} C_F + C_{bi} \tilde{\omega}_{bi} C_F) \dot{u}_J + \ddot{u}_J \left. \right]
\end{aligned}$$

For small translational and rotational motion of the rigid body to which the appendage is attached $C_{bi}^T \cong E + \tilde{\theta}^i$

$$\begin{aligned}
\therefore \{F_J\} = m_J X_F^T & \left[\left\{ C_F^T \right\} \cdot \left\{ (\ddot{\omega}_o \ddot{\omega}_o (R_o + q_i + x_i) + 2 \ddot{\omega}_o (\dot{R}_o + \dot{x}_i) \right. \right. \\
& + \ddot{\omega}_o (\dot{R}_o + \dot{q}_i + \dot{x}_i) + \ddot{R}_o + \ddot{x}_i) + \ddot{\theta}_i (\ddot{\omega}_o \ddot{\omega}_o (R_o + q_i) + 2 \ddot{\omega}_o \dot{R}_o \\
& + \ddot{\omega}_o (\dot{R}_o + \dot{q}_i) + \ddot{R}_o) + (\ddot{\omega}_o \ddot{\omega}_o + \ddot{\theta}_i (\ddot{\omega}_o \ddot{\omega}_o + \ddot{\omega}_o) - (\ddot{\omega}_o \ddot{\omega}_o + \ddot{\omega}_o) \ddot{\theta}_i^i \\
& + \ddot{\omega}_o + 2 \ddot{\omega}_o \ddot{\omega}_{bi} + \cancel{\ddot{\omega}_{bi} \ddot{\omega}_{bi}} + \ddot{\omega}_{bi}) h'_F + (\ddot{\omega}_o \ddot{\omega}_o + \ddot{\theta}_i (\ddot{\omega}_o \ddot{\omega}_o + \ddot{\omega}_o) \\
& - (\ddot{\omega}_o \ddot{\omega}_o + \ddot{\omega}_o) \ddot{\theta}_i^i + \ddot{\omega}_o + 2 \ddot{\omega}_o \ddot{\omega}_{bi} + \cancel{\ddot{\omega}_{bi} \ddot{\omega}_{bi}} + \ddot{\omega}_{bi}) C_F (r_J + u_J) \\
& \left. + (2 \ddot{\omega}_o + 2 \ddot{\theta}_i^i \ddot{\omega}_o - 2 \ddot{\omega}_o \ddot{\theta}_i^i + \ddot{\omega}_{bi}) C_F \dot{u}_J \right\} + \ddot{u}_J \Big]
\end{aligned}$$

The space station motion is assumed to be small, thus, the above equation reduces to

$$\begin{aligned}
\{F_J\} = m_J X_F^T & \left[C_F^T (\ddot{\omega}_o q_i + \ddot{R}_o + \ddot{x}_i + (\ddot{\omega}_o + \ddot{\omega}_{bi}) h'_F \right. \\
& \left. + (\ddot{\omega}_o + \ddot{\omega}_{bi})(C_F r_J) + \ddot{u}_J \right] \quad (4.10)
\end{aligned}$$

Combining the above equation for all n particles of the appendage into one large matrix equation of column size $3n$ yields

$$\begin{aligned}
[m] \{\ddot{q}\} + [K] \{q\} & = - [G] \{\dot{q}\} - [B] \{q\} \\
& + [R] \{RB\} + [s_2] \{\ddot{s}\} + \{L\} \quad (4.11)
\end{aligned}$$

$$\begin{Bmatrix} \dots \\ s \end{Bmatrix} = \begin{bmatrix} \dots \\ x_i \\ \dots \\ \omega_{bi} \end{bmatrix} \quad - \text{used to define coupling of the space station flexible modes with the cantilever modes of the fixed appendage.}$$

6 x 1

$$\begin{Bmatrix} s_2 \end{Bmatrix} = \begin{bmatrix} -\bar{m}_1 C_F^T & \bar{m}_1 C_F^T (\tilde{h}_F^1 + (C_F \tilde{r}_1)) \\ \cdot & \cdot \\ \cdot & \cdot \\ \cdot & \cdot \\ -\bar{m}_n C_F^T & \bar{m}_n C_F^T (\tilde{h}_F^n + (C_F \tilde{r}_n)) \end{bmatrix}$$

3 n x 6

$$\{L\} = 0 \quad (\text{no external forces are applied to appendages})$$

4.2.2.3 Modal Analysis

$$q = [\tau]^n$$

where $[\tau]$ - modal matrix of dimension $3n \times N_{Fi}$

n - normal modes of which there are N_{Fi}

N_{Fi} - number of normal cantilever modes used to simulate fixed appendage #i.

Assuming $\begin{bmatrix} \tau^T \\ \tau \end{bmatrix} \begin{bmatrix} m \\ \tau \end{bmatrix} = I$, equation (2) becomes

$$\left\langle \begin{aligned} & - \tau^T [R] \{RB\} - \tau^T [s_2] [\gamma_F] \{\ddot{n}_s\} \\ & + \{\dot{n}_F\} + [2\xi_F \omega_F] \{\dot{n}_F\} + [\omega_F^2] \{n_F\} \end{aligned} \right\rangle = 0 \quad (4.12)$$

where $\begin{Bmatrix} \ddot{s} \\ s \end{Bmatrix} = \begin{pmatrix} \ddot{x}_i \\ \cdot \\ \omega_{bi} \end{pmatrix} = \begin{matrix} [\gamma_F] \\ 6 \times N_s \end{matrix} \begin{Bmatrix} \ddot{n}_s \\ n_s \end{Bmatrix}$ is $N_s \times 1$

the relationship between the translational and rotational motion of the rigid body to which the appendage is attached and the normal mode accelerations of the space station.

In summary, Equation 4.12 above is generated via the following assumptions:

- (a) base motion of the fixed appendage must include translations and rotations due to both rigid body motion of the space station and flexible modes of the space station,
- (b) the fixed appendage is modeled by discrete masses; cantilever modes are used to define its modal motion,
- (c) the above equations are derived in the coordinate frame of the fixed appendage
- (d) moments of inertia of the fixed appendage are defined with respect to principal axes with origin at base of appendage
- (e) linearization of equations has resulted because of
 - (1) small flexible motions of space station
 - (2) small flexible motions of fixed array
 - (3) small rigid body motion of space station

4.2.3

ROTATING ARRAYS

Rotating arrays are modeled exactly as fixed appendages, except that the base of the rotating array may have rotational motion with respect to the rigid body of the space station to which it is attached.

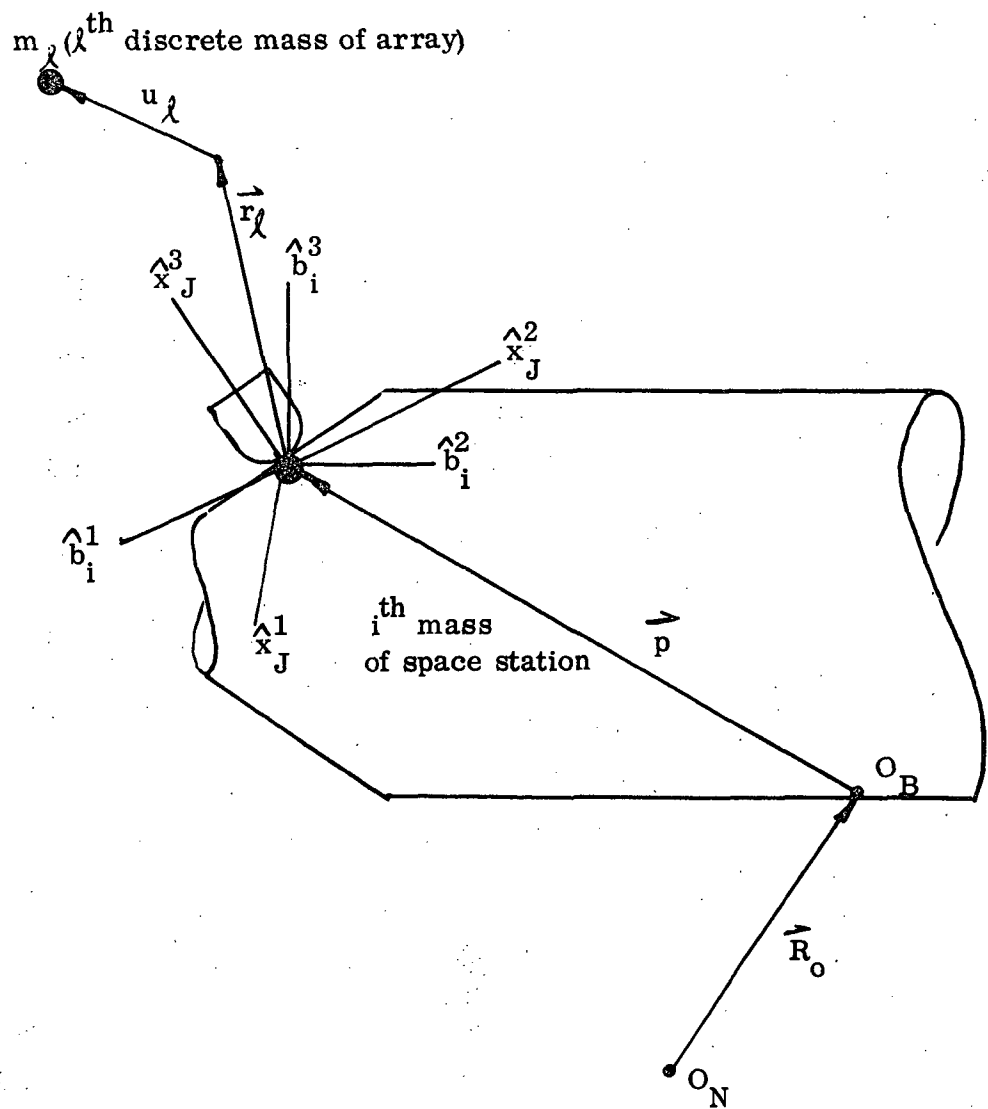


FIGURE 4-11 FLEXIBLE APPENDAGE COORDINATE SYSTEM

4.2.3.1 Coordinate Frames and Relationships

- [I] - previously defined
- [X_s] - previously defined
- [B_i] - previously defined
- [X_J] - coordinate basis which rotates with angular velocity $\vec{\omega}_J$ with respect to the rigid body of the space station to which it is attached with origin at the attachment point of the rotating array.

The relationship between [X_J] and [B_i] is defined by the direction cosine relationship

$$[B_i] = [C_J] [X_J]$$

Likewise, as shown in Reference 4.1

$$[\dot{C}_J] = [C_J] \tilde{\omega}_J$$

4.2.3.2 Equation Derivations

Again using D'Alembert's principle, the total force acting on the l^{th} mass particle of the rotating array equals

$$F_l = m_l \frac{d^2}{dt^2} \left[\vec{R}_0 + \vec{q}_i + \vec{x}_i + \vec{h}'_J + \vec{r}_l + \vec{u}_l \right]_I$$

where

- \vec{h}'_J - location of attachment point of appendage with respect to the center of mass of the i^{th} rigid body of the space station to which the appendage is attached
- \vec{r}_l - undeformed location of m_l of array
- \vec{u}_l - time dependent location of m_l with respect to undeformed location

Representative calculations, assuming \vec{h}'_J is defined in the $[B_i]$ basis and \vec{r}_ℓ and \vec{u}_ℓ are defined in the $[X_J]$ basis, are

$$\begin{aligned} \frac{d}{dt} [\vec{u}_\ell]_J &= \frac{d}{dt} \left[I^T C_o C_{bi} C_J u_\ell \right] \\ &= I^T \left[C_o \tilde{\omega}_o C_{bi} C_J u_\ell + C_o C_{bi} \tilde{\omega}_{bi} C_J u_\ell + C_o C_{bi} C_J \tilde{\omega}_J u_\ell \right. \\ &\quad \left. + C_o C_{bi} C_J \dot{u}_\ell \right] \end{aligned}$$

$$\begin{aligned} \frac{d^2}{dt^2} [\vec{u}_\ell]_I &= I^T C_o \left[\tilde{\omega}_o \tilde{\omega}_o C_{bi} C_J u_\ell + \dot{\tilde{\omega}}_o C_{bi} C_J u_\ell + 2 \tilde{\omega}_o C_{bi} \tilde{\omega}_{bi} C_J u_\ell \right. \\ &\quad + 2 \tilde{\omega}_o C_{bi} C_J \tilde{\omega}_J u_\ell + 2 \tilde{\omega}_o C_{bi} C_J \dot{u}_\ell + C_{bi} \tilde{\omega}_{bi} \tilde{\omega}_{bi} C_J u_\ell \\ &\quad + 2 C_{bi} \tilde{\omega}_{bi} C_J \dot{u}_\ell + C_{bi} \dot{\tilde{\omega}}_{bi} C_J u_\ell + 2 C_{bi} \tilde{\omega}_{bi} C_J \tilde{\omega}_J u_\ell \\ &\quad \left. + C_{bi} C_J \tilde{\omega}_J \tilde{\omega}_J u_\ell + 2 C_{bi} C_J \tilde{\omega}_J \dot{u}_\ell + C_{bi} C_J \dot{\tilde{\omega}}_J u_\ell + C_{bi} C_J \ddot{u}_\ell \right] \end{aligned}$$

$$\begin{aligned} \therefore \{F_\ell\} &= m_\ell x_J^T \left[(C_J^T C_{bi}^T) \{ \tilde{\omega}_o \tilde{\omega}_o (R_o + q_i + x_i) + 2 \tilde{\omega}_o (\dot{R}_o + \dot{x}_i) \right. \\ &\quad + \dot{\tilde{\omega}}_o (R_o + q_i + x_i) + \ddot{R}_o + \ddot{x}_i \} + \{ \tilde{\omega}_o \tilde{\omega}_o C_{bi} + \dot{\tilde{\omega}}_o C_{bi} + 2 \tilde{\omega}_o C_{bi} \tilde{\omega}_{bi} \\ &\quad + C_{bi} \tilde{\omega}_{bi} \dot{\tilde{\omega}}_{bi} + C_{bi} \dot{\tilde{\omega}}_{bi} \} h'_J + \{ \tilde{\omega}_o \tilde{\omega}_o C_{bi} C_J + \dot{\tilde{\omega}}_o C_{bi} C_J \\ &\quad + 2 \tilde{\omega}_o C_{bi} \tilde{\omega}_{bi} C_J + 2 \tilde{\omega}_o C_{bi} C_J \tilde{\omega}_J + C_{bi} \tilde{\omega}_{bi} \dot{\tilde{\omega}}_{bi} C_J + C_{bi} \dot{\tilde{\omega}}_{bi} C_J \\ &\quad + 2 C_{bi} \tilde{\omega}_{bi} C_J \tilde{\omega}_J + C_{bi} C_J \tilde{\omega}_J \tilde{\omega}_J + C_{bi} C_J \dot{\tilde{\omega}}_J \} (r_\ell + u_\ell) \\ &\quad \left. + \{ 2 \tilde{\omega}_o C_{bi} C_J + 2 C_{bi} \tilde{\omega}_{bi} C_J \} \dot{u}_\ell + 2 \tilde{\omega}_J \dot{u}_\ell + \ddot{u}_\ell \right] \end{aligned}$$

Again, ignoring products of small variables and recalling that

$$C_{bi} \approx E^{-\tilde{\theta}^i}$$

$$\begin{aligned} \therefore \{F_l\} = & m_l x_J^T \left[(C_J^T) (E + \tilde{\theta}^i) (\{\tilde{\omega}_o \tilde{\omega}_o (R_o + q_i + x_i) \right. \\ & + 2\tilde{\omega}_o (\dot{R}_o + \dot{x}_i) + \ddot{\tilde{\omega}}_o (R_o + q_i + x_i) + \ddot{R}_o + \ddot{x}_i \} + \{\tilde{\omega}_o \tilde{\omega}_o \\ & - \tilde{\omega}_o \tilde{\omega}_o \tilde{\theta}^i + \dot{\tilde{\omega}}_o - \dot{\tilde{\omega}}_o \tilde{\theta}^i + 2\tilde{\omega}_o \tilde{\omega}_{bi} + \ddot{\tilde{\omega}}_{bi} \} h'_J \\ & + \{\tilde{\omega}_o \tilde{\omega}_o C_J (r_l + u_l) - \tilde{\omega}_o \tilde{\omega}_o \tilde{\theta}^i C_J r_l + \dot{\tilde{\omega}}_o C_J (r_l + u_l) - \tilde{\omega}_o \tilde{\theta}^i C_J r_l \\ & + 2\tilde{\omega}_o \tilde{\omega}_{bi} C_J r_l + 2\tilde{\omega}_o C_J \tilde{\omega}_J (r_l + u_l) - 2\tilde{\omega}_o \tilde{\theta}^i C_J \tilde{\omega}_J r_l \\ & + \tilde{\omega}_{bi} C_J r_l + 2\omega_{bi} C_J \omega_J r_l + C_J \tilde{\omega}_J \tilde{\omega}_J (r_l + u_l) \\ & - \tilde{\theta}^i C_J \tilde{\omega}_J \tilde{\omega}_J r_l + C_J \dot{\tilde{\omega}}_J (r_l + u_l) - \tilde{\theta}^i C_J \dot{\tilde{\omega}}_J r_l + 2\tilde{\omega}_o C_J \dot{u}_l \} \\ & \left. + 2\tilde{\omega}_J \dot{u}_l + \ddot{u}_l \right] \\ = & m_l x_J^T \left[(C_J^T) (\{\tilde{\omega}_o \tilde{\omega}_o (R_o + q_i + x_i) + 2\tilde{\omega}_o (\dot{R}_o + \dot{x}_i) + \ddot{\tilde{\omega}}_o (R_o + q_i + x_i) \right. \\ & + \ddot{R}_o + \ddot{x}_i \} + \{\tilde{\omega}_o \tilde{\omega}_o - \tilde{\omega}_o \tilde{\omega}_o \tilde{\theta}^i + \dot{\tilde{\omega}}_o - \dot{\tilde{\omega}}_o \tilde{\theta}^i + 2\tilde{\omega}_o \tilde{\omega}_{bi} + \ddot{\tilde{\omega}}_{bi} \} h'_J \\ & + \tilde{\omega}_o \tilde{\omega}_o C_J (r_l + u_l) - \tilde{\omega}_o \tilde{\omega}_o \tilde{\theta}^i C_J r_l + \dot{\tilde{\omega}}_o C_J (r_l + u_l) - \tilde{\omega}_o \tilde{\theta}^i C_J r_l \\ & + 2\tilde{\omega}_o \tilde{\omega}_{bi} C_J r_l + 2\tilde{\omega}_o C_J \tilde{\omega}_J (r_l + u_l) - 2\tilde{\omega}_o \tilde{\theta}^i C_J \omega_J r_l + \tilde{\omega}_{bi} C_J r_l \\ & + 2\tilde{\omega}_{bi} C_J \omega_J r_l + C_J \tilde{\omega}_J \tilde{\omega}_J (r_l + u_l) - \cancel{\tilde{\theta}^i C_J \tilde{\omega}_J \tilde{\omega}_J r_l} + C_J \dot{\tilde{\omega}}_J (r_l + u_l) \\ & - \cancel{\tilde{\theta}^i C_J \dot{\tilde{\omega}}_J r_l} + 2\tilde{\omega}_o C_J \dot{u}_l + \tilde{\theta}^i \tilde{\omega}_o \tilde{\omega}_o (R_o + q_i + x_i) + 2\tilde{\theta}^i \omega_o (\dot{R}_o + \dot{x}_i) \end{aligned}$$

$$\begin{aligned}
& + \tilde{\theta}^i \tilde{\omega}_o (R_o + q_i + x_i) + \tilde{\theta}^i \ddot{R}_o + \tilde{\theta}^i \ddot{x}_i + \theta^i \tilde{\omega}_o \tilde{\omega}_o h'_J + \tilde{\theta}^i \dot{\tilde{\omega}}_o h'_J \\
& + \tilde{\theta}^i \tilde{\omega}_o \tilde{\omega}_o C_J r_{\ell} + \tilde{\theta}^i \dot{\tilde{\omega}}_o C_J r_{\ell} + 2\tilde{\theta}^i \tilde{\omega}_o C_J \omega_J r_{\ell} + \cancel{\tilde{\theta}^i C_J \tilde{\omega}_J \tilde{\omega}_J r_{\ell}} \\
& \left[\cancel{\tilde{\theta}^i C_J \dot{\tilde{\omega}}_J r_{\ell}} + 2\tilde{\omega}_J \dot{u}_{\ell} + \ddot{u}_{\ell} \right]
\end{aligned}$$

Small space station motion may be assumed and therefore

$$\begin{aligned}
\{F_{\ell}\} &= m_{\ell} X_J^T \left[(C_J^T) \left(\dot{\tilde{\omega}}_o q_i + \ddot{R}_o + \ddot{x}_i + \tilde{\omega}_o h'_J + \dot{\tilde{\omega}}_{bi} h'_J \right. \right. \\
& + \dot{\tilde{\omega}}_o C_J r_{\ell} + 2\tilde{\omega}_o C_J \tilde{\omega}_J r_{\ell} + \dot{\tilde{\omega}}_{bi} C_J r_{\ell} + 2\tilde{\omega}_{bi} C_J \tilde{\omega}_J r_{\ell} \quad (4.13) \\
& \left. \left. + C_J \tilde{\omega}_J \tilde{\omega}_J (r_{\ell} + u_{\ell}) + C_J \dot{\tilde{\omega}}_J (r_{\ell} + u_{\ell}) + 2\tilde{\omega}_J \dot{u}_{\ell} + \ddot{u}_{\ell} \right) \right]
\end{aligned}$$

$$\text{Letting } q = \left[u_{11}, u_{12}, u_{13}, \dots, u_{n1}, u_{n2}, u_{n3} \right]^T$$

$$\begin{aligned}
[M] \ddot{q} + [K] q &= - [G] \dot{q} - [B] q + [R] \{RB\} \\
& + \{L\} + [s_2] \{\ddot{s}\} \quad (4.14)
\end{aligned}$$

where

$$[G] = \text{Diag } (2 \bar{m}_1 \tilde{\omega}_J, 2 \bar{m}_2 \tilde{\omega}_J, \dots, 2 m_n \tilde{\omega}_J)$$

$3n \times 3n$

$$[B] = \text{Diag } (\bar{m}_1 (\dot{\tilde{\omega}}_J + \tilde{\omega}_J \tilde{\omega}_J), \dots, \bar{m}_n (\dot{\tilde{\omega}}_J + \tilde{\omega}_J \tilde{\omega}_J))$$

$3n \times 3n$

$$\left\{ \begin{matrix} \ddot{R}_o \\ \dot{\omega}_o \\ \dot{\omega}_{A1} \\ \dot{\omega}_{A2} \end{matrix} \right\}_{RB} = \begin{bmatrix} \ddot{R}_o \\ \dot{\omega}_o \\ \dot{\omega}_{A1} \\ \dot{\omega}_{A2} \end{bmatrix}_{10 \times 1}$$

$$\left\{ \omega_J \right\}_{3 \times 1} = \begin{bmatrix} C_J^* \\ C_J^* \\ C_J^* \end{bmatrix}_{3 \times 2}^T \begin{bmatrix} KG & 0 \\ 0 & 1 \end{bmatrix} \left\{ \omega_{AJ} \right\}_{2 \times 1}$$

NOTE: Motion of rotating arrays is exactly as defined in Section 4.1 with only two rotation degrees of freedom allowed.

$$\left\{ \begin{matrix} \ddot{s} \\ \dot{s} \end{matrix} \right\} = \begin{pmatrix} \ddot{x}_i \\ \dot{\omega}_{bi} \end{pmatrix}_{6 \times 1}$$

$$\left[\begin{matrix} s_2 \\ \vdots \\ \vdots \\ \vdots \end{matrix} \right]_{3n \times 6} = \left[\begin{array}{cc|c} -\bar{m}_1 C_J^T & \bar{m}_1 C_J^T & [h'_J \widetilde{+} C_J r_1] \\ \vdots & \vdots & \vdots \\ \vdots & \vdots & \vdots \\ \vdots & \vdots & \vdots \\ \hline -\bar{m}_n C_J^T & \bar{m}_n C_J^T & [h'_J \widetilde{+} C_J r_n] \end{array} \right]$$

$$\left[\begin{matrix} R_1 \\ \vdots \\ \vdots \\ \vdots \end{matrix} \right]_{3n \times 10} = \left[\begin{array}{cc|cc|c} -\bar{m}_1 C_J^T & \bar{m}_1 C_J^T & [q_i + h'_J + C_1 r_1] & \bar{m}_1 \widetilde{r}_1 C_1^{*T} \begin{bmatrix} KG & 0 \\ 0 & 1 \end{bmatrix} & 0 \\ \vdots & \vdots & \vdots & \vdots & 0 \\ \vdots & \vdots & \vdots & \vdots & 0 \\ \vdots & \vdots & \vdots & \vdots & 0 \\ \hline -\bar{m}_n C_J^T & \bar{m}_n C_J^T & [q_i + h'_J + C_1 r_n] & \bar{m}_n \widetilde{r}_n C_1^{*T} \begin{bmatrix} KG & 0 \\ 0 & 1 \end{bmatrix} & 0 \end{array} \right]$$

$$\begin{aligned} \{L\}_{3n \times 1} &= - [m] \cdot \text{Diag} \left(C_J^T (2 \tilde{\omega}_0 C_J \tilde{\omega}_J + C_J \tilde{\omega}_J \tilde{\omega}_J), \dots \right) \bar{r} \\ \bar{r}_{3n \times 1} &= \begin{bmatrix} r_{11}, r_{12}, r_{13}, \dots & & r_{n1}, r_{n2}, r_{n3} \end{bmatrix}^T \end{aligned}$$

4.2.3.3 Modal Analysis

$$q = \Phi \eta$$

$$\Phi^T [m] \Phi = I$$

$$\begin{aligned} & -\Phi^T [R] \{RB\} - \Phi^T [s_2] [\delta_R] \{\ddot{\eta}_s\} \\ & + \{\ddot{\eta}_R\} + \left[2 \zeta \omega_s \right] \{\dot{\eta}_R\} + \left[\omega_s^2 \right] \{\eta_R\} \\ & = -\Phi^T [G] \Phi \{\dot{\eta}_R\} - \Phi^T [B] \Phi \{\eta_R\} + \Phi^T \{L\} \end{aligned} \tag{4.}$$

In summary, the above equation was derived assuming

- (a) base motion of the rotating array includes translations and rotations due to both space station rigid body motion and space station flexible motion
- (b) the rotating array is modeled by discrete masses; cantilever modes are used to define its modal motion
- (c) rotational motions of the array may be constrained as previously derived in Section 4.1.
- (d) the above equations are derived in the coordinate frame of the rotating array
- (e) small motion of the rotating arrays is not assumed to further linearize the above equation

4.2.4 TOTAL SYSTEM EQUATION

The above derived equations, along with the rigid body equations of Reference 4.1 can be combined into one large matrix ordinary differential equation of the form

$$\left\langle \begin{matrix} [M] \ddot{x} + [C] \dot{x} + [K] x = P \end{matrix} \right\rangle \quad (4.16)$$

where

$$\ddot{x} = \begin{bmatrix} \ddot{R} \\ \ddot{n}_s \\ \ddot{n}_R \\ \ddot{n}_F \end{bmatrix}$$

The column dimensional size of Equation 4.16 is equal to $N_{TT} = 10 + N_s + N_R + N_F \leq 70$.

N_s - total number of simulated flexible space station modes

N_R - total number of flexible cantilever modes associated with 0, 1, or 2 rotating arrays ($= N_{R1} + N_{R2}$)

N_F - total number of flexible cantilever modes associated with 0, 1, 2, 3, or 4 fixed appendages ($= N_{F1} + N_{F2} + N_{F3} + N_{F4}$)

Before preceding with the make up of the [M], [C], [K], [X], & [P] matrices it should again be made very clear that rotational motion of the two rotating arrays is exactly as defined in Section 4.1. Only two rotational degrees of freedom are allowed. Likewise, either axis of both drivers may be locked. No attempt has been made here to recount these equation derivations, or those involving array driver gear trains, etc.

The only departure from the equations derived in Sections 4.2, 4.3 and 4.4 has been to assume that the distances from the attachment points of rotating arrays (\bar{h}'_J) and fixed appendages (\bar{h}'_F) to the center of mass is negligible. This assumption has been made since the space station will be modeled as a collection of particle masses, with moments of inertia possible for each. This places the base of each array and appendage at a mass grid pt. of the space station. Therefore:

$$\vec{q}_{FJ} = \vec{h}_{FJ}$$

$$\vec{q}_{RJ} = \vec{h}_J$$

Submatrices of $\{\ddot{x}\}$

$$\begin{matrix} \{\ddot{R}\} \\ 10 \times 1 \end{matrix} = \begin{bmatrix} \ddot{R}_0 \\ \varepsilon_0 \\ \varepsilon_{A1} \\ \varepsilon_{A2} \end{bmatrix}$$

- rigid modes of space and two rotating arrays.

$$\left\{ \begin{matrix} \dots \\ n \\ \dots \end{matrix} \right\}_R = \begin{bmatrix} \dots \\ n \\ \dots \\ n \end{bmatrix} \begin{matrix} N_{R1} \times 1 \\ \\ \\ N_{R2} \times 1 \end{matrix}$$

$$\left\{ \begin{matrix} \dots \\ n \\ \dots \end{matrix} \right\}_F = \begin{bmatrix} \dots \\ n \\ \dots \\ n \\ \dots \\ n \end{bmatrix} \begin{matrix} N_{F1} \times 1 \\ \\ N_{F2} \times 1 \\ \\ N_{F3} \times 1 \\ \\ N_{F4} \times 1 \end{matrix}$$

$$\left\{ \begin{matrix} \dots \\ n \\ \dots \end{matrix} \right\}_S = \begin{bmatrix} \dots \\ n \end{bmatrix} N_S \times 1$$

$$[M] = \begin{bmatrix} M_{11} & M_{12} & M_{13} & M_{14} \\ M_{21} & M_{22} & M_{23} & M_{24} \\ M_{31} & M_{32} & I & 0 \\ M_{41} & M_{42} & 0 & I \end{bmatrix}$$

$$C = \begin{bmatrix} 0 & 0 & 0 & 0 \\ 0 & 2\zeta_s \omega_s & 0 & 0 \\ 0 & 0 & 2\zeta_r \omega_r & 0 \\ 0 & 0 & 0 & 2\zeta_F \omega_F \end{bmatrix} + \begin{bmatrix} 0 & 0 & 0 & 0 \\ 0 & 0 & 0 & 0 \\ 0 & 0 & \begin{matrix} \Phi & T \\ R1 & G1R1 \end{matrix} & 0 \\ 0 & 0 & 0 & \begin{matrix} \Phi & T \\ R2 & G2R2 \end{matrix} \\ 0 & 0 & 0 & 0 \end{bmatrix}$$

$$P = \begin{bmatrix} P_1 & 10 \times 1 \\ P_2 & N_s \times 1 \\ P_3 & N_R \times 1 \\ P_4 & N_F \times 1 \end{bmatrix}$$

$$K = \begin{bmatrix} 0 & 0 & 0 & 0 \\ 0 & \omega_s^2 & 0 & 0 \\ 0 & 0 & \omega_R^2 & 0 \\ 0 & 0 & 0 & \omega_F^2 \end{bmatrix} + \begin{bmatrix} 0 & 0 & 0 & 0 \\ 0 & 0 & 0 & 0 \\ 0 & 0 & \phi_1^T B_1 \phi_1 & 0 \\ 0 & 0 & 0 & \phi_2^T B_2 \phi_2 \end{bmatrix}$$

As the above partitioning implies, Equation 4.16 is generated via four coupled matrix equations:

$$[M_{11}] \ddot{R} + [M_{12}] \ddot{n}_s + [M_{13}] \ddot{n}_R + [M_{14}] \ddot{n}_F = P_1 \quad (4.17)$$

$$[M_{21}] \ddot{R} + [M_{22}] \ddot{n}_s + [M_{23}] \ddot{n}_R + [M_{24}] \ddot{n}_F \quad (4.18)$$

$$+ [2 \zeta_s \omega_s] \dot{n}_s + [\omega_s^2] n_s = P_2$$

$$[M_{31}] \ddot{R} + [M_{32}] \ddot{n}_s + [I] \ddot{n}_R + 0 \quad (4.19)$$

$$+ [2 \zeta_R \omega_R] \dot{n}_R + [\omega_R^2] n_R = P_3$$

$$[M_{41}] \ddot{R} + [M_{42}] \ddot{n}_s + 0 + [I] \ddot{n}_F \quad (4.20)$$

$$+ [2 \zeta_F \omega_F] \dot{n}_F + [\omega_F^2] n_F = P_4$$

Discussing each equation in detail:

Equation 4.17 is the basic rigid body system equation of Section 4.1 with only slight modification

- (1) Forces and Torques on the system induced by the flexible appendage transient response are, in their own basis

$$\begin{array}{l}
 \hat{F}_J = - \sum_E^T M_{RJ} \Phi_{RJ} \ddot{n}_{RJ} \\
 \hat{T}_J = - \sum_E^T \tilde{r}_{RJ} M_{RJ} \Phi_{RJ} \ddot{n}_{RJ} \\
 \hat{F}_{FJ} = - \sum_E^T M_{FJ} \Phi_{FJ} \ddot{n}_{FJ} \\
 \hat{T}_{FJ} = - \sum_E^T \tilde{r}_{FJ} M_{FJ} \Phi_{FJ} \ddot{n}_{FJ}
 \end{array}
 \left. \begin{array}{l}
 \\
 \\
 \\
 \end{array} \right\}
 \begin{array}{l}
 \text{rotating} \\
 \text{appendages} \\
 J = 1, 2 \\
 \\
 \text{fixed} \\
 \text{appendages} \\
 J = 1, 2, 3, 4
 \end{array}$$

- (2) Addition of applied external torque \bar{T}_R if desired
- (3) Mass and moment of inertia of space station includes that do to any fixed appendages.
- (4) Inclusion of terms dependent upon modal acceleration of space station at attachment points of appendages, (see 4.6.3).

Partitioning equation 4.17 into four equations:

$$\begin{aligned}
 A_1 \ddot{R}_O + A_5 \ddot{\omega}_O + A_9 \dot{\omega}_{A1} + A_{13} \dot{\omega}_{A2} & \qquad (4-21) \\
 - \sum_J^2 C_J \hat{F}_J - \sum_J^4 C_{FJ} \hat{F}_{FJ} \\
 - \sum_J^2 F'_J - \sum_J^4 F'_{FJ} & = F_1
 \end{aligned}$$

$$\begin{aligned}
& A_2 \ddot{R}_O + A_6 \dot{\omega}_O + A_{10} \dot{\omega}_{A1} + A_{13} \dot{\omega}_{A2} \\
& - \sum_J^2 C_J \hat{T}_J + \sum_J^2 \tilde{r}'_J C_J \hat{F}_J - \sum_J^4 C_{FJ} \hat{T}_{FJ} + \sum_J^4 \tilde{r}'_{FJ} C_{FJ} \hat{F}_{FJ} \quad (4.22) \\
& - \sum_J^2 T'_J - \sum_J^4 T'_{FJ} = T_R + F_2
\end{aligned}$$

$$A_3 \ddot{R}_O + A_7 \dot{\omega}_O + A_{11} \dot{\omega}_{A1} + A_{15} \dot{\omega}_{A2} - T''_1 = F_3 \quad (4.23)$$

$$A_4 \ddot{R}_O + A_8 \dot{\omega}_O + A_{12} \dot{\omega}_{A1} + A_{16} \dot{\omega}_{A2} - T''_2 = F_4 \quad (4.24)$$

$$\therefore \begin{bmatrix} M_{11} \end{bmatrix} = \begin{bmatrix} A_1 & A_5 & A_9 & A_{13} \\ A_2 & A_6 & A_{10} & A_{14} \\ A_3 & A_7 & A_{11} & A_{15} \\ A_4 & A_8 & A_{12} & A_{16} \end{bmatrix}$$

10 x 10

previously defined rigid body
matrix A of Section 4.1.

$$\begin{bmatrix} M_{12} \end{bmatrix} = \sum_{i=1}^4 \begin{bmatrix} -\bar{m}_{F_i} & \bar{m}_{F_i} (C_{F_i} r_{F_i}) \\ -\bar{m}_{F_i} (C_{F_i} \tilde{r}_{F_i}) + \tilde{r}_{F_i}' - \bar{m}_{F_i} & \bar{m}_{F_i} (C_{F_i} \tilde{r}_{F_i})^2 - C_{F_i}^T C_{F_i} \tilde{r}_{F_i} \bar{m}_{F_i} (C_{F_i} \tilde{r}_{F_i}) \\ \bar{m}_{F_i} & -\bar{m}_{F_i} C_{F_i}^T \tilde{r}_{F_i} \bar{m}_{F_i} (C_{F_i} \tilde{r}_{F_i}) \end{bmatrix} \begin{bmatrix} G_{F_i}'^T \\ G_{F_i}''^T \end{bmatrix}$$

$$\sum_{j=1}^2 \begin{bmatrix} -\bar{m}_j & \bar{m}_j (C_{jJ} r_j) \\ -\bar{m}_j (C_{jJ} \tilde{r}_j) + \tilde{r}_j \bar{m}_j & \bar{m}_j (C_{jJ} \tilde{r}_j)^2 - C_{jJ}^T C_{jJ} \tilde{r}_j \bar{m}_j (C_{jJ} \tilde{r}_j) \\ 0 & 0 \end{bmatrix} \begin{bmatrix} G_{R_j}'^T \\ G_{R_j}''^T \end{bmatrix}$$

(10 x 6)

6 x N_S

$$\begin{bmatrix} M_{13} \\ 10 \times N_R \end{bmatrix} = \begin{bmatrix} + C_1 D_{R1} & + C_2 D_{R2} \\ + C_1 R_{R1} - \tilde{r}'_1 C_1 D_{R1} & + C_2 R_{R2} - \tilde{r}'_2 C_2 D_{R2} \\ 0 & 0 \end{bmatrix}$$

$3 \times N_{R1} \qquad 3 \times N_{R2}$
 $3 \times N_{R1} \qquad 3 \times N_{R2}$
 $4 \times N_{R1} \qquad 4 \times N_{R2}$
 $10 \times N_{R1} \qquad 10 \times N_{R1}$

where

$$\begin{bmatrix} D_{RJ} \\ 3 \times N_{RJ} \end{bmatrix} = \sum_E^T M_{RJ} \Phi_{RJ} \quad J = 1,2$$

$$\begin{bmatrix} R_{RJ} \\ 3 \times N_{RJ} \end{bmatrix} = \sum_E^T \tilde{r}_{RJ} M_{RJ} \Phi_{RJ} \quad J = 1,2$$

$$\begin{bmatrix} M_{14} \\ 10 \times N_F \end{bmatrix} = \begin{bmatrix} +C_{F1} D_{F1} & +C_{F2} D_{F2} & +C_{F3} D_{F3} & +C_{F4} D_{F4} \\ 3 \times N_{F1} & 3 \times N_{F2} & 3 \times N_{F3} & 3 \times N_{F4} \\ +C_{F1} R_{F1} - \tilde{r}'_{F1} C_{F1} D_{F1} & +C_{F2} R_{F2} - \tilde{r}'_{F2} C_{F2} D_{F2} & +C_{F3} R_{F3} - \tilde{r}'_{F3} C_{F3} D_{F3} & +C_{F4} R_{F4} - \tilde{r}'_{F4} C_{F4} D_{F4} \\ 3 \times N_{F1} & 3 \times N_{F2} & 3 \times N_{F3} & 3 \times N_{F4} \\ 0 & 0 & 0 & 0 \\ 4 \times N_{F1} & 4 \times N_{F2} & 4 \times N_{F3} & 4 \times N_{F4} \end{bmatrix}$$

where

$$\begin{bmatrix} D_{FJ} \\ 3 \times N_{FJ} \end{bmatrix} = \sum_E^T M_{FJ} \Phi_{FJ}$$

$$\begin{bmatrix} R_{FJ} \\ 3 \times N_{FJ} \end{bmatrix} = \sum_E^T \tilde{r}'_{FJ} M_{FJ} \Phi_{FJ}$$

$$\begin{bmatrix} P_1 \end{bmatrix}_{10 \times 1} = \begin{bmatrix} F_1 \\ T_R + F_2 \\ F_3 \\ F_4 \end{bmatrix}$$

as previously defined in Section 4.1
except for addition of external torque T_R

Equation 4.18 is the flexible modal equation for the space station. These flexible modes are excited by external forces and torques on the space station, including those which act at the attachment points of the rotating and fixed arrays.

Equations for the various hinge forces and torques are shown in Section 4.2.5.3. The above excluded linear terms in \ddot{R}_O , $\dot{\omega}_O$, $\dot{\omega}_{A1}$, $\dot{\omega}_{A2}$ are regrouped on the left-hand side of Equation 4.16 for proper coupling with the rigid body modes (forming M_{21}). Linear terms in \ddot{n}_S are regrouped on the left-hand side of Equation 4.16 for proper coupling with the space station modes (M_{22}). Likewise, linear terms in \dot{n}_R , and \dot{n}_F form M_{23} and M_{24} , respectively.

$$[M_{21}] = -\sum_{i=1}^4 \begin{bmatrix} G_{F_i} & G_{F_i}'' \\ G_{F_i}' & G_{F_i}'' \end{bmatrix} \begin{bmatrix} -\bar{m}_{F_i} & \bar{m}_{F_i} (h_{F_i} + \widetilde{C}_{F_i} r_{F_i}) \\ -\bar{m}_{F_i} (C_{F_i} r_{F_i}) & -C_{F_i} I_{F_i} C_{F_i}^T + \bar{m}_{F_i} (C_{F_i} r_{F_i}) (h_{F_i} + \widetilde{C}_{F_i} r_{F_i}) \end{bmatrix} \begin{bmatrix} 0 \\ 0 \end{bmatrix}$$

$$-\sum_{j=1}^2 \begin{bmatrix} G_{R_j} & G_{R_j} \end{bmatrix} \begin{bmatrix} I & 0 \\ 0 & C_j^{**} \end{bmatrix} \begin{bmatrix} -\bar{m}_j & \bar{m}_j (h_j + C_j r_j) \\ -\bar{m}_j \widetilde{r}_j C_j^T & -I_j C_j^T + \bar{m}_j \widetilde{r}_j C_j^T (h_j + \widetilde{C}_j r_j) \end{bmatrix} \begin{bmatrix} a_1 & a_3 \\ a_2 & a_4 \end{bmatrix} \quad (1)$$

$$(1) \quad \text{if } J=1 \quad a_3 = a_4 = 0 \quad a_1 = \bar{m}_1 C_1 \widetilde{r}_1 C_1^{*T} \begin{bmatrix} 1/\text{KG} & 0 \\ 0 & 1 \end{bmatrix}$$

$$a_2 = -(I_1 - m_1 \widetilde{r}_1 \widetilde{r}_1^T) C_1^{*T} \begin{bmatrix} 1/\text{KG} & 0 \\ 0 & 1 \end{bmatrix}$$

$$\text{if } J=2 \quad a_1 = a_2 = 0 \quad a_3 = \bar{m}_2 C_2 \widetilde{r}_2 C_2^{*T} \begin{bmatrix} 1/\text{KG} & 0 \\ 0 & 1 \end{bmatrix}$$

$$a_4 = -(I_2 - m_2 \widetilde{r}_2 \widetilde{r}_2^T) C_2^{*T} \begin{bmatrix} 1/\text{KG} & 0 \\ 0 & 1 \end{bmatrix}$$

$$\begin{bmatrix} M_{22} \end{bmatrix}_{N_s \times N_s} = \begin{bmatrix} 1 & 0 \\ 1 & \cdot \\ 0 & 1 \end{bmatrix}_{N_s \times N_s} - \sum_J^4 \begin{bmatrix} G_{F_i}' & G_{F_i}'' & 0 \\ \hline \bar{M}_{F_i} & \bar{M}_{F_i} (C_{F_i}^r) & 0 \\ \bar{M}_{F_i} (C_{F_i}^r) & \bar{M}_{F_i} (C_{F_i}^r)^2 - C_{F_i}^r C_{F_i}^r & T \end{bmatrix}_{N_s \times 10} \begin{bmatrix} G_{F_i}^{T'} \\ \hline G_{F_i}^{T''} \end{bmatrix}_{6 \times N_s}$$

$$\sum_J^2 \begin{bmatrix} G_{R_J}' & G_{R_J}'' & 0 \\ \hline -\bar{M}_J & \bar{M}_J (C_{Jr}) & 0 \\ -M_J (C_{Jr}) & M_J (C_{Jr})^2 - C_{Jr} C_{Jr} & T \end{bmatrix}_{N_s \times 10} \begin{bmatrix} G_{R_J}^{T'} \\ \hline G_{R_J}^{T''} \end{bmatrix}_{6 \times N_s}$$

10 x 6

$$\begin{bmatrix} M_{23} \end{bmatrix} = \begin{bmatrix} +\gamma_{R1}' C_1 \Sigma_E M_{R1} \phi_{R1} & +\gamma_{R2}' C_2 \Sigma_E M_{R2} \phi_{R2} \\ +\gamma_{R1}'' C_1 \Sigma_E \tau_{R1} M_{R1} \phi_{R1} & +\gamma_{R2}'' C_2 \Sigma_E \tau_{R2} M_{R2} \phi_{R2} \end{bmatrix}$$

$$= \begin{bmatrix} +G_{R1}' C_1 D_{R1} + G_{R1}'' C_1 R_{R1} & +G_{R2}' C_2 D_{R2} + G_{R2}'' C_2 R_{R2} \\ (N_s \times N_{R1}) & (N_s \times N_{R2}) \end{bmatrix}$$

(N_s x N_R)

$$\begin{bmatrix} M_{24} \end{bmatrix} = \begin{bmatrix} +G_{F1}' C_{F1} D_{F1} + G_{F1}'' C_{F1} R_{F1} & +G_{F2}' C_{F2} D_{F2} + G_{F2}'' C_{F2} R_{F2} & +G_{F3}' C_{F3} D_{F3} + G_{F3}'' C_{F3} R_{F3} & +G_{F4}' C_{F4} D_{F4} + G_{F4}'' C_{F4} R_{F4} \\ N_s \times N_{F1} & N_s \times N_{F2} & N_s \times N_{F3} & N_s \times N_{F4} \end{bmatrix}$$

where

$\begin{bmatrix} G_{RJ}' \end{bmatrix}$ - the transpose of those rows of the modal space station matrix which define the total flexural 3-dimensional displacement of the rigid body of the space station to which the j^{th} rotating appendage is attached.
($N_s \times 3$)

$\begin{bmatrix} G_{RJ}'' \end{bmatrix}$ - the transpose of those rows of the modal space station matrix which define the total flexural 3-dimensional rotation of the rigid body of the space station to which the j^{th} rotating appendage is attached.
($N_s \times 3$)

Like definitions are also true for submatrices G_{F_i}' and G_{F_i}'' at the attachment points of each fixed appendage.

$$\begin{aligned}
\begin{bmatrix} P_2 \\ N_S \times 1 \end{bmatrix} &= \sum_{i=1}^2 \begin{bmatrix} G_{E_i} \end{bmatrix} F_{R_i} + \sum_{i=1}^2 \begin{bmatrix} G_{E_i}'' \end{bmatrix} T_{R_i} + \sum_{i=1}^2 \begin{bmatrix} G_{R_i}' \end{bmatrix} (-F_{H_i}') \\
&+ \sum_{i=1}^2 \begin{bmatrix} G_{R_i}'' \end{bmatrix} (-T_i + T_{AC_i}') + \begin{bmatrix} G_{CMG}'' \end{bmatrix} T_{CMG} \\
&+ \sum_{i=1}^4 \begin{bmatrix} G_{F_i}' \end{bmatrix} (-F_{H_{F_i}}') + \sum_{i=1}^4 \begin{bmatrix} G_{F_i}'' \end{bmatrix} (-T_{H_{F_i}}')
\end{aligned}$$

where

F_{HJ}' - hinge force on the j^{th} rotating array due to rigid body motion of the array, excluding linear terms in \dot{R}_o , $\dot{\omega}_o$, $\dot{\omega}_{A1}$, $\dot{\omega}_{A2}$, \dot{n}_s

T_{AC_J}' - constraint torque exerted on spacecraft by rigid driver along constrained axis, excluding linear terms, (contains hinge torque).

T_J - hinge torque on j^{th} driver produced by control system.

$F_{H_{F_i}}'$ - hinge force on i^{th} fixed appendage excluding linear terms.

$T_{H_{F_i}}'$ - hinge torque on i^{th} fixed appendage excluding linear terms.

G_x' - modal columns (eigenvectors) associated with modal displacements at grid point to which "x" array is attached or external force or torque acts.

G_x'' - modal columns associated with modal rotations at grid point to which "x" array is attached or external force or torque acts.

Equation 4.19 is the rotating appendage modal equation in which

$$\begin{bmatrix} M_{31} \\ N_R \times 10 \end{bmatrix} = \begin{bmatrix} -\phi_{R1}^T [R_1] \\ \hline -\phi_{R2}^T [R_2] \end{bmatrix}$$

$$= \begin{bmatrix} -\phi_{R1}^T [m_{R1}] \left[\begin{array}{c|c} -\Sigma_E C_1^T & \Sigma_E C_1^T \tilde{q}_{R1} + \tilde{r}_{R1} \Sigma_E C_1^T \\ \hline \Sigma_E C_1^T & \tilde{r}_{R1} \Sigma_E C_1^* \end{array} \right] \begin{bmatrix} 1/KG & 0 \\ 0 & 1 \end{bmatrix} & 0 \\ \hline -\phi_{R2}^T [m_{R2}] \left[\begin{array}{c|c} -\Sigma_E C_2^T & \Sigma_E C_2^T \tilde{q}_{R2} + \tilde{r}_{R2} \Sigma_E C_2^T \\ \hline \Sigma_E C_2^T & \tilde{r}_{R2} \Sigma_E C_2^* \end{array} \right] \begin{bmatrix} 1/KG & 0 \\ 0 & 1 \end{bmatrix} & 0 \end{bmatrix}$$

$$= \begin{bmatrix} D_{R1}^T C_1^T & -D_{R1}^T C_1^T \tilde{q}_{R1} + R_{R1}^T C_1^T & R_{R1}^T C_1^* \begin{bmatrix} 1/KG & 0 \\ 0 & 1 \end{bmatrix} & 0 \\ \hline D_{R2}^T C_2^T & -D_{R2}^T C_2^T \tilde{q}_{R2} + R_{R2}^T C_2^T & 0 & R_{R2}^T C_2^* \begin{bmatrix} 1/KG & 0 \\ 0 & 1 \end{bmatrix} \end{bmatrix}$$

$N_R \times 3$ $N_R \times 3$ $N_R \times 2$ $N_R \times 2$

$$[M_{32}] = \begin{bmatrix} -\phi_{R1}^T & S_2 & \gamma_R^1 \\ -\phi_{R2}^T & S_2 & \gamma_R^2 \end{bmatrix}$$

$$= \begin{bmatrix} -\phi_{R1}^T [m_{R1}] & [-\Sigma_E C_1^T] & \tilde{r}_{R1} & \Sigma_E C_1^T & \left[\begin{matrix} 1 \\ \gamma_R \end{matrix} \right] \\ -\phi_{R2}^T [m_{R2}] & [-\Sigma_E C_2^T] & \tilde{r}_{R2} & \Sigma_E C_2^T & \left[\begin{matrix} 2 \\ \gamma_R \end{matrix} \right] \end{bmatrix}$$

$$= \begin{bmatrix} D_{R1}^T C_1^T G_{R1}^T + R_{R1}^T C_1^T G_{R1}^{\prime\prime T} & \\ & (N_{R1} \times N_s) \\ \hline D_{R2}^T C_2^T G_{R2}^T + R_{R2}^T C_2^T G_{R2}^{\prime\prime T} & \\ & (N_{R2} \times N_s) \end{bmatrix}$$

$$N_R \times N_s$$

N. B. $[M_{32}] = + [M_{23}]^T$

$$\begin{bmatrix} P_3 \\ N_R \times 1 \end{bmatrix} = \begin{bmatrix} T \phi_{R_1} & L_1 & N_{R_1} \times 1 \\ \hline T \phi_{R_2} & L_2 & N_{R_2} \times 1 \end{bmatrix}$$

Equation 4.20 is the modal equation for the fixed appendages

$$\begin{bmatrix} M_{41} \\ N_F \times 10 \end{bmatrix} = \begin{bmatrix} -\phi_{F1}^T [R_{F1}] \\ -\phi_{F2}^T [R_{F2}] \\ -\phi_{F3}^T [R_{F3}] \\ -\phi_{F4}^T [R_{F4}] \end{bmatrix}$$

$$\begin{bmatrix} D_{F1}^T C_{F1}^T & | & - D_{F1}^T C_{F1}^T \tilde{q}_{F1} + R_{F1}^T C_{F1}^T & | & 0 \\ \hline D_{F2}^T C_{F2}^T & | & - D_{F2}^T C_{F2}^T \tilde{q}_{F2} + R_{F2}^T C_{F2}^T & | & 0 \\ \hline D_{F3}^T C_{F3}^T & | & - D_{F3}^T C_{F3}^T \tilde{q}_{F3} + R_{F3}^T C_{F3}^T & | & 0 \\ \hline D_{F4}^T C_{F4}^T & | & - D_{F4}^T C_{F4}^T \tilde{q}_{F4} + R_{F4}^T C_{F4}^T & | & 0 \end{bmatrix}$$

$N_F \times 10$

$$\begin{bmatrix} M_{42} \end{bmatrix} = \begin{bmatrix} -\phi_{F1}^T \begin{bmatrix} S_2^{F1} \end{bmatrix} \begin{bmatrix} \gamma_{F1} \end{bmatrix} \\ \hline -\phi_{F2}^T \begin{bmatrix} S_2^{F2} \end{bmatrix} \begin{bmatrix} \gamma_{F2} \end{bmatrix} \\ \hline -\phi_{F3}^T \begin{bmatrix} S_2^{F3} \end{bmatrix} \begin{bmatrix} \gamma_{F3} \end{bmatrix} \\ \hline -\phi_{F4}^T \begin{bmatrix} S_2^{F4} \end{bmatrix} \begin{bmatrix} \gamma_{F4} \end{bmatrix} \end{bmatrix}$$

$$\begin{bmatrix} D_{F1}^T C_{F1}^T G_{F1}'^T + R_{F1}^T C_{F1}^T G_{F1}''^T \\ \hline D_{F2}^T C_{F2}^T G_{F2}'^T + R_{F2}^T C_{F2}^T G_{F2}''^T \\ \hline D_{F3}^T C_{F3}^T G_{F3}'^T + R_{F3}^T C_{F3}^T G_{F3}''^T \\ \hline D_{F4}^T C_{F4}^T G_{F4}'^T + R_{F4}^T C_{F4}^T G_{F4}''^T \end{bmatrix}$$

$N_F \times N_S$

$$\begin{matrix} \begin{bmatrix} P_4 \end{bmatrix} \\ N_F \times 1 \end{matrix} = 0 \\ \text{N. B. } \begin{bmatrix} M_{42} \end{bmatrix} = + \begin{bmatrix} M_{24} \end{bmatrix}^T$$

4.2.5 AUXILIARY EQUATIONS

4.2.5.1 When free-free modes are utilized in the definition of spacecraft flexibility it can be shown that

$$\begin{matrix}
 \left[\begin{matrix} \gamma^T \\ N_s \end{matrix} \right]_{N_s \times 6n} \cdot \left[\begin{array}{c|c} -\bar{m}_1 & \bar{m}_1 (R_o + \tilde{q}_1) \\ \hline 0 & -\bar{I}^{-1} \\ \hline -\bar{m}_2 & \bar{m}_2 (R_o + \tilde{q}_2) \\ \hline \vdots & \vdots \\ \hline \vdots & \vdots \\ \hline \vdots & \vdots \end{array} \right]_{6n \times 6} = 0
 \end{matrix}$$

Considering the first term of the product,

$$\left[\gamma^T \right] \begin{bmatrix} \bar{m}_1 \\ 0 \\ \bar{m}_2 \\ 0 \\ \vdots \\ \vdots \end{bmatrix}_{6n \times 3} = 0$$

Since for the free-free case, the spacecraft structure is in dynamic equilibrium with respect to all forces such that

$$\ddot{n}_i \sum_J \gamma_{iJ} m_J = 0 \quad (\text{Force})$$

This equilibrium condition also applies to torques.

$$\therefore \gamma^T \begin{bmatrix} 0 \\ \frac{\bar{I}^1}{\bar{I}} \\ 0 \\ \frac{\bar{I}^2}{\bar{I}} \\ \vdots \\ \vdots \end{bmatrix} = 0$$

6n x 3

Rearranging the remaining terms $m_i (R_o \hat{+} q_i)$ by letting

$$R_o^1 = R_o + \bar{q}$$

$$q_i^1 = q_i - \bar{q}$$

where \bar{q} is the constant vector from point O_B to the center of gravity of the undeformed system.

$$\therefore \gamma^T \begin{bmatrix} \frac{\bar{m}_1 (R_o^1 + q_1^1)}{\bar{m}_1} \\ 0 \\ \frac{\bar{m}_2 (R_o^1 + q_2^1)}{\bar{m}_2} \\ 0 \\ \vdots \\ \vdots \end{bmatrix} = \begin{bmatrix} \bar{m}_1 \\ 0 \\ \bar{m}_2 \\ 0 \\ \vdots \\ \vdots \end{bmatrix} \left(\sum_E R_o^1 \right) + \gamma^T \begin{bmatrix} \bar{m}_1 q_1^1 \\ 0 \\ \bar{m}_2 q_2^1 \\ 0 \\ \vdots \\ \vdots \end{bmatrix} = 0$$

The first term is zero as shown previously. The second term is also zero since

$$\sum_J \gamma_{iJ} m_J q_J^1$$

represents the moment about the center of mass which equals zero in the free-free case.

4.2.5.2 Nastran Algorithm

The integration of the system equation developed in Section 4.2.4 will be accomplished by use of the Nastran algorithm.

$$\left[\frac{M}{\Delta t^2} + \frac{C}{2\Delta t} + \frac{K}{3} \right] \{X_{\eta+2}\} = \frac{1}{3} \left[P_{\eta+2} + P_{\eta+1} + P_{\eta} \right] \\ + \left[\frac{2M}{\Delta t^2} - \frac{K}{3} \right] \{X_{\eta+1}\} + \left[-\frac{M}{\Delta t^2} + \frac{C}{2\Delta t} - \frac{K}{3} \right] \{X_{\eta}\}$$

$$\left\{ \dot{X}_{\eta} \right\} = \frac{1}{2\Delta t} \left[\left\{ X_{\eta+1} \right\} - \left\{ X_{\eta-1} \right\} \right]$$

$$\left\{ \ddot{X}_{\eta} \right\} = \frac{1}{\Delta t^2} \left[\left\{ X_{\eta+1} \right\} - 2 \left\{ X_{\eta} \right\} - \left\{ X_{\eta-1} \right\} \right]$$

* See Reference 4.7

4.2.5.3 Interaction Forces and Torques

The interaction forces (torques) which exist at the attachment points of the various arrays are calculated by summing the hinge force (torque) due to rigid body motion of the system at the attachment point and the flexible appendage transient response.

Hinge force for rotating array*:

$$F_{H_i} = m_i \left[\ddot{R}_0 + 2 \tilde{\omega}_0 \dot{R}_0 + (\tilde{\omega}_0 + \tilde{\omega}_0 \tilde{\omega}_0) (R_0 + h_i + C_i r_i) \right. \\ \left. + 2 \tilde{\omega}_0 C_i \tilde{\omega}_i r_i + C_i (\tilde{\omega}_i \tilde{\omega}_i + \tilde{\omega}_i) r_i \right] + F_i'$$

Hinge torque for rotating array*:

$$T_{H_i} = C_i \left[((C_i^T \omega_0) \tilde{\omega}_i + \tilde{\omega}_i) \begin{bmatrix} I_i \end{bmatrix} (\omega_i + C_i^T \omega_0) \right. \\ \left. + \begin{bmatrix} I_i \end{bmatrix} (\dot{\omega}_i + C_i^T \dot{\omega}_0) + \begin{bmatrix} I_i \end{bmatrix} (C_i^T \tilde{\omega}_0 C_i \omega_i) \right] \\ + C_i \tilde{r}_i C_i^T F_{H_i} + T_i'$$

Force induced by flexible appendage transient response

$$\hat{F}_i = - \left(\sum_E^T M_i \phi_i \right) \ddot{n}_i$$

Torque induced by flexible appendage transient response

$$\hat{T}_i = - \sum_E^T \tilde{r}_i M_i \phi_i \ddot{n}_i$$

* Equations for hinge forces and torques for fixed appendages are identical except that $\omega_i = 0$ (the negative of these hinge forces and torques acts on the space station). Admittedly, for the rotating case, some products have been neglected which couple ω_i with modal variables and ω_0 , basically assuming that ω_i will also be small.

Hinge force for rotating array due to space station modal accelerations of attachment point:

$$F_i' = \begin{bmatrix} \bar{m}_i & | & -\bar{m}_i (C_i \tilde{r}_i) \\ \hline & & \end{bmatrix} \begin{bmatrix} G_i'^T \\ -\tilde{r}_i^T \\ G_i^T \end{bmatrix} \ddot{n}_s$$

3 x 6 6 x N_s

Hinge torque for rotating array due to space station modal accelerations of attachment point:

$$T_i' = \begin{bmatrix} \bar{m}_i (C_i \tilde{r}_i) & | & C_i I_i C_i^T - \bar{m}_i (C_i \tilde{r}_i)^2 \\ \hline & & \end{bmatrix} \begin{bmatrix} G_i'^T \\ -\tilde{r}_i^T \\ G_i^T \end{bmatrix} \ddot{n}_s$$

3 x 6 6 x N_s

The total interaction force at the attachment point of an array is

$$F_{iNT_i} = -F_{H_i} + \hat{F}_i$$

Likewise, the total interaction torque acting on the space station due to the attachment of a flexible array is

$$T_{iNT_i} = -T_{H_i} + \hat{T}_i$$

4.3 FLEXIBLE SPINNING SPACE STATION

4.3.1 MODAL EQUATIONS

$$(1) \quad [m] \left[\ddot{q} \right] + [K] \{q\} = - [G] \{\dot{q}\} - [B] \{q\} + [R] \{RB\} + \{F'\} + \{L\}$$

where $[R]$ and $\{L\}$ are rigid body terms. If we choose $u = R_0 + q_i + x_i$ we can form the following set of equations of motion

$$(2) \quad [m] \{\ddot{u}\} + [G] \{\dot{u}\} + [K'] \{u\} = \{F'\}$$

where $[m]$ is mass matrix of the space station,

$[G]$ is skew symmetric matrix of coriolis acceleration terms

and $[K'] = [K_e] + [K_c] + [B]$

$[K_e]$ = elastic stiffness matrix

$[K_c]$ = symmetric matrix of centrifugal acceleration terms

$[B]$ = geometric stiffness matrix

The second-order matrix equation (2) can be reduced to a first order state equation (3) by introducing the following matrices

$$U = \begin{bmatrix} \dot{u} \\ u \end{bmatrix} \quad \text{and} \quad \dot{U} = \begin{bmatrix} \ddot{u} \\ \dot{u} \end{bmatrix}$$

$$(3) \quad [D] \{\dot{U}\} + [E] \{U\} = \{F\}$$

where

$$[D] = \begin{bmatrix} [0] & [m] \\ [m] & [G] \end{bmatrix}, \quad [E] = \begin{bmatrix} [m] & [0] \\ [0] & [K'] \end{bmatrix}$$

$$\text{and} \quad \{F\} = \begin{bmatrix} \{0\} \\ \{F'\} \end{bmatrix}$$

The reduced equation of motion (3) can be uncoupled by the transformation

$$(4) \quad \{U\} = [\Phi] \{Y\}, \quad \text{where } [\Phi] = \begin{bmatrix} \lambda_n & \phi^{(n)} \\ \dots & \dots \\ \phi^{(n)*} & \dots \end{bmatrix}$$

and the transformation matrix $[\Phi]$ consists of complex eigenvectors and their conjugates pairs.

$$[\Phi^{(n)}] = \left[\begin{array}{cccc} \{\phi^1\} & \{\phi^2\} & \dots & \{\phi^N\} \\ \{\phi^{1*}\} & \{\phi^{2*}\} & \dots & \{\phi^{N*}\} \end{array} \right], \quad [\lambda_n] = \text{DIAG}(-jw_1, \dots, -jw_n)$$

$$\{\phi^*\} = \text{complex conjugate of } \{\phi\},$$

$$Y \equiv \left[\begin{array}{cccc|cccc} Y_1 & Y_2 & \dots & Y_N & Y_1^* & Y_2^* & \dots & Y_N^* \end{array} \right]^T$$

where w_i are eigenvalues and ϕ^i are eigenvectors. In terms of the new coordinates Y , Equation (3) becomes

$$(5) \quad [D][\Phi] \{\dot{Y}\} + [E][\Phi] \{Y\} = \{F\}$$

Premultiplication of Equation (5) by $[\Phi^*]^T$

$$(6) \quad [\Phi^*]^T [D] \Phi \{\dot{Y}\} + [\Phi^*] [E] [\Phi] \{Y\} = [\Phi^*]^T \{F\}$$

Since $[E]$ is symmetric and $[D]$ skew symmetric, $[\Phi^*]^T [\Phi] = \text{diagonal matrix.}^{(2)}$

Writing equation (6) in simpler form

$$(7) \quad [D'] \{\dot{Y}\} + [E'] \{Y\} = [\Phi^*]^T \{F\}$$

where

$$\begin{aligned} [D'] &= [\Phi^*]^T [D] [\Phi] = \text{diagonal matrix} \\ [E'] &= [\Phi^*]^T [E] [\Phi] = \text{diagonal matrix} \end{aligned}$$

If $[\Lambda]$ is the matrix of the complex eigenvalues of the operator in Equation (7), then upon premultiplication by $[D']^{-1}$ we obtain

$$(8) \quad \{\dot{Y}\} = -[\Lambda] \{Y\} + \{\bar{F}\}$$

$$\text{where } \{\bar{F}\} = [D']^{-1} [\Phi^*]^T \{F\}$$

I = unity matrix

$$J = \sqrt{-1} I$$

and let

$$Z_i^{(1)} = (1/2)(Y_i + Y_i^*)$$

$$Z_i^{(2)} = (1/2)J (Y_i - Y_i^*)$$

$$(10) \quad \begin{bmatrix} \dot{\bar{Z}}^{(1)} \\ \dot{\bar{Z}}^{(2)} \end{bmatrix} = \begin{bmatrix} 0 & |\Lambda| \\ -|\Lambda| & 0 \end{bmatrix} \begin{bmatrix} \bar{Z}^{(1)} \\ \bar{Z}^{(2)} \end{bmatrix} + \begin{bmatrix} V \\ \end{bmatrix} \begin{bmatrix} F' \end{bmatrix}$$

where

$$\begin{bmatrix} V \\ \end{bmatrix} = 1/2 \begin{bmatrix} I & -I \\ J & -J \end{bmatrix} [D']^{-1} [\Phi^*]^T **$$

when N modes are retained

$$\bar{Z}^{(1)} \equiv \begin{bmatrix} Z_1^{(1)} \\ \vdots \\ Z_N^{(1)} \end{bmatrix}$$

$$\bar{Z}^{(2)} \equiv \begin{bmatrix} Z_1^{(2)} \\ \vdots \\ Z_N^{(2)} \end{bmatrix}$$

Modal damping may be introduced in Equation (1) by the matrix $-2\xi|\Lambda|$

$$(11) \quad \begin{bmatrix} \dot{\bar{Z}}^{(1)} \\ \dot{\bar{Z}}^{(2)} \end{bmatrix} + \begin{bmatrix} 0 & -|\Lambda| \\ |\Lambda| & 2\xi|\Lambda| \end{bmatrix} \begin{bmatrix} \bar{Z}^{(1)} \\ \bar{Z}^{(2)} \end{bmatrix} = \begin{bmatrix} V \\ \end{bmatrix} \begin{bmatrix} F' \end{bmatrix}$$

where $\xi =$ arbitrary chosen damping factor.

** See Section 4.3.6.

In terms of the new coordinates \bar{Z} , Equation (4) may be written as

$$(12) \quad \{U\} = [\Phi] \{Y\} = [\Phi] \begin{bmatrix} I & -J \\ I & J \end{bmatrix} \begin{bmatrix} \bar{Z}^{(1)} \\ \bar{Z}^{(2)} \end{bmatrix}$$

or

$$(13) \quad \{U\} = [W] [\bar{Z}]$$

where

$$[W] \equiv [\Phi] \begin{bmatrix} I & -J \\ I & J \end{bmatrix}$$

$$[\bar{Z}] \equiv \begin{bmatrix} \bar{Z}^{(1)} \\ \bar{Z}^{(2)} \end{bmatrix}$$

Equations (11) and (13) are to be implemented in the simulation.

N. B. If desired, the variation of ω_o about the nominal can be accommodated by setting

$$(14) \quad G' = \frac{\partial [G]}{\partial \omega}$$

$$(15) \quad B' = \frac{\partial [B]}{\partial \omega}$$

$$(16) \quad \Delta\omega = (\omega_o - \omega_{nom})$$

For this case (10) is modified to give

$$(10a) \quad \begin{bmatrix} \dot{\bar{Z}}^{(1)} \\ \dot{\bar{Z}}^{(2)} \end{bmatrix} + \begin{bmatrix} 0 & -|\bar{\Lambda}| \\ |\bar{\Lambda}| & 0 \end{bmatrix} \begin{bmatrix} \bar{Z}^{(1)} \\ \bar{Z}^{(2)} \end{bmatrix} = [V] [F'] - [V] ([G'] + [B']) \Delta\omega$$

4.3.2 RIGID BODY EQUATIONS

The equations developed in Section 4.3.1 will be used to simulate N complex flexible modes for the space station. The rigid body modes will not be used. Instead, the rigid body motion will be given by the Newton-Euler equations for the rotating space station taken as a rigid body.

The rigid body system given in Figure 4-12 describes the force and torque relationships which exist for two rigid appendages and a rigid body_{space station}.

Newton's and Euler's vector equations of motion for the space station can be written as

$$(17) \quad \frac{\text{Total system force equation}}{M_T \frac{d^2}{dt^2} \Big|_I (\bar{R}_O + \bar{C}) = \bar{F}_E}$$

$$(18) \quad \frac{\text{Space station moment equation}}{\frac{d}{dt} \Big|_I (\bar{I}_T \cdot \bar{\omega}_O) = \bar{T}_E}$$

where M_T = total system mass.

\bar{C} = vector from space station reference to system rigid body CG.

\bar{R}_O = location of space station reference point with respect to inertial space

\bar{I}_T = inertia dyadics of the space station about its center of mass.

$\bar{\omega}_O$ = angular velocity vector of the space station, with respect to inertial space

\bar{h}_{FJ} = location of attachment point of appendage with respect to space station reference point

\bar{r}_{FJ} = location of rigid body center of mass of appendage with respect to attachment point

Appendage 2

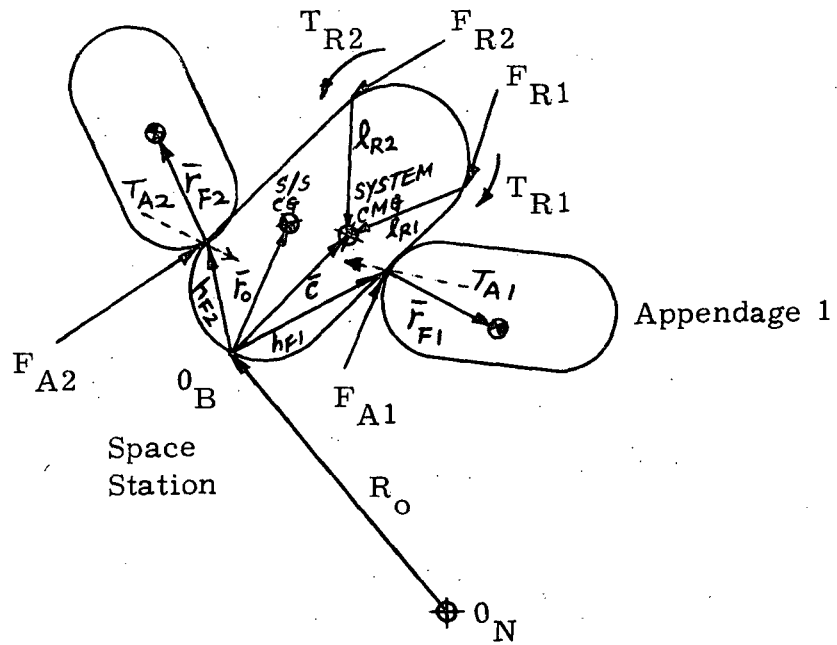


FIGURE 4-12. RIGID BODY SYSTEM CONFIGURATION

\bar{F}_{Ext} = external forces applied to space station

\bar{T}_{Ext} = external torques applied to space station

Defining \bar{R}_o and \bar{C} in the X_S frame (coordinate basis fixed to and moving with the space station taken as rigid body) and carrying out the differentiation w. r. t. time we obtain (see Section 4.2 for the following derivation conventions)

$$(19) \quad \dot{\bar{R}}_o = I^T C_o R_o, \quad \dot{\bar{C}} = I^T C_o C$$

$$(20) \quad \frac{d}{dt} \Big|_I (\dot{\bar{R}}_o + \dot{\bar{C}}) = I^T [C_o \tilde{\omega}_o R_o + C_o \dot{R}_o + C_o \tilde{\omega}_o C]$$

$$(21) \quad \frac{d^2}{dt^2} \Big|_I (\dot{\bar{R}}_o + \dot{\bar{C}}) = I^T [C_o \tilde{\omega}_o \tilde{\omega}_o R_o + C_o \tilde{\omega}_o \dot{R}_o + 2 C_o \tilde{\omega}_o \dot{R}_o + C_o \ddot{R}_o + C_o \tilde{\omega}_o \tilde{\omega}_o C + C_o \dot{\tilde{\omega}}_o C]$$

$$= X_S^T [(\tilde{\omega}_o \tilde{\omega}_o + \dot{\tilde{\omega}}_o)(R_o + C) + 2 \tilde{\omega}_o \dot{R}_o + \ddot{R}_o]$$

$$(22) \quad \frac{d}{dt} \Big|_I (\bar{I}_T \bar{\omega}_o) = I_T \dot{\omega}_o + \tilde{\omega}_o I_T \omega_o$$

Substituting equation (21) and (22) in equation (17) and (18), we obtain rigid body equations of motion for the space station

$$(23) \quad M_T (\ddot{R}_o + (\tilde{\omega}_o + \tilde{\omega}_o \tilde{\omega}_o) (R_o + C) + 2 \tilde{\omega}_o \dot{R}_o) = F_E$$

$$(24) \quad I_T \dot{\omega}_o + \tilde{\omega}_o I_T \omega_o = T_E$$

where $M_T = M_o + \sum_{i=1}^4 m_{Fi}$

$$\bar{C} = \frac{M_o \bar{r}_o + \sum_{i=1}^4 m_{Fi} (\bar{h}_{Fi} + C_{Fi} \bar{r}_{Fi})}{M_T}$$

$$I_T = I_o - M_o (\bar{r}_o - \bar{C})^2 + \sum_{i=1}^4 C_{Fi} \left[I'_{Fi} \right] C_{Fi}^T$$

$$I'_{Fi} = I_{Fi} - m_{Fi} \left(C_{Fi}^T \bar{h}_{Fi} + \bar{r}_{Fi} C_{Fi}^T \bar{C} \right)^2$$

$F_E =$ external forces (F_{Rj})
 + force due to flexible appendage motion (F_{Aj})
 + force due to flexible motion of base point of appendage ($F_{A'j}$)

$$= F_{R1} + F_{R2} + \sum_{J=1}^4 C_{FJ} (F_{AJ} + F_{A'J})$$

$$F_{AJ} = - \sum_E^T M_{FJ} W_{FJ} \dot{z}_{FJ}$$

$$F_{A'J} = m_{Fi} W_{Si} Z_S \} \text{ see section 2.5.1}$$

$T_E =$ external torques

+ torque due to flexible appendage motion

+ torque due to flexible motion of base point of appendage

$$T_E = T_{R1} + T_{R2} - (\tilde{1}_{R1}) F_1 - (\tilde{1}_{R2}) F_2$$

$$- \sum_{i=1}^4 C_{Fi} T_{Ai} + \sum_{i=1}^4 r_{Fi} C_{Fi} (F_{Ai} + F_{A'i})$$

$$- \sum_{i=1}^4 C_{Fi} I_{Fi} C_{Fi}^T W_{S_{bi}} \dot{z}_S$$

$$T_{A_i} = \sum_E^T \tilde{R}_{F_i} M_{F_i} W_{F_i} \dot{z}_{F_i}$$

T_{R_J} = externally applied torque (J = 1, 2)

F_{R_J} = externally applied forces (J = 1, 2)

M_{F_i} = mass of i^{th} appendage

M_o = mass of space station

l_{R_i} = location of application point of i^{th} external force with respect to system center of mass (negative of)

I_{F_i} = inertia matrix of i^{th} appendage

I_o = inertia matrix of space station

R_o = location of space station center of mass with respect to space station reference point

$$r_{F_i} = (r_o - h_{F_i})$$

Equation (23) and (24) may be expressed in matrix form

$$(25) \quad \begin{bmatrix} M_T & -M_T \bar{C} \\ 0 & I_T \end{bmatrix} \begin{bmatrix} \ddot{R}_o \\ \ddot{\omega}_o \end{bmatrix} + \begin{bmatrix} 0 \\ 0 \end{bmatrix} \begin{bmatrix} \dot{R}_o \\ \dot{\omega}_o \end{bmatrix} + \begin{bmatrix} 0 \\ 0 \end{bmatrix} \begin{bmatrix} \bar{R}_o \\ \bar{\theta}_o \end{bmatrix}$$

$$= \left[\frac{F_E - M_T (\tilde{\omega}_o + \tilde{\omega}_o \tilde{\omega}_o) R_o + \tilde{\omega}_o \tilde{\omega}_o \bar{C} + 2 \tilde{\omega}_o \dot{R}_o}{T_E - \tilde{\omega}_o I_T \omega_o} \right]$$

4.3.3 EQUATIONS OF FLEXIBLE APPENDAGES ATTACHED TO THE SPINNING SPACE STATION

The motion of a fixed flexible appendage is modeled as in previous derivations. Cantilevered mode shapes are used to represent the flexible appendage, whose fixed base is excited by the translational and rotational motion of the rigid body of the spinning space station, and the modal motions of the flexible space station at that point.

4.3.3.1 COORDINATE FRAMES AND RELATIONSHIPS

$[I]$ = inertially fixed coordinates

$[X_S]$ = coordinate basis fixed and moving with the space station taken as rigid body, origin at reference point O_B . (See Figure 4-13).

$[X_F]$ = coordinate basis defined with origin at attachment point of appendage and axes directed along principal axes of the appendage.

The relationship between $[I]$ and $[X_F]$ is defined by the direction cosine relationship

$$[I] = C_O C_F [X_F]$$

4.3.3.2 EQUATION DERIVATIONS

Using D'Alembert's principle, the total force acting on the j^{th} particle of the i^{th} appendage equals

$$(26) \quad \{F_j\} = m_j \frac{d^2}{dt^2} \left[\vec{a}_i + \vec{r}_j + \vec{u}_j \right]_I$$

where \vec{a}_i is the position vector of the hinge point of i^{th} fixed appendage w. r. t. inertial space

$$\vec{a}_i = I^T a_i$$

$$\vec{r}_j = I^T C_O C_F r_j$$

$$\vec{u}_j = I^T C_O C_F u_j$$

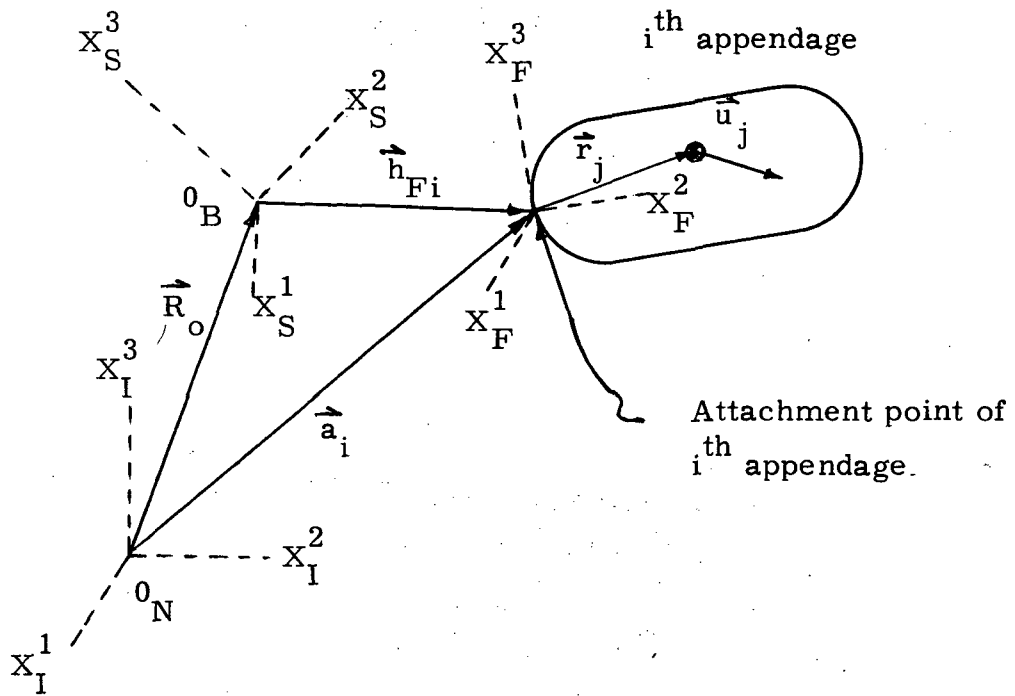


Figure 4-13 Flexible Appendage Coordinate System

$$\frac{d}{dt} \vec{r}_j = \frac{d}{dt} \left[I^T C_o C_{Fj}^r \right] = I^T \left[C_o \omega_o C_{Fj}^r \right]$$

$$\begin{aligned} \frac{d^2}{dt^2} \vec{r}_j &= \frac{d}{dt} \left[I^T C_o \tilde{\omega}_o C_{Fj}^r \right] \\ &= I^T C_o \tilde{\omega}_o \tilde{\omega}_o C_{Fj}^r + I^T C_o \dot{\tilde{\omega}}_o C_{Fj}^r \end{aligned}$$

$$\frac{d}{dt} \vec{u}_j = \frac{d}{dt} \left[I^T C_o C_{Fj}^u \right] = I^T C_o \tilde{\omega}_o C_{Fj}^u + I^T C_o \dot{C}_{Fj}^u$$

$$\begin{aligned} \frac{d^2}{dt^2} \vec{u}_j &= \frac{d}{dt} \left[I^T C_o \tilde{\omega}_o C_{Fj}^u + I^T C_o \dot{C}_{Fj}^u \right] \\ &= I^T \left[C_o \tilde{\omega}_o \tilde{\omega}_o C_{Fj}^u + C_o \dot{\tilde{\omega}}_o C_{Fj}^u + 2 C_o \tilde{\omega}_o \dot{C}_{Fj}^u + C_o \ddot{C}_{Fj}^u \right] \end{aligned}$$

Substituting the above equations in equation (26), we obtain

$$\begin{aligned} (27) \quad \left\{ F_j \right\} &= m_j I^T \left\{ \ddot{a}_i + C_o \left[(\tilde{\omega}_o \tilde{\omega}_o + \dot{\tilde{\omega}}_o) C_{Fj}^r \right. \right. \\ &\quad \left. \left. + (\tilde{\omega}_o \tilde{\omega}_o + \dot{\tilde{\omega}}_o) C_{Fj}^u + 2 \tilde{\omega}_o \dot{C}_{Fj}^u + C_{Fj} \ddot{u}_j \right] \right\} \\ &= m_j I^T C_o C_F \left\{ C_F^T C_o^T \ddot{a}_i + C_F^T \left[(\tilde{\omega}_o \tilde{\omega}_o + \dot{\tilde{\omega}}_o) C_{Fj}^r \right. \right. \\ &\quad \left. \left. + (\tilde{\omega}_o \tilde{\omega}_o + \dot{\tilde{\omega}}_o) C_{Fj}^u + 2 \tilde{\omega}_o \dot{C}_{Fj}^u \right] + \ddot{u}_j \right\} \end{aligned}$$

where $C_o^T \ddot{a}_i$ is sum of rigid body and space station modal accelerations at the attached point of i^{th} appendage

$$(28) \quad C_o^T \ddot{a}_i = (\ddot{R}_i)' + \ddot{U}_{S_i}$$

$(\ddot{R}_i)'$ ~ rigid body acceleration of the i^{th} appendage attachment point

(\ddot{U}_{S_i}) ~ space station modal acceleration of the i^{th} appendage attachment point

$$\begin{aligned}
 (29) \quad I^T C_o (\ddot{R})' &= \frac{d^2}{dt^2} \left[\vec{R}_o + \vec{h}_{F_i} \right]_I = \frac{d^2}{dt^2} \left[I^T C_o (R_o + h_{F_i}) \right] \\
 &= I^T C_o \left[\tilde{\omega}_o \tilde{\omega}_o (R_o + h_{F_i}) + \tilde{\omega}_o (R_o + h_{F_i}) + 2 \tilde{\omega}_o \dot{R}_o + \ddot{R}_o \right]
 \end{aligned}$$

Combining the above equations for all n particles of the appendage yields in matrix form

$$(30) \quad [m] \{\ddot{q}\} + [K] \{q\} = -[G] \{\dot{q}\} - [B] \{q\} + [R] \{RB\} + \{L\} + [S_2] \{\ddot{S}\}$$

3n x 3n 3n x 1

where

$$[G] = \begin{bmatrix} 2\bar{m}_1 C_F^T \tilde{\omega}_o C_F & & & 0 \\ & 2\bar{m}_2 C_F^T \tilde{\omega}_o C_F & & \\ & & \ddots & \\ 0 & & & 2\bar{m}_n C_F^T \tilde{\omega}_o C_F \end{bmatrix}$$

(3n x 3n)

$$[B] = \begin{bmatrix} \bar{m}_1 C_F^T (\tilde{\omega}_o \tilde{\omega}_o + \tilde{\omega}_o) C_F & & & \\ & \ddots & & \\ & & \ddots & \\ & & & \bar{m}_n C_F^T (\tilde{\omega}_o \tilde{\omega}_o + \tilde{\omega}_o) C_F \end{bmatrix}$$

(3n x 3n)

$$\{RB\} = \begin{bmatrix} \ddot{R}_o \\ \dot{\omega}_o \end{bmatrix}$$

(6 x 1)

$$[R] = \begin{bmatrix} -\bar{m}_1 C_F^T & \bar{m}_1 C_F^T (h_{F_i} + C_F r_1) \\ \vdots & \vdots \\ -\bar{m}_n C_F^T & \bar{m}_n C_F^T (h_{F_i} + C_F r_n) \end{bmatrix}$$

(3n x 6)

$$[L] = \begin{bmatrix} -\bar{m}_1 C_F^T \left[\tilde{\omega}_o \tilde{\omega}_o \left(R_o + h_{F_i} + C_{F_1} r_1 \right) + \tilde{\omega}_o R_o + 2 \tilde{\omega}_o \dot{R}_o \right] \\ \vdots \\ -\bar{m}_n C_F^T \left[\tilde{\omega}_o \tilde{\omega}_o \left(R_o + h_{F_i} + C_{F_n} r_n \right) + \tilde{\omega}_o R_o + 2 \tilde{\omega}_o \dot{R}_o \right] \end{bmatrix}$$

$$S = \begin{bmatrix} -\bar{m}_1 C_F^T \\ \vdots \\ -\bar{m}_n C_F^T \end{bmatrix}$$

3n x 6

Choosing $Q = \begin{bmatrix} \dot{q} \\ q \end{bmatrix}$, we reformulate equation (30) as follows

$$(31) \quad [D_F] \{\dot{Q}\} + [E_F] \{Q\} = [R] \{RB\} + [S_2] \{\ddot{S}\} + \{L\}$$

where

$$[D_F] = \begin{bmatrix} [0] & [m] \\ [m] & [G] \end{bmatrix} \quad E_F = \begin{bmatrix} [m] & [0] \\ [0] & [K] \end{bmatrix}$$

By the same reasoning as in Section 2.1.

$$(32) \quad \begin{bmatrix} \dot{\bar{Z}}(1) \\ \dot{\bar{Z}}(2) \end{bmatrix}_F + \begin{bmatrix} 0 & -|\Lambda| \\ |\Lambda| & 2\xi|\Lambda| \end{bmatrix} \begin{bmatrix} \bar{Z}(1) \\ \bar{Z}(2) \end{bmatrix}_F \\ = [V_F] [R] \{RB\} + [V_F] [S] \{\ddot{S}\} + [V_F] \{L\}$$

We can express $\{Q\}$ and $\{\ddot{S}\}$ in terms of the new coordinates \bar{Z}

$$(33) \quad \{Q\} = \begin{bmatrix} \dot{q} \\ q \end{bmatrix} = [W_F] [\bar{Z}]_F$$

$$(34) \quad \{\ddot{S}\} = [W_S] [\ddot{\bar{Z}}]_S$$

4.3.4 INTERACTION FORCES AND TORQUES

4.3.4.1 INTERACTION FORCES OF RIGID APPENDAGE

Using D'Alembert's principle in Figure 14 the interaction force of i^{th} appendage is

$$(35) \quad \vec{F}_{H_i} = -m_{F_i} \frac{d^2}{dt^2} \left[\vec{a}_i + \vec{r}_i \right]_I$$

where

$$\vec{a}_i = I^T a_i = \text{total displacement of attachment point of } i^{\text{th}} \text{ appendage with respect to inertial space (See Fig. 14)}$$

$$\vec{r}_i \equiv \text{location of C. M. of rigid appendage w. r. t. attachment point}$$

$$\vec{r}_i = I^T C_o C_{F_i} r_i$$

$$(36) \quad F_{H_i} = -m_{F_i} I^T C_o \left[C_o^T \ddot{a}_i + \left(\tilde{\omega}_o \tilde{\omega}_o + \dot{\tilde{\omega}}_o \right) C_{F_i} r_i \right]$$

$$\text{but } C_o^T \ddot{a}_i = \ddot{R}_i' + \ddot{u}_{S_i}$$

$$\text{where } \ddot{R}_i' \equiv \text{space station rigid body acceleration at attachment point } i.$$

$$\ddot{R}_i' = \left[\tilde{\omega}_o \tilde{\omega}_o (R_o + h_{F_i}) + \dot{\tilde{\omega}}_o (R_o + h_{F_i}) + 2 \tilde{\omega}_o \dot{R}_o + \ddot{R}_o \right]$$

$$\ddot{u}_{S_i} \equiv \text{space station modal acceleration at point } i \text{ (measured relative to rigid body space station motion).}$$

$$\ddot{u}_{S_i} = \begin{bmatrix} W_{S_i} \end{bmatrix} \dot{Z}_S^* \\ (3 \times 2N_S)$$

*Approximation

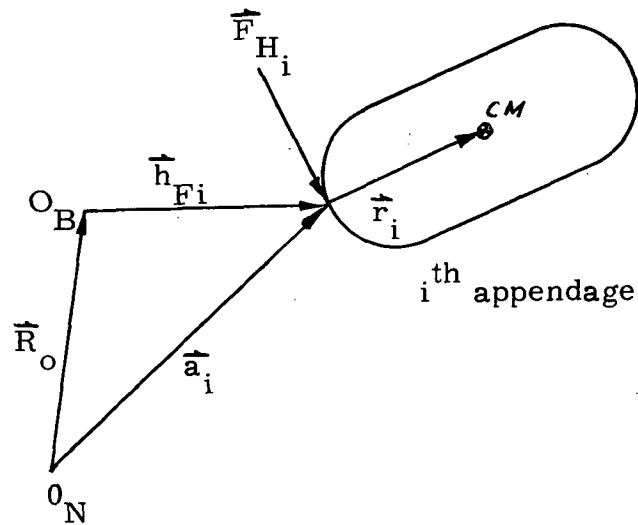


Figure 4-14 Interaction Force of Rigid Appendage to S/S

Therefore, the interaction force of a rigid appendage on the space station can be written as

$$(37) \quad F_{H_i} = \left[F_{H_i}' - m_{F_i} \left(\ddot{R}_o - \left(h_{F_i} \widetilde{C}_{F_i}^r + C_{F_i}^r \right) \dot{\omega}_o \right) \right] + F_{A_i}'$$

where

$$F_{H_i}' = -m_{F_i} \left[\tilde{\omega}_o \tilde{\omega}_o \left(R_o + h_{F_i} + C_{F_i}^r \right) + \tilde{\omega}_o R_o + 2\tilde{\omega}_o \dot{R}_o \right]$$

$$F_{A_i}' = -m_{F_i} W_{j_i} \dot{z}_s$$

4.3.4.2 INTERACTION TORQUES OF RIGID APPENDAGE

$$(38) \quad \frac{d}{dt} L_i = -\tilde{r}_i^T F_{H_i} - T_{H_i}$$

where

$$\begin{aligned} L_i &= (X_i)^T I_i (X_i) \left[(X_i)^T (\omega_o + \omega_{b_i}) \right] \\ &= \left[\left(I^T C_o \right) C_{i i} C_i^T \left(C_o^T I \right) \right] \left[\left(I^T C_o \right) (\omega_o + \omega_{b_i}) \right] \\ &= I^T C_o C_{i i} C_i^T (\omega_o + \omega_{b_i}) \\ \frac{dL_i}{dt} &= I^T \left[C_o \tilde{\omega}_o C_{i i} C_i^T (\omega_o + \omega_{b_i}) + C_o \left(C_{i i} C_i^T \right) (\dot{\omega}_o + \dot{\omega}_{b_i}) \right] \\ &= X^T \left[\tilde{\omega}_o C_{i i} C_i^T (\omega_o + \omega_{b_i}) + C_{i i} C_i^T (\dot{\omega}_o + \dot{\omega}_{b_i}) \right] \end{aligned}$$

where I_i = inertia matrix of i^{th} appendage

$\dot{\omega}_{b_i}$ \equiv modal angular acceleration at attachment point of i^{th} appendage

$$\dot{\omega}_{b_i} = \begin{bmatrix} W_{S_{b_i}} \end{bmatrix} \dot{Z}_S^* \\ (3 \times N_i)$$

Therefore, the interaction torque of i^{th} appendage of rigid motion on space station is

$$(39) \quad T_{H_i} = -\left(C_{F_i r_{F_i}} \right) F_{H_i} - C_{i i} C_i^T W_{S_{b_i}} \dot{Z}_S - C_{i i} C_i^T \dot{\omega}_o - \left(\tilde{\omega}_o C_{i i} C_i^T \right) (\omega_o + W_{S_{b_i}} Z_S)$$

*Approximation

or

$$T_{H_i} = -\left(\widetilde{C}_{F_i^r F_i}\right) F_{H_i} - (E + \omega_o) (C_{i_i}^I C_{i_i}^T) W_{S_{b_i}} \dot{Z}_S \\ - \left(C_{i_i}^I C_{i_i}^T\right) \dot{\omega}_o - \tilde{\omega}_o \left(C_{i_i}^I C_{i_i}^T\right) \omega_o$$

where E is the identity matrix.

4.3.4.3 INTERACTION FORCES AND TORQUES OF FLEXIBLE APPENDAGE

$$(40) \quad F_{A_i} = -C_{F_i} \sum_E^T M_{F_i} W_{F_i} \dot{Z}_{F_i}$$

See Section 4.3.7 for computational considerations

$$(41) \quad T_{A_i} = -C_{F_i} \sum_E^T \tilde{R}_{F_i} M_{F_i} W_{F_i} \dot{Z}_{F_i}$$

4.3.4.4 TOTAL INTERACTION FORCES AND TORQUES

The total interaction forces and torques at the attachment point of the appendages can be obtained by summing the interaction forces (torques) of the rigid and the flexible appendages at the attachment point.

$$(42) \quad F_{t_i} = F_{H_i} + F_{A_i}$$

$$(43) \quad F_{t_i} = -\left[F_{H_i}' + m_{F_i} \left(\ddot{R}_o - \left(\widetilde{h}_{F_i} + C_{F_i^r F_i} \right) \dot{\omega}_o \right) + m_{F_i} W_{S_i} \dot{Z}_S \right] \\ - C_{F_i} \sum_E^T M_{F_i} W_{F_i} \dot{Z}_{F_i}$$

$$\begin{aligned}
(44) \quad T_{t_i} &= T_{H_i} + T_{A_i} \\
&= - \left[\left(C_{F_i}^r \right)_{F_i} + (E + \tilde{\omega}_o) \left(C_{i_i}^I C_{i_i}^T \right) W_{S_{b_i}} \dot{Z}_S \right. \\
&\quad \left. + \left(C_{i_i}^I C_{i_i}^T \right) \dot{\omega}_o + \tilde{\omega}_o \left(C_{i_i}^I C_{i_i}^T \omega_o \right) \right] \\
&\quad - C_{F_i} \Sigma_E^T \tilde{R}_{F_i} M_{F_i} W_{F_i} \dot{Z}_{F_i}
\end{aligned}$$

4.3.5 TOTAL SYSTEM EQUATION

The above derived equations of motion of spinning space station with the attached appendages can be written in matrix notation as

$$(45) \quad [M] \{\ddot{X}\} + [C] \{\dot{X}\} + [K] \{X\} = \{P\}$$

where

$$M = \begin{bmatrix} M_{11} & M_{12} & M_{13} \\ M_{21} & M_{22} & M_{23} \\ M_{31} & M_{32} & M_{33} \end{bmatrix} \begin{array}{l} \leftarrow \text{Rigid Body} \\ \leftarrow \text{Space Station} \\ \leftarrow \text{Appendages} \end{array}$$

$$C = \begin{bmatrix} C_{11} & C_{12} & C_{13} \\ C_{21} & C_{22} & C_{23} \\ C_{31} & C_{32} & C_{33} \end{bmatrix}$$

$$K = \begin{bmatrix} K_{11} & K_{12} & K_{13} \\ K_{21} & K_{22} & K_{23} \\ K_{31} & K_{32} & K_{33} \end{bmatrix}$$

$$\ddot{X} = \begin{Bmatrix} \ddot{R}_O \\ \dot{\omega}_O \\ \ddot{Z}_S \\ \ddot{Z}_F \end{Bmatrix} \quad X = \begin{Bmatrix} R_O \\ \omega_O \\ Z_S \\ Z_F \end{Bmatrix} \quad P = \begin{Bmatrix} P_1 \\ \dots \\ P_2 \\ \dots \\ P_3 \end{Bmatrix}$$

For the previously derived state equations, we find that $M = O$.

Thus, the rigid body equations (25) lead to the first equation of the total system, which is

$$(46) \quad \begin{matrix} \left[C_{11} \right] \begin{Bmatrix} \ddot{R}_o \\ \dot{\omega}_o \end{Bmatrix} + \left[C_{12} \right] \begin{Bmatrix} \dot{Z}_S \end{Bmatrix} + \left[C_{13} \right] \begin{Bmatrix} \dot{Z}_F \end{Bmatrix} = \begin{Bmatrix} P_1 \end{Bmatrix} \\ (6 \times 6) \quad (6 \times 1) \quad (6 \times 2N_S) \quad (6 \times 2N_F) \quad (6 \times 1) \end{matrix}$$

where

$$\left[C_{11} \right] = \begin{bmatrix} M_T & -M_T C \\ 0 & I_T \end{bmatrix}$$

$$\left[C_{12} \right] = -\sum_{i=1}^4 \begin{bmatrix} -m_{F_i} & 0 \\ -m_{F_i} (C_{F_i} \tilde{r}_{F_i}) & -C_{i i} C_i^T \end{bmatrix} \begin{bmatrix} W_{S_i}^T \\ W_{S_{b_i}}^T \end{bmatrix}$$

$$\left[C_{13} \right] = \begin{bmatrix} C_{F1} \Sigma_E^T M_{F1} W_{F1} & \dots & C_{F4} \Sigma_E^T M_{F4} W_{F4} \\ (3 \times 2N_{F1}) & & (3 \times 2N_{F4}) \\ \hline C_{F1} \Sigma_E^T \tilde{R}_{F1} M_{F1} W_{F1} - \tilde{r}'_{F1} \Sigma_E^T M_{F1} W_{F1} & \dots & C_{F4} \Sigma_E^T \tilde{R}_{F4} M_{F4} W_{F4} \\ (3 \times 2N_{F1}) & & (3 \times 2N_{F4}) \\ \hline & & -\tilde{r}'_{F4} C_{F4} \Sigma_E^T M_{F4} W_{F4} \\ & & (3 \times 2N_{F4}) \end{bmatrix}$$

(6x2 N_F)

$$P_1 = \begin{bmatrix} F_{R1} + F_{R2} - M_T \left[(\tilde{\omega}_o + \tilde{\omega}_o \tilde{\omega}_o) R_o + \tilde{\omega}_o \tilde{\omega}_o C + 2 \tilde{\omega}_o \dot{R}_o \right] \\ T_{R1} + T_{R2} - \tilde{l}_{R1} F_{R1} - \tilde{l}_{R2} F_{R2} - \tilde{\omega}_o I_T \omega_o \end{bmatrix}$$

$$\left[K_{11} \right] = \left[K_{12} \right] = \left[K_{13} \right] = 0$$

The flexible spinning space station equation (11) leads to the second equation of the total system which is

$$(47) \quad [C_{21}] \begin{Bmatrix} \ddot{R}_o \\ \dot{\omega}_o \end{Bmatrix} + [C_{22}] \{\dot{Z}_S\} + [C_{23}] \{\dot{Z}_F\} + [K_{22}] \{Z_S\} = \{P_2\}$$

where

$$[C_{21}] = -\sum_{i=1}^4 [V_F] \begin{bmatrix} -m_{F_i} & m_{F_i} (h_{F_i} + \overline{C_{F_i}^r F_i}) \\ -(\overline{C_{F_i}^r F_i})^m_{F_i} & -C_{F_i}^I C_{F_i}^T + (\overline{C_{F_i}^r F_i})^m_{F_i} (h_{F_i} + \overline{C_{F_i}^r F_i}) \end{bmatrix}$$

$$= -\sum_{i=1}^4 \begin{bmatrix} V'_{F_i} & V''_{F_i} \end{bmatrix} \begin{bmatrix} -m_{F_i} & m_{F_i} (h_{F_i} + \overline{C_{F_i}^r F_i}) \\ -(\overline{C_{F_i}^r F_i})^m_{F_i} & -C_{F_i}^I C_{F_i}^T + (\overline{C_{F_i}^r F_i})^m_{F_i} (h_{F_i} + \overline{C_{F_i}^r F_i}) \end{bmatrix}$$

(N_S x 6) (6 x 6)

$$[C_{22}] = -\sum_{i=1}^4 \begin{bmatrix} V'_{F_i} & V''_{F_i} \end{bmatrix} \begin{bmatrix} -m_{F_i} & 0 \\ -m_{F_i} (\overline{C_{F_i}^r F_i})^m_{F_i} & -C_i^I C_i^T \end{bmatrix} \begin{bmatrix} W_{s_i}^T \\ W_{s_{b_i}}^T \end{bmatrix} + \begin{bmatrix} 1 & & 0 \\ & 1 & \\ 0 & & \dots \end{bmatrix}$$

(N_S x 6) (6 x 6)

$$[C_{23}] = \begin{bmatrix} V'_{F_1} \left(C_{F_1} \begin{matrix} T \\ \Sigma \\ E \end{matrix} M_{F_1} W_{F_1} \right) & \dots & V'_{F_4} \left(C_{F_4} \begin{matrix} T \\ \Sigma \\ E \end{matrix} M_{F_4} W_{F_4} \right) \\ V''_{F_1} \left(C_{F_1} \begin{matrix} T \\ \Sigma \\ E \end{matrix} \tilde{R}_{F_1} M_{F_1} W_{F_1} \right) & \dots & V''_{F_4} \left(C_{F_4} \begin{matrix} T \\ \Sigma \\ E \end{matrix} \tilde{R}_{F_4} M_{F_4} W_{F_4} \right) \end{bmatrix}$$

2N_S x 2N_F

Forces and torques acting on space station and exciting flexible motion include:

1. 2 external forces
2. 2 external torques
3. up to 4 hinge forces and torques due to 4 attached rigid appendages
4. up to 4 forces and torques due to flexible motion of 4 fixed appendages
5. wobble damper control torque

$$\begin{aligned}
 [P_2] &= \sum_{i=1}^4 V_{Fi}' \left[m_{Fi} (2\omega_o \dot{R}_o + \tilde{\omega}_o \tilde{\omega}_o (R_o + h_{Fi} + C_{Fi} r_{Fi}) + \dot{\omega}_o R_o) \right] \\
 &+ \sum_{i=1}^4 V_{Fi}'' \left\{ C_{Fi} (C_{Fi}^T \omega_o) I_{Fi} C_{Fi}^T \omega_o + (C_{Fi} \overline{r_{Fi}})(m_{Fi}) \left[2\omega_o \dot{R}_o + \right. \right. \\
 &\quad \left. \left. \tilde{\omega}_o R_o + \tilde{\omega}_o \tilde{\omega}_o (R_o + h_{Fi} + C_{Fi} r_{Fi}) \right] \right\} \\
 &+ \sum_{i=1}^2 V_{Ri}' F_{Ri} + \sum_{i=1}^2 V_{Ri}'' T_{Ri} + V_{WOB}'' T_{WOB}
 \end{aligned}$$

$$[K_{22}] = \begin{bmatrix} 0 & -|\bar{\lambda}| \\ |\bar{\lambda}| & 2\xi_S |\bar{\lambda}| \end{bmatrix}$$

$$[K_{21}] = [K_{23}] = 0$$

The flexible appendage equations (22) lead to the third equation of the total system, which is

$$(48) \quad \begin{bmatrix} C_{31} \end{bmatrix} \begin{Bmatrix} \ddot{R}_0 \\ \dot{\omega}_0 \end{Bmatrix} + \begin{bmatrix} C_{32} \end{bmatrix} \{\ddot{Z}_S\} + \begin{bmatrix} C_{33} \end{bmatrix} \{\ddot{Z}_F\} + \begin{bmatrix} K_{33} \end{bmatrix} \{Z_F\} = \{P_3\}$$

where

$$\begin{bmatrix} M_{31} \end{bmatrix} = \begin{bmatrix} V_{F1}'' R_{F1} \\ \vdots \\ V_{F2}'' R_{F2} \\ \vdots \\ V_{F3}'' R_{F3} \\ \vdots \\ V_{F4}'' R_{F4} \end{bmatrix} \quad M_{32} = \begin{bmatrix} V_{F1}'' S_1 \\ \vdots \\ V_{F2}'' S_2 \\ \vdots \\ V_{F3}'' S_3 \\ \vdots \\ V_{F4}'' S_4 \end{bmatrix}$$

$$\begin{bmatrix} K_{33} \end{bmatrix} = \begin{bmatrix} 0 & -|\bar{\lambda}_F| \\ |\lambda_F| & 2\xi_F |\bar{\lambda}_F| \end{bmatrix} \quad (\text{for each appendage})$$

$$\begin{bmatrix} K_{31} \end{bmatrix} = \begin{bmatrix} K_{32} \end{bmatrix} = 0$$

$$P_3 = \begin{bmatrix} V_{F1}'' L_1 \\ \vdots \\ V_{F4}'' L_4 \end{bmatrix}$$

In order to evaluate the coefficient matrices in equation (48) the transformation matrix $\begin{bmatrix} V_F \end{bmatrix}$ derived in Section 4.3.6 may be used.

For computational speed and storage considerations, the elements of $[C_{31}]$ may be obtained as follows:

(49)

$$\begin{aligned}
 \begin{bmatrix} V_F \\ R \end{bmatrix} \begin{Bmatrix} 0 \\ R \end{Bmatrix} &= \begin{bmatrix} 0 & d' \\ -d' & 0 \end{bmatrix} \begin{bmatrix} R_E(\phi_B^T) & R_E(\phi_B^T) \\ I_m(\phi_T^T) & I_m(\phi_B^T) \end{bmatrix} \begin{Bmatrix} 0 \\ R \end{Bmatrix} \\
 &= \begin{bmatrix} d' I_m(\phi_B^T) \\ -d' R_E(\phi_B^T) \end{bmatrix} [R] \\
 &= \begin{bmatrix} d' I_m(\phi_B^T) \\ -d' R_E(\phi_B^T) \end{bmatrix} [m] \begin{bmatrix} -\sum_E C_F^T & \sum_E C_F^T \tilde{h}_F + \tilde{r} \sum_E C_F^T \end{bmatrix} \\
 &\quad (2N_F \times 3n) \quad (3n \times 3n) \quad (3n \times 3) \quad (3n \times 3)
 \end{aligned}$$

Define:

$$d_{RE} = \sum_E^T [m] R_E(\phi_B)$$

$$d_{Im} = \sum_E^T [m] I_m(\phi_B)$$

$$\text{thus, } d_{RE}^T = R_E(\phi_B^T) [m] \sum_E$$

$$d_{Im}^T = I_m(\phi_B^T) [m] \sum_E$$

Also define:

$$r_{RE} = \sum_E^T \tilde{r} [m] R_E(\phi_B)$$

$$r_{Im} = \sum_E^T \tilde{r} [m] I_m(\phi_B)$$

then

$$r_{RE}^T = -R_E (\phi_B^T) [m] \tilde{r} \sum_E$$

$$r_{Im}^T = -I_m (\phi_B^T) [m] \tilde{r} \sum_E$$

In terms of the above definitions equation (49) can be written as

$$(50) \quad \begin{bmatrix} V_F \\ R \end{bmatrix} \begin{Bmatrix} 0 \\ - \\ - \end{Bmatrix} = \begin{bmatrix} d' d_{Im}^T C_F^T & -d' d_{Im}^T C_F^T \tilde{h}_F + d' r_{Im}^T C_F^T \\ -d' d_{RE}^T C_F^T & -d' d_{RE}^T C_F^T \tilde{h}_F + d' r_{RE}^T C_F^T \end{bmatrix}$$

Similarly, we have the elements of the matrix $[M_{32}]$ as

$$(51) \quad \begin{bmatrix} V_F \\ S \end{bmatrix} \begin{Bmatrix} 0 \\ - \\ S \end{Bmatrix} = \begin{bmatrix} V_F'' \end{bmatrix} [S] = \begin{bmatrix} V_F'' \end{bmatrix} \begin{bmatrix} -m_1 C_F^T & 0 \\ \vdots & \vdots \\ -m_n C_F^T & 0 \end{bmatrix} \begin{bmatrix} W_{si} \\ W_{sbi} \end{bmatrix}$$

(3n x 6) (b x N_s)

$$= - \begin{bmatrix} V_F'' \end{bmatrix} [m] \sum_E C_F^T W_{si}$$

(2N_F x 3n) (3n x N_s)

Finally, we can write equation (51) as

$$(52) \quad - \begin{bmatrix} V_F'' \end{bmatrix} [S] \begin{bmatrix} d'_{Im} (\phi_B^T) \\ - \\ d'_{RE} (\phi_B^T) \end{bmatrix} [m] \sum_E C_F^T W_{si}$$

(2N_F x 3n) (3n x N_s)

$$= \begin{bmatrix} d' d_{Im}^T C_F^T W_{si} \\ -d' d_{RE}^T C_F^T W_{si} \end{bmatrix}$$

(2N_F x N_S)

The matrix [P₃] in equation (48) can similarly be evaluated as

$$(53) \begin{bmatrix} V_F \\ L \end{bmatrix} \begin{Bmatrix} 0 \\ \vdots \end{Bmatrix} = \begin{bmatrix} V_F'' \\ L \end{bmatrix} [L]$$

$$= \begin{bmatrix} V_F'' \\ \vdots \\ V_F'' \end{bmatrix} \begin{bmatrix} -m_1 C_F^T \left[\tilde{\omega}_o \tilde{\omega}_o (R_o + h_{Fi} + C_F r_1) + \tilde{\omega}_o \dot{R}_o + 2 \tilde{\omega}_o \dot{R}_o \right] \\ \vdots \\ -m_n C_F^T \left[\tilde{\omega}_o \tilde{\omega}_o (R_o + h_{Fi} + C_F r_n) + \tilde{\omega}_o \dot{R}_o + 2 \tilde{\omega}_o \dot{R}_o \right] \end{bmatrix}$$

$$= \begin{bmatrix} d' d_{IM}^T C_F^T \left[\tilde{\omega}_o \tilde{\omega}_o (R_o + h_{Fi}) + \tilde{\omega}_o \dot{R}_o + 2 \tilde{\omega}_o \dot{R}_o \right] \\ \vdots \\ -d' d_{RE}^T C_F^T \left[\tilde{\omega}_o \tilde{\omega}_o (R_o + h_{Fi}) + \tilde{\omega}_o \dot{R}_o + 2 \tilde{\omega}_o \dot{R}_o \right] \end{bmatrix}$$

$$-V_F'' [m] \text{DIAG} (C_F^T \tilde{\omega}_o \tilde{\omega}_o C_F r_1, \dots, C_F^T \tilde{\omega}_o \tilde{\omega}_o C_F r_n)$$

4.3.6 Transformation Matrix [V]

By Definition

$$(54) \quad V = \frac{1}{2} \left[\begin{array}{c|c} -\frac{I}{J} & \frac{I}{J} \\ \hline \frac{I}{J} & -\frac{I}{J} \end{array} \right] \left[\begin{array}{c} \Phi^{*T} \\ D\Phi \end{array} \right]^{-1} \Phi^{*T}$$

where D is a skew symmetric matrix defined in equation (3)

$$(55) \quad D = \left[\begin{array}{c|c} [0] & -[m] \\ \hline [m] & [G] \end{array} \right]$$

$$(56) \text{ and } \Phi = \left[\begin{array}{c|c} \bar{\lambda}\Phi_B & \bar{\lambda}\Phi_B^* \\ \hline \Phi_B & \Phi_B^* \end{array} \right] = \left[\begin{array}{c|c} \Phi_T & \Phi_T^* \\ \hline \Phi_B & \Phi_B^* \end{array} \right]$$

where

$$\bar{\lambda} = \begin{bmatrix} \lambda_{1j} & & 0 \\ & \lambda_{2j} & \\ 0 & & \ddots \\ & & & \lambda_{Nj} \end{bmatrix}$$

$$\Phi_T = \Phi_B \bar{\lambda} \quad \Phi_B = \left[\left\{ \phi^{(1)} \right\} \left\{ \phi^{(2)} \right\} \dots \left\{ \phi^{(N)} \right\} \right]$$

$$\Phi_B^* = \left[\left\{ \phi^{(1)*} \right\} \left\{ \phi^{(2)*} \right\} \dots \left\{ \phi^{(N)*} \right\} \right]$$

$\left\{ \phi^* \right\}$ is complex conjugate of $\left\{ \phi \right\}$

Using the above defined matrices, we may formulate the following equation

$$(57) \quad \Phi^{*T} D \Phi = \left[\begin{array}{c|c} \Phi_T^{*T} & \Phi_B^{*T} \\ \hline \Phi_T & \Phi_B \end{array} \right] \left[\begin{array}{c} [0] \quad -[m] \\ [m] \quad [G] \end{array} \right] \left[\begin{array}{c|c} \Phi_T & \Phi_T^* \\ \hline \Phi_B & \Phi_B^* \end{array} \right]$$

$$= \left[\begin{array}{c|c} \Phi_B^{*T} [m] & -\Phi_T^{*T} [m] + \Phi_B^{*T} [G] \\ \hline \Phi_B^T [m] & -\Phi_T^T [m] + \Phi_B^T [G] \end{array} \right] \left[\begin{array}{c|c} \Phi_T & \Phi_T^* \\ \hline \Phi_B & \Phi_B^* \end{array} \right]$$

$$= \left[\begin{array}{c|c} \Phi_B^{*T} [m] \Phi_T - \Phi_T^{*T} [m] \Phi_B + \Phi_B^{*T} [G] \Phi_B & \Phi_B^{*T} [m] \Phi_T^* - \Phi_T^{*T} [m] \Phi_B^* + \Phi_B^{*T} [G] \Phi_B^* \\ \hline \Phi_B^T [m] \Phi_T - \Phi_T^T [m] \Phi_B + \Phi_B^T [G] \Phi_B & \Phi_B^T [m] \Phi_T^* - \Phi_T^T [m] \Phi_B^* + \Phi_B^T [G] \Phi_B^* \end{array} \right]$$

(Note that the cross terms are the complex conjugate of each other)

In order to evaluate the matrices in equation (57) we introduce the following method.

$$(58) \quad \text{Let } \psi \equiv (1/2) \Phi \begin{bmatrix} I & -J \\ I & J \end{bmatrix}$$

$$= (1/2) \begin{bmatrix} \Phi_T & \Phi_T^* \\ \Phi_B & \Phi_B^* \end{bmatrix} \begin{bmatrix} I & -J \\ I & J \end{bmatrix} = (1/2) \begin{bmatrix} \Phi_T + \Phi_T^* & J(\Phi_T^* - \Phi_T) \\ \Phi_B + \Phi_B^* & J(\Phi_B^* - \Phi_B) \end{bmatrix}$$

$$= \begin{bmatrix} R_E(\Phi_T) & I_m(\Phi_T) \\ R_E(\Phi_B) & I_m(\Phi_B) \end{bmatrix}$$

The transpose of ψ may be written as

$$(59) \quad \psi^T = 1/2 \begin{bmatrix} I & I \\ -J & J \end{bmatrix} \Phi^T$$

$$= 1/2 \begin{bmatrix} I & I \\ -J & J \end{bmatrix} \begin{bmatrix} \Phi_T^T & \Phi_B^T \\ \Phi_T^{*T} & \Phi_B^{*T} \end{bmatrix}$$

and the conjugate transpose of ψ as

$$(60) \quad \psi^{*T} = (1/2) \begin{bmatrix} I & I \\ J & -J \end{bmatrix} \begin{bmatrix} \Phi_T^{*T} & \Phi_B^{*T} \\ \Phi_T^T & \Phi_B^T \end{bmatrix}$$

$$= (1/2) \begin{bmatrix} \Phi_T^{*T} + \Phi_T^T & J(\Phi_B^{*T} - \Phi_B^T) \\ J(\Phi_T^* - \Phi_T) & \Phi_B^{*T} + \Phi_B^T \end{bmatrix}$$

$$= \begin{bmatrix} R_E(\Phi_T^T) & R_E(\Phi_B^T) \\ I_m(\Phi_T^T) & I_m(\Phi_B^T) \end{bmatrix}$$

Defining Φ in terms of ψ

$$(61) \quad \Phi = \psi \begin{bmatrix} I & & & I \\ & & & \\ & & & \\ & & & -J \end{bmatrix} (1/2)$$

$$= \begin{bmatrix} R_E(\Phi_T) & I_m(\Phi_T) \\ R_E(\Phi_B) & I_m(\Phi_B) \end{bmatrix} \begin{bmatrix} I & & & I \\ & & & \\ & & & \\ & & & -J \end{bmatrix}$$

and the conjugate transpose of Φ as

$$(62) \quad \Phi^{*T} = \begin{bmatrix} I & & & -J \\ & & & \\ & & & \\ & & & J \end{bmatrix} \begin{bmatrix} R_E(\Phi_T^T) & R_E(\Phi_B^T) \\ I_m(\Phi_T^T) & I_m(\Phi_B^T) \end{bmatrix}$$

Combining equation (2), (3), and (8), we can formulate equation (63)

$$(63) \quad \Phi^{*T} D \Phi = \begin{bmatrix} I & & & -J \\ & & & \\ & & & \\ & & & J \end{bmatrix} \begin{bmatrix} R_E(\Phi_T^T) & R_E(\Phi_B^T) \\ I_m(\Phi_T^T) & I_m(\Phi_B^T) \end{bmatrix} \begin{bmatrix} [0] & [m] \\ [m] & [G] \end{bmatrix} \begin{bmatrix} R_E(\Phi_T) & I_m(\Phi_T) \\ R_E(\Phi_B) & I_m(\Phi_B) \end{bmatrix} \begin{bmatrix} I & & & I \\ & & & \\ & & & \\ & & & -J \end{bmatrix}$$

$$= \begin{bmatrix} I & & & -J \\ & & & \\ & & & \\ & & & J \end{bmatrix} \begin{bmatrix} R_E(\Phi_T^T) & R_E(\Phi_B^T) \\ I_m(\Phi_T^T) & I_m(\Phi_B^T) \end{bmatrix} \begin{bmatrix} -[m]R_E(\Phi_B) & -[m]I_m(\Phi_B) \\ [m]R_E(\Phi_T) + [G]R_E(\Phi_B) & [m]I_m(\Phi_T) + [G]I_m(\Phi_B) \end{bmatrix}$$

$$\begin{bmatrix} I & & & I \\ & & & \\ & & & \\ & & & -J \end{bmatrix}$$

$$= \begin{bmatrix} I & & & -J \\ & & & \\ & & & \\ & & & J \end{bmatrix} \begin{bmatrix} -R_E(\Phi_T^T) [m]R_E(\Phi_B) + R_E(\Phi_B^T) ([m]R_E(\Phi_T) + [G]R_E(\Phi_B)) \\ -I_m(\Phi_T^T) [m]R_E(\Phi_B) + I_m(\Phi_B^T) ([m]R_E(\Phi_T) + [G]R_E(\Phi_B)) \\ -R_E(\Phi_T^T) [m]I_m(\Phi_B) + R_E(\Phi_B^T) ([m]I_m(\Phi_T) + [G]I_m(\Phi_B)) \\ -I_m(\Phi_T^T) [m]I_m(\Phi_B) + I_m(\Phi_B^T) ([m]I_m(\Phi_T) + [G]I_m(\Phi_B)) \end{bmatrix} \begin{bmatrix} I & & & I \\ & & & \\ & & & \\ & & & -J \end{bmatrix}$$

Substituting the following relations in equation (62)

$$\Phi_T^* = \Phi_B^{\bar{\lambda}} = \Phi_B^{\lambda(-j)}$$

$$\text{and } R_E(\Phi_T) = +I_m(\Phi_B)\lambda, \quad R_E(\Phi_T^T) = +\lambda I_m(\Phi_B^T)$$

$$I_m(\Phi_T) = -R_E(\Phi_B)\lambda, \quad I_m(\Phi_T^T) = -\lambda R_E(\Phi_B^T)$$

we obtain

$$(64) \quad \Phi^{*T} D \Phi = \begin{bmatrix} I & -J \\ I & J \end{bmatrix} \begin{bmatrix} a & c \\ b & d \end{bmatrix} \begin{bmatrix} I & J \\ J & -J \end{bmatrix}$$

where

$$a = -\lambda I_m(\Phi_B^T) [m] R_E(\Phi_B) + R_E(\Phi_B^T) \left(+ [m] I_m(\Phi_B)\lambda + [G] R_E(\Phi_B) \right)$$

$$b = +\lambda R_E(\Phi_B^T) [m] R_E(\Phi_B) + I_m(\Phi_B^T) \left(+ [m] I_m(\Phi_B)\lambda + [G] R_E(\Phi_B) \right)$$

$$c = -\lambda I_m(\Phi_B^T) [m] I_m(\Phi_B) + R_E(\Phi_B^T) \left([m] R_E(\Phi_B)\lambda + [G] I_m(\Phi_B) \right)$$

$$d = +\lambda R_E(\Phi_B^T) [m] I_m(\Phi_B) + I_m(\Phi_B^T) \left([m] R_E(\Phi_B)\lambda + [G] I_m(\Phi_B) \right)$$

Let

$$(65) \quad \Phi^{*T} D \Phi = \begin{bmatrix} e & g \\ f & h \end{bmatrix}$$

where

$$(66.) \quad \left\{ \begin{array}{l} e = (a+d) - (b+c)J \\ f = (a-d) + (b+c)J \\ g = (a-d) - (b+c)J \\ h = (a+d) + (b-c)J \end{array} \right.$$

From the orthogonality relation of eigenvectors, $\Phi^{*T} D \Phi$ should be diagonal matrix,⁽³⁾

hence,

$f = g = 0$, e and h are diagonal matrices.

Applying the above conditions in equation (66) , we have the following set of equations

$$(67) \quad \begin{cases} e & = & 2(a-bj) \\ h & = & 2(a+bj) \\ c & = & -b \\ \text{and } a & = & d \end{cases}$$

Then equation (64) becomes

$$(68) \quad \Phi^{*T} D \Phi = 2 \begin{bmatrix} a-bj & 0 \\ 0 & a+bj \end{bmatrix}$$

It can be shown that the diagonal terms of equation (57) are purely imaginary; therefore, a in equation (68) must vanish, and hence

$$(69) \quad \Phi^{*T} D \Phi = \begin{bmatrix} -2bj & 0 \\ 0 & +2bj \end{bmatrix}$$

where

$$\begin{aligned} 2bj &= -2j \left[\lambda R_E(\Phi_B^T) [m] R_E(\Phi_B) + I_M(\Phi_B^T) \left(+[m] I_m(\Phi_B) + [G] R_E(\Phi_B) \right) \right] \\ &= \Phi_B^{*T} [m] \Phi_T - \Phi_T^{*T} [m] \Phi_B + \Phi_B^{*T} [G] \Phi_B \end{aligned}$$

Substituting equation (69) in equation (54), we obtain

$$\begin{aligned} (70) \quad V &= 1/2 \begin{bmatrix} I & I \\ J & -J \end{bmatrix} \begin{bmatrix} -2bj & 0 \\ 0 & +2bj \end{bmatrix}^{-1} \Phi^{*T} \\ &= 1/2 \begin{bmatrix} I & I \\ J & -J \end{bmatrix} \begin{bmatrix} d'j & 0 \\ 0 & -d'j \end{bmatrix} \Phi^{*T} \\ &= 1/2 \begin{bmatrix} d'J & -d'J \\ d' & -d' \end{bmatrix} \Phi^{*T} \end{aligned}$$

$$\begin{aligned}
&= \frac{1}{2} \begin{bmatrix} 0 & d' \\ -d' & 0 \end{bmatrix} \begin{bmatrix} I & -I \\ J & -J \end{bmatrix} \Phi^{*T} \\
&= \frac{1}{2} \begin{bmatrix} 0 & d' \\ -d' & 0 \end{bmatrix} \begin{bmatrix} I & -I \\ J & -J \end{bmatrix} \begin{bmatrix} \Phi_T^{*T} & \Phi_B^{*T} \\ \Phi_T^T & \Phi_B^T \end{bmatrix} \\
&= \begin{bmatrix} 0 & d' \\ -d' & 0 \end{bmatrix} \begin{bmatrix} \operatorname{Re}(\Phi_T^T) & \operatorname{Re}(\Phi_B^T) \\ \operatorname{Im}(\Phi_T^T) & \operatorname{Im}(\Phi_B^T) \end{bmatrix}
\end{aligned}$$

where $\begin{bmatrix} -2bj & 0 \\ 0 & 2bj \end{bmatrix}^{-1} = \begin{bmatrix} d'j & 0 \\ 0 & -dj \end{bmatrix}$ is used.

4.3.7 Computational Considerations

$$\begin{aligned}
 F_{A_i} &= \sum_E^T M_{F_i} W_{F_i} \dot{z}_{F_i} \\
 &= [EE\dots E] \begin{bmatrix} m & o \\ o & o \end{bmatrix} \begin{bmatrix} \phi_T & \phi_T^* \\ \phi_B & \phi_B^* \end{bmatrix} \begin{bmatrix} I & -J \\ I & J \end{bmatrix} \dot{z}_{F_i} \\
 &= [E\dots E] \begin{bmatrix} m & o \\ o & o \end{bmatrix} \begin{bmatrix} 2R_E(\phi_T) & 2I_m(\phi_T) \\ 2R_E(\phi_B) & 2I_m(\phi_B) \end{bmatrix} \dot{z}_{F_i} \\
 &= [E\dots E] \begin{bmatrix} 2mR_E(\phi_T) & 2mI_m(\phi_T) \\ o & o \end{bmatrix} \dot{z}_{F_i} \\
 &= \left[\begin{array}{c|c} \sum_{j=1}^n 2m_j R_E(\phi_{Bjx}^1) \dots & \sum_{j=1}^n 2m_j I_m(\phi_{Bjx}^1) \dots \\ \hline \sum_{j=1}^n 2m_j R_E(\phi_{Bjy}^1) \dots & \sum_{j=1}^n 2m_j I_m(\phi_{Bjy}^1) \dots \\ \hline \sum_{j=1}^n 2m_j R_E(\phi_{Bjz}^1) \dots & \sum_{j=1}^n 2m_j I_m(\phi_{Bjz}^1) \dots \end{array} \right] \dot{z}_{F_i} \\
 &\hspace{15em} (3 \times 2N)
 \end{aligned}$$

Likewise -

$$\begin{aligned}
 T_{A_i} &= \sum_E^T \tilde{R}_{F_i} M_{F_i} W_{F_i} \dot{Z}_{F_i} \\
 &= [E \dots E] \left[\begin{array}{c|c} \tilde{R}_{F_i} & 0 \\ \hline 0 & 0 \end{array} \right] \left[\begin{array}{c|c} m & 0 \\ \hline 0 & 0 \end{array} \right] \left[\begin{array}{c|c} \phi_T & \phi_T^* \\ \hline \phi_B & \phi_B^* \end{array} \right] \left[\begin{array}{c|c} I & -J \\ \hline I & J \end{array} \right] \dot{Z}_{F_i} \\
 &= [E \dots E] \left[\begin{array}{c|c} 2\tilde{R}_{F_i} m R_E(\phi_T) & 2\tilde{R}_{F_i} m I_m(\phi_T) \\ \hline 0 & 0 \end{array} \right] \dot{Z}_{F_i} \\
 &= 2 \left[\begin{array}{c|c} \tilde{m}_1 \tilde{F}_1 & 0 \\ \hline 0 & \ddots \\ \tilde{m}_n \tilde{F}_n & \end{array} \right] \left[\begin{array}{c|c} R_E(\phi_T) & I_m(\phi_T) \\ \hline \end{array} \right] \dot{Z}_{F_i}
 \end{aligned}$$

4.4 REFERENCES

- Ref. 4.1 "Dynamics and Control of Flexible Space Vehicles", P. W. Likens, NASA CR 105592.
- Ref. 4.2 "Small Eccentricities or Inclinations in the Brouwer Theory of the Artificial Satellite", R. H. Lyddane, *Astronomical Journal*, Volume 68, No. 8, October 1963, P. 555.
- Ref. 4.3 Space Station Study (Phase B), Selected Control Moment Gyro Configuration Report 505, General Electric Company Avionic Controls Department, Binghamton, New York.
- Ref. 4.4 Space Station Study (Phase B), Control Moment Gyro Assembly Candidate CMG Assemblies Report 504, General Electric Company Avionic Controls Department, Binghamton, New York.
- Ref. 4.5 Space Station Study (Phase B), Control Moment Gyro Assembly Report EL 506-D, "Preliminary Synthesis and Simulation of Selected CMG Attitude Control System," General Electric Co. Avionic Controls Department, Binghamton, New York.
- Ref. 4.6 Likens, P. W., "Modal Method for Analysis of Free Rotations of Spacecraft," *AIAA Journal*, Vol. 5, #7, July 1967.
- Ref. 4.7 MacNeal, R. H., "The NASTRAN Theoretical Manual," SP-221, pg. 11.3-1 to 11.3-13, Office of Technology Utilization, NASA, Washington, D. C.

5. SOLAR ARRAY AND SPACE STATION STRUCTURAL DYNAMIC ANALYSES AND DATA

Structural dynamic analyses were performed on various solar array and space station configurations to compliment the formulation of the dynamic interactions methodology. The results of these analyses in terms of modal property definitions are required as basic input to the simulation program. Described in this report section are the performed structural analyses for two phases of the interactions study. The first study phase considered only the derivation of solar array modal properties since the space station was considered to be a rigid body. The second study phase considered the influence of space station flexibility in the dynamic interactions methodology and therefore structural mode analyses are also presented for a space station conceptual design.

5.1 PHASE I STUDY ANALYSES

The structural analyses described in this report section were performed to obtain the necessary solar array vibration mode data for use as input to the dynamic interaction analysis simulation. By direction from NASA/LRC, two solar array configurations were considered in the structural analyses; these being a rollup flexible array, configured by the Lockheed Missile and Space Corporation, and a fold out panel array, configured from a Boeing Aircraft Corporation design concept. Both arrays meet the 100 KW power requirement for the North American Rockwell Space Station. In addition, the stowage configuration of both arrays for the launch phase of flight are compatible with the present geometrical constraints imposed by the space station shroud. It is noted, however, that the design criteria for the rollup array includes the loading environment associated with an artificial "G" environment while the fold out panel array is configured for the zero "G" mode of operation only.

A discrete structural element and mass representation of the solar arrays was utilized in the analysis method of deriving the required modal data. This technical approach required the generation of large-order stiffness and mass matrices for subsequent use in a matrix displacement method of modal analysis (Reference 5.1). Details of the modal analyses and analytical results are given in the following report subsections for both the rollup and foldout panel arrays.

5.1.1 FLEXIBLE ROLLUP ARRAY

The stiffness and mass characteristics used to model the flexible array for the determination of vibration modes are based upon information received from LMSC for the North American space station flexible array concept. The array wing section (Figure 5-1) consists of a central extendible boom with inner and outer array support members attached perpendicular to the boom (Reference 5.2). Ten kapton membrane strips are tensioned between the inner and outer support members to which the solar cells are attached. Primary structural member sizes are dictated by the loading associated with the artificial "G" mode of operation which presents the most severe design condition. If the array were designed only for the zero "G" environment, a lighter weight structure would result.

The total array area (2 wing sections) is approximately 10,000 sq. ft. and the electrical power output is rated as 10 watts per sq. ft. A six inch spacing is assumed to exist between the membrane strips and each strip carries a preset tension force of 2 pounds per foot of width. The main boom and support member are specified as frames. However, they are modeled for the discrete element method of analysis as equivalent stiffness beams. The stiffness properties of the structural members are given below.

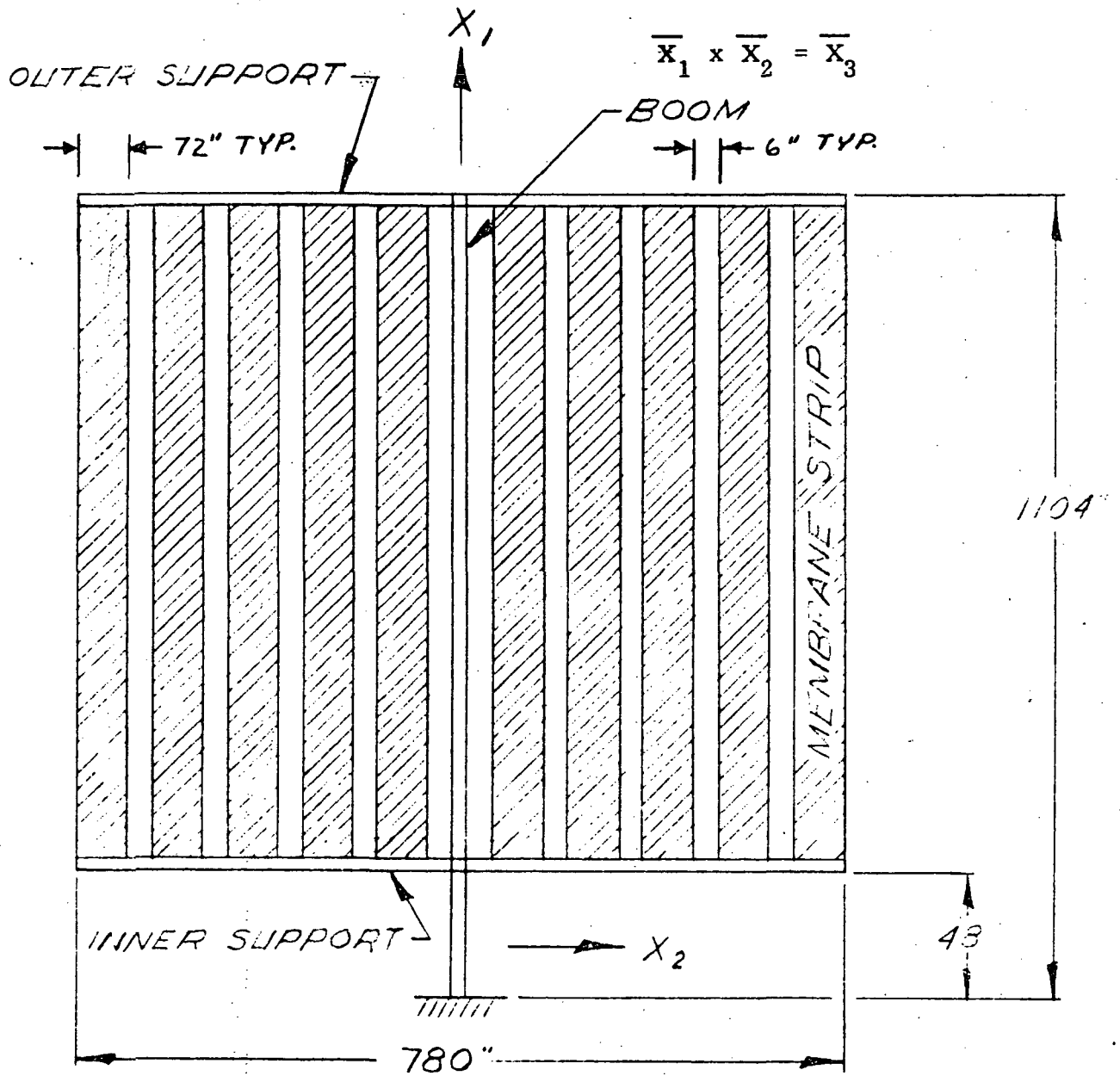


Figure 5-1. Flexible Array Wing Section Dimensions

<u>Member</u>	<u>AE</u> (lbs.)	<u>Elxi₁ *</u> (lb.-in. ²)	<u>Elxi₂ *</u> (lb.-in. ²)	<u>Elxi₃ *</u> (lb.-in. ²)	<u>JG</u> (lb.-in. ²)
Boom	11.45 x 10 ⁶		1489 x 10 ⁶	1585 x 10 ⁶	23.1 x 10 ⁶
Inner and Outer Support	23.4 x 10 ⁶	160 x 10 ⁶		840 x 10 ⁶	

*Elxi refers to moments about the Xi axis where the axis designation is shown on Figure 5-1.

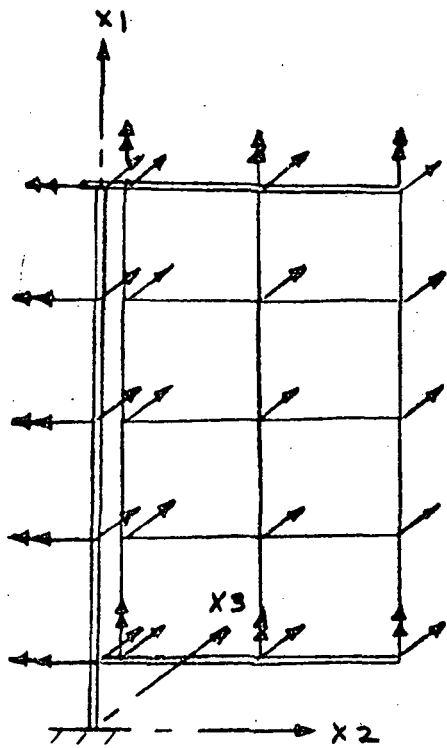
The weight distribution used for each of the structural elements are as follows:

	<u>Running Weight</u>
Boom	0.133 lb/in
Inner Support	0.958 lb/in
Outer Support	0.565 lb/in
Membrane Strips	2.45 (10 ⁻³) lbs/in ²

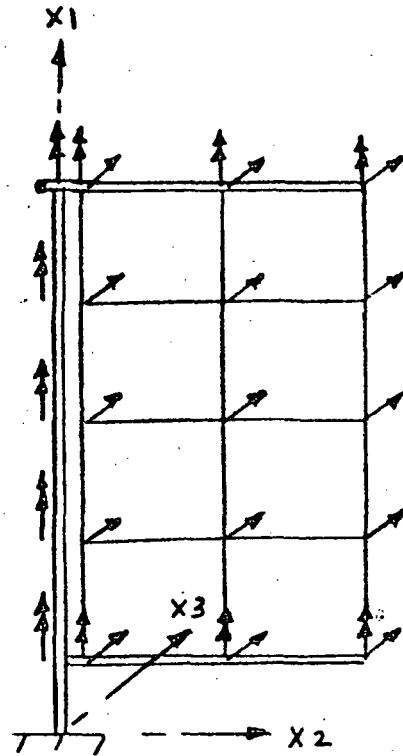
5.1.1.1 Out of Plane Motion - Array Vibration Model

In solving for the out of plane array vibration modes, advantage was taken of the structural and mass symmetry of the rollup array wing section. This enables utilizing a structural model of only one half of the wing section. By suitable adjustment of the boundary conditions along the boom centerline, the symmetric and antisymmetric modes about the boom axes were obtained. Figure 5-2 is a sketch of the finite element model similar to that used for the mathematical representation of the continuous structure.

The out of plane motion degree of freedom given the membrane nodes was an X₃ translation. The support member nodes



a) Symmetric Model



b) Antisymmetric Model

Figure 5-2 Finite Element Model Rollup Array

were allowed degrees of freedom in X_3 translation and X_1 rotation. The boom nodes were allowed to translate in the X_3 direction and rotate about the X_2 axis for the symmetrical condition, and rotate about the X_1 axis only for the antisymmetrical condition.

The discrete element model used for computing the out of plane modes is shown in Figure 5-3. A one-hundred node model was used with the boom rigidly constrained at node 100 as shown. The discrete weights derived for each of the various nodes are tabulated in Table 5-1. The weight associated with this model does not include equipment weight located on the space station tunnel.

TABLE 5-1. NODAL WEIGHTS ASSOCIATED WITH ROLLUP ARRAY DYNAMIC MODEL

Node	Weight (lbs.)
1	26.22
2-8, 11-17, 20-26, 29-35, 28-44, 47-53	11.63
56-62, 65-71, 74-80, 83-89	11.63
10, 19, 28, 37, 46, 55, 64, 73, 82	27.92
9	40.32
18, 27, 36, 45, 54, 63, 72, 81, 90	43.22
91	10.5
92, 93, 94, 95, 96, 97, 98	17.6
99	14.87
100	3.2

Ross' rectangular membrane finite element representation (Reference 5.3) was used to model the membrane strips. A pictorial sketch of this element with the forces and degrees of freedom associated with the element nodes is shown in Figure 5-4a together with the corresponding formulation of the stiffness matrix.

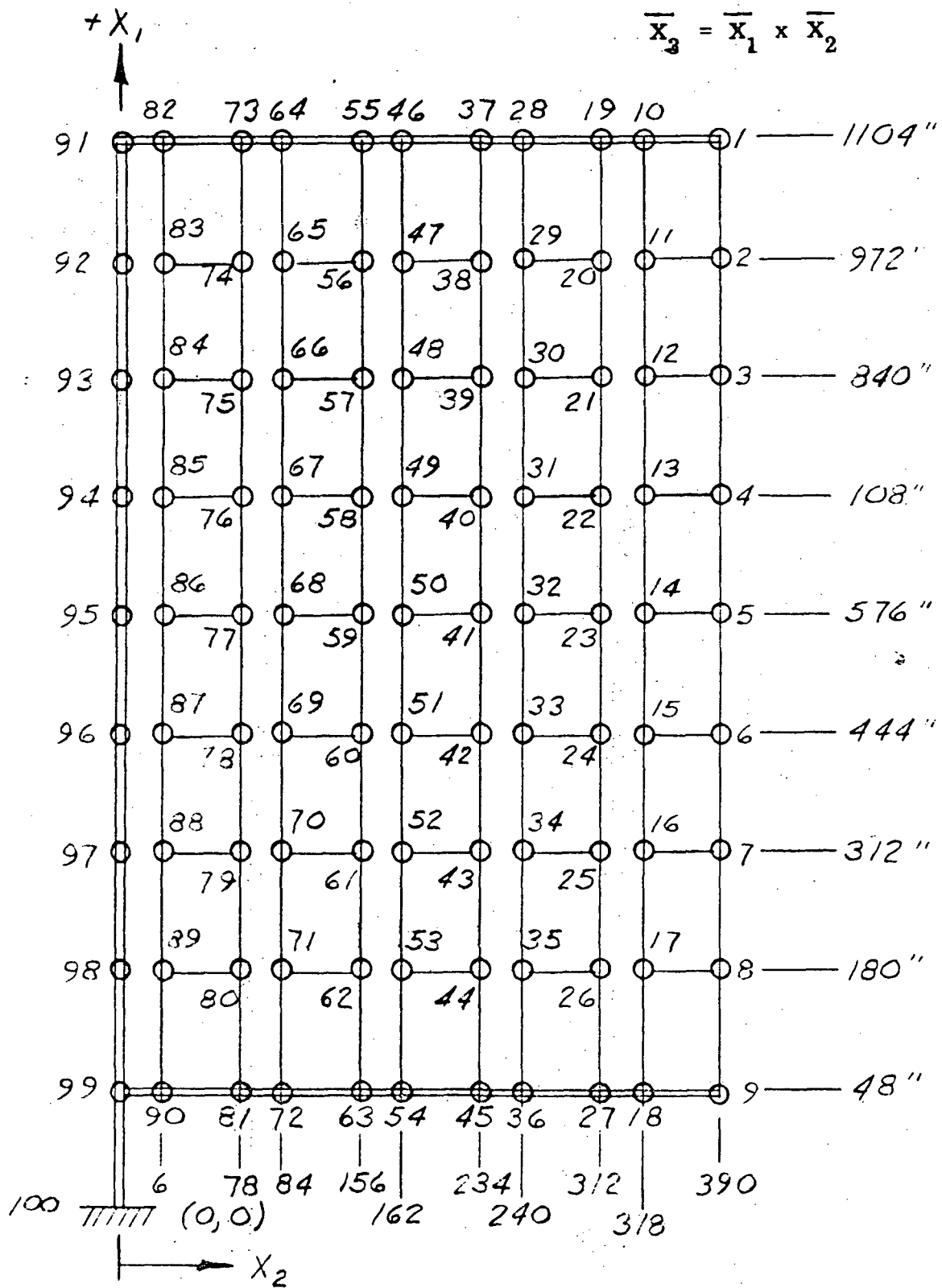


Figure 5 - 3 Dynamic Model, Rollup Array, Out of Plane Modes

$$K = \frac{T}{6 l_1} \begin{bmatrix} \mu_1 & \mu_2 & \mu_3 & \mu_4 \\ 2 & & \text{Sym.} & \\ -2 & 2 & & \\ -1 & 1 & 2 & \\ 1 & -1 & -2 & 2 \end{bmatrix}$$

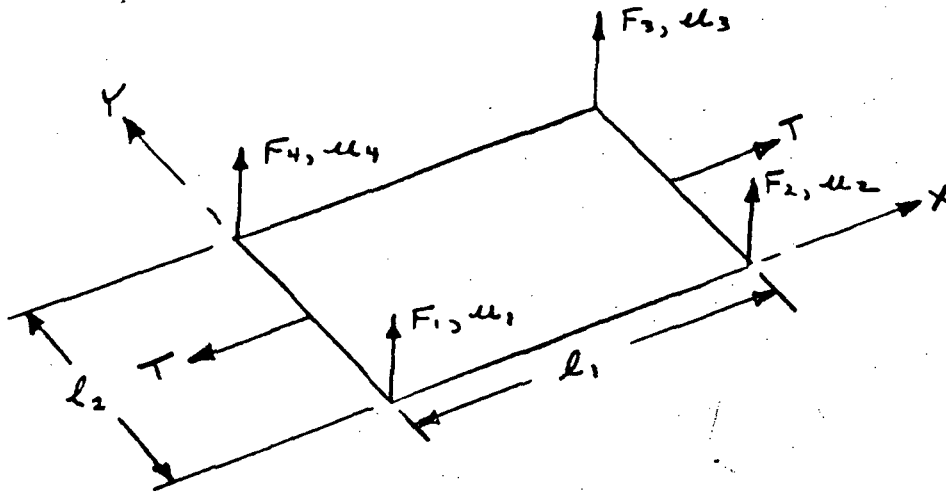


Figure 5-4a Rectangular Membrane Finite Element

$$K = \frac{2 EI}{l^3} \begin{bmatrix} \mu_1 & \theta_1 & \mu_2 & \theta_2 \\ 6 & & \text{Sym.} & \\ 3 l & 2 l^2 & & \\ -6 & -3 l^2 & 6 & \\ 3 l & l^2 & -3 l & 2 l^2 \end{bmatrix} + P/5 \begin{bmatrix} \mu_1 & \theta_1 & \mu_2 & \theta_2 \\ 6/l & & \text{Sym.} & \\ 1/2 & 2l/3 & & \\ -6/l & -1/2 & 6/l & \\ 1/2 & -1/6 & -1/2 & 2l/3 \end{bmatrix}$$

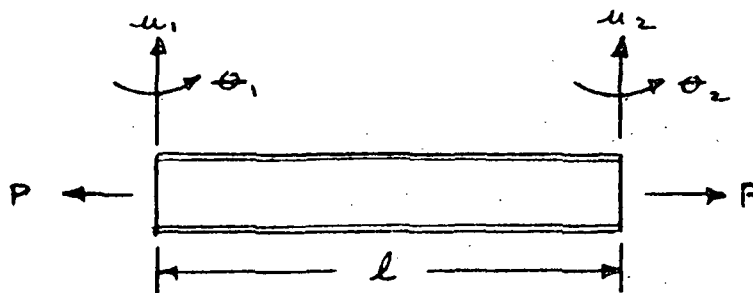


Figure 5-4b Beam Column Finite Element

Figure 5-4. Stiffness Matrices

An axial compression load due to the tensioning of the membrane strips causes a decrease in the lateral stiffness of the boom. This beam column effect was accounted for in the stiffness matrix representing the boom, although for the values of bending and torsional stiffnesses used, the effect is small. The beam columning effect on the stiffness matrix (References 5.3 and 5.4) is shown in Figure 5-4b.

5.1.1.2 In-Plane Motion - Array Vibration Model

The in-plane rollup array model had the same nodes, mass properties and geometry as the out of plane model. Only one half of the wing section was modeled since the wing section is symmetric about the boom axis. Adjustments in the boundary conditions of the boom were made to obtain both the symmetrical and antisymmetrical modes. The model is shown in Figure 5-5. The membrane finite element representation utilized triangular plate elements which are described in Reference 5.1. These elements resist in-plane forces only. The effect of membrane tension upon the elemental in-plane stiffness representation was found to be negligible by use of the stiffness derivation method given in Reference 5.5. All nodes were allowed in-plane motion degrees of freedom only. The symmetrical modes were produced by allowing the boom to deflect only in the X_1 direction, and the antisymmetrical modes were produced by allowing the boom modes to deflect only in the X_2 direction and rotate about the X_3 axis. The symmetric modes induce axial forces into the boom while the antisymmetric modes produce in-plane shear forces and bending moments. The physical characteristics of the Kapton membrane substrate that were utilized for the analysis were:

thickness = 0.004 inch

Youngs Modulus = 450,000 psi

Poisson's ratio = 0.5

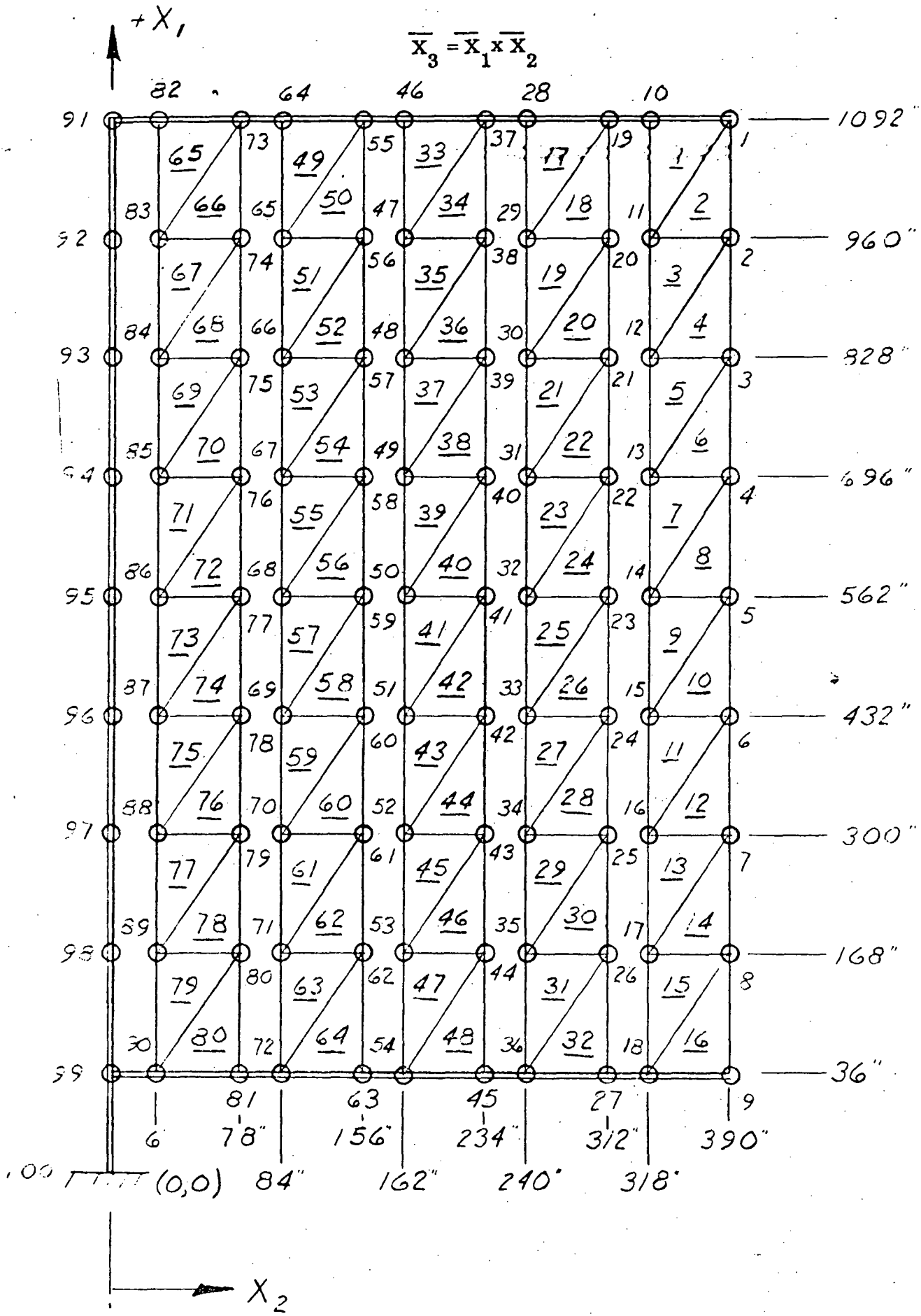


Figure 5-5 In-Plane Rollup Array Model

5.1.1.3 Rollup Array Vibration Modes

From the rollup array out of plane modal analysis, 60 symmetric and 99 antisymmetric eigenvalues were obtained with the corresponding sets of eigenvectors. It was necessary to obtain a large number of modes in order to determine those of importance to the interactions study. Many of the modes are local torsion or bending of the individual membrane strips and do not contribute significantly as external loadings upon the space station.

The first forty-one frequencies for the out of plane modes are tabulated in Tables 5-2 and 5-3 with a description of the modes. Pictorial presentations of each of the lower symmetric and antisymmetric modes along with other higher modes which are considered to be important for inclusion in the interactions study are shown in Figures 5-6 to 5-22. In determining which modes to be used for interaction computer program runs (a total of 12 modes can presently be used for both in-plane and out of plane motion), use was made to modal participation factors. For the symmetric modes, the percent participation is based on the shear at the point of structural constraint due to a base translational acceleration when the value is equal to:

$$\% \text{ participation} = \frac{(\sum m_i \phi_{in})^2}{R_n M} \times 100$$

For the antisymmetric modes, the participation is based on the moment at the point of structural constraint due to a base rotational acceleration. The percent participation is equal to:

$$\% \text{ participation} = \frac{(\sum m_i \phi_{in} r_i)^2}{R_n I_{x1}} \times 100$$

TABLE 5 - 2 LIST OF OUT OF PLANE SYMMETRIC MODE
 FREQUENCIES FOR ROLLUP ARRAY

Mode	Frequency (Hz)	Description
1	.0441	First torsion modes of membrane strips
2	.0441	
3	.0441	
4	.0441	
5	.0441	
6	.0734	First bending modes of membrane strips
7	.0762	
8	.0763	
9	.0763	
10	.0763	
11	.0864	Second torsion modes of membrane strips.
12	.0864	
13	.0864	
14	.0864	
15	.0864	
16	.1255	Third torsion modes of membrane strips.
17	.1255	
18	.1255	
19	.1255	
20	.1255	
21	.1429	Second bending modes of membrane strips
22	.1495	
23	.1497	
24	.1497	
25	.1497	
26	.1597	Fourth torsion modes of membrane strips.
27	.1597	
28	.1597	
29	.1597	
30	.1597	
31	.1878	Fifth torsion modes of membrane strips
32	.1878	
33	.1878	
34	.1878	
35	.1878	
36	.2026	First boom bending mode
37	.2086	Sixth torsion modes of membrane strips
38	.2086	
39	.2086	
40	.2086	
41	.2086	

TABLE 5 - 3 LIST OF OUT OF PLANE ANTISYMMETRIC
MODE FREQUENCIES FOR ROLLUP ARRAY

<u>Mode</u>	<u>Frequency (Hz)</u>	<u>Description</u>
1	.0439	First torsion modes of membrane strips
2	.0441	
3	.0441	
4	.0441	
5	.0441	
6	.0557 -	First torsion mode of boom
7	.0763	First bending modes of membrane strips
8	.0763	
9	.0763	
10	.0763	
11	.0863	Second torsion modes of membrane strips
12	.0864	
13	.0864	
14	.0864	
15	.0864	
16	.1082 -	First bending mode of outer support
17	.1255	Third torsion modes of membrane strips
18	.1255	
19	.1255	
20	.1255	
21	.1256	
22	.1497	Second bending modes of membrane strips
23	.1497	
24	.1497	
25	.1497	
26	.1595	
27	.1597	Fourth torsion modes of membrane strips
28	.1597	
29	.1597	
30	.1597	
31	.1620 -	Second torsion mode of boom
32	.1878	Fifth torsion modes of membrane strips
33	.1878	
34	.1878	
35	.1878	
36	.1878	
37	.2086	Sixth torsion modes of membrane strips
38	.2086	
39	.2086	
40	.2086	
41	.2086	

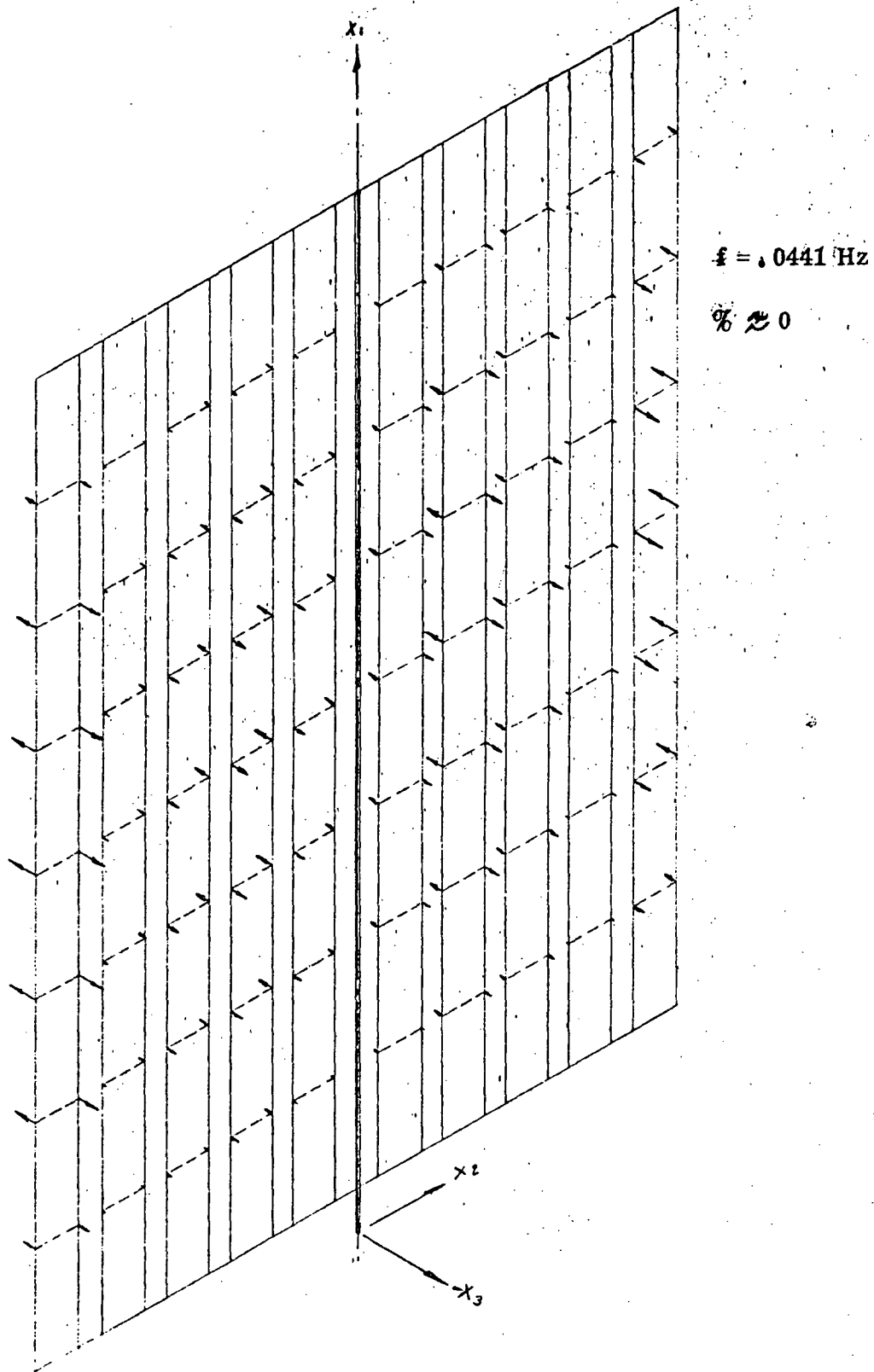
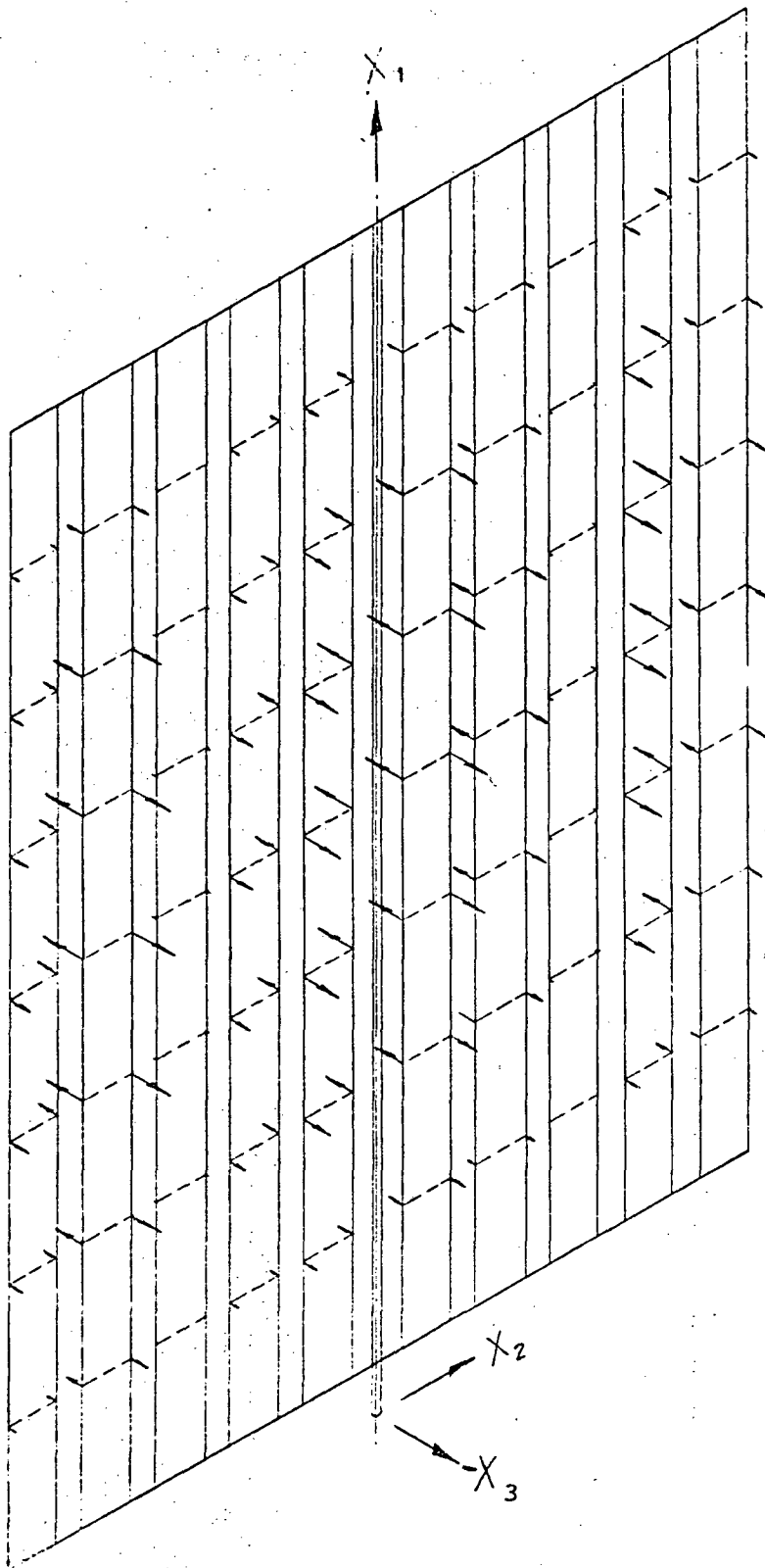


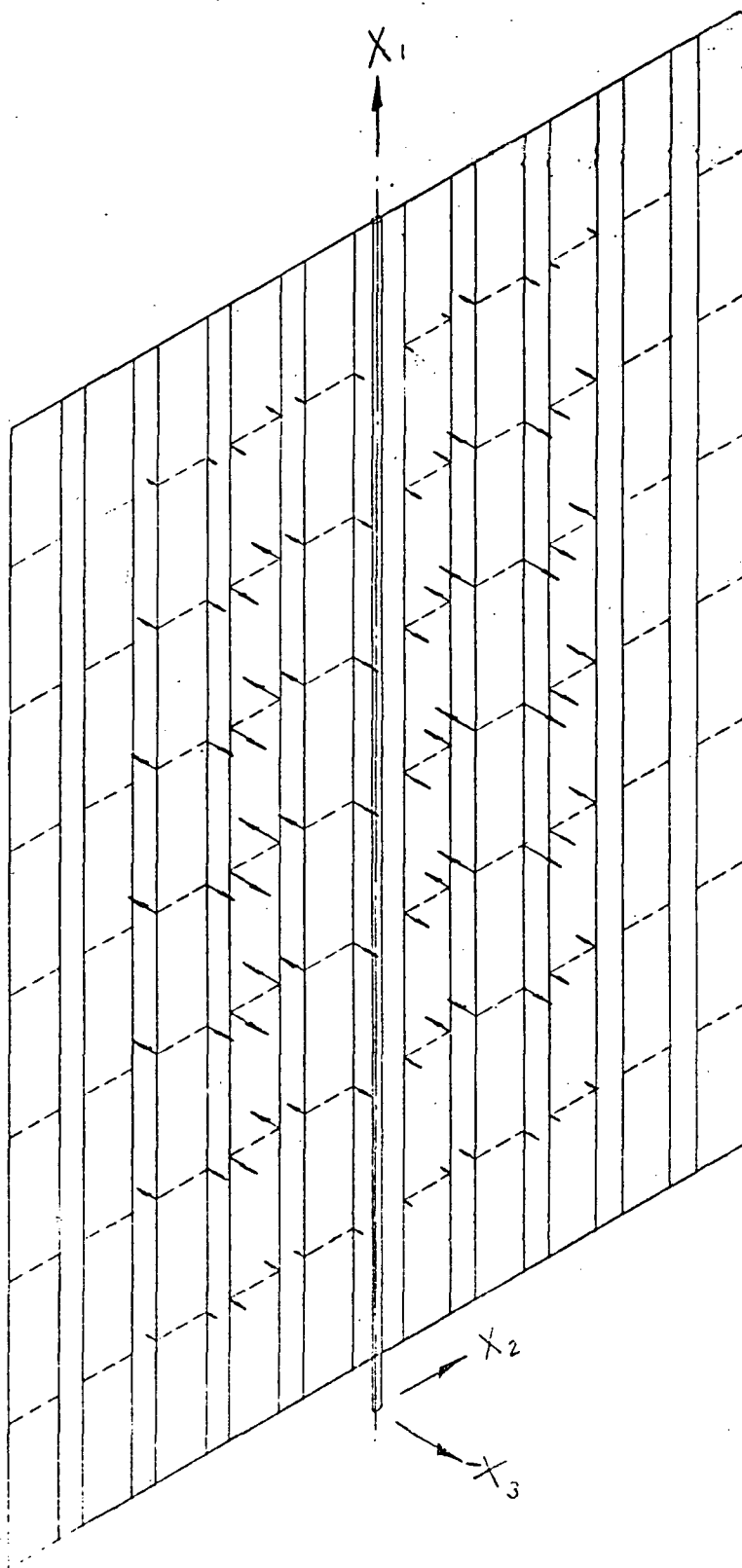
Figure 5-6. Mode 1, Rollup Array, Out of Plane, Symmetric



$f = .0441 \text{ Hz}$

$\% \approx 0$

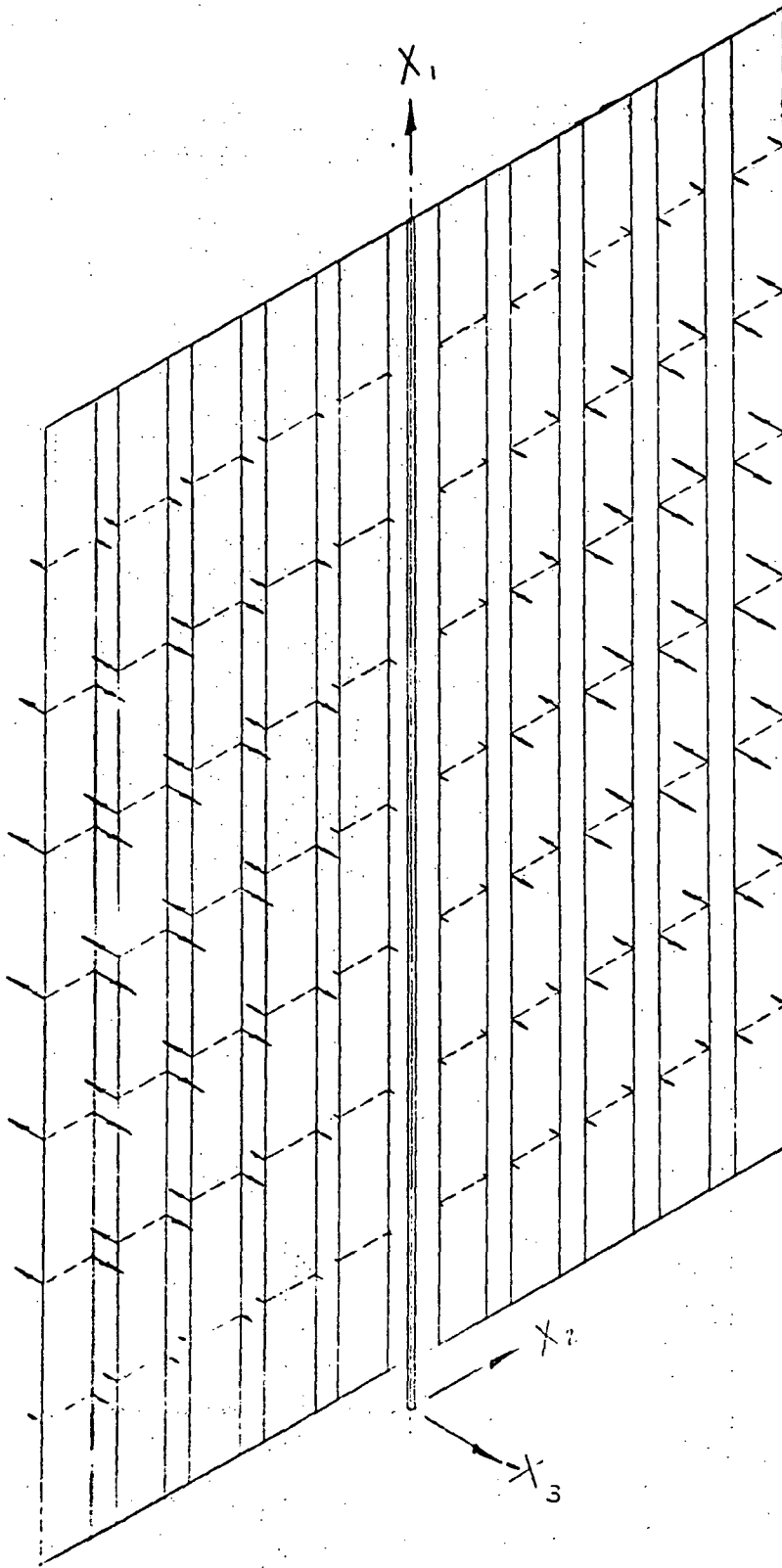
Figure 5-7. Mode 2, Rollup Array, Out of Plane, Symmetric



$f = .0441 \text{ Hz}$

$\% \approx 0$

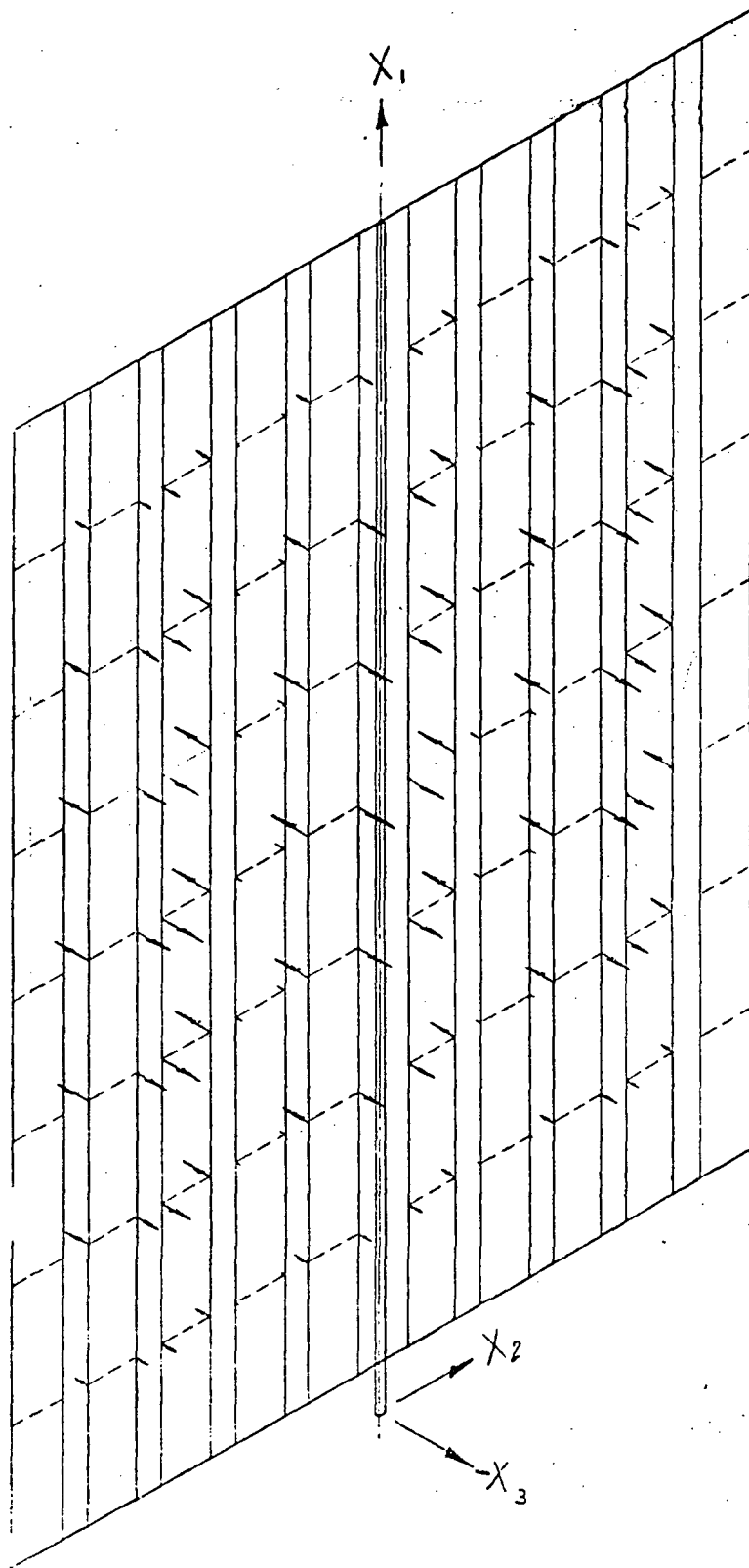
Figure 5-8. Mode 3, Rollup Array, Out of Plane, Symmetric



$f = .0441 \text{ Hz}$

$\eta_0 = .03$

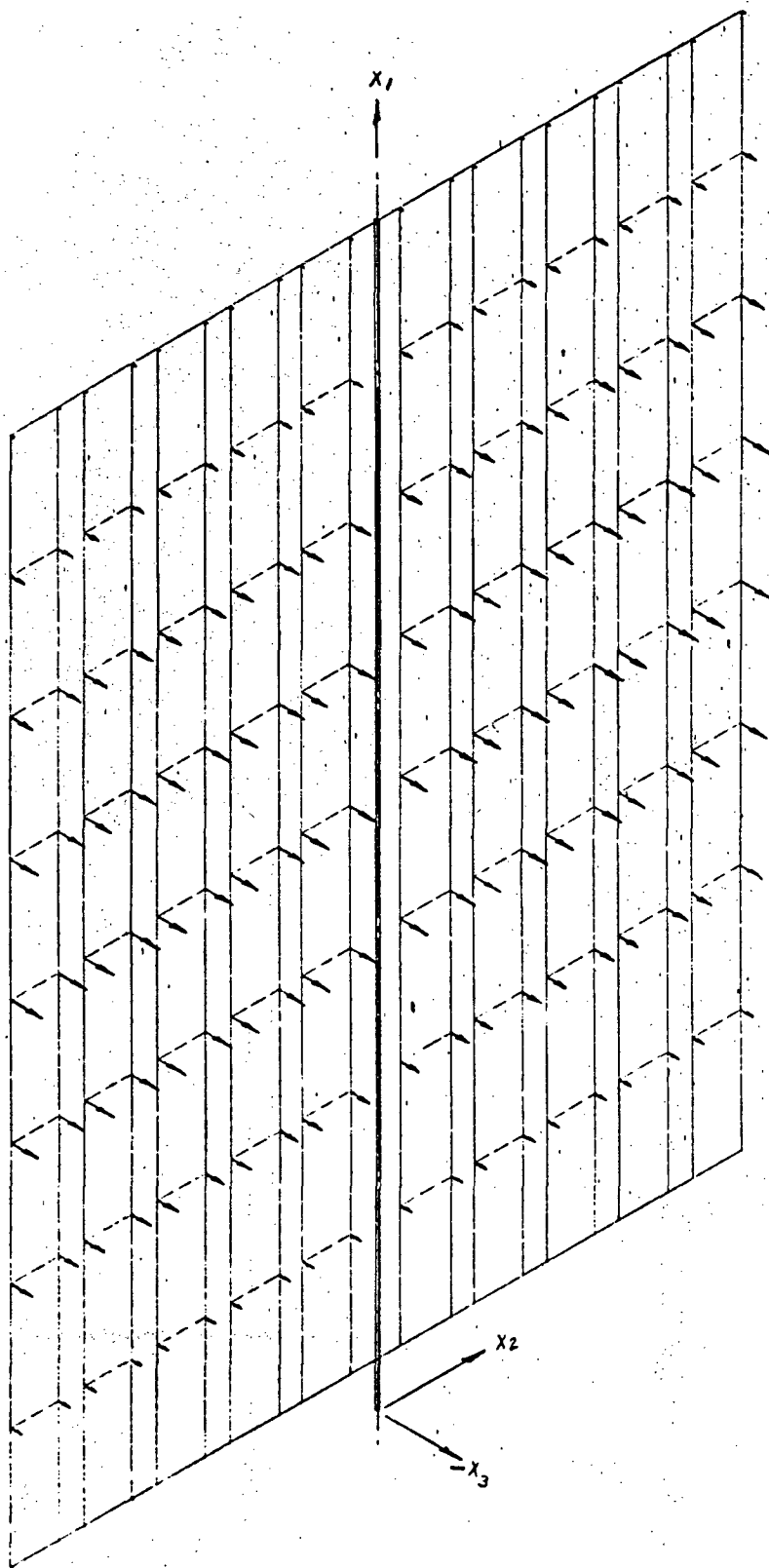
Figure 5-9. Mode 4, Rollup Array, Out of Plane, Symmetric



$f = .0441 \text{ Hz}$

$\% \approx 0$

Figure 5-10 Mode 5, Rollup Array, Out of Plane, Symmetric.



$f = .0734 \text{ Hz}$

$\phi = 50.4$

Figure 5-11 Mode 6, Rollup Array, Out of Plane, Symmetric
5-19

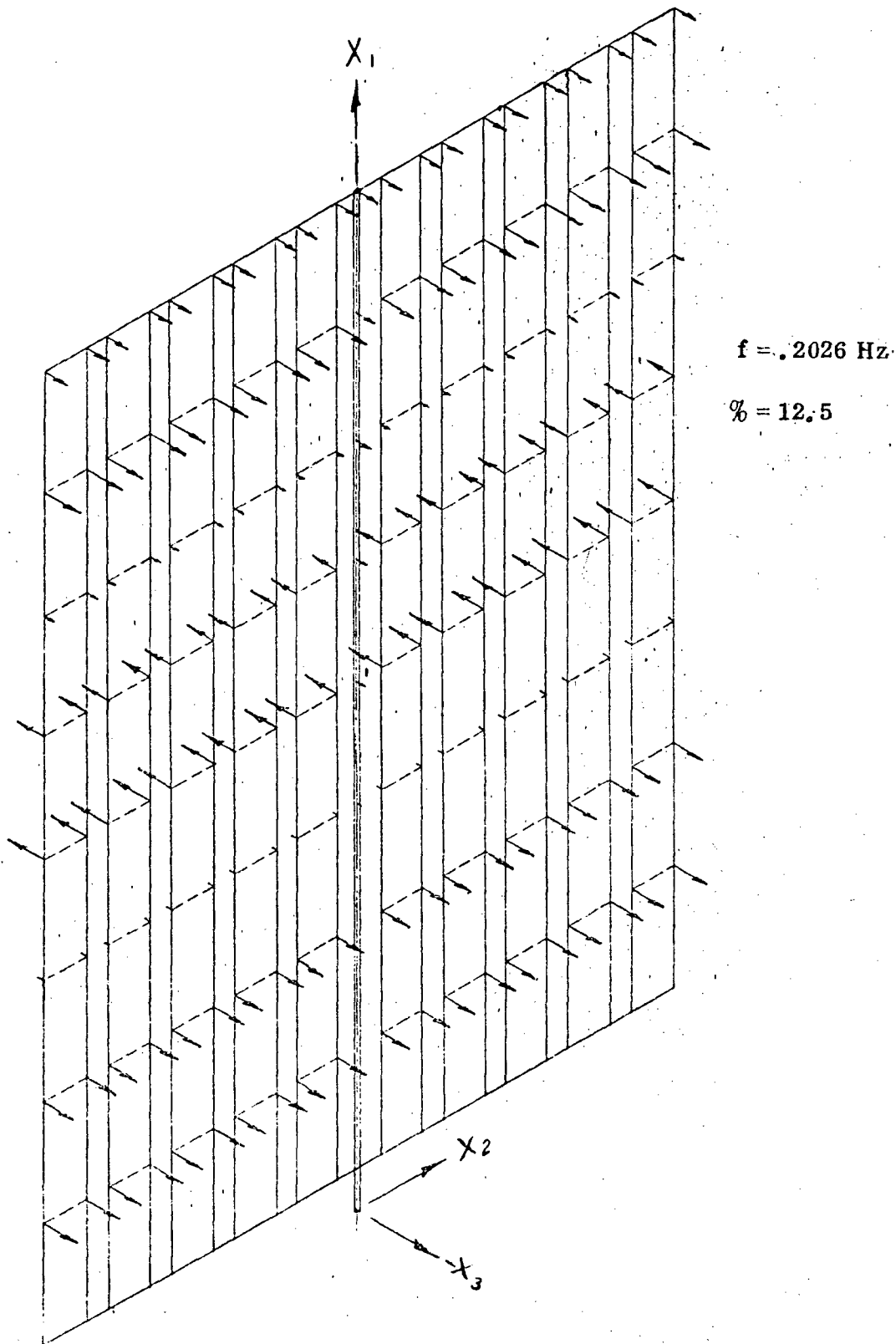


Figure 5-12 Mode 36, Rollup Array, Out of Plane, Symmetric

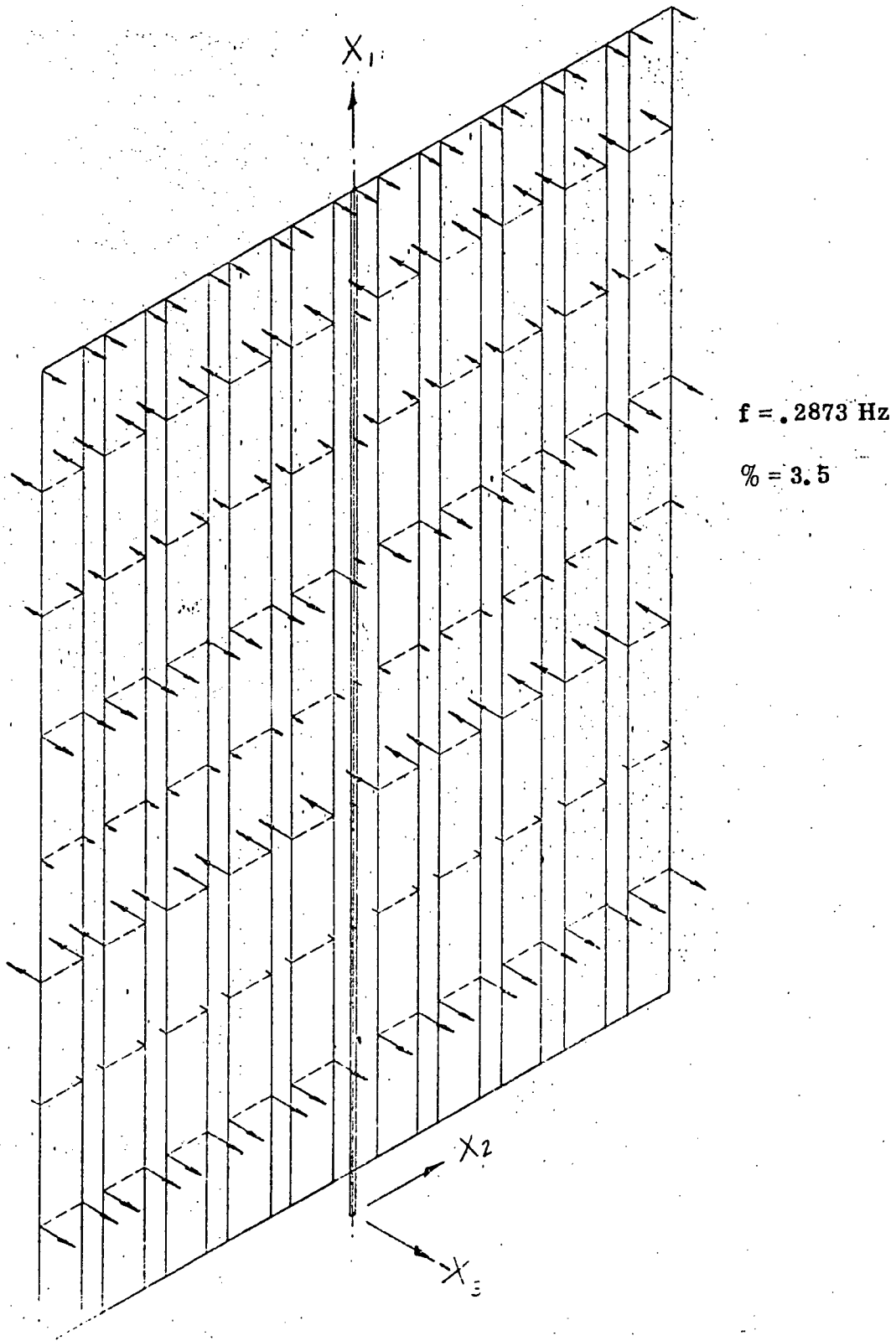


Figure 5-13 Mode 56, Rollup Array, Out of Plane, Symmetric

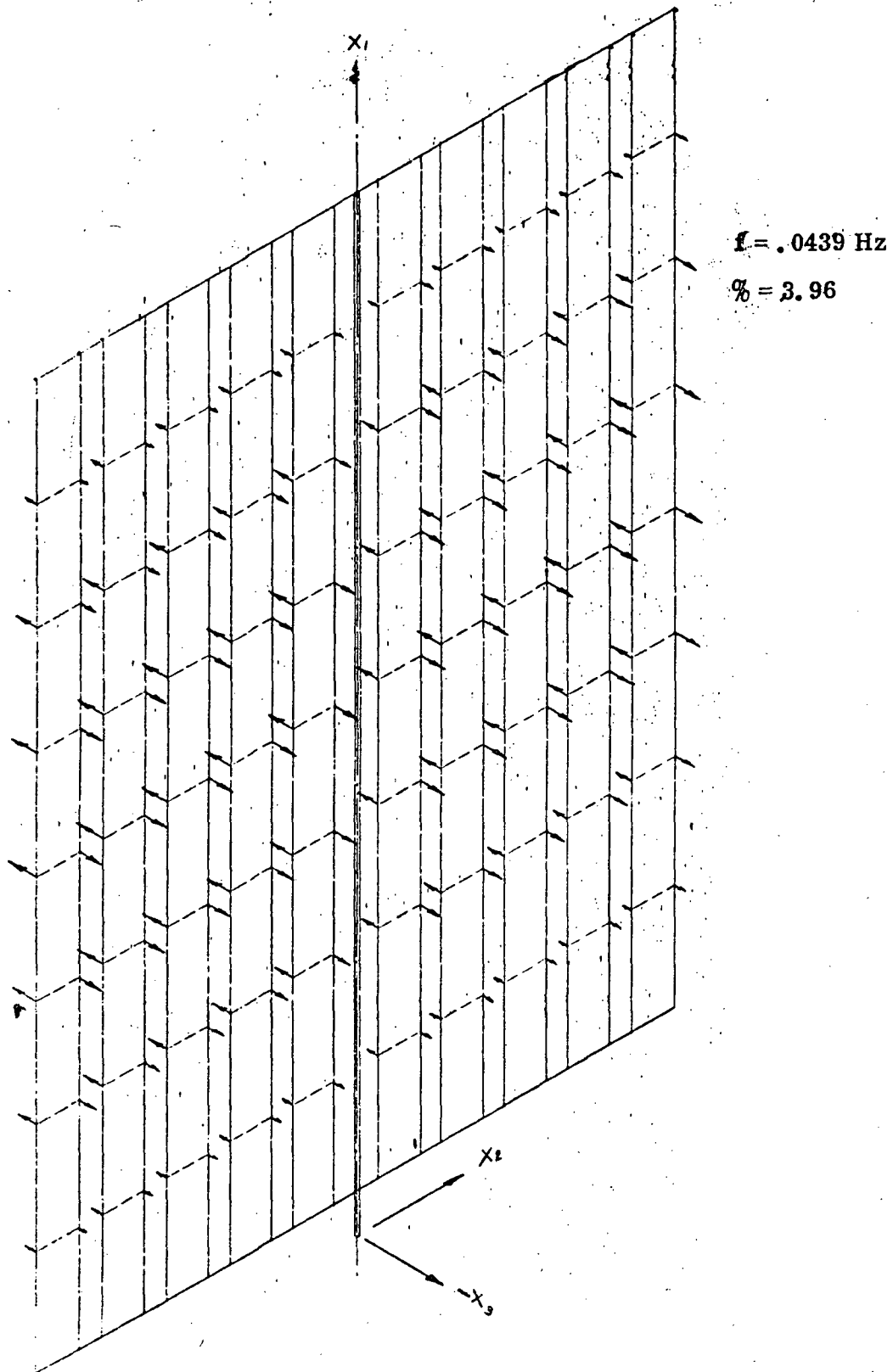
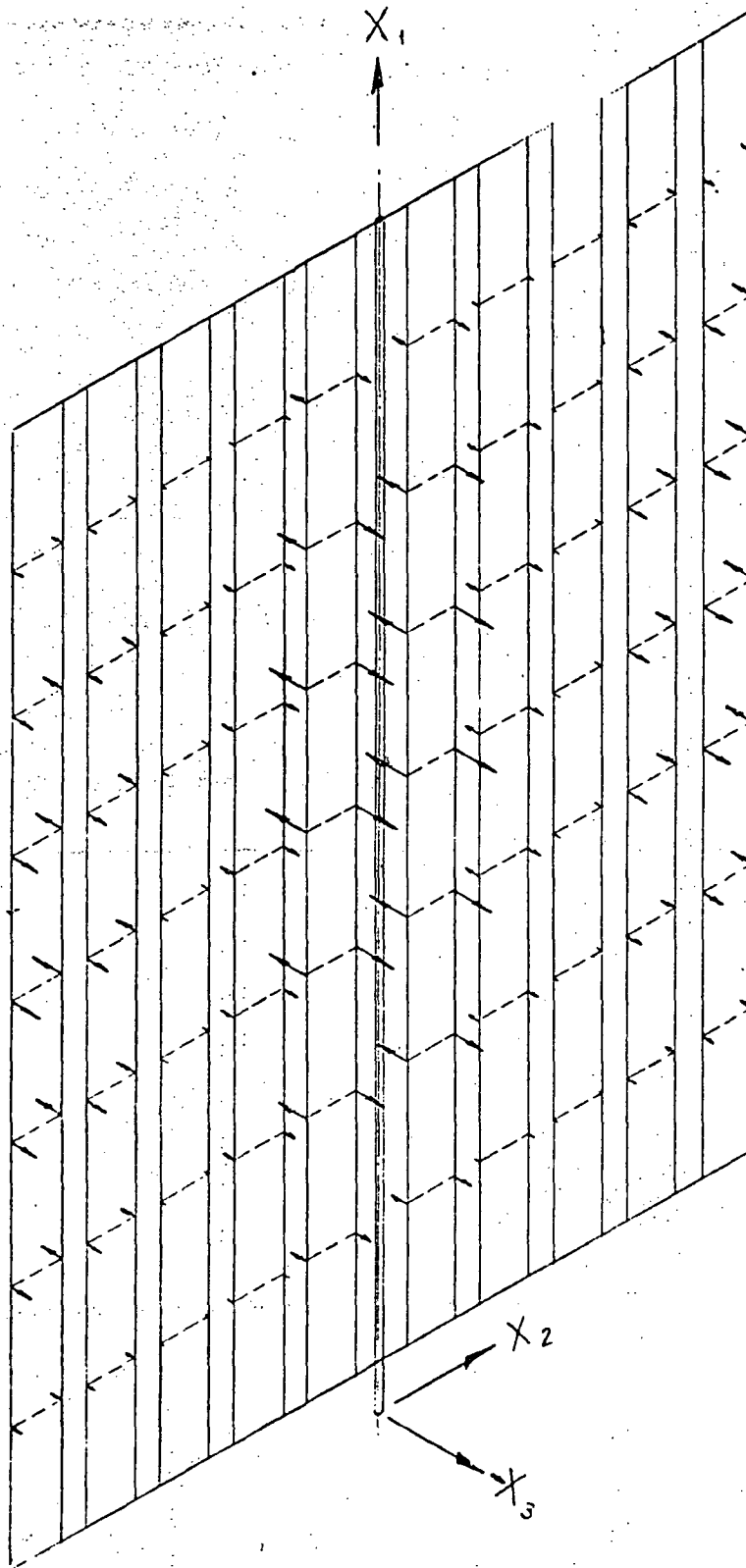


Figure 5-14 Mode 1, Rollup Array, Out of Plane, Antisymmetric



$f = .0441 \text{ Hz}$

$\% \approx 0$

Figure 5-15 Mode 2, Rollup Array, Out of Plane, Antisymmetric

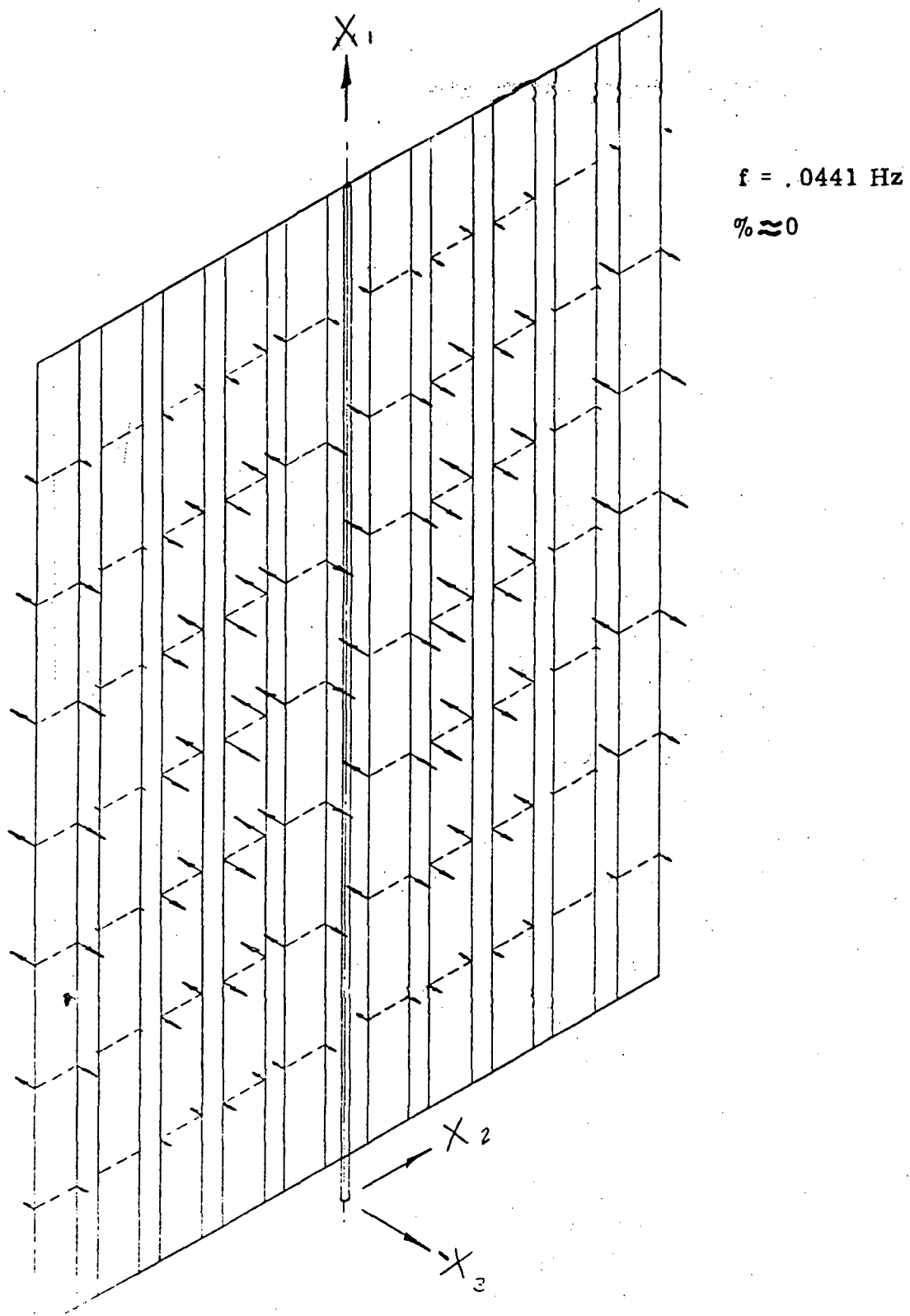
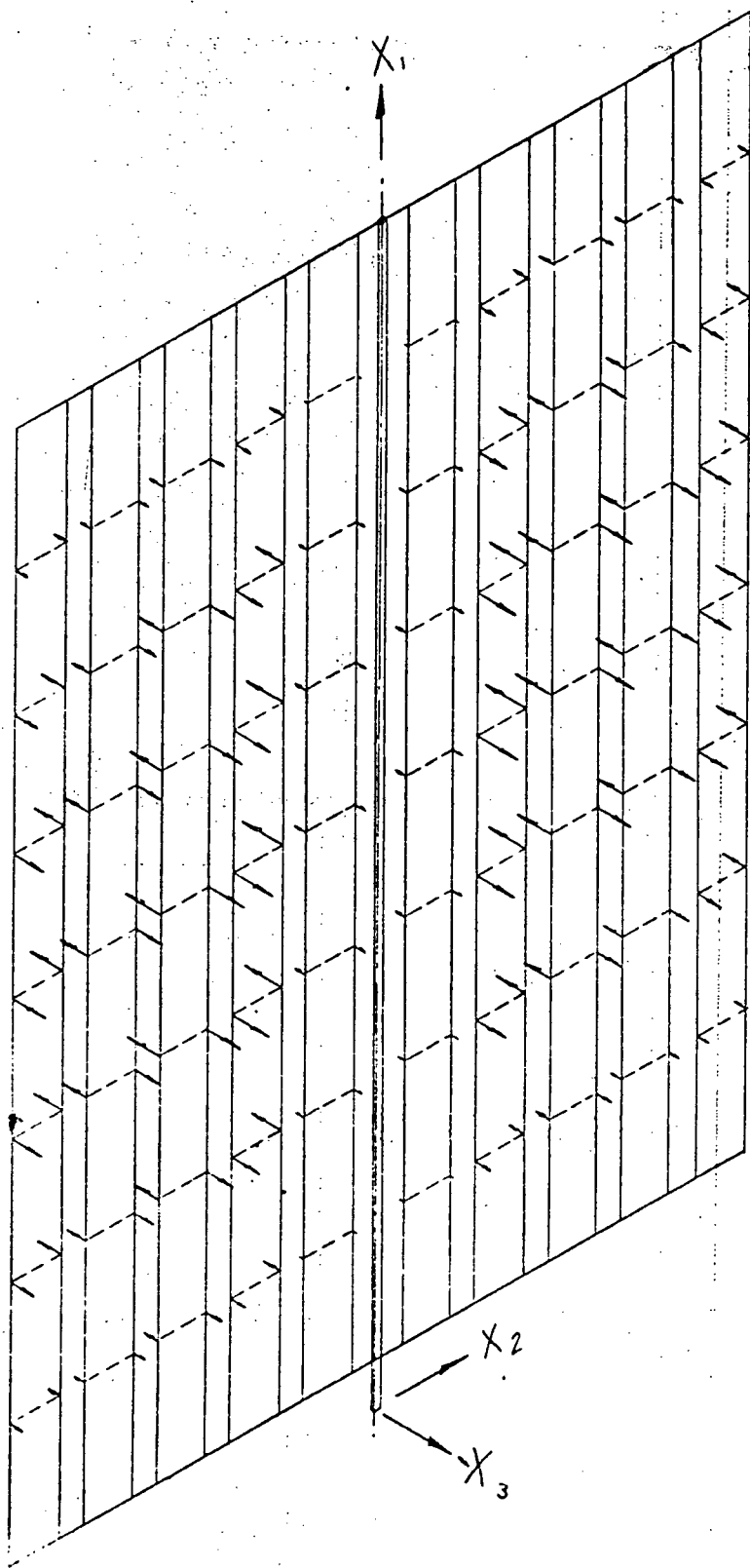


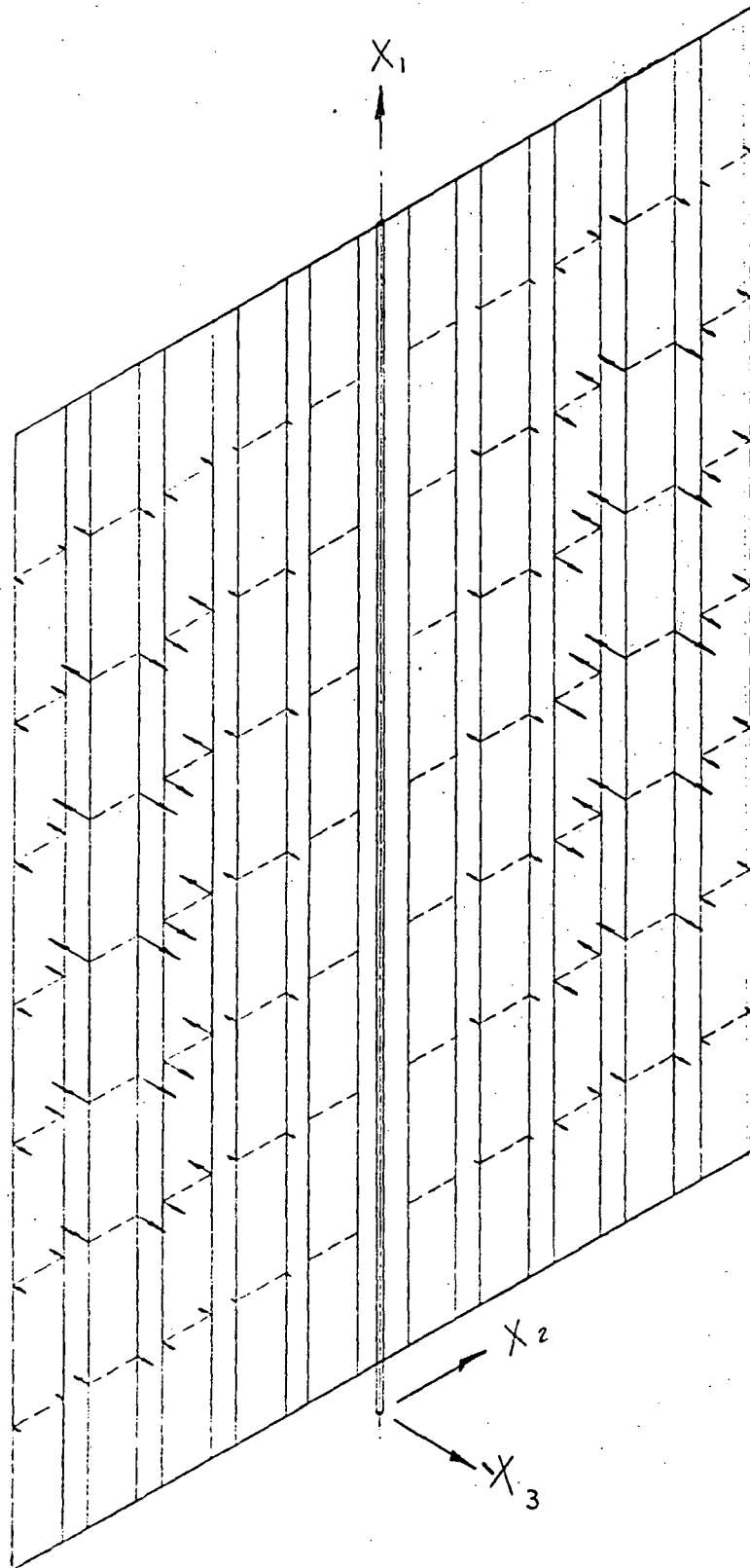
Figure 5-16 Mode 3, Rollup Array, Out of Plane, Antisymmetric



$f = .0441 \text{ Hz}$

$\% \approx 0$

Figure 5-17 Mode 4, Rollup Array, Out of Plane, Antisymmetric



$f = .0441 \text{ Hz}$

$\eta_0 \approx 0$

Figure 5-18. Mode 5, Rollup Array, Out of Plane, Antisymmetric

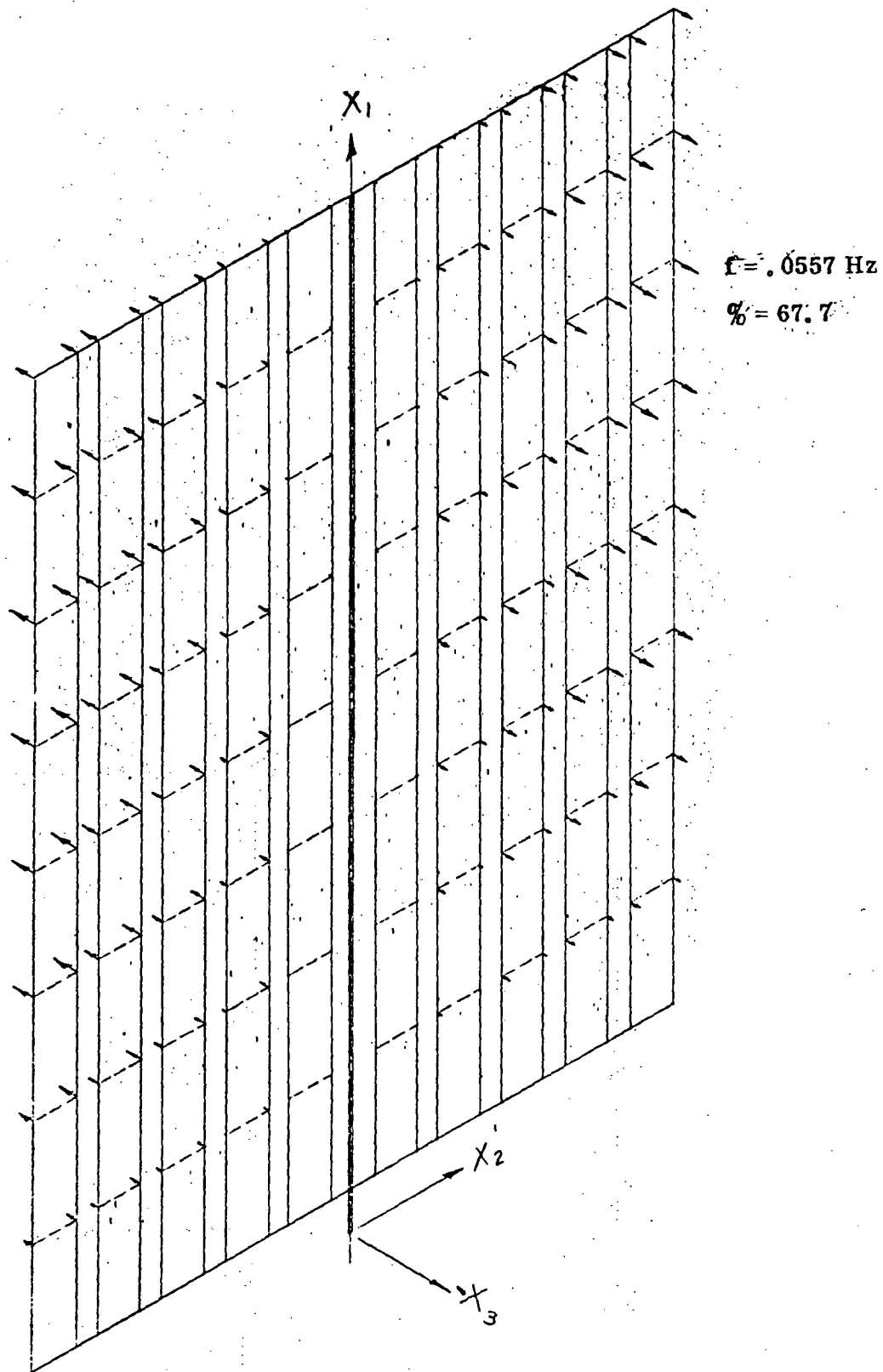


Figure 5-19 Mode 6, Rollup Array, Out of Plane, Antisymmetric

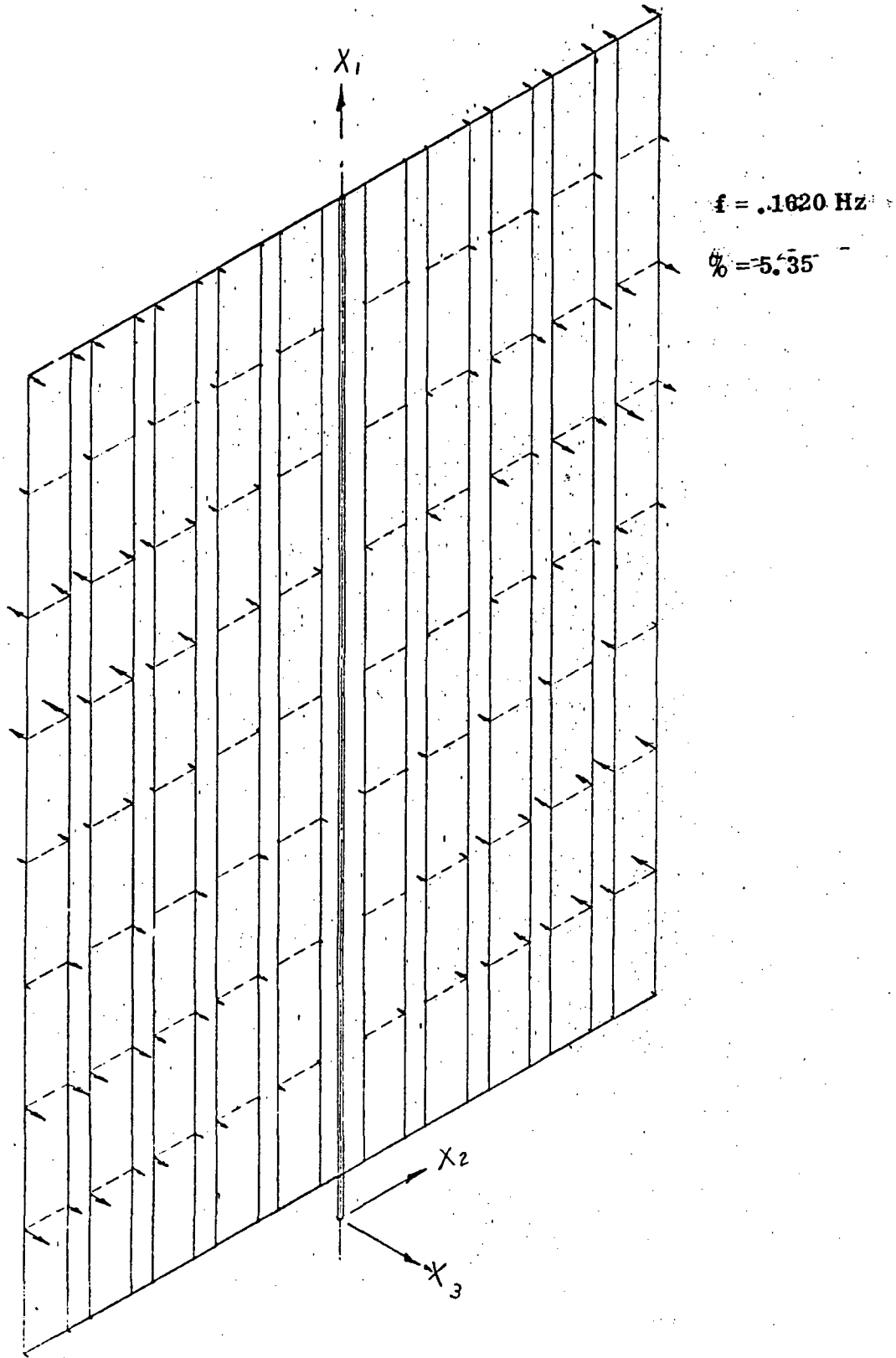


Figure 5-20 Mode 31, Rollup Array, Out of Plane, Antisymmetric

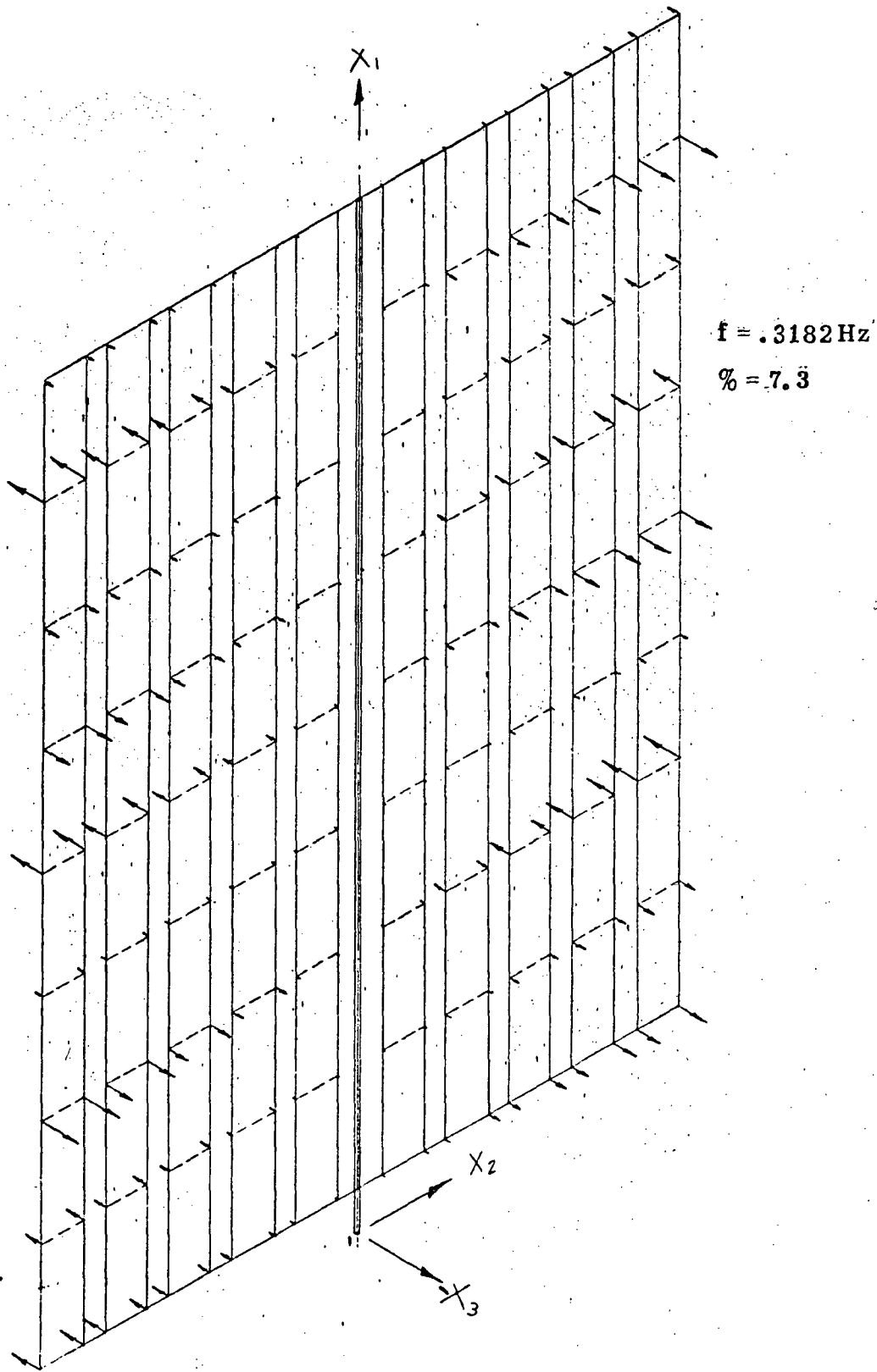


Figure 5-21 Mode 57, Rollup Array, Out of Plane, Antisymmetric

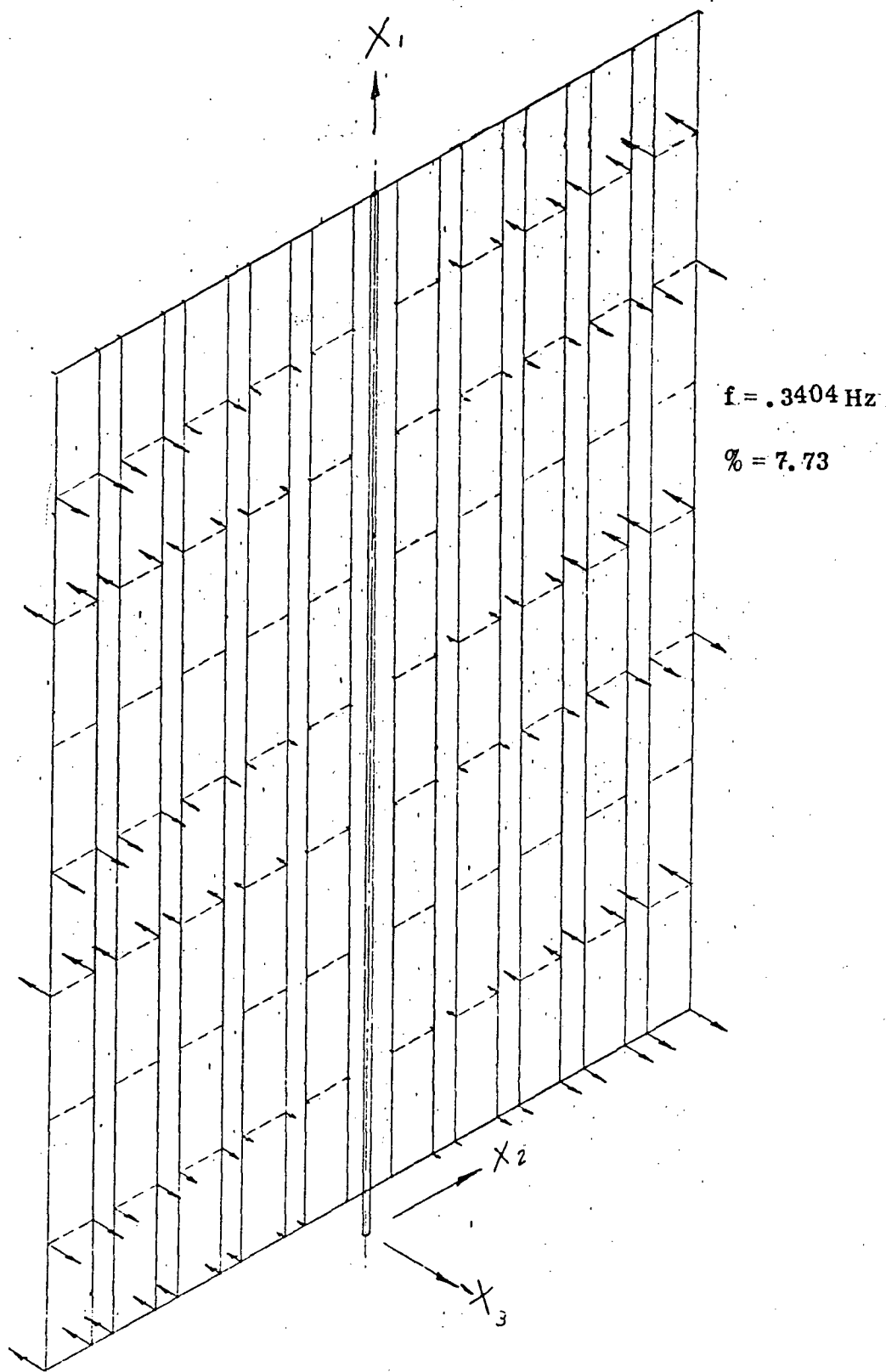


Figure 5-22. Mode 62, Rollup Array, Out of Plane, Antisymmetric

where

- m_i - mass of discrete node i (lb.-sec.²/in.)
- ϕ_{in} - deflection of node i for mode n
- R_n - generalized inertia of mode n (lb.-sec.²/in.)
- M - mass of dynamic model (lb.-sec.²/in.)
- r_i - distance along X_2 axis of mass i . (in.) (Ref. Fig. 5.1-3)
- I_{x1} - moment of inertia of dynamic model about the X_1 axis (lb.-in.-sec.²)

The participation factors for the full wing section are shown on the mode shape plots along with the frequencies. The modes which were chosen to be important for subsequent interaction analyses were antisymmetric modes 6, 31, 57 and 62 and symmetric modes 6, 36, and 56.

From the rollup array in-plane modal analysis, eigenvalues and corresponding eigenvectors were computed up to 5 Hz. Frequencies within this range should be sufficient to determine the effects of the array flexibility on the spacecraft control system. Six symmetric and eight antisymmetric modes were obtained for these cases. The frequencies for these modes are listed in Table 5-4.

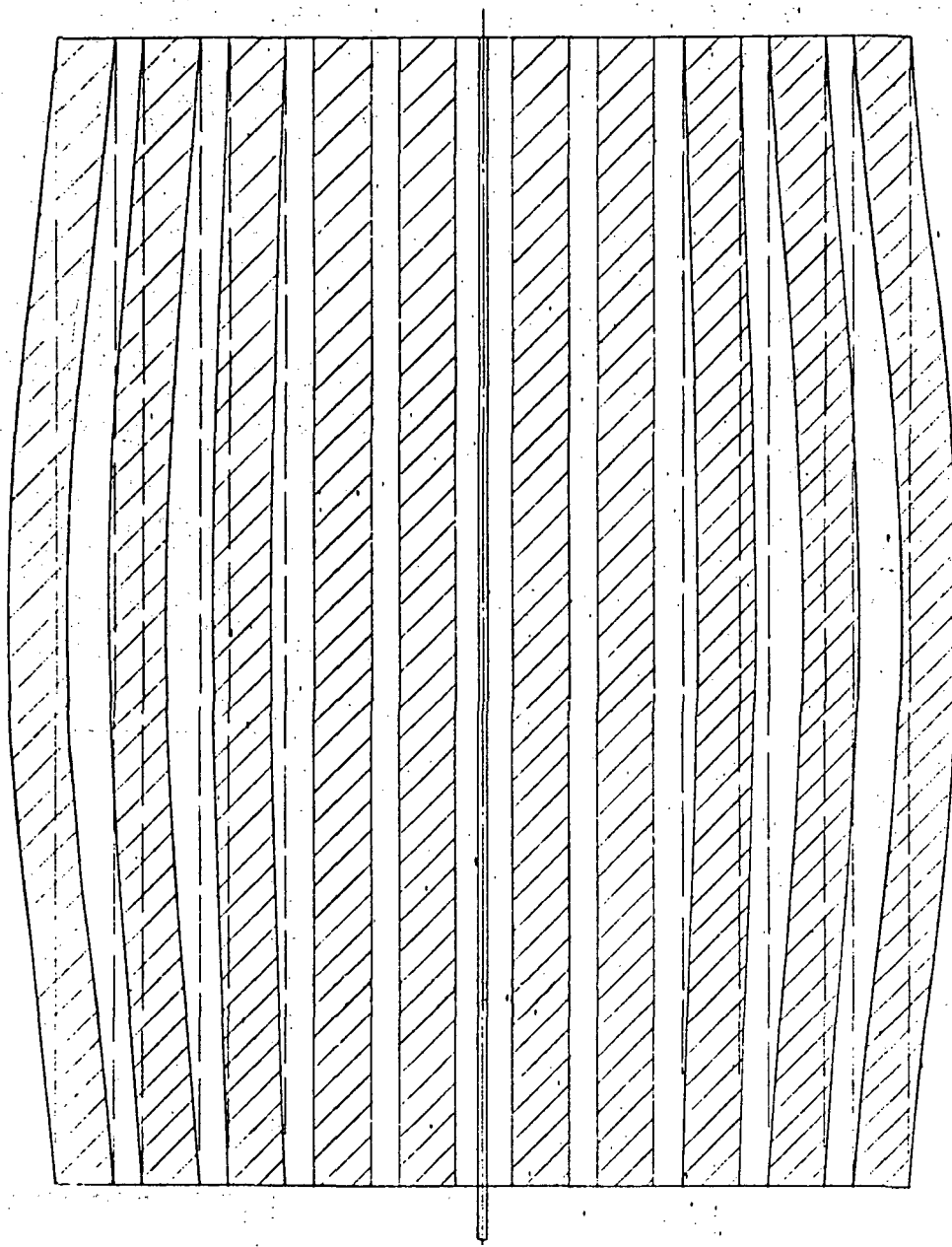
TABLE 5 - 4 FREQUENCIES OF IN-PLANE MODES FOR ROLLUP ARRAY

Mode	Frequency (Hz)	
	Symmetric	Antisymmetric
1	2.1199	.2911
2	2.2604	1.939
3	2.3825	2.177
4	2.4486	2.4139
5	2.4895	2.4757
6	2.5038	2.4999
7	-----	2.7056
8	-----	4.1198

The modal participation factors for these cases are based on axial load due to a base translational acceleration for the symmetric modes and shear load due to a base translational acceleration for the antisymmetric case. The mode shapes for the full wing section and percent modal participations are shown in Figures 5-23 to 5-29. On these figures, the solid lines are the deflected shapes while the dashed lines are the the undeflected outline of the wing section. The modes which were chosen to be important for interaction analyses are symmetric mode 2 and anti-symmetric modes 1, 2, 7 and 8. The complete list of frequencies and modal participation factors for the modes selected for use in the interaction program for the rollup array are listed in Table 5-5.

TABLE 5 —5 FREQUENCIES AND MODAL PARTICIPATION FACTORS OF ROLLUP ARRAY MODES USED IN INTERACTION ANALYSIS

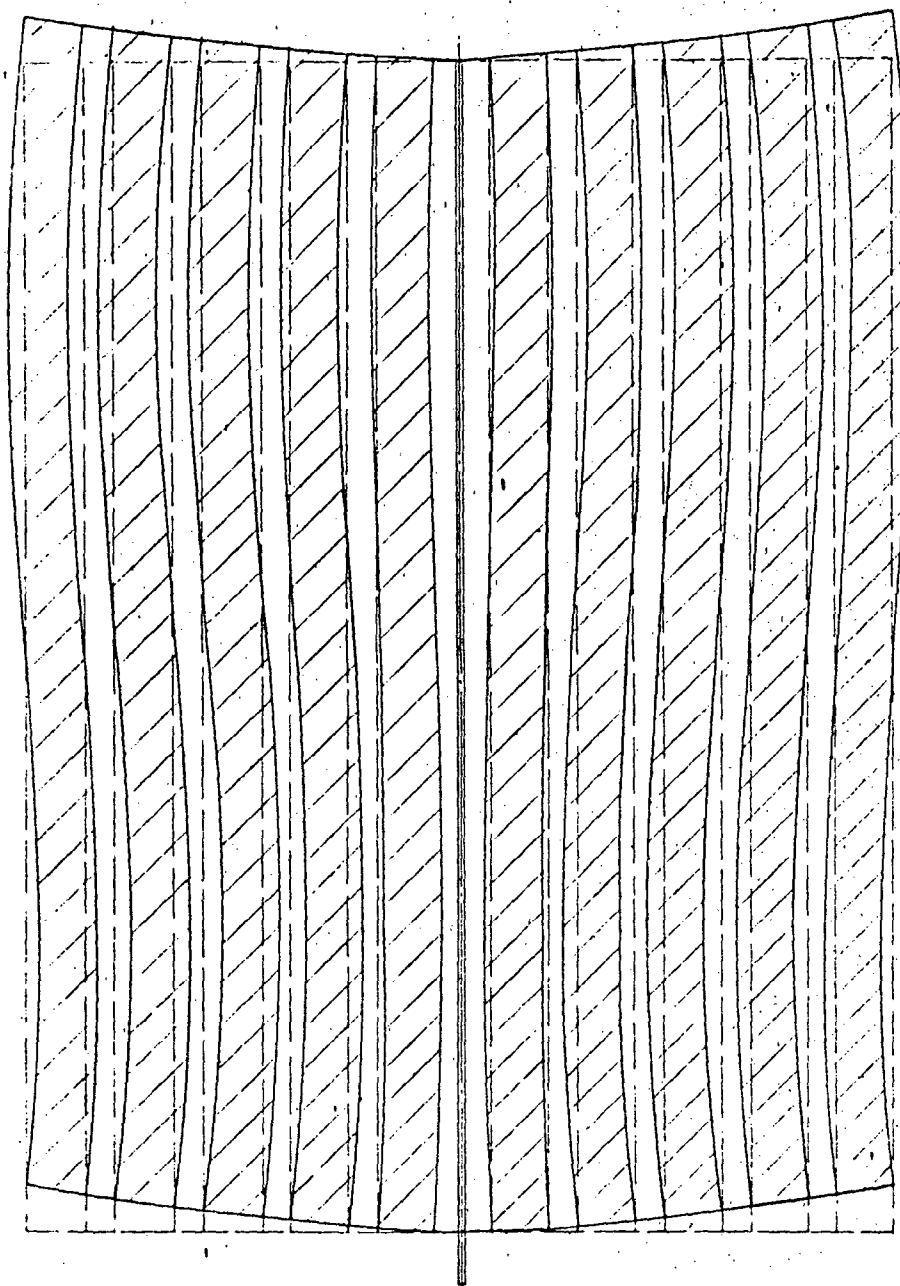
Out of Plane					
Symmetric			Antisymmetric		
Mode	Frequency (Hz)	Percent Participation	Mode	Frequency (Hz)	Percent Participation
6	.0734	50.4	6	.0557	67.7
36	.2026	12.5	31	.1620	5.35
56	.2873	3.5	57	.3182	7.3
			62	.3404	7.73
In-Plane					
Symmetric			Antisymmetric		
Mode	Frequency (Hz)	Percent Participation	Mode	Frequency (Hz)	Percent Participation
2	2.2604	57	1	.2911	55
			2	1.939	3.1
			7	2.7056	6.5
			8	4.1198	2.7



$f = 2.1199 \text{ Hz}$

$\% = .312$

Figure 5-23. Mode 1, Rollup Array, Inplane, Symmetric



$f = 2.2604 \text{ Hz}$

$\% = 57$

Figure 5-24. Mode 2, Rollup Array, Inplane, Symmetric

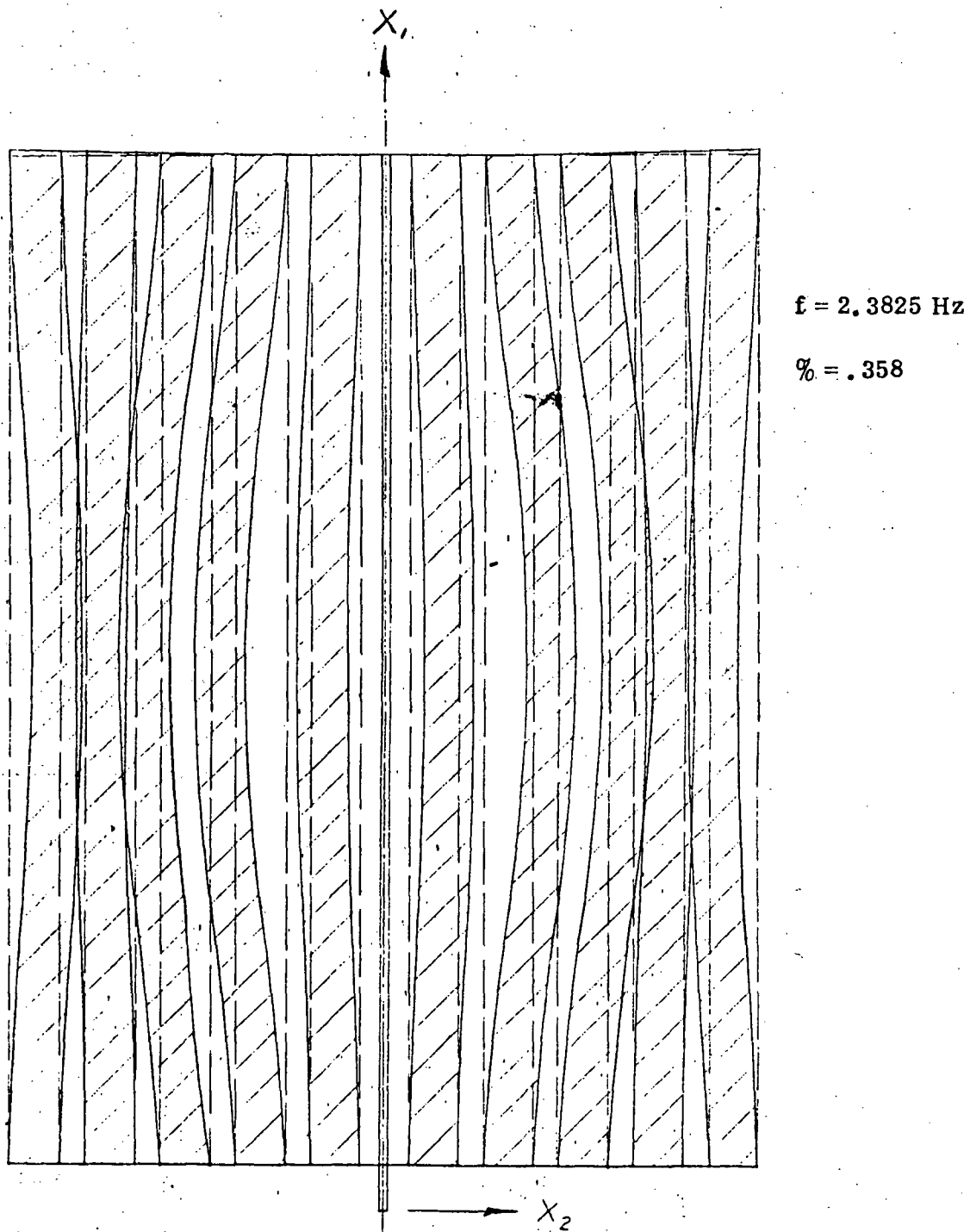
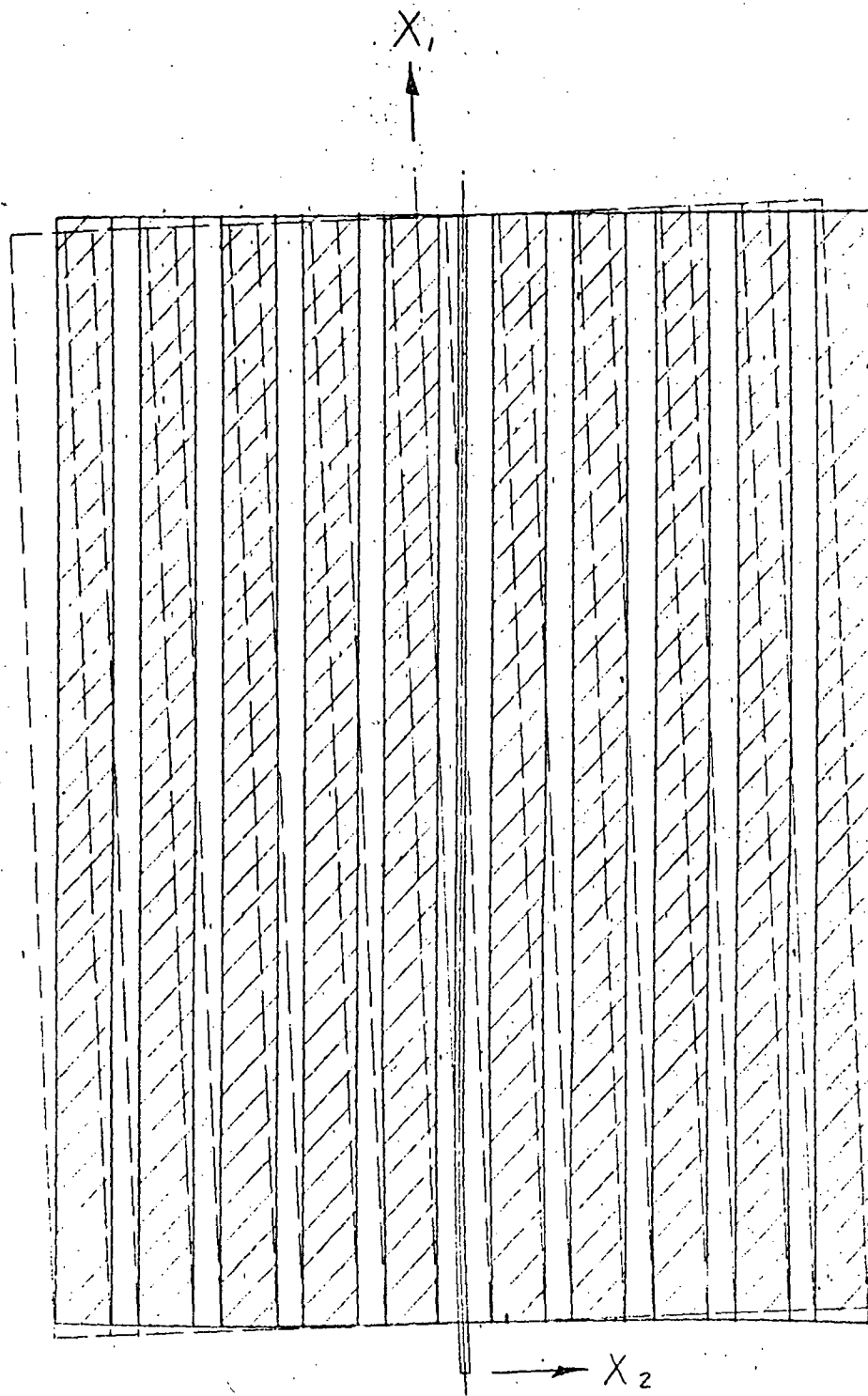


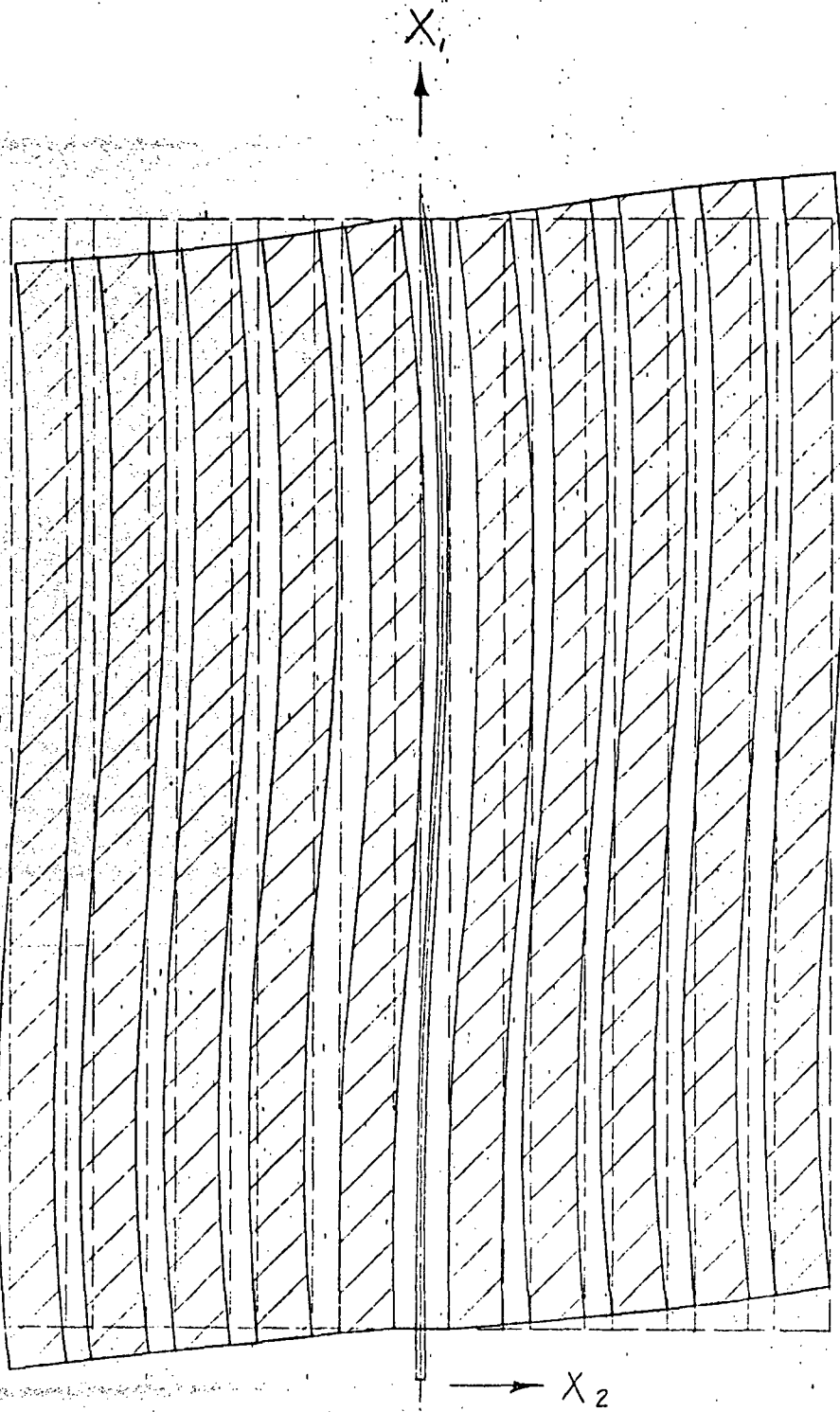
Figure 5-25. Mode 3, Rollup Array, Inplane, Symmetric



$f = .2911 \text{ Hz}$

$\% = 55$

Figure 5-26. Mode 1, Rollup Array, Inplane, Antisymmetric



$f = 1.939 \text{ Hz}$

$\% = 3.1$

Figure 5-27 Mode 2, Rollup Array, Inplane, Antisymmetric

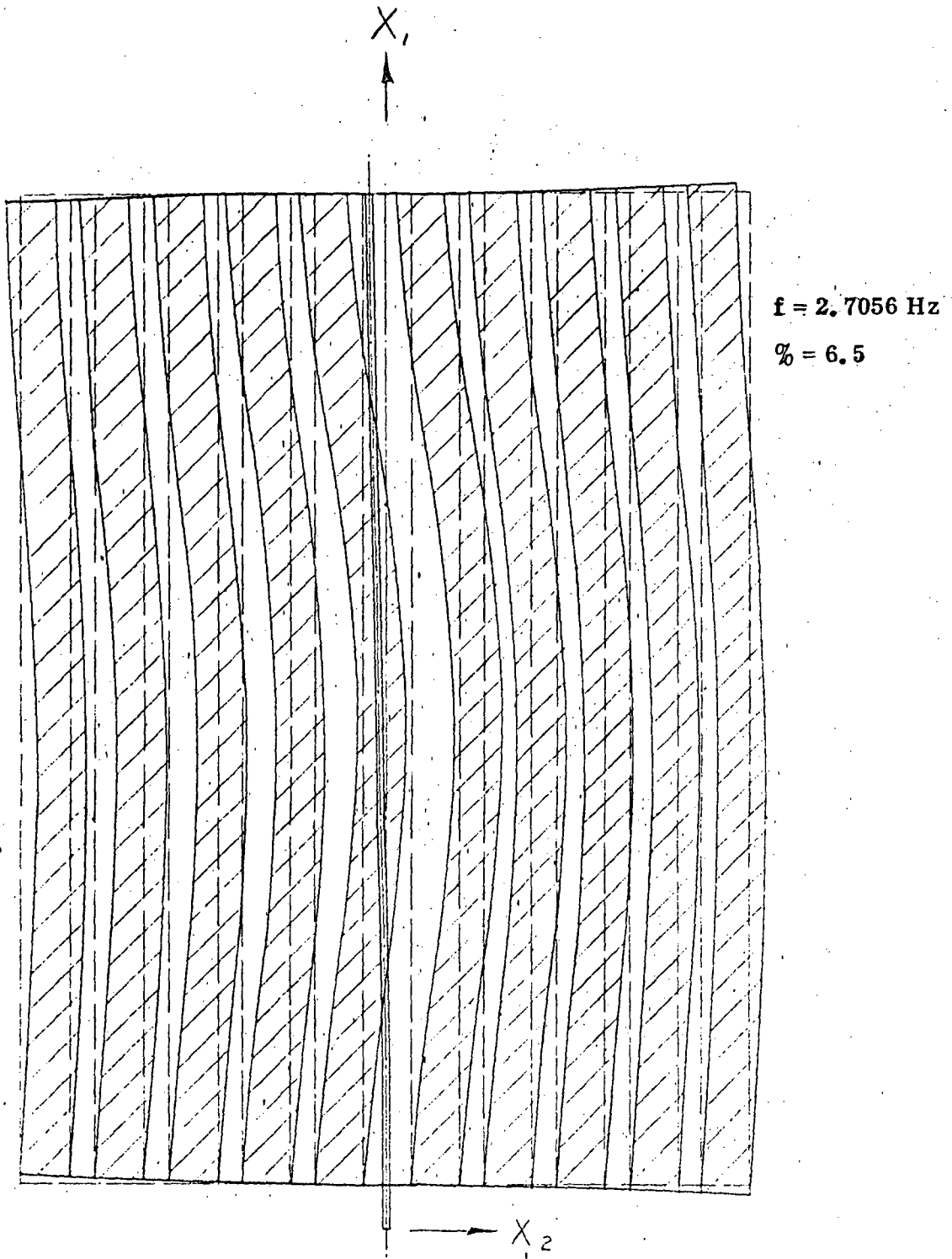


Figure 5-28. Mode 7, Rollup Array, Inplane, Antisymmetric

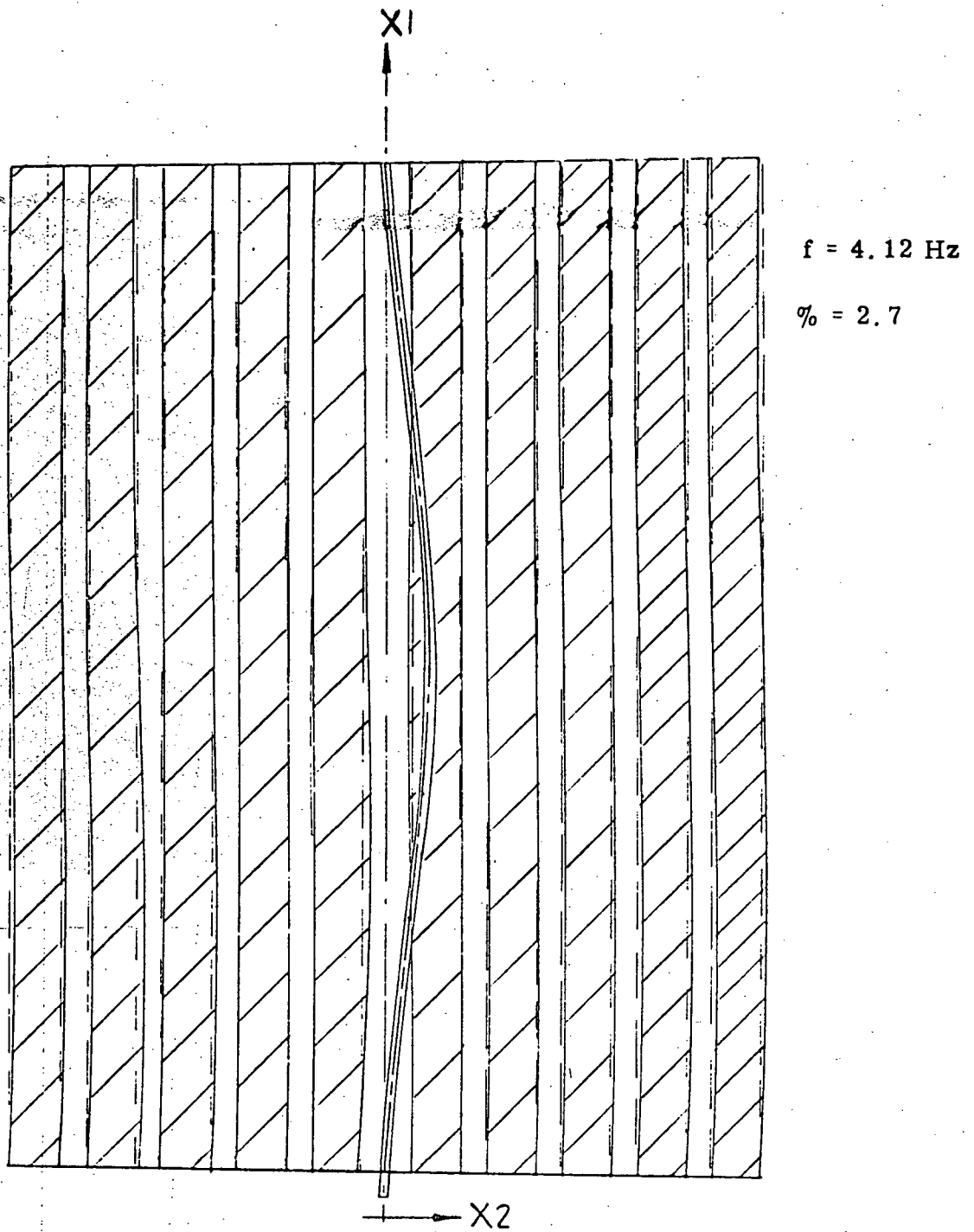


Figure 5-29. Mode 8, Rollup Array, Inplane, Antisymmetric

5.1.2 FOLDOUT PANEL ARRAY

The foldout panel array is a multipanel array consisting of a beryllium framework with a tape substrate. The array is based on a Boeing concept (Reference 5.6) for a lightweight rigid array designed for an unmanned Mars mission. The overall dimensions of one wing section of the array as modified for the space station are shown in Figure 5-30. The wing section consists of thirty panels which were required in varying lengths so as to meet the internal shroud geometry constraints for stowage during the flight launch phase. Panels 1 through 6 are hinged together and are the main load carrying members of the array. Attached to each main panel are four subpanels (such as 1A, 1B, 1C and 1D) hinged at the long side only. The entire wing section is attached to the spacecraft tunnel through members attached to main panel 1.

Each panel consists of a beryllium rectangular x-braced frame with lateral and longitudinal stiffeners as shown in Figure 5-31. Corresponding section properties are given in Figure 5-32. The overall dimensions shown are for panels 1 through 1D. The stiffeners and outer frame members are split in a horizontal plane to hold a tape membrane substrate to which the solar cells are bonded. Details of this frame construction are discussed in Reference 5.6.

Ten mill cells with six mill coverglas were used in determining the solar stack weight. The remaining weight of the array was formulated by ratioing the weight breakdown listed in Reference 5.6 by the respective areas of the 100 and 50 KW arrays. The weight breakdown and total weight of the foldout panel array used for the structural analysis is tabulated in Table 5-6.

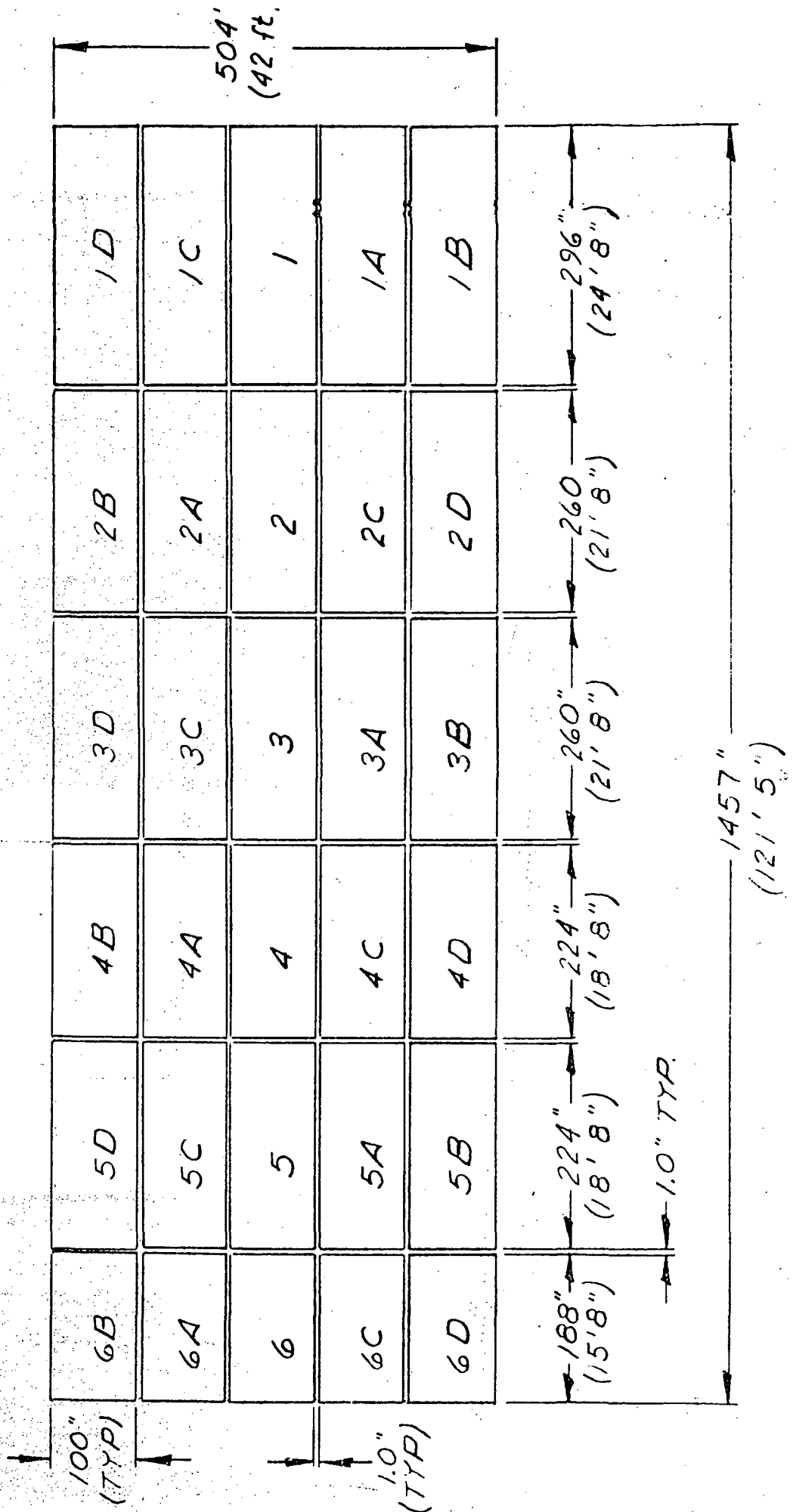


Figure 5-30. Dimensions of Wing Section of Foldout Panel Array

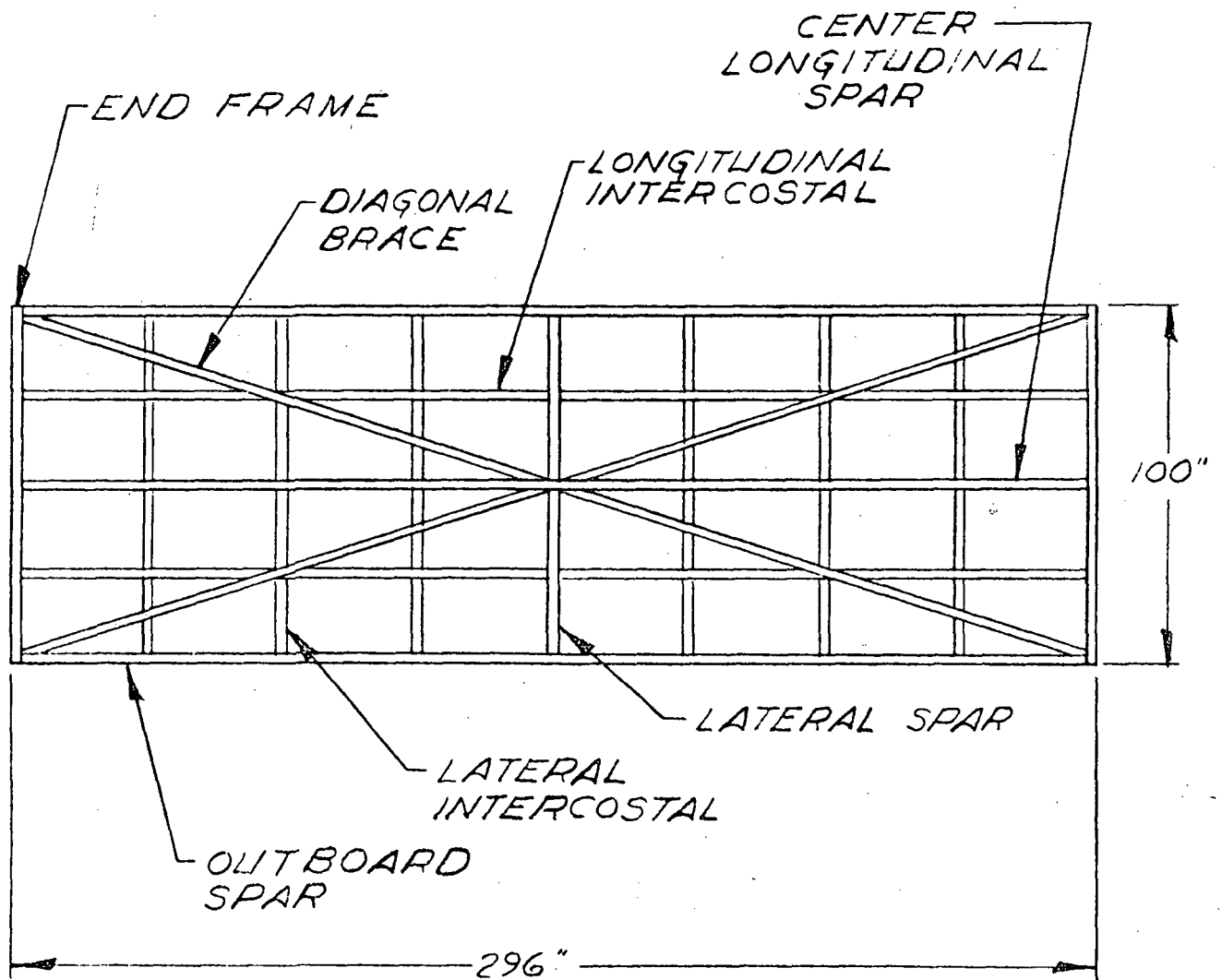
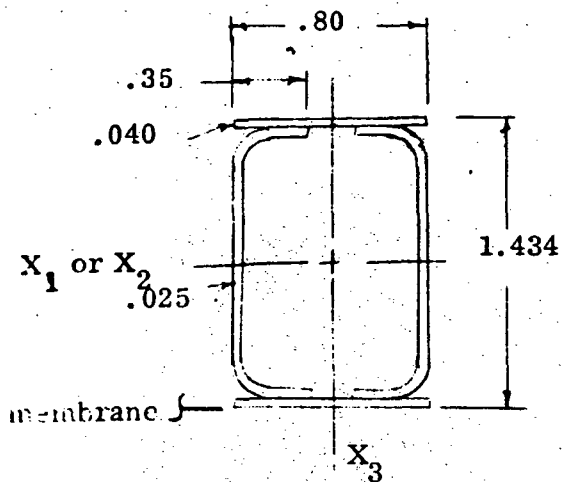


Figure 5-31. Foldout Panel Construction



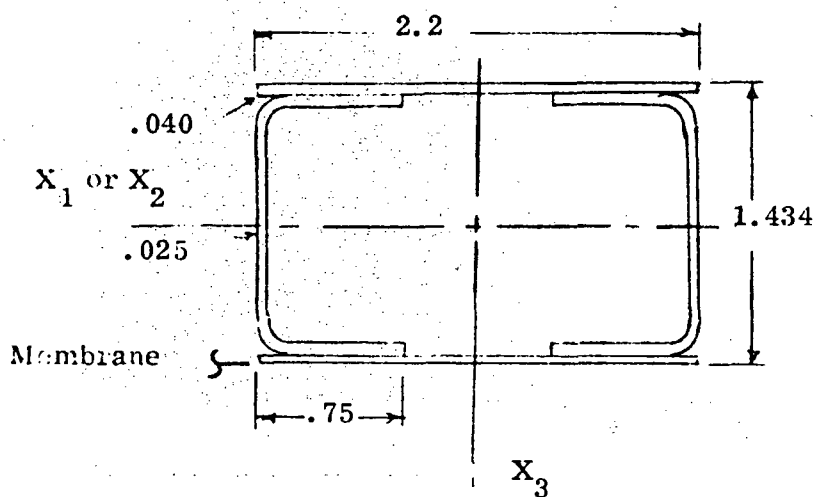
(a) Intercostals

$$A = .1642 \text{ in}^2$$

$$I_{x1} = I_{x2} = .0558 \text{ in}^4$$

$$I_{x3} = .054 \text{ in}^4$$

$$J = .0336 \text{ in}^4$$



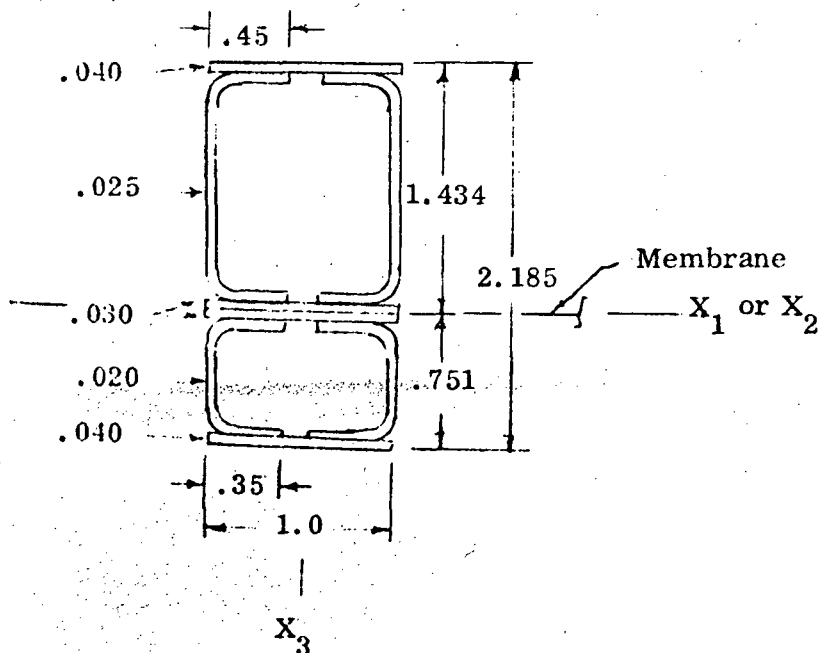
(b) Diagonals

$$A = .3162 \text{ in}^2$$

$$I_{x1} = I_{x2} = .1278 \text{ in}^4$$

$$I_{x3} = .1911 \text{ in}^4$$

$$J = .1924 \text{ in}^4$$



(c) Spars and End Frames

$$A = .3043 \text{ in}^2$$

$$I_{x1} = I_{x2} = .175 \text{ in}^2$$

$$I_{x3} = .0407 \text{ in}^4$$

$$J = .0986 \text{ in}^4$$

Material: Beryllium

$$E = 42.5 \times 10^6 \text{ lbs/in}^2$$

$$G = 20 \times 10^6 \text{ lbs/in}^2$$

Figure 5-32. Member Properties

TABLE 5 -6 WEIGHT BREAKDOWN FOR FOLDOUT PANEL ARRAY

Cell Stack, Substrate and Thermal Coating	Weight (lbs)	
Cover Glass	674	
Cover Glass Adhesive	38	
Cells	938	
Connectors	116	
Solder	8	
Substrate Adhesive	130	
Substrate	156	
Thermal Coating	190	
Total		2250
Mechanisms		
Main Hinges and Latches	60	
Auxiliary Hinges, Latches and Dampers	72	
Quadrants and Sequencers	56	
Strut Assemblies	30	
Solar Curtains	28	
Boost Tie-down System	144	
Cable, Drive and Miscellaneous	84	
Total		474
Electrical Connectors		
Busses and Diodes	194	
Pigtails and Connectors	26	
Squib Wiring	8	
Terminals and Crossover Busses	52	
Total		280
Structure		
Shear Clips	12	
Gusset Plates	34	
Diagonal Tension Ties	156	
Shear Ties	206	
Internal Fittings	38	
Main Members	2642	
Total		3088
TOTAL		6092

5. 1. 2. 1 Array Vibration Model

To derive a dynamic model of the total array and simulate all of the structural members for each foldout panel results in an unusually large problem and would be unnecessary for an adequate analytical simulation. Therefore, each panel was idealized into a simpler model. Also, since the array is symmetric, it was possible to model only one-half the array and adjust the boundary conditions of the center longitudinal spar nodes (Figure 5-31) of the main panel members in the same manner as was done for the rollup array. The dynamic model derived is shown in Figure 5-33. The construction of one panel, such as the panel bounded by nodes 1, 3, 15 and 13, can be considered as an X-braced rectangular frame with a lateral and longitudinal spar. To account for the stiffness of the remaining lateral and longitudinal intercostals of the frame (Figure 5-31), the stiffnesses of these members were distributed and added to the stiffnesses of the end frames and lateral and longitudinal intercostals. Adjacent panels of the structure are hinged and the two adjacent beams on which the hinges are located were considered as a single beam. These beams are shown as the heavy lines on Figure 5-33. The wing section is attached by struts to the space station tunnel at nodes 97 and 98 and in determining the frequencies of the model, the array was considered as rigidly constrained at nodes 97 and 98.

Mass loading for the idealized panel consists of a center mass point and a mass point at each corner. One quarter of the panel weight was allocated to the center point and the balance was divided equally between the four corners. The weight associated with the nodes of Figure 5-33 are listed in Table 5-7.

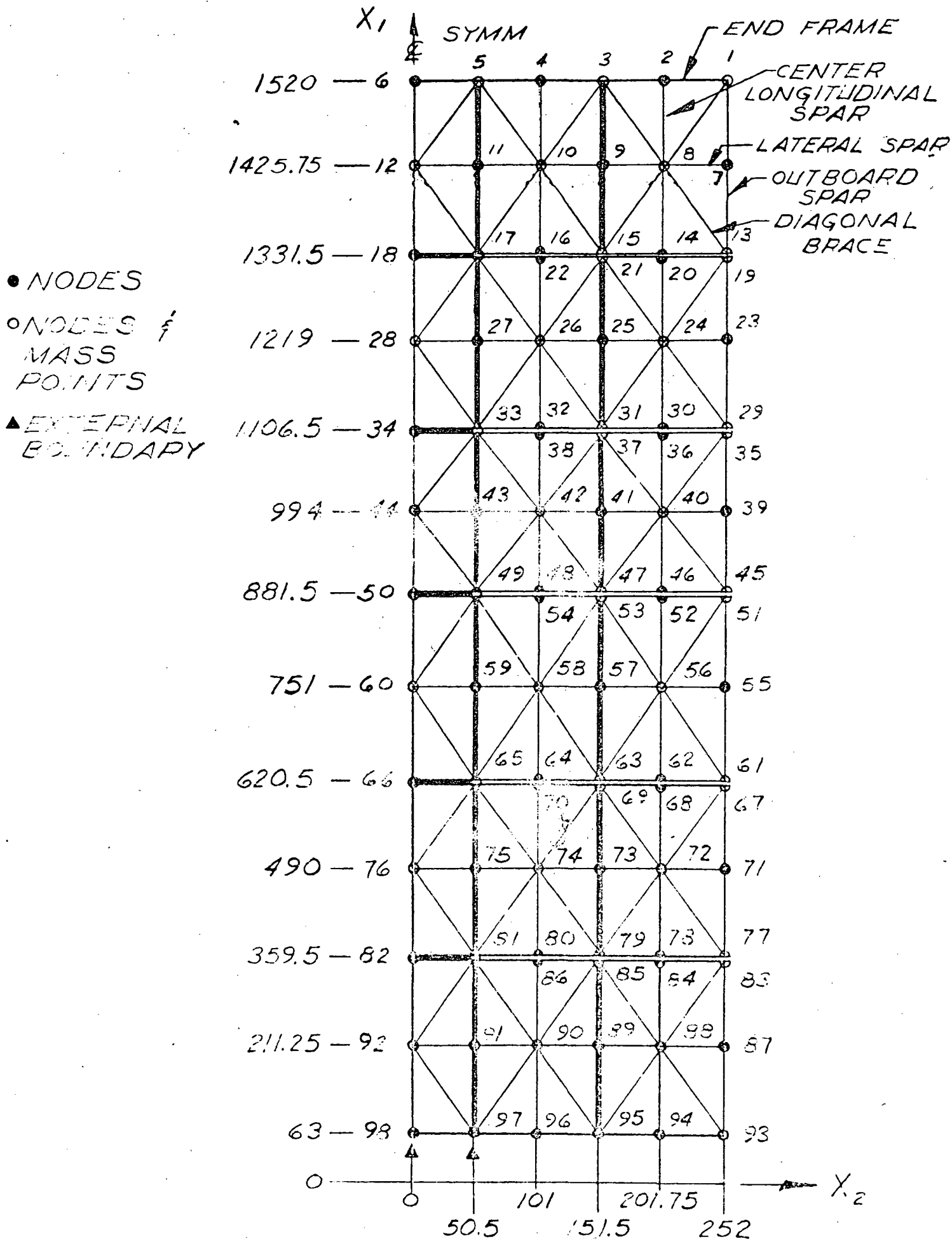


Figure 5-33. Idealized Dynamic Model for Foldout Panel Array

TABLE 5-7 NODAL WEIGHTS, FOLDOUT
 PANEL ARRAY MODEL

Nodes	Weight (lbs)
1, 13	15.4
3, 5, 15	30.8
8, 10	20.52
12	10.26
17	66.42
19, 29, 35, 45	17.81
21, 31, 37, 47	35.62
24, 26, 40, 42	23.75
28, 44	11.87
33	71.24
49	76.12
51, 61, 67, 77	20.25
53, 63, 69, 79	40.5
56, 58, 72, 74	27.0
60, 76	13.5
65	81.0
81	85.88
83, 93	22.69
85, 95, 97	45.38
88, 90	30.25
92	15.13

5.1.2.2 Foldout Panel Array Modes

Foldout panel array frequencies and corresponding modal deflections were computed up to 25 Hz. For the out of plane motions, 48 symmetric and 42 antisymmetric vibration modes were obtained. For the in-plane motions, one symmetric and five antisymmetric modes were obtained. The antisymmetric, out of plane modes represent the torsional deflections of the array while the symmetric modes represent out of plane bending deflections. For the in-plane modes, the symmetric modes represent axial deflections and the antisymmetric modes represent in-plane bending deflections. Resulting modal frequencies for the various cases are listed in Tables 5-8, 5-9, and 5-10.

Graphical presentations of selected modes and corresponding modal participation factors are given in Figures 5-34 to Figure 5-45. The participation factors are based on the same quantities as described for the rollup array modes. The displacement vectors for the out of plane modes (Figures 5-34 through 5-41) are only plotted at nodes with associated mass points. In Figure 5-42 the undeflected array is shown in dashed lines while the deflected shape is shown in solid lines. In Figures 5-43 through 5-45, only the deflected mode shapes are shown. All the modes shown are to be inputs to subsequent dynamic interaction analyses using the generated computer program. The frequencies and modal participation factors for these modes are listed in Table 5-11.

5.1.2.3 Panel Breathing Mode

As a verification of the dynamic model used, a more detailed model of one panel (Figure 5-31) was derived to analytically evaluate the fundamental panel breathing mode. It is required to maintain

TABLE 5-8. FREQUENCIES OF FOLDOUT PANEL ARRAY,
OUT OF PLANE, SYMMETRIC

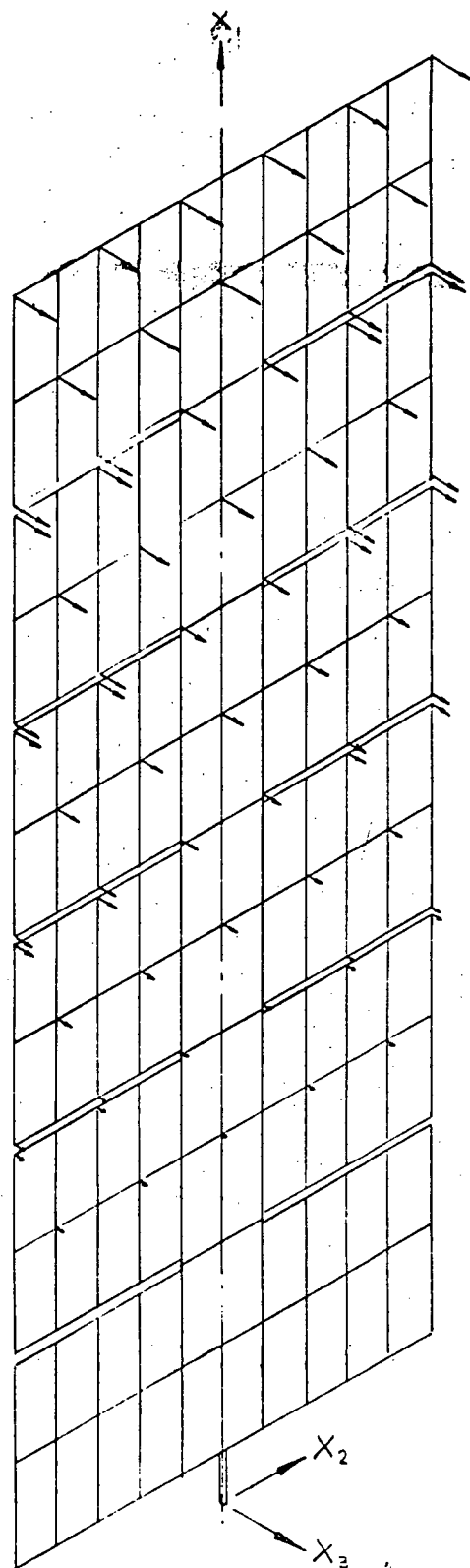
Mode	Frequency (Hz)	Mode	Frequency (Hz)
1	.0344	25	6.9385
2	.2072	26	7.0980
3	.5293	27	7.1827
4	.8861	28	7.5044
5	1.1429	29	7.6312
6	1.2950	30	7.7656
7	1.4353	31	7.8235
8	1.4971	32	7.9082
9	1.5291	33	8.3442
10	1.6078	34	8.5362
11	1.6344	35	9.4665
12	1.7653	36	10.0173
13	1.9877	37	10.0992
14	2.2596	38	11.1912
15	2.5279	39	11.9995
16	2.8494	40	12.6855
17	3.3752	41	13.3285
18	4.2284	42	13.8218
19	5.6543	43	14.0497
20	6.3315	44	14.6318
21	6.4331	45	15.6202
22	6.5716	46	16.1680
23	6.7198	47	17.5238
24	6.8655	48	18.8390

TABLE 5-9. FREQUENCIES OF FOLDOUT PANEL ARRAY,
OUT OF PLANE, ANTISYMMETRIC

Mode	Frequency (Hz)
1	.1184
2	.3606
3	.6075
4	.8607
5	1.0980
6	1.2871
7	1.5609
8	1.7386
9	1.8536
10	1.9813
11	2.1327
12	2.3362
13	3.7286
14	3.9908
15	4.2144
16	4.4811
17	4.9012
18	5.6379
19	5.7335
20	6.4064
21	6.6507
22	6.8024
23	7.0102
24	7.4163
25	7.8218
26	7.8506
27	7.9083
28	9.2626
29	9.6278
30	9.9170
31	9.9937
32	10.1300
33	10.3267
34	10.6231
35	11.2053
36	11.4311
37	11.5634
38	12.4228
39	13.2525
40	13.7070
41	14.9116
42	17.2326

TABLE 5-10. FREQUENCIES OF FOLDOUT PANEL ARRAY, IN-PLANE

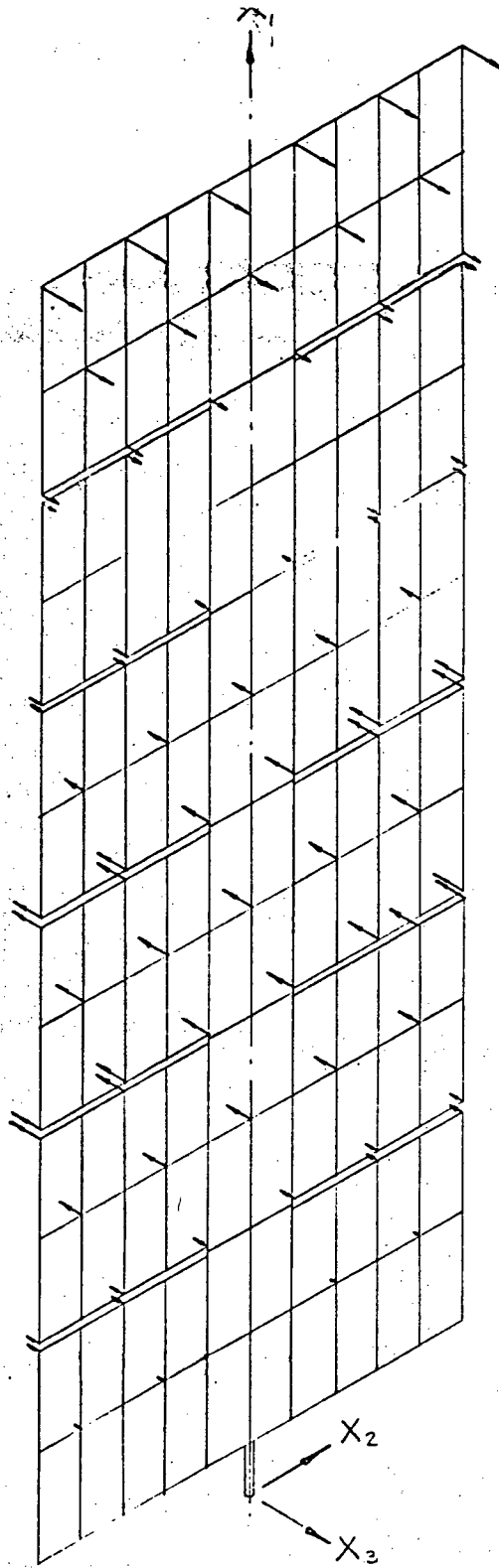
Mode	Description	Frequency (Hz)
1	Symmetric	24.76
1	Antisymmetric	1.669
2	Antisymmetric	6.934
3	Antisymmetric	13.765
4	Antisymmetric	19.771
5	Antisymmetric	23.5



$$f = .0344 \text{ Hz}$$

$$\eta_0 = 63$$

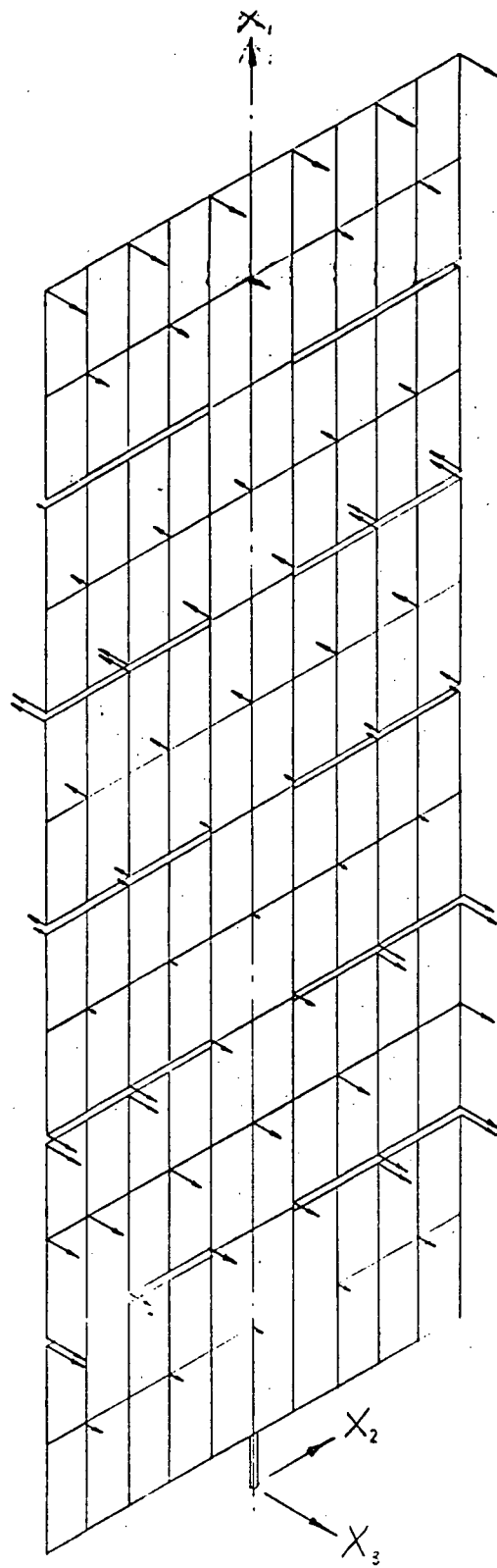
Figure 5-34. Mode 1, Foldout Panel Array, Out of Plane, Symmetric



$f = .2072 \text{ Hz}$

$\eta = 19.6$

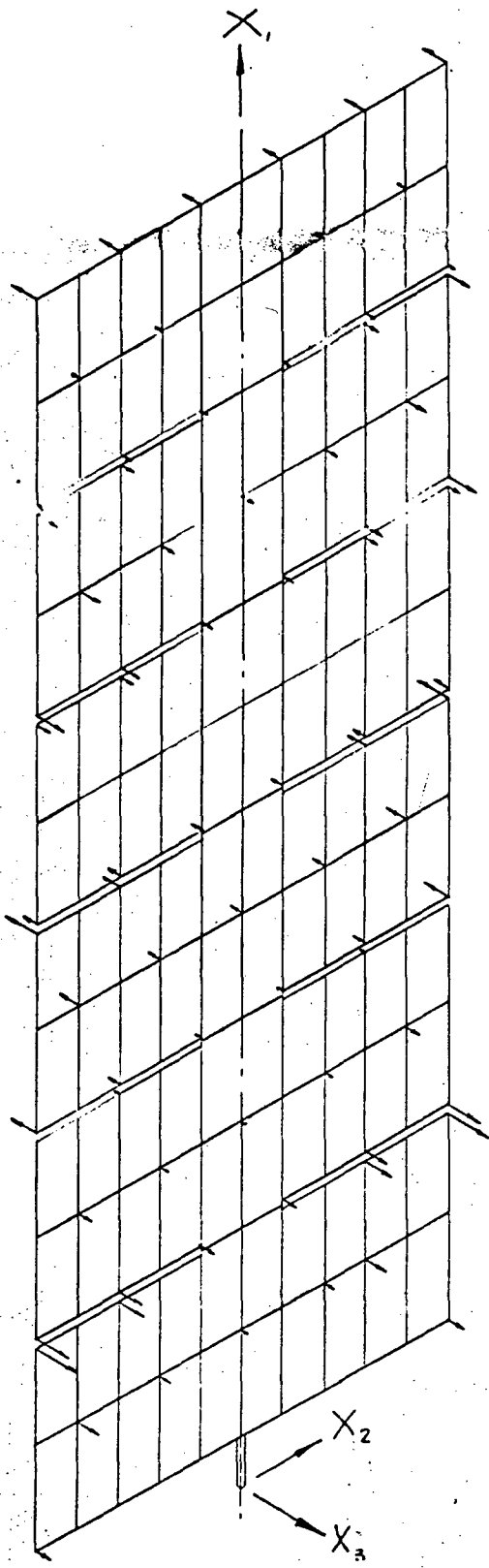
Figure 5-35. Mode 2, Foldout Panel Array, Out of Plane, Symmetric



$f = .5293 \text{ Hz}$

$\% = 7.2$

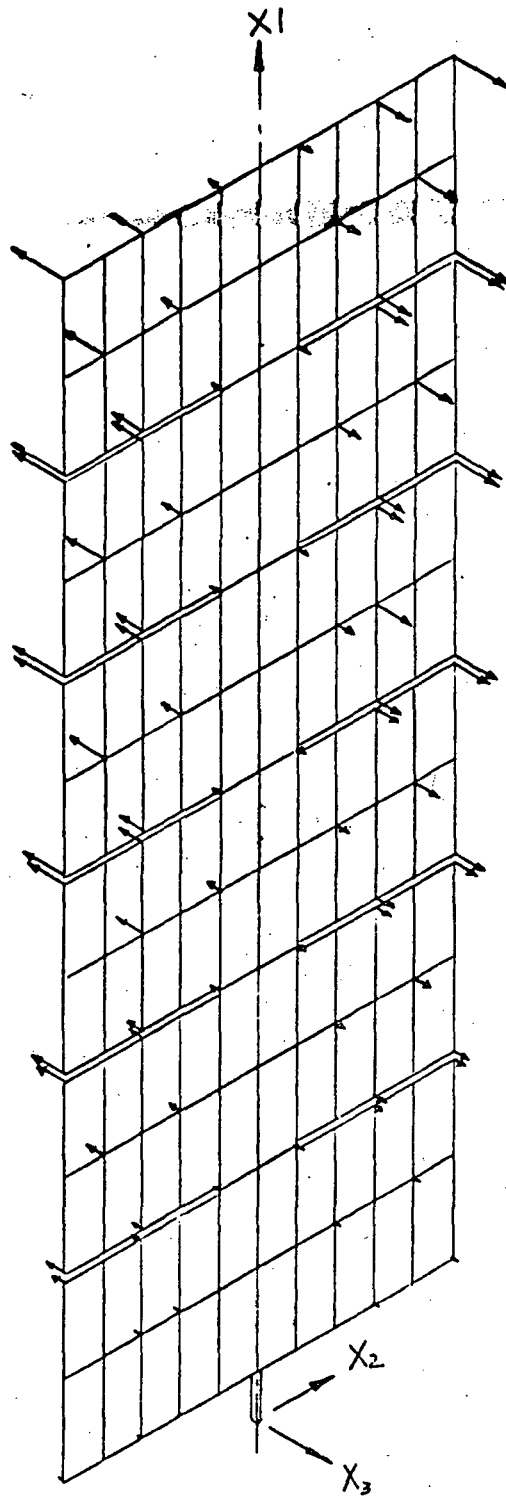
Figure 5-36 Mode 3, Foldout Panel Array, Out of Plane, Symmetric



$f = .8861 \text{ Hz}$

$\% = 3.4$

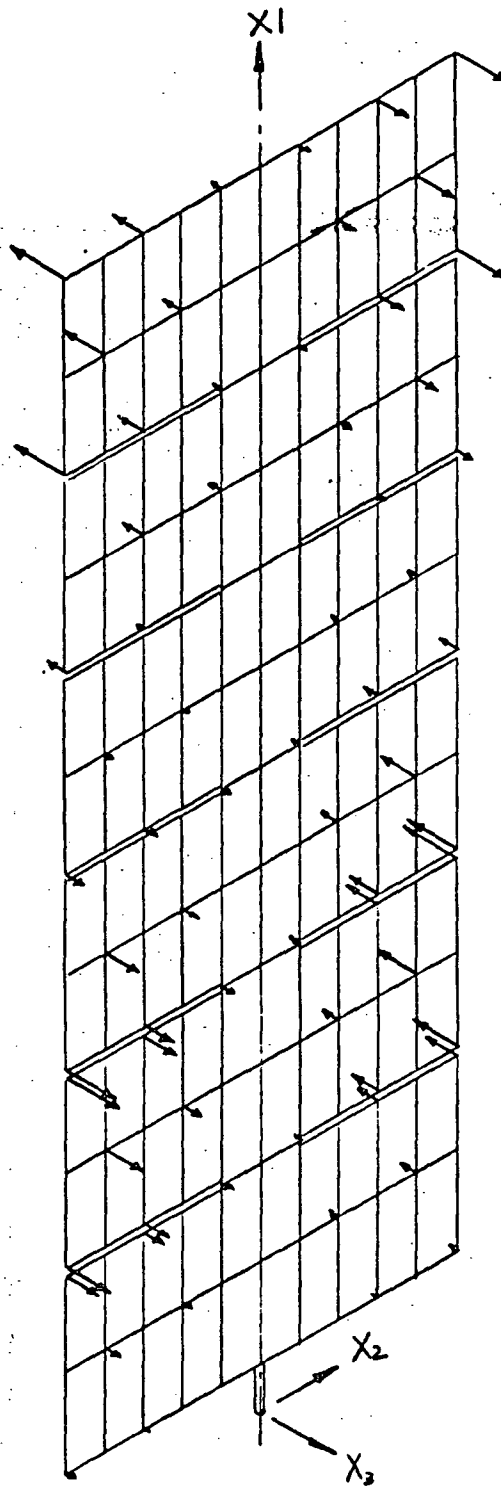
Figure 5-37 Mode 4, Foldout Panel Array, Out of Plane, Symmetric



$f = .1184 \text{ Hz}$

$\eta_0 = 78.6$

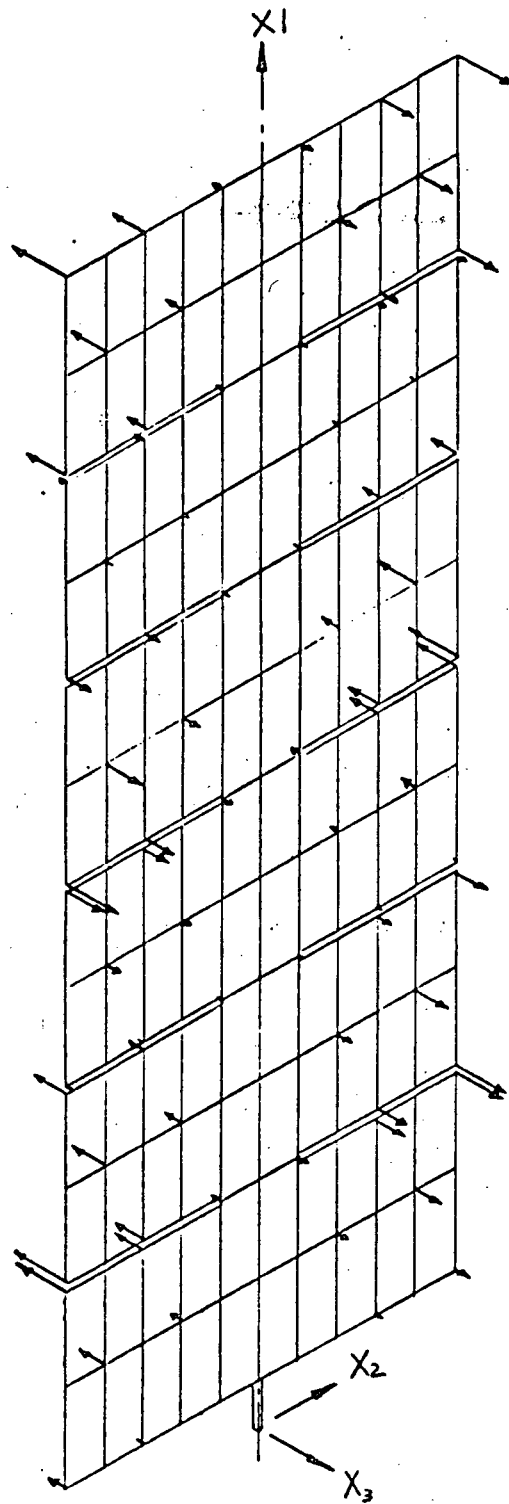
Figure 5-38 Mode 1, Foldout Panel Array, Out of Plane, Antisymmetric



$f = .3606 \text{ Hz}$

$\eta_0 = 9.4$

Figure 5-39. Mode 2, Foldout Panel Array, Out of Plane, Antisymmetric

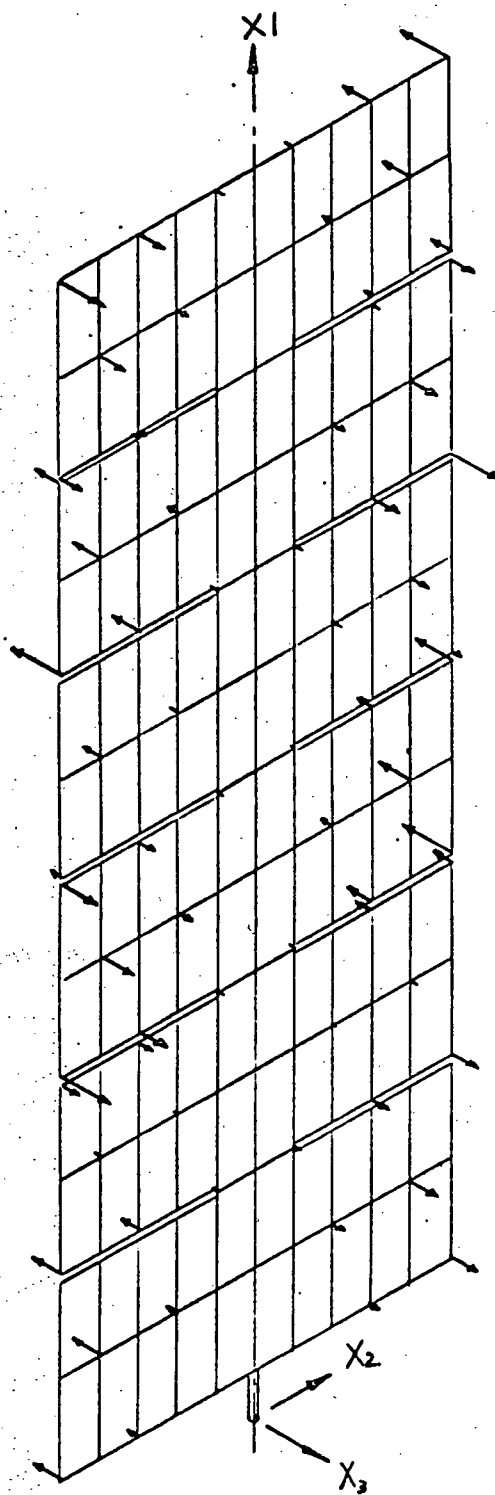


$f = .6075 \text{ Hz}$

$\eta = 3.65$

Figure 5-40 Mode 3, Foldout Panel Array, Out of Plane, Antisymmetric

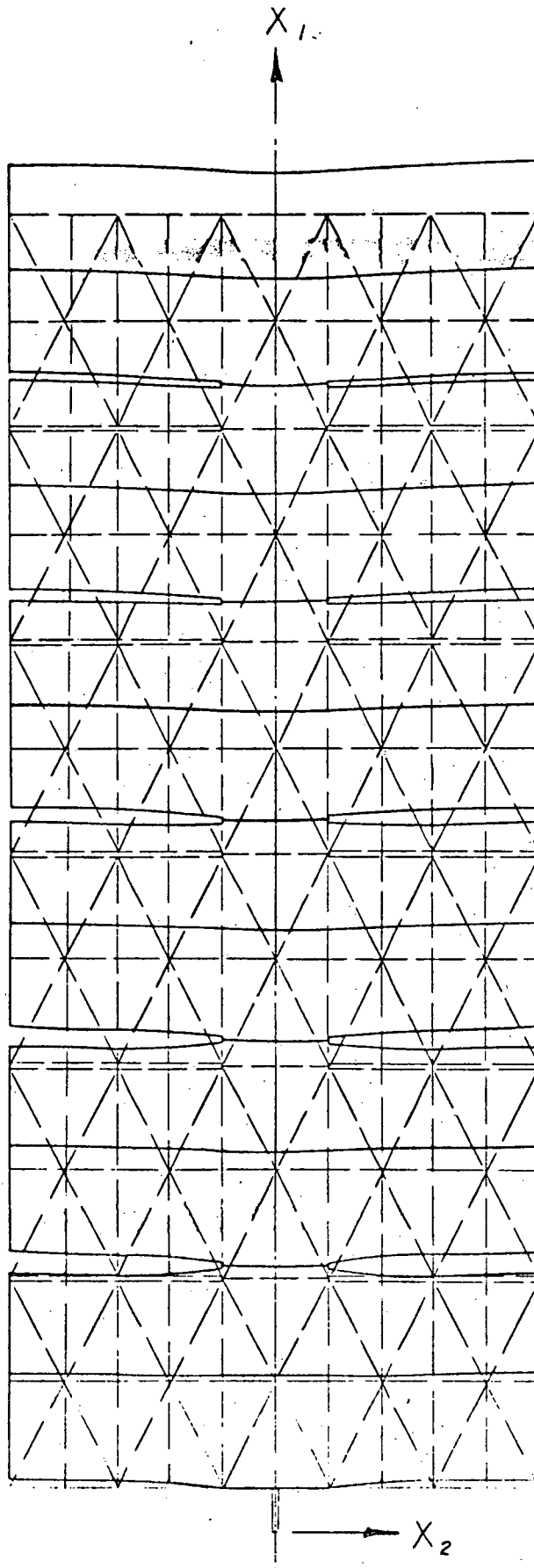
6



$f = .8607 \text{ Hz}$

$\eta_0 = 2.06$

Figure 5-41 Mode 4, Foldout Panel Array, Out of Plane, Antisymmetric

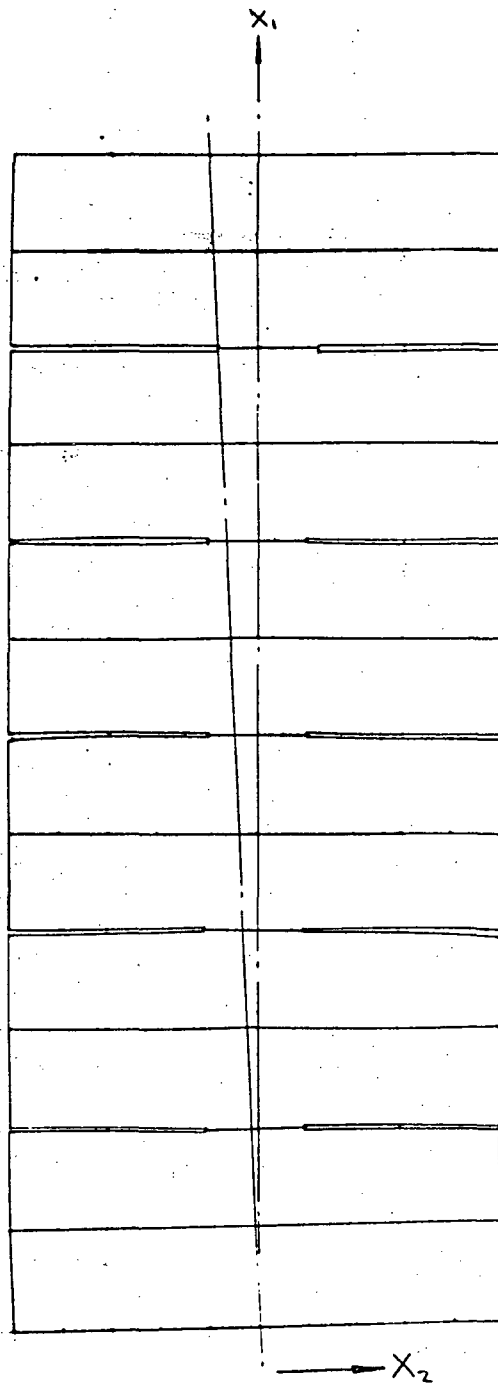


$f = 24.76 \text{ Hz}$

$\eta_0 = 83$

Figure 5-42 Mode 1, Foldout Panel Array, Inplane, Symmetric

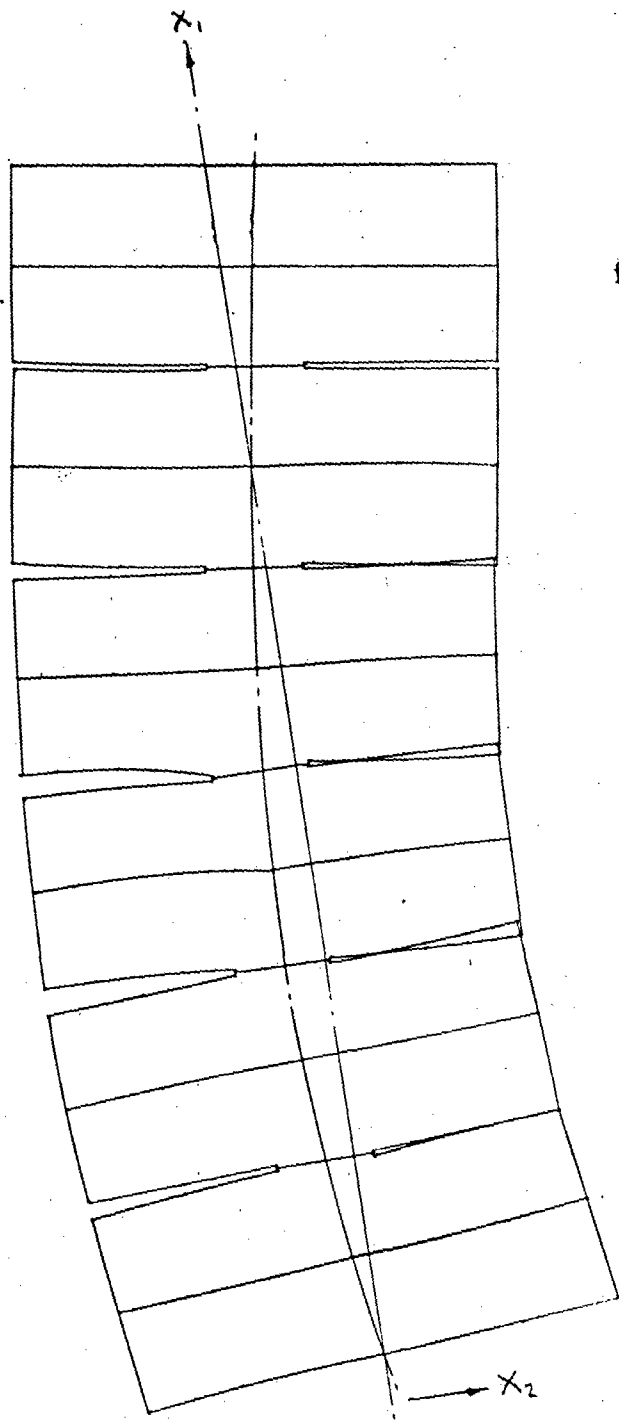
6



$f = 1.669 \text{ Hz}$

$\eta_0 = 64.5$

Figure 5-43. Mode 1, Foldout Panel Array, Inplane, Antisymmetric



$f = 6.934 \text{ Hz}$

$\eta_0 = 21.3$

Figure 5-44. Mode 2, Foldout Panel Array, Inplane, Antisymmetric

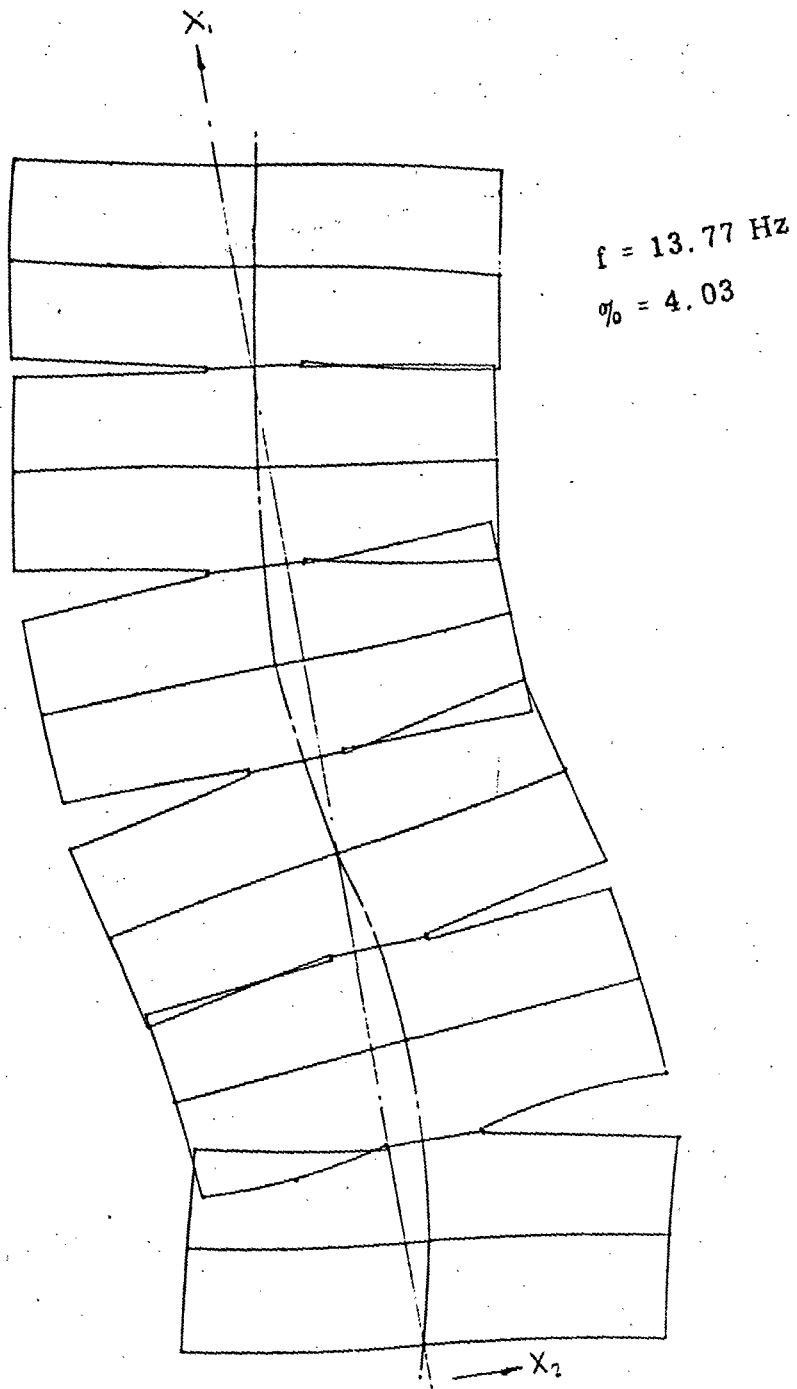


Figure 5-45 Mode 3, Foldout Panel Array, Inplane, Antisymmetric

TABLE 5-11. FOLDOUT PANEL ARRAY, MODAL PARTICIPATION FACTORS

Out of Plane						
Symmetric			Antisymmetric			
Mode	Frequency (Hz)	Percent Participation	Mode	Frequency (Hz)	Percent Participation	Percent Participation
1	.0344	63	1	.1184	78.6	
2	.2072	19.6	2	.3606	9.4	
3	.5293	7.2	3	.6075	3.65	
4	.8861	3.4	4	.8607	2.06	
In-Plane						
Symmetric			Antisymmetric			
Mode	Frequency (Hz)	Percent Participation	Mode	Frequency (Hz)	Percent Participation	Percent Participation
1	24.76	83	1	1.669	64.5	
2	---	---	2	6.934	21.3	
3	---	---	3	13.765	4.03	

an adequate frequency separation between the breathing mode and the array's out of plane modal frequencies since the model used in the array analysis did not include sufficient degrees of freedom for the description of breathing modes. The nodal numbering and dimensions of the panel model analyzed is shown on Figure 5-46. There are 53 nodes in the model and nodes 44 through 53 were rigidly constrained for the dynamic analysis. The first mode of this model was 7.634 Hz which is sufficiently separated from the array out of plane mode frequencies. The nodal weights are tabulated in Table 5-12 and the mode shape of the breathing mode is shown on Figure 5-47.

5.2 PHASE II STUDY ANALYSES

The structural analyses described were performed to obtain modal data to compliment the formulated digital simulations. The analyses were conducted on the solar array and space station configurations described in Section 2.0, which correspond to both the zero "G" and artificial "G" conditions. A requirement of the dynamic interaction analysis digital simulation is that cantilever modal data for the solar arrays and free-free modal data for the space station be initially determined and used as input. Each of the structural models and corresponding modal data is described in the following.

5.2.1 ZERO "G" SPACE STATION CONFIGURATION

The stiffness and mass properties used to represent the space station structural arrangement were those resulting from preliminary configuration studies performed by North American Rockwell (Reference 5.7). These properties were obtained from NAR and are given in Table 5-13 and Figure 5-48, comprising the total structural arrangement.

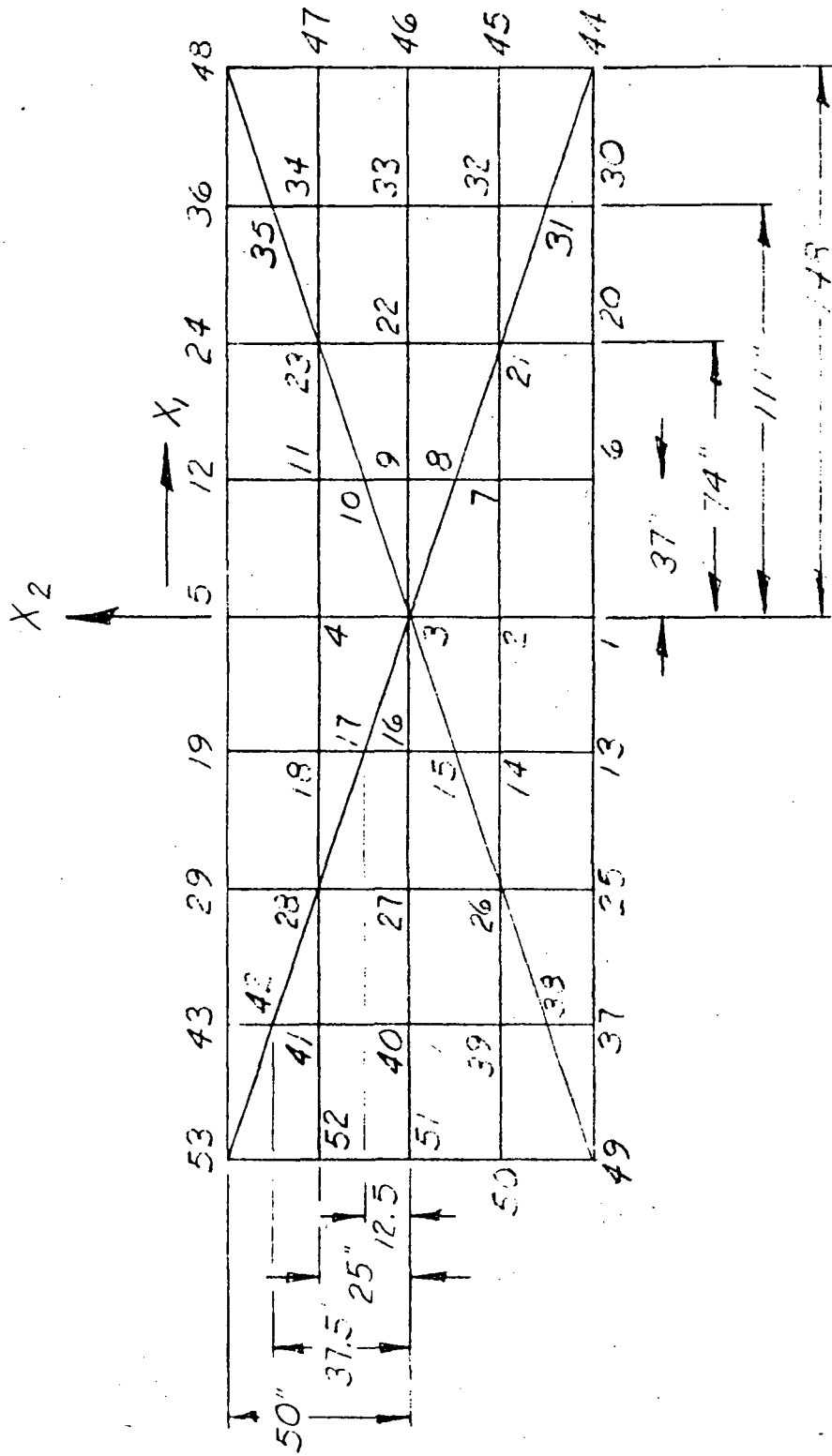


Figure 5-46 Breathing Mode Model

TABLE 5-12. NODAL WEIGHTS FOR BREATHING MODE MODEL

Node	Weight (lbs)
1, 5	2.059
2, 4	3.401
3	4.578
6, 9, 12, 13, 16, 19, 20, 24, 25, 29	1.955
7, 11, 14, 18	2.261
8, 10, 15, 17	2.066
21, 23, 26, 28	3.708
22, 27, 33, 40	3.191
30, 36, 37, 43	1.336
31, 35, 38, 42	2.064
32, 34, 39, 41	2.284

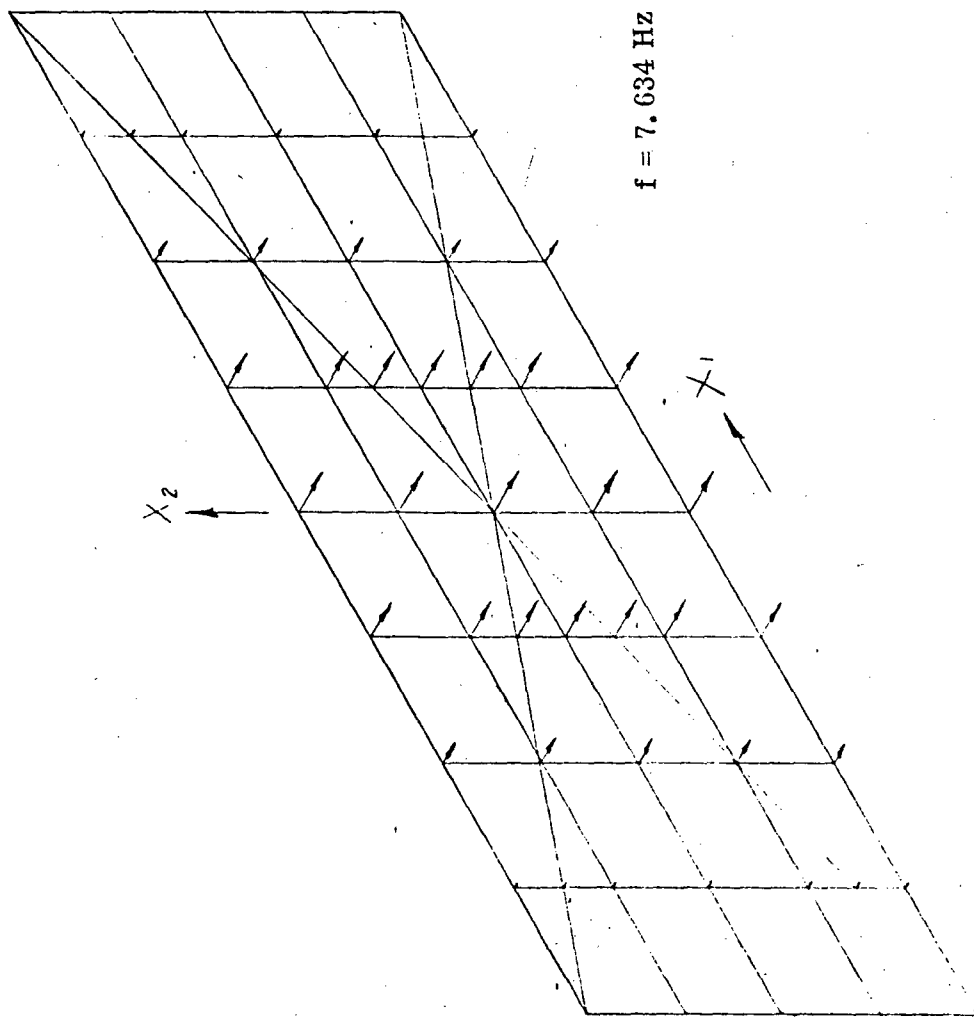
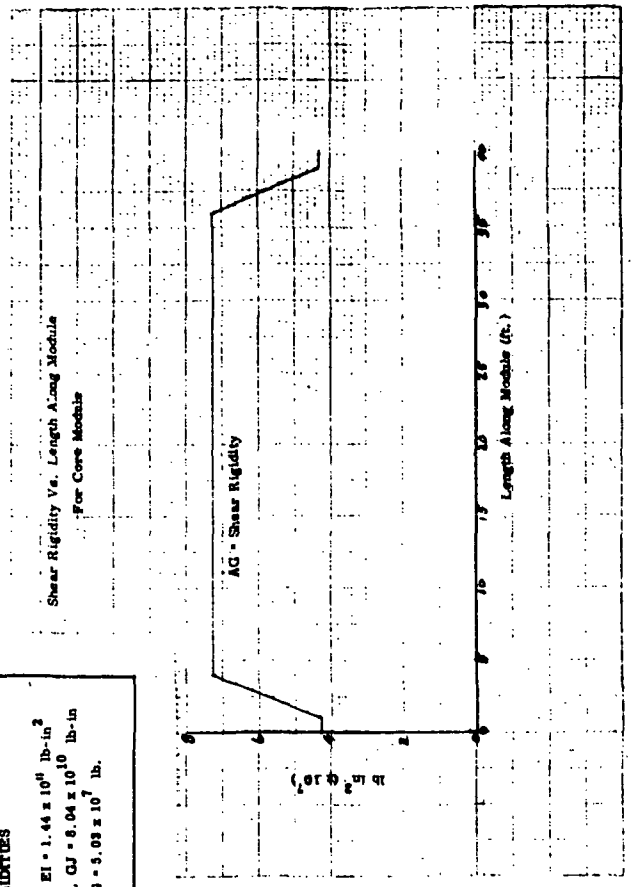
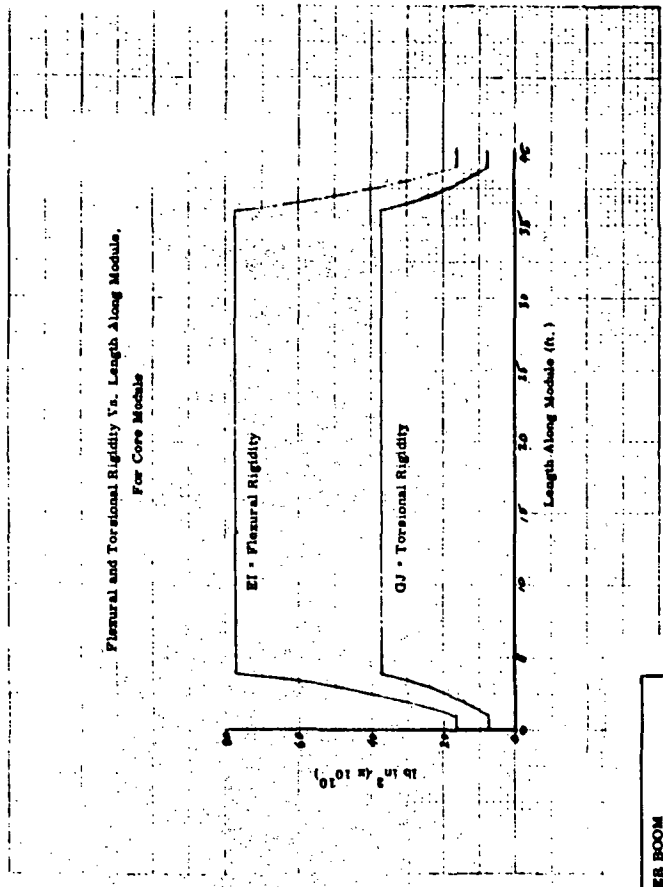


Figure 5-47 Mode 1, Foldout Panel Array, Breathing Mode



POWER BOOM RIGIDITIES

Flexural Rigidity, $EI = 1.44 \times 10^{11}$ lb-in²
 Torsional Rigidity, $GJ = 6.04 \times 10^7$ lb-in
 Shear Rigidity, $AG = 5.03 \times 10^7$ lb

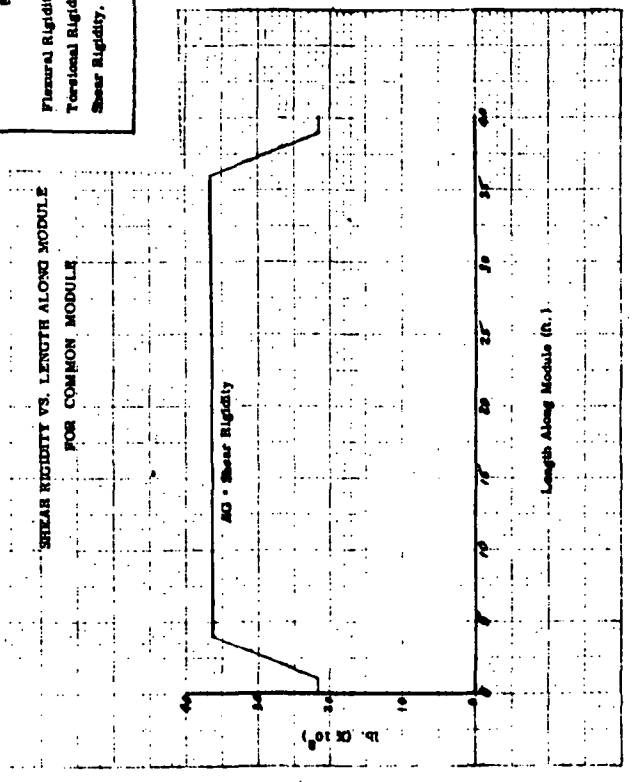
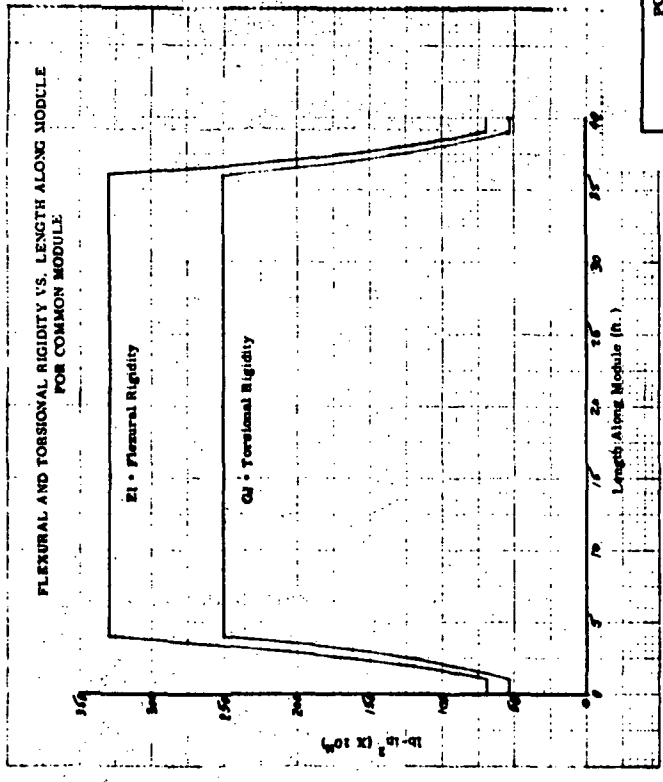


Figure 5 -48 Space Station Stiffness Properties

TABLE 5-13

Mass Properties of Zero "G" Space Station Configuration

COMPONENT	WEIGHT (LBS.)
Core Module	25,000
Common Module (8 in configuration)	25,000/module
Power Boom	17,500

A finite element model representing this configuration was derived, using a limited number of nodal points, and it is depicted in Figure 5-49. The corresponding discrete masses of the model and grid point geometry is given in Table 5-14. Each of the discrete points was allowed three translational degrees-of-freedom and one rotational degree-of-freedom, corresponding to torsion of each module. Shear flexibility was considered for appropriate degrees-of-freedom because of the relatively small length to diameter ratio of each module. The model geometry, inertial properties and stiffness properties were input to the NASTRAN program (Reference 5.12) for the determination of modal properties, i. e., frequencies, mode shapes, and modal masses. A partial list of these quantities are listed in Table 5-15. A comprehensive listing of the zero "G" modal properties, together with a graphical presentation of lower modes of vibration, are given in Appendix A to this report.

5.2.2 ARTIFICIAL "G" SPACE STATION CONFIGURATION

The artificial "G" space station configuration was discretized into the finite element model presented in Figure 5-50. Stiffness and inertial properties are similar to those presented for corresponding modules in Table 5-13 and Figure 5-48 except for the power boom and extended boom; the mass

Structural Model Of Space Station

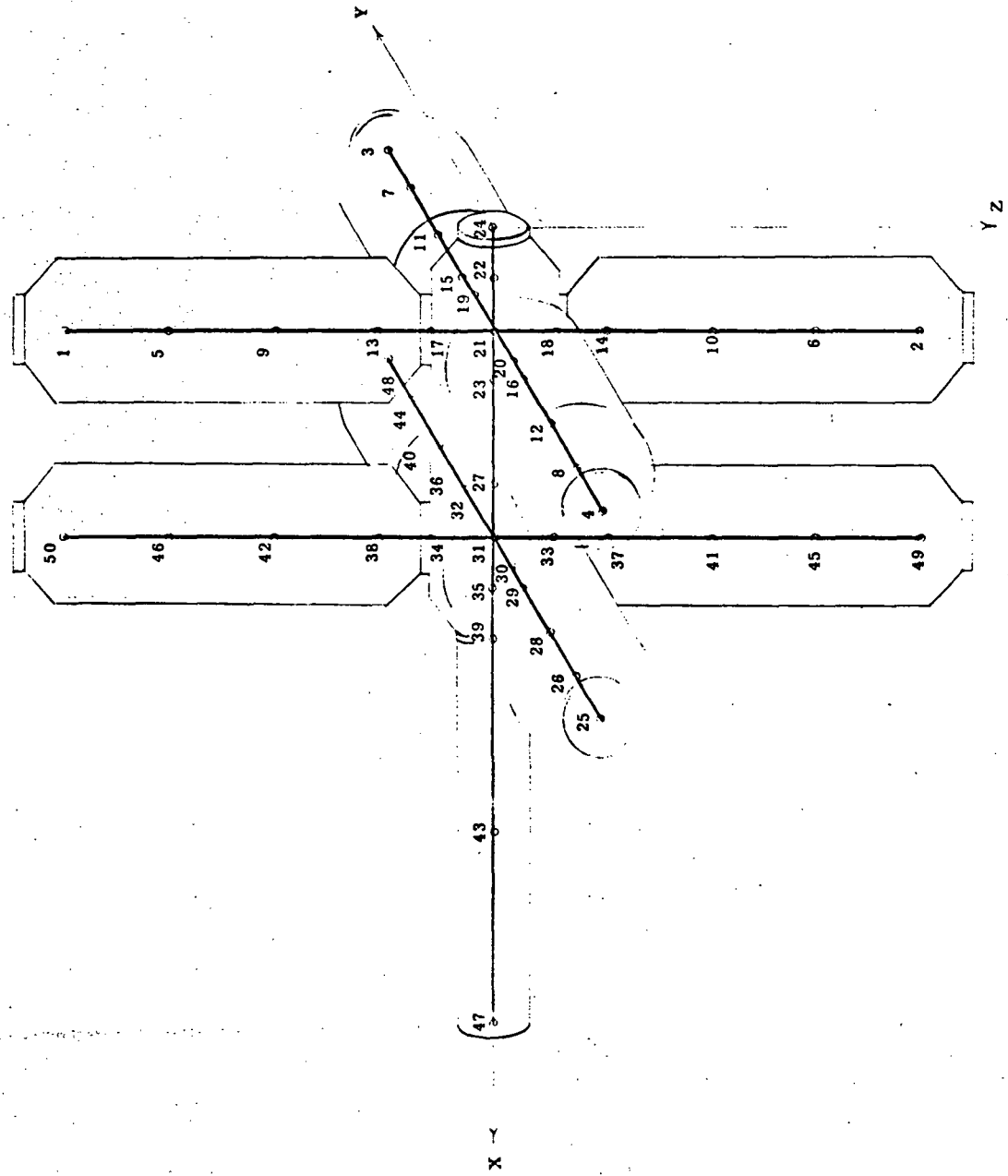


Figure 5-49

TABLE 5 -14
 Mass - Geometry Data
 Of Zero G Space Station

NODE NO.	MASS			
	(lb. -sec ²)	X	Y	Z
1	16.189	120.	0.	-492.
2	16.189	120.	0.	492.
3	16.189	120.	492.	0.
4	16.189	120.	-492.	0.
5	16.189	120.	0.	-372.
6	16.189	120.	0.	372.
7	16.189	120.	372.	0.
8	16.189	120.	-372.	0.
9	16.189	120.	0.	-252.
10	16.189	120.	0.	252.
11	16.189	120.	252.	0.
12	16.189	120.	-252.	0.
13	16.189	120.	0.	-132.
14	16.189	120.	0.	132.
15	16.189	120.	132.	0.
16	16.189	120.	-132.	0.
17	0.	120.	0.	-72.
18	0.	120.	0.	72.
19	0.	120.	72.	0.
20	0.	120.	-72.	0.
21	8.1	120.	0.	0.
22	8.1	60.	0.	0.
23	0.	180.	0.	0.
24	4.05	0.	0.	0.
25	16.189	360.	-492.	0.
26	16.189	360.	-372.	0.
27	12.15	300.	0.	0.
28	16.189	360.	-252.	0.
29	16.189	360.	-132.	0.
30	0.	360.	-72.	0.
31	8.1	360.	0.	0.
32	12.15	360.	72.	0.
33	0.	360.	0.	72.
34	0.	360.	0.	-72.
35	8.1	420.	0.	0.
36	16.189	360.	132.	0.
37	16.189	360.	0.	132.
38	16.189	360.	0.	-132.
39	12.7919	480.	0.	0.
40	16.189	360.	252.	0.
41	16.189	360.	0.	252.
42	16.189	360.	0.	-252.
43	17.4839	700.5	0.	0.
44	16.189	360.	372.	0.
45	16.189	360.	0.	372.
46	16.189	360.	0.	-372.
47	19.086	921.	0.	0.
48	16.189	360.	492.	0.
49	16.189	360.	0.	492.
50	16.189	360.	0.	-492.

Table 5-15. Modal Data, Space Station

(Zero G Configuration)

Mode	Frequency (Hz)	Generalized Mass (lb. -sec. ² /in.)
1	0.0	6.281594E 02
2	0.0	6.281594E 02
3	0.0	6.281594E 02
4	0.0	2.477312E 02
5	0.0	1.200991E 02
6	0.0	1.200991E 02
7	1.557577E 00	2.297717E 02
8	2.277407E 00	3.636589E 01
9	2.278777E 00	3.660057E 01
10	3.147397E 00	8.373244E 01
11	3.246078E 00	1.085563E 02
12	4.391578E 00	1.511882E 02
13	4.483892E 00	3.124590E 02
14	5.702700E 00	7.439223E 01
15	5.035467E 00	7.142155E 01
16	6.477557E 00	8.401511E 01
17	6.875389E 00	1.111700E 02
18	6.875395E 00	1.111700E 02
19	7.765384E 00	5.186711E 01
20	8.263874E 00	1.006247E 02
21	8.860953E 00	
22	8.935523E 00	
23	1.013241E 01	
24	1.130443E 01	
25	1.131781E 01	
26	1.475548E 01	
27	1.534728E 01	
28	1.958418E 01	
29	1.988515E 01	
30	2.277832E 01	
31	2.319455E 01	
32	2.339781E 01	
33	2.342052E 01	
34	2.490974E 01	
35	2.574709E 01	
36	2.658902E 01	
37	2.698964E 01	
38	2.752139E 01	
39	2.941002E 01	
40	2.942180E 01	
41	2.967250E 01	
42	2.967250E 01	
43	2.977396E 01	
44	2.984723E 01	
45	2.984726E 01	
46	2.992293E 01	
47	3.003922E 01	
48	3.005589E 01	
49	3.005730E 01	
50	3.027989E 01	

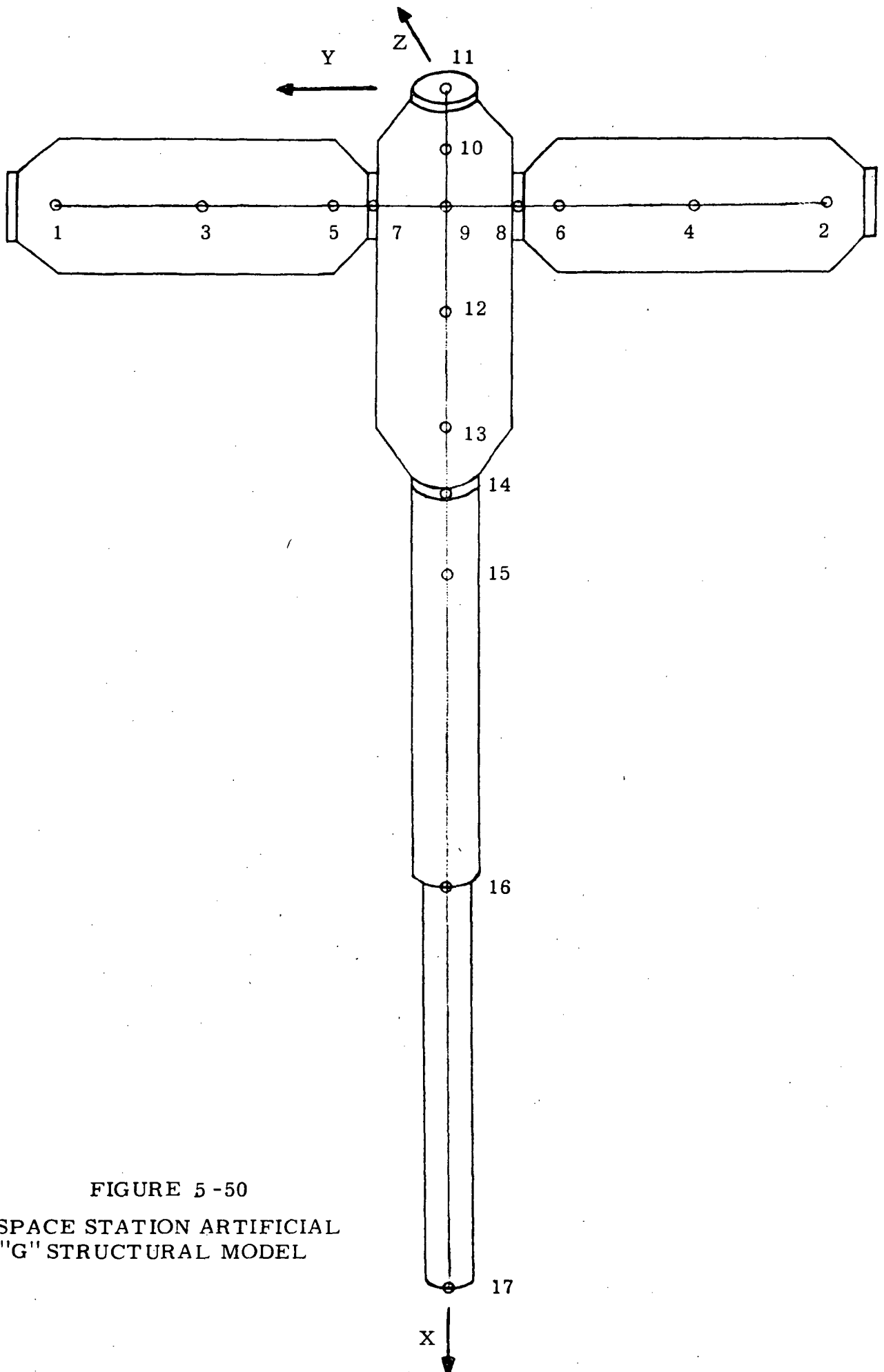


FIGURE 5-50
 SPACE STATION ARTIFICIAL
 "G" STRUCTURAL MODEL

and geometry properties for this modal are listed in Table 5-16. It was originally intended to utilize the stated capability of the NASTRAN program in the performance of the modal analysis of the spinning structure; however, initial attempts with NASTRAN failed (Version 12). An eigenvalue-eigenvector program obtained from the Jet Propulsion Laboratory (JPL) in Pasadena, California, and formulated by Dr. K. K. Gupta (Reference 5.8 and 5.9) was used. As is required for modal analysis of spinning structures, a coriolis force matrix and centrifugal force matrix were derived for the total description of the equations of equilibrium of the discretized system. A comprehensive description of typical terms in these matrices can be found in Reference 5.10. The centrifugal force matrix is a function of the motion variables while the coriolis force matrix is dependent upon the first derivatives of the motion variables. Orthogonalization of this system of equations results in complex conjugate pairs of eigenvalues (zero real part) and corresponding complex conjugate pairs of eigenvectors. The digital simulation, for the artificial "G" condition, is programmed to accept this modal data format.

For the structural configuration shown, the artificial "G" condition was attained by spinning the space station at 4 RPM about a point 44 feet outboard of the space station-solar array attachment as depicted in Figure 5-51. The coriolis force and centrifugal force matrices were computed by hand and the stiffness matrix was generated with the NASTRAN computer program. It was also determined that the influence of static spin loads upon the station's structural stiffness (beam column effect) was negligible and therefore neglected. The matrices together with the mass matrix were input into the JPL program for determination of complex eigenvalues and eigenvectors for a range of steady state spin rates. Resulting frequencies are presented in Table 5-17 for spin rates of 0, 4, 8, and 12 RPM together with

TABLE 5-16
ARTIFICIAL "G" SPACE STATION
FINITE ELEMENT MODEL DATA

NODE	MASS LB SEC ² /IN	INERTIA			NO. OF STRUCTURAL D.O.F.	D. O. F. SEQUENCE NO.
		LB	SEC ²	IN		
		x Axis	y Axis	z Axis		
1	21.578	--	66641	--	6	1-6
2	21.578	--	66641	--	6	7-12
3	21.578	--	66641	--	6	13-18
4	21.578	--	66641	--	6	19-24
5	21.578	--	66641	--	6	25-30
6	21.578	--	66641	--	6	31-36
7	--	--	--	--	6	37-42
8	--	--	--	--	6	43-48
9	15.382	41621	--	--	6	49-54
10	8.094	21886	--	--	6	55-60
11	4.047	10956	--	--	6	61-66
12	17.814	49417	--	--	6	67-72
13	15.379	41595	--	--	6	73-78
14	12.795	18700	--	--	6	79-84
15	10.632	9350			6	85-90
16	25.952	20642			6	91-96
17	.01295	10.282			6	97-102

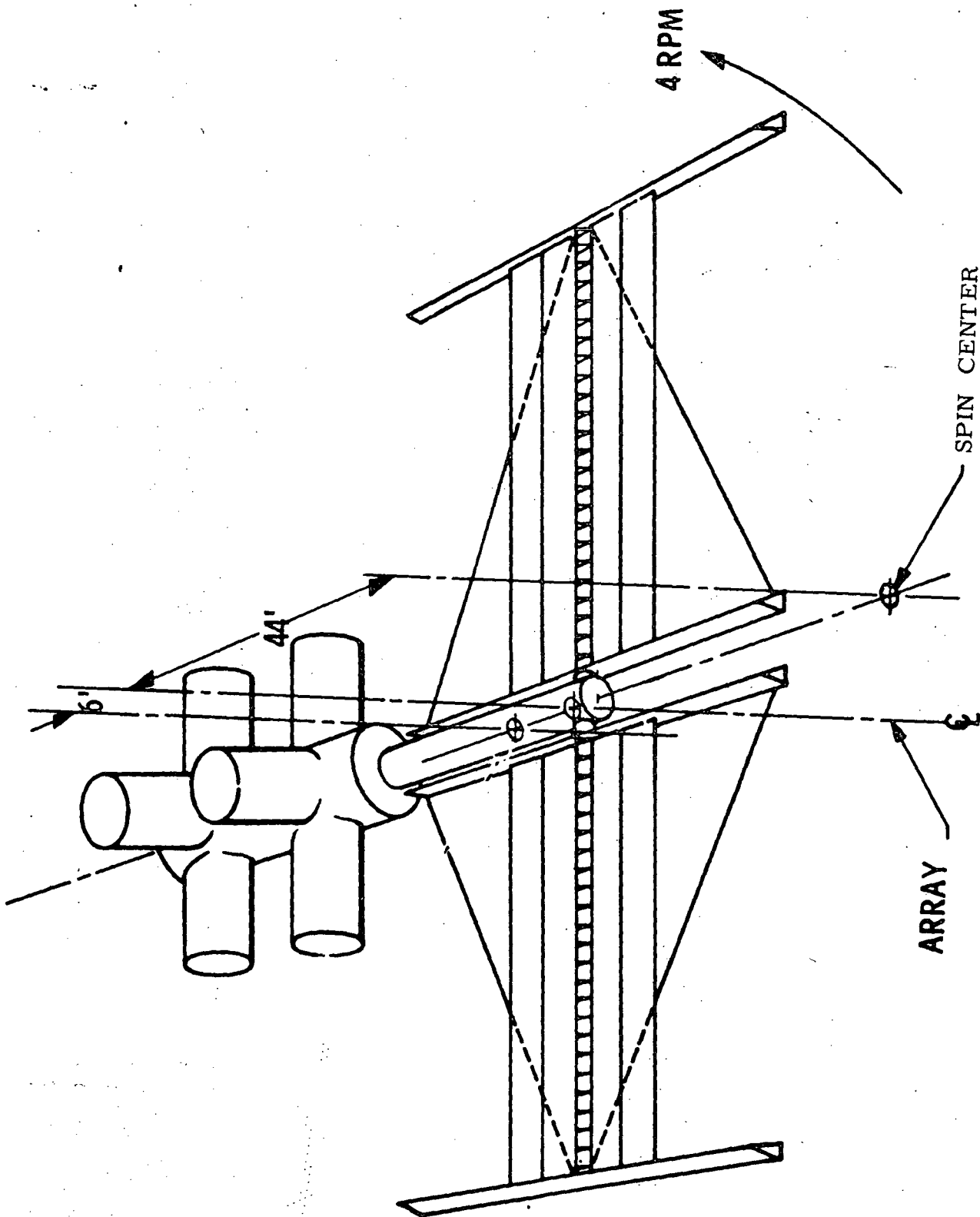


Figure 5-51. Space Station-Solar Array Artificial "G" Configuration

TABLE 5 -17
 Artificial "G" Space Station Configuration
 List of Eigen Values in Hertz

Elastic Mode No.	NASTRAN Results $\Omega = 0$	"GUPTA" Program Results			
		$\Omega = 0$	$\Omega = 4\text{RPM}$	$\Omega = 8\text{RPM}$	$\Omega = 12 \text{ RPM}$
		1	2.2967	2.2948	2.2929
2	4.2003	4.2027	4.2027	4.2026	4.2027
3	8.4202	8.4224	8.4147	8.4068	8.3914
4	8.6787	8.6711	8.6789	8.6867	8.6944

the modal frequencies obtained by NASTRAN for the same model in a zero-spin condition. It is seen that the frequency correlation between NASTRAN and Gupta's program is excellent and that the frequency change with spin rate is minimal. A comprehensive list of modal data in terms of modal deflection and graphical description of the lower frequency modes in terms of absolute deflection coefficients, are given in Appendix A to this report. Also presented are the structural degrees of freedom considered in the analysis. Examination of the shape for the second mode shows this mode is represented by out-of-the-spin-plane bending only and would not be influenced by centrifugal or coriolis forces. This explains the constant frequency results with spin rate for the second mode which is shown in Table 5-17. The general conclusion indicated by the performed modal analyses is that the spin rate does not significantly alter the zero spin modal frequencies if the zero spin modal frequencies are sufficiently separated from the spin frequency.

5.2.3 ZERO "G" SOLAR ARRAY CONFIGURATION

The rollup solar array was analyzed in a similar manner as is described for past study analyses in Section 5.1. Updates in configuration data, however, were obtained from the Lockheed Space and Missiles Company and these were incorporated into the description of the derived vibration analysis model.

The total array area (two wing sections) is approximately 10,000 square feet and the electrical power output is rated as 10 watts per square foot. The rollup array dimensions and structural components are depicted in Figure 5-52. It is comprised of 10 membrane substrates

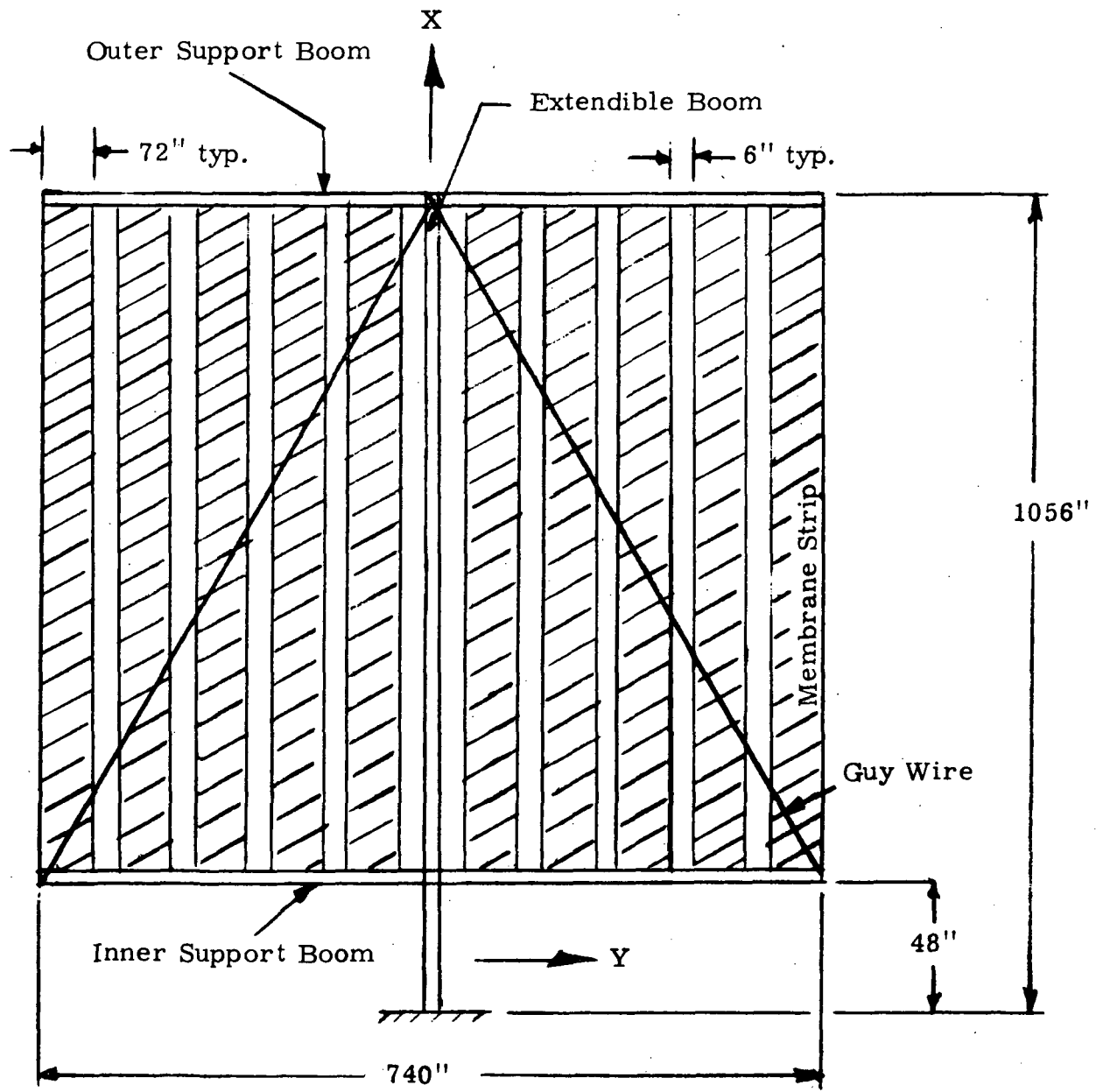


Figure 5 -52 Zero "G" Solar Array Configuration

per wing section, tensioned between an inner and outer boom by an extendible boom. Two guide wires are provided for each membrane strip and each is tensioned to 5.1 pounds. Each strip is attached to the inner boom assembly by a linear spring and tensioned to 12 pounds. A guy wire is also provided between the outboard end of the extendible boom and the extremity of the inner boom and acts as a tension load carrying member only. Pertinent stiffness and mass properties data for the array structural components are given in Table 5-18.

As was considered in Section 5.1, the symmetry properties of the solar array were utilized in the performance of its modal analysis. Only one-half of the wing section was discretized into a finite element model and it is presented in Figure 5-53. Four separate vibration conditions were established for the complete evaluation of modal properties and correspond to out-of-plane symmetric bending, out-of-plane antisymmetric bending (about the extendible boom), in-plane symmetric bending and in-plane antisymmetric bending. The NASTRAN finite element program (Reference 5.11) was utilized to obtain the modes; the four vibration conditions were obtained by constraining appropriate structural degrees-of-freedom. The nodal weights associated with the rollup array dynamic model and nodal geometry are given in Table 5-19. An assumption was made in the analyses for treating the stiffness provided by the guy wire; it was considered as a tension-compression member with only one-half of its actual tension stiffness properties. In addition, the lateral stiffness of the membrane strips was assumed to be described in terms of the tension force only. These stiffness terms were entered in the NASTRAN program by means of the "CELAS" stiffness elements.

A complete list of modal results and graphical presentation of modes for the four vibration conditions are given in Appendix A of this report. Modal participation factors, for each normal mode of the solar

TABLE 5 - 18

STIFFNESS AND MASS PROPERTIES DATA FOR ROLLUP SOLAR ARRAY

MEMBER	AE (lbs.)	EI_x^* (lb-in. ²)	EI_y^* (lb. -in. ²)	EI_z^* (lb. -in. ²)	GJ ² (lb-in. ²)	RUNNING WEIGHT (lbs/in.)
Extendible Boom (Full)	22.4×10^6		2.8×10^8	2.8×10^8		.212
Outer Support	10.4×10^6 (Y=0 to 72) 5.9×10^6 (Y=72 to 369)	9.3×10^8		3.32×10^8 (Y=0 to 72) 1.87×10^8 (Y=72 to 369)	26.8×10^6	.130
Inner Support	5.9×10^6	9.3×10^8		1.87×10^8	26.8×10^6	.115
Membrane Strip	3.33 lb/in.					.2
Guy Wire	$.203 \times 10^6$					

* - For axis system refer to Figure 5-52.

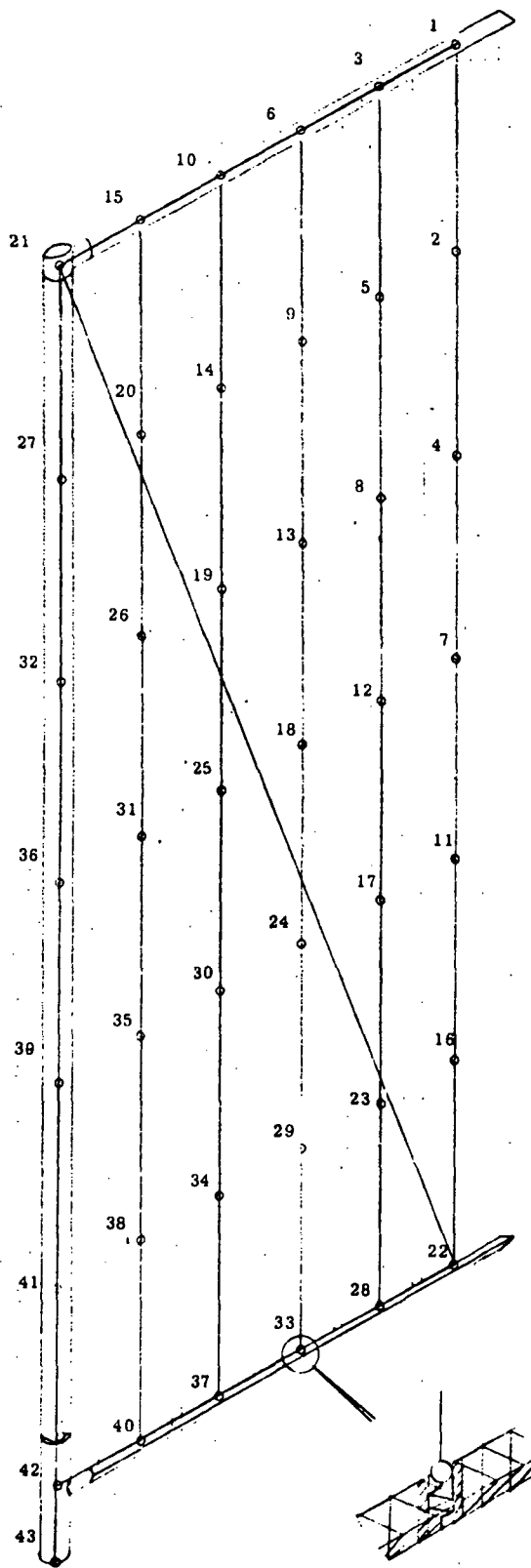


Figure 5-53
 Structural Model for Roll-up Solar
 Array Zero "G" Configuration

TABLE 5-19

Mass - Geometry Data
Of Zero G Solar Array

NODE NO.	WEIGHT(lbs.)	X	Y	Z
1	21.48	1056.	347.	0.
2	32.3	888.	347.	0.
3	26.06	1056.	275.	0.
4	32.3	720.	347.	0.
5	32.3	888.	275.	0.
6	26.06	1056.	203.	0.
7	32.3	552.	347.	0.
8	32.3	720.	275.	0.
9	32.3	888.	203.	0.
10	26.06	1056.	131.	0.
11	32.3	384.	347.	0.
12	32.3	552.	275.	0.
13	32.3	720.	203.	0.
14	32.3	888.	131.	0.
15	25.32	1056.	59.	0.
16	32.3	216.	347.	0.
17	32.3	384.	275.	0.
18	32.3	552.	203.	0.
19	32.3	720.	131.	0.
20	32.3	888.	59.	0.
21	12.74	1056.	0.	0.
22	20.84	48.	347.	0.
23	32.3	216.	275.	0.
24	32.3	384.	203.	0.
25	32.3	552.	131.	0.
26	32.3	720.	59.	0.
27	17.81	888.	0.	0.
28	24.98	48.	275.	0.
29	32.3	216.	203.	0.
30	32.3	384.	131.	0.
31	32.3	552.	59.	0.
32	17.81	720.	0.	0.
33	24.98	48.	203.	0.
34	32.3	216.	131.	0.
35	32.3	384.	59.	0.
36	17.81	552.	0.	0.
37	24.98	48.	131.	0.
38	32.3	216.	59.	0.
39	17.81	384.	0.	0.
40	24.23	48.	59.	0.
41	17.31	216.	0.	0.
42	12.30	48.	0.	0.
43	0.	0.	0.	0.

NOTE: Weights along the boom (Y = 0.) are
one half the actual weight.

array, using root constraint loads were also computed in order to determine those modes of importance for describing interaction loads. The properties of those modes having relatively large load participation factors are listed in Table 5-20.

5.2.4 ARTIFICIAL "G" SOLAR ARRAY CONFIGURATION

The rollup solar array for the artificial "G" condition consists of the same structural geometry as that of the zero "G" configuration, however, only four membrane strips are utilized-- the two on each side of and adjacent to the extendible boom. The derived finite model of the artificial "G" array is presented in Figure 5-54. Average tension in each strip during spin is increased to 340 pounds and the strips lateral deflection stiffness values are based upon this tension. The stiffness matrix for each finite element of the extendible boom was computed by hand so as to include the beam columning effect and input into the NASTRAN program by the "direct matrix input" method. Additional structural restraints are provided at the extremities of the inner boom for this spin condition and were included in the dynamic model. The stiffness matrix for the entire model was formulated by NASTRAN and the coriolis force coefficient and centrifugal force coefficient matrices were generated by hand computations. The configuration was taken to spin in a plane containing the solar arrays. These matrices, together with the mass matrix were input in the JPL program (References 5.8 and 5.9). A list of all resulting modal data for spin rates of 0, 4, 8, and 12 RPM are presented in Appendix A of this report. A list of data for those modes which were identified to have large load participation (zero spin) are presented in Table 5-21. The modal constraint forces used in the calculation of participation factor were those resulting at each point of array restraint. Table 5-22 lists the frequencies of these modes with large participation factors for each

TABLE 5-20 ROLLUP SOLAR ARRAY MODAL DATA, ZERO "G" CONFIGURATION

Direction	Type	Mode No	Frequency (Hz)	Generalized Mass ² (lb.-sec. ² /in.)	Modal Participation Factor		
					Force	Bending Moment	Torque
Out of Plane	Symmetric	1	.0925	1.36	.681	.415	
		6	.187	1.30	.003	.044	
		22	.835	.158	.119	.001	
	Anti-Symmetric	1	.0640	.609			.779
		6	.167	.547			.074
		11	.241	.689			.078
In Plane	Symmetric	26	1.35	.705	.520		
		27	3.28	.770	.165		
		28	3.49	.607	.058		
		31	6.07	.104	.062		
	Anti-Symmetric	1	.0974	1.35	.712	.514	
		6	.189	1.41	.001	.137	
		11	.265	1.46	.077	.105	
		16	.324	1.83	.055	.084	

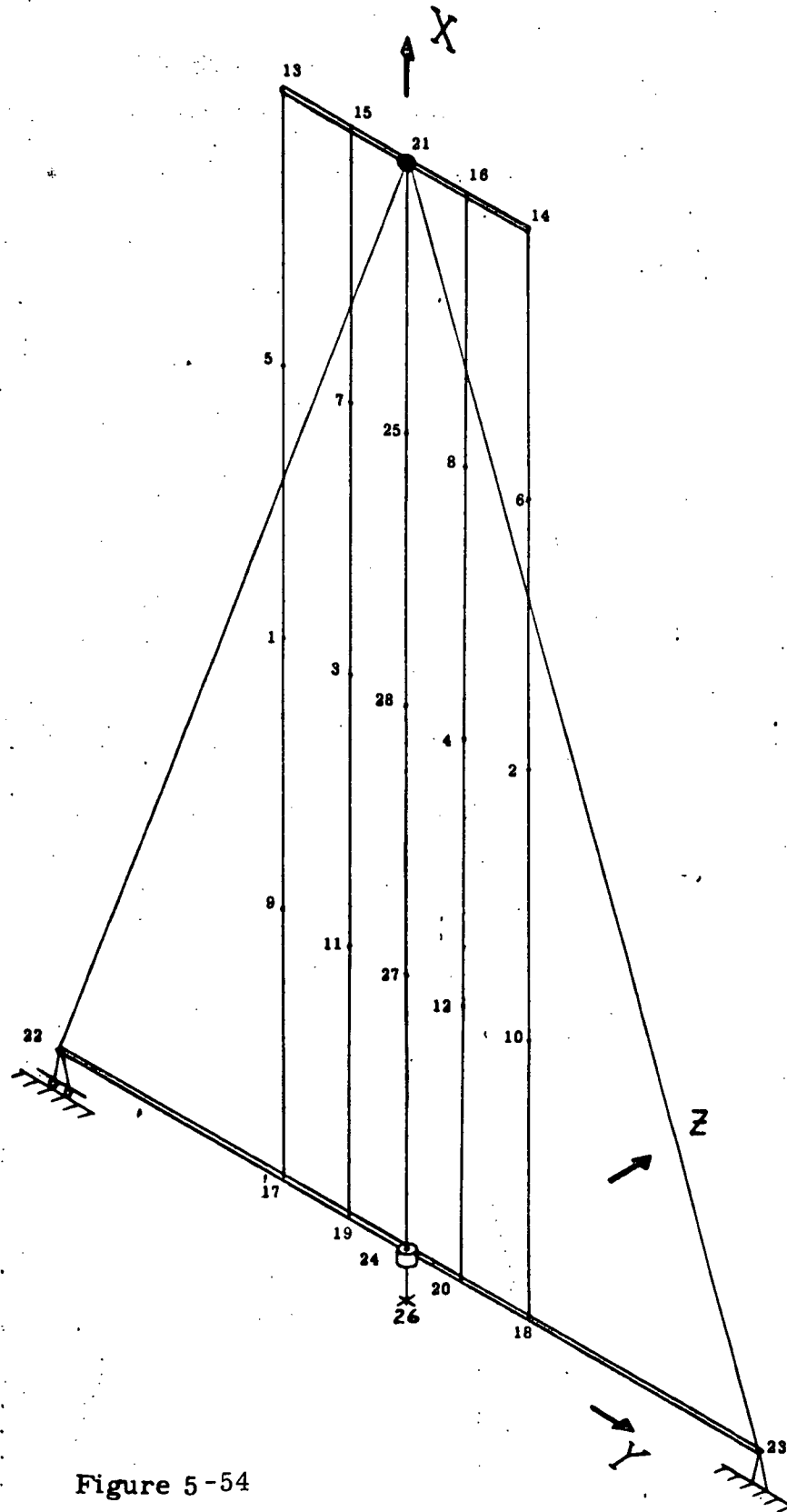


Figure 5-54
 SOLAR ARRAY ARTIFICIAL "G" STRUCTURAL MODEL

Table 5-21 Artificial "G" Solar Array,
Modal Participation Factors

Zero Spin

Out of Plane						
Symmetric			Antisymmetric			
Mode	Frequency (Hz.)	% Participation		Mode	Frequency (Hz.)	% Participation Moment
		Shear	Moment			
2	0.203	41.9	15.2	1	0.199	12.5
9	0.504	1.7	0	10	0.521	1.4
17	0.778	2.1	0	18	0.794	2.0
				19	0.905	78.6

In Plane			
Symmetric		Antisymmetric	
Mode	Frequency (Hz.)	% Participation Shear	Mode
32	3.84	76.5	3
			11
			20
			28

TABLE 5-22
ART "G" SOLAR ARRAY CONFIGURATION
LIST OF EIGENVALUES IN HERTZ

ELASTIC MODE NO.	NASTRAN RESULTS $\Omega = 0$	"GUPTA" PROGRAM RESULTS			
		$\Omega = 0$	$\Omega = 4$ RPM	$\Omega = 8$ RPM	$\Omega = 12$ RPM
1	0.1989	0.1786	0.1786	0.1787	0.1787
2	0.2032	0.1977	0.1977	0.1977	0.1977
3	0.3784	0.3768	0.3710	0.3524	0.3185
9	0.5037	0.5031	0.5025	0.5025	0.5025
10	0.5215	0.5142	0.5151	0.5151	0.5151
11	0.7045	0.7010	0.6969	0.6881	0.6716
17	0.7782	0.7774	0.7777	0.7777	0.7777
18	0.7941	0.7912	0.7911	0.7911	0.7911
19	0.9051	0.9047	0.9049	0.9049	0.9049
20	0.9349	0.9315	0.9291	0.9224	0.9090
28	1.0654	1.0544	1.0506	1.0454	1.0331
32	3.8422	3.8402	3.8413	3.8441	3.8462

Modes 1, 2, 9, 10, 17, 18, 19 are out-of-plane modes.

Modes 3, 11, 20, 28, 32 are in-plane modes.

of the considered spin rates. It is noted that out-of-plane modal frequencies are invariant with spin rate; this is due to the coriolis forces and centrifugal forces not coupling these associated motions. The in-plane modal frequencies are seen to be significantly influenced by spin rate. The zero spin frequency of mode No. 3, whose zero spin natural frequency is nearest to the highest spin frequency considered, is reduced considerably (15%) at $\Omega = 12$ RPM. It is to be emphasized that the membrane (strip) tension was considered invariant for all spin rates considered and corresponded to the LMSC average tension specified for 4 RPM. Higher spin rates would decrease this average tension, thereby further reducing frequency.

It is noted that the fundamental mode frequency obtained by the NASTRAN program is significantly different than obtained by the JPL program and cannot be explained at this time. Dr. K. K. Gupta of JPL (private communications) relates the numerical accuracies afforded by digital computers are not sufficient to accurately obtain this modal frequency by the "Givens" eigenvalue-eigenvector extraction method, contained in the NASTRAN program.

5.3 REFERENCES

- Ref. 5.1 Rosen, Richard, "STARDYNE User's Manual", Mechanics Research, Inc. Document, Los Angeles, California, January, 1970.
- Ref. 5.2 "Proposal for Large Space Station Solar Array Technology Evaluation Program - Vol. I.", LMSC A96774, Lockheed Missile and Space Company Report.
- Ref. 5.3 Coyner, J. V. and Ross, R. G., "Analysis of Performance Characteristics and Weight Variations of Large Area Roll-Up Solar Arrays", 69-WA/Ener-11, paper presented at the ASME Winter Annual Meeting, Nov. 16-20, 1969, Los Angeles, California.
- Ref. 5.4 Martin, H. C., "On the Derivation of Stiffness Matrices for the Analysis of Large Deflection and Stability Problems," Proceedings on Conference, Matrix Methods in Structural Mechanics, AFFDL-TR-66-80, October, 1965.
- Ref. 5.5 "Quarterly Report No. 3, Rollup Subsolar Array", General Electric Company Report No. GE-SSO-69SD4373, December 15, 1969.
- Ref. 5.6 "Third Quarterly Report - Large Area Solar Array", The Boeing Company Report No. D2-113355-3, July 1967.
- Ref. 5.7 "Modular Space Station-Phase B Extension, First Quarterly Review", North American Rockwell, Space Division, PDS-71-2, May 1971.
- Ref. 5.8 K. K. Gupta, "Eigenvalues of $(B - A^*) Y=O$ with Positive Definite Band Symmetric B and Band Hermitian A^* and its Application to Natural Frequency Analysis of Flexible Space Vehicles," Space Program Summary 37-60, Volume 3, Jet Propulsion Lab, Pasadena, California, December 1969.

- Ref. 5.9 K. K. Gupta, "Free Vibration Analysis of Spinning Structural Systems," International Journal for Numerical Methods in Engineering, to be published.
- Ref. 5.10 Patel, J. A., and Seltzer, S. M., "Complex Eigenvalue Solution to a Spinning Skylab Problem," NASTRAN: USERS EXPERIENCES, NASA TMX-2378, September 1971.
- Ref. 5.11 "The NASTRAN Users Manual," NASA SP-222, Section 3-4, 1970, Office of Technology Utilization, NASA, Washington, D. C.

6. SIMULATION VERIFICATION ANALYSIS

Various simplified analyses were performed to verify the formulated interactions computer program and contained methodology. These analyses were divided into two parts--one part to verify the structural dynamics methodology used (Reference 6-1) and to gain some insight into the accuracy of this methodology, and the other part to verify the various subroutines or subprograms contained within the simulation.

6.1 STRUCTURAL DYNAMICS VERIFICATION

6.1.1 SIMULATION OF FLEXIBLE APPENDAGES & RIGID SPACE STATION

A planar problem considering a structural arrangement of two uniform beams representing flexible appendages and connected to a rigid space station mass (taken to be zero) was formulated and analyzed for interaction (interface) forces caused by an applied step force. The closed form solution to this problem is presented in Reference 6-2 when using a finite number of orthogonal cantilever modes as flexible appendage degrees-of-freedom. As represented in the simulation program, this structural arrangement of two cantilevers simulates a free-free beam (Figure 6-1).

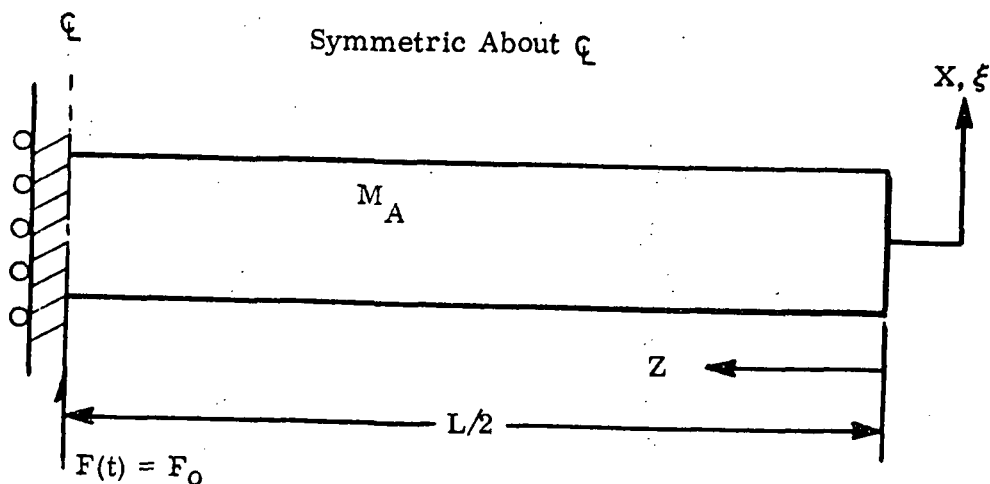


Figure 6-1. Cantilever Beam Simulation of a Free-Free Beam

An orthogonalization of the coupled motion equations of the two cantilever beams (appendages), which are formulated within the simulation from the input data, produces the comparisons shown in Figure 6-2 and Table 6-1. Figure 6-2 presents the comparison of the resulting orthogonal deflection shapes using three cantilever mode degrees-of-freedom for each beam appendage and theoretical free-free beam shapes obtained from Reference 6.3.

TABLE 6-1
 Frequency Comparison of (Uniform Beam) Cantilever + Rigid Body Mode Representation
 of a Free-Free Uniform Beam

Frequency Ratios: $f_n / f_{n,1 \text{ free-free}}$

Reference Frequency Ratios			Calculated Coupled Mode Frequency Ratios				
Symmetric Mode No., n	Free-Free Beam	Uncoupled Cantilever Beam	1 Mode Cantilever Beam + Rigid Body	2 Mode Cantilever Beam + Rigid Body	3 Mode Cantilever Beam + Rigid Body	4 Mode Cantilever Beam + Rigid Body	5 Mode Cantilever Beam + Rigid Body
1	1.000	0.632	1.0101	1.0006	1.0003	1.0000	1.0000
2	5.404	3.958	---	5.548	5.420	5.408	5.405
3	13.344	11.074	---	---	13.749	13.410	13.367
4	24.814	21.652	---	---	---	25.584	24.965
5	39.812	35.861	---	---	---	---	41.030

Table 6-1 presents the comparison of resulting frequencies using a varied number of cantilever mode degrees of freedom for each beam appendage with theoretical free-free beam frequencies.

These comparisons show the adequacy of the structural dynamics methodology that has been used in the interactions simulation; the degree of accuracy in the approximation is seen to be dependent upon the number of cantilever modes used. Transient load responses were obtained for this structural system using the formulated computer program with all control

systems inactive. Each of the cantilever beam modes was input into the program by modal descriptions of 25 discrete mass points representing 50 inertial degrees of freedom. A step force was applied at the zero-mass space station C.G. The shear force at the 1/4 span of the free-free arrangement, as obtained by the simulation, is compared with results obtained by Reference 6.4 in Figure 6-3. The entire free-free structural configuration (2 connected cantilevers) was modeled by 40 discrete mass points for input into the "direct transient method" of Reference 6.4. Comparisons are seen to be good, and as expected, higher frequency transients result in the force history obtained by Reference 6.4 since all system modes of vibration are represented. Another comparison is provided for the simulation results in Reference 6.2 and reproduced in Figure 6-4. A variable order Adams numerical integration method and the first five symmetric free-free beam modes were used to obtain the 1/4 span shear force resulting from a step input. Again, the comparison shows the simulation results to be very comparable.

6.1.2 SIMULATION OF RIGID APPENDAGES AND RIGID SPACE STATION

A simple planar problem was formulated to show verification of the rigid body dynamics solutions given by the simulation. This formulation consisted of two simulated rigid appendages connected to a simulated rigid space station and perturbed by a step force. The resulting appendage interaction forces and moments given by the simulation are compared to the exact result in Figure 6-5.

6.1.3 SIMULATION OF FLEXIBLE APPENDAGES AND FLEXIBLE SPACE STATION

A planar problem was formulated for verification purposes and consisted of three uniform beams forming a "T" arrangement (Figure 6-6). This arrangement is representative of a flexible center body (space station) and two flexible appendages (solar arrays). Stiffness and mass properties of each beam were chosen so that the center beam had an uncoupled fundamental free-free axial deflection mode frequency of 1 Hz and that the appendage beams had an

uncoupled fundamental cantilever bending frequency of 1 Hz. Initially, results were obtained from the simulation and by hand calculations using the same simulated methodology (Reference 6.2) considering one cantilever mode of each flexible appendage and a rigid center body. Corresponding shear and moment interaction histories are presented in Figure 6-7. It is seen that the solutions are coincident at time zero but are slightly different in amplitude and phase. This is attributable to integration interval used ($\Delta t = 0.05$ sec.) together with the NASTRAN numerical integration algorithm (Reference 6.4) which is coded in the simulation computer program. Although not directly applicable to the above formulated problem, the variation of amplitude, frequency and phase errors with integration sample rate per cycle of the highest system frequency resulting from use of this algorithm, were determined for a five cantilever mode representation of the flexible appendages and are presented in Figure 6-8. A higher degree of required simulation solution accuracy than that shown in Figure 6-7 therefore requires the use of a smaller integration interval.

Several methods of obtaining interaction moment solutions of the formulated problem, with the flexibility of the center body included, were used and compared with the simulation results to show the adequacy of the methodology. These solutions, together with that obtained from the simulation program are presented in Figure 6-9. Modal solutions of the structural arrangement considered as a system were obtained by the transient response solution method provided in Reference 6.5 and an independent method utilizing a variable order Adams integration method. The results shown using system modes utilize one rigid body translational degree of freedom and the first four orthogonal elastic modes. Both the modal displacement and modal acceleration methods of load calculation were considered. A solution of interaction moment produced by a coupled system response, as given by the direct transient response method of NASTRAN, is also presented. The finite element model of the "T" beam for input for the above solutions is represented by a total of 79 discrete mass

points and complete description of this model and system mode results are given in Reference 6.6. The interaction moment of the "T" beam given by the simulation reflects the use of the first 10 free-free axial deflection modes of the center body and the first two cantilever modes of the flexible appendages. The results obtained by all of the methods compare very well and show the adequacy of the methodology contained in the simulation.

6.1.4 VERIFICATION OF COMPLEX EIGENVALUE-EIGENVECTOR ROUTINE (REFERENCES 6.7 AND 6.8)

As part of the study program effort, a computer program received from the Jet Propulsion Laboratory (References 6.7 and 6.8) and formulated by Dr. K. K. Gupta, was converted for operation on the CDC 6000 Series Computer. This program has the capability of solving for the orthogonal properties of a set of coupled second order equations having non-zero coefficients of the first derivatives of the time dependent variables, which are representative of a finite element structural model in a spinning environment. A simple uniform beam problem was formulated to verify the correctness of program conversion. The finite element model and results from both the converted program and the NASTRAN program, for a zero-spin condition, are shown in Table 6-2. The comparisons show both a comparable method of orthogonalization with the similar techniques of NASTRAN and the verification of the converted program.

6.2 SUBPROGRAM VERIFICATION

The various subprograms comprising the complete digital simulation of the space station and solar arrays were verified for correctness of formulations by a number of program executions with simple structural arrangements and initializations. Each of the program executions was performed with the derived simulation of the first study phase which is described in References 6.9 and 6.10. This simulation considers the flexible dynamics of appendages and only the rigid body dynamics of the space station. The simulation resulting from the second study phase and described in Report Section 4 utilizes many of the same subprograms; and therefore, the performed subprogram verification is taken to be a partial verification of the Phase II digital simulation.

The total subprogram verification is represented by the following outline. Verification of each of the given program output quantities is made by comparison with hand computed results.

SYSTEM RIGID BODY MOTION

- Space Station Rigid Body Motion

X-, Y-, and Z- translations: due to a force input to space station
 θ_X^- , θ_Y^- , and θ_Z^- rotations: due to a force input to space station

Disturbance force input variations for check of interpolation procedure

Location variation of disturbance force, {LR}

- Solar Array Rigid Body Motion

Sun Vector Misalignment, {Sun}

Initial Attitude Error {EULER (7)}, {EULER (8)}

Solar Array Drive Selection {RBC (1)}, {RBC (2)}

θ_X^- and θ_Z^- rotations: due to a force input to space station.

SPACE STATION CONTROL DYNAMICS

- Response to Reaction Jet Control Torques

Threshold not exceeded, i. e., $\theta_\epsilon < 1/2^\circ$ {EULER (1-6)}

Threshold exceeded, i. e., $\theta_\epsilon > 1/2^\circ$

Variable SS guidance commands, {SSGTIME}, {DELTSSG}

- Response to CMG Control Torques

Threshold not exceeded, i. e., $T_{CMG_REG'D} < T_{CMG_LIMIT}$
 {EULER (1-6)}

Threshold exceeded, i. e., $T_{CMG_REG'D} > T_{CMG_LIMIT}$
 {EULER (1-6)}

Variable SS guidance commands, {SSGTIME}, {DELTSSG}

SOLAR ARRAY CONTROL DYNAMICS

- Linear OCS Response

Solar Array Drive Gear-train variation, {GEARKON}
Sun Vector Misalignment, {Sun}
Initial Attitude Error, {EULER (7)} , {EULER (8)}
Variable SA guidance commands, {SAGTIME} , {DELTSAG}

- Non-Linear OCS Response

Solar Array Drive Gear-train variation, {GEARKON}
Threshold not exceeded, i. e., $\theta_\epsilon < 5^\circ$ {EULER (7-8)}
Threshold exceeded, i. e., $\theta_\epsilon > 5^\circ$
Variable SA guidance commands, {SAGTIME} , {DELTSAG}

SYSTEM ELASTIC BODY MOTION

- Solar Array Modal Response, DEBUG (20) = .F.

Cantilever Dynamics, {RBC (1) = .T.} , {RBC (2) = .T.}
Pinned-joint Dynamics, {RBC (1) = .F.} , {RBC (2) = .F.}
Initial SA attitude error, {EULER (7)} , {EULER (8)}
Variable SA guidance commands, {SAGTIME} , {DELTSAG}

- Orbital Mechanics

Semi-major axis variation, {A}
Orbit Eccentricity variation, {E}
Orbit Inclination variation, {INC}
Orbit Initialization point, {M}, {P}, {N}

} No SS or
SA Control

The above bracketed quantities are variable names used in the various subprograms and are defined in Reference 6.9.

REFERENCES

- 6.1 "Dynamics and Control of Flexible Space Vehicles," P. W. Likens, NASA CR 105592.
- 6.2 "Integrated Dynamic Analysis of a Space Station, with Controllable Solar Arrays," J. A. Heinrichs, et al, paper presented at the 42nd Shock and Vibration Symposium.
- 6.3 D. Young and R. P. Felgar, Jr., "Tables of Characteristic Functions Representing Normal Modes of Vibration of A Beam," University of Texas Publication No. 4913, 1 July 1949.
- 6.4 "The NASTRAN Theoretical Manual," NASA-SP-221, Section 11.3, 1970., Office of Technology Utilization, NASA, Washington, D. C.
- 6.5 "The NASTRAN Users Manual," NASA SP-222, Sections 3.10 and 3.13, 1970., Office of Technology Utilization, NASA, Washington, D. C.
- 6.6 "The Study of Dynamic Interactions of Solar Cell Arrays with Space Stations and the Development of Solar Array Structural Requirements," Fairchild Industries/FSED Monthly Progress Report for October 1971, NASA/LRC Contract NAS5-10155.
- 6.7 K. K. Gupta, "Eigenvalues of $(B-\lambda A^*) Y=0$ with Positive Definite Band Symmetric B and Band Hermitian A^* and its Application to Natural Frequency Analysis of Flexible Space Vehicles," Space Programs Summary 37-60, Volume 3, Jet Propulsion Lab, Pasadena, California, December 1969.
- 6.8 K. K. Gupta, "Free Vibration Analysis of Spinning Structural Systems," International Journal for Numerical Methods in Engineering, to be published.

- 6.9 "Solar Array-Space Station Dynamic Interaction Analysis, Digital Simulation Documentation Users Manual," prepared by Fairchild Hiller Corporation, SESD, February 26, 1971, under NASA/LRC Contract NAS5-10155.
- 6.10 "Interim Report, The Study of Dynamic Interactions of Solar Arrays with Space Stations and Development of Array Structural Requirements," Fairchild Industries Report 858-IR-1, February 1971, Fairchild Industries, Germantown, Maryland.

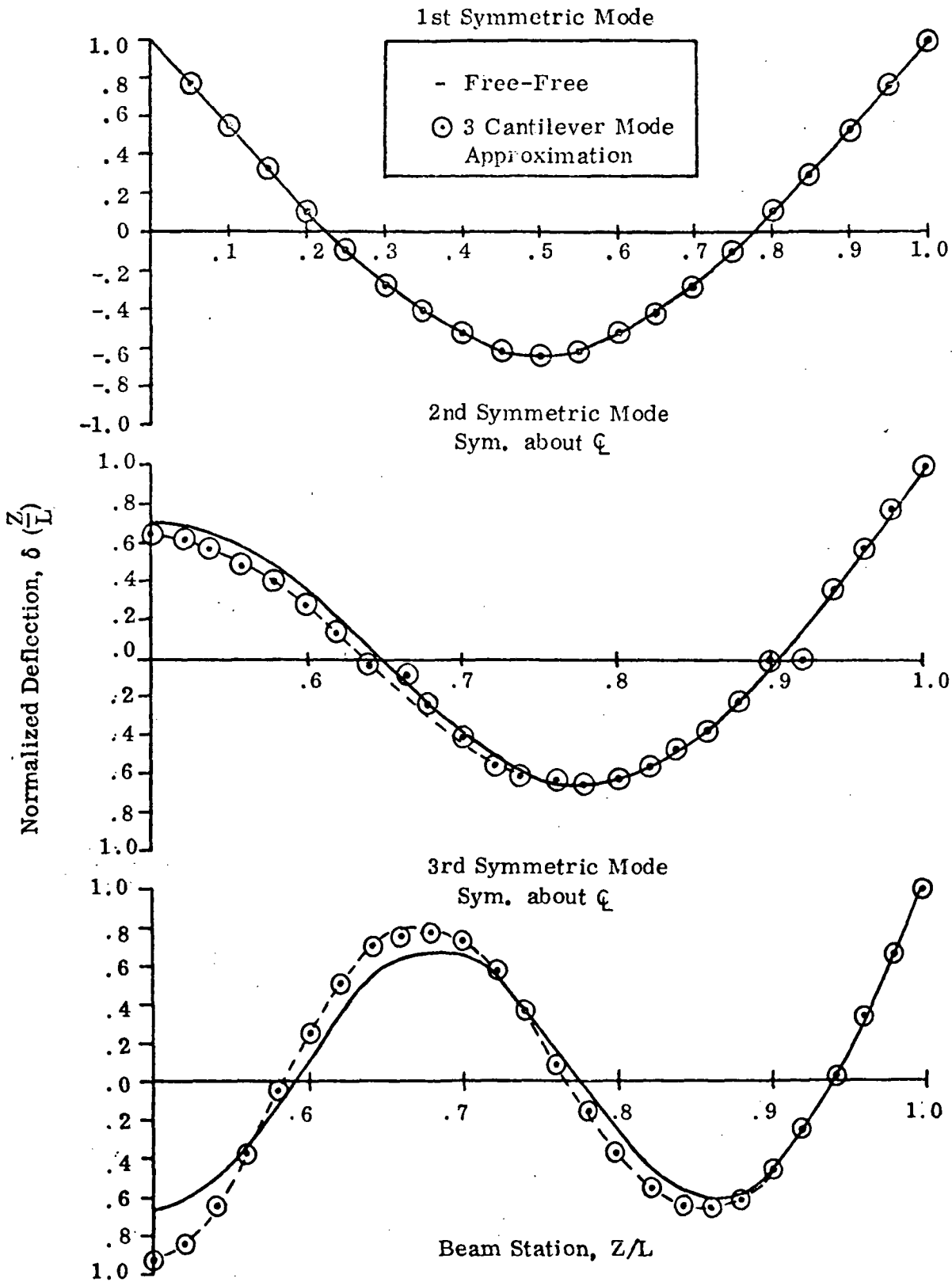


Figure 6-2. Comparison of Mode Shapes for a Free-Free Uniform Beam and a 3 Cantilever Mode Approximation

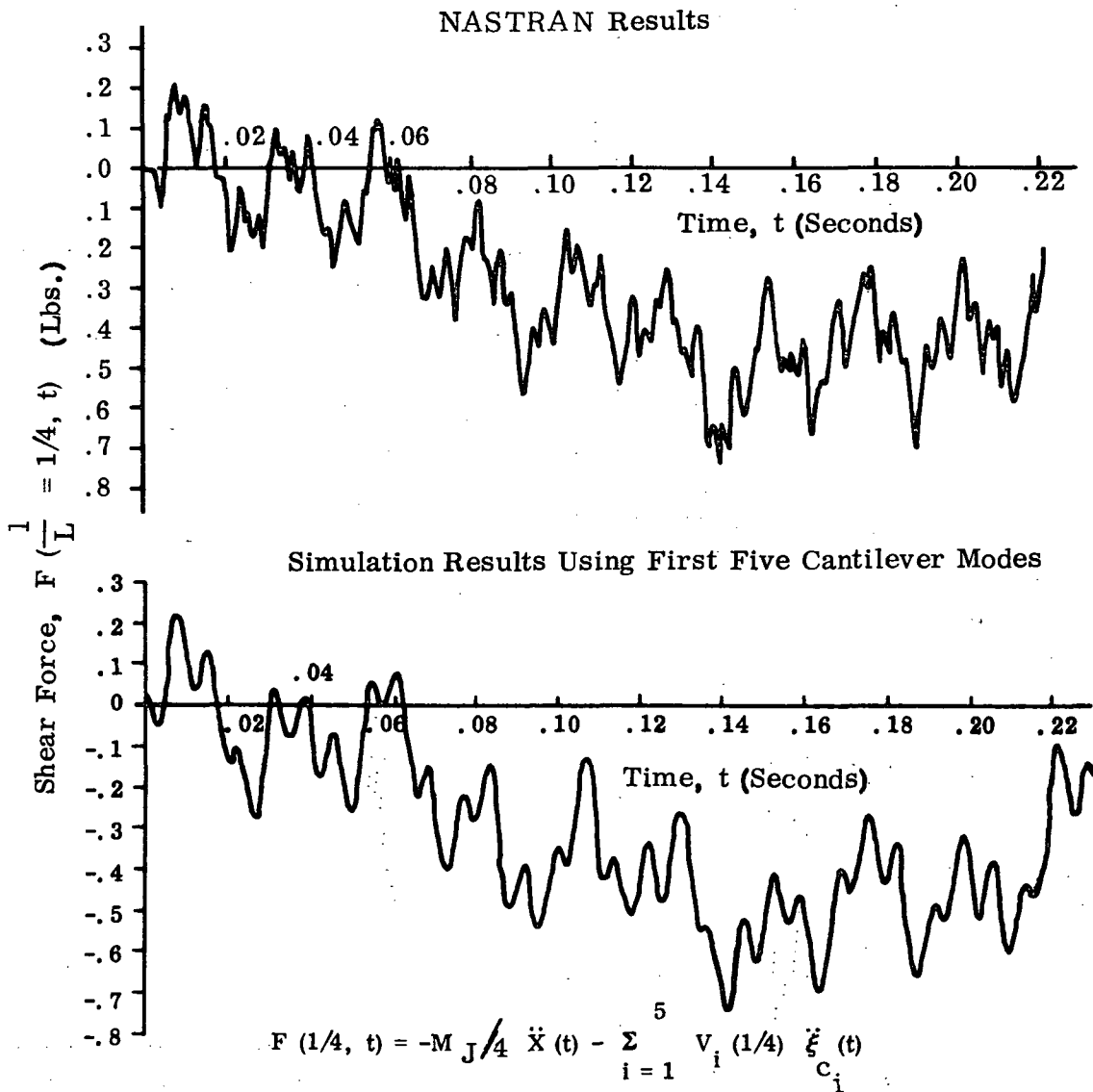
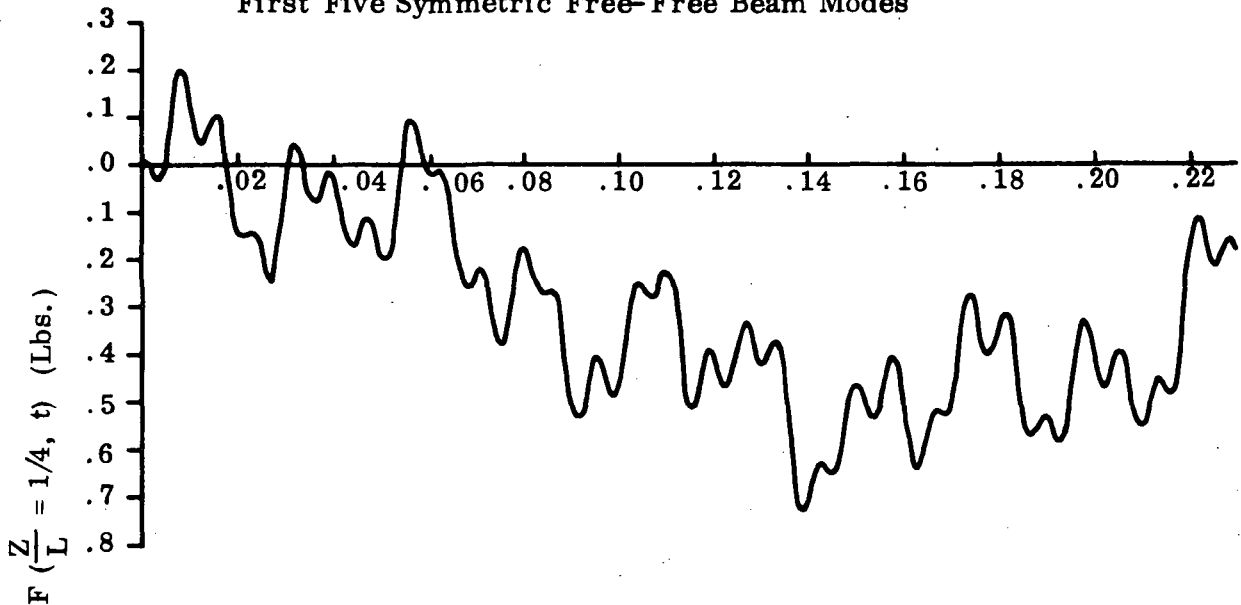


Figure 6.3 Uniform Beam Comparisons of Shear History at 1/4 Span for a Unit Step Force Applied at Mid-Span

Variable Order Adams Numerical Integration Results Using the First Five Symmetric Free-Free Beam Modes



Simulation Results Using First Five Cantilever Modes

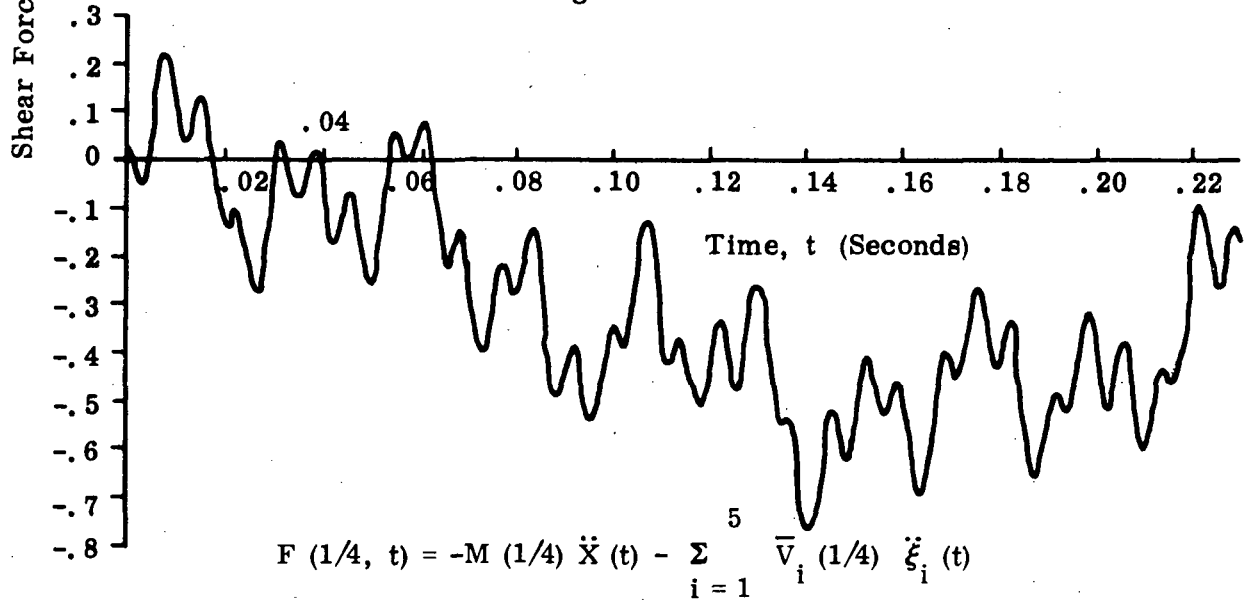


Figure 6-4. Uniform Beam Comparisons of Shear Histories @ 1/4 Span for a Unit Step Force Applied at Mid-Span

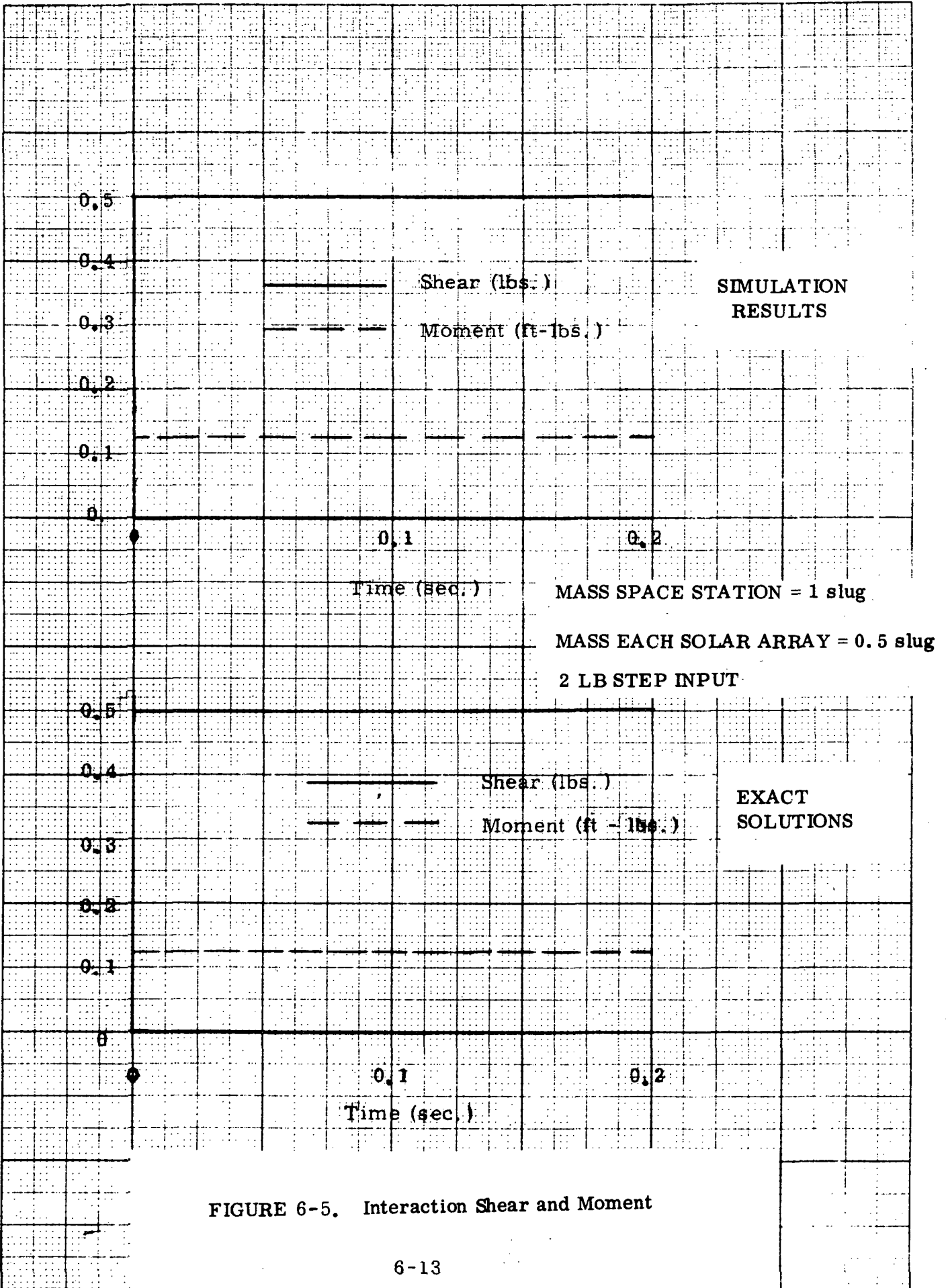


FIGURE 6-5. Interaction Shear and Moment

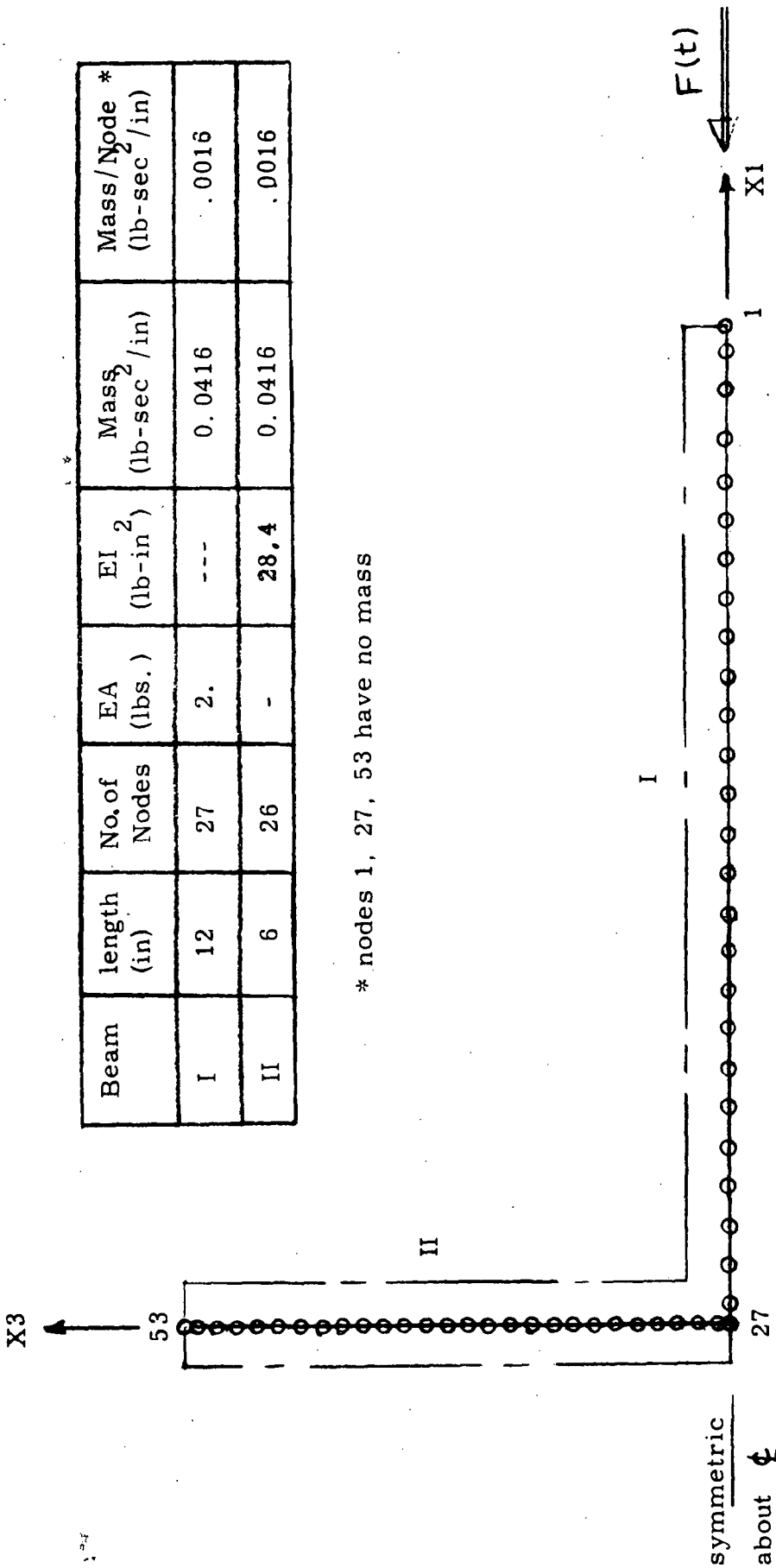
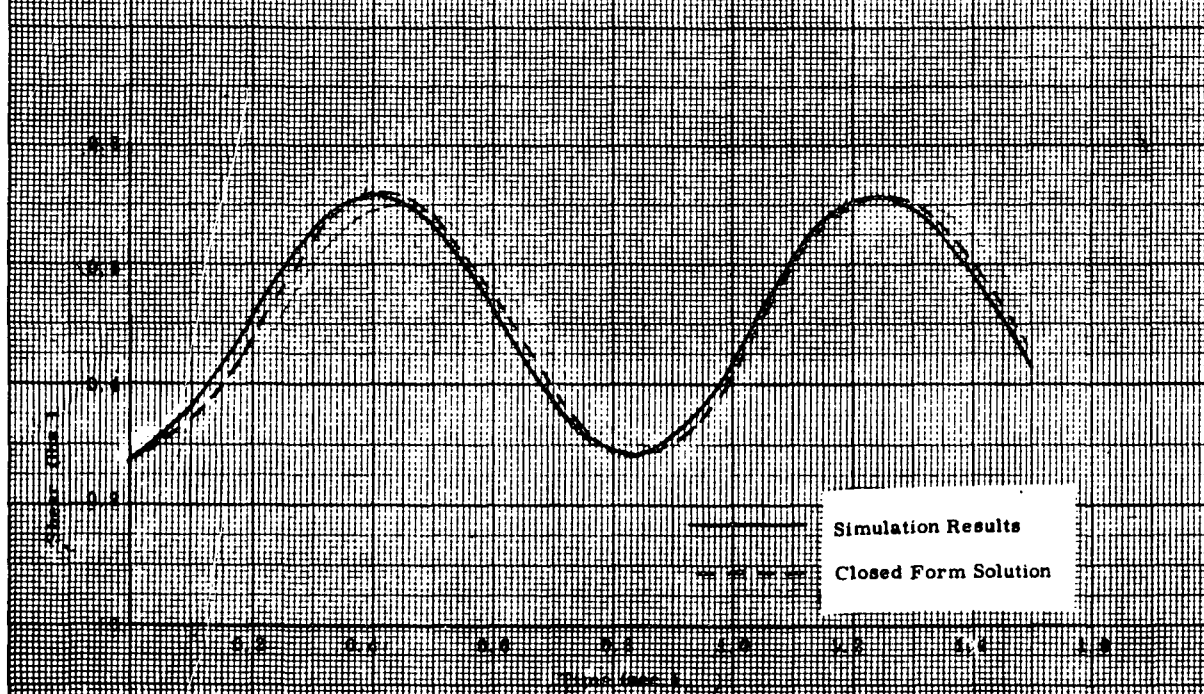
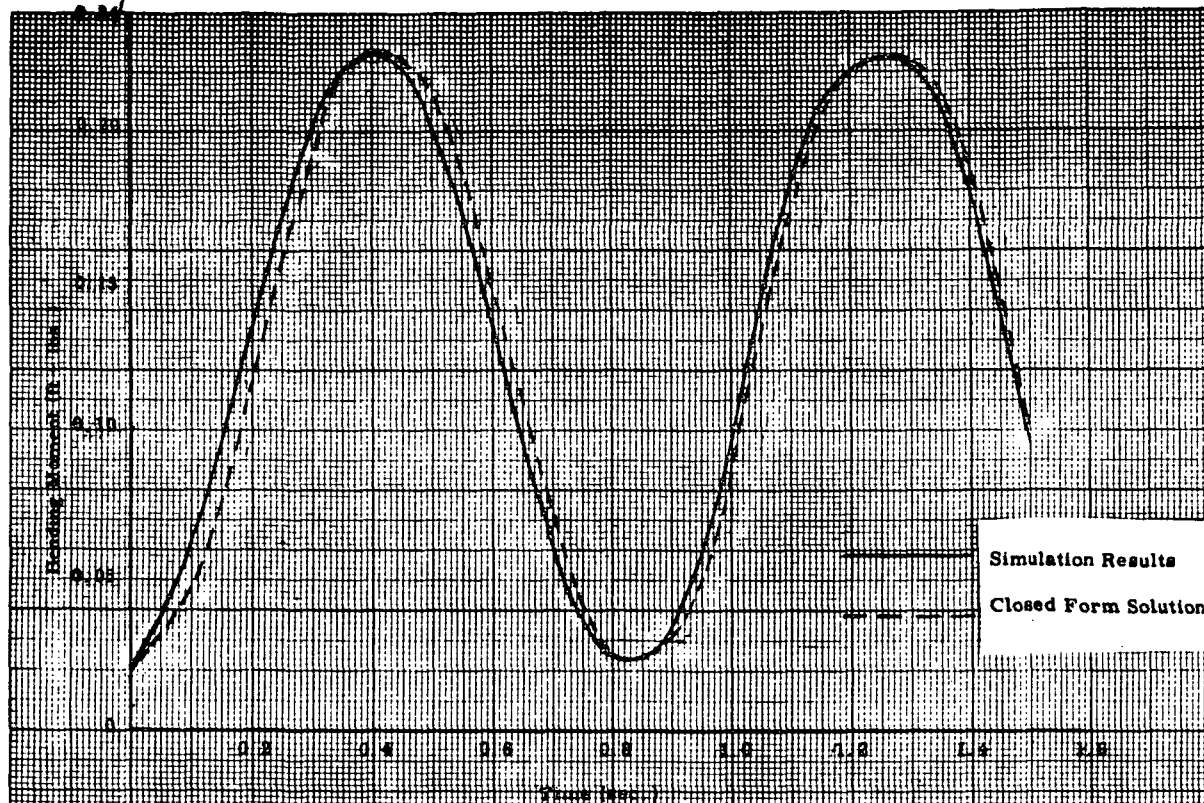


Figure 6-6. T-Beam Structural Model



**RIGID CENTER BODY AND ONE
MODE REPRESENTATION OF FIXED
APPENDAGES PERTURBED BY
A STEP FORCE HISTORY**

Figure 6-7 Interaction Forces vs. Time

FAST-RUN NUMERICAL INTEGRATION ALGORITHM
 AMPLITUDE ERROR, FREQUENCY ERROR, AND PHASE ERROR
 SAMPLING OF THE RESPONSE FREQUENCY OF OSCILLATION

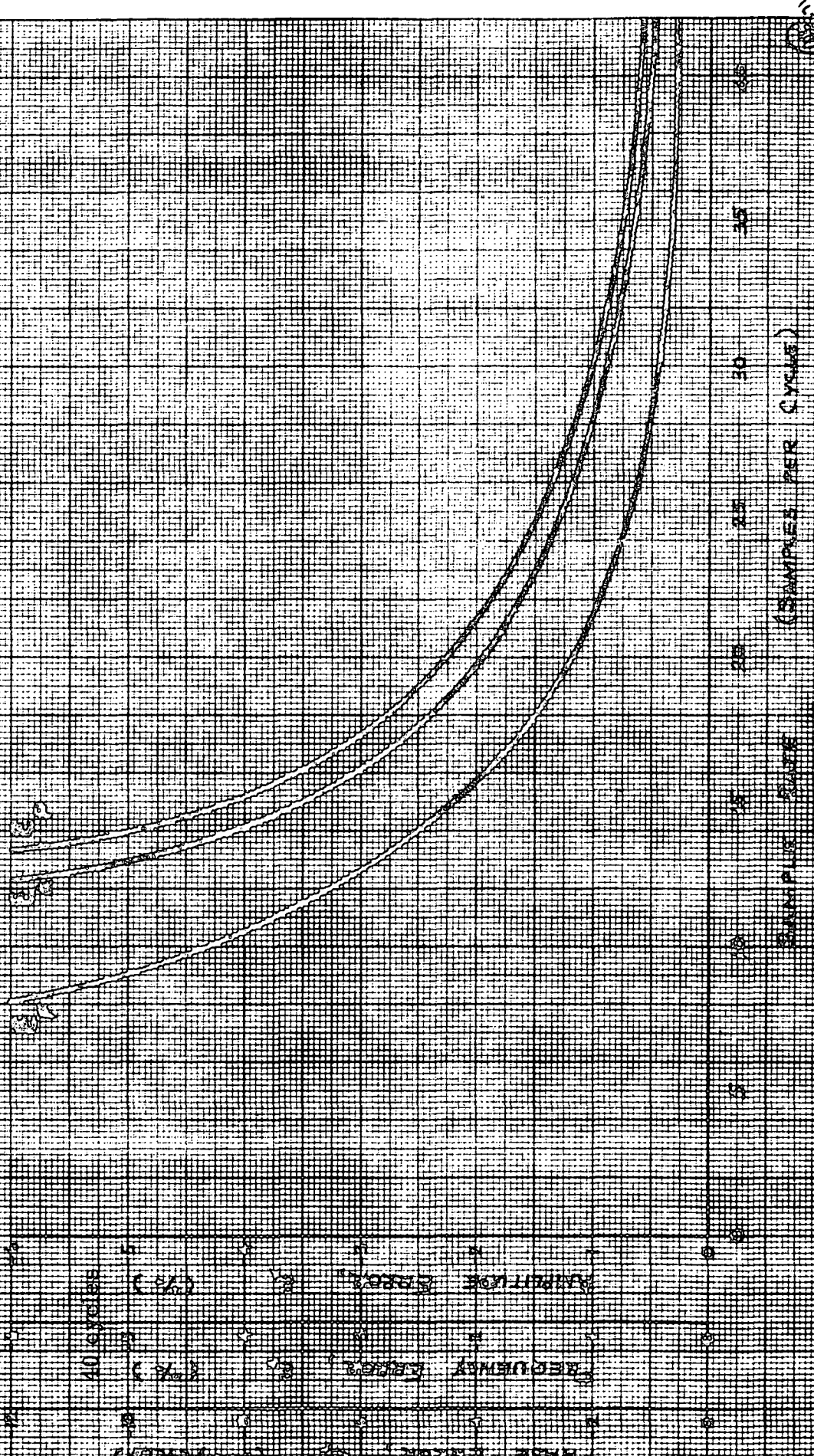


Figure 6-8

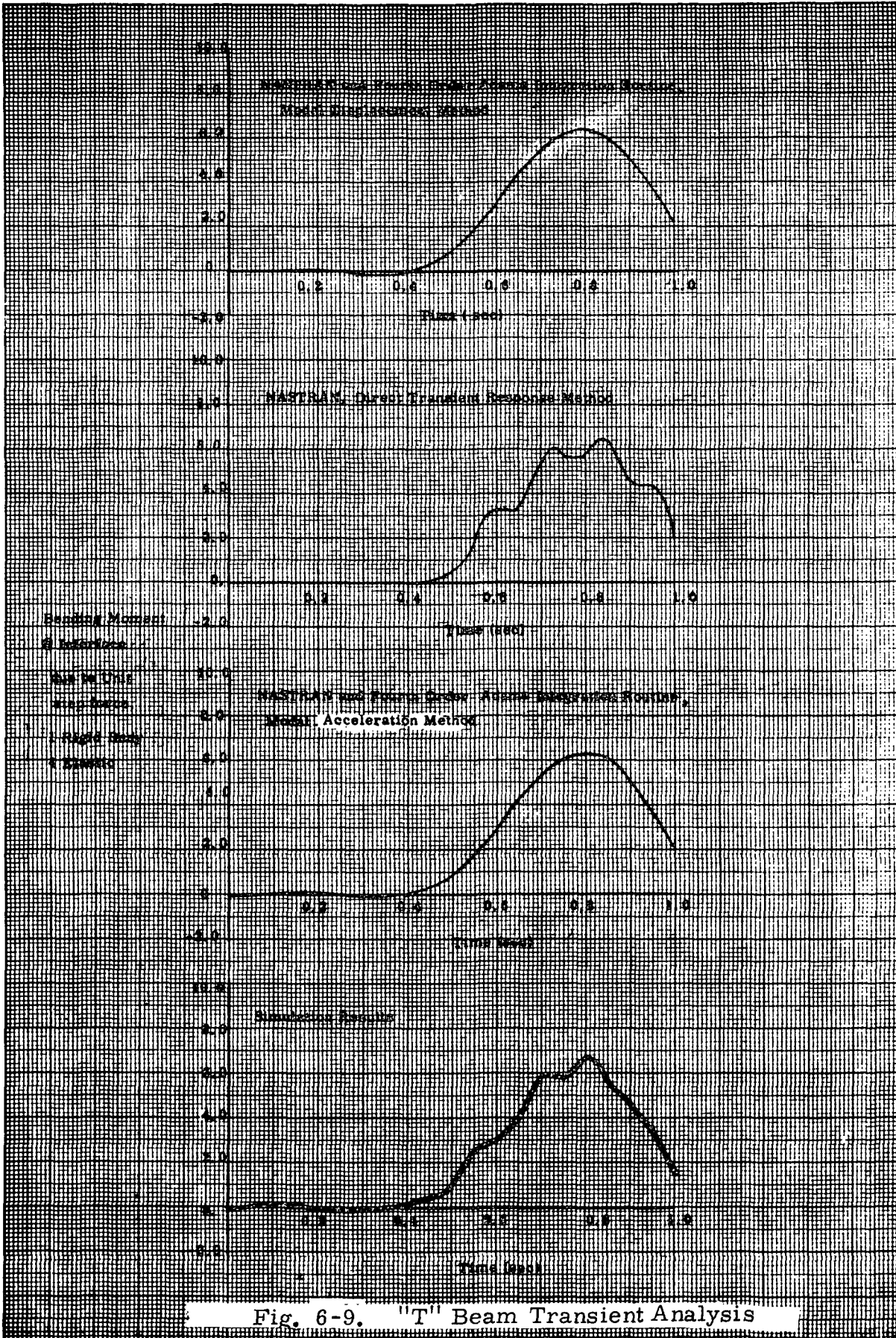
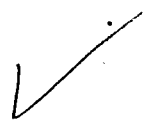
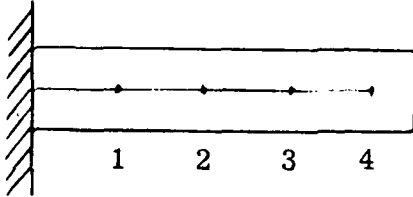


Fig. 6-9. "T" Beam Transient Analysis

TABLE 6-2
COMPARISON OF NASTRAN AND GUPTA EIGENVALUE
SOLUTIONS FOR CANTILEVER BEAM



$$\text{MASS/IN.} = 0.01 \frac{\text{LB. SEC.}^2}{\text{IN.}^2}$$

$$EI = 1 \times 10^7 \text{ LB.IN.}^2$$

FREQUENCY COMPARISON (RAD. /SEC.)

MODE	GUPTA	NASTRAN
1	55.5344	55.5349
2	357.7820	357.8042
3	1009.7656	1010.5280

MODE SHAPE COMPARISON

POINT #	MODE 1		MODE 2		MODE 3	
	GUPTA	NASTRAN	GUPTA	NASTRAN	GUPTA	NASTRAN
1	0.0925	0.0925	-0.5052	0.5052	1.0000	1.0000
2	0.3281	0.3281	-1.0000	1.0000	0.3358	0.3389
3	0.6470	0.6470	-0.5438	0.5438	-0.9656	-0.9724
4	1.0000	1.0000	0.7265	-0.7266	0.4162	0.4270

APPENDIX A

This Appendix presents detailed vibration mode data which were derived for the space station and solar array structural configurations considered in Phase 2. Analytical data are presented for the structural configurations in both Zero "G" and Artificial "G" environments. Explanations of the presented data can be found in Report Section 5. The data are presented in the following appendix sections:

- A. 1 Zero "G" Space Station Configuration page A-2
- A. 2 Zero "G" Roll-up Solar Array Configuration page A-14
- A. 3 Artificial "G" Space Station Configuration page A-36
- A. 4 Artificial "G" Roll-up Solar Array Configuration page A-65

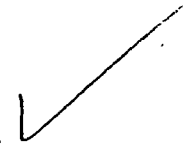
A.1 VIBRATION MODE DATA
ZERO "G" SPACE STATION CONFIGURATION

CONTENTS

<u>TABLE</u>		Page
A-1	Modal Data, Space Station, Zero "G" Configuration	A-3
A-2	Mass-Geometry Data	A-5
<u>FIGURE</u>		
A-1	Structural Model of Space Station	A-4
A-2 to A-9	Space Station Mode Shapes	A-6 to A-13

NOTE: Mode shapes shown are elastic mode shapes.
Mode 1 in Figure A-2 is the first elastic mode,
which corresponds to Mode 7 in Table A-1.

Table A-1, Modal Data, Space Station
(Zero G Configuration)



Mode	Frequency (Hz)	Generalized Mass (lb. -sec. ² /in.)
1	0.0	6.281594E 02
2	0.0	6.281594E 02
3	0.0	6.281594E 02
4	0.0	2.477313E 02
5	0.0	1.244991E 02
6	0.0	1.244991E 02
7	1.957377E 00	2.297717E 02
8	2.277407E 00	3.636589E 01
9	2.278777E 00	3.660057E 01
10	3.147397E 00	8.373204E 01
11	3.246078E 00	1.085563E 02
12	4.391578E 00	1.511882E 02
13	4.483892E 00	3.124590E 02
14	5.702710E 00	7.439223E 01
15	5.835457E 00	7.142155E 01
16	6.477457E 00	8.431511E 01
17	6.875389E 00	1.111700E 02
18	6.875395E 00	1.111700E 02
19	7.766384E 00	5.185711E 01
20	8.263874E 00	1.006247E 02
21	8.860953E 00	
22	8.935523E 00	
23	1.013241E 01	
24	1.130443E 01	
25	1.131781E 01	
26	1.475548E 01	
27	1.534728E 01	
28	1.958418E 01	
29	1.988515E 01	
30	2.277832E 01	
31	2.319455E 01	
32	2.339781E 01	
33	2.342052E 01	
34	2.490974E 01	
35	2.574709E 01	
36	2.658902E 01	
37	2.698954E 01	
38	2.752139E 01	
39	2.941022E 01	
40	2.942180E 01	
41	2.967250E 01	
42	2.967250E 01	
43	2.977394E 01	
44	2.984723E 01	
45	2.984726E 01	
46	2.992293E 01	
47	3.003922E 01	
48	3.005589E 01	
49	3.005735E 01	
50	3.027989E 01	

Structural Model Of Space Station

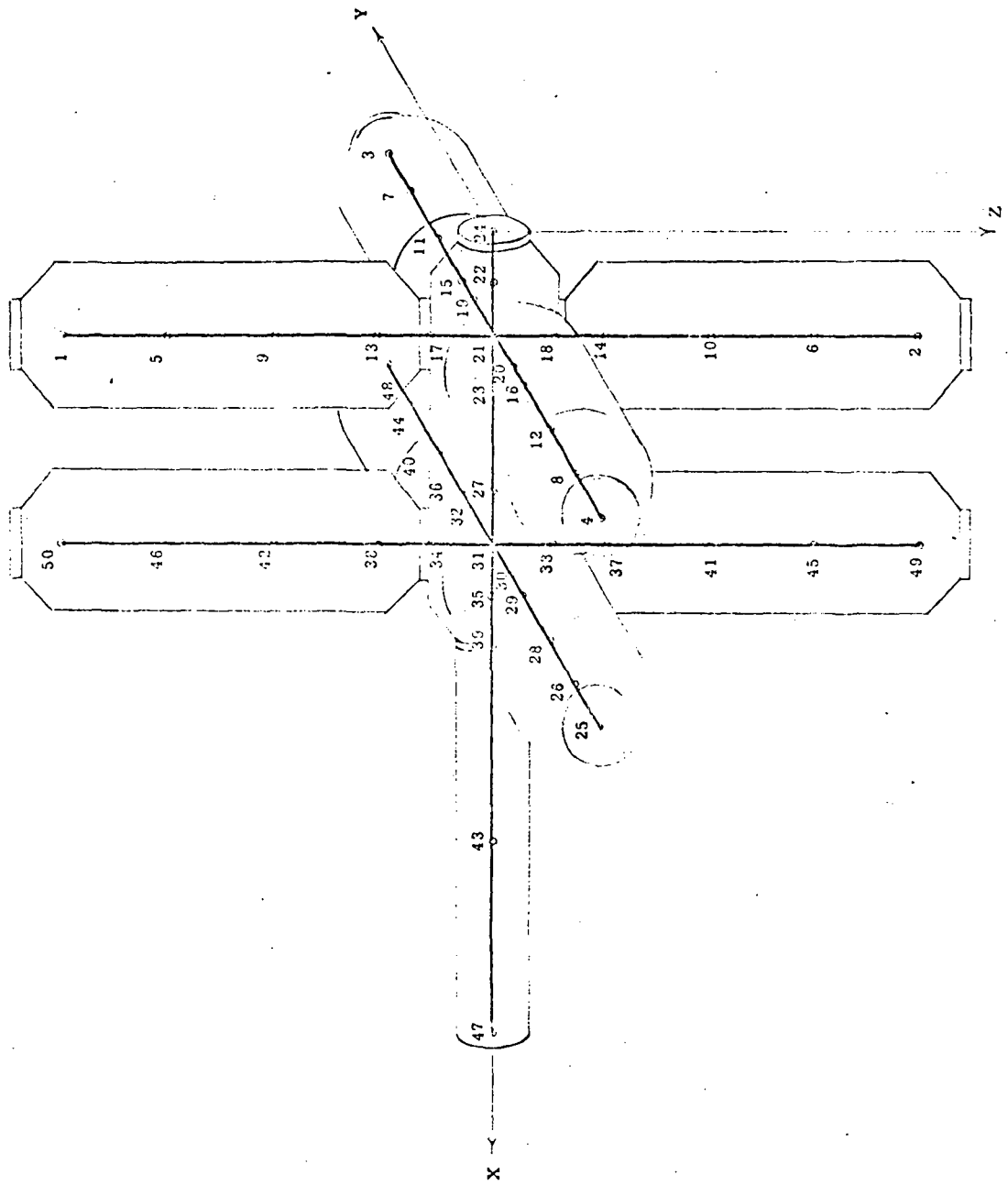


Figure A-1

TABLE A - 2
Listing of Mass - Geometry Data
Of Zero G Space Station

NODE NO.	MASS *	X	Y	Z
1	16.189	120.	0.	-492.
2	16.189	120.	0.	492.
3	16.189	120.	492.	0.
4	16.189	120.	-492.	0.
5	16.189	120.	0.	-372.
6	16.189	120.	0.	372.
7	16.189	120.	372.	0.
8	16.189	120.	-372.	0.
9	16.189	120.	0.	-252.
10	16.189	120.	0.	252.
11	16.189	120.	252.	0.
12	16.189	120.	-252.	0.
13	16.189	120.	0.	-132.
14	16.189	120.	0.	132.
15	16.189	120.	132.	0.
16	16.189	120.	-132.	0.
17	0.	120.	0.	-72.
18	0.	120.	0.	72.
19	0.	120.	72.	0.
20	0.	120.	-72.	0.
21	8.1	120.	0.	0.
22	8.1	60.	0.	0.
23	0.	180.	0.	0.
24	4.05	0.	0.	0.
25	16.189	360.	-492.	0.
26	16.189	360.	-372.	0.
27	12.15	300.	0.	0.
28	16.189	360.	-252.	0.
29	16.189	360.	-132.	0.
30	0.	360.	-72.	0.
31	8.1	360.	0.	0.
32	12.15	360.	72.	0.
33	0.	360.	0.	72.
34	0.	360.	0.	-72.
35	8.1	420.	0.	0.
36	16.189	360.	132.	0.
37	16.189	360.	0.	132.
38	16.189	360.	0.	-132.
39	12.7919	480.	0.	0.
40	16.189	360.	252.	0.
41	16.189	360.	0.	252.
42	16.189	360.	0.	-252.
43	17.4839	700.5	0.	0.
44	16.189	360.	372.	0.
45	16.189	360.	0.	372.
46	16.189	360.	0.	-372.
47	19.086	921.	0.	0.
48	16.189	360.	492.	0.
49	16.189	360.	0.	492.
50	16.189	360.	0.	-492.

* - Mass units are lb-sec²/in.

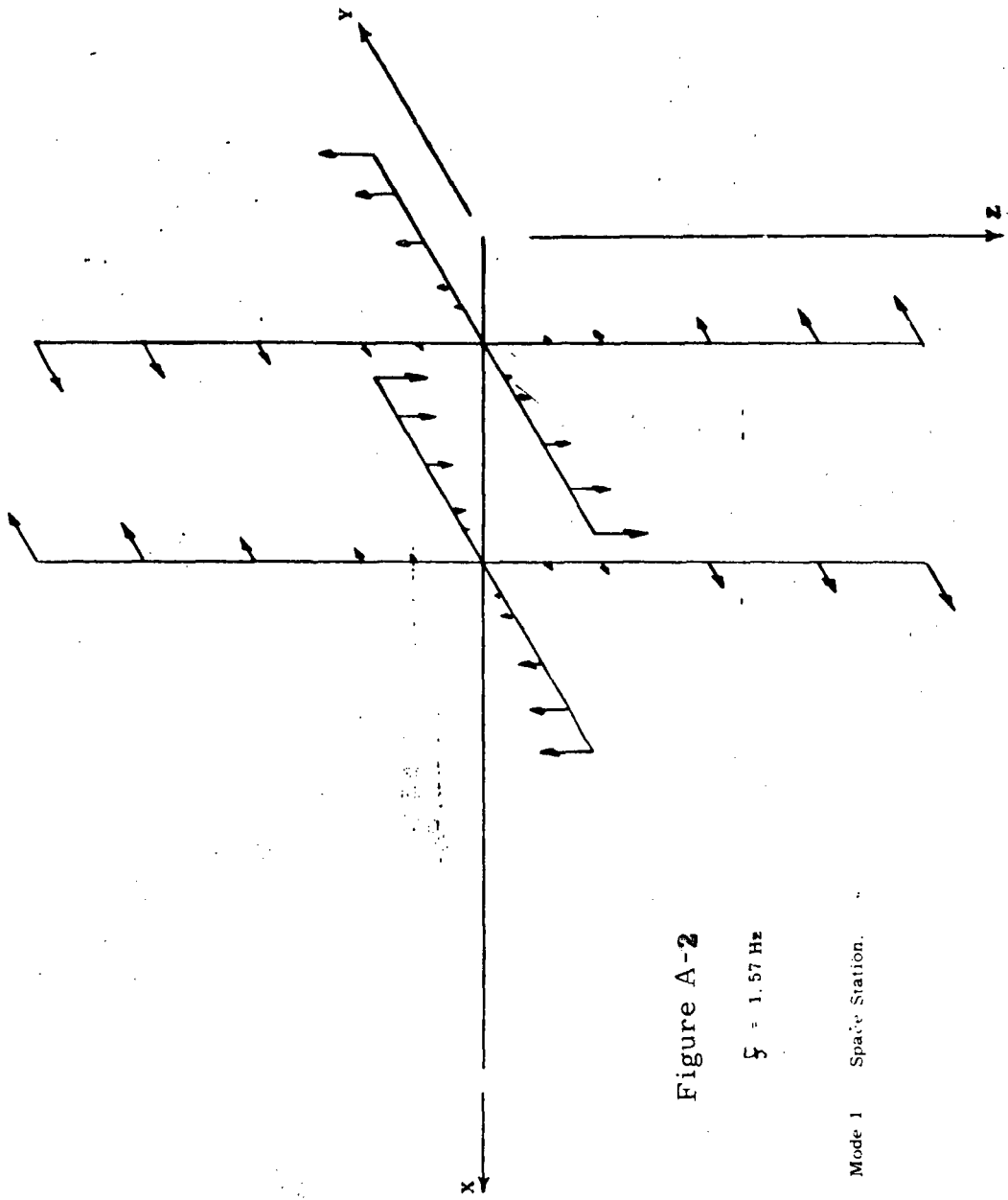


Figure A-2

$f = 1.57 \text{ Hz}$

Mode 1 Space Station.

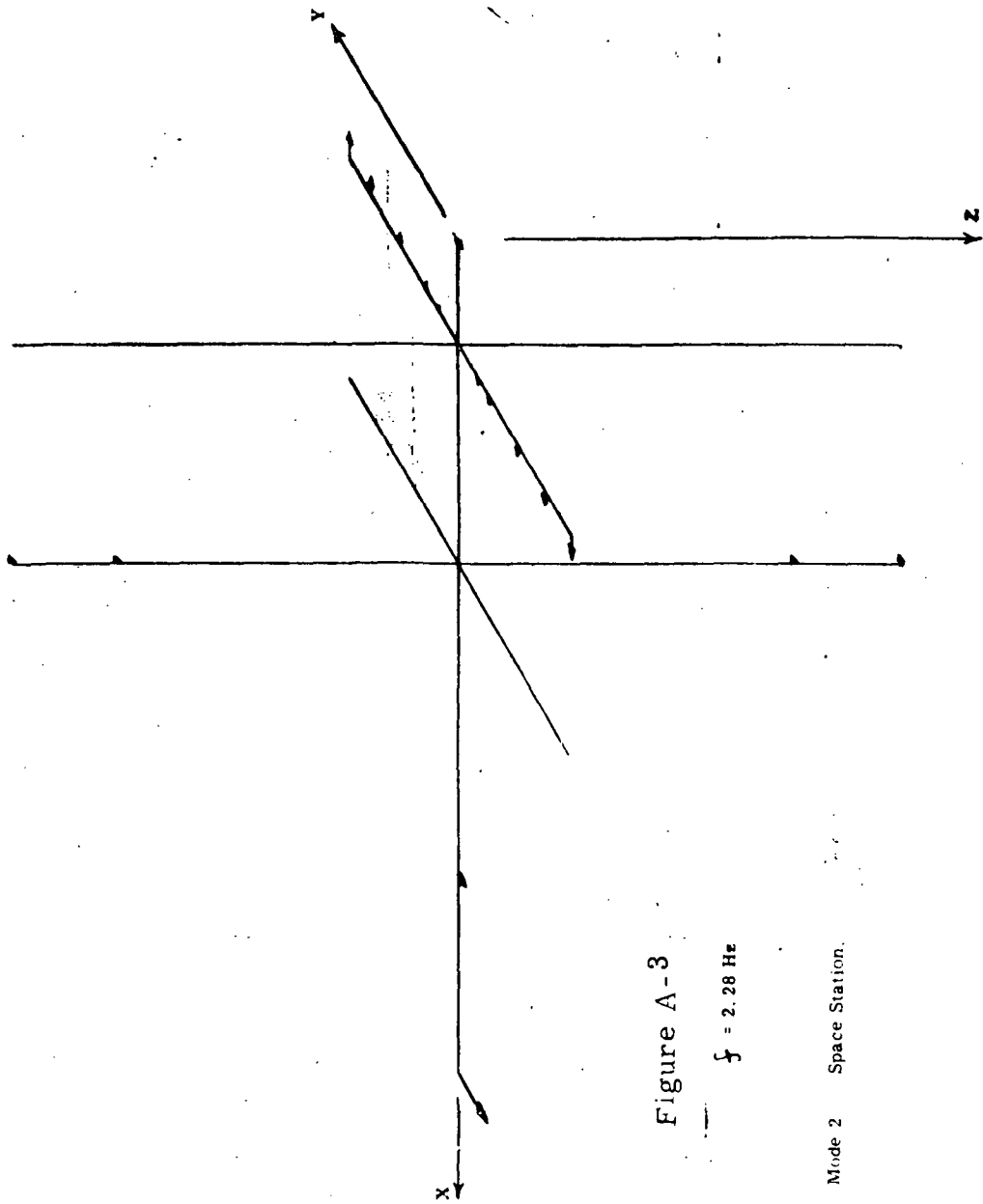


Figure A-3

$$f = 2.28 \text{ Hz}$$

Mode 2 Space Station.

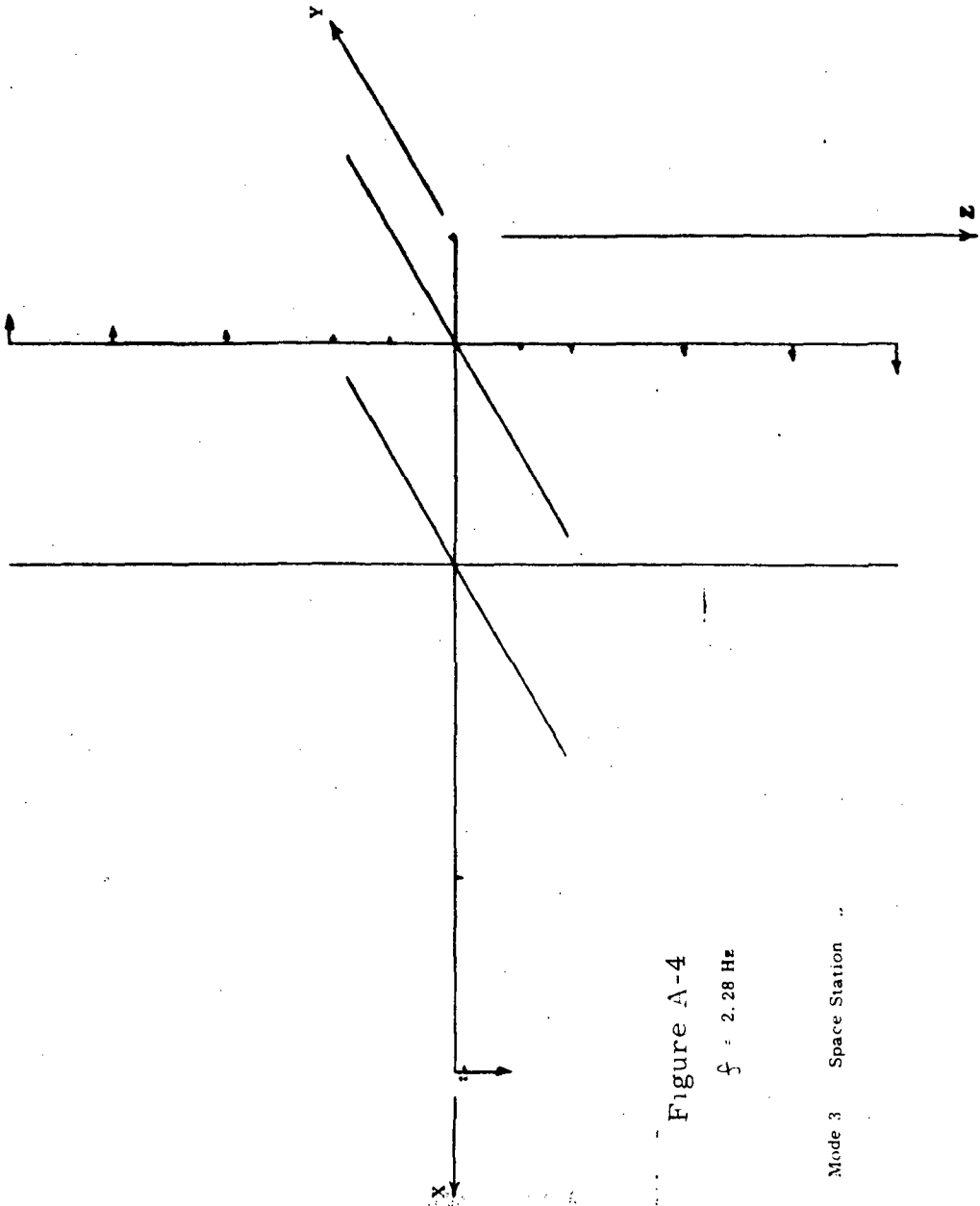


Figure A-4

$f = 2.28 \text{ Hz}$

Mode 3 Space Station

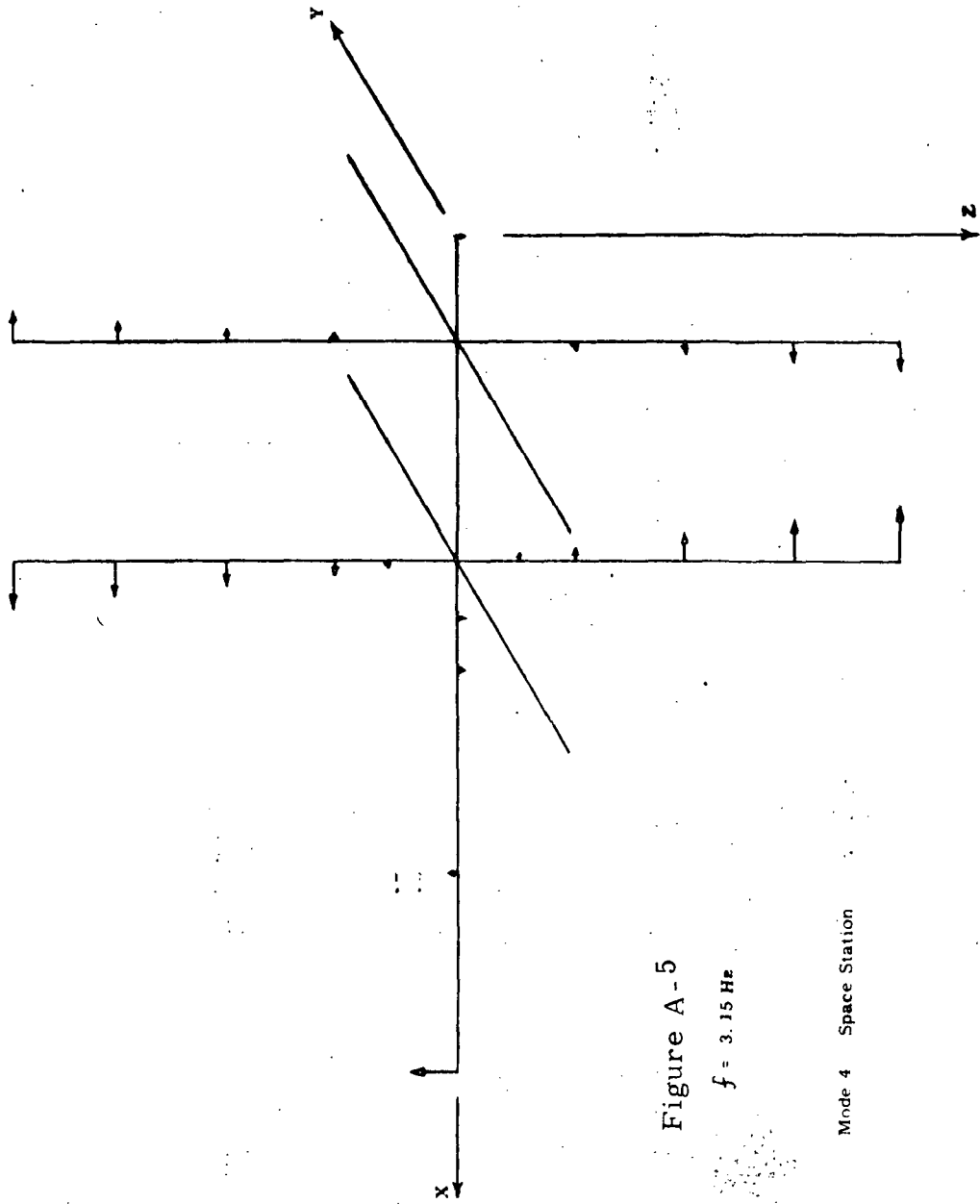


Figure A-5

$f = 3.15 \text{ Hz}$

Mode 4 Space Station

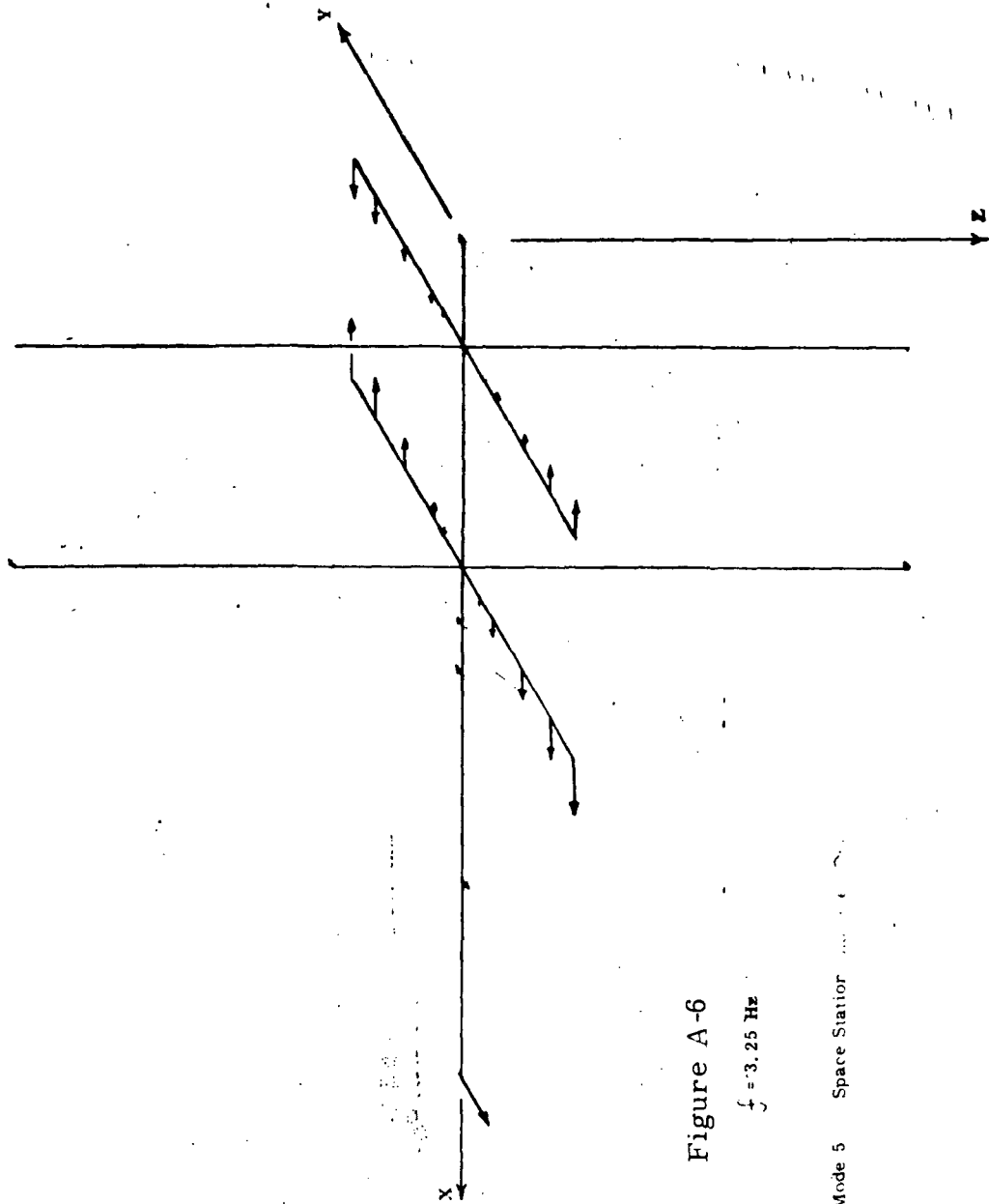


Figure A-6

$f = 3.25 \text{ Hz}$

Mode 5 Space Station

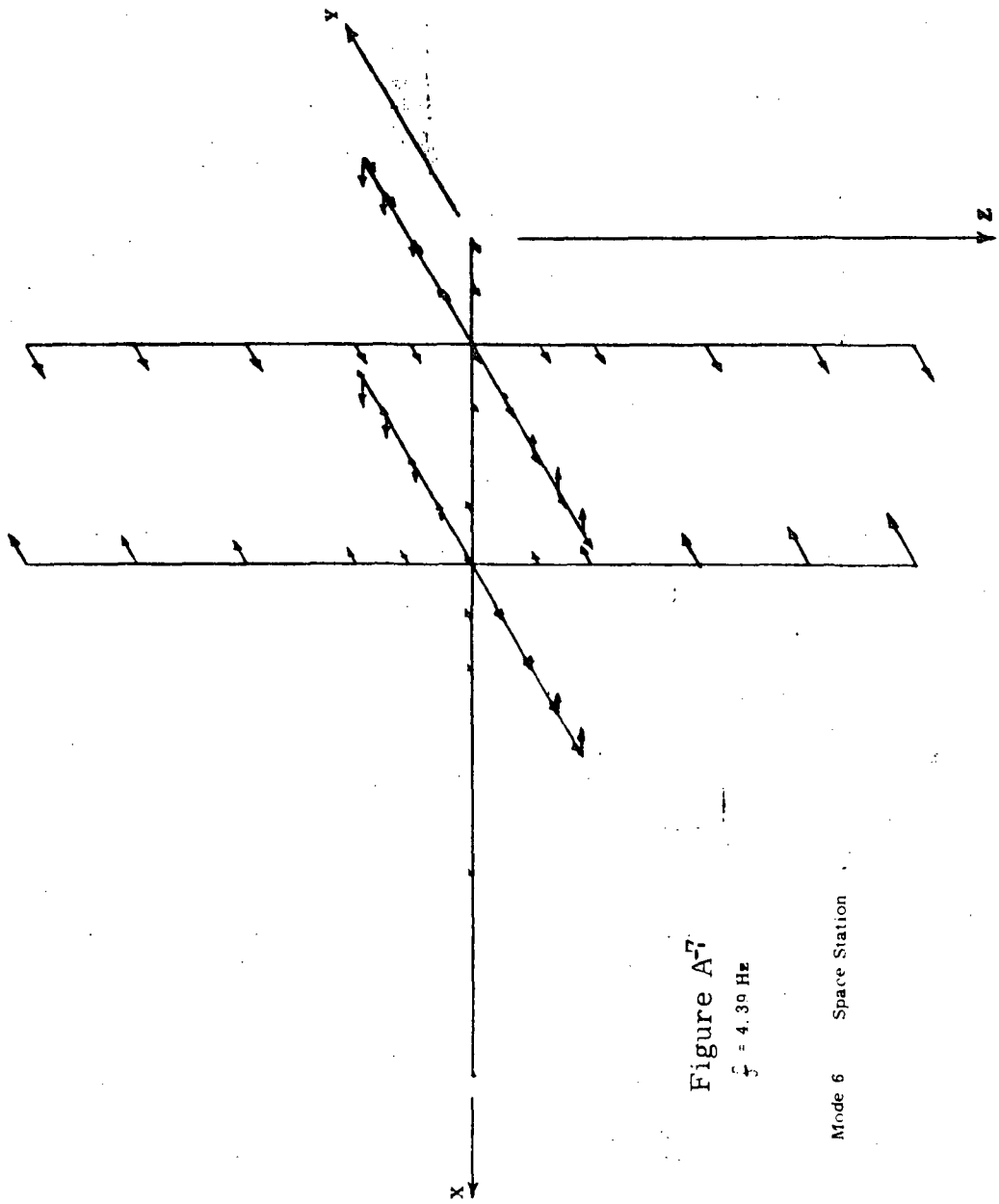


Figure A⁷

$f = 4.39 \text{ Hz}$

Mode 6 Space Station

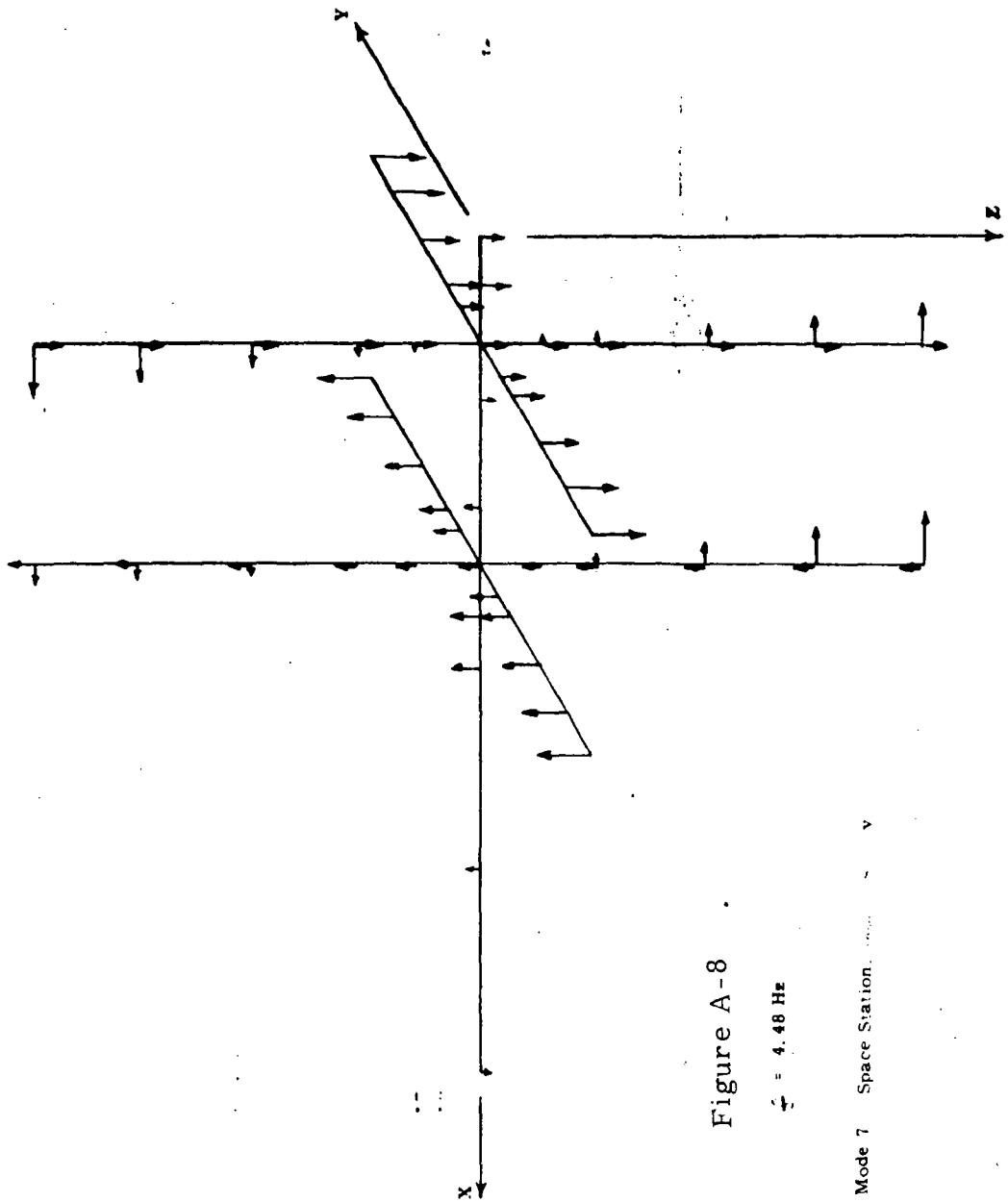


Figure A-8

$f = 4.48 \text{ Hz}$

Mode 7 Space Station

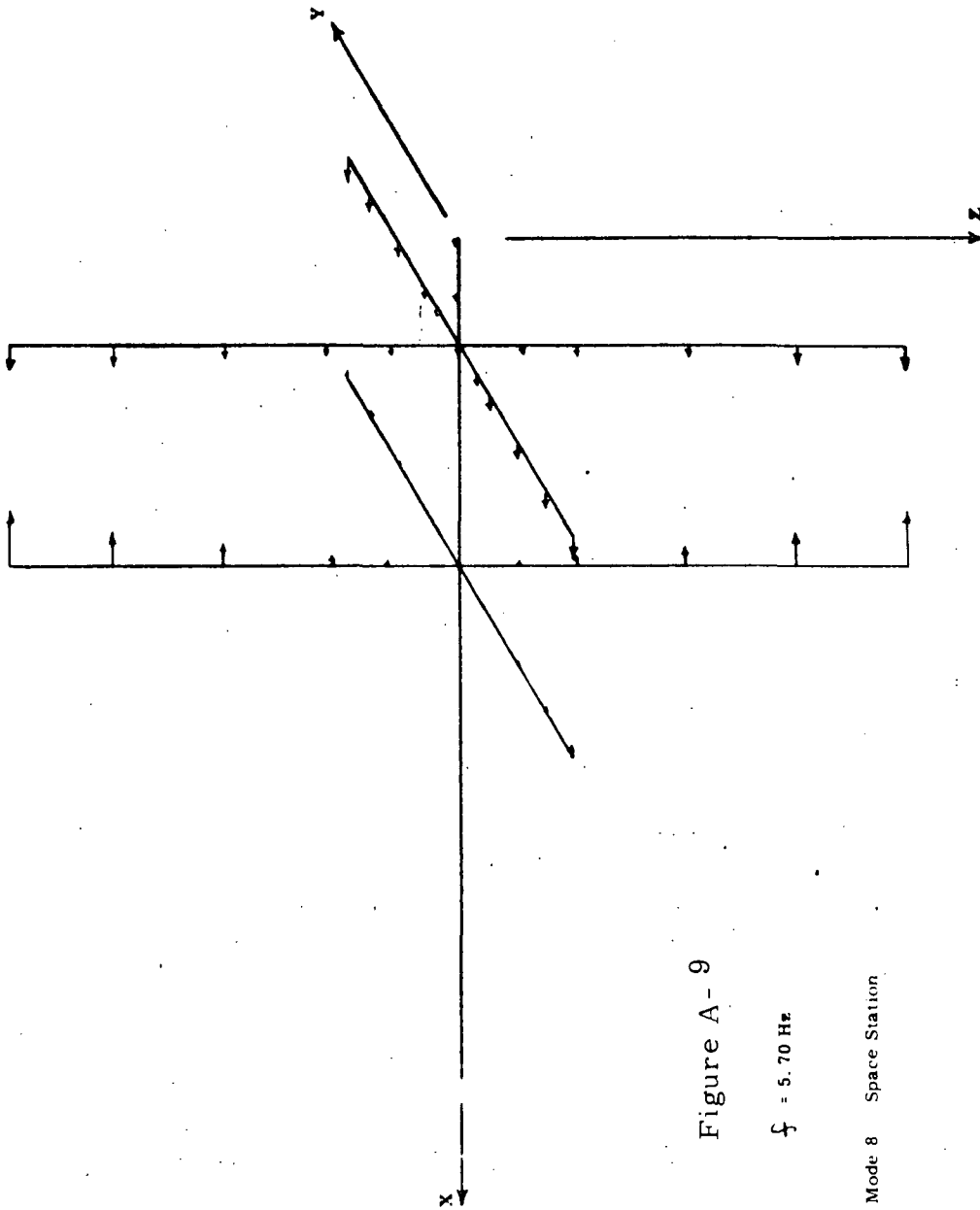


Figure A-9

$f = 5.70 \text{ Hz}$

Mode 8 Space Station

A.2 VIBRATION MODE DATA
ZERO "G" ROLLUP SOLAR ARRAY CONFIGURATION

CONTENTS

<u>TABLE</u>		<u>PAGE</u>
Table A-3	Modal Data, Solar Array Inplane, Antisymmetric	A-15
Table A-4	Modal Data, Solar Array Inplane, Symmetric	A-16
Table A-5	Modal Data, Solar Array Out-of-plane, Symmetric	A-17
Table A-6	Modal Data, Solar Array Out-of-plane, Antisymmetric	A-18
Table A-7	Mass - Geometry Data	A-20
<u>FIGURE</u>		
A-10	Structural Model	A-19
A-11 to A-14	In-plane Symmetric Mode Shapes	A-21, 24
A-15 to A-19	In-plane Antisymmetric Mode Shape	A-25, 29
A-20 to A-22	Out-of-plane Symmetric Mode Shapes	A-30, 32
A-23 to A-25	Out-of-plane Antisymmetric Mode Shapes	A-33, 35

Table A-3, Modal Data, Solar Array, Inplane, Antisymmetric, Zero G

Mode	Frequency (Hz)	Generalized Mass (lb. - sec. ² /in.)
1	9.737372E-02	1.350713E 00
2	1.035253E-01	6.274160E-01
3	1.035253E-01	4.957223E-01
4	1.035253E-01	6.000971E-01
5	1.035253E-01	6.934807E-01
6	1.687441E-01	1.409378E 00
7	1.999952E-01	9.246593E-01
8	1.999955E-01	8.365394E-01
9	1.999955E-01	9.231566E-01
10	1.999955E-01	8.366065E-01
11	2.684186E-01	1.456272E 00
12	2.628382E-01	6.936469E-01
13	2.628383E-01	6.273965E-01
14	2.628383E-01	6.923639E-01
15	2.628383E-01	6.274614E-01
16	3.237091E-01	1.832071E 00
17	3.464023E-01	9.248542E-01
18	3.464025E-01	8.365350E-01
19	3.464025E-01	9.231666E-01
20	3.464025E-01	8.366050E-01
21	3.612237E-01	1.765825E 00
22	3.663618E-01	6.936590E-01
23	3.663618E-01	4.845103E-01
24	3.663618E-01	5.731879E-01
25	3.663618E-01	5.045668E-01
26	3.891559E-01	1.503639E 00
27	5.941957E-01	8.893200E-01
28	2.523427E 00	1.298081E-01
29	3.197823E 00	8.005888E-01
30	3.495915E 00	7.669923E-01
31	3.523190E 00	6.305750E-01
32	3.528254E 00	6.607162E-01
33	4.353931E 00	1.495981E-01
34	6.507502E 00	4.571142E-01
35	6.931433E 00	2.305118E-01
36	9.297757E 00	8.740416E-01
37	1.008611E 01	7.663497E-01
38	1.013479E 01	6.293153E-01
39	1.018728E 01	6.567687E-01
40	1.240661E 01	2.131746E-01
41	1.236052E 01	4.911602E-01
42	1.496898E 01	7.352544E-01
43	1.592579E 01	7.507545E-01
44	1.600150E 01	6.193690E-01
45	1.601517E 01	6.539617E-01
46	1.772331E 01	1.098866E 00
47	1.834437E 01	4.004465E-01
48	1.965033E 01	7.068785E-01
49	2.051042E 01	7.531123E-01
50	2.056432E 01	6.381914E-01

Table A-4, Modal Data, Solar Array, Inplane, Symmetric, Zero G

Mode	Frequency (Hz)	Generalized Mass (lb.-sec. ² /in.)
1	1.035250E-01	6.471123E-01
2	1.035251E-01	6.662618E-01
3	1.035252E-01	7.732370E-01
4	1.035253E-01	3.702315E-01
5	1.035319E-01	5.658236E-01
6	1.999946E-01	8.627804E-01
7	1.999952E-01	8.883575E-01
8	1.999952E-01	6.197678E-01
9	1.999952E-01	8.961747E-01
10	1.999955E-01	6.240916E-01
11	2.828338E-01	6.471033E-01
12	2.828356E-01	4.734812E-01
13	2.828363E-01	6.536539E-01
14	2.828363E-01	6.072990E-01
15	2.828363E-01	6.702858E-01
16	3.464020E-01	8.628003E-01
17	3.464025E-01	1.045781E 00
18	3.464025E-01	7.491596E-01
19	3.464026E-01	6.347124E-01
20	3.464026E-01	8.882823E-01
21	3.863617E-01	6.470776E-01
22	3.863618E-01	7.813119E-01
23	3.863618E-01	5.618995E-01
24	3.863618E-01	4.768397E-01
25	3.863618E-01	6.663127E-01
26	1.354412E 00	7.051653E-01
27	3.278625E 00	7.702565E-01
28	3.490318E 00	6.074610E-01
29	3.519975E 00	5.617070E-01
30	3.527668E 00	6.061066E-01
31	6.072317E 00	1.035868E-01
32	6.882595E 00	4.122061E-01
33	9.511100E 00	8.556120E-01
34	1.007151E 01	6.032084E-01
35	1.014669E 01	5.632485E-01
36	1.016592E 01	6.006349E-01
37	1.280494E 01	4.343082E-01
38	1.518822E 01	7.910441E-01
39	1.590481E 01	5.698990E-01
40	1.599190E 01	5.694355E-01
41	1.601352E 01	5.922735E-01
42	1.783336E 01	5.283089E-01
43	1.987668E 01	8.288176E-01
44	2.049608E 01	5.615127E-01
45	2.055783E 01	5.868033E-01
46	2.057259E 01	5.877689E-01
47	2.154462E 01	4.647811E-01
48	2.300127E 01	1.731334E-01
49	2.315868E 01	6.691886E-01
50	2.344269E 01	5.389919E-01



Table A-5 , Modal Data, Solar Array, Out of Plane, Symmetric, Zero G

Mode	Frequency (Hz)	Generalized Mass (lb. -sec. ² /in.)
1	9.244967E-02	1.363355E 00
2	1.225755E-01	4.851304E-01
3	1.227098E-01	5.956523E-01
4	1.227105E-01	5.221769E-01
5	1.227164E-01	5.439427E-01
6	1.866132E-01	1.301536E 00
7	2.335492E-01	4.738768E-01
8	2.338332E-01	6.763698E-01
9	2.338462E-01	5.873230E-01
10	2.338475E-01	5.149174E-01
11	2.723567E-01	1.215317E 00
12	3.224205E-01	4.755982E-01
13	3.226471E-01	6.820915E-01
14	3.226523E-01	5.924900E-01
15	3.226532E-01	5.194927E-01
16	3.411543E-01	1.341820E 00
17	3.800172E-01	4.683110E-01
18	3.800961E-01	6.776543E-01
19	3.800981E-01	5.888550E-01
20	3.800984E-01	5.163653E-01
21	3.848683E-01	1.156975E 00
22	8.345175E-01	1.581258E-01
23	1.016372E 00	2.447064E-01
24	1.021062E 00	2.410409E-01
25	1.021616E 00	1.859574E-01
26	1.021757E 00	2.290614E-01
27	1.619896E 00	1.406697E-01
28	2.273774E 00	1.105896E-01
29	3.660591E 00	1.346217E-01
30	5.304781E 00	1.555309E-01
31	1.037197E 01	1.700534E-01
32	1.150986E 01	2.381182E-01
33	1.742712E 01	1.640180E-01
34	2.036168E 01	2.053636E-01
35	2.451262E 01	1.479549E-01
36	3.032007E 01	2.375647E-01
37	5.002257E 01	1.682047E-01
38	5.146941E 01	1.800458E-01
39	7.553278E 01	1.761178E-01
40	9.195334E 01	1.597598E-01
41	1.138354E 02	6.968695E-02
42	1.408519E 02	9.482276E-02

Table A-6, Modal Data, Solar Array, Out of Plane, Antisymmetric, Zero G

Mode	Frequency (Hz)	Generalized Mass (lb.-sec. ² /in.)
1	6.399534E-02	6.094149E-01
2	1.225812E-01	6.959703E-01
3	1.227031E-01	7.329165E-01
4	1.227102E-01	6.202382E-01
5	1.227106E-01	6.423883E-01
6	1.667802E-01	5.472140E-01
7	2.338042E-01	6.814334E-01
8	2.338456E-01	7.183616E-01
9	2.338476E-01	6.182398E-01
10	2.338432E-01	6.334028E-01
11	2.413185E-01	6.890857E-01
12	3.084885E-01	7.381489E-01
13	3.225234E-01	6.943066E-01
14	3.226912E-01	7.345921E-01
15	3.226535E-01	6.107412E-01
16	3.226538E-01	6.392808E-01
17	3.531117E-01	5.835944E-01
18	3.800878E-01	6.890357E-01
19	3.800975E-01	7.275511E-01
20	3.800982E-01	6.101235E-01
21	3.800984E-01	6.354181E-01
22	3.800288E-01	5.942361E-01
23	1.011542E 00	2.524251E-01
24	1.020890E 00	2.669843E-01
25	1.021528E 00	2.242702E-01
26	1.021753E 00	2.333972E-01
27	1.584146E 00	2.103242E-01
28	8.225140E 00	1.584330E-01
29	1.054482E 01	1.610069E-01
30	2.614871E 01	2.037958E-01
31	3.402454E 01	2.118104E-01
32	5.335814E 01	1.683161E-01
33	6.955161E 01	1.759176E-01
34	8.293798E 01	1.814231E-01
35	1.082325E 02	1.893509E-01

TABLE A-7

Mass - Geometry Data
Of Zero G Solar Array

NODE NO.	WEIGHT(lbs.)	X	Y	Z
1	21.48	1056.	347.	0.
2	32.3	888.	347.	0.
3	26.06	1056.	275.	0.
4	32.3	720.	347.	0.
5	32.3	888.	275.	0.
6	26.06	1056.	203.	0.
7	32.3	552.	347.	0.
8	32.3	720.	275.	0.
9	32.3	888.	203.	0.
10	26.06	1056.	131.	0.
11	32.3	384.	347.	0.
12	32.3	552.	275.	0.
13	32.3	720.	203.	0.
14	32.3	888.	131.	0.
15	25.32	1056.	59.	0.
16	32.3	216.	347.	0.
17	32.3	384.	275.	0.
18	32.3	552.	203.	0.
19	32.3	720.	131.	0.
20	32.3	888.	59.	0.
21	12.74	1056.	0.	0.
22	20.84	48.	347.	0.
23	32.3	216.	275.	0.
24	32.3	384.	203.	0.
25	32.3	552.	131.	0.
26	32.3	720.	59.	0.
27	17.81	888.	0.	0.
28	24.98	48.	275.	0.
29	32.3	216.	203.	0.
30	32.3	384.	131.	0.
31	32.3	552.	59.	0.
32	17.81	720.	0.	0.
33	24.98	48.	203.	0.
34	32.3	216.	131.	0.
35	32.3	384.	59.	0.
36	17.81	552.	0.	0.
37	24.98	48.	131.	0.
38	32.3	216.	59.	0.
39	17.81	384.	0.	0.
40	24.23	48.	59.	0.
41	17.31	216.	0.	0.
42	12.30	48.	0.	0.
43	0.	0.	0.	0.

NOTE: Weights along the boom (Y = 0.) are one half the actual weight.

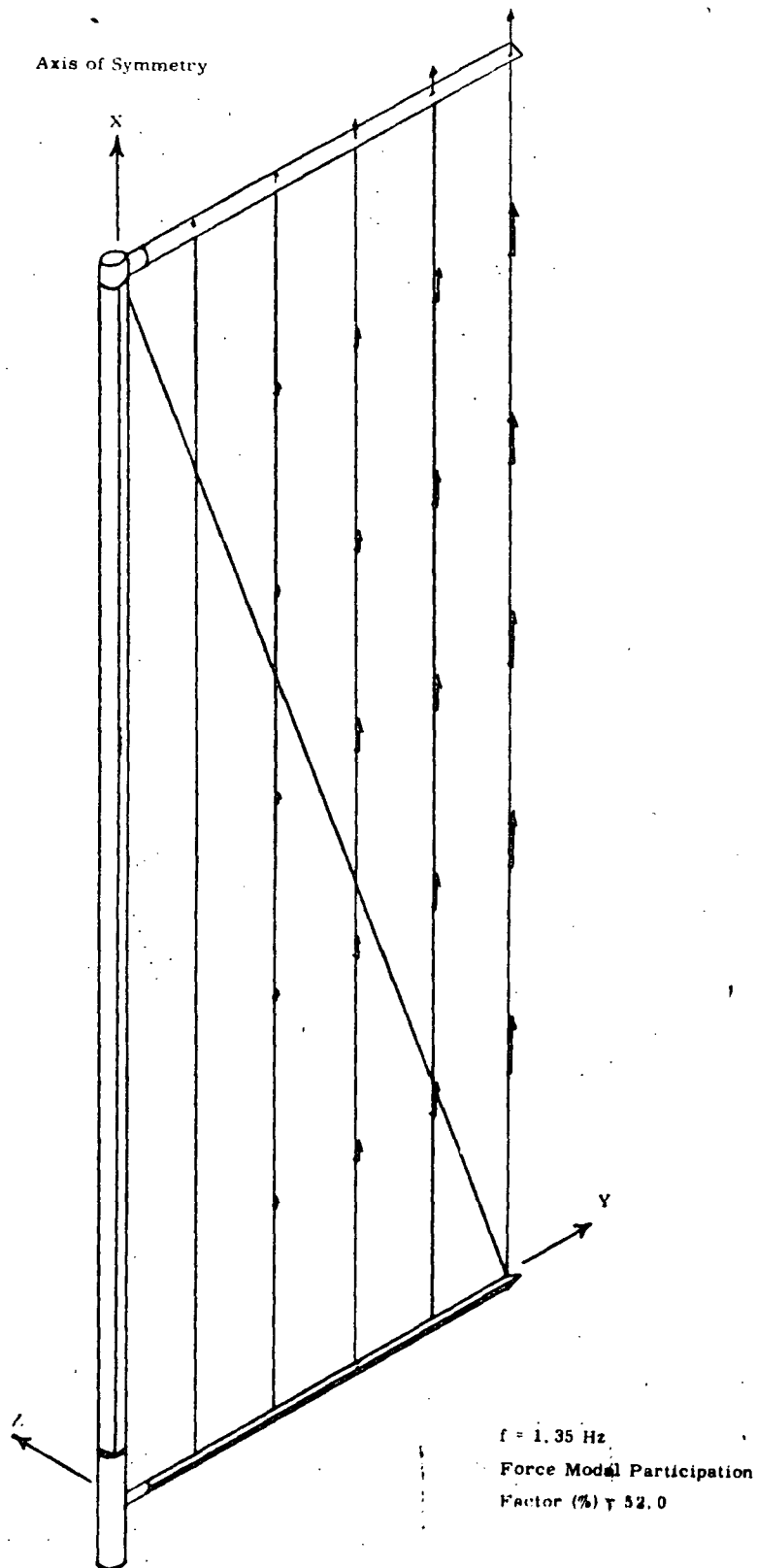


Figure A-11

Mode 26 String Solar Array, In Plane Symmetric

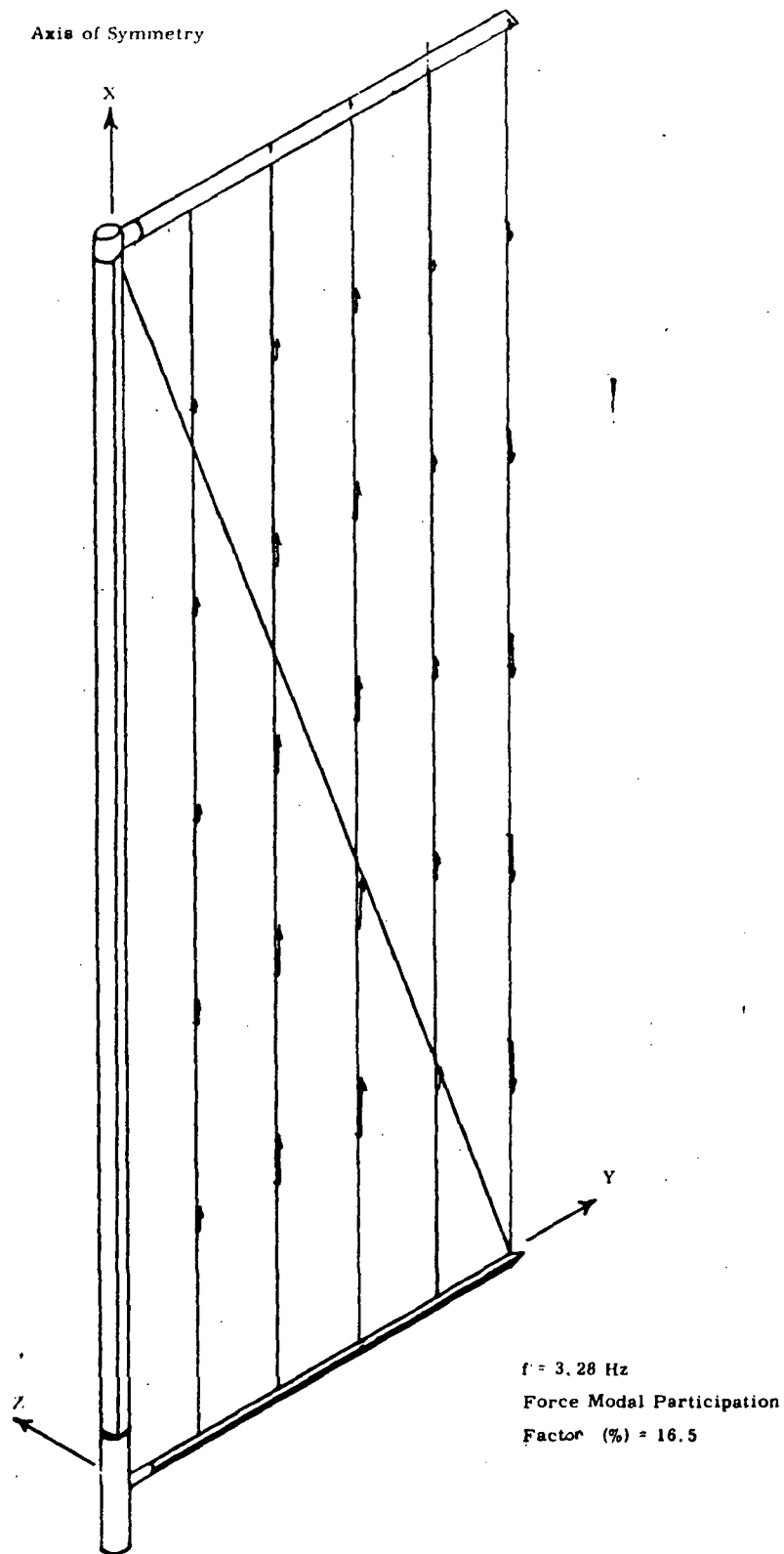


Figure A-12

Mode 27 String Solar Array, In Plane Symmetric

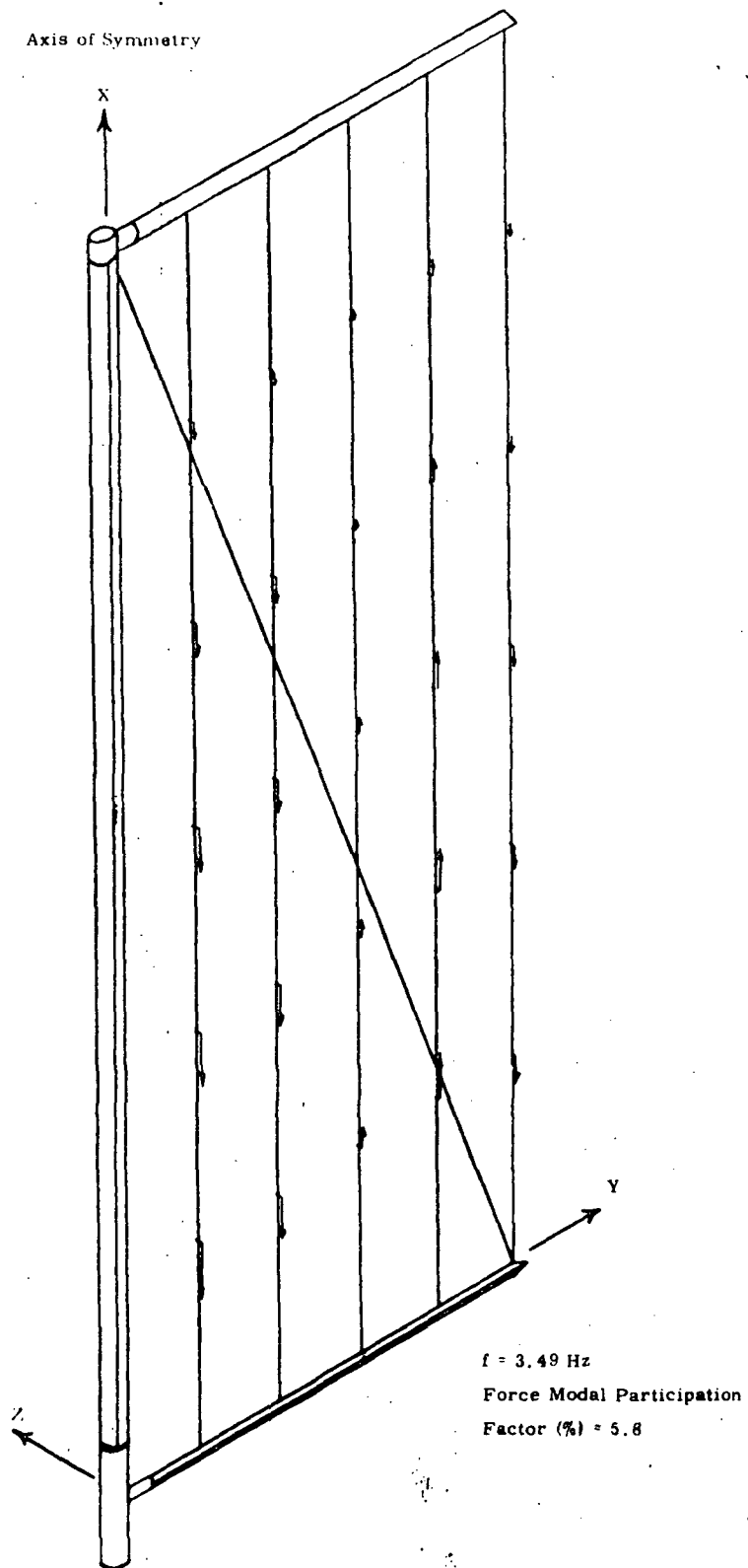


Figure A-13 Mode 28 String Solar Array, In-Plane Symmetric

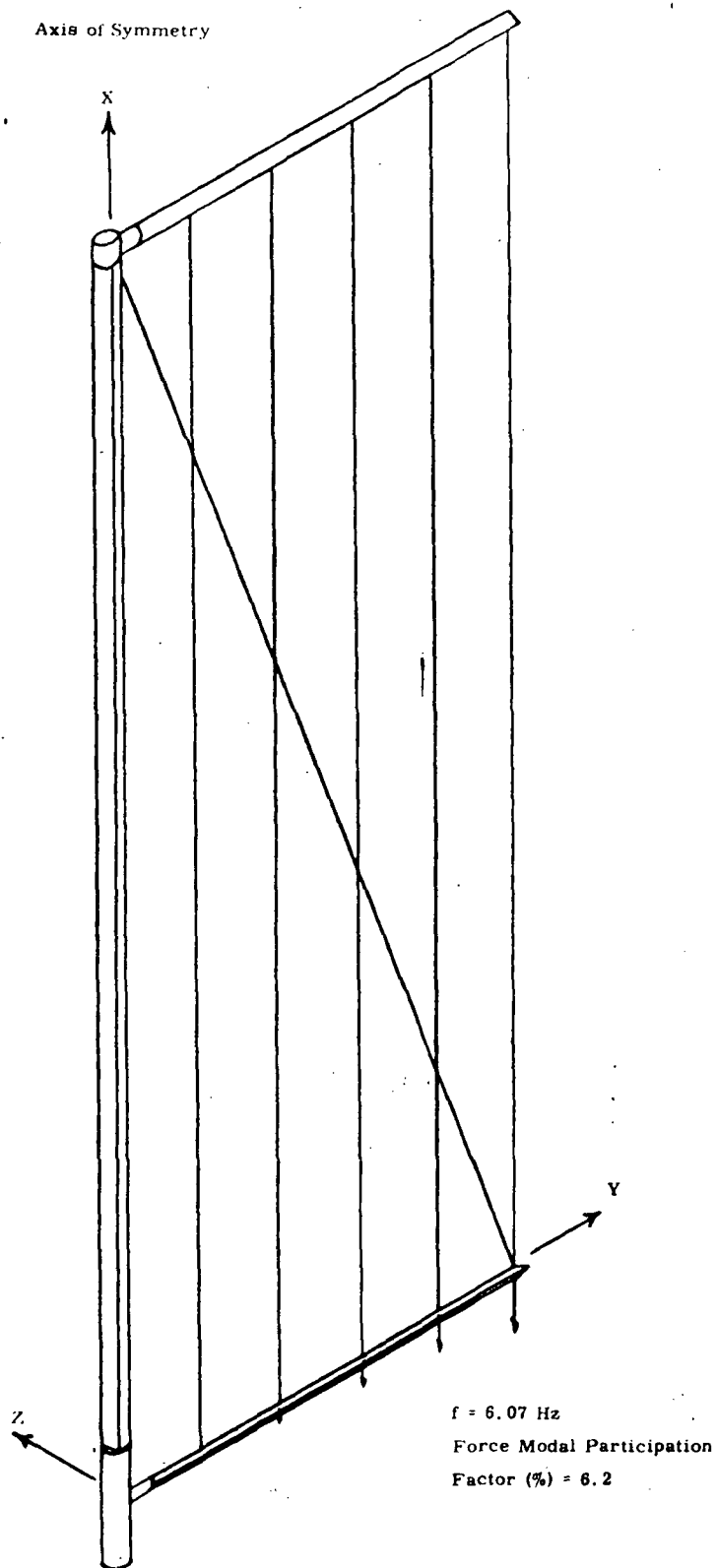


Figure A-14 Mode 31 Solar Array, In Plane Symmetric

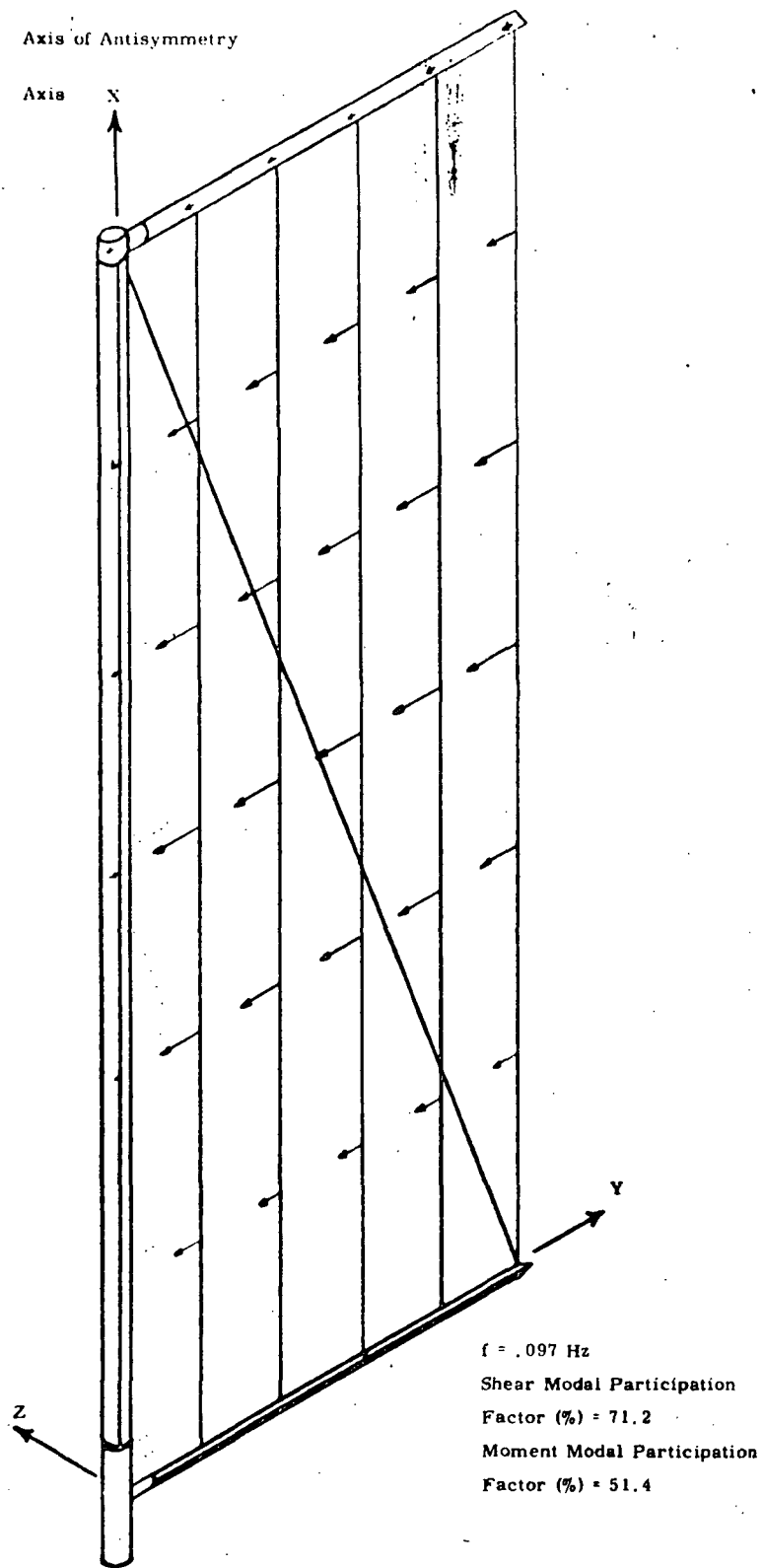


Figure A-15 Mode 1 String Solar Array, In Plane Antisymmetric

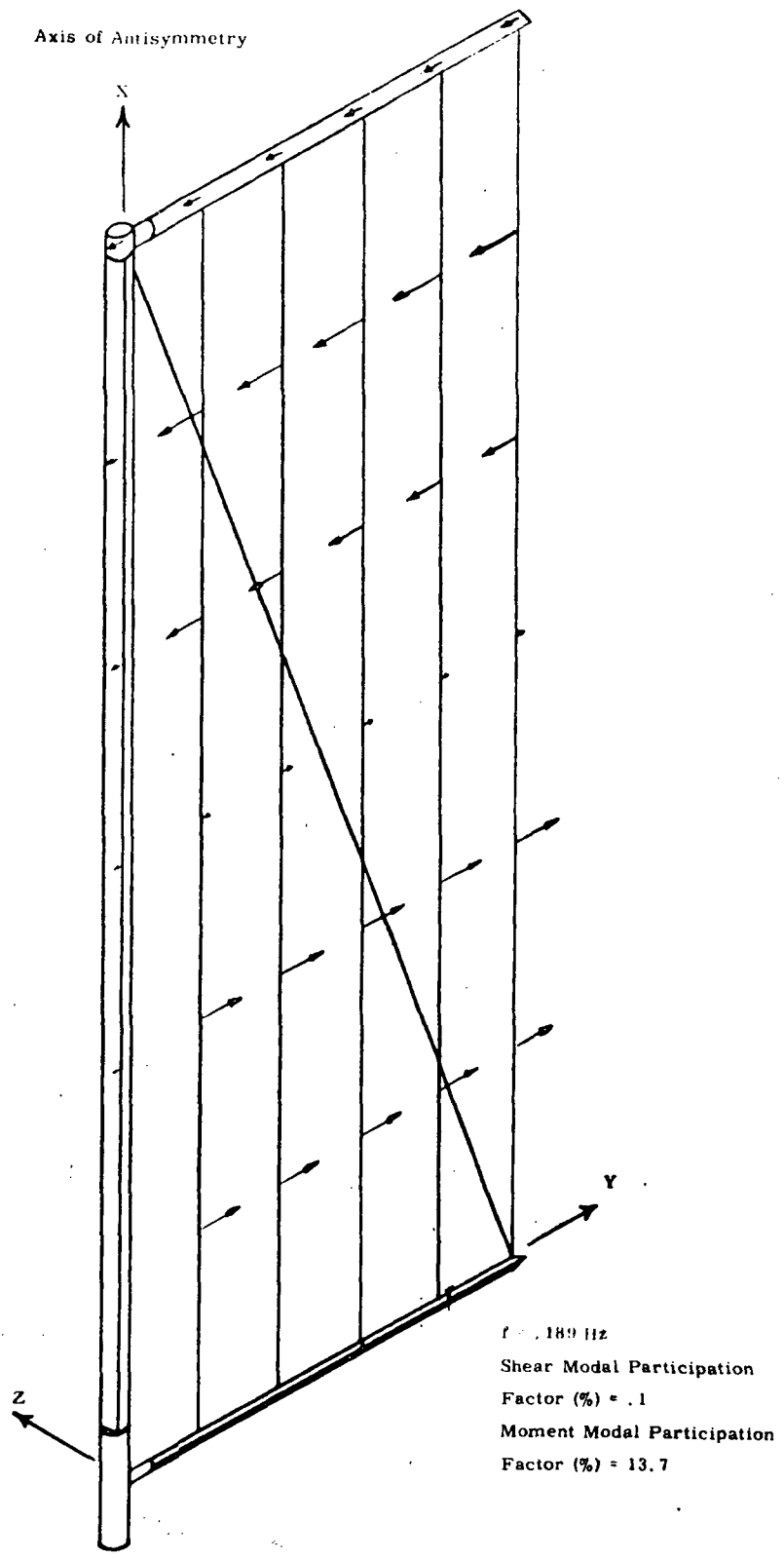


Figure A-16

Mode 6 String Solar Array, In Plane Antisymmetric

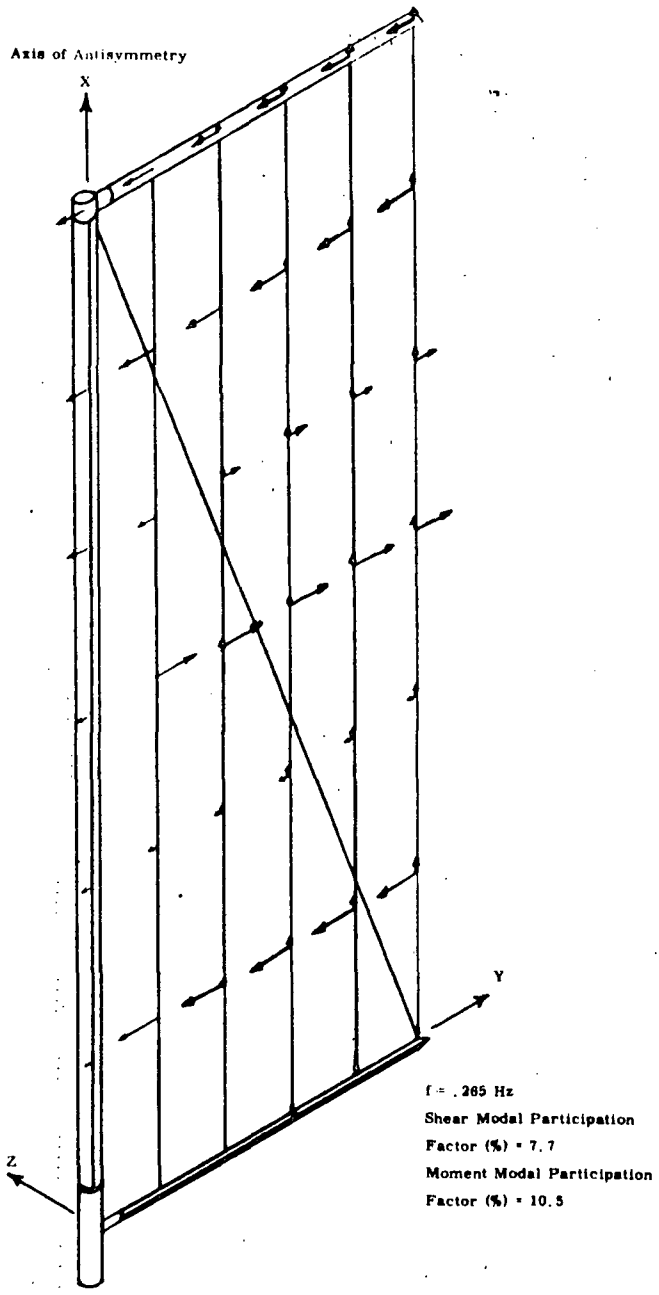


Figure A-17

Mode 11 String Solar Array, In Plane Antisymmetric

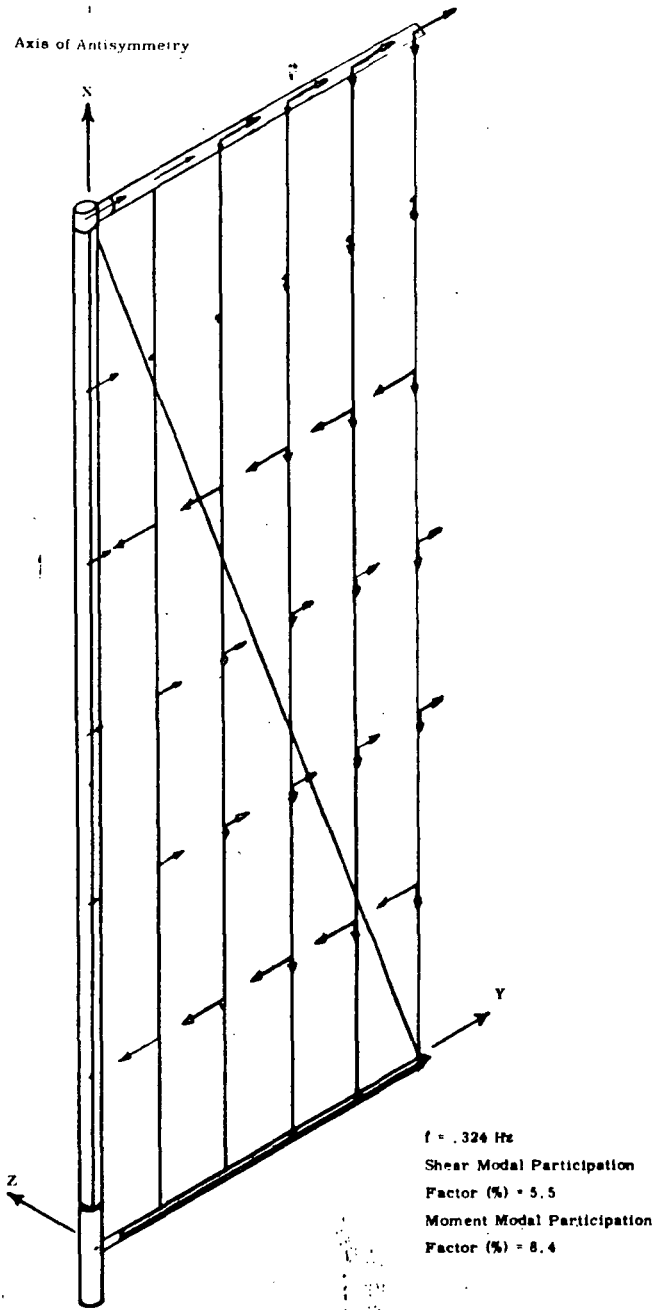


Figure A-18

Mode 16 String Solar Array, In Plane Antisymmetric

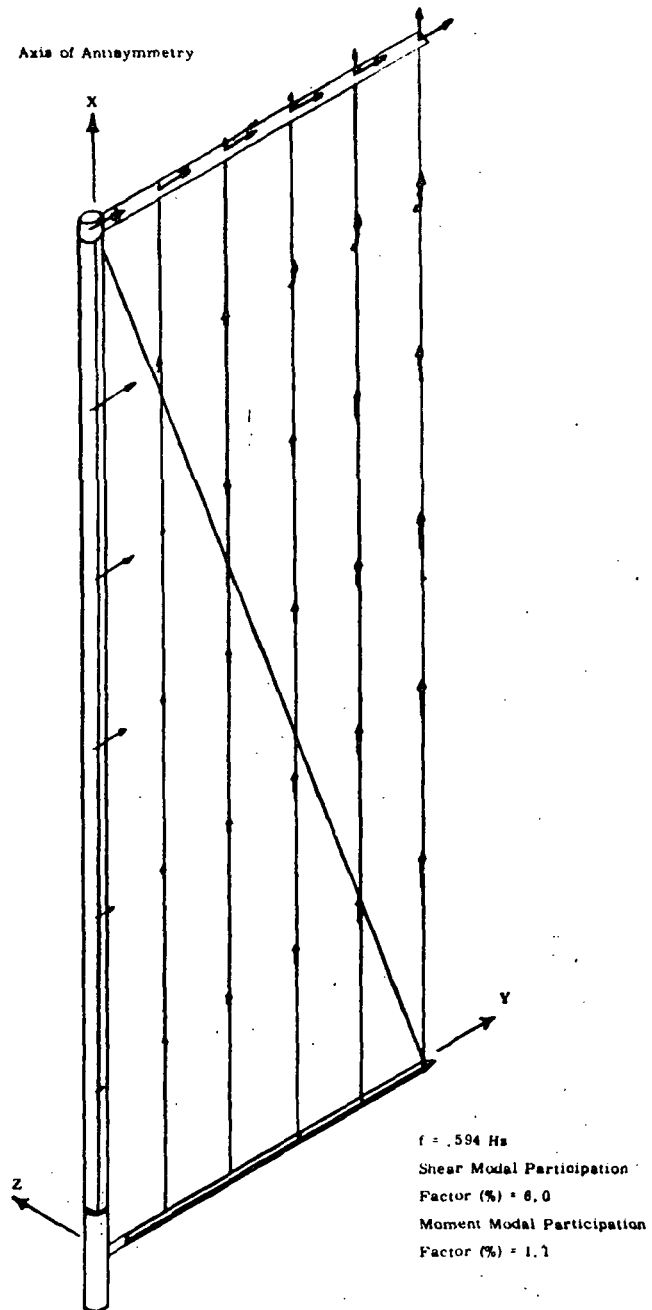


Figure A-19

Mode 27 String Solar Array, In Plane Antisymmetric

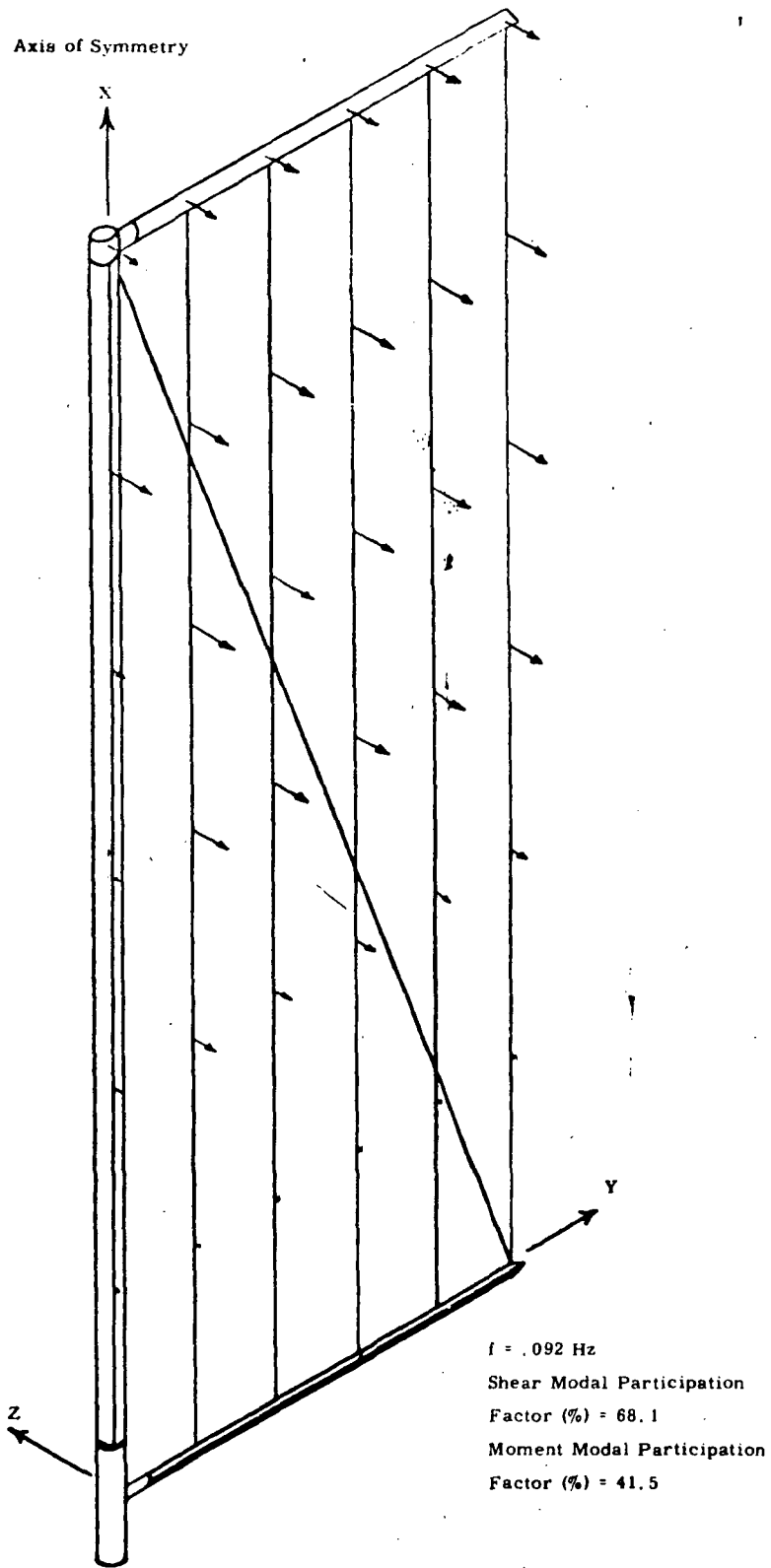


Figure A-20 Mode 1 String Solar Array, Out of Plane Symmetric

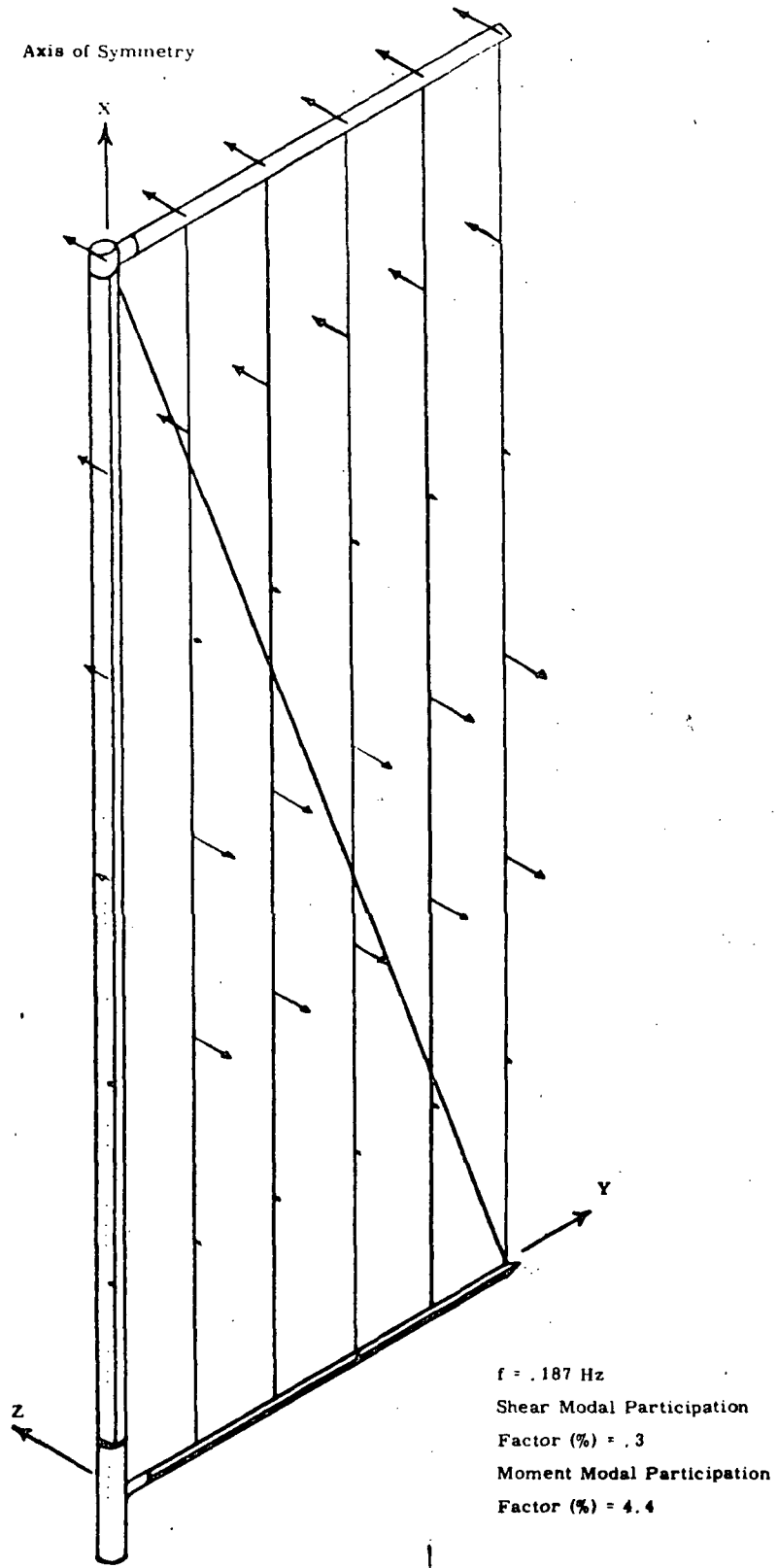


Figure A-21 Mode 6 String Solar Array, Out of Plane Symmetric

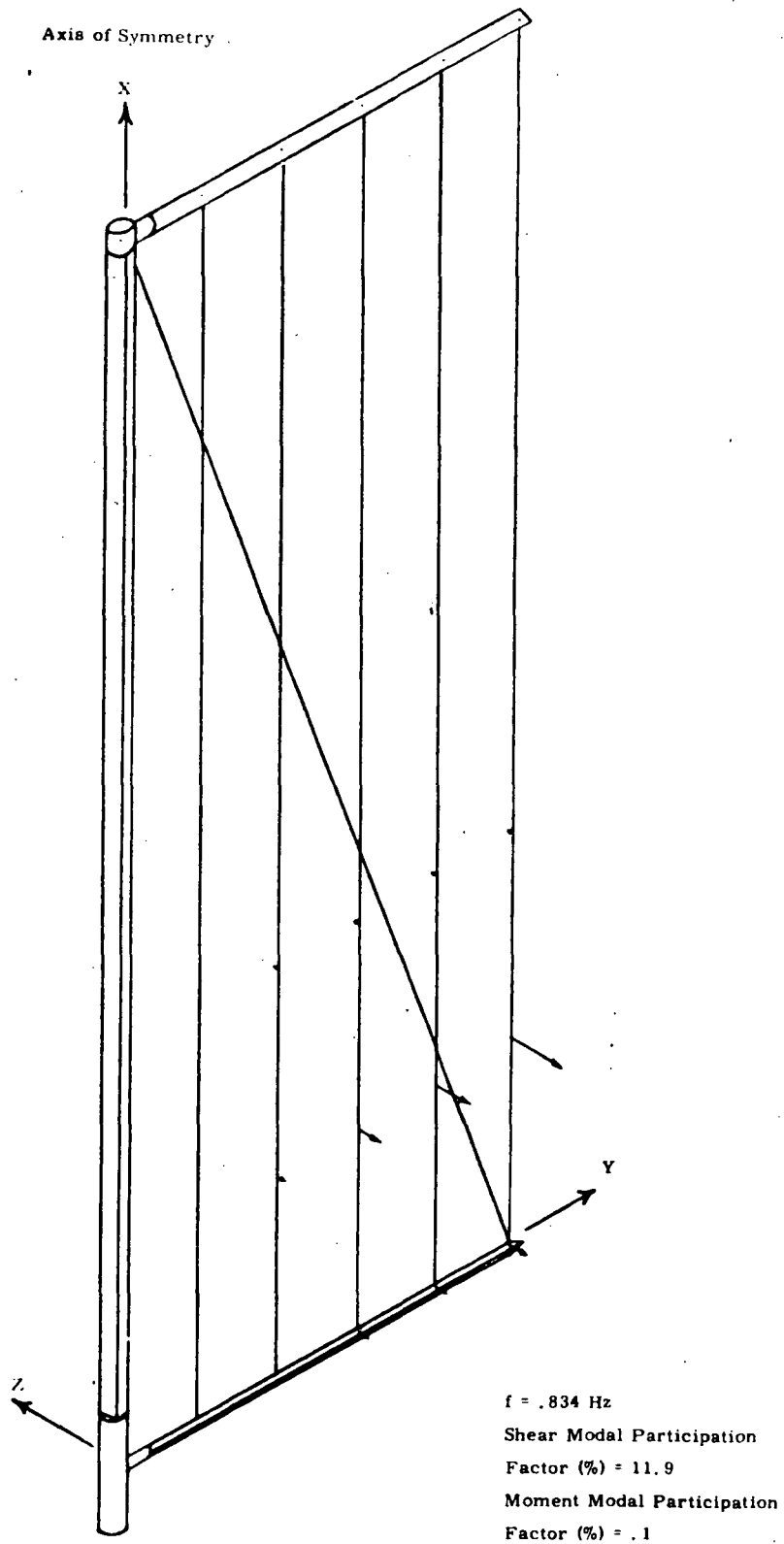


Figure A-22

Mode 22 String Solar Array, Out of Plane, Symmetric

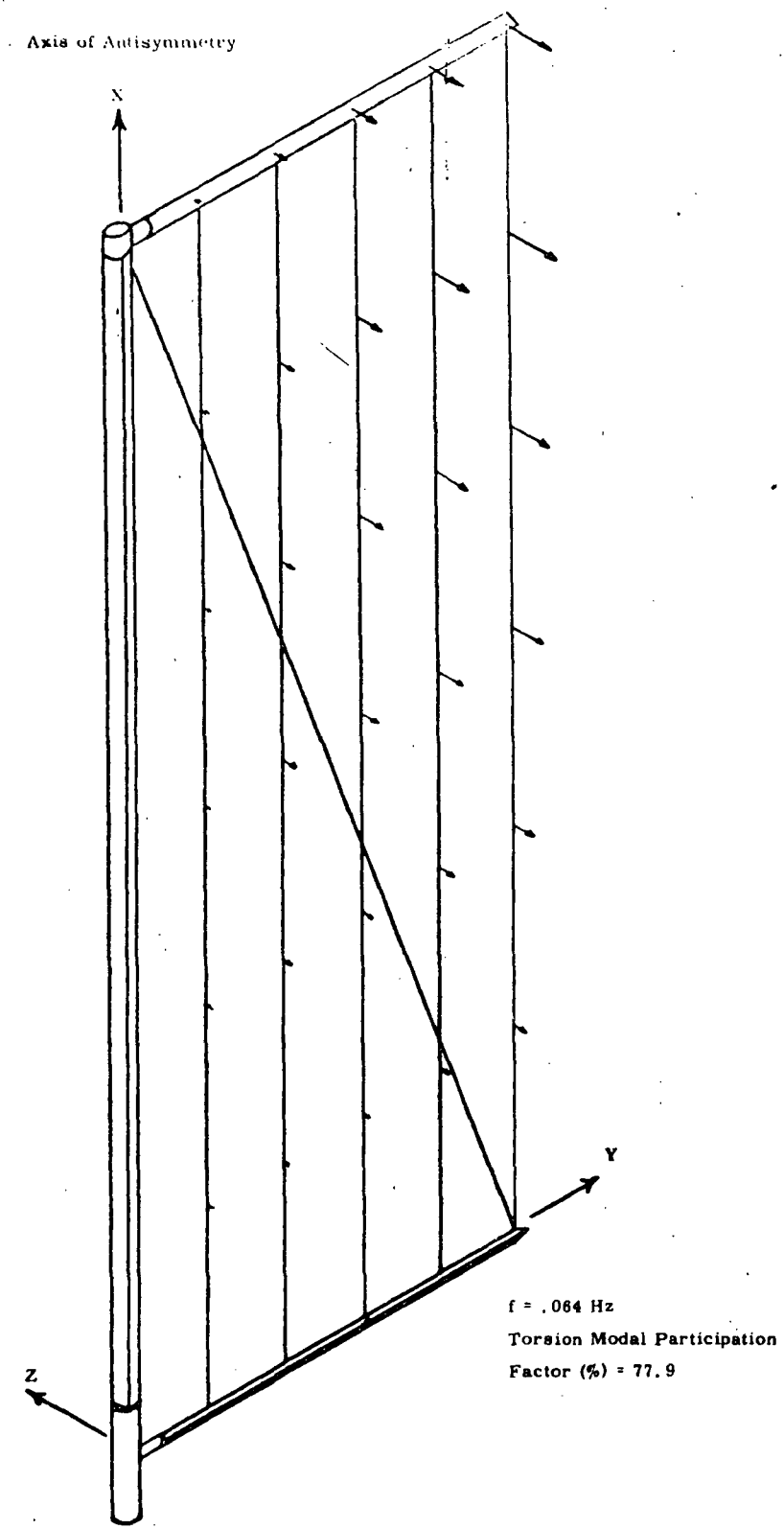


Figure A-23 Mode 1 Solar Array, Out of Plane, Antisymmetric

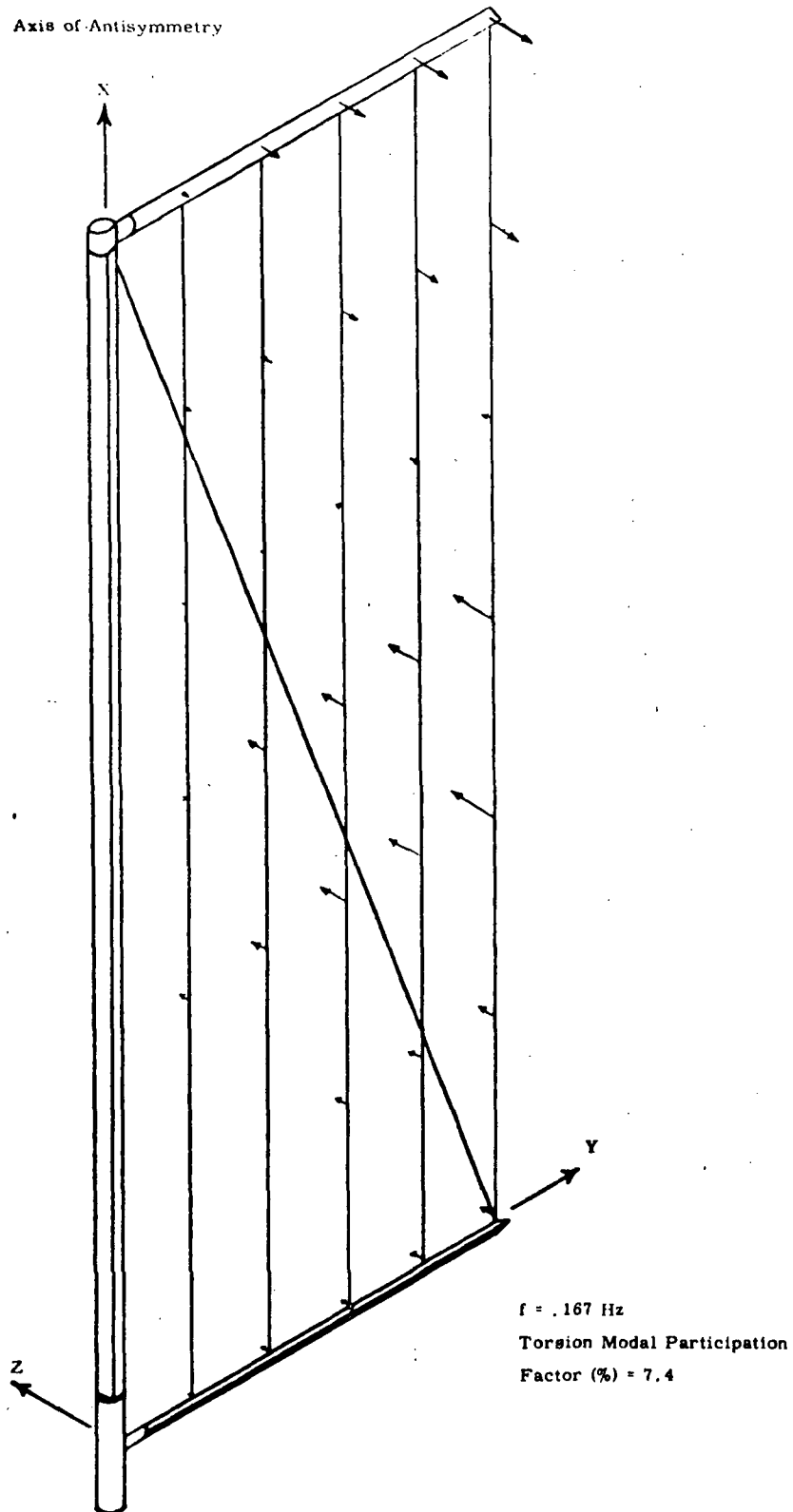


Figure A-24 Mode 6 String Solar Array, Out of Plane, Antisymmetric

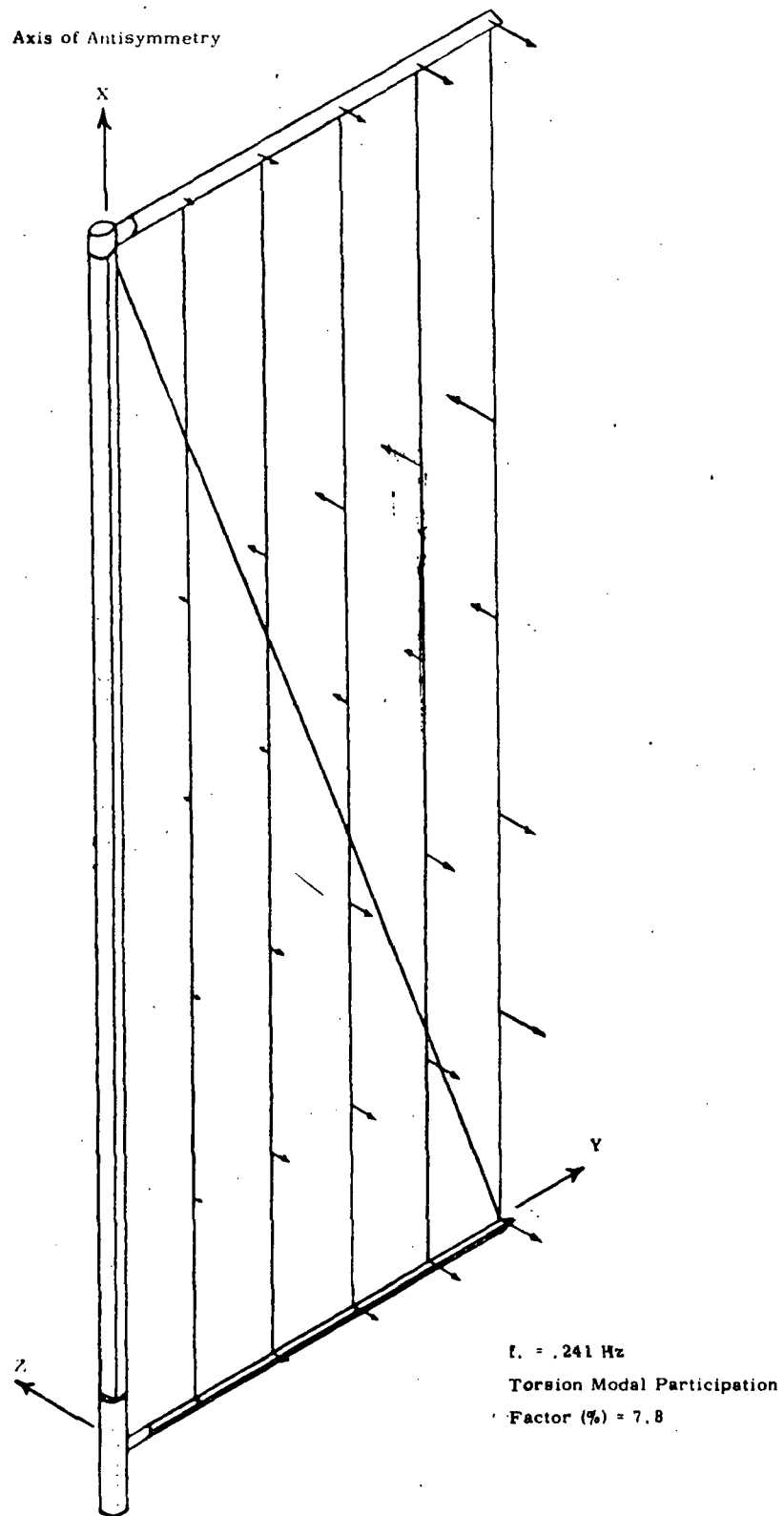


Figure A-25

Mode 11 String Solar Array, Out of Plane, Antisymmetric

A.3 VIBRATION MODE DATA
ARTIFICIAL "G" SPACE STATION CONFIGURATION

CONTENTS

<u>TABLES</u>		<u>PAGE</u>
A-8	Modal Data, Zero Spin, NASTRAN Results	A-37
A-9	Mass-Geometry Data	A-39
A-10	Structural Model Data	A-46
A-11	Coriolis Force Matrix	A-47
A-12	Centrifugal Force Matrix	A-48

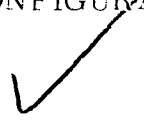
FIGURES

A-26	Structural Model	A-38
A-27 to A-32	Mode Shapes of First Six Elastic Modes (NASTRAN Results)	A-40 to A-45

NOTE: Mode 1 shown in Figure A-27 is the first elastic mode and corresponds to Mode 7 of Table A-8.

Computer Listings of Modes	JPL Eigenvalue-Eigenvector Program Results for Spin Rates of 0, 4, 8, and 12 RPM. The degree of freedom sequence numbers and their corresponding node number are described in Table A-10.	A-49
-------------------------------	---	------

TABLE A-8 MODAL DATA ARTIFICIAL "G" SPACE STATION CONFIGURATION
 ZERO SPIN, NASTRAN RESULTS



MODE	FREQUENCY (HZ)		GENERALIZED MASS (LBS:SEC ² /IN)
1	4.221942E-03	Rigid Body Modes	2.874500E 02
2	4.152642E-03		6.274835E 01
3	6.192792E-03		1.266219E 02
4	6.883873E-03		1.162889E 02
5	7.158235E-03		1.794931E 02
6	8.503952E-03		1.572773E 01
7	2.296729E 00		8.672661E 00
8	4.200339E 00		5.868550E 00
9	8.420200E 00		7.261933E 00
10	8.678653E 00		7.816177E 01
11	1.0447947E 01	7.559761E 01	
12	1.254375E 01	7.482590E 03	
13	1.532557E 01	4.555014E 01	
14	1.733156E 01	1.018629E 01	
15	2.156968E 01	2.924060E 03	
16	2.799701E 01	5.702884E 01	
17	3.031332E 01	2.432465E 05	
18	3.281332E 01	6.314181E 00	
19	3.377370E 01	7.612518E 01	
20	3.420000E 01	1.149187E 02	
21	3.922133E 01	1.977763E 00	
22	4.253050E 01	1.850132E 00	
23	5.000700E 01	3.670974E 03	
24	5.518927E 01	3.518304E 01	
25	5.629474E 01	3.503325E 00	
26	5.711957E 01	3.315749E 00	
27	6.072257E 01	8.260058E 02	
28	6.351724E 01	1.964404E 01	
29	6.399556E 01	1.996732E 04	
30	6.770356E 01	5.345604E-01	
31	7.050739E 01		
32	7.548627E 01		
33	8.357313E 01		
34	8.463323E 01		
35	8.520222E 01		
36	9.113895E 01		
37	9.125427E 01		
38	9.360021E 01		
39	9.744000E 01		
40	1.025530E 02		
41	1.037150E 02		
42	1.072331E 02		
43	1.100000E 02		
44	1.135593E 02		
45	1.195054E 02		
46	1.202260E 02		
47	1.217319E 02		
48	1.293130E 02		
49	1.247009E 02		
50	1.003121E 02		

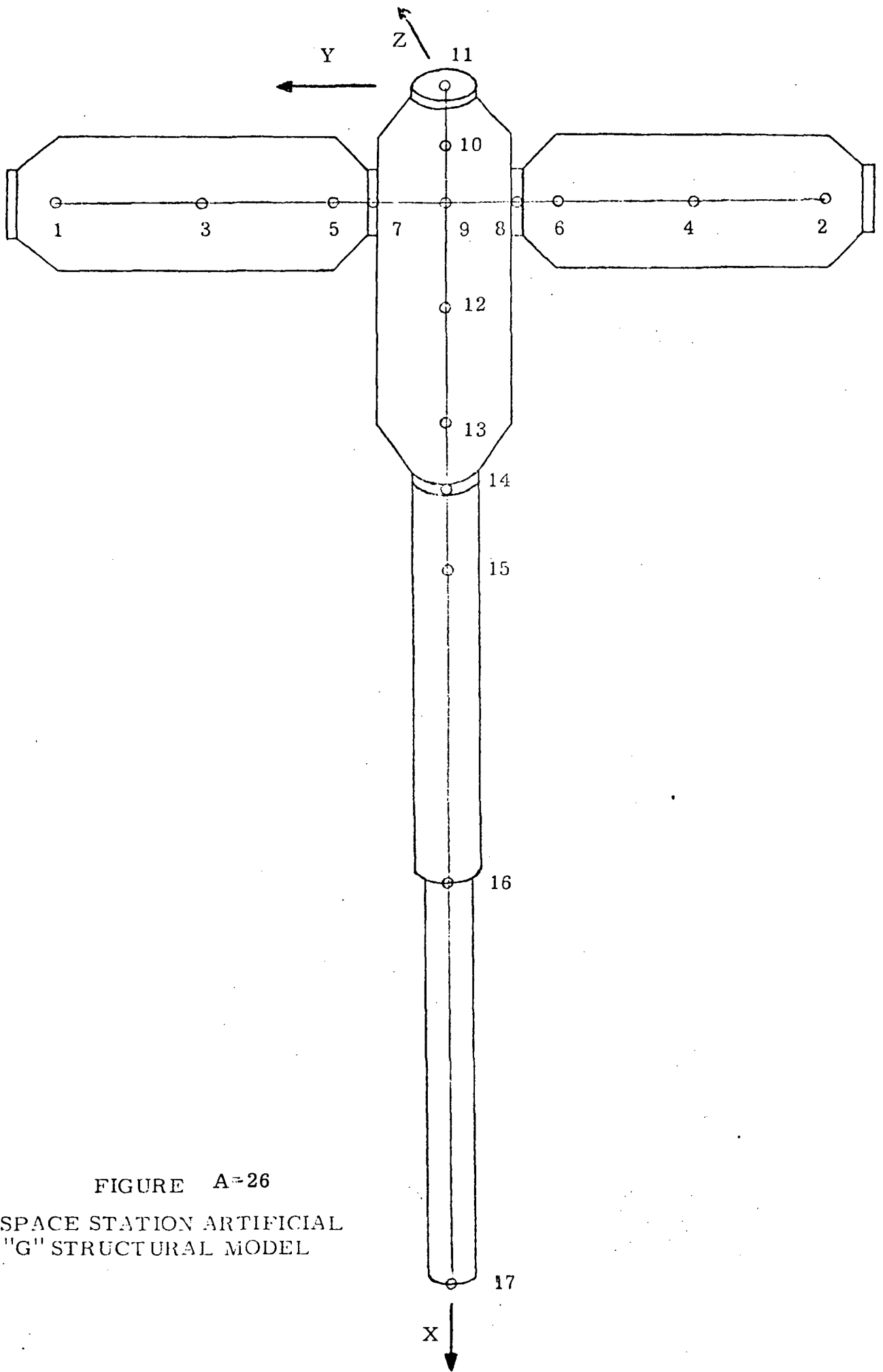


FIGURE A-26
 SPACE STATION ARTIFICIAL
 "G" STRUCTURAL MODEL

TABLE A-9
 MASS - GEOMETRY DATA
 FOR ARTIFICIAL "G" SPACE STATION

Node	Mass *	X	Y	Z
1	21.578	120.	492.	.0
2	21.578	120.	-492.	.0
3	21.578	120.	312.	.0
4	21.578	120.	-312.	.0
5	21.578	120.	132.	.0
6	21.578	120.	-132.	.0
7	0.	120.	72.	.0
8	0.	120.	-72.	.0
9	15.382	120.	.0	.0
10	8.094	60.	.0	.0
11	4.047	.0	.0	.0
12	17.814	270.	.0	.0
13	15.379	420.	.0	.0
14	12.795	480.	.0	.0
15	10.632	552.	.0	.0
16	25.952	921.0	.0	.0
17	.01295	1290.	.0	.0

* - Mass units are lb-sec²/in.

FIGURE A-27
ARTIFICIAL "G" SPACE STATION
MODE 1 FREQ. = 2.30 Hz
ZERO SPIN

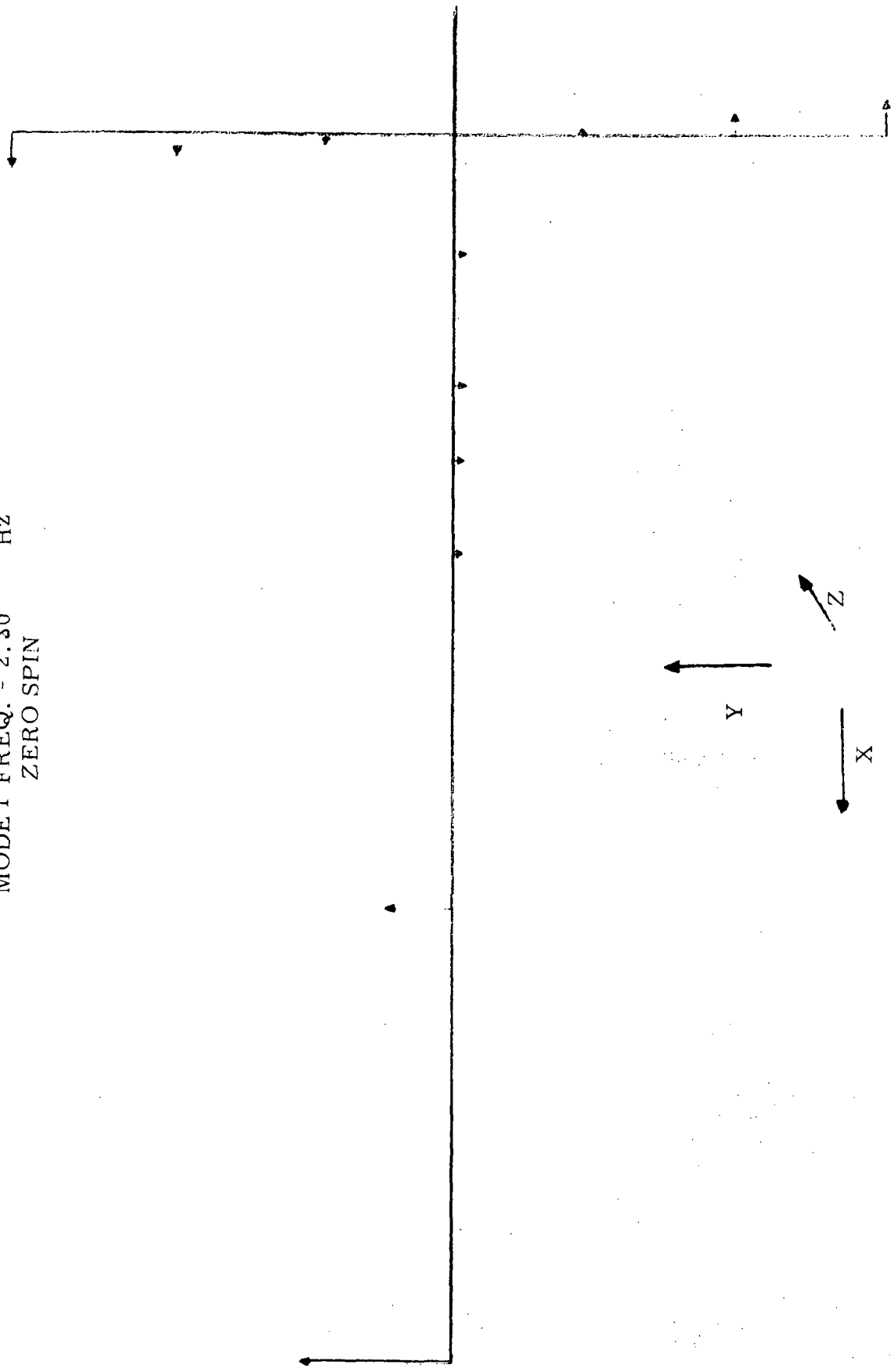


FIGURE A-28
ARTIFICIAL "G" SPACE STATION
MODE 2 FREQ. = 4.20 Hz
ZERO SPIN

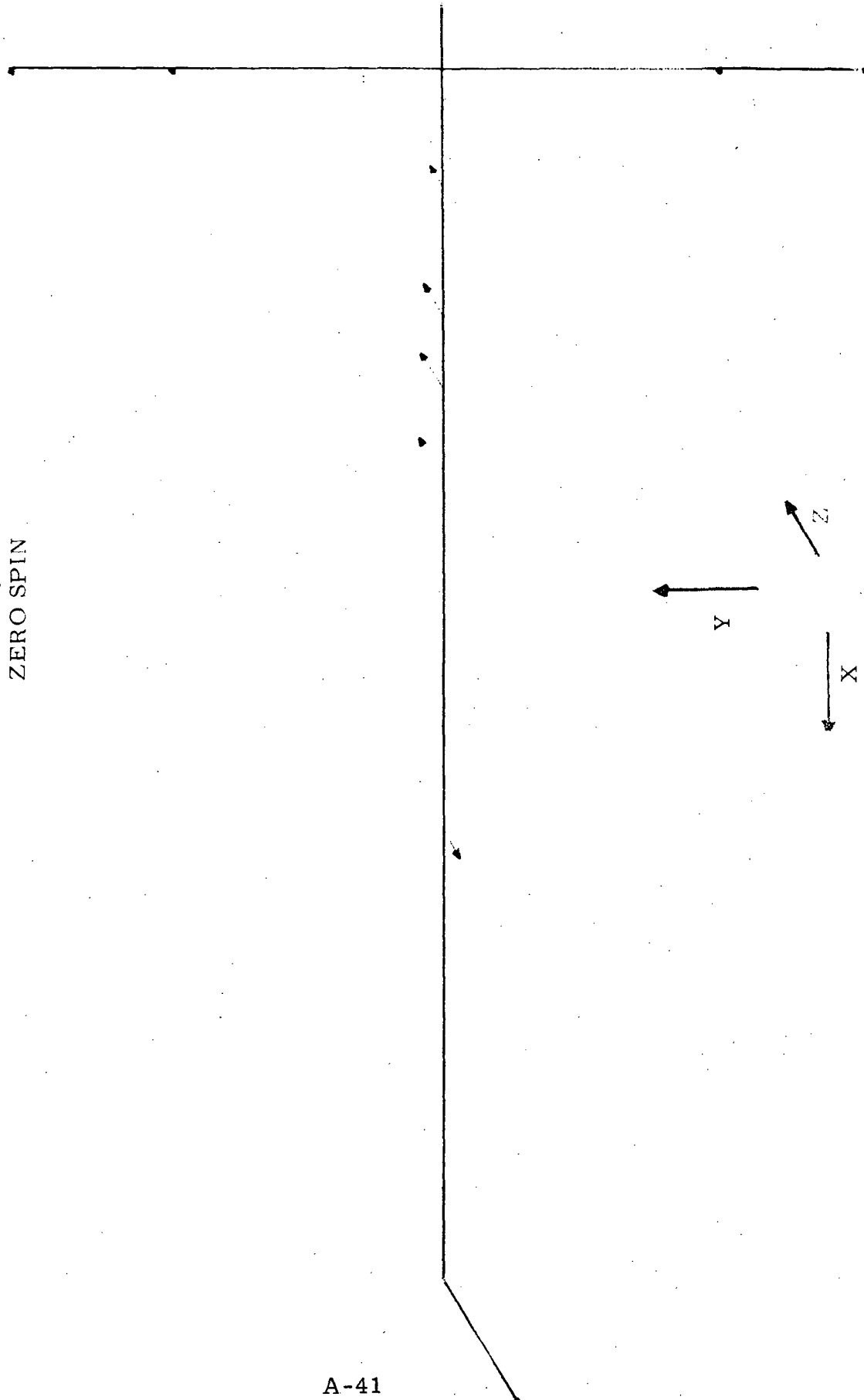


FIGURE A-29
ARTIFICIAL "G" SPACE STATION
MODE 3 FREQ. = 8.42 Hz
ZERO SPIN

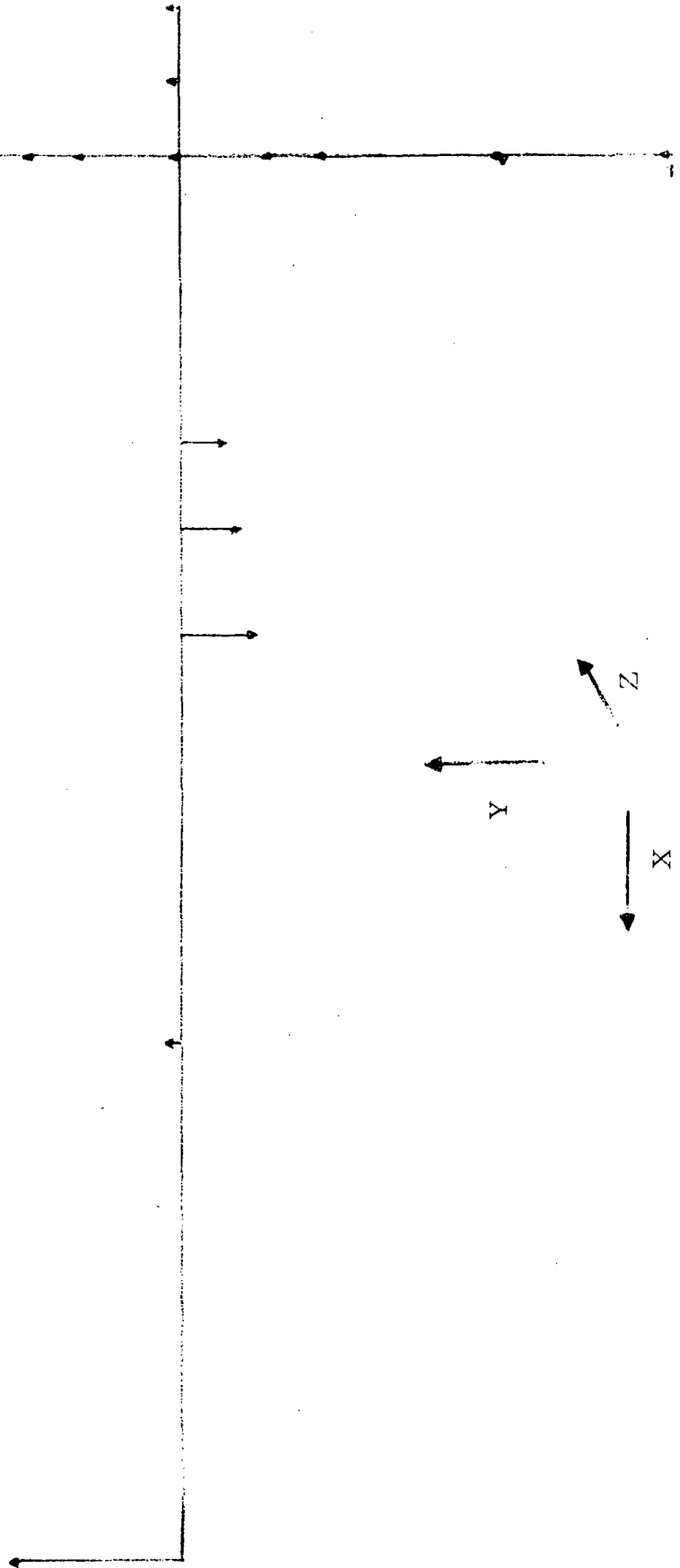


FIGURE A-30
ARTIFICIAL "G" SPACE STATION
MODE 4 FREQ. = 8.68 Hz
ZERO SPIN

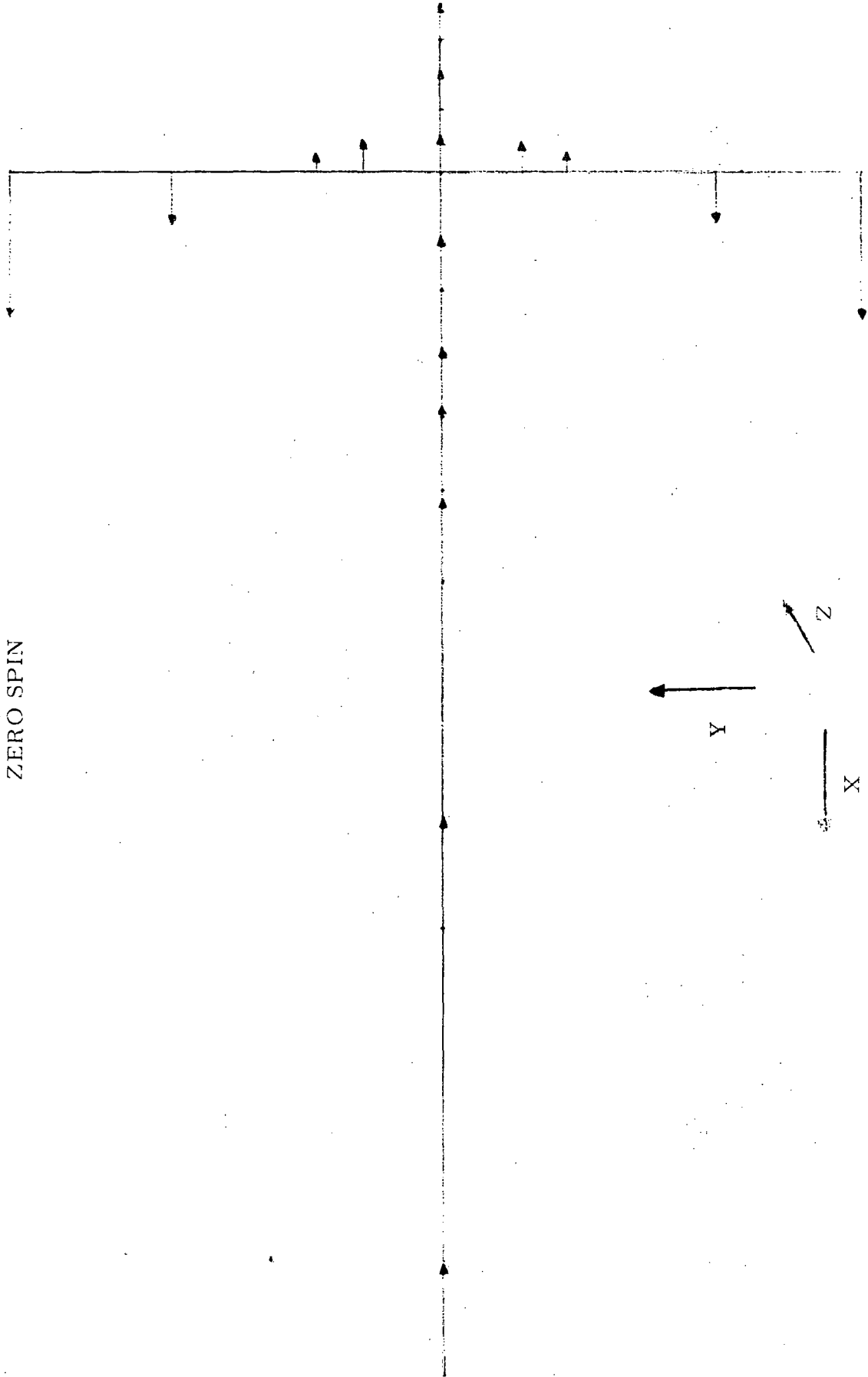


FIGURE A-31
ARTIFICIAL "G" SPACE STATION
MODE 5 FREQ. = 10.5 Hz
ZERO SPIN

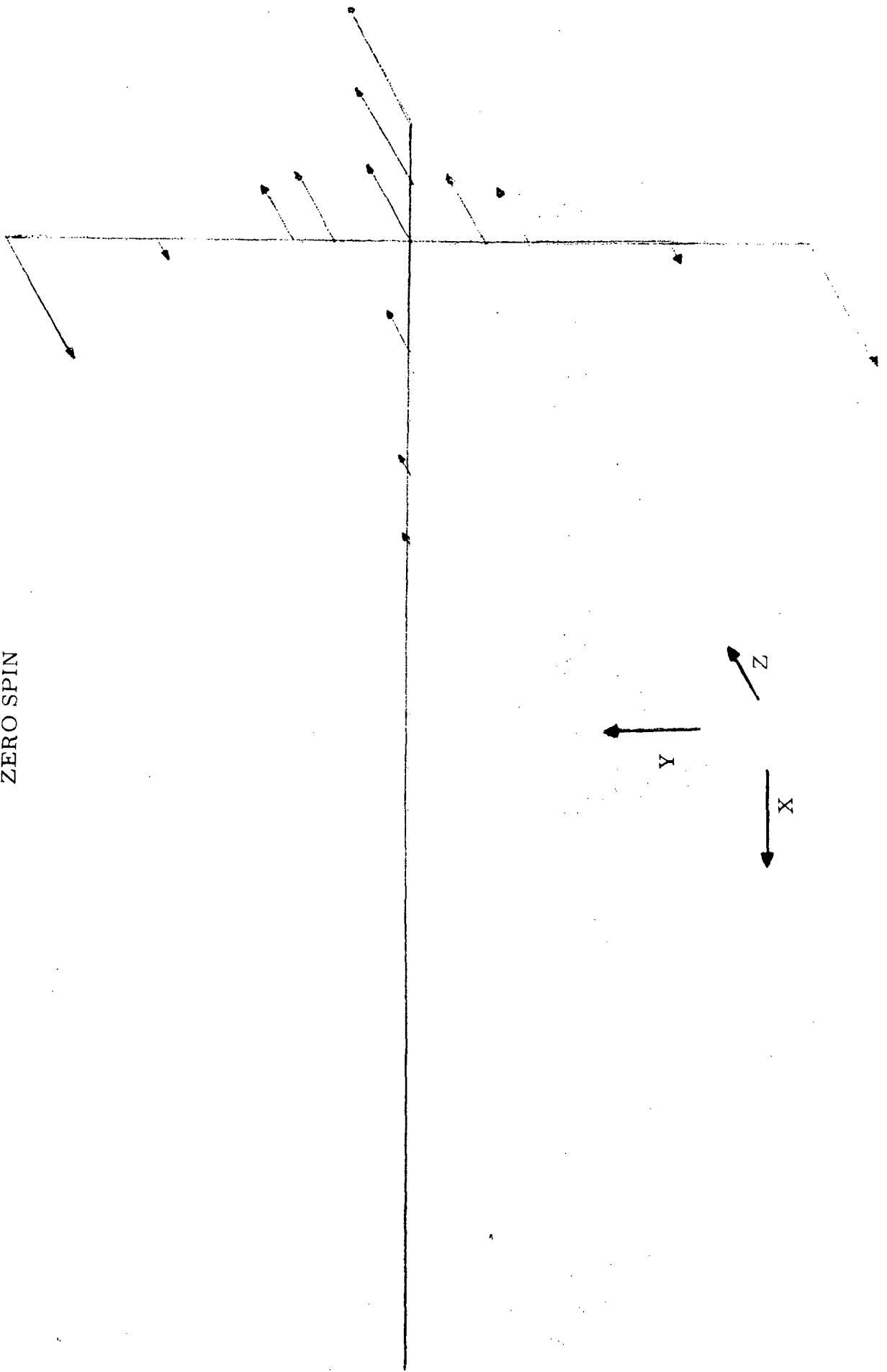


FIGURE A-32
ARTIFICIAL "G" SPACE STATION
MODE 6 FREQ. = 12.5 Hz
ZERO SPIN

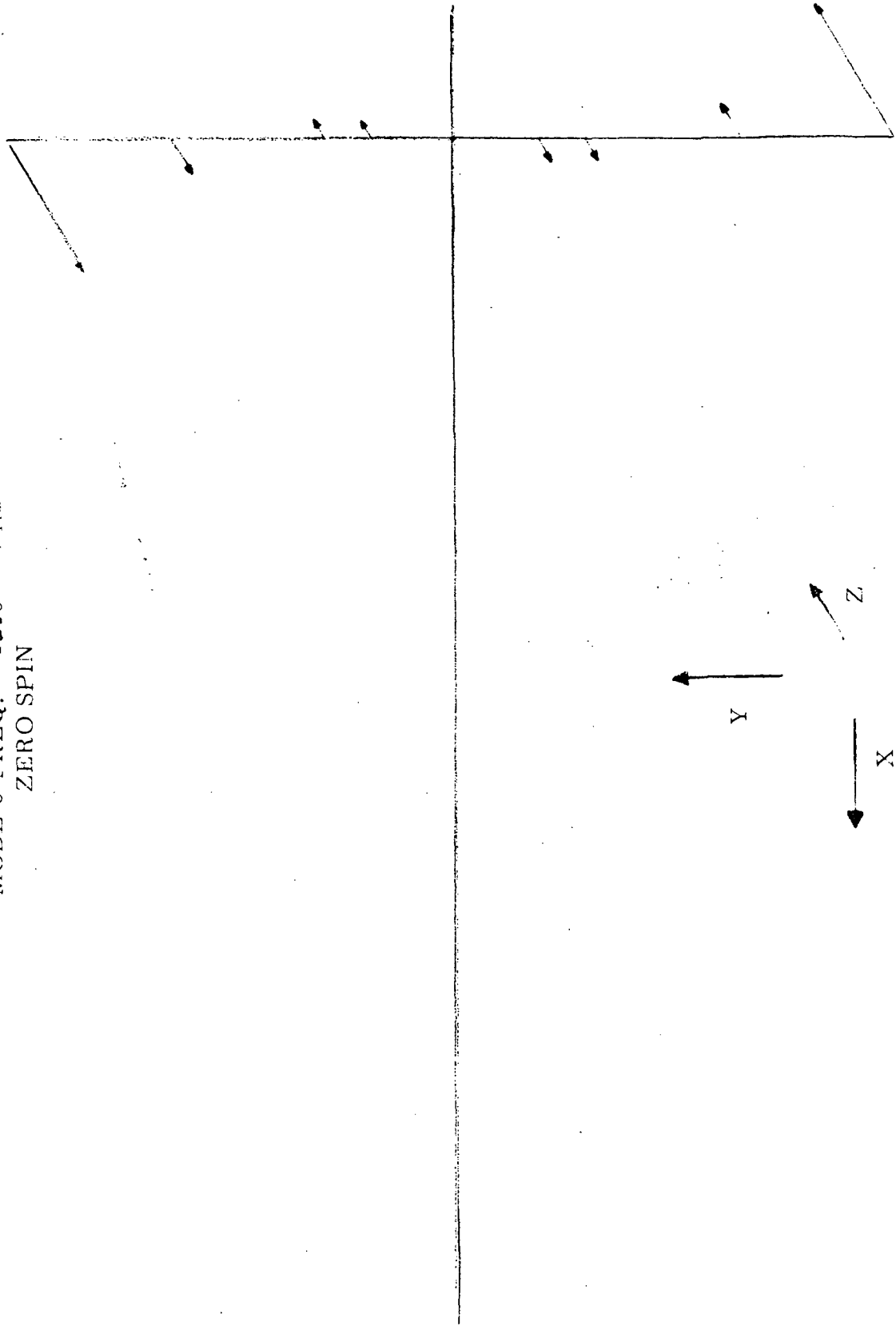


TABLE A-10
 ARTIFICIAL "G" SPACE STATION
 FINITE ELEMENT MODEL DATA

NODE	MASS LB SEC ² /IN	INERTIA			NO. OF STRUCTURAL D.O.F.	D.O.F. SEQUENCE NO.
		LB	SEC ²	IN		
		x Axis	y Axis	z Axis		
1	21.578	--	66641	--	6	1-6
2	21.578	--	66641	--	6	7-12
3	21.578	--	66641	--	6	13-18
4	21.578	--	66641	--	6	19-24
5	21.578	--	66641	--	6	25-30
6	21.578	--	66641	--	6	31-36
7	--	--	--	--	6	37-42
8	--	--	--	--	6	43-48
9	15.382	41621	--	--	6	49-54
10	8.094	21886	--	--	6	55-60
11	4.047	10956	--	--	6	61-66
12	17.814	49417	--	--	6	67-72
13	15.379	41595	--	--	6	73-78
14	12.795	18700	--	--	6	79-84
15	10.632	9350			6	85-90
16	25.952	20642			6	91-96
17	.01295	10.282			6	97-102

TABLE A-11
CORIOLIS FORCE MATRIX
(NORMALIZED TO Ω)

<u>D. O. F.</u> *			
<u>Sequence No.</u>			
1 - 3	-43.15581	0.	0.
4 - 6	0.	0.	0.
etc.	-43.15581	0.	0.
	0.	0.	0.
	-43.15581	0.	0.
	0.	0.	0.
	-43.15581	0.	0.
	0.	0.	0.
	-43.15581	0.	0.
	0.	0.	0.
	-43.15581	0.	0.
	0.	0.	0.
	0.	0.	0.
	0.	0.	0.
	0.	0.	0.
	0.	0.	0.
	0.	0.	0.
	0.	0.	0.
	-30.76417	0.	0.
	-41621.02691	0.	0.
	-16.18755	0.	0.
	-21885.53002	0.	0.
	-8.09377	0.	0.
	-10955.20496	0.	0.
	-35.62841	0.	0.
	-49417.88198	0.	0.
	-30.75889	0.	0.
	-41595.14699	0.	0.
	-25.49926	0.	0.
	-18699.30020	0.	0.
	-21.26381	0.	0.
	-9349.65010	0.	0.
	-51.90365	0.	0.
	-20642.29399	0.	0.
	-0.02588	0.	0.
100 - 102	-10.28432	0.	0.

* - Refer to Table A-10 for corresponding node number.

TABLE A-12
CENTRIFUGAL FORCE MATRIX
(NORMALIZED TO Ω^2)

D. O. F. *
Sequence No.

1 - 3	-21.57791	-21.57791	0.
4 - 6	0.	0.	0.
	-21.57791	-21.57791	0.
etc.	0.	0.	0.
	-21.57791	-21.57791	0.
	0.	0.	0.
	-21.57791	-21.57791	0.
	0.	0.	0.
	-21.57791	-21.57791	0.
	0.	0.	0.
	-21.57791	-21.57791	0.
	0.	0.	0.
	0.	0.	0.
	0.	0.	0.
	0.	0.	0.
	0.	0.	0.
	-15.38208	-15.38208	0.
	0.	0.	0.
	-8.09375	-8.09375	0.
	0.	0.	0.
	-4.04687	-4.04687	0.
	0.	0.	0.
	-17.81401	-17.81401	0.
	0.	0.	0.
	-15.37949	-15.37949	0.
	0.	0.	0.
	-12.79468	-12.79468	0.
	0.	0.	0.
	-10.63191	-10.63191	0.
	0.	0.	0.
	-25.95188	-25.95188	0.
	0.	0.	0.
	-0.01294	-0.01294	0.
100 - 102	0.	0.	0.

* - Refer to Table A-10 for corresponding node number.

Mode 1, Frequency = 2.2948 Hz, $\Omega = 0$ RPM

EFFECTIVE FOR BODY NO. = 1

EIGENVALUES = 0.14410045F 0? (rad/sec.)

REAL PART	IMAGINARY PART	0.2895E 00	-0.3381E-01	-0.7647E-05	-0.3272E-08	-0.2953E-07	-0.6066E-03	-0.2895E 00
1	1	0.2895E 00	-0.3381E-01	-0.7647E-05	-0.3272E-08	-0.2953E-07	-0.6066E-03	-0.2895E 00
2	14	-0.3381E-01	0.2895E 00	0.7647E-05	0.3272E-08	0.2953E-07	0.6066E-03	-0.3381E-01
15	10	-0.7075E-05	-0.2986E-08	-0.2949E-07	-0.6012E-03	-0.6012E-03	-0.3382E-01	-0.7080E-05
22	10	0.2973E-08	0.2949E-07	0.5012E-03	0.7399E-01	0.7399E-01	-0.6619E-05	-0.1912E-08
29	10	-0.2943E-07	-0.5801E-03	-0.7399E-01	-0.3375E-01	-0.6524E-05	0.1931E-08	-0.2943E-07
35	10	-0.5801E-03	0.3974E-01	-0.3370E-01	-0.6537E-05	-0.8929E-09	-0.2937E-07	-0.5605E-03
43	10	-0.3975E-01	-0.3371E-01	-0.6537E-05	0.9372E-09	-0.2937E-07	-0.5605E-03	-0.4130E-05
50	10	-0.3366E-01	0.6501E-05	0.2671E-10	-0.2933E-07	-0.5422E-03	-0.4145E-05	-0.1091E-02
57	10	-0.8236E-05	0.2637E-10	-0.2864E-07	-0.5429E-03	-0.4145E-05	0.3149E-01	-0.9945E-05
64	10	0.2642E-10	-0.2841E-07	-0.5430E-03	-0.4232E-05	-0.9412E-01	-0.2119E-05	0.2681E-10
71	10	-0.2799E-07	-0.2682E-03	-0.4317E-05	-0.1158E 00	0.2722E-05	0.2717E-10	-0.2598E-07
78	10	-0.2790E-04	-0.4351E-05	-0.1133E 00	0.3476E-05	-0.2732E-10	-0.2240E-07	0.1116E-03
85	10	-0.4391E-05	-0.9032E-01	0.4293E-05	0.2767E-10	-0.1732E-09	0.5425E-03	-0.4533E-05
92	10	0.3722E 00	-0.9061E-05	0.2802E-10	0.5220E-07	0.1544E-02	-0.4559E-05	0.1000F 01
99	10	-0.2739E-04	0.2926E-10	0.4876E-07	0.1729E-02	0.1544E-02	-0.4559E-05	0.1000F 01
PRIMARY PART								
1	1	0.0	0.0	0.0	0.0	0.0	0.0	0.0
2	14	0.0	0.0	0.0	0.0	0.0	0.0	0.0
15	10	0.0	0.0	0.0	0.0	0.0	0.0	0.0
22	10	0.0	0.0	0.0	0.0	0.0	0.0	0.0
29	10	0.0	0.0	0.0	0.0	0.0	0.0	0.0
35	10	0.0	0.0	0.0	0.0	0.0	0.0	0.0
43	10	0.0	0.0	0.0	0.0	0.0	0.0	0.0
50	10	0.0	0.0	0.0	0.0	0.0	0.0	0.0
57	10	0.0	0.0	0.0	0.0	0.0	0.0	0.0
64	10	0.0	0.0	0.0	0.0	0.0	0.0	0.0
71	10	0.0	0.0	0.0	0.0	0.0	0.0	0.0
78	10	0.0	0.0	0.0	0.0	0.0	0.0	0.0
85	10	0.0	0.0	0.0	0.0	0.0	0.0	0.0
92	10	0.0	0.0	0.0	0.0	0.0	0.0	0.0
99	10	0.0	0.0	0.0	0.0	0.0	0.0	0.0

EIGENVECTOR FOR ROOT NO. = 1

Mode 1, Frequency = 2.2729 Hz, Ω = 4RPM

EIGENVALUE = 0.14406738E 02 (rad/sec.)

REAL PART

1	TO	0.3613E 00	-0.2108E-01	-0.1556E-04	-0.5927E-08	-0.5179E-08	-0.7497E-03	-0.3613E 00
9	TO	-0.2116E-01	-0.1553E-04	0.5730E-08	-0.5178E-08	-0.7496E-03	0.2766E 00	-0.2110E-01
15	TO	-0.1452E-04	-0.5423E-08	-0.6170E-08	-0.7457E-03	-0.2266E 00	-0.2116E-01	-0.1452E-04
22	TO	0.5283E-08	-0.6170E-08	-0.7457E-03	0.9370E-01	-0.2110E-01	-0.1360E-04	-0.3471E-08
29	TO	-0.6156E-08	-0.7278E-03	-0.9470E-01	-0.2112E-01	-0.1371E-04	-0.3495E-08	-0.6156E-08
35	TO	-0.7278E-03	0.5054E-01	-0.2108E-01	-0.1353E-04	-0.6144E-08	-0.6144E-08	-0.7099E-03
43	TO	-0.5055E-01	-0.2109E-01	-0.1355E-04	0.1765E-08	-0.6144E-08	-0.7100E-03	-0.2343E-05
50	TO	-0.2106E-01	-0.1348E-04	0.1011E-09	-0.6135E-08	-0.6933E-03	-0.2336E-05	0.2055E-01
57	TO	-0.1378E-04	0.1014E-09	-0.4401E-08	-0.6937E-03	-0.2325E-05	0.6218E-01	-0.1402E-04
64	TO	0.1016E-09	-0.3741E-08	-0.6929E-03	-0.2576E-05	-0.1049E 00	-0.1224E-04	0.1033E-09
71	TO	-0.9988E-08	-0.4276E-03	-0.7785E-05	-0.1504E 00	-0.1066E-04	0.1048E-09	-0.1036E-07
78	TO	-0.1838E-03	-0.7969E-05	-0.1570E 00	-0.1011E-04	0.1055E-09	-0.7761E-08	-0.3693E-04
85	TO	-0.2974E-05	-0.1426E 00	-0.1033E-04	0.1071E-09	0.1416E-07	0.4262E-03	-0.3342E-05
92	TO	0.3121E 00	-0.2892E-04	0.1128E-09	0.6418E-07	0.1733E-02	-0.3456E-05	0.1000E 01
99	TO	-0.5052E-04	0.1146E-09	0.5541E-07	0.1930E-02	0.1733E-02	-0.3456E-05	0.1000E 01

IMAGINARY PART

1	TO	0.4564E-03	0.1005E-03	0.5932E-08	0.8129E-11	0.5998E-11	-0.4900E-06	0.5464E-03
9	TO	-0.9165E-04	-0.7905E-08	0.8939E-11	0.6002E-11	0.6602E-05	0.3795E-03	0.7718E-04
15	TO	0.4456E-08	0.8352E-11	0.5993E-11	-0.4438E-06	0.4304E-03	-0.6836E-04	-0.1300E-08
22	TO	0.8992E-11	0.5995E-11	0.5126E-06	0.3133E-03	0.3991E-04	0.2901E-08	0.8982E-11
29	TO	0.5980E-11	-0.2620E-06	0.3342E-03	-0.3110E-04	0.3421E-09	0.9304E-11	0.5981E-11
35	TO	0.4254E-06	0.3026E-03	0.2163E-04	0.2342E-08	0.9678E-11	0.5969E-11	-0.8764E-07
43	TO	0.3138E-03	-0.1283E-04	0.9152E-09	0.9821E-11	0.5970E-11	0.2459E-06	0.3019E-03
50	TO	0.4391E-05	0.1631E-08	0.1008E-10	0.5961E-11	0.7674E-07	0.2974E-03	-0.2120E-06
57	TO	0.1982E-08	0.1022E-10	0.5737E-11	0.7677E-07	0.2688E-03	-0.4819E-05	0.2319E-08
64	TO	0.1079E-10	0.5559E-11	0.7679E-07	0.2988E-03	0.1307E-04	0.7250E-09	0.9126E-11
71	TO	0.6086E-11	0.3951E-07	0.2768E-03	0.1650E-04	-0.1723E-09	0.6929E-11	0.5769E-11
78	TO	0.6875E-08	0.2535E-03	0.1633E-04	-0.5018E-09	0.4776E-11	0.5195E-11	-0.1223E-07
85	TO	0.1992E-03	0.1326E-04	-0.7476E-09	-0.3301E-11	0.1614E-11	-0.7142E-07	-0.1432E-03
92	TO	-0.4926E-04	0.8981E-08	-0.4098E-10	-0.7183E-11	-0.2250E-06	-0.1461E-03	-0.1355E-03
99	TO	0.3409E-08	-0.4100E-10	-0.5654E-11	-0.2381E-06	-0.2250E-06	-0.1461E-03	-0.1355E-03

FIGURE VECTOR FOR PART NO. = 2

Mode 2, Frequency = 4.2027 Hz, $\Omega = 4$ RPM

SIZE VALUE = 0.76406250E 02 (rad/sec.)

REAL PART

1	TO	7	-0.3823E-05	0.1226E-05	0.4996E-01	-0.4996E-01	-0.5194E-04	-0.1159E-02	0.8939E-08	0.3825E-05
3	TO	14	0.1226E-05	-0.4996E-01	0.5196E-04	-0.5196E-04	-0.1169E-02	0.8941E-08	-0.2237E-05	0.1222E-05
15	TO	21	-0.3988E-01	-0.4750E-04	-0.1164E-02	0.8558E-08	0.8558E-08	0.2237E-05	-0.1222E-05	-0.3985E-01
22	TO	28	0.4762E-04	-0.1164E-02	0.8560E-08	-0.7992E-06	-0.7992E-06	0.1213E-05	-0.3261E-01	-0.3058E-04
23	TO	35	-0.1155E-02	0.7222E-08	0.8011E-06	0.1213E-05	0.1213E-05	-0.3261E-01	0.3048E-04	-0.1155E-02
35	TO	42	0.7222E-08	-0.3994E-06	0.1208E-05	0.1208E-05	-0.3123E-01	-0.1474E-04	-0.1144E-02	0.6063E-08
43	TO	49	0.4014E-06	0.1208E-05	-0.3122E-01	0.1463E-04	0.1463E-04	-0.1143E-02	0.6064E-08	0.4014E-06
50	TO	56	0.1202E-05	-0.3368E-01	-0.5799E-07	-0.1142E-02	-0.1142E-02	0.5024E-08	0.1013E-08	0.9008E-06
57	TO	63	-0.9937E-01	-0.5833E-07	0.5044E-08	0.5044E-08	0.5030E-08	0.1132E-08	0.5984E-06	-0.1682E 00
64	TO	70	-0.5852E-07	-0.1149E-02	0.5044E-08	0.6806E-09	0.6806E-09	0.8353E-06	0.1309E 00	-0.6079E-07
71	TO	77	-0.9876E-03	-0.9105E-08	-0.4536E-09	-0.1291E-05	-0.1291E-05	0.2594E 00	-0.6234E-07	-0.7097E-07
78	TO	84	-0.1848E-07	0.3670E-09	-0.2501E-05	0.2501E-05	0.2501E-05	-0.6271E-07	-0.6901E-03	-0.2167E-07
85	TO	91	0.2592E-09	-0.3808E-05	0.3036E 00	-0.6307E-07	-0.6307E-07	0.2592E-09	-0.1442E-07	-0.2841E-10
92	TO	98	-0.4490E-05	-0.2267E 00	-0.6324E-07	0.2070E-02	0.2070E-02	0.2963E-08	-0.1267E-09	-0.4126E-05
93	TO	102	-0.1000E 01	-0.6324E-07	0.2068E-02	0.9807E-12	0.9807E-12	0.2963E-08	-0.1267E-09	-0.4126E-05

IMAGINARY PART

1	TO	7	-0.2571E-07	0.3250E-09	-0.1508E-03	-0.2368E-06	-0.2368E-06	-0.2144E-05	0.7608E-10	-0.1254E-07
3	TO	14	0.3825E-08	-0.2987E-04	-0.4615E-07	-0.2166E-05	-0.2166E-05	0.4513E-10	-0.1236E-07	0.7639E-09
15	TO	21	-0.1091E-03	-0.2226E-06	-0.2157E-05	0.7023E-10	0.7023E-10	-0.4653E-08	0.3410E-08	-0.3831E-04
22	TO	28	-0.4829E-07	-0.2157E-05	-0.4066E-10	-0.1402E-08	-0.1402E-08	0.1445E-08	-0.7296E-04	-0.1704E-06
23	TO	35	-0.2140E-05	0.4809E-10	0.1321E-09	0.2725E-08	0.2725E-08	-0.4772E-04	-0.5818E-07	-0.2140E-05
35	TO	42	-0.2330E-10	0.8911E-09	0.1769E-08	-0.6412E-04	-0.6412E-04	0.1225E-06	-0.2126E-05	0.2749E-10
43	TO	49	0.2247E-08	0.7399E-08	-0.5151E-04	0.6858E-07	0.6858E-07	-0.2125E-06	-0.6854E-11	0.2212E-08
50	TO	56	0.2071E-08	-0.5680E-04	-0.7902E-07	-0.2116E-05	-0.2116E-05	0.8455E-11	0.2056E-08	0.1564E-08
57	TO	63	-0.1841E-03	-0.1146E-07	-0.2125E-05	0.8450E-11	0.8450E-11	0.1313E-08	-0.1056E-08	-0.3117E-03
54	TO	70	0.2566E-07	-0.2128E-05	0.8460E-11	0.6352E-08	0.6352E-08	0.1345E-08	0.2426E-03	0.9382E-07
71	TO	77	-0.1830E-05	-0.1679E-10	0.1069E-07	-0.2543E-08	-0.2543E-08	0.4937E-03	0.4660E-07	-0.1315E-05
73	TO	84	-0.3359E-10	0.1271E-07	-0.4739E-08	0.5475E-03	0.5475E-03	-0.7174E-07	-0.9089E-06	-0.3934E-10
85	TO	91	0.1543E-07	-0.7102E-08	0.5628E-03	-0.5618E-06	-0.5618E-06	0.6541E-06	-0.2592E-10	0.2591E-07
92	TO	98	-0.8291E-08	-0.4365E-03	-0.2937E-05	0.3831E-05	0.3831E-05	0.5437E-11	-0.2592E-10	-0.7622E-08
93	TO	102	-0.1851E-02	-0.4365E-03	-0.2938E-05	0.3248E-19	0.3248E-19	0.5437E-11	-0.2592E-10	-0.7622E-08

EIGENVECTOR FOR ROOT NO. = 4

Mode 4, Frequency = 8.6789 Hz, $\Omega = 4$ RPM

EIGENVALUE = 0.54531250E-02 (rad/sec.)

REAL PART	IMAGINARY PART
1 TO 7	0.6187E-02
1 TO 7	0.5157E-02
8 TO 14	0.2133E-05
8 TO 14	-0.1046E-08
15 TO 21	0.2515E-06
15 TO 21	-0.6436E-08
22 TO 28	-0.1432E-02
22 TO 28	-0.1350E-06
29 TO 35	0.1228E-02
29 TO 35	-0.7089E-01
36 TO 42	0.1235E-02
36 TO 42	-0.1252E-00
43 TO 49	0.1254E-02
43 TO 49	0.5460E-02
50 TO 56	0.5453E-02
50 TO 56	0.1541E-05
57 TO 63	0.5991E-05
57 TO 63	0.7411E-10
64 TO 70	0.7541E-10
64 TO 70	-0.1257E-06
71 TO 77	0.5740E-07
71 TO 77	-0.3940E-04
78 TO 84	0.5150E-04
78 TO 84	-0.2070E-00
85 TO 91	0.3291E-02
85 TO 91	-0.1042E-01
92 TO 98	0.3160E-02
92 TO 98	-0.1105E-03
99 TO 102	0.1505E-02
99 TO 102	0.2890E-00
1 TO 7	0.7615E-02
1 TO 7	0.5322E-02
8 TO 14	0.5570E-02
8 TO 14	0.1870E-05
15 TO 21	0.3264E-04
15 TO 21	-0.4169E-08
22 TO 28	0.5208E-08
22 TO 28	0.3760E-08
29 TO 35	0.3633E-02
29 TO 35	-0.1541E-02
36 TO 42	0.1571E-02
36 TO 42	-0.1737E-00
43 TO 49	0.1739E-02
43 TO 49	0.4687E-02
50 TO 56	0.4509E-02
50 TO 56	-0.6655E-07
57 TO 63	0.1435E-06
57 TO 63	0.6410E-09
64 TO 70	0.6549E-06
64 TO 70	0.3580E-08
71 TO 77	0.1235E-08
71 TO 77	-0.1191E-03
78 TO 84	0.1320E-03
78 TO 84	-0.3848E-00
85 TO 91	0.4238E-03
85 TO 91	-0.7649E-01
92 TO 98	0.2695E-01
92 TO 98	-0.1759E-07
99 TO 102	0.4883E-01
99 TO 102	-0.2591E-09
1 TO 7	0.4433E-08
1 TO 7	-0.1609E-05
8 TO 14	0.3823E-08
8 TO 14	-0.5597E-08
15 TO 21	0.2523E-07
15 TO 21	0.3758E-08
22 TO 28	0.1054E-00
22 TO 28	0.7580E-02
29 TO 35	0.4991E-02
29 TO 35	-0.1046E-00
36 TO 42	0.5494E-09
36 TO 42	0.4652E-02
43 TO 49	0.3224E-09
43 TO 49	-0.5738E-07
50 TO 56	0.3455E-08
50 TO 56	0.6155E-09
57 TO 63	0.7419E-05
57 TO 63	0.3537E-08
64 TO 70	0.6190E-02
64 TO 70	-0.7449E-05
71 TO 77	0.4488E-06
71 TO 77	-0.2607E-01
78 TO 84	0.5612E-09
78 TO 84	-0.3324E-01
85 TO 91	0.1563E-08
85 TO 91	-0.4343E-09
92 TO 98	0.1656E-03
92 TO 98	-0.2592E-09
99 TO 102	0.1656E-03
99 TO 102	0.6306E-11
1 TO 7	0.2821E-08
1 TO 7	-0.4433E-08
8 TO 14	0.2891E-02
8 TO 14	-0.3823E-08
15 TO 21	0.2812E-00
15 TO 21	-0.2523E-07
22 TO 28	0.4877E-02
22 TO 28	0.1054E-00
29 TO 35	0.7456E-07
29 TO 35	0.4991E-02
36 TO 42	0.5494E-09
36 TO 42	-0.5494E-09
43 TO 49	0.3529E-08
43 TO 49	0.3224E-09
50 TO 56	0.7210E-05
50 TO 56	-0.3455E-08
57 TO 63	0.2036E-00
57 TO 63	-0.7419E-05
64 TO 70	0.6190E-02
64 TO 70	-0.6190E-02
71 TO 77	0.6056E-09
71 TO 77	-0.4488E-06
78 TO 84	0.1671E-08
78 TO 84	-0.5612E-09
85 TO 91	0.1598E-04
85 TO 91	-0.1563E-08
92 TO 98	0.5778E-00
92 TO 98	-0.1656E-03
99 TO 102	0.5778E-00
99 TO 102	-0.1656E-03
1 TO 7	0.2815E-02
1 TO 7	-0.4433E-08
8 TO 14	0.2722E-00
8 TO 14	-0.3823E-08
15 TO 21	0.5288E-02
15 TO 21	-0.2523E-07
22 TO 28	0.1703E-06
22 TO 28	0.4877E-02
29 TO 35	0.3497E-08
29 TO 35	0.7456E-07
36 TO 42	0.3529E-08
36 TO 42	-0.5494E-09
43 TO 49	0.7172E-03
43 TO 49	0.3529E-08
50 TO 56	0.2026E-00
50 TO 56	-0.7210E-05
57 TO 63	0.5395E-02
57 TO 63	-0.2036E-00
64 TO 70	0.4189E-06
64 TO 70	-0.6190E-02
71 TO 77	0.6056E-09
71 TO 77	-0.4488E-06
78 TO 84	0.1671E-08
78 TO 84	-0.5612E-09
85 TO 91	0.1598E-04
85 TO 91	-0.1563E-08
92 TO 98	0.5778E-00
92 TO 98	-0.1656E-03
99 TO 102	0.5778E-00
99 TO 102	-0.1656E-03
1 TO 7	0.2237E-02
1 TO 7	-0.4433E-08
8 TO 14	0.2299E-00
8 TO 14	-0.3823E-08
15 TO 21	0.5380E-02
15 TO 21	-0.2523E-07
22 TO 28	0.1329E-05
22 TO 28	0.4877E-02
29 TO 35	0.1696E-08
29 TO 35	0.7456E-07
36 TO 42	0.1267E-06
36 TO 42	-0.1329E-05
43 TO 49	0.5657E-03
43 TO 49	-0.1267E-06
50 TO 56	0.1482E-00
50 TO 56	0.5657E-03
57 TO 63	0.5917E-02
57 TO 63	-0.1482E-00
64 TO 70	0.1624E-04
64 TO 70	-0.1491E-00
71 TO 77	0.1227E-09
71 TO 77	0.2090E-04
78 TO 84	0.5458E-07
78 TO 84	0.1329E-09
85 TO 91	0.1938E-04
85 TO 91	0.1955E-06
92 TO 98	0.4590E-00
92 TO 98	0.2226E-04
99 TO 102	0.4590E-00
99 TO 102	0.2226E-04
1 TO 7	0.2815E-02
1 TO 7	-0.4433E-08
8 TO 14	0.2722E-00
8 TO 14	-0.3823E-08
15 TO 21	0.5288E-02
15 TO 21	-0.2523E-07
22 TO 28	0.1703E-06
22 TO 28	0.4877E-02
29 TO 35	0.3497E-08
29 TO 35	0.7456E-07
36 TO 42	0.3529E-08
36 TO 42	-0.5494E-09
43 TO 49	0.7172E-03
43 TO 49	0.3529E-08
50 TO 56	0.2026E-00
50 TO 56	-0.7210E-05
57 TO 63	0.5395E-02
57 TO 63	-0.2036E-00
64 TO 70	0.4189E-06
64 TO 70	-0.6190E-02
71 TO 77	0.6056E-09
71 TO 77	-0.4488E-06
78 TO 84	0.1671E-08
78 TO 84	-0.5612E-09
85 TO 91	0.1598E-04
85 TO 91	-0.1563E-08
92 TO 98	0.5778E-00
92 TO 98	-0.1656E-03
99 TO 102	0.5778E-00
99 TO 102	-0.1656E-03

EIGENVECTOR FOR ROOT NO. 2

Mode 2, Frequency = 4.2026 Hz, $\Omega = 8$ RPM

EIGENVALUE = 0.26406250E 02 (rad/sec.)

REAL PART

1 10 7
 8 10 14
 15 10 21
 22 10 28
 29 10 35
 36 10 42
 43 10 49
 50 10 56
 57 10 63
 64 10 70
 71 10 77
 78 10 84
 85 10 91
 92 10 98
 99 10 102

-0.373E-05
 0.120E-05
 -0.398E-01
 0.4737E-04
 -0.1155E-07
 0.7054E-08
 0.3901E-06
 -0.1185E-05
 -0.9936E-01
 -0.5875E-07
 -0.9877E-03
 0.911E-10
 -0.4476E-05
 -0.100E 01

0.1209E-05
 -0.4889E-01
 -0.4745E-04
 -0.1164E-02
 0.8382E-08
 0.7800E-06
 0.1190E-05
 -0.3121E-01
 -0.5762E-01
 -0.1147E-02
 0.4894E-08
 0.3025E-09
 -0.2520E-05
 0.3037E 00
 -0.4651E-07
 0.2068E-02

-0.5189E-04
 -0.1169E-02
 0.8270E-08
 -0.7732E-06
 0.1195E-05
 -0.3122E-01
 0.1461E-04
 -0.1142E-02
 0.4830E-08
 0.5509E-09
 -0.1315E-05
 0.2955E 00
 -0.5995E-07
 0.2270E-02
 0.8248E-12

-0.1169E-02
 0.8761E-09
 0.2195E-05
 0.1196E-05
 -0.3259E-01
 -0.1472E-04
 -0.1148E-02
 0.5905E-08
 0.9014E-09
 0.4874E-09
 0.1718E-09
 0.8097E-06
 0.7595E 00
 -0.6239E-07
 0.2520E-03
 0.2991E-08

7.8758E-08
 -0.2184E-05
 0.1204E-05
 -0.3260E-01
 0.3045E-04
 -0.1148E-02
 0.5905E-08
 0.9014E-09
 0.4874E-09
 0.5993E-06
 0.1309E 00
 -0.6270E-07
 -0.4901E-03
 -0.1431E-07
 -0.3608E-09

0.3741E-05
 0.1205E-05
 -0.3983E-01
 -0.3055E-04
 -0.1155E-02
 0.5924E-08
 0.9381E-09
 0.9927E-06
 -0.1492E 00
 -0.6142E-07
 -0.7097E-03
 -0.2157E-07
 -0.2534E-09
 -0.4108E-05

0.4434E-05
 -0.8573E-10
 -0.9659E-09
 0.3124E-08
 -0.9923E-04
 -0.2472E-05
 -0.4354E-05
 0.1799E-10
 0.3641E-09
 0.2895E-09
 0.945E-03
 -0.1433E-05
 0.9503E-05
 0.1126E-10

0.1518E-09
 -0.2487E-07
 0.6942E-08
 -0.1488E-03
 -0.1134E-06
 -0.4354E-05
 -0.1195E-10
 0.3994E-08
 -0.2171E-09
 0.4968E-06
 0.9283E-07
 -0.1861E-05
 -0.5354E-10
 0.5176E-07

IMAGINARY PART

1 10 7
 8 10 14
 15 10 21
 22 10 28
 29 10 35
 36 10 42
 43 10 49
 50 10 56
 57 10 63
 64 10 70
 71 10 77
 78 10 84
 85 10 91
 92 10 98
 99 10 102

-0.4798E-06
 -0.4434E-05
 0.1473E-09
 -0.2954E-08
 0.5402E-08
 0.1309E-03
 -0.1305E-06
 -0.4333E-05
 0.1799E-10
 0.1269E-07
 -0.5997E-09
 0.1121E-02
 -0.1124E-05
 0.7846E-05
 0.2713E-19

-0.4434E-05
 -0.8573E-10
 -0.9659E-09
 0.3124E-08
 -0.9923E-04
 -0.2472E-05
 -0.4354E-05
 0.1799E-10
 0.3641E-09
 0.2895E-09
 0.945E-03
 -0.1433E-05
 0.9503E-05
 0.1126E-10

0.3065E-03
 -0.8678E-07
 -0.4417E-05
 -0.7800E-10
 0.2813E-09
 0.3745E-08
 -0.1057E-03
 -0.1584E-06
 0.1799E-10
 0.1799E-10
 0.2117E-07
 -0.9618E-09
 0.1153E-02
 -0.5873E-03
 0.7851E-05

0.9878E-09
 -0.6423E-04
 -0.4510E-06
 -0.4417E-05
 0.0641E-10
 0.1659E-09
 0.4948E-09
 -0.1162E-02
 -0.2332E-07
 -0.4359E-05
 -0.3435E-10
 0.2541E-07
 -0.1449E-07
 -0.8939E-03
 -0.5876E-05

0.9878E-09
 -0.6423E-04
 -0.4510E-06
 -0.4417E-05
 0.0641E-10
 0.1659E-09
 0.4948E-09
 -0.1162E-02
 -0.2332E-07
 -0.4359E-05
 -0.3435E-10
 0.2541E-07
 -0.1449E-07
 -0.8939E-03
 -0.5876E-05

0.9878E-09
 -0.6423E-04
 -0.4510E-06
 -0.4417E-05
 0.0641E-10
 0.1659E-09
 0.4948E-09
 -0.1162E-02
 -0.2332E-07
 -0.4359E-05
 -0.3435E-10
 0.2541E-07
 -0.1449E-07
 -0.8939E-03
 -0.5876E-05

0.9878E-09
 -0.6423E-04
 -0.4510E-06
 -0.4417E-05
 0.0641E-10
 0.1659E-09
 0.4948E-09
 -0.1162E-02
 -0.2332E-07
 -0.4359E-05
 -0.3435E-10
 0.2541E-07
 -0.1449E-07
 -0.8939E-03
 -0.5876E-05

0.9878E-09
 -0.6423E-04
 -0.4510E-06
 -0.4417E-05
 0.0641E-10
 0.1659E-09
 0.4948E-09
 -0.1162E-02
 -0.2332E-07
 -0.4359E-05
 -0.3435E-10
 0.2541E-07
 -0.1449E-07
 -0.8939E-03
 -0.5876E-05

FIGURE VECTOR FOR POINT NO. 3 Mode 3, Frequency = 8.4068 Hz, $\Omega = 8$ RPM

FIGURE VALUE = 0.5292256E-02 (rad/sec.)

REAL PART	IMAGINARY PART
1 TO 7	0.5231E-01
8 TO 14	0.1410E-04
15 TO 21	0.6929E-07
22 TO 28	0.2409E-06
29 TO 35	0.2611E-04
36 TO 42	0.9999E-03
43 TO 49	0.1120E-01
50 TO 56	0.1066E-04
57 TO 63	0.1735E-09
64 TO 70	0.2419E-06
71 TO 77	0.4556E-03
78 TO 84	0.5597E-02
85 TO 91	0.2062E-00
92 TO 98	0.2651E-03
99 TO 105	0.5430E-00
1 TO 7	0.4101E-03
8 TO 14	0.1155E-05
15 TO 21	0.2162E-08
22 TO 28	0.1218E-09
29 TO 35	0.1498E-04
36 TO 42	0.1025E-01
43 TO 49	0.1700E-02
50 TO 56	0.402E-09
57 TO 63	0.303E-09
64 TO 70	0.1136E-00
71 TO 77	0.4440E-05
78 TO 84	0.3977E-02
85 TO 91	0.1634E-02
92 TO 98	0.3552E-09
99 TO 105	0.9157E-09
1 TO 7	0.1487E-04
8 TO 14	0.7508E-07
15 TO 21	0.2610E-06
22 TO 28	0.1327E-03
29 TO 35	0.5457E-02
36 TO 42	0.1115E-01
43 TO 49	0.1030E-04
50 TO 56	0.1700E-09
57 TO 63	0.2425E-06
64 TO 70	0.2541E-04
71 TO 77	0.5364E-03
78 TO 84	0.1541E-00
85 TO 91	0.2568E-04
92 TO 98	0.5959E-09
99 TO 105	0.4366E-07
1 TO 7	0.1161E-05
8 TO 14	0.1846E-09
15 TO 21	0.1218E-09
22 TO 28	0.2548E-04
29 TO 35	0.1026E-01
36 TO 42	0.2411E-03
43 TO 49	0.2133E-06
50 TO 56	0.2930E-09
57 TO 63	0.1140E-09
64 TO 70	0.2366E-04
71 TO 77	0.9419E-02
78 TO 84	0.1300E-07
85 TO 91	0.2485E-08
92 TO 98	0.9161E-09
99 TO 105	0.2369E-10
1 TO 7	0.7760E-07
8 TO 14	0.2650E-06
15 TO 21	0.1382E-03
22 TO 28	0.4816E-02
29 TO 35	0.1143E-01
36 TO 42	0.1031E-04
43 TO 49	0.1782E-07
50 TO 56	0.2411E-06
57 TO 63	0.1713E-04
64 TO 70	0.4804E-03
71 TO 77	0.1131E-00
78 TO 84	0.4666E-04
85 TO 91	0.3626E-09
92 TO 98	0.6363E-06
99 TO 105	0.3708E-02
1 TO 7	0.1893E-08
8 TO 14	0.1237E-09
15 TO 21	0.2849E-04
22 TO 28	0.1019E-01
29 TO 35	0.1519E-03
36 TO 42	0.2041E-06
43 TO 49	0.2849E-08
50 TO 56	0.1125E-09
57 TO 63	0.2125E-06
64 TO 70	0.1026E-01
71 TO 77	0.9714E-03
78 TO 84	0.6413E-08
85 TO 91	0.2006E-08
92 TO 98	0.2541E-10
99 TO 105	0.1355E-04
1 TO 7	0.2652E-05
8 TO 14	0.1442E-07
15 TO 21	0.2552E-01
22 TO 28	0.1113E-01
29 TO 35	0.8579E-05
36 TO 42	0.2459E-04
43 TO 49	0.3808E-06
50 TO 56	0.4185E-03
57 TO 63	0.1494E-05
64 TO 70	0.4173E-03
71 TO 77	0.2633E-01
78 TO 84	0.5050E-04
85 TO 91	0.3045E-09
92 TO 98	0.4573E-05
99 TO 105	0.1597E-02
1 TO 7	0.3379E-04
8 TO 14	0.6187E-02
15 TO 21	0.8601E-04
22 TO 28	0.3695E-06
29 TO 35	0.2623E-08
36 TO 42	0.1148E-09
43 TO 49	0.5491E-05
50 TO 56	0.1105E-01
57 TO 63	0.2314E-03
64 TO 70	0.6878E-08
71 TO 77	0.9521E-09
78 TO 84	0.2893E-08
85 TO 91	0.2633E-08
92 TO 98	0.4725E-10
99 TO 105	0.9753E-05
1 TO 7	0.5104E-01
8 TO 14	0.1140E-01
15 TO 21	0.1199E-05
22 TO 28	0.4007E-07
29 TO 35	0.2527E-06
36 TO 42	0.3955E-04
43 TO 49	0.4188E-03
50 TO 56	0.1151E-01
57 TO 63	0.1809E-04
64 TO 70	0.2330E-09
71 TO 77	0.1074E-07
78 TO 84	0.7051E-03
85 TO 91	0.6917E-03
92 TO 98	0.1000E 01
99 TO 105	
1 TO 7	0.1527E-02
8 TO 14	0.3573E-03
15 TO 21	0.8062E-06
22 TO 28	0.2644E-08
29 TO 35	0.1180E-09
36 TO 42	0.6041E-05
43 TO 49	0.1103E-01
50 TO 56	0.2177E-03
57 TO 63	0.1835E-07
64 TO 70	0.3059E-08
71 TO 77	0.1904E-10
78 TO 84	0.5232E-05
85 TO 91	0.6136E-02
92 TO 98	0.4574E-02
99 TO 105	

Mode 4. $F = 5.5 \text{ Hz}$ $\Omega = 8 \text{ RPM}$

EIGENVECTOR FOR POINT NO. = 4

EIGENVALUE = 0.54580078E 02 (rad/sec.)

REAL PART	IMAGINARY PART
1 TO 7	1 TO 7
8 TO 14	8 TO 14
15 TO 21	15 TO 21
22 TO 28	22 TO 28
29 TO 35	29 TO 35
36 TO 42	36 TO 42
43 TO 49	43 TO 49
50 TO 56	50 TO 56
57 TO 63	57 TO 63
64 TO 70	64 TO 70
71 TO 77	71 TO 77
78 TO 84	78 TO 84
85 TO 91	85 TO 91
92 TO 98	92 TO 98
99 TO 102	99 TO 102
1 TO 7	1 TO 7
8 TO 14	8 TO 14
15 TO 21	15 TO 21
22 TO 28	22 TO 28
29 TO 35	29 TO 35
36 TO 42	36 TO 42
43 TO 49	43 TO 49
50 TO 56	50 TO 56
57 TO 63	57 TO 63
64 TO 70	64 TO 70
71 TO 77	71 TO 77
78 TO 84	78 TO 84
85 TO 91	85 TO 91
92 TO 98	92 TO 98
99 TO 102	99 TO 102

Mode 1, frequency = 2.2851 Hz, $\Omega = 12$ RPM

...

...

...

7	0.2732E-00	-0.4531E-01	0.1344E-05	0.5414E-09	-0.1746E-07	-0.4746E-03	-0.2232E-00
14	-0.4531E-01	0.1344E-05	-0.5444E-09	-0.1746E-07	-0.4746E-03	0.1392E-00	-0.4526E-01
21	0.1250E-05	0.4891E-09	-0.1744E-07	-0.4678E-03	-0.1392E-00	-0.4527E-01	0.1249E-05
28	-0.4891E-09	-0.1744E-07	-0.4678E-03	-0.5590E-01	-0.4517E-01	0.1176E-05	0.3016E-09
35	-0.1740E-07	-0.4439E-03	-0.5590E-01	-0.4517E-01	0.1174E-05	-0.2994E-09	-0.1740E-07
42	-0.4439E-03	0.2978E-01	-0.4511E-01	0.1162E-05	0.1531E-09	-0.1737E-07	-0.4227E-03
49	-0.2977E-01	0.4511E-01	0.1162E-05	-0.1734E-07	-0.1531E-09	-0.4227E-03	0.4074E-05
56	-0.4506E-01	0.1156E-05	0.3360E-11	-0.1758E-07	-0.4038E-03	0.4058E-05	-0.2083E-01
63	0.1073E-04	0.3360E-11	-0.1758E-07	-0.4038E-03	0.4058E-05	-0.9505E-06	-0.9505E-06
70	0.3352E-11	0.1766E-07	-0.4038E-03	0.4860E-05	-0.3392E-02	0.3514E-05	0.3400E-11
77	-0.1407E-07	-0.1211E-03	0.5799E-05	-0.8267E-01	0.5399E-05	0.3444E-11	-0.1100E-07
84	0.1160E-03	0.6332E-05	-0.7245E-01	0.5977E-05	0.3473E-11	-0.8686E-08	0.2488E-03
91	0.7297E-05	-0.3087E-01	0.6044E-05	0.3567E-11	0.4325E-09	0.6500E-03	0.1234E-04
98	0.4270E-07	-0.4055E-05	0.3973E-11	0.4207E-07	0.1565E-02	0.1245E-04	0.1000E-01
105	-0.2073E-04	0.4004E-11	0.4311E-07	0.1543E-02	0.1565E-02	0.1245E-04	0.1000E-01
112	0.1952E-02	0.1302E-04	-0.3753E-08	-0.1146E-10	-0.7340E-10	-0.4680E-05	0.2132E-03
119	-0.3269E-03	0.5474E-08	-0.1162E-10	-0.7340E-10	-0.1203E-05	0.1025E-02	-0.2753E-04
126	-0.1724E-09	-0.1090E-10	-0.7332E-10	-0.4417E-05	0.2670E-05	-0.2860E-03	0.3418E-08
133	0.1102E-10	-0.7332E-10	0.9866E-06	0.3077E-03	-0.6330E-04	0.7506E-10	-0.8742E-11
140	-0.7315E-10	-0.3390E-05	-0.1034E-03	-0.2195E-03	0.1606E-08	-0.8749E-11	-0.7315E-10
147	0.1256E-04	0.1324E-03	-0.1256E-03	0.5067E-09	-0.5502E-11	-0.7300E-10	-0.2410E-05
154	-0.8721E-04	0.1868E-03	0.1171E-08	-0.5592E-11	-0.7300E-10	-0.7039E-06	-0.9436E-05
161	-0.1560E-03	0.8273E-09	-0.3604E-11	-0.7290E-10	-0.1690E-05	-0.3048E-05	-0.5663E-04
168	-0.3555E-08	-0.1916E-11	-0.7340E-10	-0.1490E-05	0.2817E-05	0.2778E-04	-0.7966E-08
175	-0.9869E-12	-0.7359E-10	-0.1490E-05	-0.2763E-03	-0.3078E-03	0.1098E-07	-0.9843E-12
182	-0.6211E-10	-0.4895E-06	-0.4857E-03	-0.3108E-03	0.1944E-07	-0.3444E-11	-0.5077E-10
189	0.3540E-04	-0.6394E-03	-0.2750E-03	0.2271E-07	0.1608E-10	-0.4162E-10	0.8284E-06
196	-0.9073E-03	-0.1622E-03	0.2307E-07	-0.2272E-10	0.1608E-10	0.2265E-05	-0.2331E-02
203	0.1407E-02	-0.1637E-07	-0.9699E-10	0.1537E-09	0.5593E-05	-0.2333E-02	0.3552E-02
210	-0.7339E-07	-0.9603E-10	-0.1551E-09	0.5556E-05	0.5556E-05	-0.2333E-02	0.3552E-02

EIGENVECTOR FOR ROOT NO. = 2 Mode 2, frequency = 4.2027 Hz, $\Omega = 12$ RPM

EIGENVALUE = 0.26406250E 07 (rad/sec)

REAL PART	IMAGINARY PART						
1 Y 7	0.3641E-05	0.1142E-05	-0.4962E-01	-0.5351E-04	-0.1144E-02	0.8770E-08	0.4101E-05
4 Y 14	0.1167E-05	-0.4861E-01	0.5353E-04	-0.1143E-02	0.8133E-08	-0.2082E-05	0.1151E-05
15 Y 21	-0.4027E-01	-0.4899E-02	-0.1139E-02	0.8436E-08	0.2479E-05	0.1168E-05	-0.4075E-01
22 Y 28	0.4891E-04	-0.1139E-02	0.8774E-03	-0.5548E-06	0.1154E-05	-0.3279E-01	-0.3144E-04
29 Y 35	-0.1130E-02	0.7245E-02	0.9988E-06	0.1162E-05	-0.3279E-01	0.3139E-04	-0.1130E-02
36 Y 42	0.7468E-09	-0.2502E-04	-0.1153E-05	-0.3137E-01	-0.1151E-05	-0.1123E-02	0.6212E-08
43 Y 49	0.5840E-06	0.1157E-05	-0.3136E-01	-0.1504E-04	-0.1123E-02	0.6321E-08	0.1649E-06
50 Y 56	0.1150E-05	-0.3022E-01	-0.5609E-07	-0.1117E-02	0.5222E-09	0.1748E-06	0.8315E-06
57 Y 63	-0.9800E-01	-0.5630E-07	-0.1122E-02	0.5348E-08	0.1929E-05	0.5082E-06	-0.1654E 00
64 Y 70	-0.5655E-07	-0.1124E-02	0.5406E-08	0.1263E-06	0.8652E-05	0.1272E 00	-0.5871E-07
71 Y 77	-0.9647E-03	-0.8342E-05	0.9374E-07	-0.1127E-05	-0.2524E 00	-0.6023E-07	-0.5877E-03
78 Y 84	0.1747E-07	0.8141E-07	-0.2273E-05	0.2871E 00	-0.6024E-07	-0.4679E-03	-0.2056E-07
85 Y 91	0.6760E-07	-0.2486E-05	0.2925E 00	-0.6172E-07	0.2793E-02	-0.1787E-07	0.2631E-07
92 Y 98	-0.3434E-05	-0.2553E 00	-0.6752E-07	0.2060E-02	0.4524E-02	0.1102E-07	-0.2833E-05
99 Y 102	-0.1000E 01	-0.6252E-07	0.1099E-02	0.1471E-09			
1 Y 7	-0.2840E-07	-0.4427E-07	-0.6529E-04	-0.1758E-06	-0.5069E-05	0.1142E-09	-0.8928E-07
4 Y 14	-0.2810E-07	0.2222E-04	-0.1208E-06	-0.5088E-06	-0.2465E-09	-0.8690E-08	-0.4032E-07
15 Y 21	-0.3516E-04	-0.1505E-04	-0.5048E-06	0.0974E-10	-0.4417E-07	-0.2731E-07	0.1149E-06
22 Y 28	-0.1084E-06	-0.5043E-04	-0.2289E-09	0.5118E-08	-0.3443E-07	-0.1433E-04	-0.7137E-07
29 Y 35	-0.5009E-04	0.4512E-10	-0.9672E-09	-0.2832E-07	-0.1427E-04	-0.4431E-07	-0.5009E-06
36 Y 42	-0.1658E-09	0.6371E-02	-0.3728E-07	-0.1195E-04	-0.6247E-09	-0.4976E-06	-0.5533E-11
43 Y 49	-0.1420E-09	-0.2923E-07	-0.1544E-04	0.6764E-08	-0.4975E-05	-0.11064E-09	0.4353E-09
50 Y 56	-0.3060E-07	-0.1745E-04	0.4953E-07	-0.6952E-06	-0.5229E-10	0.4457E-08	-0.2714E-07
57 Y 63	-0.4323E-04	0.2489E-04	-0.4972E-06	-0.6301E-10	0.4924E-09	-0.2300E-07	-0.7310E-04
64 Y 70	0.3584E-06	-0.4991E-06	-0.7182E-10	0.1513E-07	-0.3237E-07	0.5659E-04	0.5446E-06
71 Y 77	-0.4273E-06	0.2094E-10	0.2662E-07	-0.2273E-07	-0.1122E-02	-0.3911E-06	-0.3063E-06
78 Y 84	0.8020E-10	0.3701E-07	-0.1483E-07	0.1277E-05	0.3444E-07	-0.2101E-09	0.1045E-07
85 Y 91	0.3926E-07	-0.9036E-09	0.1309E-03	-0.1432E-03	0.1151E-05	0.1004E-09	0.6670E-09
92 Y 98	0.3247E-09	-0.1075E-02	-0.8504E-05	0.9045E-06	0.4412E-12	0.6907E-07	-0.6670E-09
99 Y 102	-0.4380E-03	-0.8507E-05	0.8915E-06	-0.1789E-16			0.3326E-08

STEINVECTIOR FOR ROHT N7.= 4

Mode 4, frequency = 8.6944 Hz, $\Omega = 12$ RPM

STEINVALUE= 0.54628006E 02 (rad/sec)

REAL PART

1	TO	7	0.9012E 00	0.8419E-02	0.2569E-05	-0.2611E-07	-0.9893E-15	-0.3245E-02	0.9108E 00
8	TO	14	0.8210E-02	0.7808E-05	0.1361E-07	-0.9893E-06	0.3273E-17	0.3370E 00	0.9546E-02
15	TO	21	0.7082E-06	-0.2160E-07	-0.8728E-06	-0.2913E-07	0.3403E 00	0.8393E-02	0.1016E-04
22	TO	28	0.8866E-08	-0.8788E-06	0.2941E-02	-0.8964E-01	0.8627E-17	0.1095E-04	-0.1100E-07
29	TO	35	-0.9402E-06	-0.1784E-02	-0.3968E-01	0.8556E-02	0.1132E-15	0.2973E-08	-0.9402E-05
35	TO	42	-----	-0.1787E 00	0.8592E-02	0.1130E-04	-0.3421E-15	-0.9130E-03	-0.9239E-03
43	TO	49	0.1791E 00	0.8558E-02	0.1143E-04	0.1373E-08	-0.9133E-15	0.8234E-03	-0.2093E 00
50	TO	56	0.8558E-02	0.1149E-04	0.5300E-09	-0.8937E-06	-0.5795E-15	-0.2121E 00	0.8936E-02
57	TO	63	-0.4282E-04	0.5471E-09	-0.3100E-06	-0.6532E-05	-0.2134E 00	0.9328E-02	-0.9730E-04
64	TO	70	0.5581E-09	-0.9073E-06	-0.5530E-05	-0.3088E 00	0.2507E-17	0.1170E-03	0.7382E-09
71	TO	77	-0.4808E-06	-0.4301E 00	-0.3940E 00	-0.9989E-02	0.1497E-15	0.8917E-09	0.5302E-07
73	TO	84	-0.8032E-04	-0.4301E 00	-0.1514E-01	0.1359E-03	0.9631E-15	0.3997E-04	-0.8026E-04
85	TO	91	-0.4770E 00	-0.1895E-01	0.6914E-04	0.1153E-08	0.1416E-15	-0.2489E-04	-0.6606E 00
82	TO	98	-0.1250E-02	-0.8025E-02	0.1935E-08	0.1959E-05	0.4577E-17	-0.6659E 00	-0.3378E-02
83	TO	102	-0.1088E-02	0.2038E-02	0.1587E-06	-0.3153E-04	-----	-----	-----

IMAGINARY PART

1	TO	7	0.3241E 00	0.2320E-01	0.6021E-05	0.1072E-07	0.1583E-17	-0.1210E-02	0.4129E 00
8	TO	14	0.2491E-01	-0.4788E-06	0.5321E-08	0.1689E-07	0.1496E-17	0.1137E 00	0.2253E-01
15	TO	21	0.4021E-05	0.1189E-07	0.1660E-07	-0.1087E-02	0.1531E 00	0.2359E-01	-0.3726E-05
22	TO	28	0.7090E-09	0.1661E-07	0.1338E-02	-0.4987E-01	0.2123E-15	0.1685E-05	0.1396E-07
29	TO	35	0.1605E-07	-0.6746E-02	-0.4633E-01	0.2172E-01	-0.2109E-15	0.1103E-07	0.1605E-07
34	TO	42	0.8051E-03	-0.8017E-01	0.2060E-01	0.8089E-06	0.1522E-17	0.1559E-07	-0.3266E-03
43	TO	49	-0.8144E-01	0.2082E-01	-0.1350E-05	0.1394E-07	0.1555E-17	0.3529E-03	-0.9337E-01
50	TO	56	0.2001E-01	-0.2082E-06	0.1551E-07	0.1526E-07	-0.3214E-17	-0.9450E-01	0.2198E-01
57	TO	63	0.6286E-07	0.1610E-07	0.1550E-07	-0.3323E-04	-0.8493E-17	0.2398E-01	0.1572E-05
44	TO	70	0.1642E-07	0.1577E-07	-0.3347E-04	-0.1332E 00	-0.2715E-17	-0.1859E-05	0.1670E-07
71	TO	77	0.5502E-08	-0.5199E-03	-0.1673E 00	-0.1146E 00	0.1997E-17	0.1623E-07	-0.3305E-08
73	TO	84	-0.5810E-03	-0.1817E 00	-0.31462E 00	-0.1660E-05	0.1542E-15	-0.7414E-08	-0.4615E-03
85	TO	91	-0.2004E 00	-0.1605E 00	-0.1125E-05	0.1239E-07	-0.7033E-15	0.6905E-04	-0.2742E 00
82	TO	98	0.1177E 00	-0.2463E-07	-0.5693E-09	-0.5401E-09	0.7311E-17	-0.6659E-04	-0.2742E 00
83	TO	102	-0.4090E-07	-0.5662E-05	0.1370E-10	-0.4308E-07	-----	-0.2747E 00	0.2076E 00

A. 4 VIBRATION MODE DATA
ARTIFICIAL "G" ROLLUP SOLAR ARRAY CONFIGURATION

CONTENTS

<u>TABLES</u>		<u>PAGE</u>
A-13	Modal Data, Zero Spin, NASTRAN Results	A-66
A-14	Mass-Geometry Data	A-68
A-15	Structural Model Data	A-81
A-16	Coriolis Force Matrix	A-83
A-17	Centrifugal Force Matrix	A-84
 <u>FIGURES</u>		
A-33	Structural Model	A-67
A-34to A-45	Mode Shapes, Zero Spin, NASTRAN Results	A-69 to A-80
Computer Listings of Modes	JPL Eigenvalue-Eigenvector Program Results for Spin Rates of 0, 4, 8, and 12 RPM. The degree of freedom sequence numbers and their corresponding node number are described in Table A-15.	A-85 to A-132

TABLE A-13 MODAL DATA, ARTIFICIAL "G" SOLAR ARRAY CONFIGURATION

ZERO SPIN, NASTRAN RESULTS

MODE	FREQUENCY (HZ)	GENERALIZED MASS (LBS·SEC ² /IN)
1	1.988690E-01	7.167556E-01
2	2.031515E-01	1.292258E 00
3	3.784189E-01	1.063949E 00
4	3.979775E-01	1.001644E 00
5	3.980261E-01	6.105757E-01
6	3.980299E-01	9.539251E-01
7	3.980302E-01	6.210912E-01
8	3.980324E-01	6.018445E-01
9	5.036502E-01	1.465514E 00
10	5.214531E-01	9.017351E-01
11	7.044816E-01	1.066769E 00
12	7.353594E-01	9.928919E-01
13	7.354488E-01	5.991474E-01
14	7.354546E-01	6.097919E-01
15	7.354608E-01	3.408555E-01
16	7.354647E-01	4.339064E-01
17	7.731657E-01	1.038958E 00
18	7.941298E-01	6.538786E-01
19	9.051450E-01	8.818594E-01
20	9.348565E-01	1.096124E 00
21	9.609272E-01	5.915505E-01
22	9.609300E-01	6.108234E-01
23	9.609315E-01	9.547644E-01
24	9.609319E-01	6.211393E-01
25	9.609702E-01	9.569576E-01
26	9.713216E-01	1.036751E 00
27	9.772314E-01	6.586445E-01
28	1.065360E 00	1.054537E 00
29	1.652814E 00	2.813135E-01
30	2.106756E 00	4.305415E-01
31	2.825887E 00	
32	3.842224E 00	
33	4.707289E 00	
34	5.006941E 00	
35	5.713924E 00	
36	5.790833E 00	
37	6.093275E 00	
38	6.099439E 00	
39	6.462175E 00	
40	8.135055E 00	
41	8.675979E 00	
42	9.569734E 00	
43	1.006908E 01	
44	1.067541E 01	
45	1.136669E 01	
46	1.143346E 01	
47	1.267509E 01	
48	1.302590E 01	
49	1.485096E 01	
50	1.497922E 01	

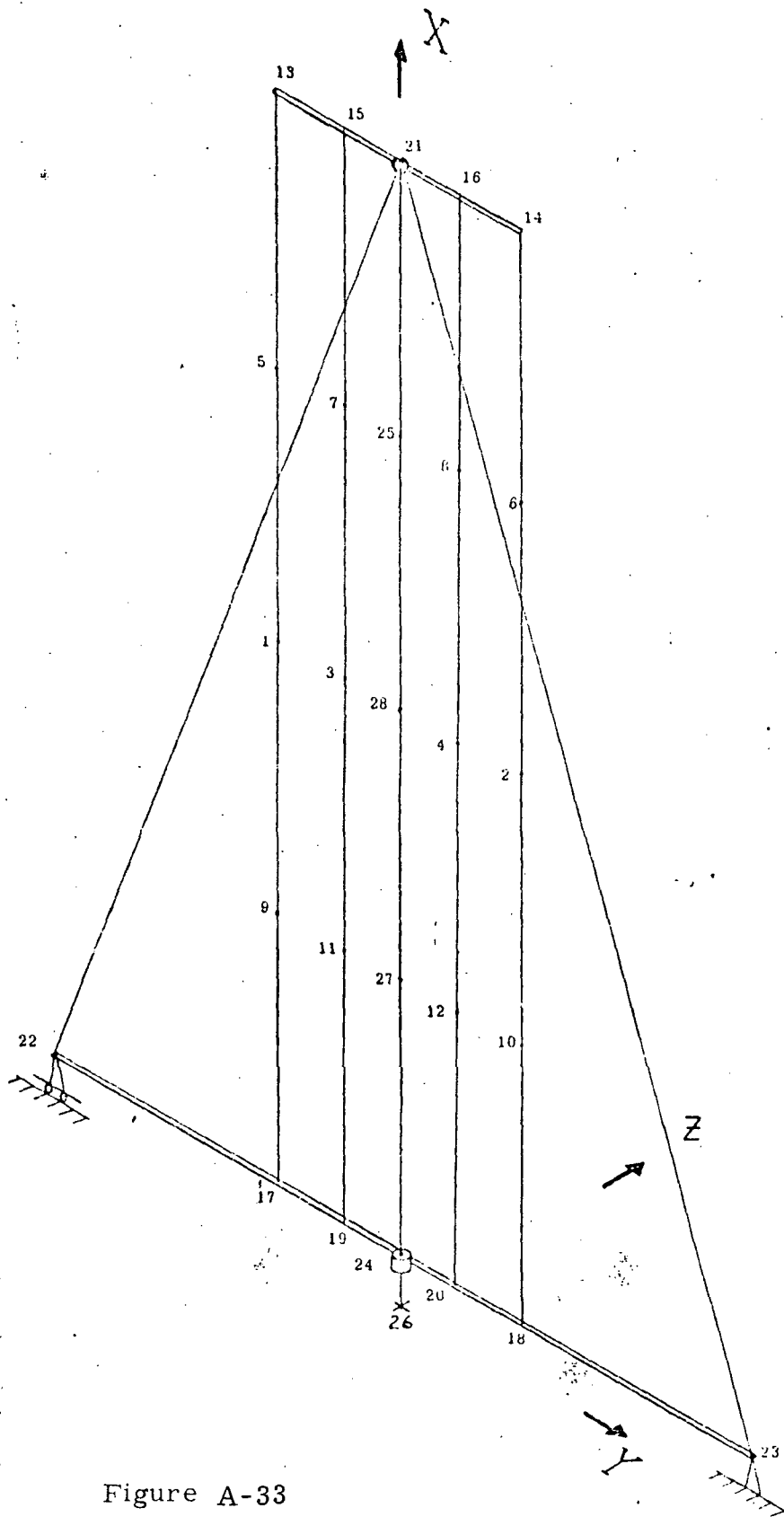


Figure A-33

SOLAR ARRAY ARTIFICIAL "G" STRUCTURAL MODEL

TABLE A-14
 MASS-GEOMETRY DATA
 FOR ARTIFICIAL "G" SOLAR ARRAY

Node	Mass*	X	Y	Z
1	.1252	552.	-130.5	.0
2	.1252	552.	130.5	.0
3	.1252	552.	-58.5	.0
4	.1252	552.	58.5	.0
5	.1252	804.	-130.5	.0
6	.1252	804.	130.5	.0
7	.1252	804.	-58.5	.0
8	.1252	804.	58.5	.0
9	.1252	300.	-130.5	.0
10	.1252	300.	130.5	.0
11	.1252	300.	-58.5	.0
12	.1252	300.	58.5	.0
13	.1394	1056.	-130.5	.0
14	.1394	1056.	130.5	.0
15	.0897	1056.	-58.5	.0
16	.0897	1056.	58.5	.0
17	.8609	48.	-130.5	.0
18	.8609	48.	130.5	.0
19	.0822	48.	-58.5	.0
20	.0822	48.	58.5	.0
21	.1418	1056.	.0	.0
22	.7873	48.	-369.0	.0
23	0.	48.	369.0	.0
24	.0996	48.	.0	.0
25	.1383	804.	.0	.0
26	0.	.0	.0	.0
27	.1383	300.	.0	.0
28	.1383	552.	.0	.0

* - Mass units are lb-sec²/in.

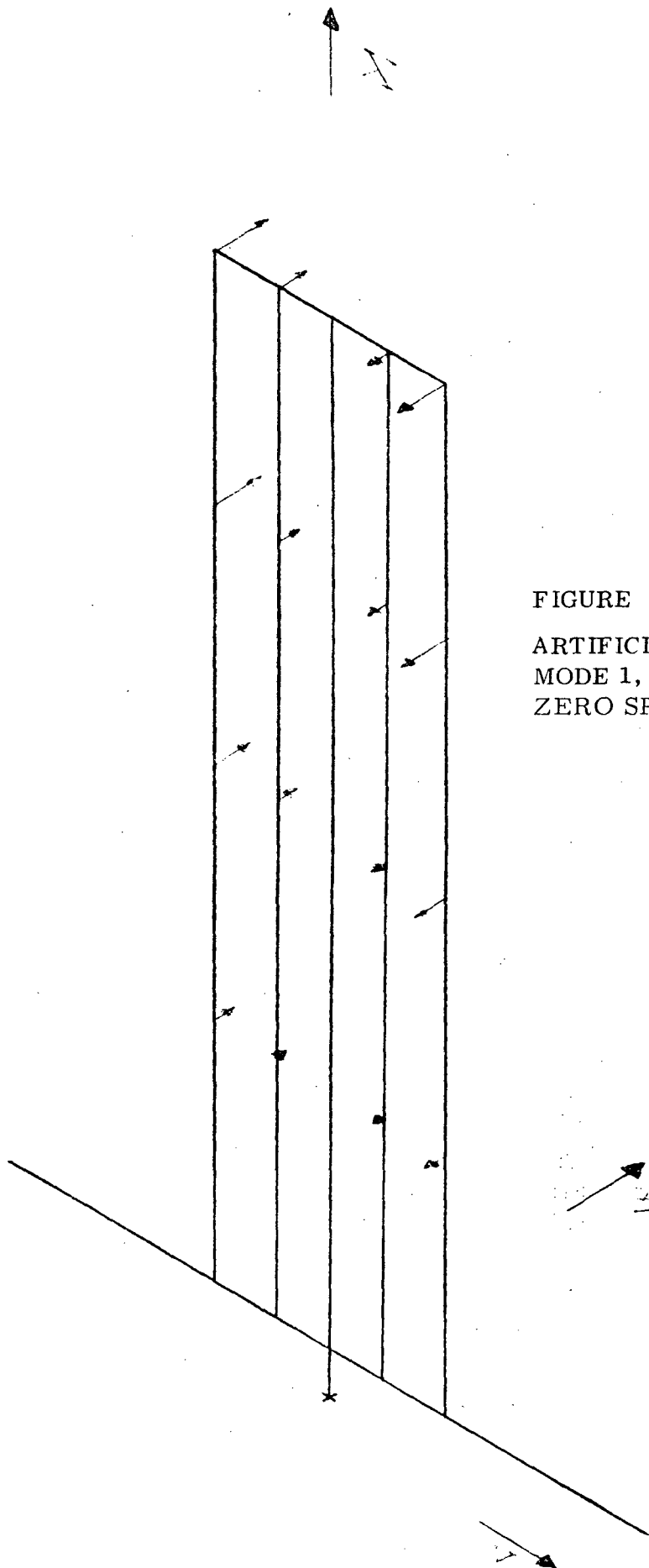


FIGURE A-34

ARTIFICIAL "G" SOLAR ARRAY
MODE 1, FREQUENCY = 0.199 Hz
ZERO SPIN

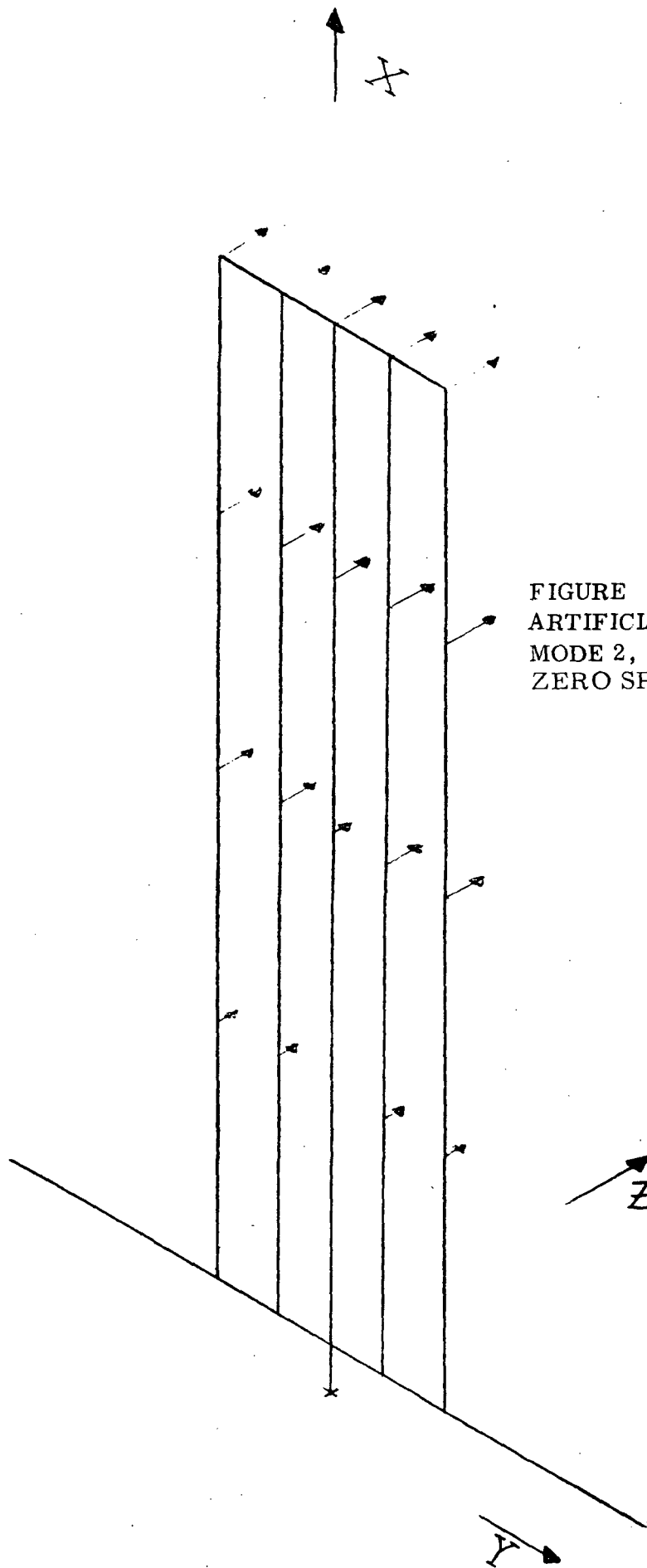
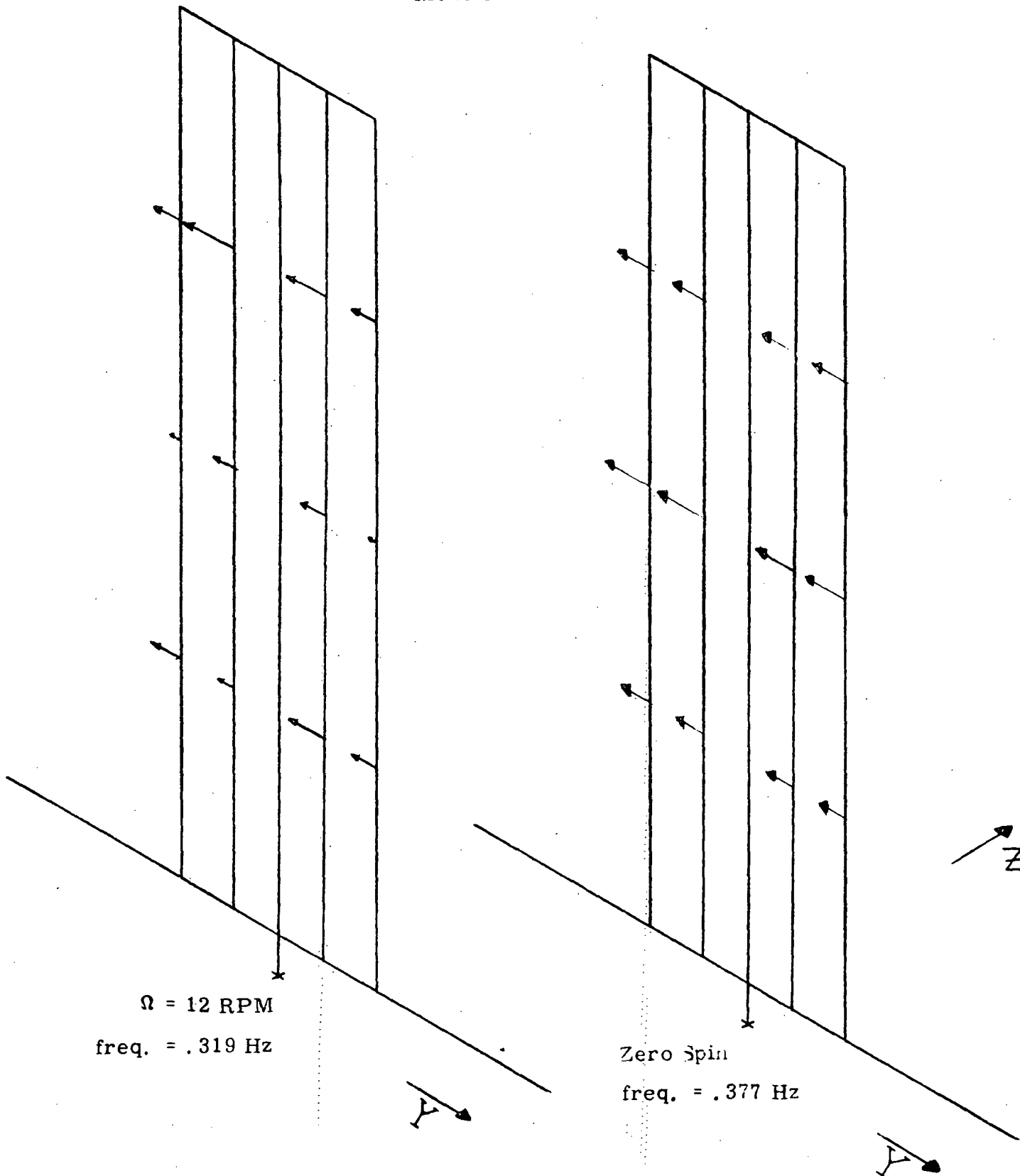


FIGURE A-35
ARTIFICIAL "G" SOLAR ARRAY
MODE 2, FREQUENCY = 0.203 Hz
ZERO SPIN

Figure A-36
Artificial "G" Solar Array
Mode 3



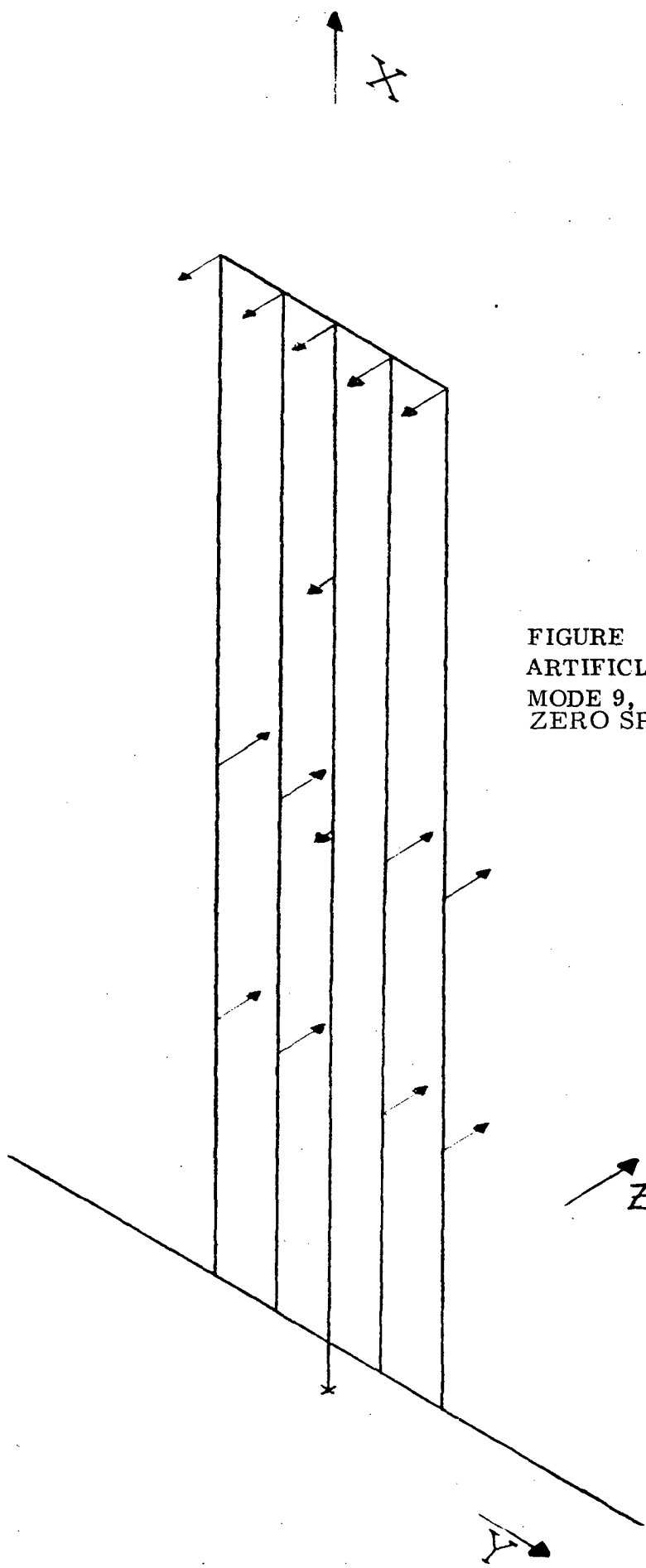


FIGURE A-37
ARTIFICIAL "G" SOLAR ARRAY
MODE 9, FREQUENCY = 0.504 Hz
ZERO SPIN

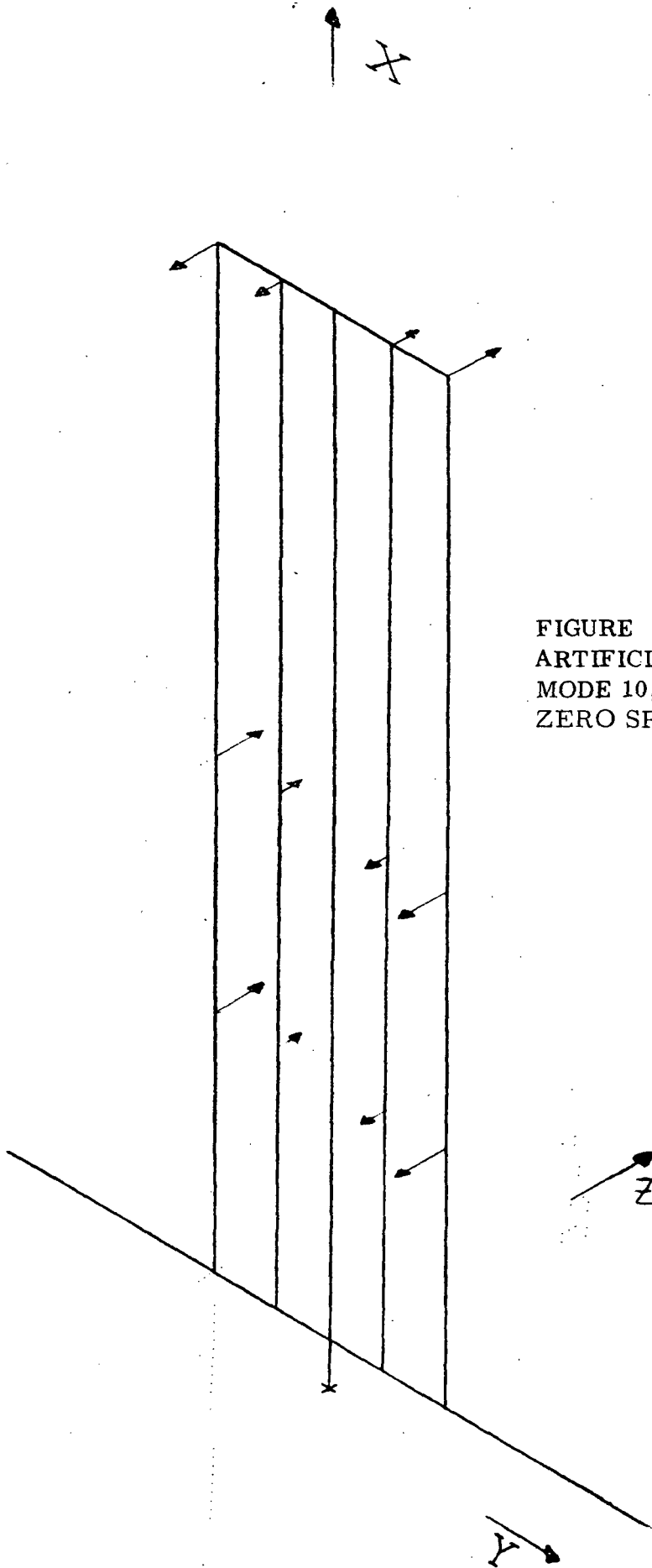


FIGURE A-38
ARTIFICIAL "G" SOLAR ARRAY
MODE 10, FREQUENCY = 0.521 Hz
ZERO SPIN

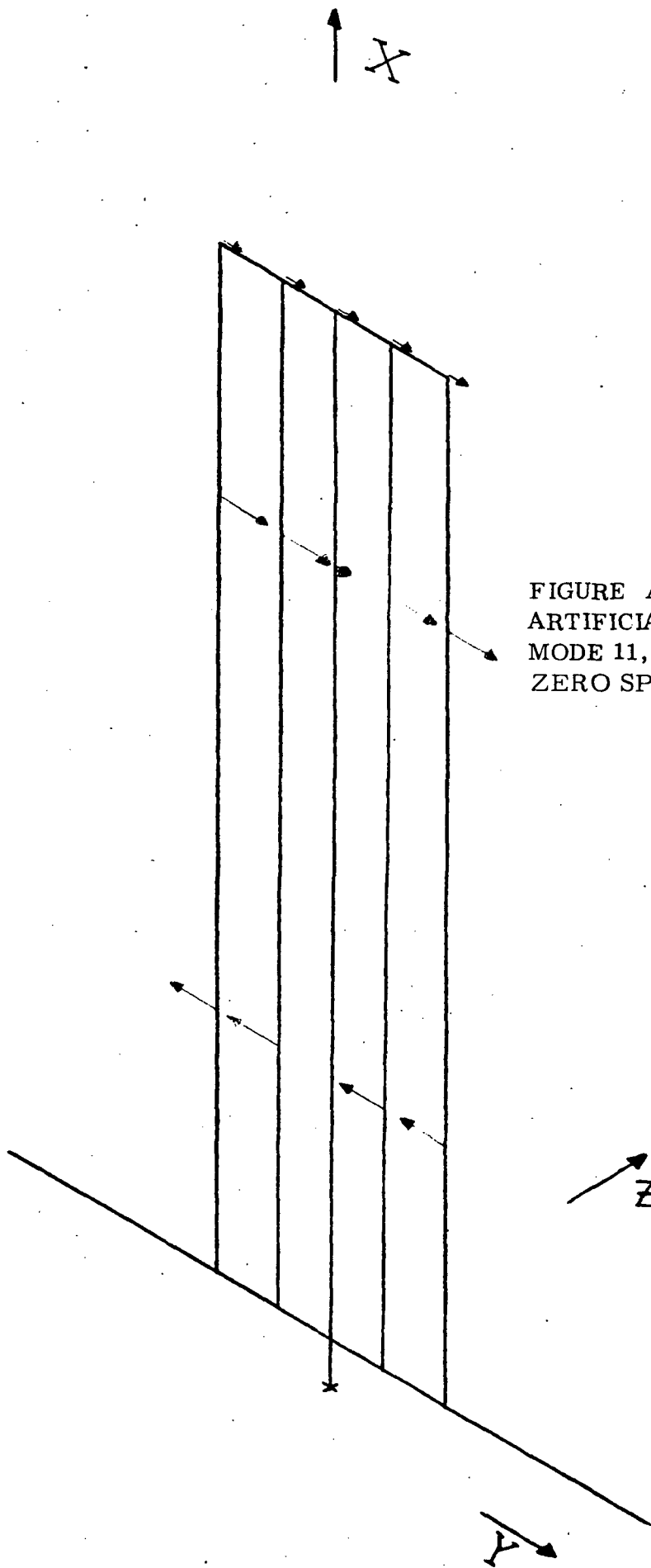


FIGURE A-39
ARTIFICIAL "G" SOLAR ARRAY
MODE 11, FREQUENCY = 0.704 Hz
ZERO SPIN

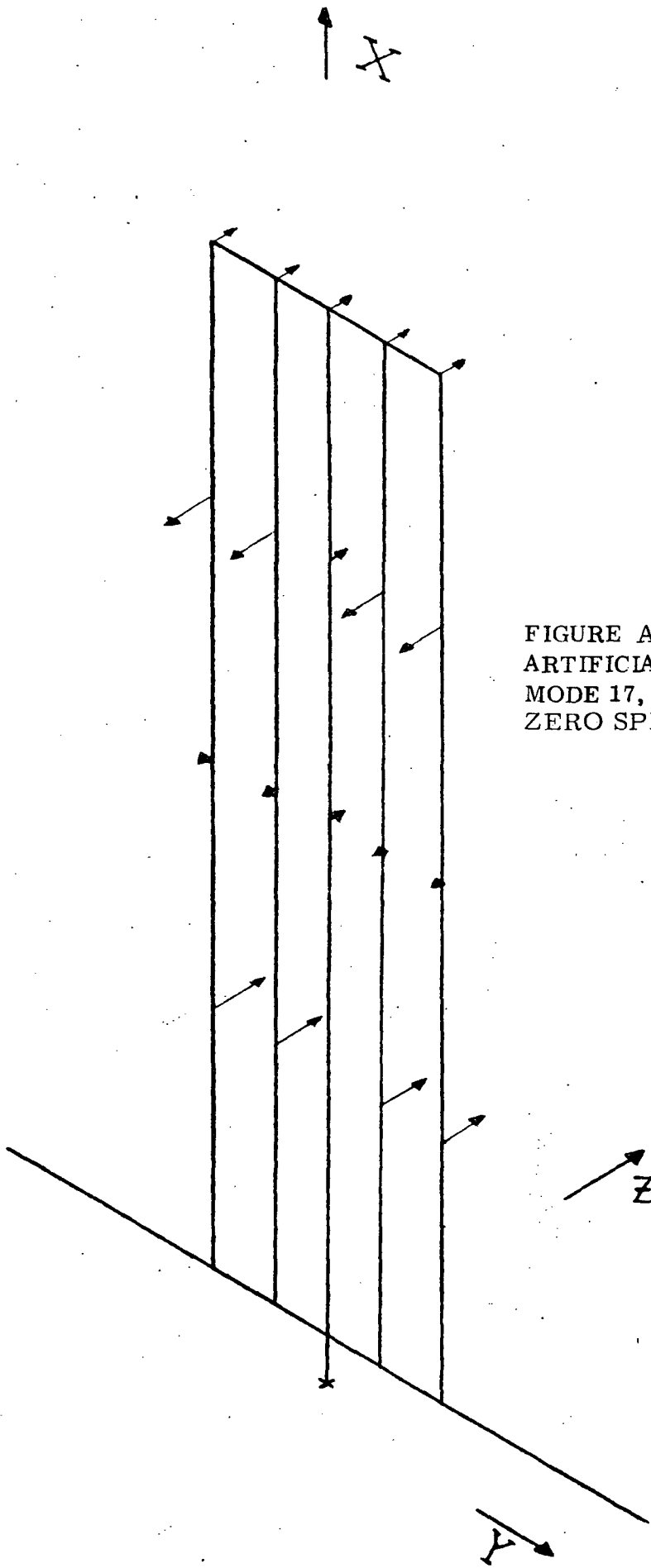


FIGURE A-40
ARTIFICIAL "G" SOLAR ARRAY
MODE 17, FREQUENCY = 0.778 Hz
ZERO SPIN

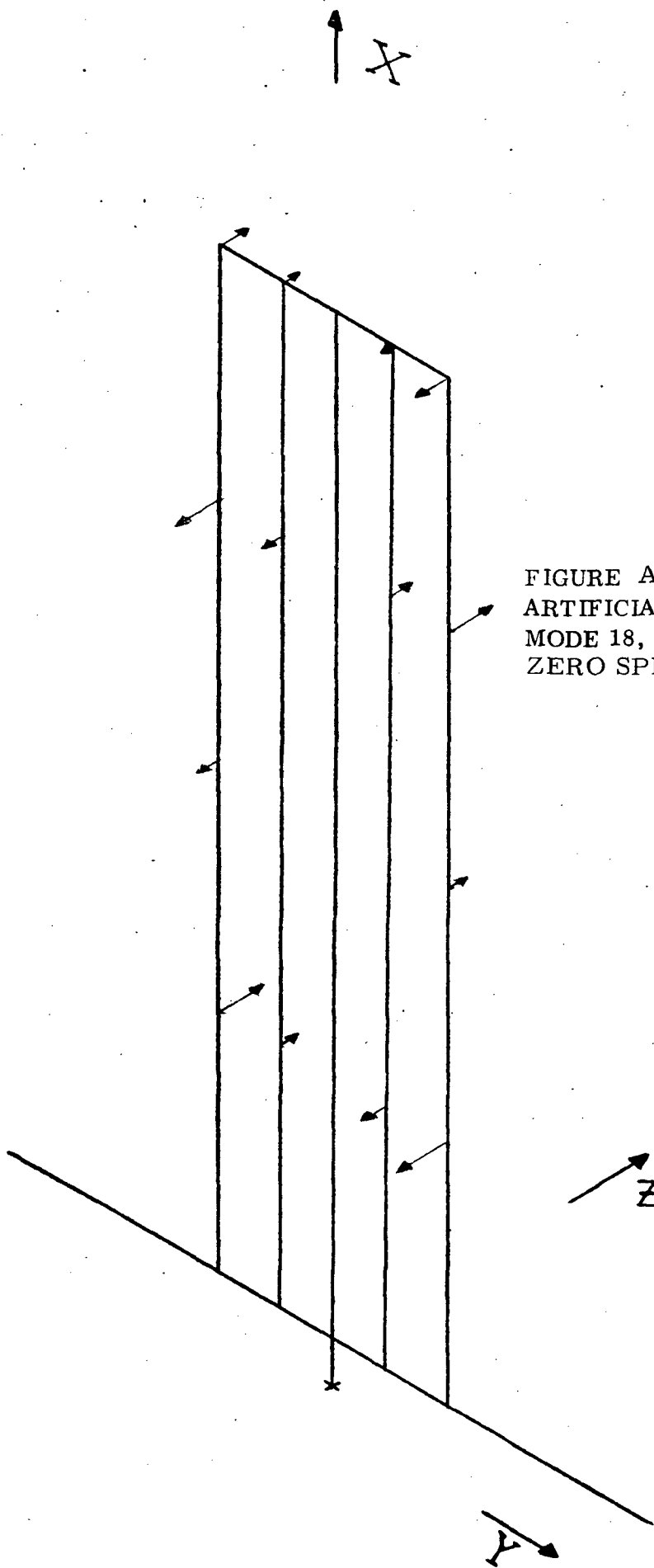


FIGURE A-41
ARTIFICIAL "G" SOLAR ARRAY
MODE 18, FREQUENCY = 0.794 Hz
ZERO SPIN

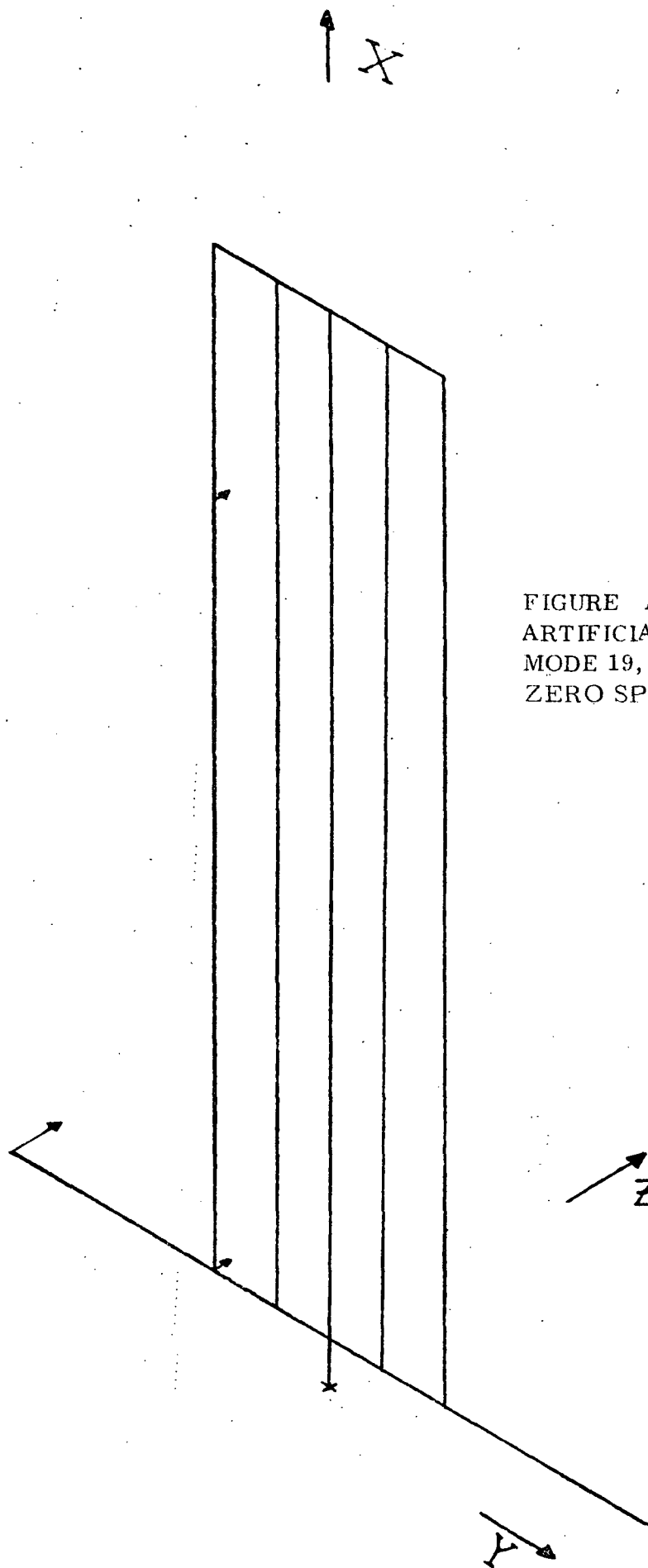


FIGURE A-42
ARTIFICIAL "G" SOLAR ARRAY
MODE 19, FREQUENCY = 0.905 Hz
ZERO SPIN

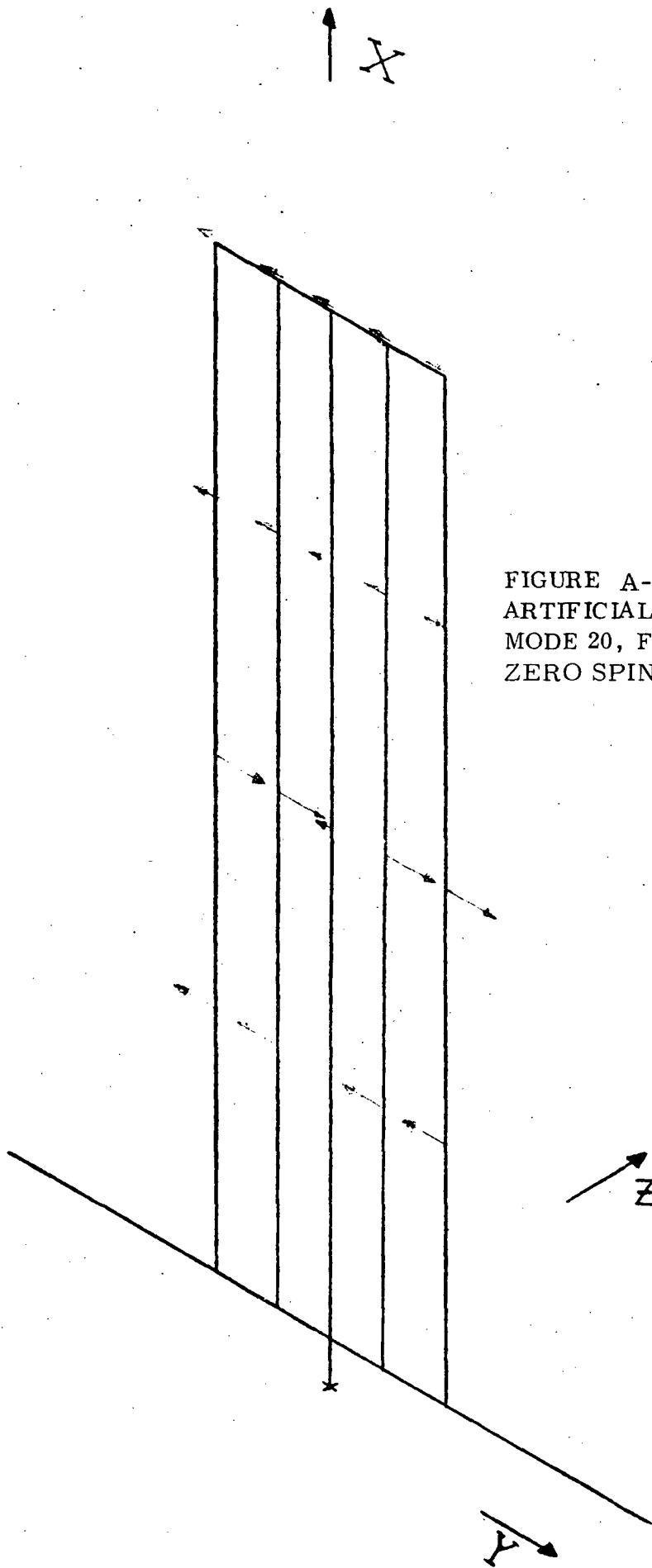


FIGURE A-43
ARTIFICIAL "G" SOLAR ARRAY
MODE 20, FREQUENCY = 0.935 Hz
ZERO SPIN

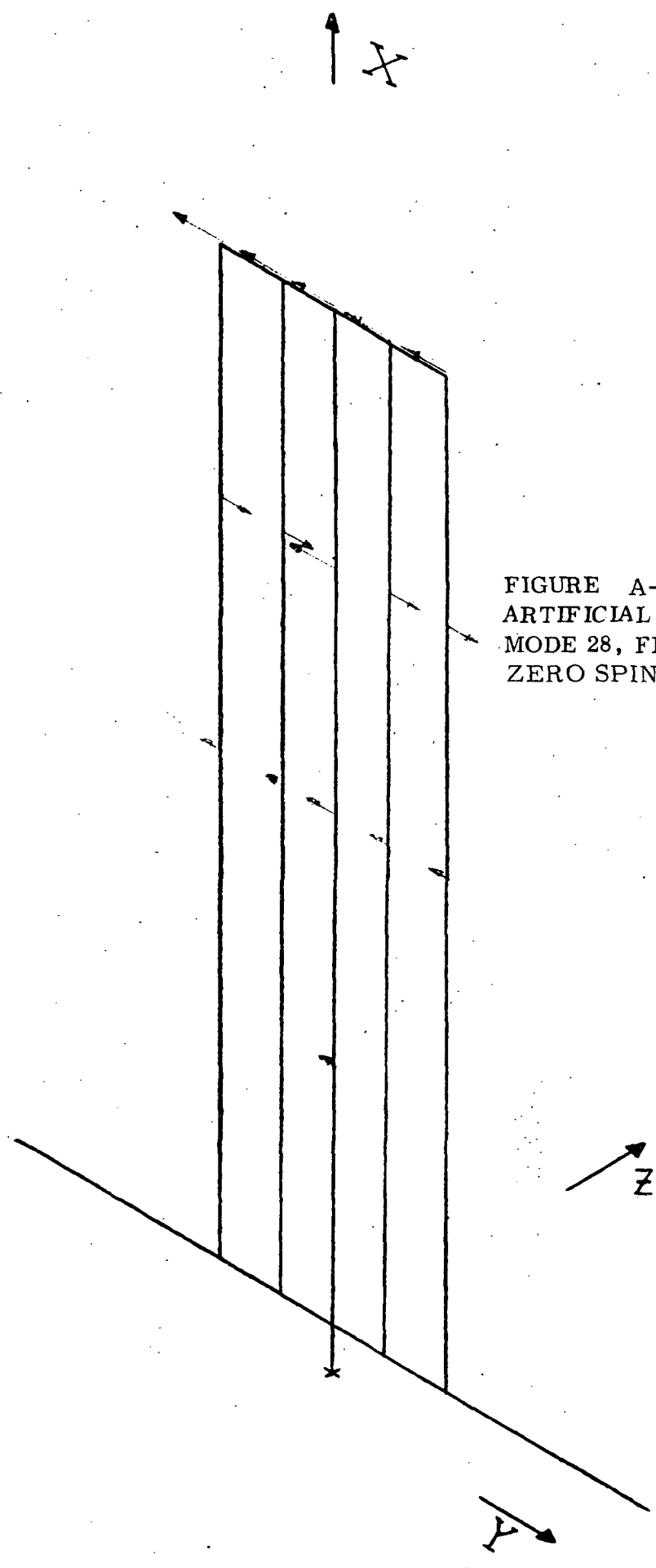


FIGURE A-44
ARTIFICIAL "G" SOLAR ARRAY
MODE 28, FREQUENCY = 1.07 Hz
ZERO SPIN

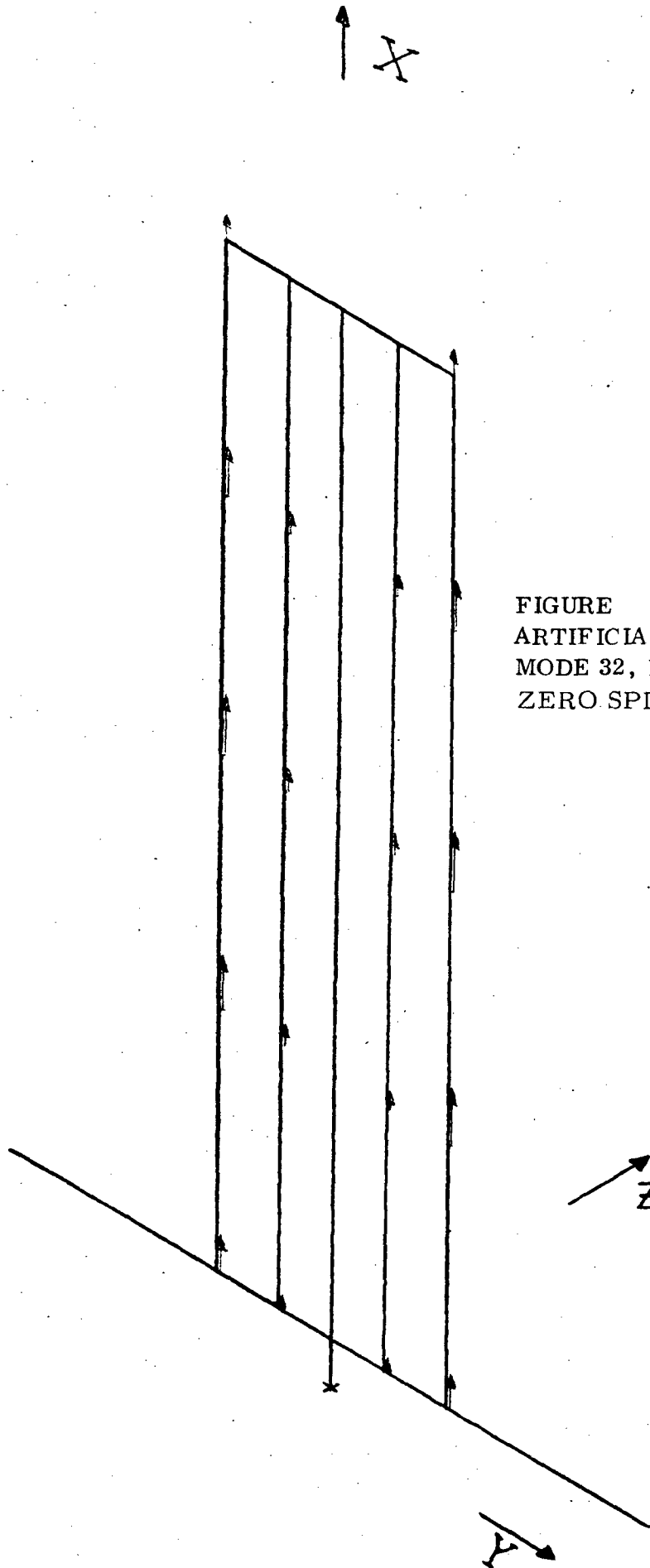


FIGURE A-45
ARTIFICIAL "G" SOLAR ARRAY
MODE 32, FREQUENCY = 3.84 Hz
ZERO SPIN

TABLE A-15
 Artificial "G" Solar Array
 Finite Element Model Data

Node	Mass lb-sec ² /in	No. of Structural D. O. F.	D. O. F. Sequence No.
1	0.1252	3	1 - 3
2	0.1252	3	4 - 6
3	0.1252	3	7 - 9
4	0.1252	3	10 - 12
5	0.1252	3	13 - 15
6	0.1252	3	16 - 18
7	0.1252	3	19 - 21
8	0.1252	3	22 - 24
9	0.1252	3	25 - 27
10	0.1252	3	28 - 30
11	0.1252	3	31 - 33
12	0.1252	3	34 - 36
13	0.1394	5	37 - 41
14	0.1394	5	42 - 46
15	0.0897	5	47 - 51
16	0.0897	5	52 - 56
17	0.8609	5	57 - 61
18	0.8609	5	62 - 66
19	0.0822	5	67 - 71
20	0.0822	5	72 - 76
21	0.1418	6	77 - 82
22	0.7873	5	83 - 87
23	0.0	3	88 - 90
24	0.0996	6	91 - 96

(TABLE A-15- CONTINUED)
 Artificial "G" Solar Array
 Finite Element Model Data

Node	Mass lb-sec ² /in	No. of Structural D.O.F.	D.O.F. Sequence No.
25	0.1383	6	97 - 102
26	0.0	0	-----
27	0.1383	6	103 - 108
28	0.1383	6	109 - 114

TABLE A-16
CORIOLIS FORCE MATRIX
(NORMALIZED TO Ω)

D. O. F. *			
<u>Sequence No.</u>			
1 - 3	-0.25043	0.	0.
4 - 6	-0.25043	0.	0.
	-0.25043	0.	0.
e t c.	-0.25043	0.	0.
	-0.25043	0.	0.
	-0.25043	0.	0.
	-0.25043	0.	0.
	-0.25043	0.	0.
	-0.25043	0.	0.
	-0.25043	0.	0.
	-0.25043	0.	0.
	-0.25043	0.	0.
	-0.25043	0.	0.
	-0.27878	0.	0.
	0.	0.	-0.27878
	0.	0.	0.
	0.	-0.17940	0.
	0.	0.	0.
	-0.17940	0.	0.
	0.	0.	-1.72184
	0.	0.	0.
	0.	-1.72184	0.
	0.	0.	0.
	-0.16439	0.	0.
	0.	0.	-0.16439
	0.	0.	0.
	0.	-0.28364	0.
	0.	0.	0.
	0.	0.	0.
	0.	0.	0.
	0.	0.	0.
	-0.19928	0.	0.
	0.	0.	0.
	-0.27652	0.	0.
	0.	0.	0.
	-0.27652	0.	0.
	0.	0.	0.
	-0.27652	0.	0.
	0.	0.	0.
112 - 114	0.	0.	0.

* - Refer to Table A-15 for corresponding node number.

TABLE A-17
CENTRIFUGAL FORCE MATRIX
(NORMALIZED TO Ω^2)

D.. O. F. *			
<u>Sequence No.</u>			
1 - 3	-0.12527	-0.12527	0.
4 - 6	-0.12527	-0.12527	0.
etc.	-0.12527	-0.12527	0.
	-0.12527	-0.12527	0.
	-0.12527	-0.12527	0.
	-0.12527	-0.12527	0.
	-0.12527	-0.12527	0.
	-0.12527	-0.12527	0.
	-0.12527	-0.12527	0.
	-0.12527	-0.12527	0.
	-0.12527	-0.12527	0.
	-0.12527	-0.12527	0.
	-0.13939	-0.13939	0.
	0.	0.	-0.13939
	-0.13939	0.	0.
	0.	-0.08970	-0.08970
	0.	0.	0.
	-0.08970	-0.08970	0.
	0.	0.	-0.86092
	-0.86092	0.	0.
	0.	-0.86092	-0.86092
	0.	0.	0.
	-0.08219	-0.08219	0.
	0.	0.	-0.08219
	-0.08219	0.	0.
	0.	-0.14192	-0.14192
	0.	0.	0.
	0.	-0.78787	0.
	0.	0.	0.
	0.	0.	0.
	-0.09964	-0.09964	0.
	0.	0.	0.
	-0.13836	-0.13836	0.
	0.	0.	0.
	-0.13836	-0.13836	0.
	0.	0.	0.
	-0.13836	-0.13836	0.
112 - 114	0.	0.	0.

* - Refer to TableA-15 for corresponding node number.

EIGENVECTOR FOR ROOT NO. 1 Mode 1, frequency = 0.1786 Hz, Ω = 0 RPM

EIGENVALUE = 0.11224365E 01 (rad/sec)

REAL PART	IMAGINARY PART						
1 TO 7	0.1039E-06	0.2416E-02	-0.9595E 00	-0.7518E-08	0.2416E-02	0.9600E 00	0.5577E-07
9 TO 14	0.2416E-02	-0.4295E 00	0.1730E-09	0.2416E-02	0.4311E 00	0.9106E-07	0.1473E-02
15 TO 21	-0.1300E 01	-0.2727E-07	0.1473E-02	0.9997E 00	0.5032E-07	0.1473E-02	-0.4481E 00
22 TO 28	-0.7054E-03	0.1473E-02	0.4481E 00	0.6355E-07	0.1007E-02	-0.3953E 00	-0.2191E-07
29 TO 35	0.1007E-02	0.3948E 00	0.4535E-07	0.1707E-02	-0.1769E 00	-0.1651E-07	0.1007E-02
36 TO 42	0.1775E 00	0.5435E-07	0.1216E-05	-0.5859E 00	0.4488E-02	0.4648E-09	-0.4402E-07
43 TO 49	0.1219E-05	0.5855E 00	0.4488E-02	0.3245E-09	0.2231E-07	0.1218E-05	-0.2628E 00
50 TO 56	0.4488E-02	0.6076E-09	-0.2017E-07	0.1219E-05	0.2623E 00	0.4488E-02	0.3407E-09
57 TO 63	0.3711E-07	0.1388E-07	-0.1754E-02	0.1416E-04	-0.5963E-10	-0.3301E-07	0.8839E-03
64 TO 70	0.8499E-03	0.2105E-05	-0.1155E-10	0.2907E-07	0.1376E-07	-0.7559E-03	0.1331E-04
71 TO 77	0.2374E-09	-0.3021E-07	0.1150E-10	0.5130E-03	0.7259E-05	0.2540E-09	0.1322E-09
78 TO 84	0.1219E-05	-0.2511E-03	0.4488E-02	0.4543E-06	0.3525E-09	0.1425E-07	-0.5149E-02
85 TO 91	0.1427E-04	0.1924E-12	-0.1671E-09	-0.6389E-05	0.1824E-12	-0.1669E-09	0.5770E-11
92 TO 98	0.1365E-07	-0.3369E-04	0.1125E-04	0.8895E-06	0.7900E-09	0.9511E-10	0.1451E-05
99 TO 105	-0.1536E-03	0.3369E-02	0.2507E-06	-0.3360E-08	0.3905E-10	0.1175E-05	-0.1260E-03
106 TO 112	0.1131E-02	0.6977E-07	0.6670E-09	0.6355E-10	0.2371E-05	-0.1285E-03	0.2250E-02
113 TO 114	0.1868E-09	0.3245E-11					
IMAGINARY PART							
1 TO 7	0.0	0.0	0.0	0.0	0.0	0.0	0.0
9 TO 14	0.0	0.0	0.0	0.0	0.0	0.0	0.0
15 TO 21	0.0	0.0	0.0	0.0	0.0	0.0	0.0
22 TO 28	0.0	0.0	0.0	0.0	0.0	0.0	0.0
29 TO 35	0.0	0.0	0.0	0.0	0.0	0.0	0.0
36 TO 42	0.0	0.0	0.0	0.0	0.0	0.0	0.0
43 TO 49	0.0	0.0	0.0	0.0	0.0	0.0	0.0
50 TO 56	0.0	0.0	0.0	0.0	0.0	0.0	0.0
57 TO 63	0.0	0.0	0.0	0.0	0.0	0.0	0.0
64 TO 70	0.0	0.0	0.0	0.0	0.0	0.0	0.0
71 TO 77	0.0	0.0	0.0	0.0	0.0	0.0	0.0
78 TO 84	0.0	0.0	0.0	0.0	0.0	0.0	0.0
85 TO 91	0.0	0.0	0.0	0.0	0.0	0.0	0.0
92 TO 98	0.0	0.0	0.0	0.0	0.0	0.0	0.0
99 TO 105	0.0	0.0	0.0	0.0	0.0	0.0	0.0
106 TO 112	0.0	0.0	0.0	0.0	0.0	0.0	0.0
113 TO 114	0.0	0.0	0.0	0.0	0.0	0.0	0.0

EIGENVECTOR FOR ROOT NO. 2 Mode 2, frequency = 0.1977 Hz, $\Omega = 0$ RPM

EIGENVALUE = 0.12421875F 01 (rad/sec)

REAL PART	7	0.1393E-09	0.3345E-05	-0.5144E 00	-0.1597E-10	0.3345E-05	-0.6533E 00	0.8857E-10
1 TO 14	0.3345E-05	-0.5524E 00	-0.1070E-11	0.3345E-05	0.3345E-05	-0.6147E 00	0.1247E-09	0.2049E-05
15 TO 21	-0.6975E 00	-0.3773E-10	0.2048E-05	-0.1792E 00	-0.8506E-10	0.6934E-10	0.2049E-05	-0.7423E 00
22 TO 28	-0.1304E-10	0.2049E-05	-0.8269E 00	0.5997E-10	0.1399E-05	-0.2863E 00	-0.2324E-10	-0.3171E-10
29 TO 35	0.1399E-05	-0.3613E 00	0.7877E-10	0.1399E-05	-0.3067E 00	0.1399E-05	0.1399E-05	0.1399E-05
36 TO 42	0.3404E 00	0.7877E-10	-0.1616E-08	-0.7841E 00	-0.8259E-03	0.6602E-12	-0.6522E-10	-0.6522E-10
43 TO 49	0.1621E-08	-0.1000E 01	-0.8287E-03	0.4781E-12	0.3293E-10	0.1619E-08	-0.8436E 00	-0.8436E 00
50 TO 56	-0.8262E-03	0.5920E-12	-0.3015E-10	0.1621E-08	-0.8403E 00	-0.8282E-03	0.5047E-12	0.5047E-12
57 TO 63	0.4251E-10	0.1815E-10	-0.4916E-02	0.1593E-04	-0.8615E-13	-0.4379E-10	0.1154E-10	0.1154E-10
64 TO 70	-0.1973E-02	0.7387E-05	-0.1031E-12	0.3811E-10	0.1799E-10	-0.3805E-02	0.1457E-04	0.1457E-04
71 TO 77	0.3148E-12	-0.3975E-10	0.1503E-10	-0.2507E-02	0.7865E-05	0.3385E-12	0.1713E-12	0.1713E-12
78 TO 84	0.1620E-08	-0.5919E 00	-0.8270E-03	0.1239E-02	0.5318E-12	0.1865E-10	-0.8775E-02	-0.8775E-02
85 TO 91	0.1639E-04	0.2332E-15	-0.2242E-12	0.8714E-05	0.2332E-15	-0.2242E-12	0.1234E-12	0.1234E-12
92 TO 98	0.1794E-10	-0.3042E-02	0.1100E-04	0.1233E-03	0.11032E-11	0.1234E-12	0.8770E-14	0.8770E-14
99 TO 105	-0.5849E 00	-0.6176E-03	0.1178E-02	-0.4293E-11	0.5062E-13	0.1530E-08	0.1896E-08	0.1896E-08
106 TO 112	-0.1985E-03	0.6347E-03	0.9690E-11	0.4225E-13	0.3022E-08	-0.3093E 00	-0.1020E 00	-0.1020E 00
113 TO 114	0.9838E-03	0.4244E-14	0.9690E-11	0.4225E-13	0.3022E-08	-0.3093E 00	-0.4081E-03	-0.4081E-03
IMAGINARY PART	1 TO 7	0.0	0.0	0.0	0.0	0.0	0.0	0.0
8 TO 14	0.0	0.0	0.0	0.0	0.0	0.0	0.0	0.0
15 TO 21	0.0	0.0	0.0	0.0	0.0	0.0	0.0	0.0
22 TO 28	0.0	0.0	0.0	0.0	0.0	0.0	0.0	0.0
29 TO 35	0.0	0.0	0.0	0.0	0.0	0.0	0.0	0.0
36 TO 42	0.0	0.0	0.0	0.0	0.0	0.0	0.0	0.0
43 TO 49	0.0	0.0	0.0	0.0	0.0	0.0	0.0	0.0
50 TO 56	0.0	0.0	0.0	0.0	0.0	0.0	0.0	0.0
57 TO 63	0.0	0.0	0.0	0.0	0.0	0.0	0.0	0.0
64 TO 70	0.0	0.0	0.0	0.0	0.0	0.0	0.0	0.0
71 TO 77	0.0	0.0	0.0	0.0	0.0	0.0	0.0	0.0
78 TO 84	0.0	0.0	0.0	0.0	0.0	0.0	0.0	0.0
85 TO 91	0.0	0.0	0.0	0.0	0.0	0.0	0.0	0.0
92 TO 98	0.0	0.0	0.0	0.0	0.0	0.0	0.0	0.0
99 TO 105	0.0	0.0	0.0	0.0	0.0	0.0	0.0	0.0
106 TO 112	0.0	0.0	0.0	0.0	0.0	0.0	0.0	0.0
113 TO 114	0.0	0.0	0.0	0.0	0.0	0.0	0.0	0.0

EIGENVECTORS FOR ROTATION: Mode 11, frequency = 0.7010 Hz, $\Omega = 0$ RPM

EIGENVALUE = 0.44042060E 01 (rad/sec)

REAL PART		IMAGINARY PART	
1	7	0.4422E-03	0.9822E-01
8	14	0.6332E-03	-0.5844E-01
15	21	0.1312E-03	0.4743E-00
22	28	-0.3052E-03	-0.2316E-01
29	35	-0.4742E-03	0.1204E-03
36	42	0.3472E-01	0.7136E-02
43	49	0.8623E-03	-0.2623E-07
50	56	0.7122E-03	-0.4070E-03
57	63	0.5822E-03	0.2491E-05
64	70	0.3732E-04	0.3540E-06
71	77	0.7042E-04	-0.2933E-04
78	84	0.7172E-03	-0.7631E-05
85	91	-0.1064E-07	0.8950E-12
92	98	-0.2574E-05	0.4277E-06
99	105	0.1132E-04	0.2300E-07
106	112	0.5442E-03	-0.5159E-07
113	119	0.4892E-13	0.2522E-35
1	7	0.0	0.0
8	14	0.0	0.0
15	21	0.0	0.0
22	28	0.0	0.0
29	35	0.0	0.0
36	42	0.0	0.0
43	49	0.0	0.0
50	56	0.0	0.0
57	63	0.0	0.0
64	70	0.0	0.0
71	77	0.0	0.0
78	84	0.0	0.0
85	91	0.0	0.0
92	98	0.0	0.0
99	105	0.0	0.0
106	112	0.0	0.0
113	119	0.0	0.0
1	7	0.2923E-01	0.7592E-03
8	14	0.6423E-03	-0.2522E-02
15	21	0.4145E-00	0.3083E-03
22	28	-0.1136E-00	-0.9931E-00
29	35	-0.1195E-03	0.1578E-00
36	42	0.5974E-05	0.7180E-07
43	49	0.7126E-02	0.4108E-03
50	56	0.2702E-07	-0.5873E-05
57	63	-0.6909E-04	0.3503E-06
64	70	0.9236E-06	-0.2959E-05
71	77	0.6994E-06	0.3340E-09
78	84	0.1719E-05	0.7655E-05
85	91	-0.6111E-06	0.3952E-12
92	98	-0.1285E-07	0.9593E-08
99	105	-0.4048E-03	-0.9770E-09
106	112	0.1979E-04	0.2195E-03
113	119	0.0	0.0
1	7	0.0	0.0
8	14	0.0	0.0
15	21	0.0	0.0
22	28	0.0	0.0
29	35	0.0	0.0
36	42	0.0	0.0
43	49	0.0	0.0
50	56	0.0	0.0
57	63	0.0	0.0
64	70	0.0	0.0
71	77	0.0	0.0
78	84	0.0	0.0
85	91	0.0	0.0
92	98	0.0	0.0
99	105	0.0	0.0
106	112	0.0	0.0
113	119	0.0	0.0

EIGENVECTOR FOR ROOT NO. = 17 Mode 17, frequency = 0.7774 Hz, $\Omega = 0$ RPM.

EIGENVALUE = 0.49343094F 01 (rad/sec)

REAL PART		IMAGINARY PART	
7	0.49008E-05	0.2759E-02	0.7402E-01
8	-0.1759E-01	-0.1730E-01	0.2593E-05
14	0.9072E 00	0.7483E-05	-0.1656E-01
15	0.3706E-05	-0.5688E-02	0.8941E 00
22	0.4695E-01	-0.7654E 00	-0.4544E-05
28	-0.9117E 00	-0.9704E-05	-0.1427E-04
35	-0.1418E-04	-0.1905E-01	0.1303E-04
42	0.1230E-04	-0.7467E-07	0.4682E-05
49	0.5979E-06	0.3200E-06	0.1775E-02
56	-0.4893E-03	-0.1682E-05	-0.1851E-02
63	0.5172E-08	-0.4474E-04	0.2599E-06
70	-0.1419E-04	-0.1977E-01	0.1305E-04
77	-0.1960E-04	0.2310E-11	-0.1531E-08
84	0.3219E-06	0.1708E-03	-0.8775E-05
91	-0.4130E-02	0.9351E-05	-0.1711E-06
98	0.2040E-05	-0.1594E-04	0.1454E-04
105	0.1370E-04	0.2742E-09	0.1237E-08
112	0.0	0.0	0.0
119	0.0	0.0	0.0
126	0.0	0.0	0.0
133	0.0	0.0	0.0
140	0.0	0.0	0.0
147	0.0	0.0	0.0
154	0.0	0.0	0.0
161	0.0	0.0	0.0
168	0.0	0.0	0.0
175	0.0	0.0	0.0
182	0.0	0.0	0.0
189	0.0	0.0	0.0
196	0.0	0.0	0.0
203	0.0	0.0	0.0
210	0.0	0.0	0.0
217	0.0	0.0	0.0
224	0.0	0.0	0.0
231	0.0	0.0	0.0
238	0.0	0.0	0.0
245	0.0	0.0	0.0
252	0.0	0.0	0.0
259	0.0	0.0	0.0
266	0.0	0.0	0.0
273	0.0	0.0	0.0
280	0.0	0.0	0.0
287	0.0	0.0	0.0
294	0.0	0.0	0.0
301	0.0	0.0	0.0
308	0.0	0.0	0.0
315	0.0	0.0	0.0
322	0.0	0.0	0.0
329	0.0	0.0	0.0
336	0.0	0.0	0.0
343	0.0	0.0	0.0
350	0.0	0.0	0.0
357	0.0	0.0	0.0
364	0.0	0.0	0.0
371	0.0	0.0	0.0
378	0.0	0.0	0.0
385	0.0	0.0	0.0
392	0.0	0.0	0.0
399	0.0	0.0	0.0
406	0.0	0.0	0.0
413	0.0	0.0	0.0
420	0.0	0.0	0.0
427	0.0	0.0	0.0
434	0.0	0.0	0.0
441	0.0	0.0	0.0
448	0.0	0.0	0.0
455	0.0	0.0	0.0
462	0.0	0.0	0.0
469	0.0	0.0	0.0
476	0.0	0.0	0.0
483	0.0	0.0	0.0
490	0.0	0.0	0.0
497	0.0	0.0	0.0
504	0.0	0.0	0.0
511	0.0	0.0	0.0
518	0.0	0.0	0.0
525	0.0	0.0	0.0
532	0.0	0.0	0.0
539	0.0	0.0	0.0
546	0.0	0.0	0.0
553	0.0	0.0	0.0
560	0.0	0.0	0.0
567	0.0	0.0	0.0
574	0.0	0.0	0.0
581	0.0	0.0	0.0
588	0.0	0.0	0.0
595	0.0	0.0	0.0
602	0.0	0.0	0.0
609	0.0	0.0	0.0
616	0.0	0.0	0.0
623	0.0	0.0	0.0
630	0.0	0.0	0.0
637	0.0	0.0	0.0
644	0.0	0.0	0.0
651	0.0	0.0	0.0
658	0.0	0.0	0.0
665	0.0	0.0	0.0
672	0.0	0.0	0.0
679	0.0	0.0	0.0
686	0.0	0.0	0.0
693	0.0	0.0	0.0
700	0.0	0.0	0.0
707	0.0	0.0	0.0
714	0.0	0.0	0.0
721	0.0	0.0	0.0
728	0.0	0.0	0.0
735	0.0	0.0	0.0
742	0.0	0.0	0.0
749	0.0	0.0	0.0
756	0.0	0.0	0.0
763	0.0	0.0	0.0
770	0.0	0.0	0.0
777	0.0	0.0	0.0
784	0.0	0.0	0.0
791	0.0	0.0	0.0
798	0.0	0.0	0.0
805	0.0	0.0	0.0
812	0.0	0.0	0.0
819	0.0	0.0	0.0
826	0.0	0.0	0.0
833	0.0	0.0	0.0
840	0.0	0.0	0.0
847	0.0	0.0	0.0
854	0.0	0.0	0.0
861	0.0	0.0	0.0
868	0.0	0.0	0.0
875	0.0	0.0	0.0
882	0.0	0.0	0.0
889	0.0	0.0	0.0
896	0.0	0.0	0.0
903	0.0	0.0	0.0
910	0.0	0.0	0.0
917	0.0	0.0	0.0
924	0.0	0.0	0.0
931	0.0	0.0	0.0
938	0.0	0.0	0.0
945	0.0	0.0	0.0
952	0.0	0.0	0.0
959	0.0	0.0	0.0
966	0.0	0.0	0.0
973	0.0	0.0	0.0
980	0.0	0.0	0.0
987	0.0	0.0	0.0
994	0.0	0.0	0.0
1001	0.0	0.0	0.0
1008	0.0	0.0	0.0
1015	0.0	0.0	0.0
1022	0.0	0.0	0.0
1029	0.0	0.0	0.0
1036	0.0	0.0	0.0
1043	0.0	0.0	0.0
1050	0.0	0.0	0.0
1057	0.0	0.0	0.0
1064	0.0	0.0	0.0
1071	0.0	0.0	0.0
1078	0.0	0.0	0.0
1085	0.0	0.0	0.0
1092	0.0	0.0	0.0
1099	0.0	0.0	0.0
1106	0.0	0.0	0.0
1113	0.0	0.0	0.0
1120	0.0	0.0	0.0
1127	0.0	0.0	0.0
1134	0.0	0.0	0.0
1141	0.0	0.0	0.0
1148	0.0	0.0	0.0
1155	0.0	0.0	0.0
1162	0.0	0.0	0.0
1169	0.0	0.0	0.0
1176	0.0	0.0	0.0
1183	0.0	0.0	0.0
1190	0.0	0.0	0.0
1197	0.0	0.0	0.0
1204	0.0	0.0	0.0
1211	0.0	0.0	0.0
1218	0.0	0.0	0.0
1225	0.0	0.0	0.0
1232	0.0	0.0	0.0
1239	0.0	0.0	0.0
1246	0.0	0.0	0.0
1253	0.0	0.0	0.0
1260	0.0	0.0	0.0
1267	0.0	0.0	0.0
1274	0.0	0.0	0.0
1281	0.0	0.0	0.0
1288	0.0	0.0	0.0
1295	0.0	0.0	0.0
1302	0.0	0.0	0.0
1309	0.0	0.0	0.0
1316	0.0	0.0	0.0
1323	0.0	0.0	0.0
1330	0.0	0.0	0.0
1337	0.0	0.0	0.0
1344	0.0	0.0	0.0
1351	0.0	0.0	0.0
1358	0.0	0.0	0.0
1365	0.0	0.0	0.0
1372	0.0	0.0	0.0
1379	0.0	0.0	0.0
1386	0.0	0.0	0.0
1393	0.0	0.0	0.0
1400	0.0	0.0	0.0
1407	0.0	0.0	0.0
1414	0.0	0.0	0.0
1421	0.0	0.0	0.0
1428	0.0	0.0	0.0
1435	0.0	0.0	0.0
1442	0.0	0.0	0.0
1449	0.0	0.0	0.0
1456	0.0	0.0	0.0
1463	0.0	0.0	0.0
1470	0.0	0.0	0.0
1477	0.0	0.0	0.0
1484	0.0	0.0	0.0
1491	0.0	0.0	0.0
1498	0.0	0.0	0.0
1505	0.0	0.0	0.0
1512	0.0	0.0	0.0
1519	0.0	0.0	0.0
1526	0.0	0.0	0.0
1533	0.0	0.0	0.0
1540	0.0	0.0	0.0
1547	0.0	0.0	0.0
1554	0.0	0.0	0.0
1561	0.0	0.0	0.0
1568	0.0	0.0	0.0
1575	0.0	0.0	0.0
1582	0.0	0.0	0.0
1589	0.0	0.0	0.0
1596	0.0	0.0	0.0
1603	0.0	0.0	0.0
1610	0.0	0.0	0.0
1617	0.0	0.0	0.0
1624	0.0	0.0	0.0
1631	0.0	0.0	0.0
1638	0.0	0.0	0.0
1645	0.0	0.0	0.0
1652	0.0	0.0	0.0
1659	0.0	0.0	0.0
1666	0.0	0.0	0.0
1673	0.0	0.0	0.0
1680	0.0	0.0	0.0
1687	0.0	0.0	0.0
1694	0.0	0.0	0.0
1701	0.0	0.0	0.0
1708	0.0	0.0	0.0
1715	0.0	0.0	0.0
1722	0.0	0.0	0.0
1729	0.0	0.0	0.0
1736	0.0	0.0	0.0
1743	0.0	0.0	0.0
1750	0.0	0.0	0.0
1757	0.0	0.0	0.0
1764	0.0	0.0	0.0
1771	0.0	0.0	0.0
1778	0.0	0.0	0.0
1785	0.0	0.0	0.0
1792	0.0	0.0	0.0
1799	0.0	0.0	0.0
1806	0.0	0.0	0.0
1813	0.0	0.0	0.0
1820	0.0	0.0	0.0
1827	0.0	0.0	0.0
1834	0.0	0.0	0.0
1841	0.0	0.0	0.0
1848	0.0	0.0	0.0
1855	0.0	0.0	0.0
1862	0.0	0.0	0.0
1869	0.0	0.0	0.0
1876	0.0	0.0	0.0
1883	0.0	0.0	0.0
1890	0.0	0.0	0.0
1897	0.0	0.0	0.0
1904	0.0	0.0	0.0
1911	0.0	0.0	0.0
1918	0.0	0.0	0.0
1925	0.0	0.0	0.0
1932	0.0	0.0	0.0
1939	0.0	0.0	0.0
1946	0.0	0.0	0.0
1953	0.0	0.0	0.0
1960	0.0	0.0	0.0
1967	0.0	0.0	0.0
1974	0.0	0.0	0.0
1981	0.0	0.0	0.0
1988	0.0	0.0	0.0
1995	0.0	0.0	0.0
2002	0.0	0.0	0.0
2009	0.0	0.0	0.0
2016	0.0	0.0	0.0
2023	0.0	0.0	0.0
2030	0.0	0.0	0.0
2037	0.0	0.0	0.0
2044	0.0	0.0	0.0
2051	0.0	0.0	0.0
2058	0.0	0.0	0.0
2065	0.0	0.0	0.0
2072	0.0	0.0	0.0
2079	0.0	0.0	0.0
2086	0.0	0.0	0.0
2093	0.0	0.0	0.0
2100	0.0	0.0	0.0
2107	0.0	0.0	0.0
2114	0.0	0.0	0.0
2121	0.0	0.0	0.0
2128	0.0	0.0	0.0
2135	0.0	0.0	0.0
2142	0.0	0.0	0.0
2149	0.0	0.0	0.0
2156	0.0	0.0	0.0
2163	0.0	0.0	0.0
2170	0.0	0.0	0.0
2177	0.0	0.0	0.0
2184	0.0	0.0	0.0
2191	0.0	0.0	0.0

EIGENVECTOR FOR ROOT NO. = IR Mode 18, frequency = 0.7912 Hz, $\Omega = 0$ RPM

EIGENVALUE = 0.69716355F 01 (rad/sec)

REAL PART		IMAGINARY PART							
1	7	-0.1375E-05	-0.8993E-02	-0.1155E 00	0.1919E-05	-0.4196E-02	0.8353E-01	-0.5662E-05	
8	14	0.1699E-06	0.6572E-01	0.8995E-04	0.1790E-01	-0.1246E 00	-0.2135E-04	-0.2401E-01	
15	21	-0.7415E 00	0.2607E-05	0.1703E-01	0.8700E 00	-0.1076E-05	0.1035E-01	-0.5150E 00	
28	28	0.1280E-05	-0.1783E-01	0.9311E 00	-0.8433E-06	-0.1009E-01	0.8922E 01	0.7979E-06	
29	35	-0.3806E-02	-0.1000E 01	-0.1565E-06	0.2721E-02	0.6663E 00	0.3303E-04	0.2759E-01	
36	42	-0.9431E 00	-0.3309E-05	-0.2073E-05	-0.3501E-01	0.2660E-03	-0.2255E-04	0.3760E-05	
43	49	-0.2043E-05	0.3669E-01	0.2672E-03	-0.2181E-07	-0.1615E-05	-0.2055E-05	-0.1504E-01	
50	56	0.2666E-03	-0.2942E-07	0.1610E-05	-0.2043E-05	0.1544E-01	0.2676E-03	-0.3512E-07	
57	63	0.2150E-06	0.1272E-06	-0.1591E-02	0.1451E-04	-0.1074E-08	0.1993E-05	0.2172E-07	
64	70	0.5865E-03	0.1375E-05	-0.7005E-09	0.2177E-06	0.1290E-06	-0.6315E-03	0.1100E-04	
71	77	0.1372E-08	-0.2900E-06	0.1046E-06	0.3675E-03	0.5053E-05	0.8981E-09	0.2926E-09	
78	84	-0.2066E-05	-0.2170E-03	0.2675E-03	-0.1192E-06	-0.3086E-07	0.1279E-05	-0.5698E-02	
85	91	0.1732E-06	0.8607E-17	-0.8400E-09	-0.3179E-05	0.8697E-12	-0.8379E-09	0.6903E-10	
92	98	0.1265E-06	-0.3645E-04	0.8469E-05	0.1053E-05	0.7195E-08	0.7161E-09	0.2117E-04	
99	105	-0.2415E-03	0.2037E-03	-0.6509E-07	-0.5931E-07	0.2921E-09	0.1127E-04	-0.1894E-03	
106	112	0.7337E-04	0.3076E-06	0.5870E-07	0.4369E-09	0.2046E-04	-0.2351E-03	0.2395E-03	
113	119	0.9309E-07	0.9130E-10						
IMAGINARY PART									
1	7	0.0	0.0	0.0	0.0	0.0	0.0	0.0	
8	14	0.0	0.0	0.0	0.0	0.0	0.0	0.0	
15	21	0.0	0.0	0.0	0.0	0.0	0.0	0.0	
22	28	0.0	0.0	0.0	0.0	0.0	0.0	0.0	
29	35	0.0	0.0	0.0	0.0	0.0	0.0	0.0	
36	42	0.0	0.0	0.0	0.0	0.0	0.0	0.0	
43	49	0.0	0.0	0.0	0.0	0.0	0.0	0.0	
50	56	0.0	0.0	0.0	0.0	0.0	0.0	0.0	
57	63	0.0	0.0	0.0	0.0	0.0	0.0	0.0	
64	70	0.0	0.0	0.0	0.0	0.0	0.0	0.0	
71	77	0.0	0.0	0.0	0.0	0.0	0.0	0.0	
78	84	0.0	0.0	0.0	0.0	0.0	0.0	0.0	
85	91	0.0	0.0	0.0	0.0	0.0	0.0	0.0	
92	98	0.0	0.0	0.0	0.0	0.0	0.0	0.0	
99	105	0.0	0.0	0.0	0.0	0.0	0.0	0.0	
106	112	0.0	0.0	0.0	0.0	0.0	0.0	0.0	
113	119	0.0	0.0	0.0	0.0	0.0	0.0	0.0	

EIGENVECTOR FOR POINT NO. = 19 Mode 19, frequency = 0.9047 Hz, $\Omega = 0$ RPM

FIGURE VALUES = 0.56845703E 01 (rad/sec)

REAL PART		IMAGINARY PART						
1	7	0.5162E-06	-0.1928E-01	0.6491E 00	0.7858E-06	-0.2187E-02	-0.5776E-01	-0.2181E-05
4	14	-0.7346E-03	-0.8994E 00	0.4477E-06	-0.6992E-03	-0.6334E-01	-0.8240E-06	0.1151E-01
15	21	-0.1231E 00	0.9723E-06	0.3703E-02	0.6231E-01	-0.3698E-06	0.3799E-03	-0.4993E-01
22	28	-0.5022E-06	0.3610E-03	0.2237E-01	-0.3957E-06	-0.7677E-03	-0.4988E 00	0.5419E-05
29	35	-0.7686E-03	-0.2196E-01	-0.1918E-04	0.2119E-02	0.1000E 01	0.3289E-06	0.2119E-02
34	42	0.9320E-02	-0.1218E-05	-0.1080E-04	0.7926E-07	-0.3699E-04	-0.8998E-09	0.1190E-05
43	49	-0.1975E-04	-0.6716E-02	-0.3499E-04	-0.8223E-08	-0.5628E-06	-0.1077E-04	0.2622E-03
50	56	-0.3697E-04	-0.9292E-08	-0.5510E-06	-0.1075E-04	-0.4089E-02	-0.3691E-04	-0.8926E-03
57	63	-0.2394E-06	-0.8677E-07	-0.5274E-02	0.5947E-04	-0.8097E-09	0.2961E-06	-0.5439E-07
64	70	0.2067E-02	0.4469E-05	-0.8169E-10	-0.1453E-06	-0.8953E-07	-0.2429E-02	0.4593E-04
71	77	-0.1439E-09	0.2180E-06	-0.7121E-07	0.1277E-02	0.1903E-04	-0.2491E-08	-0.3547E-03
78	84	-0.1075E-04	-0.1899E-02	-0.3694E-04	0.2470E-05	-0.1011E-07	-0.9033E-07	-0.2295E-01
85	91	0.7511E-04	0.5179E-12	0.1905E-08	-0.1523E-04	0.5179E-12	0.1902E-08	-0.1584E-10
92	98	-0.8438E-07	-0.1609E-03	0.3149E-04	0.4957E-05	-0.4728E-08	-0.2891E-09	-0.8922E-03
99	105	-0.1306E-02	-0.1920E-04	0.2109E-05	0.6063E-08	-0.9844E-10	-0.6607E-05	-0.9123E-03
106	112	0.1621E-04	0.1935E-05	-0.3412E-07	-0.2036E-09	-0.1193E-04	-0.9491E-03	-0.1494E-05
113	114	0.3851E-06	0.2159E-09	0.0	0.0	0.0	0.0	0.0
1	7	0.0	0.0	0.0	0.0	0.0	0.0	0.0
4	14	0.0	0.0	0.0	0.0	0.0	0.0	0.0
15	21	0.0	0.0	0.0	0.0	0.0	0.0	0.0
22	28	0.0	0.0	0.0	0.0	0.0	0.0	0.0
29	35	0.0	0.0	0.0	0.0	0.0	0.0	0.0
34	42	0.0	0.0	0.0	0.0	0.0	0.0	0.0
43	49	0.0	0.0	0.0	0.0	0.0	0.0	0.0
50	56	0.0	0.0	0.0	0.0	0.0	0.0	0.0
57	63	0.0	0.0	0.0	0.0	0.0	0.0	0.0
64	70	0.0	0.0	0.0	0.0	0.0	0.0	0.0
71	77	0.0	0.0	0.0	0.0	0.0	0.0	0.0
78	84	0.0	0.0	0.0	0.0	0.0	0.0	0.0
85	91	0.0	0.0	0.0	0.0	0.0	0.0	0.0
92	98	0.0	0.0	0.0	0.0	0.0	0.0	0.0
99	105	0.0	0.0	0.0	0.0	0.0	0.0	0.0
106	112	0.0	0.0	0.0	0.0	0.0	0.0	0.0
113	114	0.0	0.0	0.0	0.0	0.0	0.0	0.0

FIGENVECTOR FOR ROOT NO. 20

Mode 20, frequency = 0.9315 Hz, $\Omega = 0$ RPM

FIGENVALIIF= 0.5953073F 01 (rad/sec)

REAL PART	IMAGINARY PART
1 TO 7	0.1000E 01
8 TO 14	-0.9853E-01
15 TO 21	0.3401E 00
22 TO 28	0.1305E-01
29 TO 35	0.2316E-03
36 TO 42	-0.2672E 00
43 TO 49	0.1943E-01
50 TO 56	0.1559E-07
57 TO 63	-0.1130E-09
64 TO 70	0.6013E-04
71 TO 77	0.4085E-06
78 TO 84	0.4205E-06
85 TO 91	0.1557E-02
92 TO 98	0.6166E-08
99 TO 105	0.2249E-11
106 TO 112	0.9449E-06
113 TO 114	0.2857E-04
115 TO 116	0.2045E-04
117 TO 118	0.1399E-07
119 TO 120	0.3331E-07
121 TO 122	-0.1383E-06
123 TO 124	0.1634E-09
125 TO 131	0.0
132 TO 138	0.0
139 TO 145	0.0
146 TO 152	0.0
153 TO 159	0.0
160 TO 166	0.0
167 TO 173	0.0
174 TO 180	0.0
181 TO 187	0.0
188 TO 194	0.0
195 TO 201	0.0
202 TO 208	0.0
209 TO 215	0.0
216 TO 222	0.0
223 TO 229	0.0
230 TO 236	0.0
237 TO 243	0.0
244 TO 250	0.0
251 TO 257	0.0
258 TO 264	0.0
265 TO 271	0.0
272 TO 278	0.0
279 TO 285	0.0
286 TO 292	0.0
293 TO 299	0.0
300 TO 306	0.0
307 TO 313	0.0
314 TO 320	0.0
321 TO 327	0.0
328 TO 334	0.0
335 TO 341	0.0
342 TO 348	0.0
349 TO 355	0.0
356 TO 362	0.0
363 TO 369	0.0
370 TO 376	0.0
377 TO 383	0.0
384 TO 390	0.0
391 TO 397	0.0
398 TO 404	0.0
405 TO 411	0.0
412 TO 418	0.0
419 TO 425	0.0
426 TO 432	0.0
433 TO 439	0.0
440 TO 446	0.0
447 TO 453	0.0
454 TO 460	0.0
461 TO 467	0.0
468 TO 474	0.0
475 TO 481	0.0
482 TO 488	0.0
489 TO 495	0.0
496 TO 502	0.0
503 TO 509	0.0
510 TO 516	0.0
517 TO 523	0.0
524 TO 530	0.0
531 TO 537	0.0
538 TO 544	0.0
545 TO 551	0.0
552 TO 558	0.0
559 TO 565	0.0
566 TO 572	0.0
573 TO 579	0.0
580 TO 586	0.0
587 TO 593	0.0
594 TO 600	0.0
601 TO 607	0.0
608 TO 614	0.0
615 TO 621	0.0
622 TO 628	0.0
629 TO 635	0.0
636 TO 642	0.0
643 TO 649	0.0
650 TO 656	0.0
657 TO 663	0.0
664 TO 670	0.0
671 TO 677	0.0
678 TO 684	0.0
685 TO 691	0.0
692 TO 698	0.0
699 TO 705	0.0
706 TO 712	0.0
713 TO 719	0.0
720 TO 726	0.0
727 TO 733	0.0
734 TO 740	0.0
741 TO 747	0.0
748 TO 754	0.0
755 TO 761	0.0
762 TO 768	0.0
769 TO 775	0.0
776 TO 782	0.0
783 TO 789	0.0
790 TO 796	0.0
797 TO 803	0.0
804 TO 810	0.0
811 TO 817	0.0
818 TO 824	0.0
825 TO 831	0.0
832 TO 838	0.0
839 TO 845	0.0
846 TO 852	0.0
853 TO 859	0.0
860 TO 866	0.0
867 TO 873	0.0
874 TO 880	0.0
881 TO 887	0.0
888 TO 894	0.0
895 TO 901	0.0
902 TO 908	0.0
909 TO 915	0.0
916 TO 922	0.0
923 TO 929	0.0
930 TO 936	0.0
937 TO 943	0.0
944 TO 950	0.0
951 TO 957	0.0
958 TO 964	0.0
965 TO 971	0.0
972 TO 978	0.0
979 TO 985	0.0
986 TO 992	0.0
993 TO 999	0.0
1000 TO 1006	0.0
1007 TO 1013	0.0
1014 TO 1020	0.0
1021 TO 1027	0.0
1028 TO 1034	0.0
1035 TO 1041	0.0
1042 TO 1048	0.0
1049 TO 1055	0.0
1056 TO 1062	0.0
1063 TO 1069	0.0
1070 TO 1076	0.0
1077 TO 1083	0.0
1084 TO 1090	0.0
1091 TO 1097	0.0
1098 TO 1104	0.0
1105 TO 1111	0.0
1112 TO 1118	0.0
1119 TO 1125	0.0
1126 TO 1132	0.0
1133 TO 1139	0.0
1140 TO 1146	0.0
1147 TO 1153	0.0
1154 TO 1160	0.0
1161 TO 1167	0.0
1168 TO 1174	0.0
1175 TO 1181	0.0
1182 TO 1188	0.0
1189 TO 1195	0.0
1196 TO 1202	0.0
1203 TO 1209	0.0
1210 TO 1216	0.0
1217 TO 1223	0.0
1224 TO 1230	0.0
1231 TO 1237	0.0
1238 TO 1244	0.0
1245 TO 1251	0.0
1252 TO 1258	0.0
1259 TO 1265	0.0
1266 TO 1272	0.0
1273 TO 1279	0.0
1280 TO 1286	0.0
1287 TO 1293	0.0
1294 TO 1300	0.0
1301 TO 1307	0.0
1308 TO 1314	0.0
1315 TO 1321	0.0
1322 TO 1328	0.0
1329 TO 1335	0.0
1336 TO 1342	0.0
1343 TO 1349	0.0
1350 TO 1356	0.0
1357 TO 1363	0.0
1364 TO 1370	0.0
1371 TO 1377	0.0
1378 TO 1384	0.0
1385 TO 1391	0.0
1392 TO 1398	0.0
1399 TO 1405	0.0
1406 TO 1412	0.0
1413 TO 1419	0.0
1420 TO 1426	0.0
1427 TO 1433	0.0
1434 TO 1440	0.0
1441 TO 1447	0.0
1448 TO 1454	0.0
1455 TO 1461	0.0
1462 TO 1468	0.0
1469 TO 1475	0.0
1476 TO 1482	0.0
1483 TO 1489	0.0
1490 TO 1496	0.0
1497 TO 1503	0.0
1504 TO 1510	0.0
1511 TO 1517	0.0
1518 TO 1524	0.0
1525 TO 1531	0.0
1532 TO 1538	0.0
1539 TO 1545	0.0
1546 TO 1552	0.0
1553 TO 1559	0.0
1560 TO 1566	0.0
1567 TO 1573	0.0
1574 TO 1580	0.0
1581 TO 1587	0.0
1588 TO 1594	0.0
1595 TO 1601	0.0
1602 TO 1608	0.0
1609 TO 1615	0.0
1616 TO 1622	0.0
1623 TO 1629	0.0
1630 TO 1636	0.0
1637 TO 1643	0.0
1644 TO 1650	0.0
1651 TO 1657	0.0
1658 TO 1664	0.0
1665 TO 1671	0.0
1672 TO 1678	0.0
1679 TO 1685	0.0
1686 TO 1692	0.0
1693 TO 1699	0.0
1700 TO 1706	0.0
1707 TO 1713	0.0
1714 TO 1720	0.0
1721 TO 1727	0.0
1728 TO 1734	0.0
1735 TO 1741	0.0
1742 TO 1748	0.0
1749 TO 1755	0.0
1756 TO 1762	0.0
1763 TO 1769	0.0
1770 TO 1776	0.0
1777 TO 1783	0.0
1784 TO 1790	0.0
1791 TO 1797	0.0
1798 TO 1804	0.0
1805 TO 1811	0.0
1812 TO 1818	0.0
1819 TO 1825	0.0
1826 TO 1832	0.0
1833 TO 1839	0.0
1840 TO 1846	0.0
1847 TO 1853	0.0
1854 TO 1860	0.0
1861 TO 1867	0.0
1868 TO 1874	0.0
1875 TO 1881	0.0
1882 TO 1888	0.0
1889 TO 1895	0.0
1896 TO 1902	0.0
1903 TO 1909	0.0
1910 TO 1916	0.0
1917 TO 1923	0.0
1924 TO 1930	0.0
1931 TO 1937	0.0
1938 TO 1944	0.0
1945 TO 1951	0.0
1952 TO 1958	0.0
1959 TO 1965	0.0
1966 TO 1972	0.0
1973 TO 1979	0.0
1980 TO 1986	0.0
1987 TO 1993	0.0
1994 TO 2000	0.0



EIGENVECTORS FOR ROT N1 = 28

Mode 28, Frequency = 1.0544 Hz, $\Omega = 0$ RPM

EIGENVALUE = 0.56254893E 01 (rad/sec.)

REAL PART	1	7	14	21	28	35	42	49	56	63	70	77	84	91	98	105	112	119	126
1	0.7450E-02	-0.1000E 01	-0.1493E 00	-0.7259E-02	-0.9997E 00	-0.2204E 00	-0.9997E 00	-0.1493E 00	-0.7259E-02	-0.9997E 00	-0.2204E 00	-0.9997E 00	-0.1493E 00	-0.7259E-02	-0.9997E 00	-0.2204E 00	-0.9997E 00	-0.1493E 00	-0.7259E-02
7	-0.9099E 00	-0.1771E 00	-0.3477E-02	-0.9993E 00	-0.2458E 00	0.5122E-02	0.9993E 00	-0.3477E-02	-0.9993E 00	-0.2458E 00	0.5122E-02	0.9993E 00	-0.3477E-02	-0.9993E 00	-0.2458E 00	0.5122E-02	0.9993E 00	-0.3477E-02	-0.9993E 00
14	0.1604E 00	-0.1056E-01	0.9554E 00	0.2458E 00	0.3717E-02	0.779E 00	0.2458E 00	0.3717E-02	0.9554E 00	0.1604E 00	-0.1056E-01	0.9554E 00	0.2458E 00	0.3717E-02	0.779E 00	0.2458E 00	0.3717E-02	0.9554E 00	0.1604E 00
21	-0.5111E-02	0.1726E 00	0.1533E-02	0.3717E-02	0.1380E 00	0.4779E 00	0.3717E-02	0.1533E-02	0.5111E-02	0.1726E 00	0.1533E-02	0.5111E-02	0.1726E 00	0.1533E-02	0.3717E-02	0.1380E 00	0.4779E 00	0.3717E-02	0.5111E-02
28	0.3768E 00	0.1416E-01	0.4235E-01	0.1380E 00	0.1380E 00	0.6779E-02	0.1380E 00	0.4235E-01	0.3768E 00	0.1416E-01	0.4235E-01	0.1380E 00	0.4235E-01	0.3768E 00	0.1416E-01	0.4235E-01	0.1380E 00	0.4235E-01	0.3768E 00
35	0.1452E 00	-0.1332E-02	0.5861E-06	0.1332E-02	0.1332E-02	0.6779E-02	0.1332E-02	0.1452E 00	0.1452E 00	-0.1332E-02	0.5861E-06	0.1332E-02	0.1452E 00	-0.1332E-02	0.5861E-06	0.1332E-02	0.1452E 00	-0.1332E-02	0.5861E-06
42	0.4243E-01	0.1083E-03	-0.6629E-02	0.1083E-03	0.1083E-03	-0.6629E-02	0.1083E-03	0.4243E-01	0.1083E-03	0.1083E-03	-0.6629E-02	0.1083E-03	0.4243E-01	0.1083E-03	0.1083E-03	-0.6629E-02	0.1083E-03	0.1083E-03	-0.6629E-02
49	0.6657E-06	-0.1750E-03	0.2615E-03	-0.1750E-03	-0.1750E-03	0.2615E-03	-0.1750E-03	0.6657E-06	-0.1750E-03	-0.1750E-03	0.2615E-03	-0.1750E-03	0.6657E-06	-0.1750E-03	-0.1750E-03	0.2615E-03	-0.1750E-03	-0.1750E-03	0.2615E-03
56	-0.4807E-04	-0.2214E-06	0.1937E-05	-0.2214E-06	-0.2214E-06	0.1937E-05	-0.2214E-06	-0.4807E-04	-0.2214E-06	-0.2214E-06	0.1937E-05	-0.2214E-06	-0.4807E-04	-0.2214E-06	-0.2214E-06	0.1937E-05	-0.2214E-06	-0.2214E-06	0.1937E-05
63	0.5025E-04	0.5550E-04	-0.1517E-03	0.5550E-04	0.5550E-04	-0.1517E-03	0.5550E-04	0.5025E-04	0.5550E-04	0.5550E-04	-0.1517E-03	0.5550E-04	0.5025E-04	0.5550E-04	0.5550E-04	-0.1517E-03	0.5550E-04	0.5550E-04	-0.1517E-03
70	-0.8210E-04	-0.5550E-04	0.1517E-03	-0.5550E-04	-0.5550E-04	0.1517E-03	-0.5550E-04	-0.8210E-04	-0.5550E-04	-0.5550E-04	0.1517E-03	-0.5550E-04	-0.8210E-04	-0.5550E-04	-0.5550E-04	0.1517E-03	-0.5550E-04	-0.5550E-04	0.1517E-03
77	0.4241E-01	-0.1408E-02	0.6071E-06	0.1408E-02	0.1408E-02	-0.6071E-06	0.1408E-02	0.4241E-01	0.1408E-02	0.1408E-02	-0.6071E-06	0.1408E-02	0.4241E-01	0.1408E-02	0.1408E-02	-0.6071E-06	0.1408E-02	0.1408E-02	-0.6071E-06
84	-0.2500E-05	0.5281E-10	-0.1999E-05	0.2500E-05	0.2500E-05	-0.1999E-05	0.2500E-05	-0.2500E-05	0.5281E-10	0.5281E-10	-0.1999E-05	0.2500E-05	-0.2500E-05	0.5281E-10	0.5281E-10	-0.1999E-05	0.2500E-05	0.2500E-05	-0.1999E-05
91	0.5992E-03	0.3295E-04	0.6425E-05	0.3295E-04	0.3295E-04	0.6425E-05	0.3295E-04	0.5992E-03	0.3295E-04	0.3295E-04	0.6425E-05	0.3295E-04	0.5992E-03	0.3295E-04	0.3295E-04	0.6425E-05	0.3295E-04	0.3295E-04	0.6425E-05
98	0.4250E-06	-0.4005E-05	-0.5595E-04	-0.4005E-05	-0.4005E-05	-0.5595E-04	-0.4005E-05	0.4250E-06	-0.4005E-05	-0.4005E-05	-0.5595E-04	-0.4005E-05	0.4250E-06	-0.4005E-05	-0.4005E-05	-0.5595E-04	-0.4005E-05	-0.4005E-05	-0.5595E-04
105	0.2896E-08	0.1636E-04	0.5595E-04	0.1636E-04	0.1636E-04	0.5595E-04	0.1636E-04	0.2896E-08	0.1636E-04	0.1636E-04	0.5595E-04	0.1636E-04	0.2896E-08	0.1636E-04	0.1636E-04	0.5595E-04	0.1636E-04	0.1636E-04	0.5595E-04
IMAGINARY PART	1	7	14	21	28	35	42	49	56	63	70	77	84	91	98	105	112	119	126
1	0.0	0.0	0.0	0.0	0.0	0.0	0.0	0.0	0.0	0.0	0.0	0.0	0.0	0.0	0.0	0.0	0.0	0.0	0.0
7	0.0	0.0	0.0	0.0	0.0	0.0	0.0	0.0	0.0	0.0	0.0	0.0	0.0	0.0	0.0	0.0	0.0	0.0	0.0
14	0.0	0.0	0.0	0.0	0.0	0.0	0.0	0.0	0.0	0.0	0.0	0.0	0.0	0.0	0.0	0.0	0.0	0.0	0.0
21	0.0	0.0	0.0	0.0	0.0	0.0	0.0	0.0	0.0	0.0	0.0	0.0	0.0	0.0	0.0	0.0	0.0	0.0	0.0
28	0.0	0.0	0.0	0.0	0.0	0.0	0.0	0.0	0.0	0.0	0.0	0.0	0.0	0.0	0.0	0.0	0.0	0.0	0.0
35	0.0	0.0	0.0	0.0	0.0	0.0	0.0	0.0	0.0	0.0	0.0	0.0	0.0	0.0	0.0	0.0	0.0	0.0	0.0
42	0.0	0.0	0.0	0.0	0.0	0.0	0.0	0.0	0.0	0.0	0.0	0.0	0.0	0.0	0.0	0.0	0.0	0.0	0.0
49	0.0	0.0	0.0	0.0	0.0	0.0	0.0	0.0	0.0	0.0	0.0	0.0	0.0	0.0	0.0	0.0	0.0	0.0	0.0
56	0.0	0.0	0.0	0.0	0.0	0.0	0.0	0.0	0.0	0.0	0.0	0.0	0.0	0.0	0.0	0.0	0.0	0.0	0.0
63	0.0	0.0	0.0	0.0	0.0	0.0	0.0	0.0	0.0	0.0	0.0	0.0	0.0	0.0	0.0	0.0	0.0	0.0	0.0
70	0.0	0.0	0.0	0.0	0.0	0.0	0.0	0.0	0.0	0.0	0.0	0.0	0.0	0.0	0.0	0.0	0.0	0.0	0.0
77	0.0	0.0	0.0	0.0	0.0	0.0	0.0	0.0	0.0	0.0	0.0	0.0	0.0	0.0	0.0	0.0	0.0	0.0	0.0
84	0.0	0.0	0.0	0.0	0.0	0.0	0.0	0.0	0.0	0.0	0.0	0.0	0.0	0.0	0.0	0.0	0.0	0.0	0.0
91	0.0	0.0	0.0	0.0	0.0	0.0	0.0	0.0	0.0	0.0	0.0	0.0	0.0	0.0	0.0	0.0	0.0	0.0	0.0
98	0.0	0.0	0.0	0.0	0.0	0.0	0.0	0.0	0.0	0.0	0.0	0.0	0.0	0.0	0.0	0.0	0.0	0.0	0.0
105	0.0	0.0	0.0	0.0	0.0	0.0	0.0	0.0	0.0	0.0	0.0	0.0	0.0	0.0	0.0	0.0	0.0	0.0	0.0
112	0.0	0.0	0.0	0.0	0.0	0.0	0.0	0.0	0.0	0.0	0.0	0.0	0.0	0.0	0.0	0.0	0.0	0.0	0.0
119	0.0	0.0	0.0	0.0	0.0	0.0	0.0	0.0	0.0	0.0	0.0	0.0	0.0	0.0	0.0	0.0	0.0	0.0	0.0
126	0.0	0.0	0.0	0.0	0.0	0.0	0.0	0.0	0.0	0.0	0.0	0.0	0.0	0.0	0.0	0.0	0.0	0.0	0.0

EIGENVECTORS FOR POINT NO. = 3 Mode 3, Frequency = 0.3710 Hz, $\alpha = 4$ RPM

EIGENVALUES = 0.2330932AF 01 (rad/sec.)

REAL PART	IMAGINARY PART
1 TO 7	0.75957E-03
8 TO 14	-0.4827E-02
15 TO 21	-0.8113E-01
22 TO 28	-0.1871E-01
29 TO 35	-0.3571E-04
36 TO 42	-0.4117E-00
43 TO 49	-0.6747E-01
50 TO 56	-0.9622E-03
57 TO 63	-0.9406E-07
64 TO 70	-0.5292E-04
71 TO 77	-0.2692E-06
78 TO 84	-0.9613E-03
85 TO 91	-0.1616E-07
92 TO 98	-0.1296E-04
99 TO 105	-0.1811E-04
106 TO 112	-0.2447E-07
113 TO 114	-0.2494E-00
1 TO 7	0.7865E-03
8 TO 14	-0.2970E-00
15 TO 21	-0.2074E-00
22 TO 28	-0.7569E-03
29 TO 35	-0.1619E-00
36 TO 42	-0.5594E-04
43 TO 49	-0.1917E-05
50 TO 56	-0.2279E-05
57 TO 63	-0.0
64 TO 70	-0.1123E-07
71 TO 77	-0.5410E-06
78 TO 84	-0.0
85 TO 91	-0.3014E-05
92 TO 98	-0.0
99 TO 105	-0.0
106 TO 112	-0.0
113 TO 114	-0.5646E-06
1 TO 7	-0.2521E-03
8 TO 14	-0.4862E-01
15 TO 21	-0.4798E-00
22 TO 28	-0.3349E-03
29 TO 35	-0.3210E-00
36 TO 42	-0.2122E-04
43 TO 49	-0.2530E-06
50 TO 56	-0.9631E-03
57 TO 63	-0.7492E-06
64 TO 70	-0.1195E-04
71 TO 77	-0.3722E-08
78 TO 84	-0.2537E-05
85 TO 91	-0.1338E-08
92 TO 98	-0.2596E-07
99 TO 105	-0.4995E-05
106 TO 112	-0.7195E-06
113 TO 114	-0.2569E-02
1 TO 7	-0.2035E-00
8 TO 14	-0.7128E-03
15 TO 21	-0.1214E-00
22 TO 28	-0.5159E-03
29 TO 35	-0.1144E-00
36 TO 42	-0.2136E-05
43 TO 49	-0.5471E-04
50 TO 56	-0.1637E-06
57 TO 63	-0.4390E-05
64 TO 70	-0.0
71 TO 77	-0.1102E-05
78 TO 84	-0.0
85 TO 91	-0.1558E-06
92 TO 98	-0.1915E-05
99 TO 105	-0.1139E-05
106 TO 112	-0.5031E-03
113 TO 114	-0.0
1 TO 7	-0.1190E-03
8 TO 14	-0.6012E-01
15 TO 21	-0.6194E-00
22 TO 28	-0.3614E-01
29 TO 35	-0.3313E-04
36 TO 42	-0.2995E-05
43 TO 49	-0.9885E-03
50 TO 56	-0.1516E-01
57 TO 63	-0.3753E-05
64 TO 70	-0.7441E-04
71 TO 77	-0.6551E-06
78 TO 84	-0.5992E-06
85 TO 91	-0.1634E-04
92 TO 98	-0.6841E-06
99 TO 105	-0.7633E-06
106 TO 112	-0.1278E-02
113 TO 114	-0.3020E-04
1 TO 7	-0.5524E-03
8 TO 14	-0.3090E-03
15 TO 21	-0.0
22 TO 28	-0.5474E-03
29 TO 35	-0.2573E-01
36 TO 42	-0.2008E-03
43 TO 49	-0.0
50 TO 56	-0.1367E-05
57 TO 63	-0.7490E-06
64 TO 70	-0.0
71 TO 77	-0.1332E-06
78 TO 84	-0.4112E-05
85 TO 91	-0.2626E-06
92 TO 98	-0.3599E-05
99 TO 105	-0.1599E-03
106 TO 112	-0.0
113 TO 114	-0.0

EIGENVECTORS FOR POINT NO. = 10

Mode 10, Frequency = 0.5151 Hz, $\Omega = 4$ RPM

EIGENVALUE = 7.32766947E 01 (rad/sec.)

duces from available

REAL PART	IMAGINARY PART						
1	1	0.7464E-07	0.1242E-02	-0.8716E-07	0.2130E-07	0.1194E-02	0.9144E-00
2	2	0.1176E-02	-0.5059E-00	0.1529E-02	0.1176E-02	0.2009E-00	0.1948E-02
3	3	0.1123E-00	-0.1922E-08	0.1195E-07	-0.1017E-00	0.4025E-07	0.5081E-01
4	4	0.3492E-09	0.2360E-02	0.4546E-00	0.5625E-07	0.2375E-02	-0.1463E-07
5	5	0.2376E-02	-0.1616E-00	0.4275E-07	0.1465E-02	0.4020E-07	0.1455E-02
6	6	-0.5698E-01	0.7713E-07	0.1402E-05	0.9093E-00	-0.7457E-07	-0.6223E-07
7	7	0.1400E-01	-0.1000E-01	-0.7557E-02	0.4485E-00	0.3135E-07	0.4479E-00
8	8	-0.7657E-02	0.5759E-02	-0.2740E-07	0.1400E-05	-0.4487E-02	0.4686E-00
9	9	0.3523E-07	0.1508E-07	-0.9194E-02	0.7915E-04	-0.6373E-13	0.9599E-09
10	10	0.4053E-02	0.1040E-04	-0.8724E-10	0.3129E-07	0.1699E-07	0.5909E-04
11	11	0.2543E-09	-0.3359E-07	0.1252E-07	0.2418E-02	0.3507E-04	0.1353E-09
12	12	0.1401E-05	-0.9101E-03	-0.7455E-02	-0.2188E-05	0.4958E-09	-0.2991E-01
13	13	0.9558E-04	0.1678E-12	-0.1896E-09	-0.3769E-04	0.1579E-12	0.6897E-11
14	14	0.1492E-07	-0.1961E-07	0.5377E-04	0.5960E-05	0.8681E-09	0.1411E-05
15	15	-0.1609E-02	-0.5728E-02	-0.1554E-05	-0.3523E-08	0.3698E-10	-0.1273E-02
16	16	-0.1874E-02	0.2675E-05	0.7405E-08	0.5570E-10	0.2843E-05	-0.3802E-02
17	17	0.1237E-06	0.3264E-11				
18	18	-0.6054E-05	0.5640E-06	0.0	-0.3632E-05	0.2912E-05	-0.3341E-05
19	19	0.7344E-05	0.0	-0.3344E-05	0.1834E-05	0.0	-0.1431E-05
20	20	0.0	-0.3060E-05	-0.3078E-05	0.0	-0.3375E-05	0.0
21	21	-0.3574E-05	0.1214E-05	0.0	-0.3077E-05	-0.2447E-05	-0.3077E-05
22	22	0.3484E-05	0.0	-0.1898E-05	-0.7097E-06	0.0	0.1991E-05
23	23	0.0	-0.4134E-09	0.7447E-11	0.0	0.0	-0.4231E-05
24	24	0.8246E-11	0.0	0.0	0.1842E-11	-0.3061E-09	0.0
25	25	0.0	-0.9430E-12	-0.3107E-09	0.8175E-11	0.0	0.9844E-12
26	26	0.6372E-09	0.2684E-11	0.0	0.0	0.3017E-11	-0.1327E-12
27	27	0.0	0.6733E-11	-0.3115E-11	0.22691E-09	0.1710E-11	0.0
28	28	0.6733E-11	0.2720E-09	0.5421E-12	0.0	0.0	-0.6945E-09
29	29	0.9055E-11	0.0	0.0	0.0	0.0	0.0
30	30	0.0	0.0	-0.5916E-11	0.0	0.4570E-13	-0.2799E-09
31	31	0.1009E-11	0.0	0.0	0.0	0.0	0.0
32	32	0.0	0.0	0.0	0.0	0.4420E-14	0.1158E-10
33	33	0.0	0.0	0.0	0.0	-0.1954E-09	0.1768E-11
34	34	0.0	0.0	-0.3372E-14	-0.2200E-09	0.5617E-12	0.0
35	35	0.0	0.1466E-06	0.0	0.0	0.2894E-12	0.0

EIGENVECTOR FOR POINT NO. = 17

Mode 17, Frequency = 0.7777 Hz, $\Omega = 4$ RPM

EIGENVALUE = 3.48864746E 01 (rad/sec.)

REAL PART		IMAGINARY PART	
I	J	I	J
1	7	1	7
2	14	2	14
3	21	3	21
4	28	4	28
5	35	5	35
6	42	6	42
7	49	7	49
8	56	8	56
9	63	9	63
10	70	10	70
11	77	11	77
12	84	12	84
13	91	13	91
14	98	14	98
15	105	15	105
16	112	16	112
17	119	17	119
18	126	18	126
19	133	19	133
20	140	20	140
21	147	21	147
22	154	22	154
23	161	23	161
24	168	24	168
25	175	25	175
26	182	26	182
27	189	27	189
28	196	28	196
29	203	29	203
30	210	30	210
31	217	31	217
32	224	32	224
33	231	33	231
34	238	34	238
35	245	35	245
36	252	36	252
37	259	37	259
38	266	38	266
39	273	39	273
40	280	40	280
41	287	41	287
42	294	42	294
43	301	43	301
44	308	44	308
45	315	45	315
46	322	46	322
47	329	47	329
48	336	48	336
49	343	49	343
50	350	50	350
51	357	51	357
52	364	52	364
53	371	53	371
54	378	54	378
55	385	55	385
56	392	56	392
57	399	57	399
58	406	58	406
59	413	59	413
60	420	60	420
61	427	61	427
62	434	62	434
63	441	63	441
64	448	64	448
65	455	65	455
66	462	66	462
67	469	67	469
68	476	68	476
69	483	69	483
70	490	70	490
71	497	71	497
72	504	72	504
73	511	73	511
74	518	74	518
75	525	75	525
76	532	76	532
77	539	77	539
78	546	78	546
79	553	79	553
80	560	80	560
81	567	81	567
82	574	82	574
83	581	83	581
84	588	84	588
85	595	85	595
86	602	86	602
87	609	87	609
88	616	88	616
89	623	89	623
90	630	90	630
91	637	91	637
92	644	92	644
93	651	93	651
94	658	94	658
95	665	95	665
96	672	96	672
97	679	97	679
98	686	98	686
99	693	99	693
100	700	100	700
101	707	101	707
102	714	102	714
103	721	103	721
104	728	104	728
105	735	105	735
106	742	106	742
107	749	107	749
108	756	108	756
109	763	109	763
110	770	110	770
111	777	111	777
112	784	112	784
113	791	113	791
114	798	114	798
115	805	115	805
116	812	116	812
117	819	117	819
118	826	118	826
119	833	119	833
120	840	120	840
121	847	121	847
122	854	122	854
123	861	123	861
124	868	124	868
125	875	125	875
126	882	126	882
127	889	127	889
128	896	128	896
129	903	129	903
130	910	130	910
131	917	131	917
132	924	132	924
133	931	133	931
134	938	134	938
135	945	135	945
136	952	136	952
137	959	137	959
138	966	138	966
139	973	139	973
140	980	140	980
141	987	141	987
142	994	142	994
143	1001	143	1001
144	1008	144	1008
145	1015	145	1015
146	1022	146	1022
147	1029	147	1029
148	1036	148	1036
149	1043	149	1043
150	1050	150	1050
151	1057	151	1057
152	1064	152	1064
153	1071	153	1071
154	1078	154	1078
155	1085	155	1085
156	1092	156	1092
157	1099	157	1099
158	1106	158	1106
159	1113	159	1113
160	1120	160	1120
161	1127	161	1127
162	1134	162	1134
163	1141	163	1141
164	1148	164	1148
165	1155	165	1155
166	1162	166	1162
167	1169	167	1169
168	1176	168	1176
169	1183	169	1183
170	1190	170	1190
171	1197	171	1197
172	1204	172	1204
173	1211	173	1211
174	1218	174	1218
175	1225	175	1225
176	1232	176	1232
177	1239	177	1239
178	1246	178	1246
179	1253	179	1253
180	1260	180	1260
181	1267	181	1267
182	1274	182	1274
183	1281	183	1281
184	1288	184	1288
185	1295	185	1295
186	1302	186	1302
187	1309	187	1309
188	1316	188	1316
189	1323	189	1323
190	1330	190	1330
191	1337	191	1337
192	1344	192	1344
193	1351	193	1351
194	1358	194	1358
195	1365	195	1365
196	1372	196	1372
197	1379	197	1379
198	1386	198	1386
199	1393	199	1393
200	1400	200	1400

EIGENVECTOR FOR POINT N7. = 18

Mode 18, Frequency = 0.7911 Hz, Ω = 4 RPM

EIGENVALUE = 0.49705811E 01 (rad/sec)

REAL PART		IMAGINARY PART	
1	7	-0.1537E-05	-0.4999E-01
9	14	-0.5113E-04	0.1011E-05
15	21	-0.4924E-00	0.1812E-01
22	28	0.1445E-05	0.1700E-01
29	35	-0.3661E-02	0.1499E-00
36	42	-0.7533E-00	-0.1918E-06
43	49	-0.2181E-05	-0.2717E-05
50	56	0.2554E-03	-0.2551E-03
57	63	0.2487E-06	0.1816E-05
64	70	0.5654E-03	-0.1449E-02
71	77	0.1591E-09	-0.7809E-09
78	84	-0.2185E-05	0.1216E-06
85	91	0.2166E-04	0.2555E-03
92	98	0.1444E-06	-0.0933E-09
99	105	-0.2254E-03	0.8113E-05
106	112	-0.7005E-04	-0.7423E-07
113	119	0.7293E-07	0.6668E-07
1	7	0.1433E-04	0.1637E-04
9	14	-0.2262E-05	0.0
15	21	0.5359E-05	-0.1763E-04
22	28	0.2634E-04	0.4923E-05
29	35	0.1605E-06	0.0
36	42	0.0	-0.2755E-05
43	49	-0.1633E-03	-0.1634E-09
50	56	0.0	0.0
57	63	-0.2260E-04	-0.3576E-08
64	70	0.0	-0.1407E-10
71	77	-0.1605E-10	-0.2927E-11
78	84	-0.1538E-09	0.0
85	91	0.0	0.2225E-10
92	98	-0.1324E-10	0.0
99	105	0.0	0.0
106	112	0.0	0.1705E-12
113	119	0.0	0.2527E-14
1	7	-0.4822E-02	0.2044E-05
9	14	-0.9639E-01	-0.1979E-01
15	21	-0.1205E-05	0.4345E-00
22	28	-0.1053E-01	-0.6488E-06
29	35	0.3459E-00	0.2641E-02
36	42	0.2554E-03	-0.3355E-01
43	49	-0.1823E-05	-0.2459E-07
50	56	0.1476E-01	-0.2191E-05
57	63	-0.1140E-09	0.1305E-04
64	70	0.1474E-06	0.2764E-06
71	77	0.4904E-05	0.3471E-03
78	84	-0.3489E-07	-0.1493E-05
85	91	0.0484E-12	-0.4191E-05
92	98	0.8221E-08	0.1045E-05
99	105	0.3303E-09	-0.6704E-07
106	112	0.2305E-04	0.5625E-03
113	119	0.0	0.0
1	7	0.1698E-04	0.8437E-05
9	14	0.0	0.1287E-04
15	21	0.9371E-05	0.0
22	28	0.5492E-05	-0.1109E-04
29	35	0.0	-0.1577E-04
36	42	0.0	0.0
43	49	-0.3770E-08	-0.9151E-11
50	56	0.0	-0.1549E-09
57	63	-0.1607E-10	0.0
64	70	-0.2267E-10	-0.4272E-09
71	77	0.0	0.0
78	84	-0.1419E-11	0.0
85	91	-0.2230E-10	0.0
92	98	-0.3880E-08	-0.7338E-12
99	105	-0.1147E-10	-0.2165E-09
106	112	0.0	-0.1804E-10
113	119	0.0	0.0
1	7	0.7488E-01	-0.6194E-06
9	14	-0.2637E-05	0.2594E-01
15	21	0.1097E-01	-0.2720E-00
22	28	0.1700E-01	0.8821E-06
29	35	0.7653E-06	0.2907E-01
36	42	-0.2544E-07	0.3677E-05
43	49	-0.2195E-05	-0.1514E-01
50	56	0.2554E-03	-0.2833E-07
57	63	-0.1140E-06	0.9341E-07
64	70	0.5903E-03	0.1072E-04
71	77	0.1065E-08	0.1110E-08
78	84	0.1383E-06	-0.5131E-02
85	91	-0.9911E-09	0.5635E-10
92	98	0.8330E-09	0.1281E-04
99	105	0.1283E-04	-0.1823E-03
106	112	-0.2255E-03	0.1322E-03
113	119	0.0	0.0
1	7	0.0	0.3363E-05
9	14	0.8796E-06	-0.1608E-05
15	21	0.1945E-04	0.0
22	28	0.0	0.3812E-05
29	35	-0.3030E-04	0.775E-07
36	42	0.3025E-11	-0.3010E-09
43	49	-0.1696E-09	0.0
50	56	0.0	-0.5345E-11
57	63	-0.1899E-08	0.2745E-11
64	70	0.0	0.0
71	77	0.1278E-10	-0.3773E-09
78	84	-0.2230E-10	0.0
85	91	-0.3880E-08	0.0
92	98	-0.1147E-10	-0.3705E-09
99	105	0.0	-0.3161E-11
106	112	0.0	0.0
113	119	0.0	0.0

EIGENVECTOR FOR ROOT N1 = 20

Mode 20, Frequency = 0.9291 Hz, $\Omega = 4$ RPM

EIGENVALUE = 0.58375244E 01 (rad/sec.)

REAL PART	IMAGINARY PART					
1 10 7	0.1000E 01	0.4845E-01	0.3290E-03	0.6205E 00	-0.6421E-01	-0.1456E-03
9 10 14	-0.2506E 00	-0.1595E-03	0.4274E 00	-0.2750E-01	-0.5165E-03	-0.6696E 00
15 10 21	0.2266E-03	0.5235E-03	-0.1030E-01	-0.2532E-03	0.8703E-01	0.3993E-02
22 10 28	0.2540E-03	0.8473E-01	0.1437E-03	-0.2977E 00	-0.6194E-01	0.1457E-03
29 10 35	-0.2879E 00	0.2564E-01	-0.1471E 00	0.2039E 00	0.5431E-04	-0.2561E 00
35 10 42	-0.1125E-01	-0.7641E-03	0.6814E-03	-0.7821E-04	-0.5125E-05	-0.7298E-03
43 10 50	0.8564E-03	-0.7835E-04	-0.4932E-05	-0.3517E-03	0.6512E-03	-0.7851E-04
57 10 56	-0.2140E-09	-0.5712E-05	0.3584E-03	0.5554E-03	0.2263E-08	-0.5611E-05
57 10 56	0.4893E-04	0.2785E-04	-0.1933E-04	-0.1420E-06	-0.4267E-04	0.1770E-04
64 10 70	0.1329E-05	0.5778E-08	-0.1230E-06	0.5071E-04	0.2214E-05	0.1343E-06
71 10 77	0.3208E-06	-0.4239E-04	0.2301E-04	0.1110E-05	0.2074E-06	0.1975E-06
79 10 84	0.6547E-03	-0.7866E-04	0.6107E-08	0.4900E-06	-0.2860E-04	-0.3596E-04
85 10 91	0.3065E-07	0.3970E-11	-0.2074E-06	-0.6792E-05	0.2860E-04	-0.3596E-04
92 10 98	0.2731E-04	0.1555E-05	0.1120E-07	0.1133E-07	-0.2075E-06	0.1098E-07
99 10 105	0.3466E-04	0.2554E-07	0.3628E-06	-0.6438E-07	0.1600E-06	0.3502E-02
105 10 112	0.6149E-07	-0.2322E-06	0.1415E-04	0.1215E-06	0.2519E-02	0.4578E-04
113 10 114	0.2628E-09	0.2386E-05		0.1216E-06	0.8494E-04	0.6489E-07
IMAGINARY PART						
1 10 7	-0.7737E-03	0.3443E-02	0.0	-0.6296E-03	0.0	-0.3223E-03
9 10 14	0.1553E-02	0.0	-0.5094E-03	-0.1933E-02	0.3306E-03	-0.3071E-03
15 10 21	0.0	-0.7958E-04	0.4515E-03	0.0	-0.2754E-03	0.0
22 10 28	-0.2030E-03	0.2673E-03	0.0	-0.1735E-04	0.0	-0.1720E-04
29 10 35	0.1100E-02	0.0	-0.9437E-05	-0.3047E-03	-0.1448E-04	0.5276E-03
35 10 42	0.0	-0.3765E-05	-0.3111E-07	0.0	-0.1346E-07	-0.3414E-05
43 10 50	-0.7401E-07	0.0	0.0	0.8578E-09	-0.8607E-07	0.0
57 10 56	0.0	-0.9173E-09	-0.2851E-05	-0.7916E-07	0.0	0.6003E-08
57 10 56	0.0	-0.6596E-08	0.0	0.0	0.0	-0.2134E-08
57 10 56	0.0	0.0	0.9409E-09	-0.7095E-06	-0.6281E-09	0.0
71 10 77	-0.1344E-07	-0.6446E-06	-0.3127E-09	0.0	0.0	0.1270E-07
73 10 84	-0.8262E-07	0.0	0.0	0.0	-0.3912E-09	-0.8024E-08
95 10 91	0.0	0.0	0.1559E-07	0.0	0.0	0.0
97 10 98	-0.4831E-08	0.0	0.0	-0.2493E-09	-0.1468E-07	-0.2345E-06
99 10 105	0.0	0.0	0.0	0.0	-0.2606E-05	-0.2806E-07
105 10 112	0.0	0.0	0.0	-0.8216E-10	-0.2244E-07	0.0
113 10 114	0.0	0.0	0.7110E-11	-0.2348E-05	0.0	0.0



EIGENVALUES FOR PART NO. 28

Mode 28. Frequency = 1.051 Hz. $\Omega = 4$ RPM

EIGENVALUES 0.56011606F 01 (rad/sec.)

REAL PART	IMAGINARY PART
1 7	0.1199E-01
8 7	-0.9094E-00
14 7	-0.2431E-01
15 7	-0.1605E-01
22 7	-0.7770E-02
23 7	0.2778E-00
34 7	0.2210E-01
43 7	0.1860E-00
50 7	0.8831E-00
57 7	0.1895E-02
64 7	-0.6294E-05
71 7	0.1477E-04
78 7	0.1185E-00
85 7	-0.3125E-05
92 7	0.2098E-03
99 7	0.7418E-04
105 7	0.5524E-07
112 7	0.3731E-09
113 7	0.2141E-03
1 7	0.2507E-03
3 7	-0.3214E-02
15 7	0.0
22 7	-0.1072E-02
23 7	-0.4004E-02
34 7	0.0
43 7	-0.3163E-05
50 7	0.0
57 7	-0.1155E-04
64 7	0.0
71 7	-0.1140E-06
78 7	-0.3150E-05
85 7	0.0
92 7	-0.3444E-07
99 7	0.0
105 7	0.0
112 7	0.0
113 7	0.1510E-09
1 7	-0.2027E-01
8 7	-0.5434E-02
14 7	0.8074E-00
15 7	0.3314E-01
22 7	0.6309E-02
23 7	0.2722E-00
34 7	-0.1871E-03
43 7	0.1301E-03
50 7	-0.9432E-07
57 7	0.3273E-04
64 7	0.7249E-07
71 7	-0.2737E-05
78 7	0.1424E-03
85 7	0.8001E-07
92 7	-0.1581E-04
99 7	-0.1102E-04
105 7	0.8000E-06
112 7	0.1170E-03
113 7	0.2418E-04
1 7	0.2532E-03
3 7	0.3247E-02
15 7	0.0
22 7	-0.3225E-03
23 7	-0.2457E-02
34 7	0.0
43 7	0.2555E-05
50 7	-0.1581E-05
57 7	0.0
64 7	-0.6873E-05
71 7	0.0
78 7	-0.3750E-07
85 7	0.0
92 7	0.1419E-04
99 7	0.0
105 7	-0.1532E-08
112 7	-0.3393E-04
113 7	-0.1829E-05
1 7	-0.1157E-01
8 7	-0.9989E-00
14 7	0.3314E-01
15 7	0.6309E-02
22 7	0.2722E-00
34 7	-0.1871E-03
43 7	0.1301E-03
50 7	-0.9432E-07
57 7	0.3273E-04
64 7	0.7249E-07
71 7	-0.2737E-05
78 7	0.1424E-03
85 7	0.8001E-07
92 7	-0.1581E-04
99 7	-0.1102E-04
105 7	0.8000E-06
112 7	0.1170E-03
113 7	0.2418E-04
1 7	0.5133E-02
3 7	0.0
15 7	-0.1073E-02
22 7	0.4052E-02
23 7	0.0
34 7	-0.3336E-03
43 7	-0.2624E-05
50 7	-0.3433E-05
57 7	0.0
64 7	-0.1235E-03
71 7	-0.9447E-07
78 7	0.2077E-07
85 7	0.0
92 7	-0.7505E-08
99 7	0.0
105 7	-0.3071E-08
112 7	-0.1871E-04
113 7	-0.1829E-05
1 7	0.3455E-03
3 7	0.3704E-02
15 7	0.0
22 7	-0.3883E-03
23 7	-0.2333E-02
34 7	0.0
43 7	0.1644E-05
50 7	0.0
57 7	-0.1811E-06
64 7	0.0
71 7	-0.6981E-04
78 7	0.2255E-07
85 7	0.0
92 7	-0.3054E-05
99 7	0.0
105 7	-0.1733E-05
112 7	0.0
113 7	0.0

EIGENVECTOR FOR ROOT NO.= 2

Mode 2. Frequency = 0.1977 Hz, $\Omega = 8$ RPM

EIGENVALUE= 0.12424011E 01 (rad/sec.)

REAL PART	7	0.2047E-09	0.2169E-05	-0.5096E 00	-0.3265E-10	0.2169E-05	0.2169E-05	0.6463E 00	0.1286E-09
1 TO 7	0.2047E-09	0.2169E-05	-0.5096E 00	-0.3265E-10	0.2169E-05	0.2169E-05	0.6463E 00	0.1286E-09	
8 TO 14	0.2439E-05	-0.5463E 00	-0.6307E-11	0.2439E-05	-0.6081E 00	0.1884E-09	0.1884E-09	0.1562E-05	
15 TO 21	-0.6855E 00	-0.1562E-05	0.1562E-05	-0.6855E 00	0.1023E-09	0.1712E-05	0.1712E-05	-0.7372E 00	
22 TO 28	-0.2473E-10	0.1712E-05	-0.5214E 00	0.1218E-09	-0.1033E-06	-0.2843E 00	-0.2843E 00	-0.4964E-10	
29 TO 35	-0.1083E-06	-0.3050E 00	0.8534E-10	-0.1664E-05	-0.3050E 00	0.3472E-10	0.3472E-10	0.1664E-05	
36 TO 42	-0.3381E 00	0.1266E-09	0.1266E-09	-0.3381E 00	-0.8276E-03	0.1039E-11	0.1039E-11	-0.1072E-09	
43 TO 49	0.2352E-08	-0.1000E 01	-0.8305E-03	0.7766E-12	0.5392E-10	0.2350E-08	0.2350E-08	-0.8432E 00	
50 TO 56	-0.8279E-03	0.9539E-12	-0.4998E-10	0.2352E-08	-0.9402E 00	-0.8300E-03	-0.8300E-03	0.8279E-12	
57 TO 63	0.6131E-10	0.2582E-10	-0.4918E-02	0.1598E-04	-0.1131E-12	-0.6339E-10	-0.6339E-10	0.1643E-10	
64 TO 70	-0.1969E-02	0.7332E-05	-0.1404E-12	0.5429E-10	0.2557E-10	-0.3803E-02	-0.3803E-02	0.1460E-04	
71 TO 77	0.4546E-12	-0.5694E-10	0.2137E-10	-0.2503E-02	0.7872E-05	0.4929E-12	0.4929E-12	0.2404E-12	
78 TO 84	0.2351E-05	-0.8917E 00	-0.8238E-03	0.1239E-02	0.8894E-12	0.2653E-10	0.2653E-10	-0.8791E-02	
85 TO 91	0.1637E-04	0.3198E-15	-0.3299E-12	0.8691E-05	0.3198E-15	-0.3287E-12	-0.3287E-12	0.1229E-13	
92 TO 98	0.2536E-10	-0.3039E-02	0.1102E-04	0.1232E-03	0.1466E-11	0.1734E-12	0.1734E-12	0.2693E-08	
99 TO 105	-0.5844E 00	-0.6185E-03	0.1178E-02	-0.5908E-11	0.7101E-13	0.2163E-08	0.2163E-08	-0.1019E 00	
106 TO 112	-0.1991E-03	0.6343E-03	0.1226E-10	0.1161E-12	0.4267E-08	-0.3091E 00	-0.3091E 00	-0.4090E-03	
113 TO 114	0.9835E-03	0.6012E-14							
IMAGINARY PART									
1 TO 7	-0.1317E-08	0.3927E-08	0.0	-0.1317E-08	0.1174E-08	0.0	0.0	-0.2783E-08	
8 TO 14	0.2151E-08	0.0	-0.2784E-08	0.1008E-08	0.0	-0.1012E-08	-0.1012E-08	0.3117E-08	
15 TO 21	0.0	-0.1012E-08	0.6463E-09	0.0	-0.1963E-08	0.1565E-08	0.1565E-08	0.0	
22 TO 28	-0.1963E-08	0.5285E-09	0.0	0.1052E-09	-0.2600E-08	0.0	0.0	0.1053E-09	
29 TO 35	0.1541E-08	0.0	-0.1672E-08	-0.9982E-09	0.0	-0.1672E-08	-0.1672E-08	0.1521E-08	
36 TO 42	0.0	-0.4865E-11	-0.1742E-13	0.0	0.0	-0.4348E-13	-0.4348E-13	-0.4697E-11	
43 TO 49	-0.1924E-13	0.0	0.0	0.4108E-13	-0.2104E-11	0.0	0.0	0.0	
50 TO 56	0.0	-0.2815E-13	-0.2073E-11	-0.1833E-13	0.0	-0.1305E-11	-0.1305E-11	0.2713E-13	
57 TO 63	0.4367E-15	0.0	0.6267E-14	0.0	-0.6503E-14	0.0	0.0	-0.4217E-14	
64 TO 70	0.0	0.0	-0.3326E-14	0.0	-0.6736E-15	0.0	0.0	0.0	
71 TO 77	-0.1286E-13	-0.5780E-12	0.0	0.0	0.0	0.1241E-13	0.1241E-13	-0.1160E-11	
78 TO 84	-0.1779E-13	0.0	0.0	0.0	-0.1394E-15	-0.2796E-14	-0.2796E-14	0.0	
85 TO 91	0.0	0.0	0.1176E-13	0.0	0.0	-0.1135E-13	-0.1135E-13	-0.8289E-13	
92 TO 98	-0.2091E-14	0.0	0.0	0.0	-0.1185E-15	-0.9189E-12	-0.9189E-12	-0.1136E-13	
99 TO 105	0.0	0.0	0.0	0.7864E-17	-0.4248E-12	-0.1290E-13	-0.1290E-13	0.0	
106 TO 112	0.0	0.0	0.1318E-16	-0.7330E-12	-0.7619E-14	0.0	0.0	0.0	
113 TO 114	0.0	0.2965E-22							

EIGENVECTOR FOR ROOT N1. = 3

Mode 3. Frequency = 0.3524 Hz, $\Omega = 8$ RPM

EIGENVALUE = 0.22144775F U1 (rad/sec.)

REAL PART	7	0.1236E-02	-0.2601E 00	0.4525E-03	0.1315E-02	-0.1500F 00	-0.2957E-02	0.1071E-02
1	10	-0.1713E 00	0.4280E-02	0.1121E-02	-0.4434E-01	0.1507E-01	0.1087E-02	-0.5129E 00
8	10	-0.3375E-02	-0.1306E 00	-0.3038E 00	-0.9728E-02	0.9261E-03	-0.2980E 00	0.3774E-02
15	10	0.1049E-02	0.2245E 00	0.2414E-01	0.7494E-03	-0.2786E 00	-0.2987E-02	0.1093F-02
22	10	-0.2725E 00	-0.1152E-01	0.1049E-02	-0.3192E 00	0.1032E-01	0.1027E-02	-0.2399E 00
29	10	0.3791E-01	-0.5768E-03	-0.3167E-02	-0.2655E-05	0.3071E-07	-0.5869E-05	0.2393E-03
36	10	-0.3163E-02	0.5651E-05	0.3443E-07	-0.1826E-05	-0.1996E-03	-0.3164E-02	-0.4340E-06
43	10	0.3119E-07	-0.3973E-05	0.1089E-03	-0.3162E-02	0.3222E-05	0.3223E-07	-0.1783E-05
50	10	0.3580E-04	-0.6537E-05	0.1121E-06	-0.8655E-09	-0.4679E-06	0.2816E-05	-0.3674E-05
57	10	0.1049E-08	-0.3154E-10	0.8346E-07	-0.3514E-04	-0.6398E-05	0.2943E-07	-0.8605E-09
64	10	-0.3004E-06	0.6693E-05	-0.4305E-05	0.3857E-08	-0.4215E-10	-0.3820E-07	-0.1198E-04
71	10	0.3153E-07	0.1395E-05	0.3102E-07	-0.2234E-08	-0.2654E-05	-0.7755E-05	-0.1291E-06
78	10	0.1950E-06	0.5410E-12	0.7736E-06	0.8378E-11	0.5410E-12	-0.2435E-07	-0.9155E-06
85	10	-0.5133E-05	0.7440E-08	-0.1011F-09	-0.6484E-09	-0.1887E-06	-0.9130F-05	-0.1972E-02
92	10	0.9091E-06	0.2164E-07	-0.1641E-08	-0.6019E-05	-0.3526E-05	0.2968E-04	0.6406E-06
99	10	0.6671E-08	-0.1872E-08	-0.4989E-06	-0.6237E-05	-0.5514E-03	0.6855E-06	0.1366E-07
106	10	0.6320E-10	-0.4319E-05					
IMAGINARY PART								
1	10	0.3176E-03	0.4493E 00	0.0	0.9188E-03	0.1769E 00	0.0	0.7844E-03
8	10	0.1211E 00	0.0	0.6462E-03	0.1256E 00	0.0	0.7767E-03	0.8584E 00
15	10	0.0	0.8480E-03	-0.5122E 00	0.0	0.6709E-03	0.4354E 00	0.0
22	10	0.6081E-03	0.3948E 00	0.0	0.5136E-03	0.4287E 00	0.0	0.7657E-03
29	10	0.4653E 00	0.0	0.6675E-03	0.5025E 00	0.0	0.6171E-03	0.4468E 00
36	10	0.0	-0.1693F-03	-0.5441E-02	0.0	0.0	-0.2306E-05	0.1717E-03
43	10	-0.5450E-02	0.0	0.0	-0.1866E-05	-0.3169E-04	-0.5446E-02	0.0
50	10	0.0	-0.1145E-05	0.5617E-04	-0.5449E-02	0.0	0.0	-0.1081E-05
57	10	0.0	-0.2943F-04	0.0	0.0	-0.1761E-06	0.1320E-03	-0.1817E-04
64	10	0.0	0.7557F-04	-0.4125E-06	0.0	-0.2829E-04	0.0	0.0
71	10	-0.5955E-06	0.0	-0.2302E-04	0.0	0.0	-0.1089E-05	0.1158E-04
78	10	0.0	0.0	0.0	0.0	-0.5355E-06	-0.3220E-04	0.0
85	10	0.0	0.0	0.6014E-06	0.0	0.0	0.1037E-05	0.1081E-05
92	10	-0.2716E-04	0.0	0.0	0.0	-0.1446E-05	0.9133E-05	-0.5288E-02
99	10	0.0	0.0	0.0	-0.1532E-05	0.3866E-05	-0.1895E-02	0.0
106	10	0.0	0.0	-0.1058E-04	0.6585E-05	-0.4299E-02	0.0	0.0
113	10	0.0	-0.7085E-05					

FIGURE VECTOR FOR POINT NO. = 9, Mode 9, Frequency = 0.5025 Hz, $\Omega = 8$ RPM

EIGENVALUE = 0.31574402E 01 (rad/sec.)

REAL PART		IMAGINARY PART	
1	7	0.4196E-06	0.3547E-02
8	14	0.3547E-02	-0.9697E-00
15	21	0.4790E-00	-0.1223E-06
22	28	-0.3545E-07	0.3552E-02
29	35	0.3745E-02	0.7443E-00
36	42	-0.4808E-00	0.1650E-06
43	49	0.4239E-05	0.4230E-05
50	56	0.2835E-04	0.3040E-04
57	63	0.1077E-06	0.4239E-05
64	70	-0.1154E-03	0.6014E-05
71	77	0.7800E-05	0.9520E-07
78	84	0.4238E-05	-0.3145E-03
85	91	0.3417E-05	0.3397E-05
92	98	0.4520E-07	0.6380E-04
99	105	-0.7119E-01	-0.3171E-06
106	112	0.7545E-05	0.2235E-04
113	119	0.1117E-03	-0.1063E-07
1	7	-0.1471E-04	0.1987E-09
8	14	0.9291E-05	0.7690E-05
15	21	0.0	0.0
22	28	-0.1284E-04	0.6335E-05
29	35	-0.1198E-06	0.0
36	42	0.0	-0.9442E-05
43	49	0.4989E-10	0.7367E-05
50	56	0.0	0.0
57	63	0.3737E-06	0.1153E-10
64	70	0.0	0.4935E-10
71	77	0.3951E-10	0.0
78	84	0.4850E-10	0.1577E-08
85	91	0.0	0.0
92	98	0.5895E-11	0.1829E-10
99	105	0.0	0.3137E-11
106	112	0.0	0.0
113	119	0.0	-0.3236E-10
1	7	0.0	0.0
8	14	0.0	0.0
15	21	0.0	0.0
22	28	0.0	0.0
29	35	0.0	0.0
36	42	0.0	0.0
43	49	0.0	0.0
50	56	0.0	0.0
57	63	0.0	0.0
64	70	0.0	0.0
71	77	0.0	0.0
78	84	0.0	0.0
85	91	0.0	0.0
92	98	0.0	0.0
99	105	0.0	0.0
106	112	0.0	0.0
113	119	0.0	0.0
1	7	0.0	0.0
8	14	0.0	0.0
15	21	0.0	0.0
22	28	0.0	0.0
29	35	0.0	0.0
36	42	0.0	0.0
43	49	0.0	0.0
50	56	0.0	0.0
57	63	0.0	0.0
64	70	0.0	0.0
71	77	0.0	0.0
78	84	0.0	0.0
85	91	0.0	0.0
92	98	0.0	0.0
99	105	0.0	0.0
106	112	0.0	0.0
113	119	0.0	0.0

EIGENVECTOR FOR POINT NO.= 11 Mode 11, Frequency = 0.6881 Hz; $\Omega = 8\text{RPM}$

EIGENVALUE= 0.43236084E 01 (rad/sec.)

REAL PART		IMAGINARY PART	
7	0.3790E-03	0.9779E-01	-0.3194E-03
8	0.5181E-02	-0.1174E-01	0.2641E-02
14	0.5456E-01	0.4385E-03	0.1513E-01
15	-0.2928E-03	0.3805E 00	0.1858E-03
21	-0.4435E 00	0.1264E-01	-0.9590E 00
22	0.1009E-01	0.1283E-03	0.6560E-01
28	0.3889E-02	0.3901E-02	0.8558E-07
29	0.7714E-07	0.6528E-07	0.3253E-03
35	0.1067E-03	-0.3211E-03	-0.2363E-04
42	0.1992E-05	0.8456E-05	0.8931E-06
43	0.1067E-03	0.8997E-06	0.9876E-05
49	0.1024E-05	-0.8195E-05	-0.2161E-07
56	0.3940E-02	0.6348E-07	0.6057E-05
57	0.1992E-05	-0.2711E-04	-0.1718E-06
63	0.1067E-03	0.1663E-11	0.1584E-07
64	0.1067E-03	0.7212E-06	0.1663E-11
70	0.1067E-03	-0.9475E-05	-0.2746E-07
77	0.1067E-03	-0.6626E-08	0.1256E-04
84	0.1067E-03	-0.2411E-04	-0.1655E-07
85	0.1067E-03	-0.2711E-04	-0.9927E-06
91	0.1067E-03	0.1663E-11	0.1718E-06
92	0.1067E-03	0.7212E-06	0.1584E-07
98	0.1255E-04	0.4294E-07	-0.2746E-07
105	0.1051E-07	-0.8135E-07	0.1256E-04
106	0.1051E-07	0.4984E-05	-0.1655E-07
112	0.0	0.0	0.0
113	0.0	0.0	0.0
114	0.0	0.0	0.0
1	-0.4048E-03	0.4352E-02	-0.1394E-03
8	-0.1391E-01	0.0	-0.9504E-02
15	0.0	-0.7723E-03	-0.9241E-04
22	-0.6096E-03	-0.3339E-01	0.3733E-01
29	-0.3153E-01	0.0	0.1074E-02
36	0.0	0.4424E-03	0.3017E-01
42	0.0	-0.5119E-04	0.0
43	-0.5122E-04	0.0	0.3890E-06
49	0.0	0.2700E-06	-0.5122E-04
56	0.8387E-05	-0.1656E-06	0.0
57	0.0	0.0	0.5654E-07
63	0.7763E-07	0.4851E-05	-0.1424E-06
64	-0.5121E-04	0.0	0.0
70	0.0	0.0	0.0
77	0.0	0.0	0.0
78	0.0	0.0	0.0
84	0.0	0.0	0.0
85	0.0	0.0	0.0
91	0.0	0.0	0.0
92	0.0	0.0	0.0
99	0.0	0.0	0.0
105	0.0	0.0	0.0
106	0.0	0.0	0.0
112	0.0	0.0	0.0
113	0.0	0.0	0.0
114	0.0	0.0	0.0
1	0.0	0.1847E-01	-0.1234E-03
8	-0.1612E-02	0.0	0.2384E-01
15	-0.3345E-01	-0.6739E-03	0.0
21	0.0	-0.2754E-01	0.4967E-03
28	0.4329E-03	0.0	0.3452E-01
35	0.1044E-05	0.0	-0.7929E-05
42	-0.5121E-04	-0.1452E-05	0.0
43	0.0	0.0	-0.4184E-07
49	0.0	0.5654E-07	-0.8711E-07
56	0.0	-0.1424E-06	0.0
57	0.0	0.0	0.0
63	-0.1151E-06	0.0	-0.1896E-06
64	-0.1645E-06	0.0	0.0
70	0.1105E-06	0.0	0.2905E-06
77	0.1011E-05	0.0	-0.7938E-05
84	0.4408E-05	0.1169E-05	0.0
85	0.0	0.1162E-04	0.0
91	0.0	0.0	0.0
92	0.0	0.0	0.0
99	0.0	0.0	0.0
105	0.0	0.0	0.0
106	0.0	0.0	0.0
112	0.0	0.0	0.0
113	0.0	0.0	0.0
114	0.0	0.0	0.0

FIGURE VECTOR FOR ROOT NO. = 17

Mode 17, Frequency = 0.7777 Hz, $\Omega = 8$ RPM

EIGENVALUE = 0.48804740E 01 (rad/sec.)

REAL PART

1	10	7	-0.3051E-05	-0.2057E-01	0.7159E-01	0.4390E-05	-0.9714E-02	0.1068E-01	-0.1281E-05
8	10	14	0.4328E-03	-0.1660E-01	0.2200E-05	0.4269E-01	0.3337E-01	-0.5442E-05	0.5827E-01
15	10	21	0.9227E 00	0.6126E-05	0.4178E-01	0.7425E 00	-0.2405E-05	0.2504E-01	0.9753E 00
22	10	28	0.3034E-05	-0.4422E-01	0.9665E 00	-0.1286E-05	-0.2508E-01	-0.9513E 00	0.1841E-05
29	10	35	-0.1013E-01	-0.7580E 00	-0.4919E-05	0.4971E-02	-0.1000E 01	0.7681E-06	0.6786E-01
36	10	42	-0.9673E 00	-0.7721E-05	-0.4977E-05	-0.2330E-01	0.1331E-04	-0.5256E-07	0.7608E-05
43	10	49	-0.4908E-05	-0.1961E-01	0.1442E-04	-0.5083E-07	-0.3774E-05	-0.4935E-05	-0.2233E-01
50	10	56	0.1366E-04	-0.5933E-07	0.3761E-05	-0.4908E-05	-0.2065E-01	0.1469E-04	-0.5862E-07
57	10	63	0.5041E-06	0.2973E-06	0.1742E-02	-0.1501E-04	-0.2402E-08	-0.4419E-06	0.1909E-06
64	10	70	-0.4686E-03	-0.1653E-05	-0.1635E-08	0.5453E-06	0.3017E-06	0.7666E-03	-0.1192E-04
71	10	77	0.3229E-08	-0.4676E-06	0.2486E-06	-0.2426E-03	-0.5269E-05	0.2104E-08	0.2311E-08
78	10	84	-0.4915E-05	-0.2151E-01	0.1444E-04	0.6864E-04	-0.7144E-07	0.2827E-06	0.6004E-02
85	10	91	-0.1430E-04	0.2087E-11	-0.1968E-08	0.3900E-05	0.2087E-11	-0.1963E-08	0.1175E-09
92	10	98	0.2957E-06	0.1620E-03	-0.8636E-05	-0.6150E-05	0.1682E-07	0.1730E-08	0.2621E-04
99	10	105	-0.5316E-02	0.1046E-04	0.5577E-04	-0.1393E-06	0.6872E-09	0.2635E-04	0.3386E-02
106	10	112	0.2584E-05	-0.1466E-04	0.1375E-06	0.1167E-08	0.4792E-04	0.4288E-02	0.6507E-05
113	10	114	0.1567E-04	0.2053E-09	0.1375E-06	0.1167E-08	0.4792E-04	0.4288E-02	0.6507E-05

IMAGINARY PART

1	10	7	0.1421E-04	0.7183E-04	0.0	-0.8237E-05	0.7375E-04	0.0	-0.2963E-04
8	10	14	-0.5061E-05	0.0	-0.1197E-03	0.5517E-04	0.0	-0.8615E-04	-0.1499E-04
15	10	21	0.0	-0.6708E-04	0.2796E-04	0.0	-0.4766E-04	0.8227E-04	0.0
22	10	28	0.3239E-04	0.1044E-04	0.0	0.5031E-04	0.3027E-04	0.0	0.2031E-04
29	10	35	-0.3127E-05	0.0	-0.9985E-05	-0.6754E-04	0.0	-0.1362E-03	-0.2178E-05
36	10	42	0.0	-0.1486E-07	-0.7726E-09	0.0	0.0	0.2190E-11	-0.1253E-07
43	10	49	-0.7950E-09	0.0	0.0	-0.2598E-10	-0.1492E-07	-0.7758E-09	0.0
50	10	56	0.0	-0.2116E-11	-0.1412E-07	-0.7953E-09	0.0	0.0	-0.1444E-10
57	10	63	-0.9125E-08	-0.1257E-09	0.0	0.0	-0.6926E-10	-0.7661E-08	0.1818E-10
64	10	70	0.0	0.0	0.6125E-10	-0.3118E-08	-0.1048E-09	0.0	0.0
71	10	77	-0.6327E-10	-0.2500E-08	-0.1008E-10	0.0	0.0	0.5002E-10	-0.1468E-07
78	10	84	-0.7856E-09	0.0	0.0	0.0	-0.6005E-11	-0.1052E-09	0.0
85	10	91	0.0	0.0	0.9199E-10	0.0	0.0	-0.7898E-10	-0.1456E-08
92	10	98	-0.6188E-10	0.0	0.0	0.0	-0.3113E-11	-0.1507E-07	-0.8907E-10
99	10	105	0.0	0.0	0.0	-0.4469E-12	-0.8473E-08	-0.1013E-09	0.0
106	10	112	0.0	0.0	0.0	-0.1375E-07	-0.1319E-09	0.0	0.0
113	10	114	0.0	0.8087E-14	0.5678E-12	-0.1375E-07	-0.1319E-09	0.0	0.0

EIGENVECTOR FOR ROOT NO.= 15

Mode 18, Frequency = 0.7911 Hz, $\Omega = 8$ RPM

EIGENVALUE= 0.49705811E 01 (rad/sec.)

REAL PART		IMAGINARY PART	
1	10	7	7
8	10	14	14
15	10	21	21
22	10	28	28
29	10	35	35
36	10	42	42
43	10	49	49
50	10	56	56
57	10	63	63
64	10	70	70
71	10	77	77
78	10	84	84
85	10	91	91
92	10	98	98
99	10	105	105
106	10	112	112
113	10	114	114
IMAGINARY PART			
1	10	7	7
8	10	14	14
15	10	21	21
22	10	28	28
29	10	35	35
36	10	42	42
43	10	49	49
50	10	56	56
57	10	63	63
64	10	70	70
71	10	77	77
78	10	84	84
85	10	91	91
92	10	98	98
99	10	105	105
106	10	112	112
113	10	114	114

0.1562E-05	-0.1275E-01	-0.4999E-01	0.2158E-05	-0.5623E-02	0.7488E-01	-0.6660E-06	
-0.1222E-02	-0.7211E-01	0.1075E-05	0.2016E-01	-0.8530E-01	-0.2733E-05	0.2535E-01	
-0.3224E-00	0.3042E-05	0.1680E-01	0.8343E 00	-0.1225E-05	0.1083E-01	-0.2720E 00	
-0.1511E-05	-0.1693E-01	0.7499E 00	-0.6684E-06	-0.9494E-02	0.1000E 01	0.9067E-06	
-0.2154E-02	-0.9491E 00	-0.2454E-06	0.2927E-02	0.3459E 00	0.3736E-06	0.2654E-01	
-0.7533E 00	-0.3888E-05	-0.2177E-05	-0.3355E-01	0.2558E-03	-0.2648E-07	0.3830E-05	
-0.2150E-05	0.3313E-01	0.2551E-03	-0.2560E-07	-0.1900E-05	-0.2154E-05	-0.1514E-01	
0.2558E-03	-0.2988E-07	0.1893E-05	-0.2139E-05	0.1476E-01	-0.2554E-03	-0.2950E-07	
0.2672E-06	0.1568E-06	-0.1449E-02	0.1306E-04	-0.1165E-08	0.2376E-06	0.9899E-07	
0.5954E-03	0.1272E-05	-0.7998E-09	0.2826E-06	0.1573E-06	-0.5903E-03	0.1072E-04	
0.1716E-08	-0.2455E-06	0.1289E-06	0.3471E-03	0.4905E-05	0.1179E-08	0.1170E-08	
-0.2143E-04	-0.1934E-03	0.2555E-03	-0.1483E-06	-0.3596E-07	0.1549E-06	-0.5131E-02	
0.1683E-04	0.9484E-12	-0.1098E-08	-0.4191E-05	0.9484E-12	-0.1095E-08	0.5874E-10	
0.1532E-06	-0.3391E-04	0.8113E-05	0.1005E-05	0.8699E-08	0.8709E-09	0.1352E-04	
-0.1254E-03	0.1941E-03	-0.7423E-07	-0.7009E-07	0.3444E-09	0.1351E-04	-0.1823E-03	
0.7235E-04	0.3010E-06	0.7008E-07	0.5693E-09	0.2444E-04	-0.2255E-03	0.1322E-03	
-0.7235E-07	0.1208E-09						
IMAGINARY PART							
1	10	7	7				
8	10	14	14				
15	10	21	21				
22	10	28	28				
29	10	35	35				
36	10	42	42				
43	10	49	49				
50	10	56	56				
57	10	63	63				
64	10	70	70				
71	10	77	77				
78	10	84	84				
85	10	91	91				
92	10	98	98				
99	10	105	105				
106	10	112	112				
113	10	114	114				

FIG. VFCIOR FOR ROOT NO. = 19 Mode 19. Frequency = 0.9049 Hz. $\Omega = 8$ RPM

EIGENVALUE = 0.56554858E 01 (rad/sec.)

REAL PART

1	TO	7	-0.3135E-06	-0.2118E-02	0.6762E 00	0.3353E-06	-0.5446E-04	-0.5878E-01	-0.1271E-06
8	TO	14	0.1836E-04	-0.9142E 00	0.1552E-06	0.2147E-04	-0.5480E-01	-0.5134E-06	0.1364E-02
15	TO	21	-0.1147E 00	0.5253E-06	0.3416E-03	0.5855E-01	-0.2406E-06	0.3400E-04	-0.4384E-01
22	TO	28	0.2543E-06	0.3219E-04	0.2368E-01	-0.1157E-06	-0.1417E-03	-0.5136E 00	0.1337E-06
29	TO	35	-0.1419E-03	-0.2090E-01	-0.2574E-07	0.1669E-03	0.1000F 01	0.4707E-07	0.1669E-03
36	TO	42	0.1769E-02	-0.7206E-06	-0.1607E-06	-0.2771E-02	-0.7305E-05	-0.4945E-08	0.7047E-06
43	TO	49	-0.1535E-06	-0.4669E-02	-0.7232E-05	-0.4718E-08	-0.3505E-06	-0.1559E-06	-0.3296E-02
50	TO	56	0.7295E-05	-0.5530E-08	0.3430E-06	-0.1534E-06	-0.4148E-02	-0.7254E-05	-0.5424E-08
57	TO	63	0.7957E-07	0.3362E-07	0.5396E-02	-0.5030E-04	-0.2559E-09	-0.6637E-07	0.2161E-07
64	TO	70	-0.1980E-02	-0.4082E-05	-0.9112E-10	0.7570E-07	0.3351E-07	0.2162E-02	-0.3956E-04
71	TO	77	0.6385E-09	-0.5913E-07	0.2812E-07	-0.1160E-02	-0.1640E-04	0.3987E-09	0.2103E-09
73	TO	84	-0.6827E-04	-0.3723E-02	-0.7281E-05	0.1168E-04	-0.06621E-08	0.3396E-07	0.2025E-01
85	TO	91	0.5011E-13	-0.3724E-09	-0.3724E-09	0.1386E-04	0.5011E-13	-0.3721E-09	0.1055E-10
92	TO	98	0.3341E-07	0.1461E-03	-0.2858E-04	-0.4457E-05	0.1906E-08	0.1606E-09	0.2727E-05
99	TO	105	-0.9261E-03	-0.1196E-04	0.9797E-05	-0.1282E-07	0.6304E-10	0.2665E-05	0.9628E-03
105	TO	112	-0.2148E-04	-0.1936E-05	0.1343E-07	0.1133E-09	0.4711E-05	0.8611E-03	-0.1673E-04
113	TO	114	0.3687E-05	0.4485E-10					

IMAGINARY PART

1	TO	7	0.2961E-05	-0.2440E-05	0.0	-0.1222E-06	-0.2941E-06	0.0	-0.6584E-07
8	TO	14	0.7766E-06	0.0	-0.7021E-07	-0.7474E-07	0.0	-0.1911E-05	0.2538E-05
15	TO	21	0.0	-0.5677E-06	0.3873E-06	0.0	0.8747E-07	-0.1862E-06	0.0
22	TO	28	0.9003E-07	0.1713E-06	0.0	0.1261E-06	0.2201E-06	0.0	0.1264E-06
29	TO	35	0.2609E-06	0.0	-0.1529E-06	0.6100E-06	0.0	-0.1529E-06	0.2994E-06
36	TO	42	0.0	-0.2680E-08	0.5380E-10	0.0	0.0	0.5273E-11	-0.2508E-08
43	TO	49	0.8154E-10	0.0	0.0	-0.9853E-11	-0.3223E-08	0.6227E-10	0.0
50	TO	56	0.0	0.3666E-11	-0.3125E-08	0.7328E-10	0.0	0.0	-0.6107E-11
57	TO	63	-0.1086E-08	0.3350E-11	0.0	0.0	-0.9815E-11	-0.1498E-08	-0.4128E-11
64	TO	70	0.0	0.0	0.8674E-11	-0.7301E-09	0.0	0.0	0.0
71	TO	77	0.1259E-10	-0.6577E-09	-0.2499E-11	0.0	-0.5539E-12	0.0	-0.3338E-08
73	TO	84	0.6779E-10	0.0	0.0	0.0	0.0	0.1086E-10	0.0
85	TO	91	0.0	0.0	0.1551E-10	0.0	-0.6269E-12	0.5048E-12	0.0
92	TO	98	-0.2368E-11	0.0	0.0	0.0	0.0	-0.1377E-10	-0.3115E-09
99	TO	105	0.0	0.0	0.0	0.0	-0.2369E-12	-0.3416E-08	0.1386E-09
106	TO	112	0.0	0.0	0.0	-0.1778E-13	-0.1841E-08	0.1015E-09	0.0
113	TO	114	0.0	0.5406E-14	0.4405E-12	-0.3165E-08	0.1262E-09	0.0	0.0

FIGURE VECTOR FOR 5001 NO. = 20

Mode 20, Frequency = 0.9824 Hz, $\Omega = 8$ RPM



EIGENVALUE = 0.57954712E 01 (rad/sec.)

REAL PART	IMAGINARY PART
1 TO 7	0.9832E-05
8 TO 14	0.3591E-05
15 TO 21	0.7206E-02
22 TO 28	0.6249E-04
29 TO 35	-0.2347E-02
36 TO 42	-0.3495E-02
43 TO 49	0.1335E-01
50 TO 56	0.3239E-04
57 TO 63	0.2419E-03
64 TO 70	-0.1910E-04
71 TO 77	0.1942E-05
78 TO 84	0.1334E-01
85 TO 91	-0.6900E-06
92 TO 98	0.5760E-04
99 TO 105	0.1206E-04
106 TO 112	-0.1518E-04
113 TO 114	0.2798E-10
1 TO 7	0.1000E 01
8 TO 14	-0.3059E-01
15 TO 21	0.1318E-03
22 TO 28	0.6718E-01
29 TO 35	0.3574E-12
36 TO 42	0.2567E-03
43 TO 49	0.5219E-04
50 TO 56	0.2201E-05
57 TO 63	0.7218E-04
64 TO 70	0.3564E-07
71 TO 77	0.1559E-03
78 TO 84	0.1028E-04
85 TO 91	0.3758E-12
92 TO 98	0.1573E-05
99 TO 105	0.1621E-06
106 TO 112	0.2055E-07
113 TO 114	0.2026E-04
1 TO 7	0.3398E-02
8 TO 14	0.3232E-02
15 TO 21	0.0
22 TO 28	0.4761E-03
29 TO 35	0.0
36 TO 42	0.6415E-04
43 TO 49	0.0
50 TO 56	0.3274E-06
57 TO 63	0.1990E-07
64 TO 70	0.0
71 TO 77	0.9208E-05
78 TO 84	0.0
85 TO 91	0.0
92 TO 98	0.0
99 TO 105	0.0
106 TO 112	0.0
113 TO 114	0.1890E-08
1 TO 7	0.4238E-03
8 TO 14	-0.2201E-04
15 TO 21	-0.8146E-01
22 TO 28	-0.2281E-02
29 TO 35	0.9151E-04
36 TO 42	0.1333E-01
43 TO 49	0.3225E-06
50 TO 56	0.1451E-03
57 TO 63	0.5334E-04
64 TO 70	0.4301E-06
71 TO 77	0.5731E-04
78 TO 84	0.3210E-06
85 TO 91	-0.1702E-05
92 TO 98	-0.2899E-06
99 TO 105	0.4631E-08
106 TO 112	0.3023E-04
113 TO 114	0.0
1 TO 7	-0.1055E-02
8 TO 14	-0.3234E-02
15 TO 21	0.0
22 TO 28	-0.6836E-04
29 TO 35	-0.9116E-03
36 TO 42	0.0
43 TO 49	0.5028E-06
50 TO 56	0.7972E-06
57 TO 63	0.0
64 TO 70	-0.9402E-05
71 TO 77	0.0
78 TO 84	0.0
85 TO 91	0.0
92 TO 98	0.0
99 TO 105	-0.1059E-09
106 TO 112	-0.1365E-04
113 TO 114	0.0
1 TO 7	0.4972E 00
8 TO 14	0.5652E-02
15 TO 21	-0.6191E-04
22 TO 28	-0.2345E 00
29 TO 35	0.2544E-01
36 TO 42	0.3251E-06
43 TO 49	-0.1637E-05
50 TO 56	0.1334E-01
57 TO 63	0.2901E-04
64 TO 70	0.3608E-06
71 TO 77	0.1687E-06
78 TO 84	0.6982E-04
85 TO 91	-0.1185E-04
92 TO 98	0.8128E-08
99 TO 105	0.1400E-06
106 TO 112	0.2952E-05
113 TO 114	0.3768E-12
1 TO 7	0.1304E-04
8 TO 14	0.4061E 00
15 TO 21	0.3295E-02
22 TO 28	-0.1200E-03
29 TO 35	0.2195E 00
36 TO 42	0.3197E-04
43 TO 49	-0.1637E-05
50 TO 56	0.1334E-01
57 TO 63	0.2901E-04
64 TO 70	0.3608E-06
71 TO 77	0.1687E-06
78 TO 84	0.6982E-04
85 TO 91	-0.1185E-04
92 TO 98	0.8128E-08
99 TO 105	0.1400E-06
106 TO 112	0.2952E-05
113 TO 114	0.3768E-12
1 TO 7	0.1055E-02
8 TO 14	-0.3234E-02
15 TO 21	0.0
22 TO 28	-0.6836E-04
29 TO 35	-0.9116E-03
36 TO 42	0.0
43 TO 49	0.5028E-06
50 TO 56	0.7972E-06
57 TO 63	0.0
64 TO 70	-0.9402E-05
71 TO 77	0.0
78 TO 84	0.0
85 TO 91	0.0
92 TO 98	0.0
99 TO 105	-0.1059E-09
106 TO 112	-0.1365E-04
113 TO 114	0.0
1 TO 7	0.3067E-02
8 TO 14	-0.1396E-03
15 TO 21	0.6689E-01
22 TO 28	-0.1006E-01
29 TO 35	-0.8650E-04
36 TO 42	-0.1810E-05
43 TO 49	0.1334E-01
50 TO 56	0.3207E-06
57 TO 63	-0.2362E-03
64 TO 70	0.2166E-04
71 TO 77	0.1839E-05
78 TO 84	0.7872E-04
85 TO 91	-0.1701E-05
92 TO 98	0.3682E-06
99 TO 105	0.5160E-02
106 TO 112	0.1255E-04
113 TO 114	0.0
1 TO 7	-0.9293E-03
8 TO 14	-0.7802E-03
15 TO 21	0.0
22 TO 28	-0.6774E-04
29 TO 35	0.9051E-03
36 TO 42	-0.6313E-04
43 TO 49	0.0
50 TO 56	0.3206E-06
57 TO 63	-0.3111E-07
64 TO 70	0.0
71 TO 77	-0.2070E-04
78 TO 84	0.0
85 TO 91	-0.2139E-06
92 TO 98	-0.1771E-04
99 TO 105	0.2700E-06
106 TO 112	0.0
113 TO 114	0.0

EIGENVALUE= 0.65686035E 01 (rad/sec.)

REAL PART

1	TO	7	0.8533E-02	-0.9999E 00	-0.1790E 00	-0.8337E-02	-0.9985E 00	-0.9345E-01	0.3900E-02	
9	TO	14	-0.9992E 00	-0.1573E 00	-0.4001E-02	-0.9986E 00	-0.1189E 00	0.1246E-01	0.9446E 00	
15	TO	21	0.1758E 00	-0.1206E-01	0.9439E 00	0.9259E-01	0.5845E-02	0.9437E 00	0.1538E 00	
22	TO	28	-0.5839E-02	0.9434E 00	0.1165E 00	0.4357E-02	0.3332E 00	0.1107E 00	-0.4393E-02	
29	TO	35	0.3119E 00	0.9112E-01	0.1835E-02	0.3327E 00	0.1368E 00	-0.2054E-02	0.3322E 00	
36	TO	42	0.9602E-01	0.1609E-01	0.5995E-01	-0.8616E-03	0.8140E-06	-0.1143E-03	-0.1547E-01	
43	TO	49	0.6004E-01	-0.6956E-03	0.7163E-06	0.1059E-03	0.7641E-02	0.6001E-01	-0.8241E-03	
50	TO	56	-0.7668E-06	0.1231E-03	-0.7530E-02	0.6004E-01	-0.7456E-03	0.6421E-06	0.1190E-03	
57	TO	63	0.7451E-04	-0.1532E-03	0.1517E-05	-0.1313E-05	0.5893E-05	-0.3386E-03	-0.1051E-03	
64	TO	70	-0.3022E-04	-0.1259E-06	0.2574E-05	-0.2879E-03	-0.1582E-03	0.6560E-04	-0.1005E-05	
71	TO	77	0.5101E-06	-0.4406E-04	-0.1366E-03	-0.1213E-04	-0.3876E-06	0.5312E-05	-0.8254E-06	
78	TO	84	-0.5002E-01	-0.7822E-03	0.6553E-06	0.4789E-05	0.1411E-03	-0.1363E-03	0.4883E-03	
85	TO	91	-0.1401E-05	0.2901E-10	-0.3414E-05	0.2532E-06	-0.2991E-10	-0.3423E-05	-0.4282E-07	
92	TO	98	-0.1621E-03	0.1796E-04	-0.6479E-06	-0.6942E-06	-0.9123E-05	-0.6507E-06	0.8500E-02	
99	TO	105	0.3211E-03	0.4657E-06	0.3535E-05	0.1846E-03	-0.2585E-06	-0.1440E-01	0.4353E-03	
106	TO	112	0.2429E-06	-0.2184E-05	-0.5643E-04	-0.4754E-06	-0.1683E-01	0.8098E-03	0.3343E-06	
113	TO	114	0.1775E-08	0.5638E-04						
IMAGINARY PART										
1	TO	7	0.6149E-03	-0.1037E-01	0.0	0.6166E-03	0.1036E-01	0.0	0.6814E-03	
9	TO	14	-0.5331E-02	0.0	0.6816E-03	0.5567E-02	0.0	-0.2183E-02	0.7496E-02	
15	TO	21	0.0	-0.2177E-02	-0.7189E-02	0.0	-0.2088E-02	0.3881E-02	0.0	
22	TO	28	-0.2087E-02	-0.3723E-02	0.0	-0.7716E-03	0.7784E-02	0.0	-0.7678E-03	
29	TO	35	-0.7472E-02	0.0	-0.7384E-03	0.4659E-02	0.0	-0.7370E-03	-0.4460E-02	
36	TO	42	0.0	-0.1578E-03	-0.4844E-05	0.0	0.0	-0.1745E-05	-0.1527E-03	
43	TO	49	-0.5415E-05	0.0	0.0	0.1673E-05	-0.4788E-04	-0.5016E-05	0.0	
50	TO	56	0.0	-0.1092E-05	-0.4692E-04	-0.5241E-05	0.0	0.0	0.1062E-05	
57	TO	63	0.5254E-06	-0.2816E-07	0.0	0.0	-0.9625E-08	-0.1407E-07	-0.4528E-07	
64	TO	70	0.0	0.0	0.1392E-07	0.1032E-05	-0.1939E-07	0.0	0.0	
71	TO	77	0.1572E-08	0.8970E-06	-0.2940E-07	0.0	0.0	0.3713E-08	-0.1184E-04	
78	TO	84	-0.5128E-05	0.0	0.0	0.0	-0.5227E-08	-0.1620E-07	0.0	
85	TO	91	0.0	0.0	0.1500E-08	0.0	0.0	-0.7123E-08	0.7657E-06	
92	TO	98	-0.1641E-07	0.0	0.0	0.0	-0.7535E-09	-0.3269E-06	-0.3253E-05	
99	TO	105	0.0	0.0	0.0	-0.4790E-08	0.4604E-05	-0.2298E-05	0.0	
106	TO	112	0.0	0.0	-0.9266E-08	0.7475E-05	-0.3136E-05	0.0	0.0	
113	TO	114	0.0	0.6712E-09						

Mode 32, Frequency = 3.8441 Hz, $\Omega = 8$ RPM

EIGENVALUES FOR PART 02 = 32

EIGENVALUE = 0.24153225E 02 (rad/sec.)

REAL PART	IMAGINARY PART
1 TO 97	0.4493E-01
8 TO 14	0.2329E-01
15 TO 21	0.5655E-03
22 TO 28	0.2753E-02
29 TO 35	0.6449E-01
36 TO 42	0.2791E-03
43 TO 49	0.2782E-01
50 TO 56	0.1222E-02
57 TO 63	0.2234E-01
64 TO 70	0.1332E-04
71 TO 77	0.3133E-03
78 TO 84	0.2782E-01
85 TO 91	0.6009E-07
92 TO 98	0.1630E-02
99 TO 105	0.2503E-03
106 TO 112	0.2225E-07
113 TO 114	0.1499E-07
1 TO 7	0.9890E 00
8 TO 14	0.1498E-01
15 TO 21	0.0
22 TO 28	0.3009E 00
29 TO 35	0.3504E-01
36 TO 42	0.0
43 TO 49	0.4295E-03
50 TO 56	0.0
57 TO 63	0.5740E 00
64 TO 70	0.0
71 TO 77	0.6234E-02
78 TO 84	0.4441E-03
85 TO 91	0.0
92 TO 98	0.1139E-02
99 TO 105	0.0
106 TO 112	0.0
113 TO 114	0.0
1 TO 7	0.4347E-01
8 TO 14	0.0
15 TO 21	0.8359E 00
22 TO 28	0.1293E-01
29 TO 35	0.0
36 TO 42	0.4865E 00
43 TO 49	0.0
50 TO 56	0.2991E-02
57 TO 63	0.1916E-03
64 TO 70	0.0
71 TO 77	0.2283E 00
78 TO 84	0.0
85 TO 91	0.0
92 TO 98	0.0
99 TO 105	0.0
106 TO 112	0.0
113 TO 114	0.7634E-07
1 TO 7	0.8113E-03
8 TO 14	0.4449E-02
15 TO 21	0.5668E-01
22 TO 28	0.5630E-03
29 TO 35	0.4937E-01
36 TO 42	0.2780E-01
43 TO 49	0.8387E-07
50 TO 56	0.2472E-02
57 TO 63	0.1043E-04
64 TO 70	0.2769E-03
71 TO 77	0.1532E-02
78 TO 84	0.4713E-07
85 TO 91	0.3292E-03
92 TO 98	0.9227E-06
99 TO 105	0.5228E-06
106 TO 112	0.1479E-04
113 TO 114	0.0
1 TO 7	0.3046E-01
8 TO 14	0.2339E-01
15 TO 21	0.8497E-03
22 TO 28	0.1629E 00
29 TO 35	0.2191E-01
36 TO 42	0.3755E-04
43 TO 49	0.1998E-03
50 TO 56	0.2782E-01
57 TO 63	0.5054E-08
64 TO 70	0.1018E-01
71 TO 77	0.1027E-04
78 TO 84	0.1354E-05
85 TO 91	0.5955E-07
92 TO 98	0.4207E-06
99 TO 105	0.5123E-04
106 TO 112	0.2189E-02
113 TO 114	0.0
1 TO 7	0.6769E-01
8 TO 14	0.8125E-03
15 TO 21	0.9844E-02
22 TO 28	0.6432E-01
29 TO 35	0.8783E-03
36 TO 42	0.1540E-06
43 TO 49	0.1736E-01
50 TO 56	0.2053E-04
57 TO 63	0.2390E-03
64 TO 70	0.1682E-02
71 TO 77	0.8861E-08
78 TO 84	0.1315E-03
85 TO 91	0.3453E-09
92 TO 98	0.4638E-04
99 TO 105	0.1314E-02
106 TO 112	0.4987E-03
113 TO 114	0.0
1 TO 7	0.8130E-03
8 TO 14	0.3207E-01
15 TO 21	0.1929E-01
22 TO 28	0.8778E-03
29 TO 35	0.5150E-01
36 TO 42	0.3976E-03
43 TO 49	0.2782E-01
50 TO 56	0.3616E-07
57 TO 63	0.4282E-01
64 TO 70	0.9529E-05
71 TO 77	0.3919E-03
78 TO 84	0.2188E-02
85 TO 91	0.4058E-03
92 TO 98	0.3168E-02
99 TO 105	0.5399E-02
106 TO 112	0.2695E-03
113 TO 114	0.0
1 TO 7	0.4249E-01
8 TO 14	0.0
15 TO 21	0.3012E 00
22 TO 28	0.3934E-01
29 TO 35	0.0
36 TO 42	0.0
43 TO 49	0.1818E 00
50 TO 56	0.0
57 TO 63	0.4507E-02
64 TO 70	0.1490E-03
71 TO 77	0.0
78 TO 84	0.6234E-02
85 TO 91	0.1523E-05
92 TO 98	0.0
99 TO 105	0.6494E-02
106 TO 112	0.6608E-01
113 TO 114	0.1768E-02
1 TO 7	0.9989E 00
8 TO 14	0.1460E-01
15 TO 21	0.0
22 TO 28	0.9371E 00
29 TO 35	0.1365E-01
36 TO 42	0.0
43 TO 49	0.4862E-02
50 TO 56	0.4398E-03
57 TO 63	0.0
64 TO 70	0.2284E 00
71 TO 77	0.0
78 TO 84	0.4509E-02
85 TO 91	0.1055E-03
92 TO 98	0.0
99 TO 105	0.6493E-02
106 TO 112	0.0
113 TO 114	0.7764E-05
1 TO 7	0.3534E 00
8 TO 14	0.3890E-01
15 TO 21	0.0
22 TO 28	0.9382E 00
29 TO 35	0.1353E-01
36 TO 42	0.0
43 TO 49	0.4853E-02
50 TO 56	0.4516E-03
57 TO 63	0.0
64 TO 70	0.6741E 00
71 TO 77	0.0
78 TO 84	0.8421E-01
85 TO 91	0.0
92 TO 98	0.1048E-01
99 TO 105	0.1895E-02
106 TO 112	0.0
113 TO 114	0.0

VECTOR FOR PORT NO. = 1 Mode 1, frequency = 0.1787 Hz, $\Omega = 12$ RPM

STATE VALUE = 0.11227112E 01 (rad/sec)

REAL PART	IMAGINARY PART
1 TO 7	0.1250E-06
8 TO 14	0.4246E 00
15 TO 21	-0.1000E-07
22 TO 28	-0.1076E-07
29 TO 35	-0.2342E-03
36 TO 42	0.1775E 00
43 TO 49	0.1425E-05
50 TO 56	0.4431E-02
57 TO 63	0.3702E-07
64 TO 70	0.9485E-03
71 TO 77	0.2750E-09
78 TO 84	0.1428E-05
85 TO 91	0.1425E-04
92 TO 98	0.1500E-07
99 TO 105	-0.1534E-03
106 TO 112	0.1123E-02
113 TO 114	0.1834E-05
1 TO 7	-0.9711E-06
8 TO 14	0.1967E-05
15 TO 21	0.0
22 TO 28	-0.1609E-05
29 TO 35	0.1499E-05
36 TO 42	0.0
43 TO 49	-0.1849E-10
50 TO 56	0.0
57 TO 63	-0.1273E-05
64 TO 70	0.0
71 TO 77	-0.1216E-10
78 TO 84	-0.1702E-10
85 TO 91	0.0
92 TO 98	-0.1378E-11
99 TO 105	0.0
106 TO 112	0.0
113 TO 114	0.0
1 TO 7	0.1381E-02
8 TO 14	0.4313E 00
15 TO 21	0.6409E-07
22 TO 28	-0.7342E-03
29 TO 35	-0.1769E 00
36 TO 42	0.5851E 00
43 TO 49	0.4481E-02
50 TO 56	0.3436E-07
57 TO 63	-0.1727E-02
64 TO 70	0.2102E-05
71 TO 77	-0.3411E-07
78 TO 84	0.2911E-03
85 TO 91	0.1829E-12
92 TO 98	0.3044E-04
99 TO 105	0.2364E-02
106 TO 112	0.8422E-07
113 TO 114	0.3564E-11
1 TO 7	-0.9709E-06
8 TO 14	0.7741E-06
15 TO 21	0.0
22 TO 28	0.2249E-06
29 TO 35	-0.1053E-05
36 TO 42	0.0
43 TO 49	0.3699E-10
50 TO 56	-0.1759E-10
57 TO 63	0.0
64 TO 70	0.5932E-11
71 TO 77	-0.2990E-11
78 TO 84	0.0
85 TO 91	0.1107E-10
92 TO 98	0.0
99 TO 105	0.0
106 TO 112	0.0
113 TO 114	0.2407E-19
1 TO 7	0.2584E-07
8 TO 14	0.1515E-02
15 TO 21	0.9097E 00
22 TO 28	0.7265E-07
29 TO 35	0.9047E-03
36 TO 42	-0.5851E 00
43 TO 49	0.4481E-02
50 TO 56	0.1428E-05
57 TO 63	0.1414E-04
64 TO 70	0.3235E-07
71 TO 77	0.5123E-03
78 TO 84	0.4556E-06
85 TO 91	-0.6389E-05
92 TO 98	0.8942E-06
99 TO 105	-0.3353E-08
106 TO 112	0.6821E-10
113 TO 114	0.0
1 TO 7	0.8679E-06
8 TO 14	0.0
15 TO 21	-0.1609E-05
22 TO 28	-0.2560E-05
29 TO 35	0.0
36 TO 42	0.0
43 TO 49	-0.1865E-08
50 TO 56	0.0
57 TO 63	-0.6128E-11
64 TO 70	-0.6255E-12
71 TO 77	0.0
78 TO 84	-0.1284E-12
85 TO 91	0.0
92 TO 98	-0.1033E-12
99 TO 105	-0.3578E-09
106 TO 112	-0.6659E-11
113 TO 114	0.0
1 TO 7	0.9604E 00
8 TO 14	0.1193E-06
15 TO 21	0.1080E-02
22 TO 28	-0.3953E 00
29 TO 35	-0.2166E-07
36 TO 42	0.6831E-09
43 TO 49	0.1427E-05
50 TO 56	0.4482E-02
57 TO 63	-0.3841E-07
64 TO 70	-0.7548E-03
71 TO 77	0.3006E-09
78 TO 84	0.1578E-07
85 TO 91	-0.2021E-09
92 TO 98	0.8701E-09
99 TO 105	0.1017E-09
106 TO 112	0.1277E-05
113 TO 114	-0.1281E-03
1 TO 7	0.0
8 TO 14	-0.7758E-06
15 TO 21	0.1448E-05
22 TO 28	0.0
29 TO 35	-0.1270E-05
36 TO 42	-0.3910E-10
43 TO 49	-0.1659E-10
50 TO 56	0.0
57 TO 63	-0.1232E-08
64 TO 70	0.0
71 TO 77	0.1178E-10
78 TO 84	-0.2651E-11
85 TO 91	-0.1072E-10
92 TO 98	-0.7988E-09
99 TO 105	-0.1125E-10
106 TO 112	0.0
113 TO 114	0.0



EIGENVECTOR FOR RUMT NO. 2

Mode 2, frequency = 0.1977 Hz, $\Omega = 12$ RPM

EIGENVALUE = 0.12424011E 01 (rad/sec)

REAL PART	7	0.2725E-09	0.2559E-05	-0.5936E-00	-0.5572E-10	0.2559E-05	0.2559E-05	-0.6463E 00	0.1580E-09
1 10	7	0.2725E-09	0.2559E-05	-0.5936E-00	-0.5572E-10	0.2559E-05	0.2559E-05	-0.6463E 00	0.1580E-09
2 10	14	-0.3451E-05	-0.5463E-00	-0.1735E-01	0.2724E-05	-0.4351E-00	0.2243E-09	0.2243E-09	0.1866E-05
15 10	21	-0.0035E 00	-0.3787E-10	-0.1356E-01	0.2724E-05	-0.0035E 00	-0.2447E-05	-0.2447E-05	-0.7372E 00
22 10	28	-0.3560E-10	-0.1966E-05	-0.8214E-01	0.1315E-09	-0.3560E-10	-0.5922E-06	-0.2843E 00	-0.6192E-10
29 10	35	-0.5923E-06	-0.3590E 00	-0.1104E-01	0.9705E-05	-0.5923E-06	-0.3046E 00	-0.4056E-10	0.1532E-05
36 10	42	-0.3331E-00	-0.1659E-04	-0.2604E-01	-0.7836E 00	-0.3331E-00	-0.8276E-03	0.1320E-11	-0.1449E-09
43 10	49	-0.2610E-08	-0.1030E 01	-0.5305E-01	0.1034E-11	-0.2610E-08	0.7254E-10	0.2608E-08	-0.8432E 00
50 10	56	-0.8279E-03	0.1255E-11	-0.5836E-11	0.2613E-08	-0.8279E-03	-0.9402E 00	-0.8300E-03	-0.1121E-11
57 10	63	-0.6749E-10	-0.2754E-10	-0.4918E-11	0.1598E-04	-0.6749E-10	-0.1012E-12	-0.7009E-10	0.1755E-10
64 10	70	-0.1969E-02	0.7382E-05	-0.1363E-11	0.5926E-10	-0.1969E-02	0.2724E-10	-0.3803E-02	0.1460E-04
71 10	77	0.5016E-12	-0.6170E-10	-0.2808E-11	-0.2503E-02	0.5016E-12	0.7872E-05	0.5511E-12	0.2507E-12
78 10	84	0.2639E-08	-0.8917E 00	-0.2288E-01	0.1239E-02	0.2639E-08	0.1231E-11	0.2837E-10	-0.8791E-02
85 10	91	0.1637E-04	0.3198E-15	-0.3731E-17	0.8691E-05	0.1637E-04	0.3198E-15	-0.3729E-12	0.1279E-13
92 10	98	0.2705E-10	-0.3039E-02	-0.1102E-01	0.1232E-03	0.2705E-10	0.1562E-11	0.1812E-12	0.2867E-08
99 10	105	-0.3544E 00	-0.6184E-03	-0.1178E-01	-0.5500E-11	-0.3544E 00	0.7483E-13	0.2282E-08	-0.1019E 00
106 10	112	-0.1991E-03	0.6343E-03	-0.1290E-11	0.1216E-12	-0.1991E-03	0.4495E-08	-0.3091E 00	-0.4090E-03
113 10	119	0.0525E-02	0.6409E-14	0.0	0.0	0.0525E-02	0.0	0.0	0.0
IMAGINARY PART									
1 10	7	-0.1507E-08	0.7930E-08	0.0	-0.1837E-08	-0.1507E-08	0.1533E-08	0.0	-0.1464E-07
8 10	14	0.5386E-08	0.0	-0.4451E-08	0.1436E-08	0.5386E-08	0.0	-0.1481E-08	0.6223E-08
15 10	21	0.0	-0.1490E-08	0.7601E-08	0.0	-0.1490E-08	-0.9837E-08	0.3805E-08	0.0
22 10	28	-0.3201E-08	0.7201E-04	0.0	0.9251E-09	-0.3201E-08	0.0	0.9254E-09	0.0
29 10	35	0.3582E-08	0.0	-0.1525E-07	0.9984E-08	0.3582E-08	0.0	-0.2414E-08	0.2956E-08
36 10	42	0.0	-0.9219E-11	-0.3605E-13	0.0	0.0	0.0	-0.8315E-13	-0.8905E-11
43 10	49	-0.4038E-13	0.0	0.0	0.7873E-13	-0.4038E-13	-0.3935E-11	0.0	0.0
50 10	56	0.0	-0.5395E-13	-0.3875E-11	-0.3981E-13	0.0	0.0	0.5204E-13	-0.7985E-14
57 10	63	-0.2773E-11	0.7687E-15	0.0	-0.1233E-11	-0.2773E-11	-0.1337E-13	-0.2689E-11	0.0
64 10	70	0.0	0.0	-0.1297E-13	0.0	0.0	-0.1190E-14	0.0	0.0
71 10	77	-0.2656E-13	-0.1184E-11	-0.6336E-14	0.0	-0.2656E-13	0.0	0.2578E-13	-0.2124E-11
78 10	84	-0.3748E-13	0.0	0.0	0.0	-0.3748E-13	-0.2760E-15	-0.5672E-14	0.0
85 10	91	0.0	0.0	-0.2412E-13	0.0	0.0	0.0	-0.2342E-13	0.1535E-12
92 10	98	-0.3939E-14	0.0	0.0	0.0	-0.3939E-14	-0.2142E-15	-0.1666E-11	-0.2132E-13
99 10	105	0.0	0.0	0.0	0.4423E-17	0.0	-0.7653E-12	-0.2331E-13	0.0
106 10	112	0.0	0.0	0.0	-0.1321E-11	0.0	-0.3644E-13	0.0	0.0
113 10	119	0.0	0.5898E-22	-0.2419E-10	-0.1381E-13	0.0	-0.3644E-13	0.0	0.0

EIGENVECTOR FOR ROOT NO. = 3 Mode 3, frequency = 0.3185, Q = 12 RPM

EIGENVALUE = 0.2009766E 01 (rad/sec)

REAL PART

1	Y0	7	0.5659E-03	0.1229E-01	0.1406E-03	-0.8988E-01	0.1173E-02	-0.2207E-03
4	Y0	14	-0.4207E-02	0.1013E-02	-0.3523E-00	0.4517E-02	0.4041E-03	-0.5950E-00
15	Y0	21	0.4759E-02	-0.2001E-02	-0.1070E-02	-0.3875E-04	-0.9983E-00	0.5896E-02
22	Y0	28	0.2463E-03	0.2088E-02	0.5171E-03	-0.6886E-00	-0.6687E-02	0.1698E-03
29	Y0	35	-0.5325E-03	-0.2247E-03	-0.3633E-00	0.4242E-01	0.7693E-03	-0.7117E-00
36	Y0	42	0.1528E-02	0.4715E-04	0.4562E-02	-0.8103E-05	0.4205E-06	0.3944E-04
43	Y0	49	0.4566E-02	0.2695E-04	0.1365E-06	-0.5524E-04	0.4560E-02	0.1799E-05
50	Y0	56	0.1384E-06	-0.5624E-06	0.4280E-04	-0.1725E-04	0.1318E-06	-0.4819E-06
57	Y0	63	0.8374E-04	0.2204E-04	-0.1227E-06	0.4899E-06	-0.8500E-04	0.1380E-04
64	Y0	70	-0.2314E-06	0.3545E-05	0.4261E-06	0.3796E-04	-0.3544E-06	-0.1656E-08
71	Y0	77	0.5475E-06	-0.2131E-04	0.1731E-04	0.1106E-08	0.5789E-06	-0.5150E-05
78	Y0	84	0.4502E-02	0.4633E-05	-0.1312E-06	-0.1080E-05	0.2407E-04	0.6389E-06
85	Y0	91	-0.2805E-06	-0.2805E-06	0.7716E-06	0.8563E-12	-0.7482E-06	-0.5060E-06
92	Y0	98	0.2121E-04	-0.3625E-06	0.8674E-09	0.1412E-07	-0.3944E-05	0.4915E-02
99	Y0	105	-0.7544E-05	0.9484E-07	-0.5529E-07	-0.6166E-06	0.1940E-02	-0.8612E-05
106	Y0	112	0.3195E-07	0.4065E-07	0.1170E-04	-0.3025E-05	-0.1524E-04	0.6211E-07
113	Y0	114	0.4447E-03	0.6276E-05				
1	Y0	7	0.2244E-02	0.9936E-01	0.0	0.1645E-02	0.0	0.2024E-02
4	Y0	14	-0.9746E-01	0.0	0.2644E-02	0.2208E-00	0.1981E-02	0.1056E-00
15	Y0	21	0.0	0.1526E-02	0.6061E-01	0.0	0.5837E-01	0.0
22	Y0	28	0.2375E-02	0.2674E-00	0.0	0.1502E-00	0.0	0.1606E-02
29	Y0	35	0.7900E-01	0.0	-0.1044E-02	0.0	0.2172E-02	0.2625E-00
36	Y0	42	0.0	-0.1504E-04	-0.1798E-02	0.0	0.4417E-05	-0.2335E-04
43	Y0	49	-0.1799E-02	0.0	0.0	-0.3175E-04	-0.1798E-02	0.0
50	Y0	56	0.0	-0.1899E-06	0.4110E-05	0.0	0.0	0.8095E-08
57	Y0	63	-0.1305E-04	-0.5767E-05	0.0	0.3506E-06	0.3405E-05	-0.6075E-05
64	Y0	70	0.0	0.0	-0.3020E-06	-0.2877E-04	0.0	0.0
71	Y0	77	-0.1803E-06	0.1954E-04	-0.7026E-05	0.0	-0.6143E-07	-0.9592E-05
78	Y0	84	-0.1746E-02	0.0	0.0	-0.4257E-06	-0.1050E-04	0.0
85	Y0	91	0.0	0.0	-0.9326E-07	0.0	0.0	-0.9344E-06
92	Y0	98	-0.9399E-05	0.0	0.0	-0.5269E-06	-0.1297E-06	-0.1618E-02
99	Y0	105	0.0	0.0	0.0	-0.1066E-05	-0.7058E-05	0.0
106	Y0	112	0.0	0.0	-0.2871E-05	-0.3922E-05	-0.5135E-03	0.0
113	Y0	114	0.0	-0.2305E-05	-0.5523E-05	-0.1212E-02	0.0	0.0

IMAGINARY PART

EIGENVECTOR FOR MODE NO. 9

Mode 9, frequency = 0.5025 Hz, $\Omega = 12$ RPM

EIGENVALUE = 0.315744E-01 (rad/sec)

REAL PART

1	10	7	-0.4535E-04	0.2549E-01	0.6321E-00	-0.3571E-04	0.2932E-02	-0.1352E-00	0.3528E-04
3	10	14	0.1115E-01	-0.5897E-00	0.4258E-04	0.2433E-01	0.8027E-00	-0.3269E-04	0.1192E-01
15	10	21	0.4790E-00	-0.2844E-04	-0.2522E-03	-0.2221E-00	0.2527E-04	0.3855E-02	-0.1000E-01
22	10	28	0.3512E-04	0.1163E-01	0.7443E-00	0.6068E-05	-0.1215E-02	-0.5214E-00	-0.1787E-05
29	10	35	-0.1417E-02	-0.4642E-00	-0.1596E-04	-0.9250E-02	-0.4952E-00	0.1238E-04	-0.7894E-02
36	10	42	-0.4609E-00	-0.4798E-00	0.8431E-06	-0.9223E-01	0.2597E-04	-0.2201E-08	0.4768E-06
43	10	49	0.8511E-06	-0.8450E-01	0.3040E-04	-0.2222E-08	-0.2800E-06	0.8504E-06	-0.9030E-01
50	10	56	0.2835E-04	-0.3939E-08	0.2766E-06	0.2532E-06	-0.8671E-01	0.3124E-04	-0.3876E-08
57	10	63	0.4370E-07	0.3387E-07	-0.1169E-02	0.6014E-05	0.1161E-10	-0.4381E-07	0.2168E-07
64	10	70	-0.1154E-03	0.2066E-05	0.6178E-11	0.3695E-07	0.3369E-07	-0.7857E-03	0.4676E-05
71	10	77	0.8641E-10	-0.5918E-07	0.2823E-07	-0.3143E-03	0.3397E-05	0.8942E-10	-0.2011E-11
78	10	84	0.5130E-00	-0.0555E-01	0.3109E-04	0.6380E-04	-0.5570E-08	0.3443E-07	-0.2986E-02
85	10	91	0.8417E-05	0.5055E-12	-0.2806E-09	-0.3171E-06	0.5055E-12	-0.2809E-09	-0.3526E-11
92	10	98	0.3354E-07	-0.5346E-03	0.4021E-05	0.2235E-04	0.1835E-08	0.1807E-10	0.3470E-05
99	10	105	-0.7119E-01	0.2326E-04	0.7870E-04	-0.1213E-07	0.5130E-11	0.3180E-05	-0.1815E-01
106	10	112	0.7545E-05	0.1659E-03	0.1544E-07	0.1751E-11	0.5379E-05	-0.4733E-01	0.1541E-04
113	10	114	0.1117E-03	0.2682E-10	0.1544E-07	0.1751E-11	0.5379E-05	-0.4733E-01	0.1541E-04

IMAGINARY PART

1	10	7	-0.5235E-04	-0.2112E-01	0.0	0.1617E-05	-0.1630E-01	0.0	0.1418E-04
3	10	14	0.2009E-01	0.0	-0.2443E-04	0.1637E-01	0.0	-0.3377E-04	-0.1145E-01
15	10	21	0.0	0.4733E-05	-0.8954E-02	0.0	0.1341E-04	0.1090E-01	0.0
22	10	28	-0.1442E-04	0.8981E-02	0.0	0.6010E-05	0.1260E-02	0.0	0.6992E-05
29	10	35	-0.3879E-07	0.0	0.4543E-04	-0.3014E-02	0.0	0.3889E-04	0.2534E-02
36	10	42	0.0	-0.2079E-08	-0.3931E-08	0.0	0.0	-0.5127E-10	0.4005E-08
43	10	49	-0.6632E-08	0.0	0.0	-0.8128E-10	-0.4505E-08	0.0	-0.3377E-10
50	10	56	0.0	-0.4679E-10	-0.7781E-09	-0.5387E-08	0.0	0.0	0.6168E-09
57	10	63	0.1390E-08	-0.6377E-09	0.0	0.0	0.1400E-10	0.1656E-08	0.0
64	10	70	0.0	0.0	-0.1426E-10	0.2124E-09	-0.8325E-09	0.0	0.0
71	10	77	0.1245E-10	0.3247E-09	0.8194E-09	0.0	0.0	-0.1584E-10	-0.2168E-08
78	10	84	-0.5410E-08	0.0	0.0	0.0	-0.2863E-10	-0.6571E-11	0.0
85	10	91	0.0	0.0	-0.1585E-10	0.0	0.0	0.1883E-10	-0.1541E-09
92	10	98	0.2008E-11	0.0	0.0	0.0	0.1088E-11	-0.2050E-08	0.4526E-08
99	10	105	0.0	0.0	0.0	0.0	-0.9034E-09	0.5547E-08	0.0
106	10	112	0.0	0.0	0.0	-0.4220E-10	0.1108E-07	0.0	0.0
113	10	114	0.0	-0.3625E-12	0.0	-0.1585E-08	0.0	0.0	0.0

Mode 10, frequency = 0.5151 Hz, $\Omega = 12$ RPM

EIGENVECTOR FOR ROOT NO. = 10

EIGENVALUE = 0.32366943E C1 (rad/sec)

REAL PART

1	10	7	-0.1309E-04	0.9355E-02	-0.6734E-03	0.2972E-03	0.9168E-00	0.1301E-04
2	10	14	0.2776E-02	-0.5753E-04	0.1417E-04	0.9009E-00	-0.1061E-04	0.4126E-02
3	10	21	0.1123E-00	-0.7275E-05	-0.4955E-03	0.9941E-05	0.9424E-03	0.5083E-01
4	10	28	0.1057E-04	-0.4260E-02	0.4554E-00	-0.5666E-03	0.2169E-00	-0.8190E-06
5	10	35	-0.6635E-03	0.1615E-00	-0.3192E-02	0.4202E-01	0.5467E-05	-0.2039E-02
6	10	42	-0.6688E-01	-0.2783E-07	0.9483E-00	-0.7657E-02	-0.2179E-09	0.1225E-07
7	10	49	-0.2762E-06	-0.1033E-01	-0.7657E-02	-0.1219E-07	-0.2765E-06	0.4470E-00
8	10	56	-0.7657E-02	-0.2821E-09	-0.7596E-08	-0.4487E-00	-0.7656E-02	-0.9442E-10
9	10	63	-0.7688E-08	-0.2791E-08	-0.9156E-02	0.1833E-10	0.7829E-08	-0.1770E-08
10	10	70	0.4053E-02	0.1045E-04	0.1829E-10	-0.2767E-08	-0.3831E-02	0.6909E-04
11	10	77	-0.6642E-10	0.6733E-08	-0.2352E-05	0.2144E-02	-0.6574E-10	-0.7836E-10
12	10	84	-0.2764E-06	-0.9131E-03	-0.7655E-02	-0.2195E-05	-0.2882E-08	-0.2901E-01
13	10	91	0.8558E-04	0.1673E-12	0.4037E-10	0.1679E-12	0.4006E-10	-0.4826E-11
14	10	98	-0.2750E-08	-0.1561E-03	0.5377E-04	-0.1633E-09	-0.5359E-10	-0.2893E-06
15	10	105	-0.1409E-02	-0.5726E-02	-0.1554E-05	-0.2080E-10	-0.2278E-06	-0.1273E-02
16	10	112	-0.1874E-02	0.2675E-05	-0.1342E-08	-0.4359E-10	-0.1606E-02	-0.3802E-02
17	10	119	0.1237E-06	0.3665E-11				

IMAGINARY PART

1	10	7	-0.1737E-04	-0.7065E-02	0.0	-0.3938E-02	0.0	0.6758E-05
2	10	14	0.7044E-02	0.0	-0.1214E-04	0.3462E-02	-0.1177E-04	-0.4067E-02
3	10	21	0.0	0.3234E-05	-0.2272E-02	0.0	0.4059E-02	0.0
4	10	28	-0.7933E-05	0.0	0.2331E-05	0.9374E-03	0.0	0.3345E-05
5	10	35	-0.1661E-03	0.0	0.1106E-02	0.0	0.1030E-04	0.1090E-02
6	10	42	0.0	-0.2735E-10	0.1043E-09	0.0	-0.3681E-11	0.8694E-09
7	10	49	0.7344E-10	-0.0	-0.1592E-10	0.27106E-09	0.4624E-10	0.0
8	10	56	0.0	-0.1261E-11	0.0	0.0	0.0	-0.3211E-11
9	10	63	-0.2517E-09	-0.2755E-10	0.4903E-10	0.0	-0.2659E-09	0.8799E-11
10	10	70	0.0	0.0	-0.6681E-10	-0.3031E-10	0.0	0.0
11	10	77	-0.2151E-11	-0.8067E-10	0.0	0.0	0.2736E-11	0.2251E-09
12	10	84	0.4646E-10	0.0	0.0	0.5156E-12	-0.1438E-10	0.0
13	10	91	0.0	0.0	0.0	0.0	-0.2225E-11	0.8975E-11
14	10	98	-0.5824E-11	0.0	0.0	-0.1041E-12	0.1723E-09	-0.9739E-10
15	10	105	0.0	0.0	0.0	0.8916E-10	-0.8871E-10	0.0
16	10	112	0.0	0.0	-0.6173E-14	0.1513E-09	-0.8722E-11	0.0
17	10	119	0.0	0.4151E-16				

Mode 11, frequency = 0.6716 Hz, $\Omega = 12$ RPM

11

FIGURE VECTOR FOR POINT No. = 11

EIGENVALUE = 0.42200928E 01 (rad/sec)

REAL PART	IMAGINARY PART					
1 TO 7	0.1464E-01	0.2133E-01	0.4699E-04	0.4272E-01	0.1986E-01	-0.2486E-03
8 TO 14	-0.1403E-01	0.5235E-05	-0.6420E-02	-0.1257E-01	-0.2537E-02	0.3157E-02
15 TO 21	-0.8744E-03	0.5678E-01	0.1690E-01	-0.1107E-02	-0.2057E-01	-0.2775E-01
22 TO 28	-0.7280E-03	0.8191E-02	0.1489E-02	0.5340E-02	-0.1237E-01	0.9025E-03
29 TO 35	-0.3138E-01	-0.1193E-02	-0.3157E-01	0.3723E-01	0.6640E-03	0.9393E-01
36 TO 42	0.6067E-02	-0.1726E-03	-0.6506E-02	0.3499E-07	-0.1675E-06	0.2634E-03
43 TO 49	-0.6506E-02	0.2026E-05	-0.1450E-05	-0.1283E-03	-0.6506E-02	-0.4126E-05
50 TO 56	-0.3399E-07	-0.1511E-05	-0.6506E-02	-0.2890E-06	0.3217E-07	-0.2225E-05
57 TO 63	-0.9234E-04	-0.1601E-04	-0.1238E-05	-0.2890E-06	0.9550E-04	-0.9288E-05
64 TO 70	-0.3924E-06	-0.8272E-04	-0.5217E-04	-0.1547E-04	0.4538E-06	-0.9239E-08
71 TO 77	-0.7900E-06	0.5214E-04	-0.2484E-04	-0.3226E-08	-0.8177E-06	-0.4950E-05
78 TO 84	-0.6505E-02	-0.2185E-05	0.3263E-07	-0.2600E-05	-0.1887E-04	0.4494E-05
85 TO 91	-0.1444E-07	0.1900E-11	0.7253E-06	0.1000E-11	0.7653E-06	-0.2623E-06
92 TO 98	-0.1506E-04	0.1234E-07	-0.5880E-08	-0.2011E-09	-0.3790E-05	-0.5378E-02
99 TO 105	-0.4933E-06	0.2681E-07	-0.5375E-08	-0.6410E-05	-0.1191E-02	-0.5062E-07
106 TO 112	0.3092E-08	-0.7825E-09	-0.7538E-05	-0.2710E-05	0.2821E-06	0.1910E-07
113 TO 114	0.1192E-05	-0.8974E-05				
1 TO 7	-0.2975E-03	-0.7446E-01	0.0	0.1616E-01	0.0	-0.1288E-03
8 TO 14	0.3443E-02	0.0	0.1780E-01	0.0	-0.3742E-03	-0.9908E 00
15 TO 21	0.0	0.2447E-03	-0.4604E 00	-0.1336E-03	-0.4154E 00	0.0
22 TO 28	0.3585E-03	-0.3544E 00	0.0	0.1000E 01	0.0	0.1899E-03
29 TO 35	0.4730E 00	0.0	-0.1199E-03	0.0	-0.1115E-03	0.3694E 00
36 TO 42	0.0	-0.4674E-03	-0.1395E-03	0.0	-0.3109E-05	0.5584E-03
43 TO 49	-0.1266E-03	0.0	-0.3653E-05	-0.2294E-03	-0.1304E-03	0.0
50 TO 56	0.0	-0.3696E-05	0.2728E-03	0.0	0.0	-0.4197E-05
57 TO 63	-0.6728E-04	0.1513E-04	0.0	-0.7511E-06	0.2974E-04	0.1209E-04
64 TO 70	0.0	0.0	-0.5323E-06	0.1906E-04	0.0	0.0
71 TO 77	-0.7396E-06	-0.1161E-04	0.1561E-04	0.0	-0.3615E-06	0.1317E-04
78 TO 84	-0.1777E-03	0.0	0.0	-0.4741E-05	0.1882E-04	0.0
85 TO 91	0.0	0.0	0.7987E-06	0.0	0.4527E-06	0.3412E-06
92 TO 98	0.1854E-04	0.0	0.0	0.9554E-06	0.1037E-04	0.1902E-02
99 TO 105	0.0	0.0	-0.9037E-05	0.3817E-05	0.1855E-02	0.0
106 TO 112	0.0	0.0	0.4562E-05	0.3314E-02	0.0	0.0
113 TO 114	0.0	0.2912E-07				

9

EIGENVECTOR FOR FOOT NO. 17 Mode 17, frequency = 0.7777 Hz, $\beta = 12$ RPM

EIGENVALUE = 0.48364746E 01 (rad/sec)

REAL PART	1 TO 7	8 TO 14	15 TO 21	22 TO 28	29 TO 35	36 TO 42	43 TO 49	50 TO 56	57 TO 63	64 TO 70	71 TO 77	78 TO 84	85 TO 91	92 TO 98	99 TO 105	106 TO 112	113 TO 114
	0.323E-01	-0.264E-01	0.247E-05	0.7159E-01	0.4931E-05	-0.1262E-01	0.1068E-01	-0.1518E-05									
	-0.2651E-02	-0.1663E-01	0.2477E-05	0.2477E-05	0.4449E-01	0.3337E-01	-0.5991E-05	0.5565E-01									
	0.9227E 00	0.6727E-05	0.3672E-04	0.3672E-04	0.7425E 00	-0.2587E-05	0.2399E-01	0.9753E 00									
	0.3313E-05	-0.3665E-01	0.9665F 00	0.9665F 00	-0.1429E-05	-0.2057E-01	-0.9513F 00	0.1986E-05									
	-0.4326E-02	-0.7580F 00	-0.6896E-06	-0.6896E-06	0.6754E-02	-0.1000E 01	0.8191E-06	0.5779E-01									
	-0.4665E-05	-0.8576E-05	-0.4730E-05	-0.4730E-05	-0.2330E-01	0.1331E-04	-0.5833E-07	0.8448E-05									
	0.1366E-04	-0.1961E-01	0.1442E-04	0.1442E-04	-0.4195E-05	-0.4195E-05	0.4679E-05	-0.2233E-01									
	0.6035E-06	0.6590E-07	0.4179E-05	0.4179E-05	-0.4645E-05	-0.2065E-01	0.1469E-04	-0.6508E-07									
	-0.4866E-03	0.3495E-06	0.1742E-02	0.1742E-02	-0.1501E-04	-0.2354E-08	-0.5376E-06	0.2207E-06									
	0.3933E-08	-0.1653E-05	-0.1741E-08	-0.1741E-08	0.6329E-06	0.3506E-06	0.7666E-03	-0.1192E-04									
	-0.4685E-05	-0.5506E-06	0.2873E-06	0.2873E-06	-0.2426E-03	-0.5269E-05	0.2709E-08	0.2600E-08									
	-0.1930E-04	-0.2151E-01	0.1444E-04	0.1444E-04	0.6884E-04	-0.7966E-07	0.3454E-06	0.6004E-02									
	0.3417E-05	0.1420E-03	-0.2517E-08	-0.2517E-08	0.3900E-05	0.2087E-11	-0.2512E-08	0.1304E-09									
	-0.5315E-02	0.1746E-04	-0.8636E-05	-0.8636E-05	-0.6150E-05	0.1940E-07	0.1936E-08	0.3010E-04									
	0.2584E-05	-0.1456E-04	0.5577E-04	0.5577E-04	-0.1557E-06	0.7653E-09	0.3007E-04	0.3386E-02									
	0.1567E-04	0.2672E-09	0.1559E-06	0.1559E-06	0.1310E-08	0.5436E-04	0.4288E-02	0.6507E-05									
IMAGINARY PART																	
	0.4083E-04	0.9233E-04	0.0	0.0	-0.7116E-05	0.1108E-03	0.0	-0.3776E-04									
	-0.2332E-04	0.0	-0.1821E-03	-0.1821E-03	0.8574E-04	0.0	-0.1182E-03	0.1138E-04									
	0.3010E-04	-0.8778E-04	0.2293E-04	0.2293E-04	0.0	-0.6739E-04	0.1208E-03	0.0									
	0.4719E-05	0.0	0.0	0.0	0.6593E-04	0.1481E-04	0.0	0.1449E-04									
	-0.8483E-04	-0.2483E-07	-0.2039E-04	-0.2039E-04	-0.9196E-04	0.0	-0.1854E-03	0.3818E-05									
	0.0	0.0	-0.9118E-09	-0.9118E-09	0.0	0.0	0.4411E-10	-0.2055E-07									
	0.0	0.2754E-10	0.0	0.0	-0.9101E-10	-0.2757E-07	-0.8885E-09	0.0									
	-0.1692E-07	-0.1273E-09	-0.2623E-07	-0.2623E-07	-0.8768E-09	0.0	0.0	-0.5490E-10									
	0.0	0.0	0.1041E-09	0.1041E-09	0.0	-0.1180E-09	-0.1445E-07	-0.1347E-11									
	-0.1216E-09	-0.5274E-08	0.2546E-10	0.2546E-10	-0.6300E-08	-0.1197E-09	0.0	0.0									
	0.0	0.0	0.0	0.0	0.0	-0.9633E-11	0.9898E-10	-0.2819E-07									
	0.0	0.0	0.1654E-09	0.1654E-09	0.0	0.0	-0.1100E-09	0.0									
	-0.8151E-10	0.0	0.0	0.0	0.0	-0.4695E-11	-0.1432E-09	-0.2767E-08									
	0.0	0.0	0.0	0.0	0.0	-0.1615E-07	-0.2906E-07	0.2717E-09									
	0.0	0.0	0.2011E-11	0.2011E-11	-0.8247E-12	-0.1615E-07	0.1645E-09	0.0									
	0.0	0.2810E-13	-0.2660E-07	-0.2660E-07	0.0	0.2021E-09	0.0	0.0									

EIGENVECTOR FOR ROOT NO. = 18

Mode 18, frequency = 0.7911 Hz, $\Omega = 12$ RPM

EIGENVALUE = 0.49705811E 01 (rad/sec)

REAL PART		IMAGINARY PART	
1	10	7	7
9	11	14	14
15	12	21	21
22	13	28	28
29	14	35	35
36	15	42	42
43	16	49	49
50	17	56	56
57	18	63	63
64	19	70	70
71	20	77	77
78	21	84	84
85	22	91	91
92	23	98	98
99	24	105	105
106	25	112	112
113	26	119	119
120	27	126	126
127	28	133	133
134	29	140	140
141	30	147	147
148	31	154	154
155	32	161	161
162	33	168	168
169	34	175	175
176	35	182	182
183	36	189	189
190	37	196	196
197	38	203	203
204	39	210	210
211	40	217	217
218	41	224	224
225	42	231	231
232	43	238	238
239	44	245	245
246	45	252	252
253	46	259	259
260	47	266	266
267	48	273	273
274	49	280	280
281	50	287	287
288	51	294	294
295	52	301	301
302	53	308	308
309	54	315	315
316	55	322	322
323	56	329	329
330	57	336	336
337	58	343	343
344	59	350	350
351	60	357	357
358	61	364	364
365	62	371	371
372	63	378	378
379	64	385	385
386	65	392	392
393	66	399	399
400	67	406	406
407	68	413	413
414	69	420	420
421	70	427	427
428	71	434	434
435	72	441	441
442	73	448	448
449	74	455	455
456	75	462	462
463	76	469	469
470	77	476	476
477	78	483	483
484	79	490	490
491	80	497	497
498	81	504	504
505	82	511	511
512	83	518	518
519	84	525	525
526	85	532	532
533	86	539	539
540	87	546	546
547	88	553	553
554	89	560	560
561	90	567	567
568	91	574	574
575	92	581	581
582	93	588	588
589	94	595	595
596	95	602	602
603	96	609	609
610	97	616	616
617	98	623	623
624	99	630	630
631	100	637	637
638	101	644	644
645	102	651	651
652	103	658	658
659	104	665	665
666	105	672	672
673	106	679	679
680	107	686	686
687	108	693	693
694	109	700	700
701	110	707	707
708	111	714	714
715	112	721	721
722	113	728	728
729	114	735	735
736	115	742	742
743	116	749	749
750	117	756	756
757	118	763	763
764	119	770	770
771	120	777	777
778	121	784	784
785	122	791	791
792	123	798	798
799	124	805	805
806	125	812	812
813	126	819	819
820	127	826	826
827	128	833	833
834	129	840	840
841	130	847	847
848	131	854	854
855	132	861	861
862	133	868	868
869	134	875	875
876	135	882	882
883	136	889	889
890	137	896	896
897	138	903	903
904	139	910	910
911	140	917	917
918	141	924	924
925	142	931	931
932	143	938	938
939	144	945	945
946	145	952	952
953	146	959	959
960	147	966	966
967	148	973	973
974	149	980	980
981	150	987	987
988	151	994	994
995	152	1001	1001
1002	153	1008	1008
1009	154	1015	1015
1016	155	1022	1022
1023	156	1029	1029
1030	157	1036	1036
1037	158	1043	1043
1044	159	1050	1050
1051	160	1057	1057
1058	161	1064	1064
1065	162	1071	1071
1072	163	1078	1078
1079	164	1085	1085
1086	165	1092	1092
1093	166	1099	1099
1100	167	1106	1106
1107	168	1113	1113
1114	169	1120	1120
1121	170	1127	1127
1128	171	1134	1134
1135	172	1141	1141
1142	173	1148	1148
1149	174	1155	1155
1156	175	1162	1162
1163	176	1169	1169
1170	177	1176	1176
1177	178	1183	1183
1184	179	1190	1190
1191	180	1197	1197
1198	181	1204	1204
1205	182	1211	1211
1212	183	1218	1218
1219	184	1225	1225
1226	185	1232	1232
1233	186	1239	1239
1240	187	1246	1246
1247	188	1253	1253
1254	189	1260	1260
1261	190	1267	1267
1268	191	1274	1274
1275	192	1281	1281
1282	193	1288	1288
1289	194	1295	1295
1296	195	1302	1302
1303	196	1309	1309
1310	197	1316	1316
1317	198	1323	1323
1324	199	1330	1330
1331	200	1337	1337
1338	201	1344	1344
1345	202	1351	1351
1352	203	1358	1358
1359	204	1365	1365
1366	205	1372	1372
1373	206	1379	1379
1380	207	1386	1386
1387	208	1393	1393
1394	209	1400	1400
1401	210	1407	1407
1408	211	1414	1414
1415	212	1421	1421
1422	213	1428	1428
1429	214	1435	1435
1436	215	1442	1442
1443	216	1449	1449
1450	217	1456	1456
1457	218	1463	1463
1464	219	1470	1470
1471	220	1477	1477
1478	221	1484	1484
1485	222	1491	1491
1492	223	1498	1498
1499	224	1505	1505
1506	225	1512	1512
1513	226	1519	1519
1520	227	1526	1526
1527	228	1533	1533
1534	229	1540	1540
1541	230	1547	1547
1548	231	1554	1554
1555	232	1561	1561
1562	233	1568	1568
1569	234	1575	1575
1576	235	1582	1582
1583	236	1589	1589
1590	237	1596	1596
1597	238	1603	1603
1604	239	1610	1610
1611	240	1617	1617
1618	241	1624	1624
1625	242	1631	1631
1632	243	1638	1638
1639	244	1645	1645
1646	245	1652	1652
1653	246	1659	1659
1660	247	1666	1666
1667	248	1673	1673
1674	249	1680	1680
1681	250	1687	1687
1688	251	1694	1694
1695	252	1701	1701
1702	253	1708	1708
1709	254	1715	1715
1716	255	1722	1722
1723	256	1729	1729
1730	257	1736	1736
1737	258	1743	1743
1744	259	1750	1750
1751	260	1757	1757
1758	261	1764	1764
1765	262	1771	1771
1772	263	1778	1778
1779	264	1785	1785
1786	265	1792	1792
1793	266	1799	1799
1794	267	1806	1806
1805	268	1813	1813
1812	269	1820	1820
1819	270	1827	1827
1826	271	1834	1834
1833	272	1841	1841
1840	273	1848	1848
1847	274	1855	1855
1854	275	1862	1862
1861	276	1869	1869
1868	277	1876	1876
1875	278	1883	1883
1882	279	1890	1890
1889	280	1897	1897
1896	281	1904	1904
1903	282	1911	1911
1910	283	1918	1918
1917	284	1925	1925
1924	285	1932	1932
1931	286	1939	1939
1938	287	1946	1946
1945	288	1953	1953
1952	289	1960	1960
1959	290	1967	1967
1966	291	1974	1974
1973	292	1981	1981
1980	293	1988	1988
1987	294	1995	1995
1994	295	2002	2002
2001	296	2009	2009
2008	297	2016	2016
2015	298	2023	2023
2022	299	2030	2030
2029	300	2037	2037
2036	301	2044	2044
2043	302	2051	2051
2050	303	2058	2058
2057	304	2065	2065
2064	305	2072	2072
2071	306	2079	2079
2078	307	2086	2086
2085	308	2093	2093
2092	309	2100	2100
2099	310	2107	2107
2106	311	2114	2114
2113	312	2121	2121
2120	313	2128	2128
2127	314	2135	2135
2134	315	2142	2142
2141	316	2149	2149
2148	317	2156	2156
2155	318	2163	2163
2162	319	2170	2170
2169	320	2177	2177
2176	321	2184	2184
2183	322	2191	2191
2190	323	2198	2198
2197	324	2205	2205
2204	325	2212	2212
2211	326	2219	2219
2218	327		

EIGENVECTOR FOR ROOT NO.= 10 Mode 19, frequency = 0.8049 Hz, $\Omega = 12$ RPM

FIGENVALUE= 0.56854658E 01 (rad/sec)

REAL PART		IMAGINARY PART	
1	7	0.5428E-03	0.6762E-00
9	14	-0.5142E-06	0.4012E-06
15	21	0.1424E-05	0.1433E-03
22	28	0.6869E-06	0.1879E-03
29	35	0.7425E-03	-0.2388E-01
36	42	0.1769E-02	-0.1862E-05
43	49	-0.1828E-05	-0.7232E-05
50	56	-0.7295E-05	-0.1513E-07
57	63	0.7144E-07	0.5396E-02
64	70	-0.1880E-02	-0.4498E-09
71	77	0.3699E-09	-0.7712E-07
78	84	-0.1829E-05	-0.3723E-02
85	91	-0.6827E-04	0.5011E-13
92	98	-0.5719E-07	0.1461E-03
99	105	-0.9361E-03	0.9787E-05
106	112	-0.2144E-04	-0.1938E-05
113	119	0.3687E-05	0.1118E-08
1	7	-0.2429E-05	0.0
8	14	-0.8027E-06	-0.3143E-05
15	21	0.0	0.2087E-05
22	28	-0.1069E-05	0.0
29	35	0.6015E-05	0.6911E-06
36	42	0.0	-0.5322E-09
43	49	-0.4044E-09	0.0
50	56	0.0	-0.9932E-08
57	63	-0.4052E-08	0.0
64	70	0.0	0.2034E-10
71	77	-0.2422E-10	-0.1543E-10
78	84	-0.4686E-09	0.0
85	91	0.0	0.3724E-10
92	98	-0.3085E-10	0.0
99	105	0.0	0.0
106	112	0.0	0.1346E-12
113	119	0.0	0.1976E-13
1	7	0.6683E-02	-0.6355E-05
9	14	0.9037E-03	-0.1007E-04
15	21	0.5855E-01	0.0
22	28	-0.2000E-06	-0.5398E-06
29	35	0.6888E-03	0.5803E-05
36	42	-0.2771E-02	0.0
43	49	-0.1311E-07	-0.1231E-09
50	56	0.1826E-06	-0.4428E-09
57	63	-0.5030E-04	0.0
64	70	0.9738E-07	-0.2353E-10
71	77	-0.1160E-02	-0.4524E-10
78	84	0.1168E-04	0.0
85	91	0.1386E-04	-0.2250E-11
92	98	-0.4457E-05	0.0
99	105	0.3264E-08	-0.3198E-10
106	112	-0.3344E-07	-0.1452E-11
113	119	0.26230E-09	-0.7344E-08
1	7	0.0	-0.1967E-04
8	14	0.7898E-06	0.0
15	21	-0.1470E-05	0.1335E-05
22	28	0.0	-0.5455E-05
29	35	-0.2678E-06	0.0
36	42	0.9169E-10	0.0
43	49	-0.4944E-09	-0.1038E-07
50	56	0.0	0.0
57	63	-0.3449E-08	-0.2353E-10
64	70	0.0	-0.4524E-10
71	77	0.1872E-10	0.0
78	84	-0.5493E-10	0.0
85	91	-0.3198E-10	-0.2250E-11
92	98	-0.1319E-07	0.0
99	105	-0.1202E-09	-0.1452E-11
106	112	0.0	-0.7344E-08
113	119	0.0	-0.1060E-09
1	7	-0.5878E-01	0.0
9	14	-0.1420E-05	0.4251E-05
15	21	0.4829E-03	0.2739E-05
22	28	-0.5136E 00	0.0
29	35	0.1746E-06	-0.5392E-06
36	42	-0.1359E-07	0.3129E-05
43	49	-0.1838E-05	-0.2237E-08
50	56	-0.7254E-05	0.0
57	63	-0.5528E-07	-0.7495E-10
64	70	0.2162E-02	-0.4508E-11
71	77	0.8741E-10	0.0
78	84	0.5772E-07	-0.1241E-07
85	91	-0.1242E-09	0.0
92	98	0.3438E-09	-0.5493E-10
99	105	0.5618E-05	-0.3198E-10
106	112	0.8611E-03	-0.1319E-07
113	119	0.0	-0.1202E-09

EIGENVALUE = 0.64309668E 01 (rad/sec)

REAL PART	IMAGINARY PART
1 10 7	0.3920E-02
2 10 14	-0.9545E-03
3 10 21	0.1470E 00
4 10 28	-0.6089E-02
5 10 35	0.3131E 00
6 10 42	0.7836E-01
7 10 49	0.7612E-01
8 10 56	0.5805E-06
9 10 63	0.2828E-03
10 10 70	-0.1981E-04
11 10 77	0.2224E-05
12 10 84	0.7610E-01
13 10 91	-0.4431E-06
14 10 98	-0.1173E-03
15 10 105	0.1956E-03
16 10 112	0.1768E-06
17 10 119	0.1350E-05
18 10 126	0.1351E-06
19 10 133	0.9284E-03
20 10 140	-0.8347E-02
21 10 147	0.0
22 10 154	-0.3065E-02
23 10 161	-0.1142E-01
24 10 168	0.0
25 10 175	-0.7611E-05
26 10 182	0.0
27 10 189	-0.2016E-05
28 10 196	-0.8076E-08
29 10 203	0.0
30 10 210	-0.3561E-07
31 10 217	-0.7372E-05
32 10 224	0.0
33 10 231	0.0
34 10 238	-0.3360E-07
35 10 245	0.0
36 10 252	0.0
37 10 259	0.0
38 10 266	0.0
39 10 273	0.0
40 10 280	0.0
41 10 287	0.0
42 10 294	0.0
43 10 301	0.0
44 10 308	0.0
45 10 315	0.0
46 10 322	0.0
47 10 329	0.0
48 10 336	0.0
49 10 343	0.0
50 10 350	0.0
51 10 357	0.0
52 10 364	0.0
53 10 371	0.0
54 10 378	0.0
55 10 385	0.0
56 10 392	0.0
57 10 399	0.0
58 10 406	0.0
59 10 413	0.0
60 10 420	0.0
61 10 427	0.0
62 10 434	0.0
63 10 441	0.0
64 10 448	0.0
65 10 455	0.0
66 10 462	0.0
67 10 469	0.0
68 10 476	0.0
69 10 483	0.0
70 10 490	0.0
71 10 497	0.0
72 10 504	0.0
73 10 511	0.0
74 10 518	0.0
75 10 525	0.0
76 10 532	0.0
77 10 539	0.0
78 10 546	0.0
79 10 553	0.0
80 10 560	0.0
81 10 567	0.0
82 10 574	0.0
83 10 581	0.0
84 10 588	0.0
85 10 595	0.0
86 10 602	0.0
87 10 609	0.0
88 10 616	0.0
89 10 623	0.0
90 10 630	0.0
91 10 637	0.0
92 10 644	0.0
93 10 651	0.0
94 10 658	0.0
95 10 665	0.0
96 10 672	0.0
97 10 679	0.0
98 10 686	0.0
99 10 693	0.0
100 10 700	0.0
101 10 707	0.0
102 10 714	0.0
103 10 721	0.0
104 10 728	0.0
105 10 735	0.0
106 10 742	0.0
107 10 749	0.0
108 10 756	0.0
109 10 763	0.0
110 10 770	0.0
111 10 777	0.0
112 10 784	0.0
113 10 791	0.0
114 10 798	0.0
115 10 805	0.0
116 10 812	0.0
117 10 819	0.0
118 10 826	0.0
119 10 833	0.0
120 10 840	0.0
121 10 847	0.0
122 10 854	0.0
123 10 861	0.0
124 10 868	0.0
125 10 875	0.0
126 10 882	0.0
127 10 889	0.0
128 10 896	0.0
129 10 903	0.0
130 10 910	0.0
131 10 917	0.0
132 10 924	0.0
133 10 931	0.0
134 10 938	0.0
135 10 945	0.0
136 10 952	0.0
137 10 959	0.0
138 10 966	0.0
139 10 973	0.0
140 10 980	0.0
141 10 987	0.0
142 10 994	0.0
143 10 1001	0.0
144 10 1008	0.0
145 10 1015	0.0
146 10 1022	0.0
147 10 1029	0.0
148 10 1036	0.0
149 10 1043	0.0
150 10 1050	0.0
151 10 1057	0.0
152 10 1064	0.0
153 10 1071	0.0
154 10 1078	0.0
155 10 1085	0.0
156 10 1092	0.0
157 10 1099	0.0
158 10 1106	0.0
159 10 1113	0.0
160 10 1120	0.0
161 10 1127	0.0
162 10 1134	0.0
163 10 1141	0.0
164 10 1148	0.0
165 10 1155	0.0
166 10 1162	0.0
167 10 1169	0.0
168 10 1176	0.0
169 10 1183	0.0
170 10 1190	0.0
171 10 1197	0.0
172 10 1204	0.0
173 10 1211	0.0
174 10 1218	0.0
175 10 1225	0.0
176 10 1232	0.0
177 10 1239	0.0
178 10 1246	0.0
179 10 1253	0.0
180 10 1260	0.0
181 10 1267	0.0
182 10 1274	0.0
183 10 1281	0.0
184 10 1288	0.0
185 10 1295	0.0
186 10 1302	0.0
187 10 1309	0.0
188 10 1316	0.0
189 10 1323	0.0
190 10 1330	0.0
191 10 1337	0.0
192 10 1344	0.0
193 10 1351	0.0
194 10 1358	0.0
195 10 1365	0.0
196 10 1372	0.0
197 10 1379	0.0
198 10 1386	0.0
199 10 1393	0.0
200 10 1400	0.0
201 10 1407	0.0
202 10 1414	0.0
203 10 1421	0.0
204 10 1428	0.0
205 10 1435	0.0
206 10 1442	0.0
207 10 1449	0.0
208 10 1456	0.0
209 10 1463	0.0
210 10 1470	0.0
211 10 1477	0.0
212 10 1484	0.0
213 10 1491	0.0
214 10 1498	0.0
215 10 1505	0.0
216 10 1512	0.0
217 10 1519	0.0
218 10 1526	0.0
219 10 1533	0.0
220 10 1540	0.0
221 10 1547	0.0
222 10 1554	0.0
223 10 1561	0.0
224 10 1568	0.0
225 10 1575	0.0
226 10 1582	0.0
227 10 1589	0.0
228 10 1596	0.0
229 10 1603	0.0
230 10 1610	0.0
231 10 1617	0.0
232 10 1624	0.0
233 10 1631	0.0
234 10 1638	0.0
235 10 1645	0.0
236 10 1652	0.0
237 10 1659	0.0
238 10 1666	0.0
239 10 1673	0.0
240 10 1680	0.0
241 10 1687	0.0
242 10 1694	0.0
243 10 1701	0.0
244 10 1708	0.0
245 10 1715	0.0
246 10 1722	0.0
247 10 1729	0.0
248 10 1736	0.0
249 10 1743	0.0
250 10 1750	0.0
251 10 1757	0.0
252 10 1764	0.0
253 10 1771	0.0
254 10 1778	0.0
255 10 1785	0.0
256 10 1792	0.0
257 10 1799	0.0
258 10 1806	0.0
259 10 1813	0.0
260 10 1820	0.0
261 10 1827	0.0
262 10 1834	0.0
263 10 1841	0.0
264 10 1848	0.0
265 10 1855	0.0
266 10 1862	0.0
267 10 1869	0.0
268 10 1876	0.0
269 10 1883	0.0
270 10 1890	0.0
271 10 1897	0.0
272 10 1904	0.0
273 10 1911	0.0
274 10 1918	0.0
275 10 1925	0.0
276 10 1932	0.0
277 10 1939	0.0
278 10 1946	0.0
279 10 1953	0.0
280 10 1960	0.0
281 10 1967	0.0
282 10 1974	0.0
283 10 1981	0.0
284 10 1988	0.0
285 10 1995	0.0
286 10 2002	0.0
287 10 2009	0.0
288 10 2016	0.0
289 10 2023	0.0
290 10 2030	0.0
291 10 2037	0.0
292 10 2044	0.0
293 10 2051	0.0
294 10 2058	0.0
295 10 2065	0.0
296 10 2072	0.0
297 10 2079	0.0
298 10 2086	0.0
299 10 2093	0.0
300 10 2100	0.0
301 10 2107	0.0
302 10 2114	0.0
303 10 2121	0.0
304 10 2128	0.0
305 10 2135	0.0
306 10 2142	0.0
307 10 2149	0.0
308 10 2156	0.0
309 10 2163	0.0
310 10 2170	0.0
311 10 2177	0.0
312 10 2184	0.0
313 10 2191	0.0
314 10 2198	0.0
315 10 2205	0.0
316 10 2212	0.0
317 10 2219	0.0
318 10 2226	0.0
319 10 2233	0.0
320 10 2240	0.0
321 10 2247	0.0
322 10 2254	0.0
323 10 2261	0.0
324 10 2268	0.0
325 10 2275	0.0
326 10 2282	0.0
327 10 2289	0.0
328 10 2296	0.0
329 10 2303	0.0
330 10 2310	0.0
331 10 2317	0.0
332 10 2324	0.0
333 10 2331	0.0
334 10 2338	0.0
335 10 2345	0.0
336 10 2352	0.0
337 10 2359	0.0
338 10 2366	0.0
339 10 2373	0.0
340 10 2380	0.0
341 10 2387	0.0
342 10 2394	0.0
343 10 2401	0.0
344 10 2408	0.0
345 10 2415	0.0
346 10 2422	0.0
347 10 2429	0.0
348 10 2436	0.0
349 10 2443	0.0
350 10 2450	0.0
351 10 2457	0.0
352 10 2464	0.0
353 10 2471	0.0
354 10 2478	0.0
355 10 2485	0.0
356 10 2492	0.0
357 10 2499	0.0
358 10 2506	0.0
359 10 2513	0.0
360 10 2520	0.0
361 10 2527	0.0
362 10 2534	0.0
363 10 2541	0.0
364 10 2548	0.0
365 10 2555	0.0
366 10 2562	0.0
367 10 2569	0.0
368 10 2576	0.0
369 10 2583	0.0
370 10 2590	0.0
371 10 2597	0.0
372 10 2604	0.0
373 10 2611	0.0
374 10 2618	0.0
375 10 2625	0.0
376 10 2632	0.0
377 10 2639	0.0
378 10 2646	0.0
379 10 2653	0.0
380 10 2660	0.0
381 10 2667	0.0
382 10 2674	0.0
383 10 2681	0.0
384 10 2688	0.0
385 10 2695	0.0
386 10 2702	0.0
387 10 2709	0.0
388 10 2716	0.0
389 10 2723	0.0
390 10 2730	0.0
391 10 2737	0.0
392 10 2744	0.0
393 10 2751	0.0
394 10 2758	0.0
395 10 2765	0.0
396 10 2772	0.0
397 10 2779	0.0
398 10 2786	0.0
399 10 2793	0.0
400 10 2800	0.0
401 10 2807	0.0
402 10 2814	0.0
403 10 2821	0.0
404 10 2828	0.0
405 10 2835	0.0
406 10 2842	0.0
407 10 2849	0.0
408 10 2856	0.0
409 10 2863	0.0
410 10 2870	0.0
411 10 2877	0.0
412 10 2884	0.0
413 10 2891	0.0
414 10 2898	0.0
415 10 2905	0.0
416 10 2912	0.0
417 10 2919	0.0
418 10 2926	0.0
419 10 2933	0.0
420 10 2940	0.0
421 10 2947	0.0

EIGENVECTOR FOR ROOT NO. 32

Mode 32, frequency = 3.8462 Hz, $\Omega = 12$ RPM

EIGENVALUE = 0.24166260E 02 (rad/sec)

REAL PART	IMAGINARY PART
1 TO 7	0.5914E-02
1 TO 14	-0.4292E-01
15 TO 21	-0.6953E-01
22 TO 28	-0.2684E-01
29 TO 35	-0.8032E-01
36 TO 42	-0.5974E-02
43 TO 49	-0.4111E-01
50 TO 56	0.8316E-06
57 TO 63	-0.1205E-00
64 TO 70	0.7016E-04
71 TO 77	-0.1118E-02
78 TO 84	-0.4111E-01
85 TO 91	0.4045E-06
92 TO 98	0.2453E-02
99 TO 105	0.1702E-07
106 TO 112	0.1583E-05
113 TO 114	0.1024E-06
1 TO 7	0.1069E 00
8 TO 14	0.3729E-01
15 TO 21	0.0
22 TO 28	-0.2666E 00
29 TO 35	0.9714E-01
36 TO 42	0.0
43 TO 49	0.5344E-02
50 TO 56	0.0
57 TO 63	-0.6664E 00
64 TO 70	0.0
71 TO 77	-0.6163E-02
78 TO 84	0.5354E-02
85 TO 91	0.0
92 TO 98	-0.3946E-03
99 TO 105	0.0
106 TO 112	0.0
113 TO 114	0.0
1 TO 7	0.5914E-02
8 TO 14	-0.4292E-01
15 TO 21	-0.6953E-01
22 TO 28	-0.2684E-01
29 TO 35	-0.8032E-01
36 TO 42	-0.5974E-02
43 TO 49	-0.4111E-01
50 TO 56	0.8316E-06
57 TO 63	-0.1205E-00
64 TO 70	0.7016E-04
71 TO 77	-0.1118E-02
78 TO 84	-0.4111E-01
85 TO 91	0.4045E-06
92 TO 98	0.2453E-02
99 TO 105	0.1702E-07
106 TO 112	0.1583E-05
113 TO 114	0.1024E-06
1 TO 7	0.9871E 00
8 TO 14	0.3640E-01
15 TO 21	0.0
22 TO 28	-0.4012E 00
29 TO 35	0.3388E-01
36 TO 42	0.0
43 TO 49	0.4777E-02
50 TO 56	0.5345E-02
57 TO 63	0.0
64 TO 70	-0.2259E 00
71 TO 77	0.0
78 TO 84	0.0
85 TO 91	0.6419E-02
92 TO 98	0.0
99 TO 105	-0.44831E-05
106 TO 112	0.0
113 TO 114	-0.4689E-01
1 TO 7	0.5525E-02
8 TO 14	-0.1347E 00
15 TO 21	-0.1995E-01
22 TO 28	0.5965E-02
29 TO 35	-0.1111E 00
36 TO 42	-0.1095E-02
43 TO 49	-0.4110E-01
50 TO 56	0.2458E-06
57 TO 63	-0.1350E 00
64 TO 70	0.6477E-04
71 TO 77	0.1242E-02
78 TO 84	0.3295E-02
85 TO 91	-0.1290E-02
92 TO 98	-0.1156E-01
99 TO 105	0.9366E-02
106 TO 112	0.1831E-02
113 TO 114	0.0
1 TO 7	0.8450E-01
8 TO 14	0.5221E-02
15 TO 21	-0.4457E-01
22 TO 28	-0.7957E-01
29 TO 35	0.5969E-02
36 TO 42	0.1048E-05
43 TO 49	-0.4479E-01
50 TO 56	-0.1396E-03
57 TO 63	-0.8303E-03
64 TO 70	0.2829E-02
71 TO 77	0.6040E-07
78 TO 84	-0.1979E-03
85 TO 91	-0.2352E-08
92 TO 98	0.7057E-04
99 TO 105	-0.4982E-02
106 TO 112	0.2915E-02
113 TO 114	0.0
1 TO 7	0.1051E 00
8 TO 14	0.0
15 TO 21	-0.2980E 00
22 TO 28	0.9756E-01
29 TO 35	0.0
36 TO 42	-0.1771E 00
43 TO 49	0.0
50 TO 56	-0.4455E-02
57 TO 63	-0.4843E-03
64 TO 70	0.0
71 TO 77	0.0
78 TO 84	0.2022E-04
85 TO 91	0.0
92 TO 98	-0.6770E-05
99 TO 105	-0.2867E-01
106 TO 112	0.3423E-02
113 TO 114	0.0
1 TO 7	0.5193E-01
8 TO 14	-0.6684E-01
15 TO 21	0.6007E-02
22 TO 28	0.3404E 00
29 TO 35	-0.2400E-01
36 TO 42	-0.7017E-01
43 TO 49	-0.1856E-03
50 TO 56	0.3934E-03
57 TO 63	0.2103E-02
64 TO 70	-0.5393E-07
71 TO 77	-0.1510E-01
78 TO 84	0.8692E-05
85 TO 91	-0.1897E-02
92 TO 98	0.9981E-03
99 TO 105	0.1641E-02
106 TO 112	0.1291E-06
113 TO 114	0.0
1 TO 7	0.3499E 00
8 TO 14	0.9479E-01
15 TO 21	0.0
22 TO 28	0.9042E 00
29 TO 35	0.3368E-01
36 TO 42	-0.4799E 00
43 TO 49	0.0
50 TO 56	0.2955E-02
57 TO 63	-0.3570E-03
64 TO 70	0.0
71 TO 77	0.6159E-02
78 TO 84	-0.6893E-03
85 TO 91	-0.6416E-02
92 TO 98	0.4587E-02
99 TO 105	0.0
106 TO 112	0.0
113 TO 114	0.0